NOAA Atlas NESDIS 38

WORLD OCEAN ATLAS 1998
VOLUME 12: Nutrients and Chlorophyll of the Indian Ocean

Margarita E. Conkright
Todd D. O'Brien
Sydney Levitus
Timothy P. Boyer
Cathy Stephens
John I. Antonov

National Oceanographic Data Center
Ocean Climate Laboratory

Silver Spring, MD
December 1998

1998 International Year of the Ocean

National Oceanographic Data Center

Additional copies of this publication, as well as information about NODC data holdings, and services, are available on request directly from NODC. NODC information and data are also available over the Internet through the NODC World Wide Web site.

National Oceanographic Data Center
User Services Team
NOAA/NESDIS E/OC1
SSMC-III, 4th Floor
1315 East-West Highway
Silver Spring, MD 20910-3282

Telephone: (301)713-3277

Fax: (301)713-3302

E-mail: services@nodc.noaa.gov

NODC World Wide Web site: http://www.nodc.noaa.gov/

Contents

List of Tables

List of Figures

APPENDIX A

APPENDIX B

APPENDIX C

APPENDIX D

APPENDIX E

APPENDIX F

APPENDIX G

APPENDIX H

Preface

The oceanographic analyses described by this atlas series expand on earlier works, *e.g.* the *World Ocean Atlas 1994* (WOA94) and *Climatological Atlas of the World Ocean*. Previously published oceanographic objective analyses have proven to be of great utility to the oceanographic, climate research, and operational environmental forecasting communities. Such analyses are used as boundary and/or initial conditions in numerical ocean circulation models and atmosphere-ocean models, for verification of numerical simulations of the ocean, as a form of "sea truth" for satellite measurements such as altimetric observations of sea surface height, for computation of nutrient fluxes by Ekman transport, and for planning oceanographic expeditions.

We have expanded our earlier analyses to include an all-data annual analysis of chlorophyll, monthly analyses of oxygen, and seasonal analyses of nutrients. Additional data for these variables have become available and there is a need for such analyses of these data in order to:

1)   study the role of biogeochemical cycles in determining how the earth's climate system works, particularly the vulnerability of ocean ecosystems to climate change (IPCC, 1996);

2)   help verify remotely sensed estimates of chlorophyll (SeaWIFS, ADEOS missions) which requires knowledge of *in situ* variables such as chlorophyll and plankton;

3)   provide the most comprehensive set of oceanographic databases and products based on these data to the international research and forecasting communities.

We continue preparing climatological analyses on a one-degree grid. This is because higher resolution analyses are not justified for all the variables we are working with and we wish to produce a set of analyses for which all variables have been analyzed in the same manner. High-resolution analyses as typified by the work of Boyer and Levitus (1997) will be published as separate atlases.

In the acknowledgment section of this publication we have expressed our view that creation of global ocean profile and plankton databases and analyses are only possible through the cooperation of scientists, data managers, and scientific administrators throughout the international scientific community. I would also like to thank my colleagues and the staff of the Ocean Climate Laboratory of NODC for their dedication to the project leading to publication of this atlas series. Their integrity and thoroughness have made this database possible. It is my belief that the development and management of national and international oceanographic data archives is best performed by scientists who are actively working with the historical data.

Sydney Levitus
National Oceanographic Data Center
Silver Spring, MD
December 1998

Acknowledgments

WORLD OCEAN ATLAS 1998, VOLUME 12:
Nutrients and Chlorophyll of the Indian Ocean

Margarita E. Conkright, Todd D. O'Brien, Sydney Levitus,
Timothy P. Boyer, Cathy Stephens, and John I. Antonov
National Oceanographic Data Center
Silver Spring, MD

ABSTRACT

This atlas contains maps of the distribution of objectively analyzed fields of phosphate, nitrate, silicate, and chlorophyll at selected standard depth levels of the Indian Ocean on a one-degree grid. Maps for all-data annual and seasonal compositing periods are presented at standard depth levels. The fields used to generate these maps were computed by objective analysis of historical data. Data distribution maps are presented for all-data annual and seasonal compositing periods at selected standard levels.

1. INTRODUCTION

This atlas is an analysis of all historical nutrient and chlorophyll profile data available from the National Oceanographic Data Center (NODC) and World Data Center-A (WDC-A) for Oceanography, Silver Spring, Maryland, plus data gathered as a result of several data management projects including:

a) the Intergovernmental Oceanographic Commission (IOC) Global Oceanographic Data Archaeology and Rescue (GODAR) project;

b) the NODC Oceanographic Data Archaeology and Rescue (NODAR) project;

c) the NODC Global Ocean Database project (GODB).

Data used in this atlas have been analyzed in a consistent, objective manner on a one-degree latitude-longitude grid at standard oceanographic levels between the surface and ocean bottom to a maximum depth of 5500m for the nutrients and to 100m depth for chlorophyll. The procedures used are very similar to, but not identical with those used to produce earlier analyses (Levitus, 1982; Levitus and Boyer, 1994a,b; Levitus *et al*, 1994a; Conkright *et al.,* 1994a). Annual and seasonal analyses have been computed for phosphate, nitrate, silicate, and chlorophyll.

Objective analyses shown in this atlas are limited by the nature of the data base (data are non-synoptic and scattered in space) and characteristics of the objective analysis techniques, and the grid used. These limitations and characteristics will be discussed below.

Since the publication of WOA94, substantial amounts of additional historical data have become available. However, even with these additional data, we are still hampered in a number of ways by a lack of data. Because of the lack of data, we are forced to examine the annual cycle by compositing all data regardless of the year of observation. In some areas, quality control is made difficult by the limited number of data. Data may exist in an area for only one season, thus precluding any representative annual analysis. In some areas there may be a reasonable spatial distribution of data points on which to base an analysis, but there may be only a few (perhaps only one) data in each one-degree latitude-longitude square.

2. DATA AND DATA DISTRIBUTION

Data sources and quality control procedures are briefly described below. For further information on the data sources used in WOA98 refer to the World Ocean Database 1998 (WOD98) series (Conkright *et al.,* 1998a,b; Levitus *et al.,* 1998a). The quality control procedures we have used in preparing these analyses are outlined by Conkright *et al.* (1998c).

2.1 Data sources

Historical Ocean Station Data (OSD) nutrient and chlorophyll profiles used in this project were obtained from the NODC/WDC-A archives, as well as all data gathered as a result of the NODAR and GODAR projects.

Appendix A shows the geographic distribution of all historical phosphate observations at selected standard depth levels. Appendix B shows the distribution of historical phosphate observations at selected standard depth levels for individual seasons. Appendix C shows the geographic distribution of all historical nitrate observations at selected standard depth levels and Appendix D shows the distribution for individual seasons. Appendix E shows the geographic distribution of all historical silicate observations at selected standard depth levels and Appendix F shows the distribution for individual seasons. Appendix G shows the geographic distribution of all historical chlorophyll observations at selected standard depth levels and Appendix H shows the distribution for individual seasons. In all data distribution maps that appear in the appendices, a small dot indicates a one-degree square containing one to four observations and a large dot indicates a square containing five or more observations.

We define the terms "standard level data" and "observed level data" here so the reader can understand the various data distribution figures, summary figures, and tables we present in this atlas. We refer to the actual measured value of an oceanographic variable *in situ* (Latin for "in place") as an "observation," and to the depth at which such a measurement was made as the "observed level depth." We may refer to such data as "observed level data." Before the development of oceanographic instrumentation that measure at high frequencies in the vertical, oceanographers often attempted to make measurements at selected "standard levels" in the water column. Sverdrup *et al.* (1942) presented the suggestions of the International Association of Physical Oceanography (IAPSO) as to which depths oceanographic measurements should be made or interpolated to for analysis. Different nations or institutions have a slightly different set of standard levels defined. For many purposes, including preparation of this atlas, observed level data are interpolated to standard observation levels, if such data do not occur exactly at a standard observation levels. We have prepared objective analyses at the NODC standard levels as given in Table 1 and added levels at 3500, 4500, and 5500 m. Section 3.1 discusses the vertical interpolation procedures used in our work.

2.2 Data quality control

Quality control of the data is a major task, the difficulty of which is directly related to lack of data (in some areas) upon which to base statistical checks. Consequently certain empirical criteria were applied, and as part of the last processing step, subjective judgment was used. Individual data, and in some cases entire profiles or cruises, have been flagged because these data produced features that were judged to be non-representative or in error. As part of our work, we have made available *World Ocean Database 1998* (WOD98) which contains both observed level profile data as well as standard level profile data with various quality control flags applied. Our knowledge of the variability of the world ocean now includes a greater appreciation and understanding of the ubiquity of eddies, rings, and lenses in some parts of the world ocean as well as interannual and interdecadal variability of water mass properties associated with modal variability of the atmosphere such as the North Atlantic Oscillation and El Nino/Southern Oscillation Therefore, we have simply flagged data, not eliminated them. Thus, individual investigators can make their own decision regarding the representativeness or correctness of the data. Investigators studying the distribution of features such as eddies will be interested in those data that we may regard as unrepresentative for the preparation of the analyses shown in this atlas.

2.2a Duplicate elimination

Because data are received from many sources, sometimes the same data set is received at NODC/WDC-A more than once but with slightly different time and/or position and/or data values, and hence are not easily identified as duplicate stations. Therefore, our databases were checked for the presence of exact and "near" exact replicates using eight different criteria. The first checks involve identifying stations with exact position/date/time and data values; the next checks involve offsets in position/date/time. Profiles identified as duplicates in the checks with a large offset were individually verified to ensure they were indeed duplicate profiles.

All but one profile from each set of replicate profiles was eliminated at the first step of our processing.

2.2b Range checks and gradient checks

Range checking (checking whether data is within set minimum and maximum values as a function of depth) was performed on all data as a first error check to flag and eliminate from further use the relatively few data that seemed to be grossly in error. Range checks were prepared for individual regions of the world ocean. Conkright *et al.* (1998c) and Conkright *et al.* (1994) detail the quality control procedures and include tables showing the ranges selected for each basin.

A check as to whether excessive gradients occur in the data were made for each variable in WOD98 both in terms of positive and negative gradients.

2.2c Statistical checks

Statistical checks were performed as follows. All data for each variable (irrespective of season), at each standard level, were averaged by five-degree latitude-longitude squares to produce a record of the number of observations, mean, and standard deviation in each square. Statistics were computed for the annual and seasonal compositing periods. Below 50 m depth, if data were more than three standard deviations from the mean, the data were flagged and eliminated from further use in our objective analyses. Above 50 m depth, a five-standard-deviation criterion was used in five-degree squares that contained any land area. In selected five-degrees squares that are close to land areas, a four-standard-deviation check was used. In all other squares a three-standard-deviation criterion was used.

The reason for the weaker criterion in coastal and near-coastal regions is the exceptionally large variability in the coastal five-degree square statistics for some variables. Frequency distributions of some variables in some coastal regions are observed to be skewed or bimodal. Thus to avoid eliminating possibly good data in highly variable environments, the standard deviation criteria were weakened.

The total number of nutrient and chlorophyll measurements in each cast, as well as the total number of observations exceeding the criterion, were recorded. If more than two observations in a cast were found to exceed the standard deviation criterion, then the entire cast was flagged. This check was imposed after tests indicated that surface data from particular casts (which upon inspection appeared to be erroneous) were being flagged but deeper data were not. Other situations were found where erroneous data from the deeper portion of a cast were flagged, while near-surface data from the same cast were not flagged because of larger natural variability in surface layers. One reason for this was the decrease of the number of observations with depth and the resulting change in sample statistics. The standard-deviation check was applied twice to the data set for each compositing period. Individual flags were set for each period.

In summary, first the five-degree square statistics were computed, and the elimination procedure described above was used to provide a preliminary data set. Next, new five-degree-square statistics were computed from this preliminary data set and used with the same statistical check to produce a new, "clean" data set. The reason for applying the statistical check twice was to flag (and eliminate from further use), in the first round, any grossly erroneous or non-representative data from the data set that would artificially increase the variances. The second check is then more effective in eliminating smaller, but still erroneous or non-representative, observations. The standard deviation for phosphate observations at 500 meters depth on a one-degree latitude-longitude square are shown in Figure 1a; the standard error of the mean for the same depth is shown in Figure 1b.

2.2d Subjective flagging of data

The data were averaged by one-degree squares for input to the objective analysis program. After initial objective analyses were computed, the input set of one-degree means still contained suspicious data contributing to unrealistic distributions, yielding intense bull's-eyes or gradients. Examination of these features indicated that some of them were due to particular oceanographic cruises. In such cases, data from an entire cruise were eliminated from further use by setting a flag on each profile from the cruise. In other cases, individual profiles or measurements were found to cause these features and were eliminated from use.

2.2e Representativeness of the data

Another quality control issue is data representativeness. The general paucity of data forces the compositing of all historical data to produce "climatological" fields. In a given one-degree square, there may be data from a month or season of one particular year, while in the same or a nearby square there may be data from an entirely different year. If there is large interannual variability in a region where scattered sampling in time has occurred, then one can expect the analysis to reflect this. Because the observations are scattered randomly with respect to time, except for a few limited areas, the results cannot, in a strict sense, be considered a true long-term climatological average.

We present smoothed analyses of historical means, based (in certain areas) on relatively few observations. We believe, however, that useful information about the oceans can be gained through our procedures and that the large-scale features are representative of the real ocean. We believe that, if a hypothetical global synoptic set of ocean data (nutrients and chlorophyll) existed, and one were to smooth this data to the same degree as we have smoothed the historical means overall, the large-scale features would be similar to our results. Some differences would certainly occur because of interannual-to-decadal-scale variability.

To clarify discussions of the amount of available data, quality control techniques, and representativeness of the data, the reader should examine in detail the maps showing the distribution of data (Appendices A-H) and the *World Ocean Database 1998* atlas series which shows the distribution of oceanographic stations as a function of year and instrument type. These maps are provided to give the reader a quick, simple way of examining the historical data distributions. Basically, the data diminish in number with increasing depth. In the upper ocean, the all-data annual mean distributions are quite good for defining large-scale features, but for the seasonal periods, the data base is inadequate for some regions. With respect to the deep ocean, in some areas the distribution of observations may

be adequate for some diagnostic computations but inadequate for other purposes. If an isolated deep basin or some region of the deep ocean has only one observation, then no horizontal gradient computations are meaningful. However, useful information is provided by the observation in the computation of other quantities (*e.g.*, a volumetric mean over a major ocean basin).

3. DATA PROCESSING PROCEDURES

3.1 Vertical interpolation to standard levels

Vertical interpolation of observed level data to standard levels followed procedures in UNESCO (1991). These procedures are in part based on the work of Reiniger and Ross (1968). Four observed level values surrounding the standard level values were used, two values from above the standard level and two values below the standard level. The pair of values furthest from the standard level are termed "exterior " points and the pair of values closest to the standard level are termed "interior" points. Paired parabolas were generated via Lagrangian interpolation. A reference curve was fitted to the four data points and used to define unacceptable interpolations caused by "overshooting" in the interpolation. When there were too few data points above or below the standard level to apply the Reiniger-Ross technique, we used a three-point Lagrangian interpolation. If three points were not available (either two above and one below or vice-versa), we used linear interpolation. In the event that an observation occurred exactly at the depth of a standard level, then a direct substitution was made. Table 1 provides the range of acceptable distances for which observed level data could be used for interpolation to a standard level.

3.2 Methods of analysis

3.2a Overview

An objective analysis scheme of the type described by Barnes (1964) was used to produce the fields shown in this atlas. This scheme had its origins in the work of Cressman (1959). In WOA94, the Barnes (1973) scheme was used. This required only one "correction" to the first-guess field at each grid point in comparison to the successive correction method of Cressman (1959) and Barnes (1964). This was to minimize computer time used in the processing. Barnes (1994) recommends a return to a multi-pass analysis when computer time is not an issue. Based on our own experience we agree with this assessment. The single pass analysis, used in WOA94, caused an artificial front in the Southeastern Pacific Ocean in a data sparse area (Anne Marie Treguier, personal communication). The analysis scheme used in generating WOA98 analyses uses a three-pass "correction" which eliminates this artificial front.

Inputs to the analysis scheme were one-degree square means

of data values at standard levels (for whatever period and variable being analyzed), and a first-guess value for each square. For instance, one-degree square means for our annual analysis were computed using all available data regardless of date of observation. For July, we used all historical July data regardless of year of observation.

Analysis was the same for all standard depth levels. Each one-degree latitude-longitude square value was defined as being representative of its square. The 360x180 gridpoints are located at the intersection of half-degree lines of latitude and longitude. An influence radius was then specified. At those grid points where there was an observed mean value, the difference between the mean and the first-guess field was computed. Next, a correction to the first-guess value at all gridpoints was computed as a distance-weighted mean of all gridpoint difference values that lie within the area around the gridpoint defined by the influence radius. Mathematically, the correction factor derived by Barnes (1964) is given by the expression

$$ C_{i,j} = \frac{\sum\limits_{s=1}^{n} W_s Q_s}{\sum\limits_{s=1}^{n} W_s} \qquad (1) $$

in which

(i,j) =   **coordinates of a gridpoint in the east-west and north-south directions respectively;**

$C_{i,j}$ =   **the correction factor at gridpoint coordinates (i,j);**

n =   **the number of observations that fall within the area around the point i,j defined by the influence radius;**

Q_s =   **the difference between the observed mean and the first-guess at the Sth point in the influence area;**

W_s =   **exp $(-E\, r^2 R^{-2})$ for $r \le R$; 0 for $r > R$;**

r =   **distance of the observation from the gridpoint;**

R =   **influence radius;**

E =   **4.**

The derivation of the weight function, W_s, will be presented in the following section. At each gridpoint we computed an

analyzed value $G_{i,j}$ as the sum of the first-guess, $F_{i,j}$, and the correction $C_{i,j}$. The expression for this is

$$G_{i,j} = F_{i,j} + C_{i,j} \qquad (2)$$

If there were no data points within the area defined by the influence radius, then the correction was zero, the first-guess field was left unchanged, and the analyzed value was simply the first-guess value. This correction procedure was applied at all gridpoints to produce an analyzed field. The resulting field was first smoothed with a median filter (Tukey, 1974; Rabiner *et al.*, 1975) and then smoothed with a five-point smoother of the type described by Shuman (1957). The choice of first-guess fields is important and we discuss our procedures in section 3.2e.

The analysis scheme is based on the work of several researchers analyzing meteorological data. Bergthorsson and Doos (1955) computed corrections to a first-guess field using various techniques: one assumed that the difference between a first-guess value and an analyzed value at a gridpoint was the same as the difference between an observation and a first-guess value at a nearby observing station. All the observed differences in an area surrounding the gridpoint were then averaged and added to the gridpoint first-guess value to produce an analyzed value. Cressman (1959) applied a distance-related weight function to each observation used in the correction in order to give more weight to observations that occur closest to the gridpoint. In addition, Cressman introduced the method of performing several iterations of the analysis scheme using the analysis produced in each iteration as the first-guess field for the next iteration. He also suggested starting the analysis with a relatively large influence radius and decreasing it with successive iterations so as to analyze smaller scale phenomena with each pass.

Sasaki (1960) introduced a weight function that was specifically related to the density of observations, and Barnes (1964, 1973) extended the work of Sasaki. The weight function of Barnes (1964) has been used here. The objective analysis scheme we used is in common use by the mesoscale meteorological community. Several studies of objective analysis techniques have been made. Achtemeier (1987) examined the "concept of varying influence radii for a successive corrections objective analysis scheme." Seaman (1983) compared the "objective analysis accuracies of statistical interpolation and successive correction schemes." Smith and Leslie (1984) performed an "error determination of a successive correction type objective analysis scheme." Smith *et al.* (1986) made "a comparison of errors in objectively analyzed fields for uniform and non-uniform station distribution."

3.2b Derivation of Barnes' (1964) weight function

The principle upon which Barnes' (1964) weight function is derived is that "the two-dimensional distribution of an atmospheric variable can be represented by the summation of an infinite number of independent harmonic waves, that is, by a Fourier integral representation". If $f(x,y)$ is the variable, then in polar coordinates (r,θ), a smoothed or filtered function $h(x,y)$ can be defined:

$$h(x,y) = \frac{1}{2\pi} \int_0^{2\pi} \int_0^\infty \eta f(x + r\cos\theta, y + r\sin\theta) d(r^2/4K) d\theta \quad (3)$$

in which r is the radial distance from a gridpoint whose coordinates are (x,y). The weight function is defined as

$$\eta = \exp(-r^2/4K) \qquad (4)$$

which resembles the Gaussian distribution. The shape of the weight function is determined by the value of K, which depends on the distribution of data. The determination of K follows. The weight function has the property that

$$\frac{1}{2\pi} \int_0^{2\pi} \int_0^\infty \eta \, d\left(\frac{r^2}{4K}\right) d\theta = 1. \qquad (5)$$

This property is desirable because in the continuous case (3) the application of the weight function to the distribution $f(x,y)$ will not change the mean of the distribution. However, in the discrete case (1), we only sum the contributions to within the distance R. This introduces an error in the evaluation of the filtered function, because the condition given by (5) does not apply. The error can be pre-determined and set to a reasonably small value in the following manner. If one carries out the integration in (5) with respect to θ, the remaining integral can be rewritten as

$$\int_0^R \eta \, d\left(\frac{r^2}{4K}\right) + \int_R^\infty \eta \, d\left(\frac{r^2}{4K}\right) = 1. \qquad (6)$$

Defining the second integral as ϵ yields

$$\int_0^R \exp\left(-\frac{r^2}{4K}\right) d\left(\frac{r^2}{4K}\right) = 1 - \epsilon \qquad (7)$$

in which

$$e = \exp(-R^2/4K)$$

Levitus (1982) chose $\epsilon = 0.02$, which implies with respect to (6) the representation of 98 percent of the influence of any data around the gridpoint in the area defined by the influence radius, R. In terms of the weight function used in the evaluation of (1) this choice leads to a value of E=4 since

$$E = R^2 / 4K = -\ln \epsilon.$$

Thus,

$$K = R^2/16.$$

The choice of ϵ and the specification of R determine the shape of the weight function.

Barnes (1964) proposed using this scheme in an iterative fashion similar to Cressman (1959). Levitus (1982) used a four iteration scheme with a variable influence radius for each pass. Conkright $et~al.$ (1994a) used a one-iteration scheme. WOA98 uses a three iteration scheme with a variable influence radius. The three influence radii are 888, 666, and 444 km.

3.2c Derivation of Barnes' (1964) response function

It is desirable to know the response of a data set to the interpolation procedure applied to it. Following Barnes (1964) we let

$$f(x) = A\sin(ax) \qquad (8)$$

in which $a = 2\pi/\lambda$ with λ being the wavelength of a particular Fourier component, and substitute this function into equation (3) along with the expression for η in equation (4). Then

$$g(x) = D(A\sin(ax)) = Df(x) \qquad (9)$$

in which D is the response function for one application of the analysis. The phase of each Fourier component is not changed by the interpolation procedure. The results of an analysis pass are used as the first-guess for the next analysis pass in an iterative fashion. The response function after N iterations as derived by Barnes (1964) is

$$g_n = f(x)D\sum_{n=1}^{N=1}(1-D)^{n-1} \qquad (10)$$

Equation (10) differs trivially from that given by Barnes. The difference is due to our first-guess field being defined as a zonal average, annual mean or seasonal mean, whereas Barnes used the first application of the analysis as a first-

guess. Barnes (1964) also showed that applying the analysis scheme in an iterative fashion will result in convergence of the analyzed field to the observed data field. However, it is not desirable to approach the observed data too closely, because at least seven or eight gridpoints are needed to represent a Fourier component.

The response function given in (10) is useful in two ways: it is informative to know what Fourier components make up the analyses, and the computer programs used in generating the analyses can be checked for correctness by comparison with (10).

3.2d Choice of response function

The distribution of observations (see appendices) at different depths and for the different averaging periods, are not regular in space or time. At one extreme, regions exist in which every one-degree square contains data and no interpolation needs to be performed. At the other extreme are regions in which few if any data exist. Thus, with variable data spacing the average separation distance between gridpoints containing data is a function of geographical position and averaging period. However, if we computed and used a different average separation distance for each variable at each depth and each averaging period, we would be generating analyses in which the wavelengths of observed phenomena might differ from one depth level to another and from one season to another. In WOA94, a fixed influence radius of 555 kilometers was used to allow uniformity in the analysis of all variables. For these analyses, a three-pass analysis, based on Barnes (1964), with influence radii of 888, 666 and 444 km was used.

Inspection of (1) shows that the difference between the analyzed field and the first-guess at any gridpoint is proportional to the sum of the weighted-differences between the observed mean and first-guess at all gridpoints containing data within the influence area.

The reason for using the five-point smoother and the median smoother is that our data are not evenly distributed in space. As the analysis moves from regions containing data to regions devoid of data, small-scale discontinuities may develop. The five-point and median smoothers are used to eliminate these discontinuities. The five-point smoother does not affect the phase of the Fourier components that comprise an analyzed field.

The response function for the analyses presented in this atlas is given in Table 2 and Figure 2. For comparison purposes, the response function used by Levitus (1982) and Conkright $et~al.$ (1994a) are also presented. The response function represents the smoothing inherent in the objective analysis described above plus the effects of one application of the five-point smoother and one application of a five-point median smoother. The effect of varying the amount of smoothing in North Atlantic sea surface temperature (SST)

fields has been quantified by Levitus (1982) for a particular case. In a region of strong SST gradient such as the Gulf Stream, the effect of smoothing can easily be responsible for differences between analyses exceeding 1.0 °C.

To avoid the problem of the influence region extending across land or sills to adjacent basins, the objective analysis program uses basin "identifiers" to preclude the use of data from adjacent basins. Table 3 lists these basins and the depth at which no exchange of information between basins is allowed during the objective analysis of data, i.e., "depths of mutual exclusion." Some regions are nearly, but not completely, isolated topographically. Because some of these nearly isolated basins have water mass properties that are different from surrounding basins, we have chosen to treat these as isolated basins as well. Not all such basins have been identified because of the complicated structure of the sea floor. In Table 3, a region marked with a "*" can interact with adjacent basins except for special areas such as the Isthmus of Panama.

3.2e First-guess field determination

For all variables and compositing periods, there are gaps in the data coverage. In some parts of the world ocean, there exist adjacent basins whose water mass properties are individually nearly homogeneous but have distinct basin-to-basin differences. Spurious features can be created when an influence area extends over two basins of this nature (basins are listed in Table 3). Our choice of first-guess field attempts to minimize the creation of these features. To provide a first-guess field for the annual analysis at any standard level, we first zonally averaged the observed data in each one-degree latitude belt by individual ocean basins. An annual analysis of a variable was then used as the first-guess for each seasonal analysis.

We then reanalyzed the data for each variable using the newly produced analyses as first-guess fields described as follows and as shown in Fig. 3. A new annual mean was computed as the mean of the four seasons for the upper 500 m, and the zonal average below 500 m depth. This new annual mean was used as the first-guess field for new seasonal analyses. This procedure produces slightly smoother means. More importantly we recognize that fairly large data-void regions exist, in some cases to such an extent that a seasonal analysis in these regions is not meaningful. We are interested in computing integral quantities such as heat storage that are deviations from annual means. Geographic distribution of observations for the all-data annual periods (see appendices) is excellent for upper layers of the ocean. By using an all-data annual mean, first-guess field regions where data exists for only one season will show no contribution to the annual cycle. By contrast, if we used a zonal average for each season, then, in those latitudes where gaps exist, the first-guess field would be heavily biased by the few data points that exist. If these were anomalous data in some way, an entire basin-

wide belt might be affected.

One advantage of producing "global" fields for a particular compositing period (even though some regions are data void) is that such analyses can be modified by investigators for use in modeling studies. For example, England (1992) noted that the temperature distribution produced by Levitus (1982) for the Antarctic is too high (due to a lack of winter data for the Southern Hemisphere) to allow for the formation of Antarctic Intermediate Water in an ocean general circulation model. By decreasing the temperature of the "observed" field the model was able to produce this water mass.

3.3 Choice of objective analysis procedures

Optimum interpolation (Gandin, 1963) has been used by some investigators to objectively analyze oceanographic data. We recognize the power of this technique but have not used it to produce analyzed fields. As described by Gandin (1963), optimum interpolation is used to analyze synoptic data using statistics based on historical data. In particular, second-order statistics such as correlation functions are used to estimate the distribution of first order parameters such as means. We attempt to map most fields in this atlas based on relatively sparse data sets. By necessity we must composite all data regardless of year of observation, to have enough data to produce a global, hemispheric, or regional analysis for a particular month or season. Because of the paucity of data, we prefer not to use an analysis scheme that is based on second order statistics. In addition, as Gandin has noted, there are two limiting cases associated with optimum interpolation. The first is when a data distribution is dense. In this case, the choice of interpolation scheme makes little difference. The second case is when data are sparse. In this case, an analysis scheme based on second order statistics is of questionable value. For additional information on objective analysis procedures see Thiebaux and Pedder (1987) and Daley (1991).

3.4 Choice of spatial grid

The analyses that comprise WOA98 have been computed using a new land-sea topography to define ocean depths at each grid point (ETOPO5, 1988). From the ETOPO5 mask, a quarter-degree mask was created based on ocean bottom depth and land criteria. If four or more 5-minute square values out of a possible nine in a one-quarter-degree box were defined as land, then the quarter-degree gridbox was defined to be land. If no more than two of the 5-minute squares had the same depth value in a quarter-degree box, then the average value of the 5-minute ocean depths in that box was defined to be the depth of the quarter-degree gridbox. If three or more 5-minute squares out of the nine had a common bottom depth, then the depth of the quarter-degree box was set to the most common depth value. The same method was used to go from a quarter-degree to a one-degree resolution. In the one-degree

7

resolution case, at least four points out of a possible sixteen (in a one-degree square) had to be land in order for the one-degree square to remain land and three out of sixteen had to have the same depth for the ocean depth to be set. These criteria yielded a mask that was then modified by :

a)   Connecting the Isthmus of Panama,

b)   maintaining an opening in the Straits of Gibraltar and in the English Channel,

c)   connecting the Kamchatka Peninsula and the Baja Peninsula to their respective continents.

The quarter-degree mask was created as an intermediate step to ensure consistency between the present work and future high resolution analysis of temperature and salinity.

4. RESULTS

4.1 Computation of annual and seasonal fields

After completion of all of our analyses we define a final annual climatology as the average of the four seasonal analyses in the upper 500 m of the ocean for nutrients, and the average surface analyses for chlorophyll. Below 500 m depth we define the annual climatology as the annual analysis with the zonal average as the first guess field.

4.2 Explanation of standard level figures

All figures showing standard level analyses in this atlas series use similar symbols for displaying information. Continents are indicated as solid - black areas. Ocean areas shallower than the standard depth level being displayed are gray. Gridpoints for which there were less than four one-degree-square values available to correct the first-guess are indicated by an X. "H" and "L" indicate locations of the absolute maximum and minimum of the entire field. All figures were computer drafted.

4.3 Standard level analyses

Global distributions of annual mean nutrients and chlorophyll at standard analysis levels are presented in Appendices A, C, E, and G.   Seasonal analyses are presented in Appendices B, D, F, and H.

4.4 Contents of the *World Ocean Atlas 1998* CD-ROM

This atlas presents data for selected standard levels in the Indian Ocean. Associated with this atlas, is a CD-ROM containing the following digital fields for the world ocean:

(a)   fields containing the number of observations by one-degree squares as a function of depth;

(b)   one-degree annual objectively analyzed nutrient fields at 33 standard levels (5500 m) and objectively analyzed chlorophyll fields at 7 standard levels (100m depth);

(c)   one-degree seasonal objectively analyzed nutrient fields at 14 standard levels (500 m depth) and surface objectively analyzed chlorophyll fields;

(d)   one-degree seasonal minus annual nutrient analyses at 14 standard levels and surface seasonal minus annual chlorophyll fields;

(e)   one-degree fields of the annual standard deviation of nutrients at 33 standard depth levels and chlorophyll at 7 standard depth levels;

(f)   one-degree fields of the seasonal standard deviation of nutrients at 14 standard depth levels and seasonal standard deviation of chlorophyll at the surface;

(g)   one-degree fields of the annual standard error of the mean for nutrients at 33 standard depth levels and chlorophyll at 7 standard depth levels;

(h)   one-degree fields of the seasonal standard error of the mean at 14 standard depth levels and chlorophyll at 7 standard depth levels;

(i)   one-degree fields of the unanalyzed annual nutrient mean field at 33 standard depth levels   and chlorophyll at 7 standard depth levels;

(j)   one-degree fields of the unanalyzed seasonal mean field at 14 standard depth levels and chlorophyll at the surface;

(k)   one-degree nutrient unanalyzed annual mean minus objectively analyzed mean values at 33 standard depth levels and chlorophyll at 7 standard depth levels. These fields represent the combined interpolation and smoothing "error" of our analyses. An example of these statistics is shown in Fig. 4;

(l)   one-degree unanalyzed seasonal mean minus objectively analyzed seasonal mean values at 14 standard levels and chlorophyll at the surface;

(m)   land-sea file used in the analysis;

(n)   definition of ocean basin masks used in the analysis

The sample standard deviation in a gridbox was computed using:

$$s = \sqrt{\dfrac{\displaystyle\sum_{n=1}^{N} (x_n - \overline{x})^2}{N - 1}} \qquad (11)$$

in which x_n= the nth data value in the gridbox, $\overline{x}$ =mean of all data values in the gridbox, and N= total number of data values in the gridbox. The standard error of the mean was computed by dividing the standard deviation by the square root of the number of observations in each gridbox.

5. SUMMARY

In the preceding sections we have described the results of a project to objectively analyze all historical nutrient and chlorophyll data archived at NODC/WDC-A, including substantial amounts of data gathered as a result of the NODC and IOC data archaeology and rescue projects. We desire to build a set of climatological analyses that are as similar as possible in all respects for all variables including relatively data sparse variables such as nutrients. This provides investigators with a consistent set of analyses to work with.

One advantage of the analysis techniques used in this atlas is that we know the amount of smoothing by objective analyses as given by the response function in Table 2 and Figure 2. We believe this to be an important function for constructing and describing a climatology of any geophysical parameter. Particularly when computing anomalies from a standard climatology, it is important that the synoptic field be smoothed to the same extent as the climatology, to prevent generation of spurious anomalies simply through differences in smoothing. A second reason is that purely diagnostic computations require a minimum of seven or eight gridpoints to represent any Fourier component with accuracy. Higher order derivatives will require more smoothing.

We have attempted to create objectively analyzed fields and data sets that can be used as a "black box." We emphasize that some quality control procedures used are subjective. For those users who wish to make their own choices, all the data used in our analyses are available both at standard depth levels as well as observed depth levels (*World Ocean Database 1998* CD-ROM set - Conkright *et al.*, 1998c). The results presented in this atlas show some features that are suspect and may be due to nonrepresentative or incorrect data that were not flagged by the quality control techniques used. Although we have attempted to eliminate as many of these features as possible by flagging the data which

generate these features some obviously remain. Some may eventually turn out not to be artifacts but rather to represent real features, not yet capable of being described in a meaningful way due to lack of data.

6. FUTURE WORK

Our analyses will be updated when justified by additional observations. As more data are received at NODC/WDC-A, we will also be able to produce improved annual and seasonal climatologies for each variable.

References

Achtemeier, G. L., 1987: On the concept of varying influence radii for a successive corrections objective analysis. *Monthly Weather Review,* 11, 1761-1771.

Barnes, S. L., 1964: A technique for maximizing details in numerical weather map analysis. *J. App. Meteor.,* 3, 396-409.

_____ 1973: Mesoscale objective map analysis using weighted time series observations. *NOAA Technical Memorandum ERL* NSSL-62, 60 pp.

_____ 1994: Applications of the Barnes Objective Analysis Scheme, Part III: Tuning for Minimum Error. *J. Atmosph. and Oceanic Tech.* 11:1459-1479.

Bergthorsson, P., and B. Doos, 1955: Numerical Weather map analysis. *Tellus,* 7, 329-340.

Boyer, T.P., and S. Levitus, 1997: *Objective Analyses of temperature and salinity for the world ocean on a 1/4 °grid. NOAA/NESDIS Atlas 11.* U.S. Gov. Printing Office, Wash., D.C., 62 pp.

Conkright, M. E., Levitus, S., and Boyer, T. P., 1994a: *World Ocean Atlas 1994, Vol 1: Nutrients.* National Oceanic and Atmospheric Administration, Wash., D.C., 150 pp.

Conkright, M.E., Boyer, T. P., and S. Levitus, 1994b: Quality control and processing of historical oceanographic nutrient data. *NOAA Technical Report NESDIS 79,* 75 pp.

Conkright, M.E. , T.P. Boyer, S. Levitus, D. Johnson, T. O'Brien, C. Stephens, R. Gelfeld, 1998a: *World Ocean Database 1998, Volume 6: Temporal Distribution of Ocean Station Data (Bottle) Nutrient profiles. NOAA Atlas NESDIS 23,* U.S. Government Printing Office, Wash., D.C., 296 pp.

Conkright M.E., T. O'Brien, L. Stathoplos, C. Stephens, T.P. Boyer, D. Johnson, S. Levitus, R. Gelfeld, 1998b: *World Ocean Database 1998, Volume 8: Temporal Distribution of Ocean Station Data (Bottle) Chlorophyll Profiles and Plankton Data. NOAA Atlas NESDIS 25,* U.S. Government Printing Office, Wash., D.C.,

Conkright, M. E., S. Levitus, T. O'Brien, T.P. Boyer, C. Stephens, D. Johnson, L. Stathoplos, O. Baranova, J. Antonov, R. Gelfeld, J. Burney, J. Rochester, and C. Forgy, 1998c: *World Ocean Database 1998 CD-ROM Data Set Documentation.* National Oceanographic Data Center, Silver Spring, MD, 43 pp.

Cressman, G. P., 1959: An operational objective analysis scheme. *Mon. Wea. Rev.,* 87, 329-340.

Daley, R., 1991: *Atmospheric Data Analysis.* Cambridge University Press, Cambridge, 457 pp.

England, M.H., 1992: On the formation of Antarctic Intermediate and Bottom Water in Ocean general circulation models. *J. Phys. Oceanogr., 22, 918- 926.*

ETOPO5, 1988: Data Announcements 88-MGG-02, Digital relief of the Surface of the Earth. NOAA, National Geophysical Data Center, Boulder, CO.

Intergovernmental Panel on Climate Change, 1996: *Climate Change 1995 - The Science of Climate Change, Contribution of Working Group I to thte Second Assessment Report of the Intergovernmental Panel on Climate Change.* Editors J.J. Houghton, L.G. Meiro Filho, B.A. Callander, N. Harris, A. Kattenberg, and K. Maskell. Cambridge University Press, Cambridge, UK, 572 pp.

Gandin, L.S., 1963: *Objective Analysis of Meteorological fields.* Gidrometeorol Izdat, Leningrad (translation by Israel program for Scientific Translations, Jerusalem, 1966); 242 pp.

Levitus, S., 1982: *Climatological Atlas of the World Ocean,* NOAA Professional Paper No. 13, U.S. Gov. Printing Office, 173 pp.

Levitus, S., R. Gelfeld, T. Boyer, and D. Johnson, 1994b: *Results of the NODC Oceanographic Data Archaeology and Rescue Projects.* Key to Oceanographic Records Documentation No. 19, NODC, Wash., D.C. , 73 pp.

Levitus, S., T.P. Boyer, M.E. Conkright, T. O'Brien, J. Antonov, C. Stephens, L. Stathoplos, D. Johnson, and R. Gelfeld, 1998a: *World Ocean Database 1998 Volume 1: Introduction.* NOAA Atlas NESDIS 18, U.S. Government Printing Office, Wash., D.C., 346 pp.

Rabiner, L. R., M. R. Sambur, and C. E. Schmidt, 1975: *Applications of a nonlinear smoothing algorithm to speech processing, IEEE Trans. on Acoustics, Speech and Signal Processing,* Vol. Assp-23, 552-557.

Reiniger, R.F., and C.F. Ross, 1968: A method of interpolation with application to oceanographic data. *Deep-Sea Res.,* 9, 185-193.

Sasaki, Y., 1960: An objective analysis for determining initial conditions for the primitive equations. Ref. 60-1 6T, Atmospheric Research Lab., Univ. of Oklahoma Research Institute, Norman, 23 pp.

Seaman, R. S., 1983. Objective Analysis accuracies of statistical interpolation and successive correction schemes. *Australian Meteor. Mag.,* 31, 225-240.

Shuman, F. G., 1957: Numerical methods in weather prediction: II. Smoothing and filtering. *Mon. Wea. Rev.,* 85, 357-361.

Smith, D. R., and F. Leslie, 1984: Error determination of a successive correction type objective analysis scheme. *J Atm. and Oceanic Tech.,* 1, 121-130.

Smith, D.R., M.E. Pumphry, and J.T. Snow, 1986: A comparison of errors in objectively analyzed fields for uniform and nonuniform station distribution, *J. Atm. Oceanic Tech.,* 3, 84-97.

Sverdrup, H.U., M.W. Johnson, and R.H. Fleming, 1942: *The Oceans: Their physics, chemistry, and general biology.* Prentice Hall, 1060 pp.

Thiebaux, H.J., M.A. Pedder, 1987: *Spatial Objective Analysis: with applications in atmospheric science.* Academic Press, 299 pp.

Tukey, J. W., 1974: Nonlinear (nonsuperposable) methods for smoothing data, in *"Cong. Rec.",* 1974 EASCON, 673 pp.

UNESCO, 1991: *Processing of Oceanographic Station Data.* Imprimerie des Presses Unibversitaires de France, Imprimerie des Presses Universitaires de France, Vendome, 138 pp.

Table 1. Acceptable distances (m) for defining interior and exterior values used in the Reiniger-Ross scheme for interpolating observed level data to standard levels.

Standard Level number	Standard depths (m)	Acceptable distances (m) for interior values	Acceptable distances (m) for exterior values
1	0	5	200
2	10	50	200
3	20	50	200
4	30	50	200
5	50	50	200
6	75	50	200
7	100	50	200
8	125	50	200
9	150	50	200
10	200	50	200
11	250	100	200
12	300	100	200
13	400	100	200
14	500	100	400
15	600	100	400
16	700	100	400
17	800	100	400
18	900	200	400
19	1000	200	400
20	1100	200	400
21	1200	200	400
22	1300	200	1000
23	1400	200	1000
24	1500	200	1000
25	1750	200	1000
26	2000	1000	1000
27	2500	1000	1000
28	3000	1000	1000
29	3500	1000	1000
30	4000	1000	1000
31	4500	1000	1000
32	5000	1000	1000
33	5500	1000	1000

Table 2. Response function of the objective analysis scheme as a function of wavelength for WOA98 and earlier analyses.

Wavelength*	Levitus (1982)	WOA94	WOA98
$360\Delta X$	1.000	0.999	1.000
$180\Delta X$	1.000	0.997	0.999
$120\Delta X$	1.000	0.994	0.999
$90\Delta X$	1.000	0.989	0.998
$72\Delta X$	1.000	0.983	0.997
$60\Delta X$	1.000	0.976	0.995
$45\Delta X$	1.000	0.957	0.992
$40\Delta X$	0.999	0.946	0.990
$36\Delta X$	0.999	0.934	0.987
$30\Delta X$	0.996	0.907	0.981
$24\Delta X$	0.983	0.857	0.969
$20\Delta X$	0.955	0.801	0.952
$18\Delta X$	0.923	0.759	0.937
$15\Delta X$	0.828	0.671	0.898
$12\Delta X$	0.626	0.532	0.813
$10\Delta X$	0.417	0.397	0.698
$9\Delta X$	0.299	0.315	0.611
$8\Delta X$	0.186	0.226	0.500
$6\Delta X$	3.75×10^{-2}	0.059	0.229
$5\Delta X$	1.34×10^{-2}	0.019	0.105
$4\Delta X$	1.32×10^{-3}	2.23×10^{-3}	2.75×10^{-2}
$3\Delta X$	2.51×10^{-3}	1.90×10^{-4}	5.41×10^{-3}
$2\Delta X$	5.61×10^{-7}	5.30×10^{-7}	1.36×10^{-6}

* For $\Delta X = 111$ km

Table 3. Basins defined for objective analysis and the shallowest standard depth level for which each basin is defined.

BASIN	STANDARD DEPTH LEVEL	BASIN	STANDARD DEPTH
Aleutian Basin	28	Gulf of Mexico	26
Andaman Basin	25	Hudson Bay	1
Arabian Sea	30	Indian Ocean	1 *
Arctic Ocean	1 *	Java Sea	6
Argentine Basin	31	Kara Sea	8
Atlantic Indian Basin	31	Marianas Basin	30
Atlantic Ocean	1 *	Mascarene Basin	30
Baffin Bay	14	Mediterranean Sea	1 *
Baltic Sea	1	North Caribbean	26
Banda Sea	23	North American Basin	29
Barents Sea	28	Pacific Ocean	1 *
Bay of Bengal	1 *	Persian Gulf	1
Beaufort Sea	28	Philippine Sea	30
Black Sea	1	Red Sea	1
Brazil Basin	31	Sea of Okhotsk	19
Caribbean Sea	23	Sea of Japan	1
Caspian Sea	1	Somali Basin	30
Celebes Sea	25	South China Sea	28
Central Indian Ocean	29	Southeast Pacific	29
Chile Basin	30	Southeast Indian	29
Coral Sea	29	Southeast Atlantic	29
Crosat Basin	30	Southern Ocean	1 *
East Indian Ocean	29	Southwest Atlantic	29
East Mediterranean	16	Sulu Sea	10
East Caroline Basin	30	Tasman Sea	30
Fiji Basin	29	West Mediterranean	19
Guatemala Basin	29	West European Basin	29
Guinea Basin	30		

Basins marked with a "" can interact with adjacent basins

14
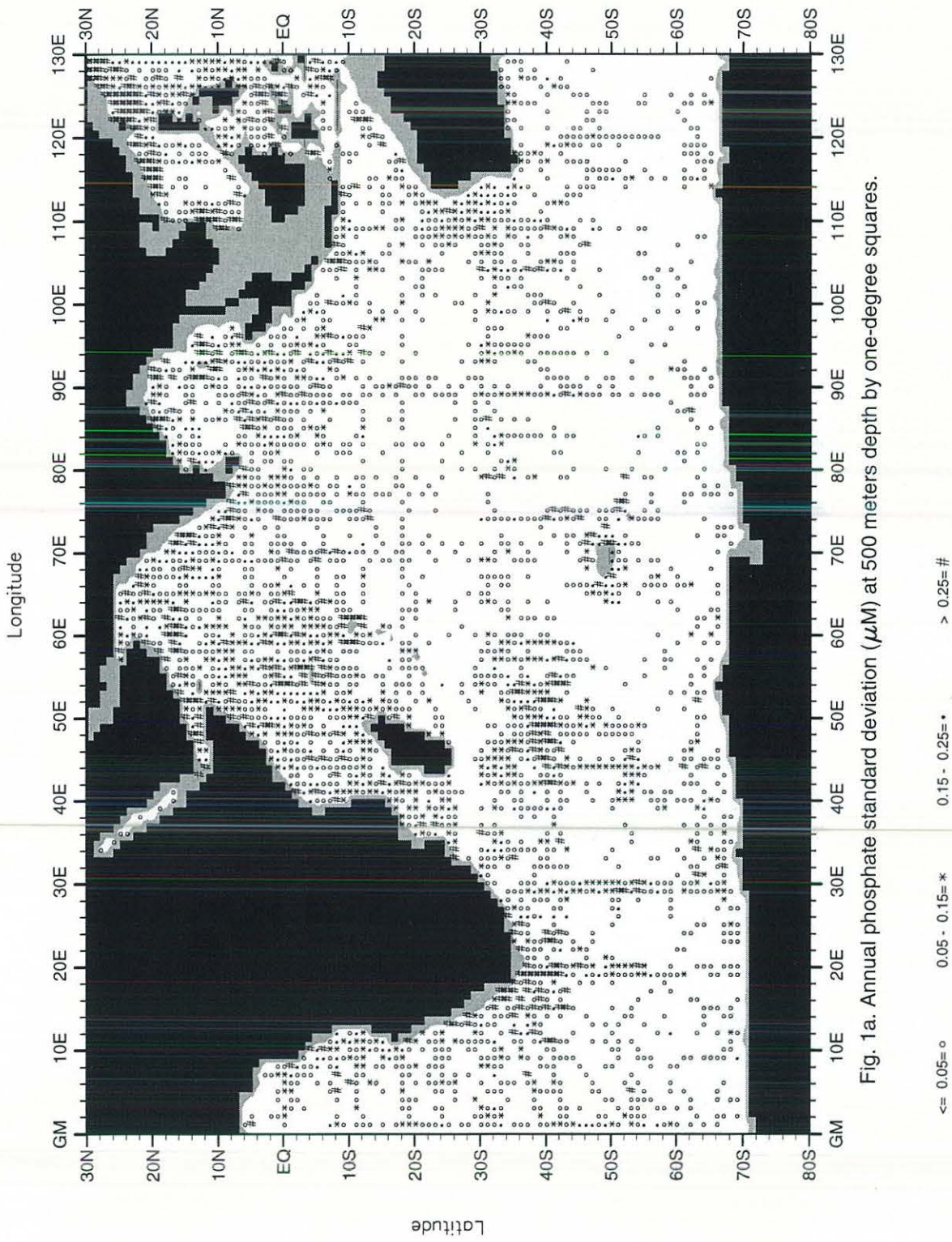
Fig. 1a. Annual phosphate standard deviation (μM) at 500 meters depth by one-degree squares.

<= 0.05 = o   0.05 - 0.15 = *   0.15 - 0.25 = •   > 0.25 = #

15

Fig. 1b. Annual phosphate standard error of the mean (μM) at 500 meters depth by one-degree squares

<= 0.05= ○   0.05 - 0.15= *   0.15 - 0.25= •   > 0.25= #
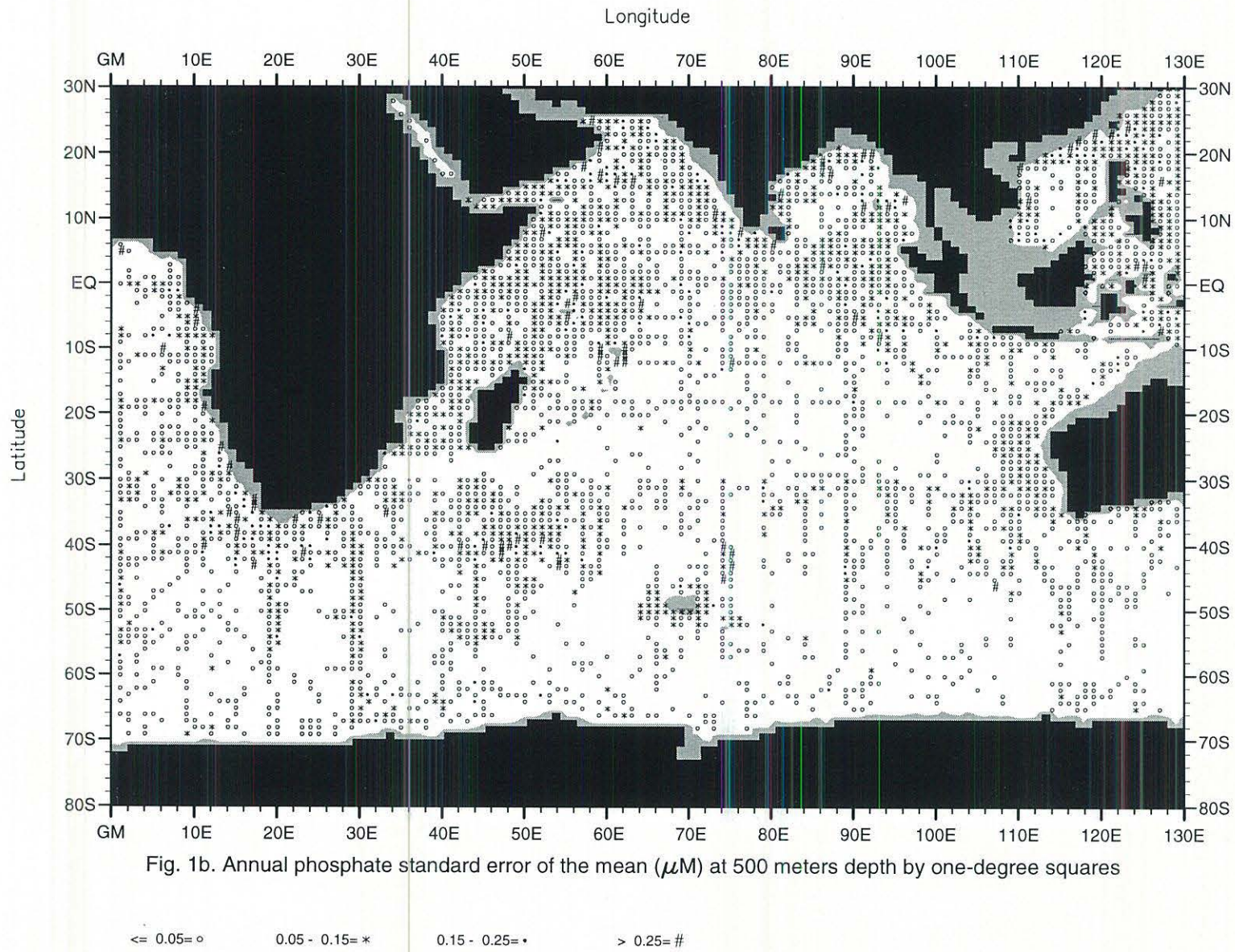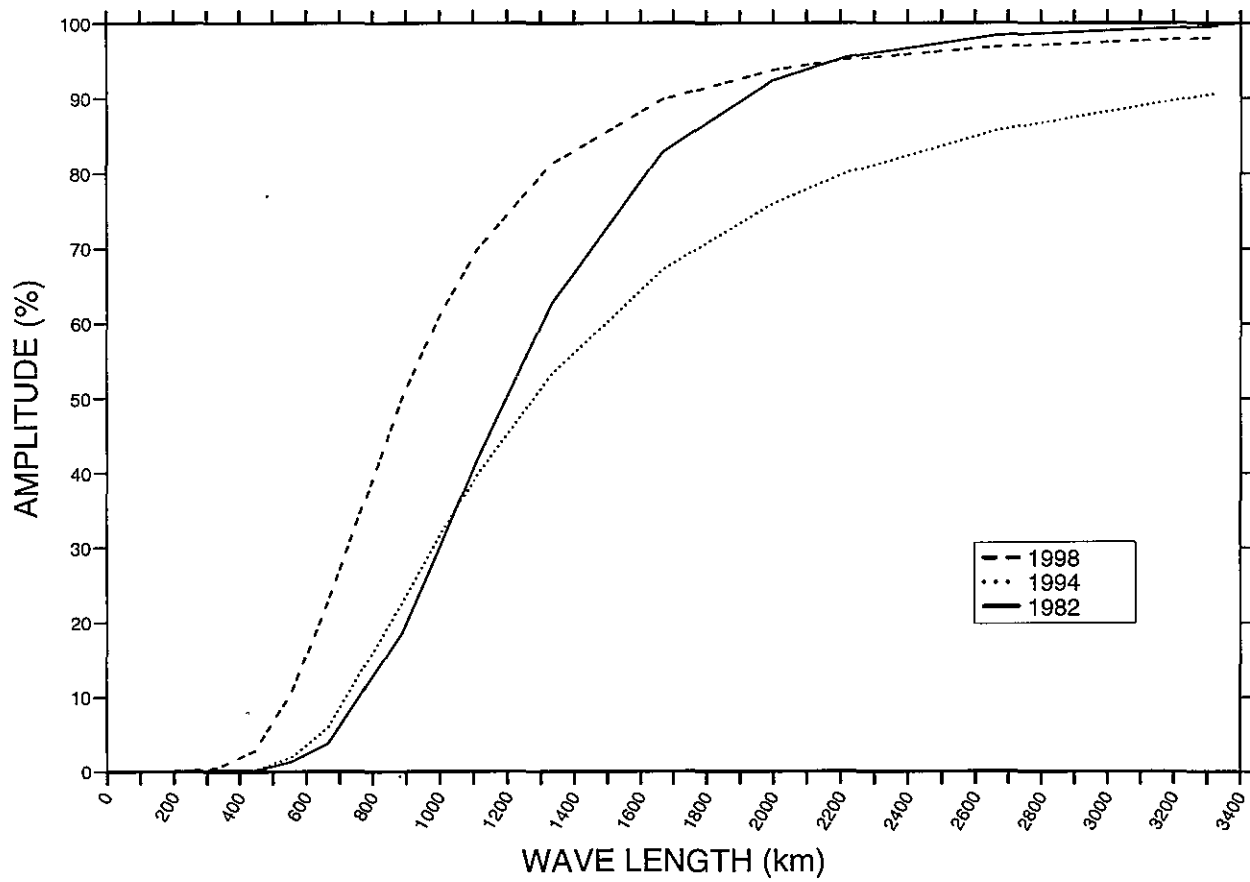
Figure 2. Response function of the WOA98, WOA94, and Levitus (1982) objective analysis schemes.

Zonal Average

Annual mean (analyzed) ──── Z >500 meters ──→ | Annual mean |

Seasonal mean (analyzed)

Z ≤ 500 meters (NO_3, PO_4, Si)
Z = surface (Chlorophyll)

average of four seasons

| Annual mean |

- - - -   Used as first guess field for calculating mean
─────   Averaged mean
▭   Final mean value
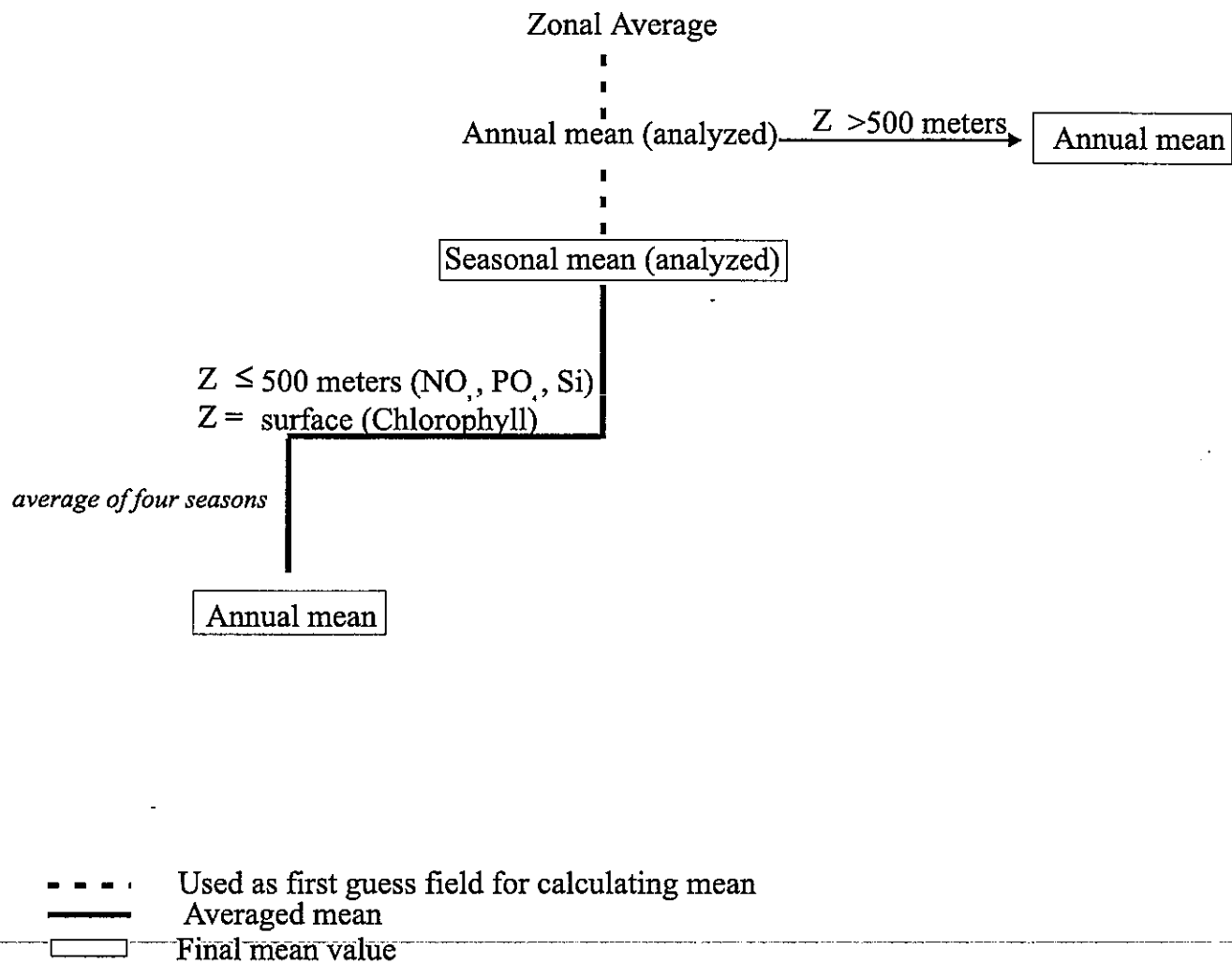
Figure 3. Scheme used in computing annual and seasonal objectively analyzed means for a variable.
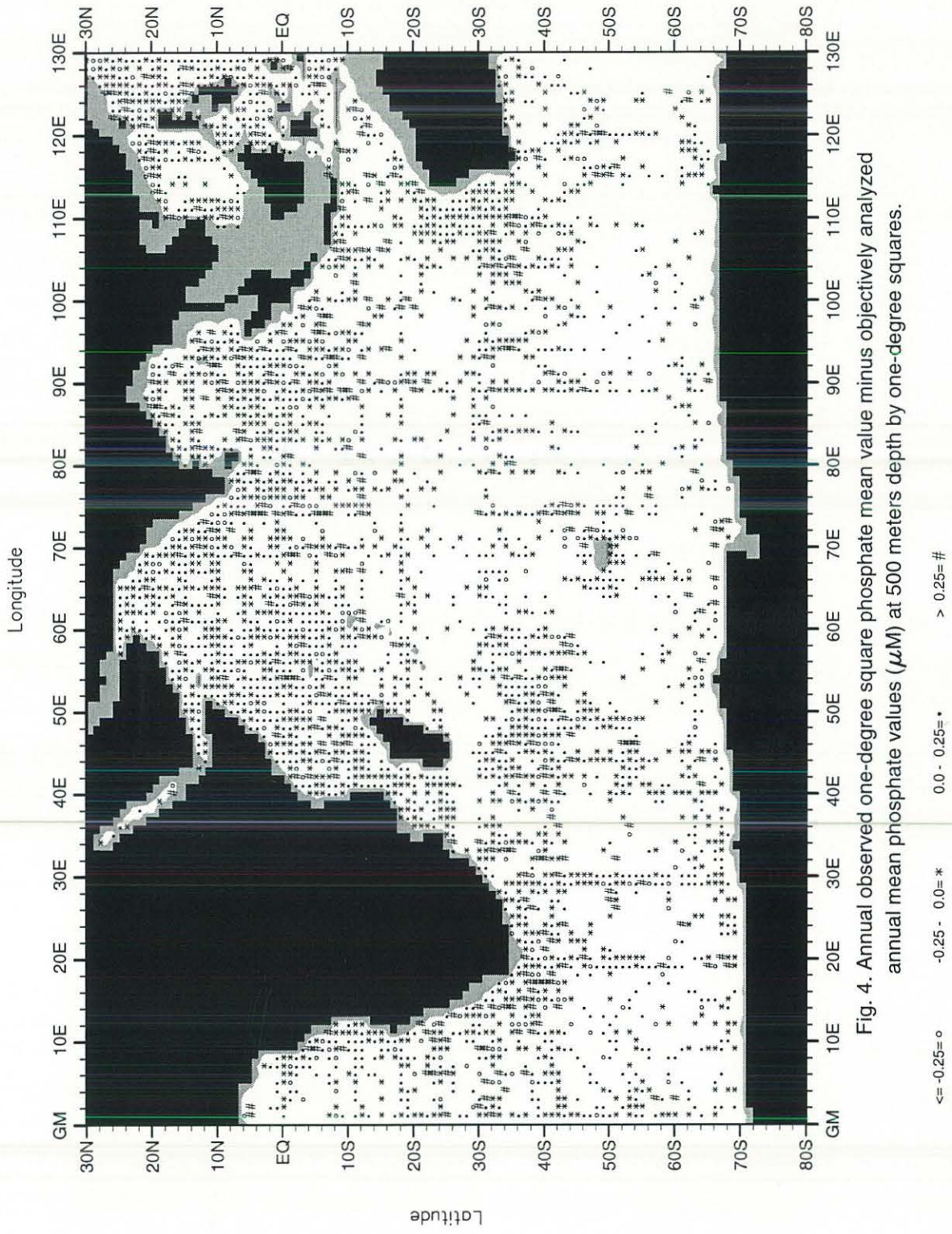
Fig. 4. Annual observed one-degree square phosphate mean value minus objectively analyzed annual mean phosphate values (μM) at 500 meters depth by one-degree squares.

$<= -0.25 = \circ$ $-0.25 - 0.0 = *$ $0.0 - 0.25 = \cdot$ $> 0.25 = \#$

APPENDICES

In each data distribution figure in each appendix, a small dot indicates a one-degree square containing 1-4 observations and a large dot indicates a one-degree square containing five or more observations.

In each figure showing an objectively analyzed mean, gridpoints for which there were less than four one-degree square values available to correct the first-guess are indicated by an "x".

Longitude
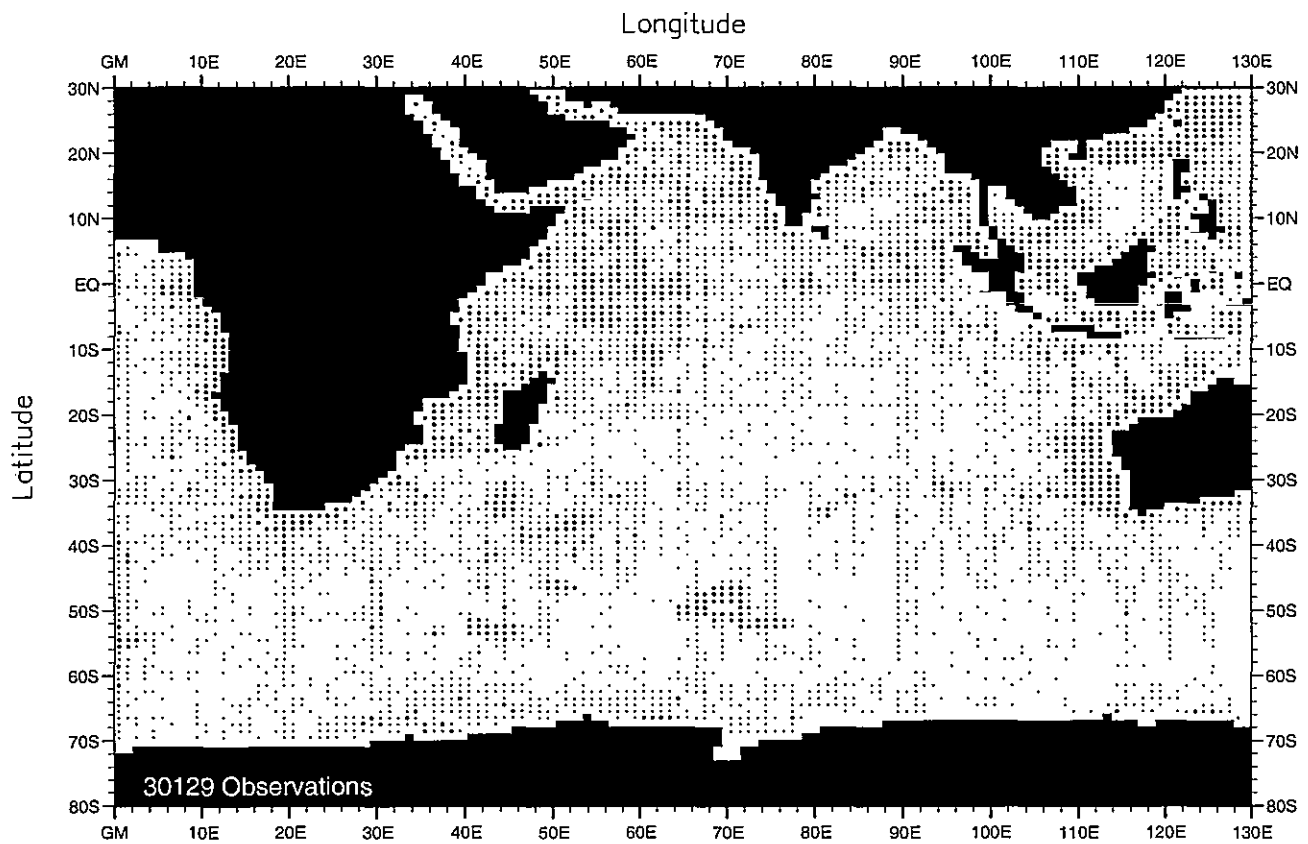
Fig. A1.   Annual phosphate observations at the surface .
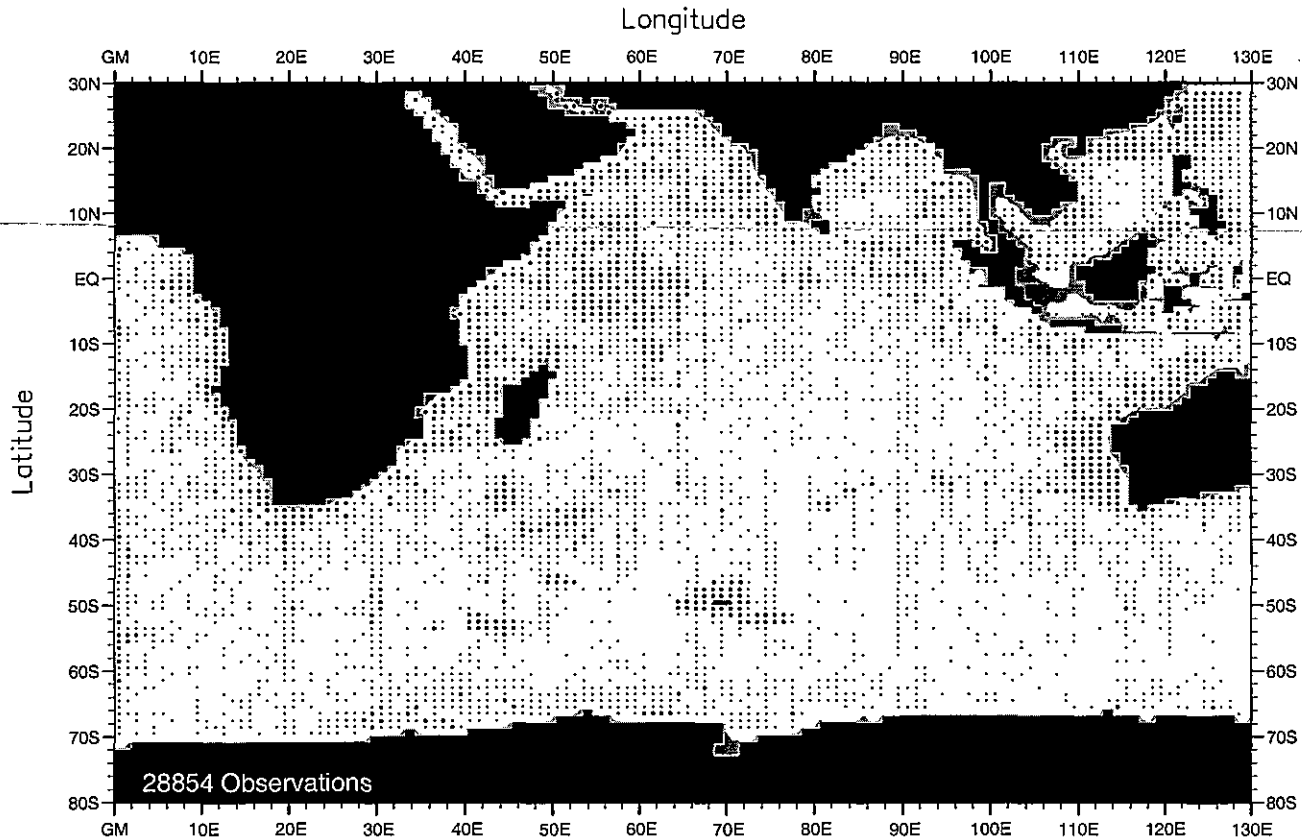
Fig. A2.   Annual phosphate observations at   50 m. depth .

21

Longitude
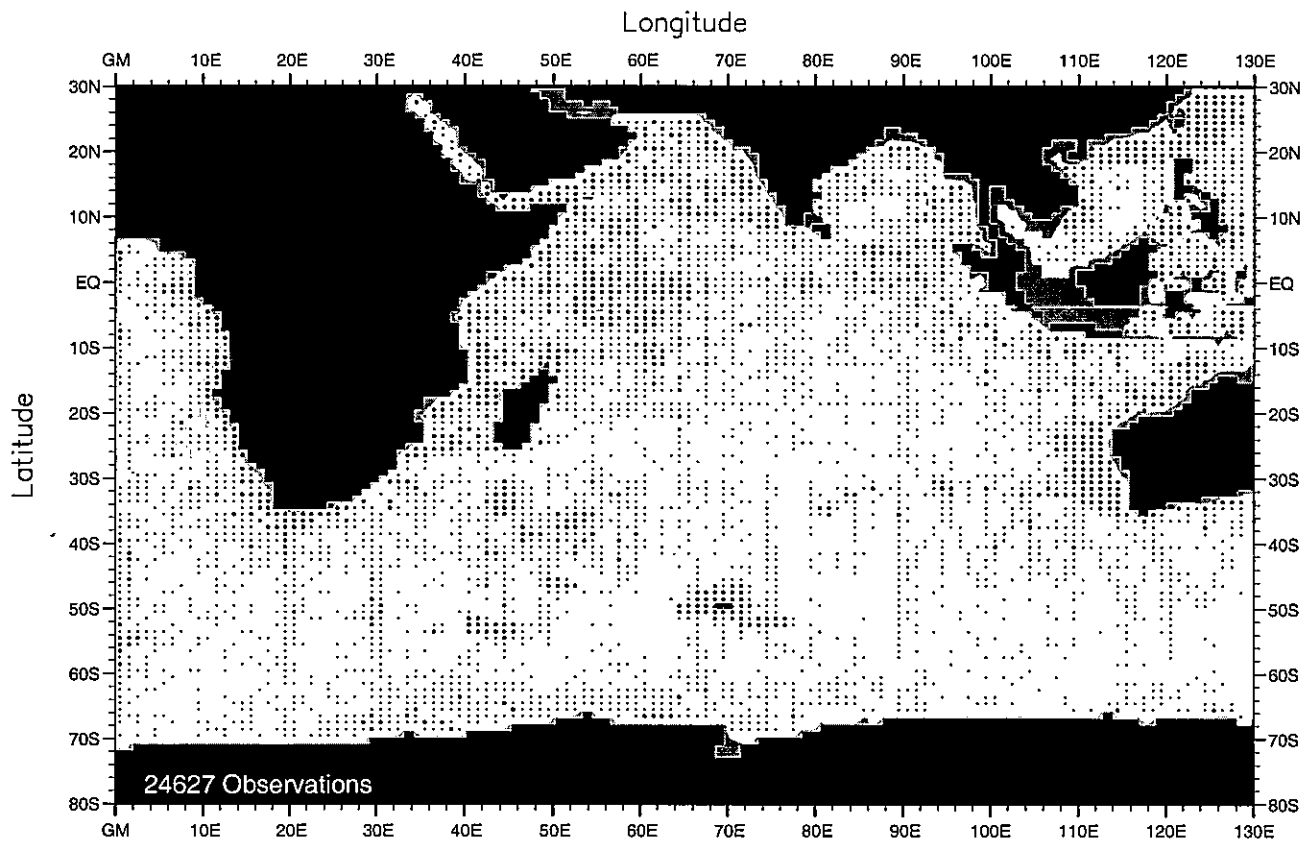
Fig. A3. Annual phosphate observations at 75 m. depth .

Longitude
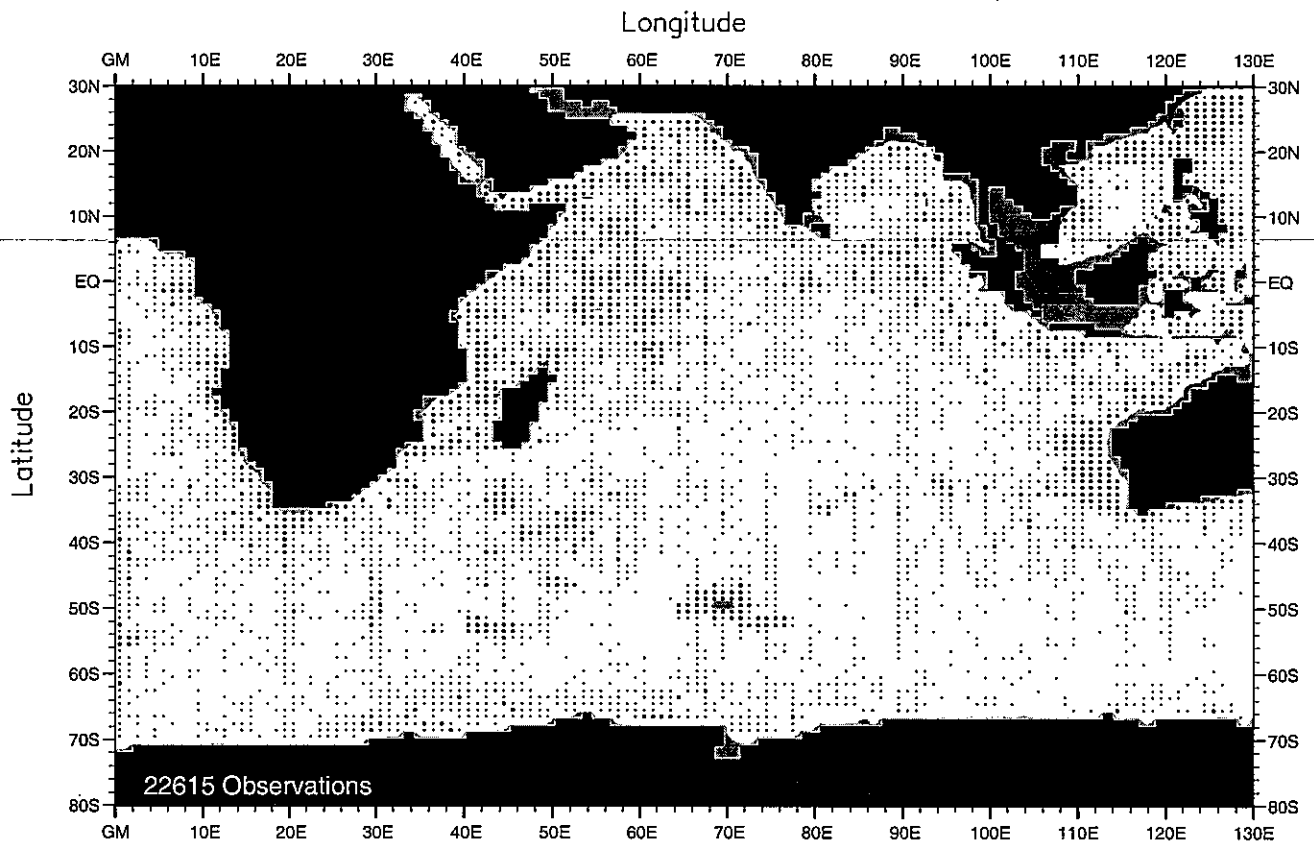
Fig. A4. Annual phosphate observations at 100 m. depth .
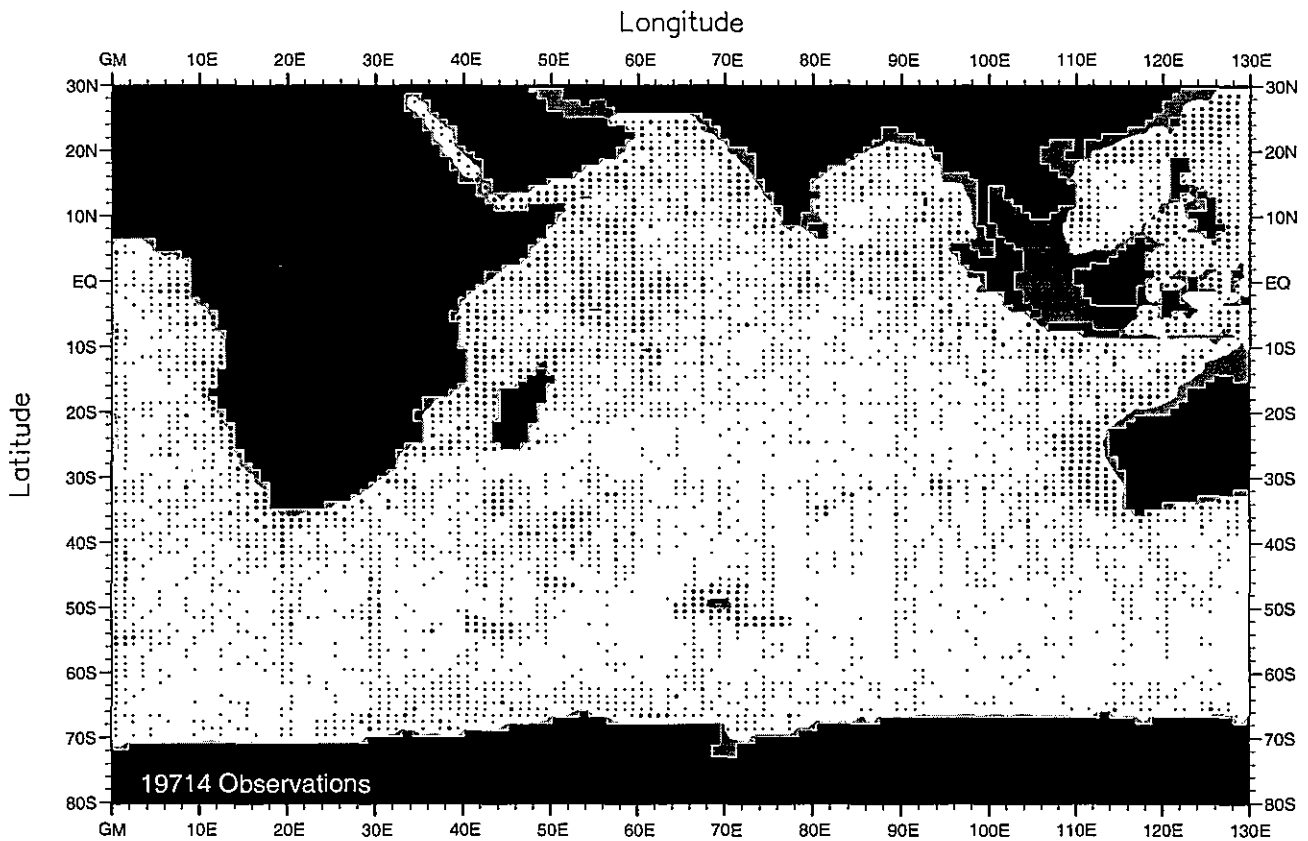
Fig. A5.   Annual phosphate observations at 150 m. depth .
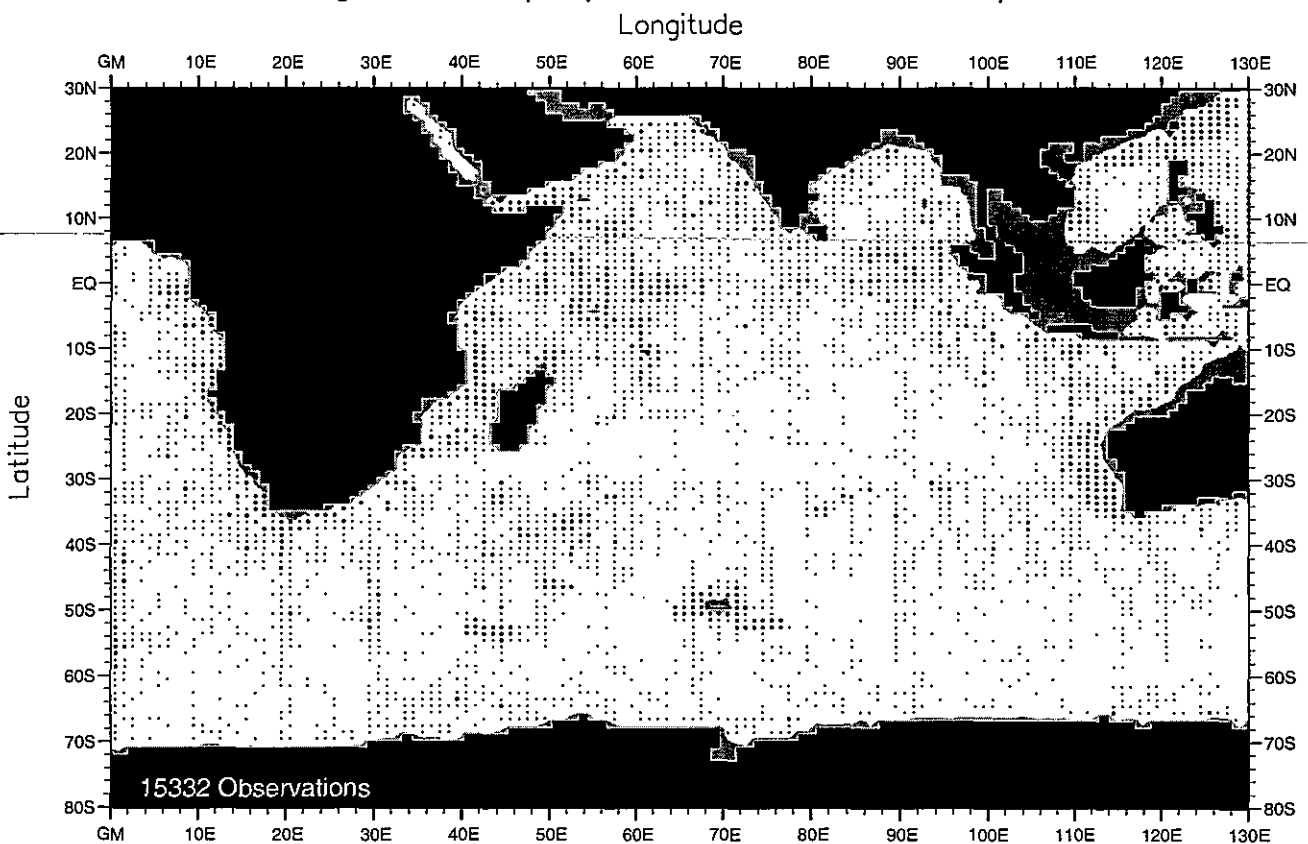
Fig. A6.   Annual phosphate observations at 200 m. depth .
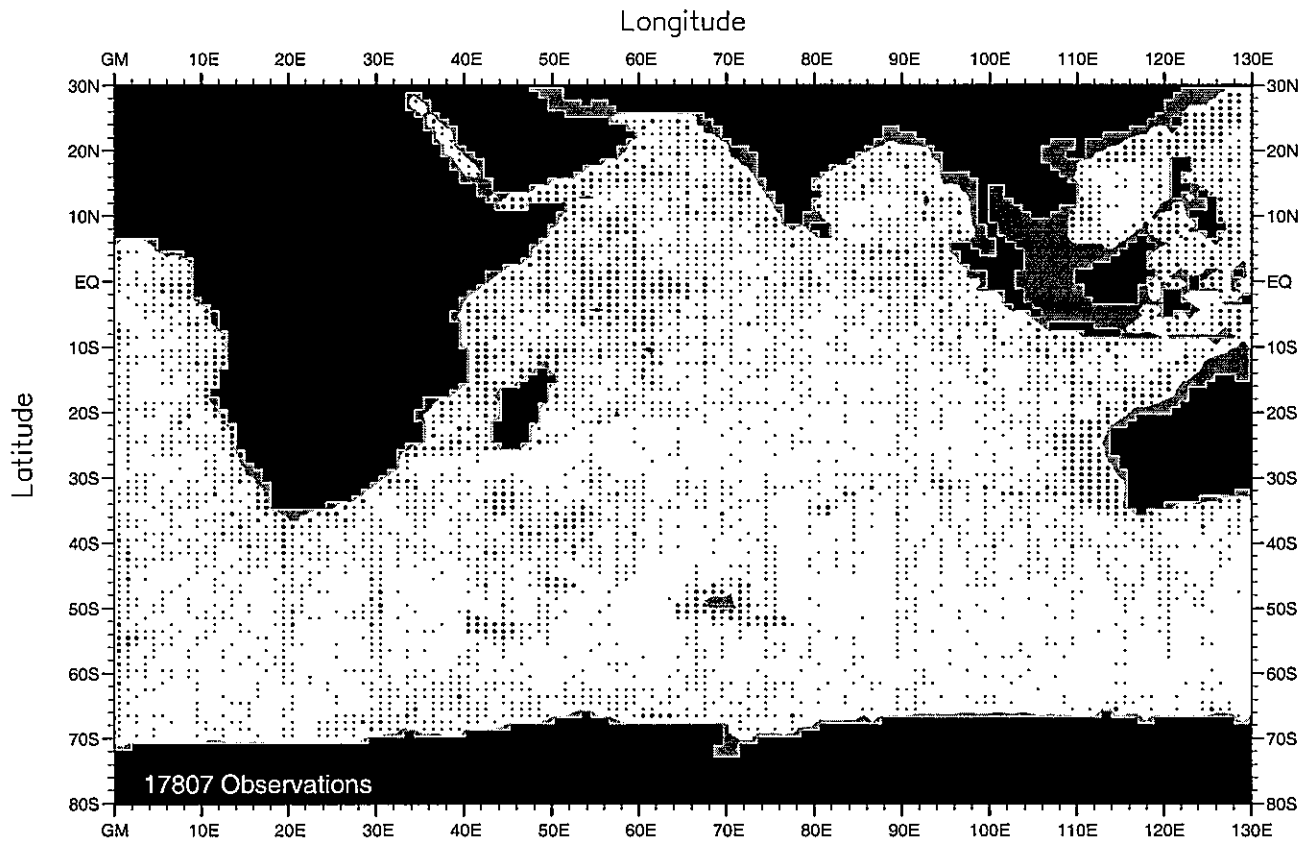
Fig. A7. Annual phosphate observations at 250 m. depth .
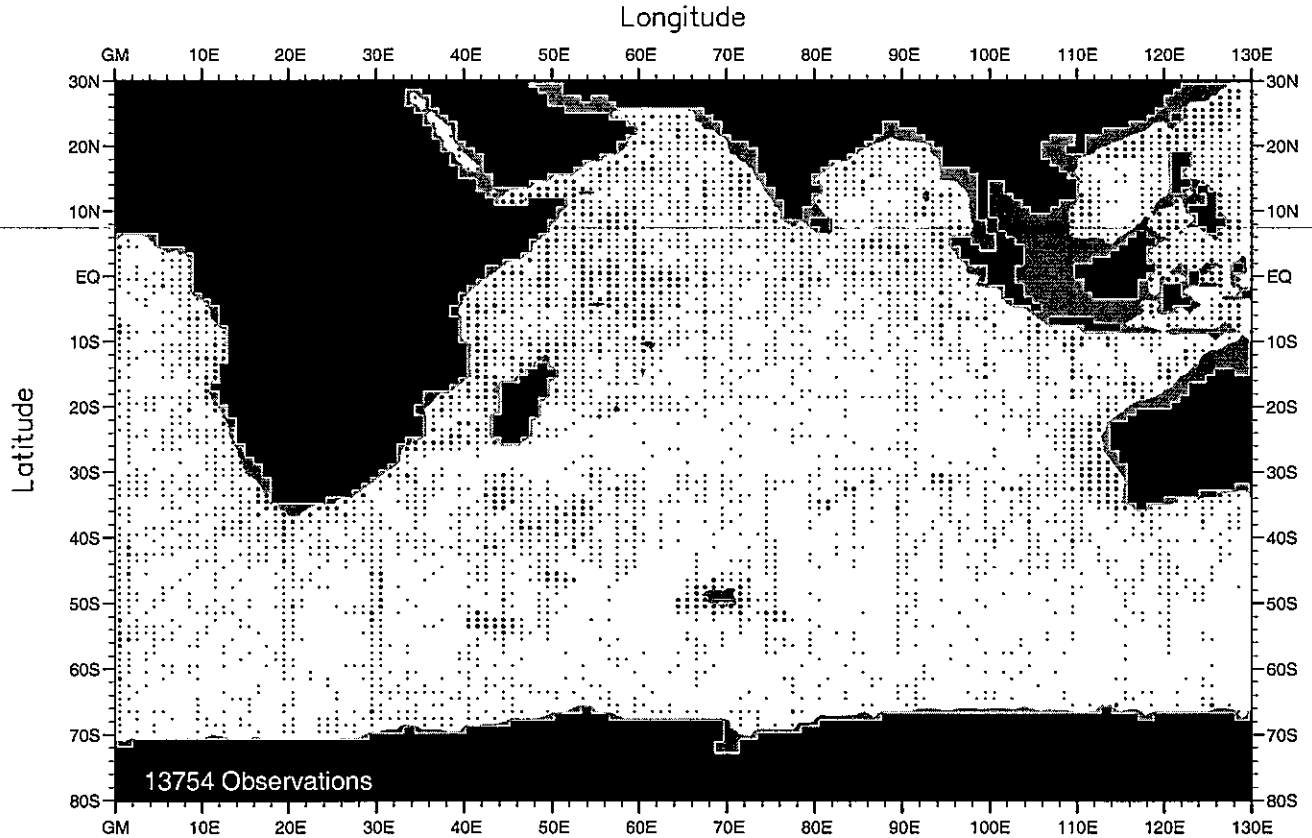
Fig. A8. Annual phosphate observations at 400 m. depth .
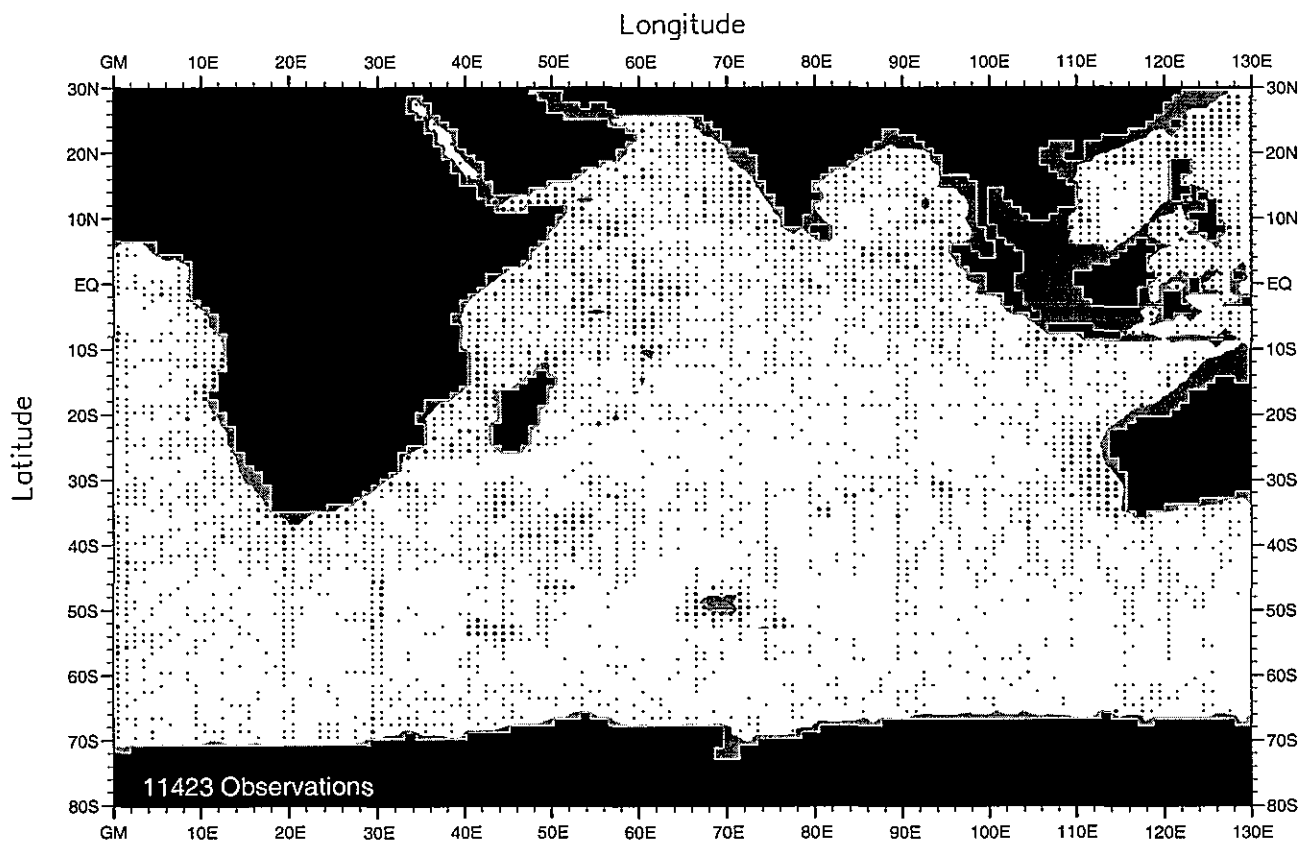
Fig. A9. Annual phosphate observations at 500 m. depth .
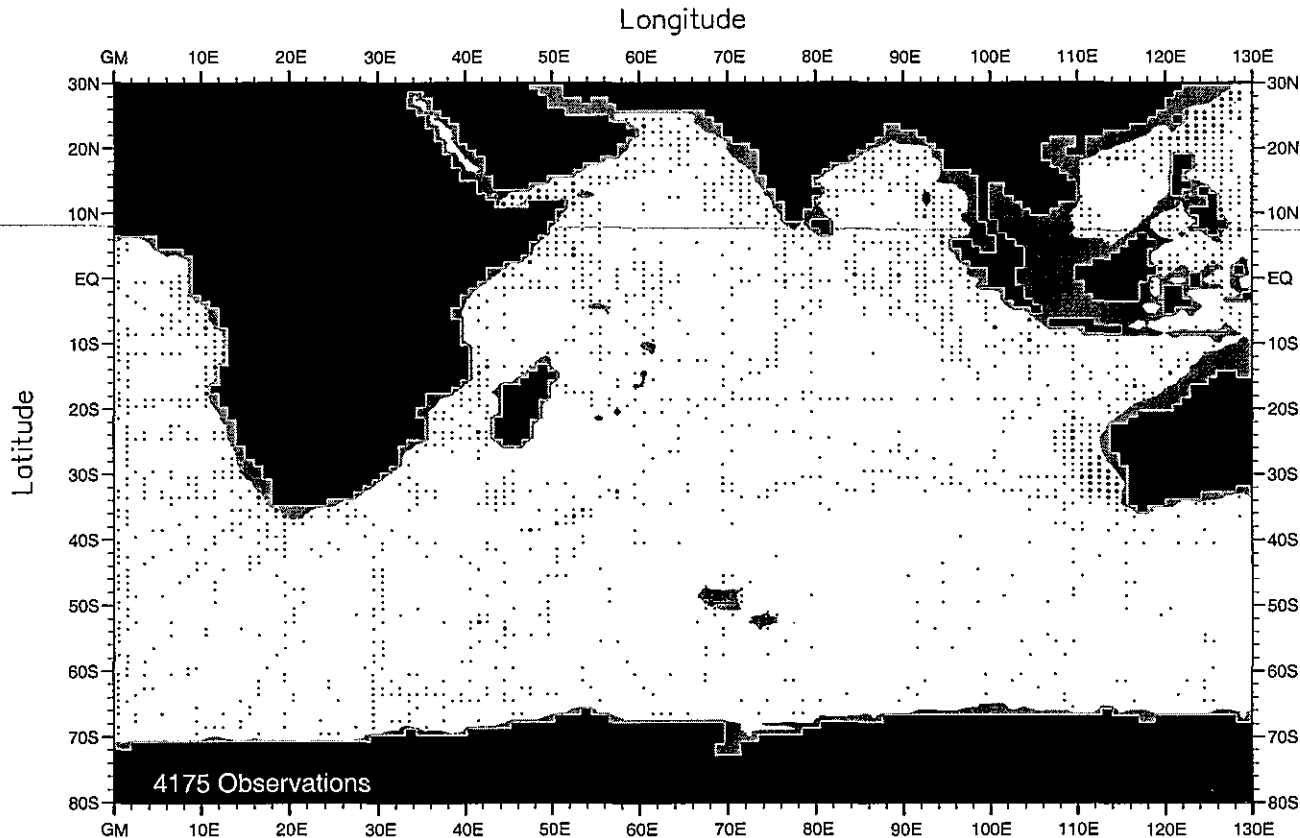
Fig. A10. Annual phosphate observations at 700 m. depth .
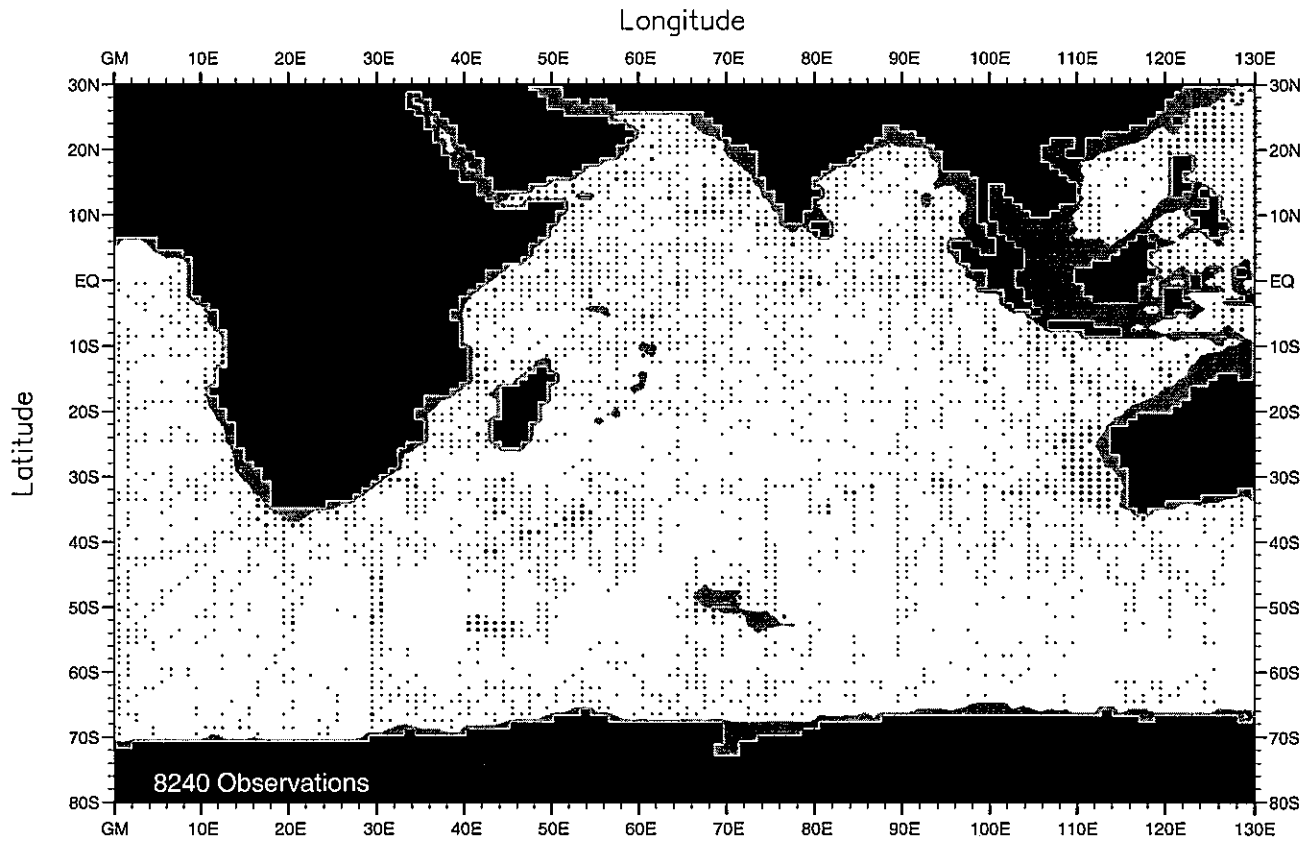
Fig. A11.   Annual phosphate observations at 1000 m. depth .
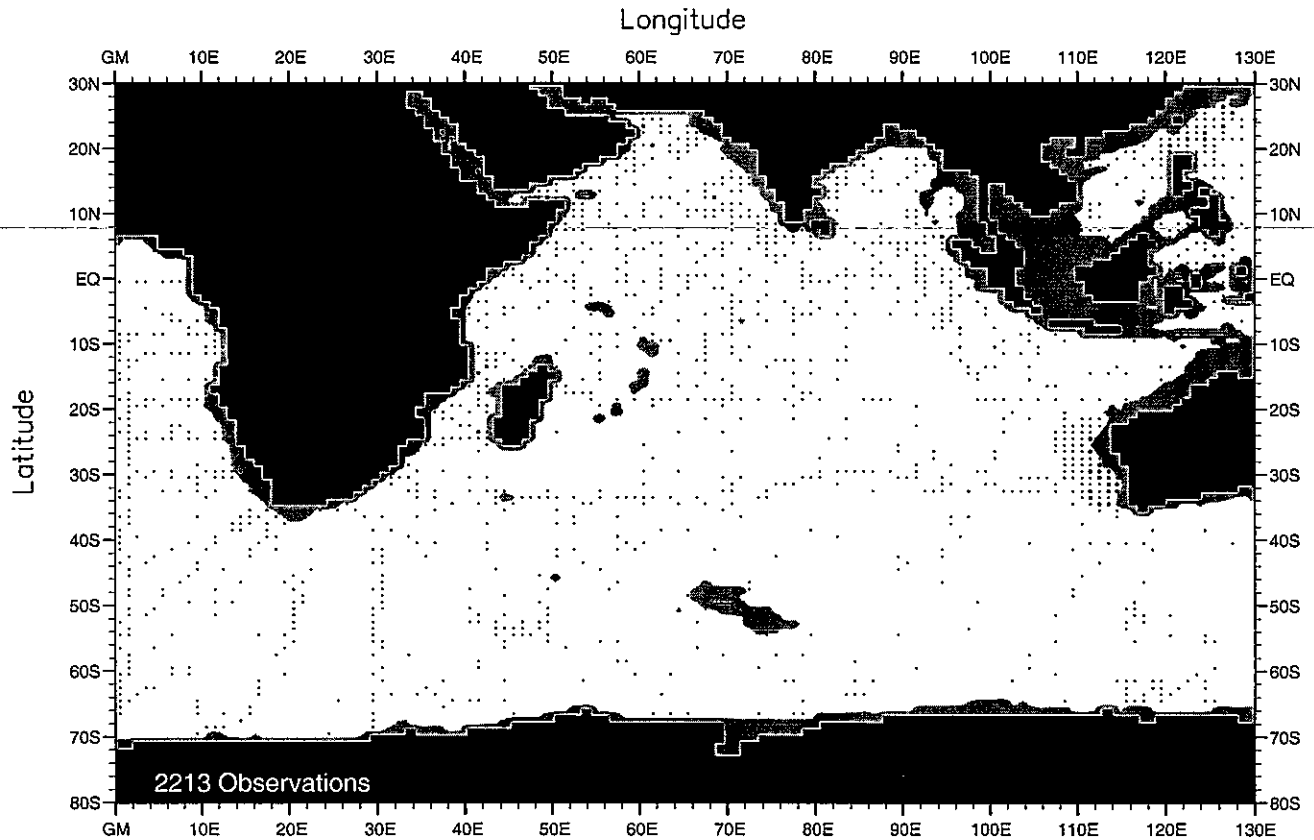
Fig. A12.   Annual phosphate observations at 1500 m. depth .

Longitude
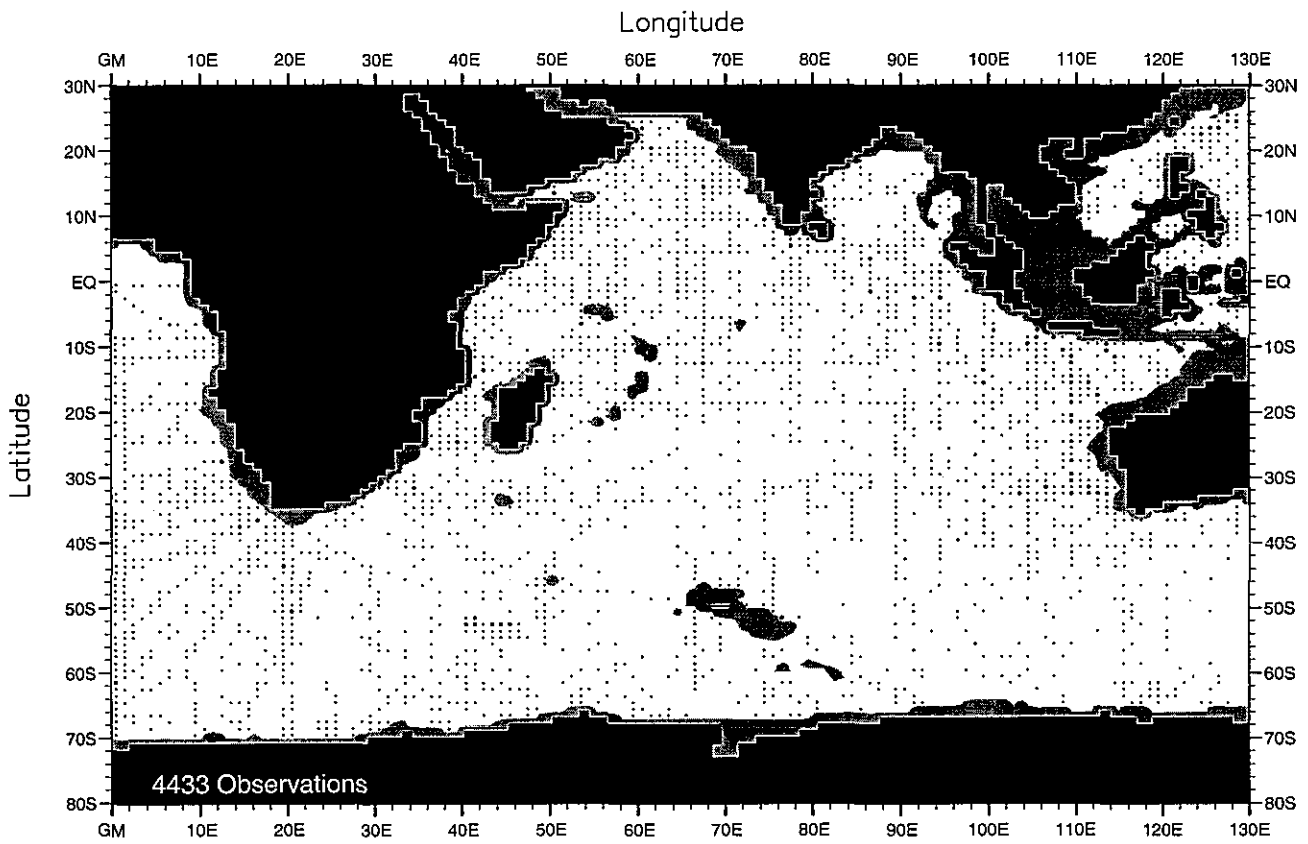
Fig. A13. Annual phosphate observations at 2000 m. depth .

Longitude
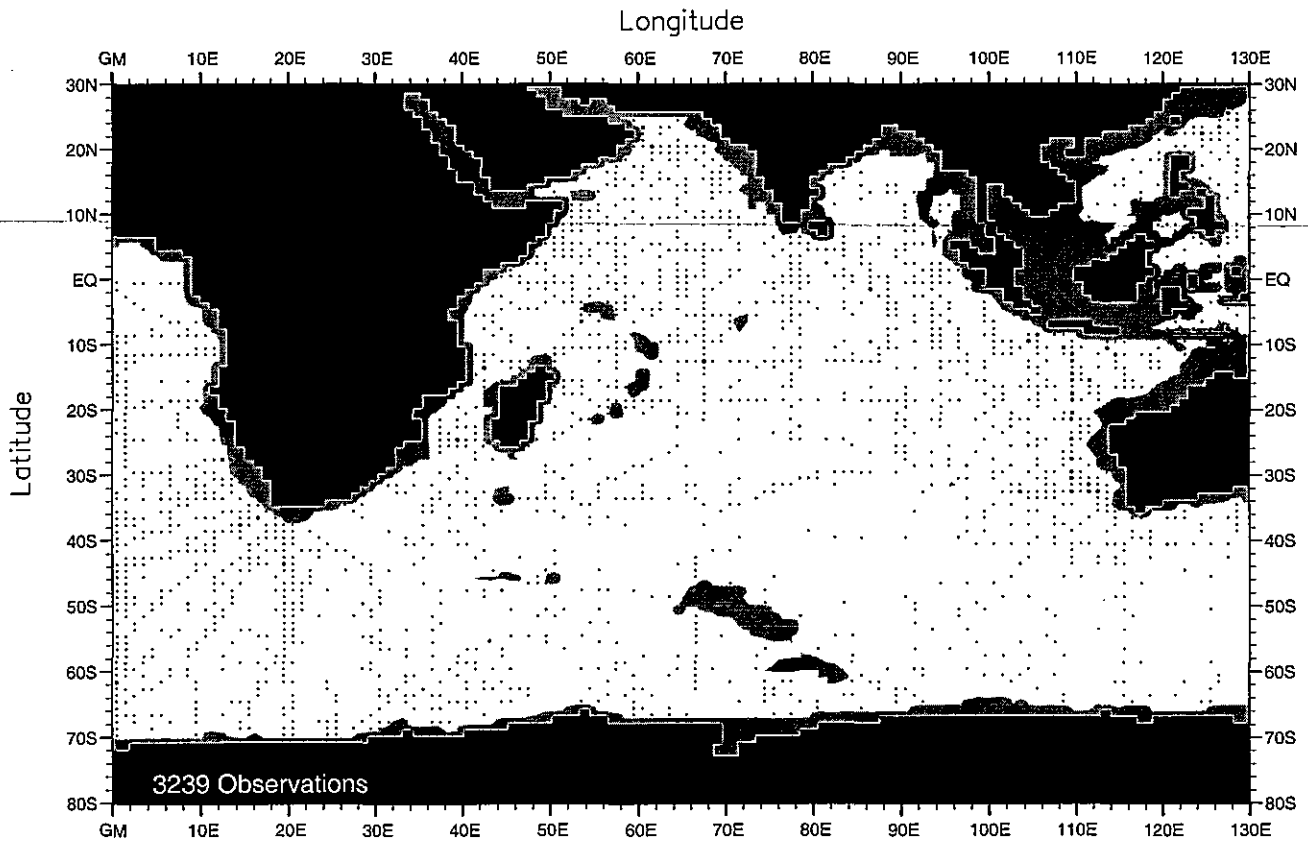
Fig. A14. Annual phosphate observations at 2500 m. depth .

27
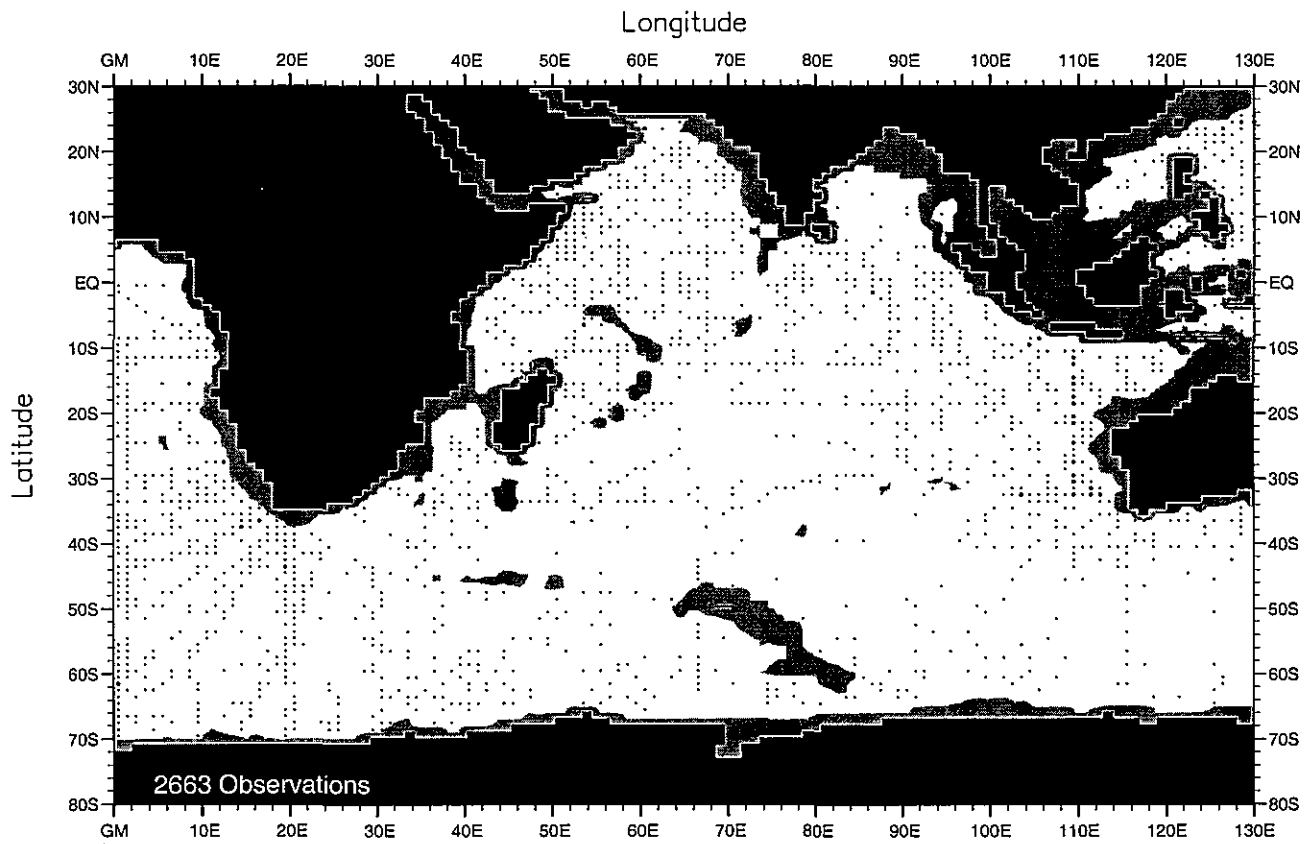
Fig. A15. Annual phosphate observations at 3000 m. depth .
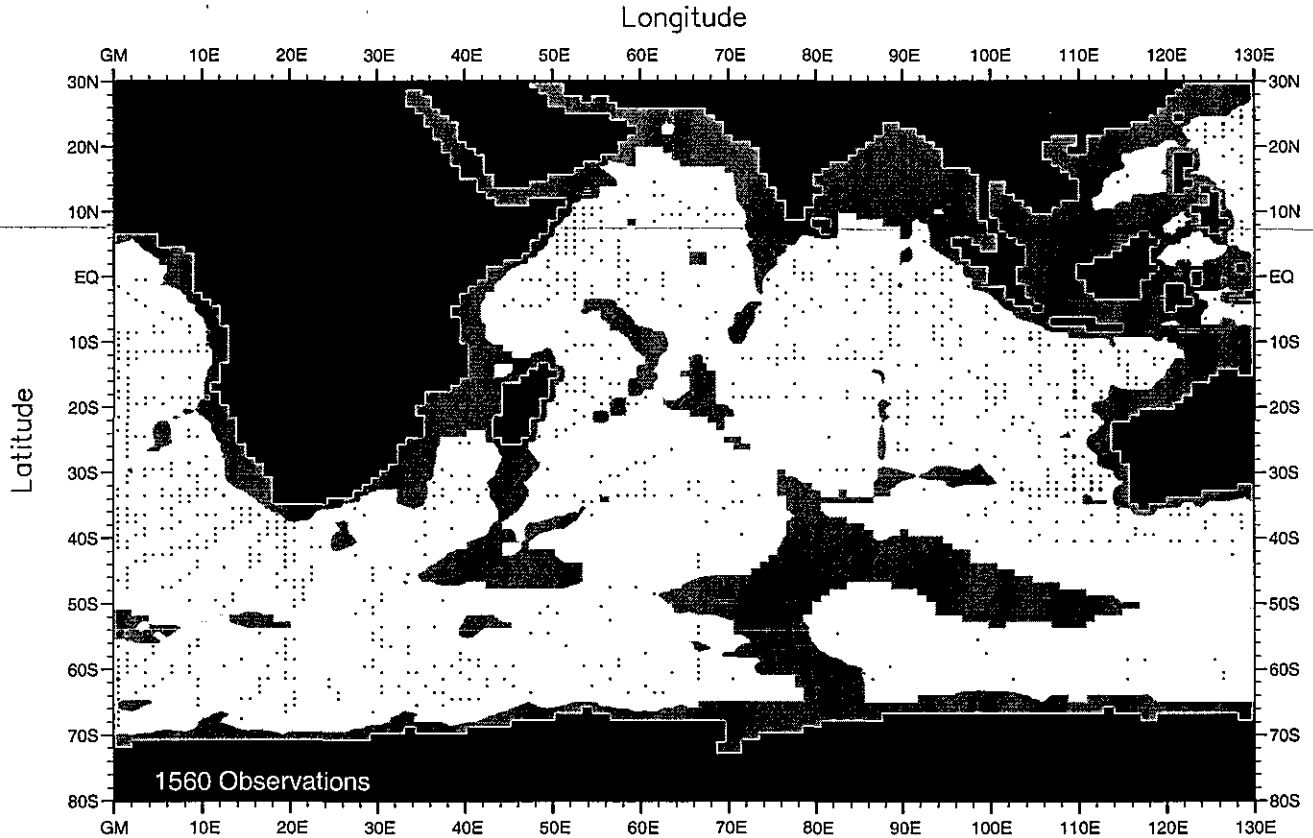
Fig. A16. Annual phosphate observations at 4000 m. depth .

28
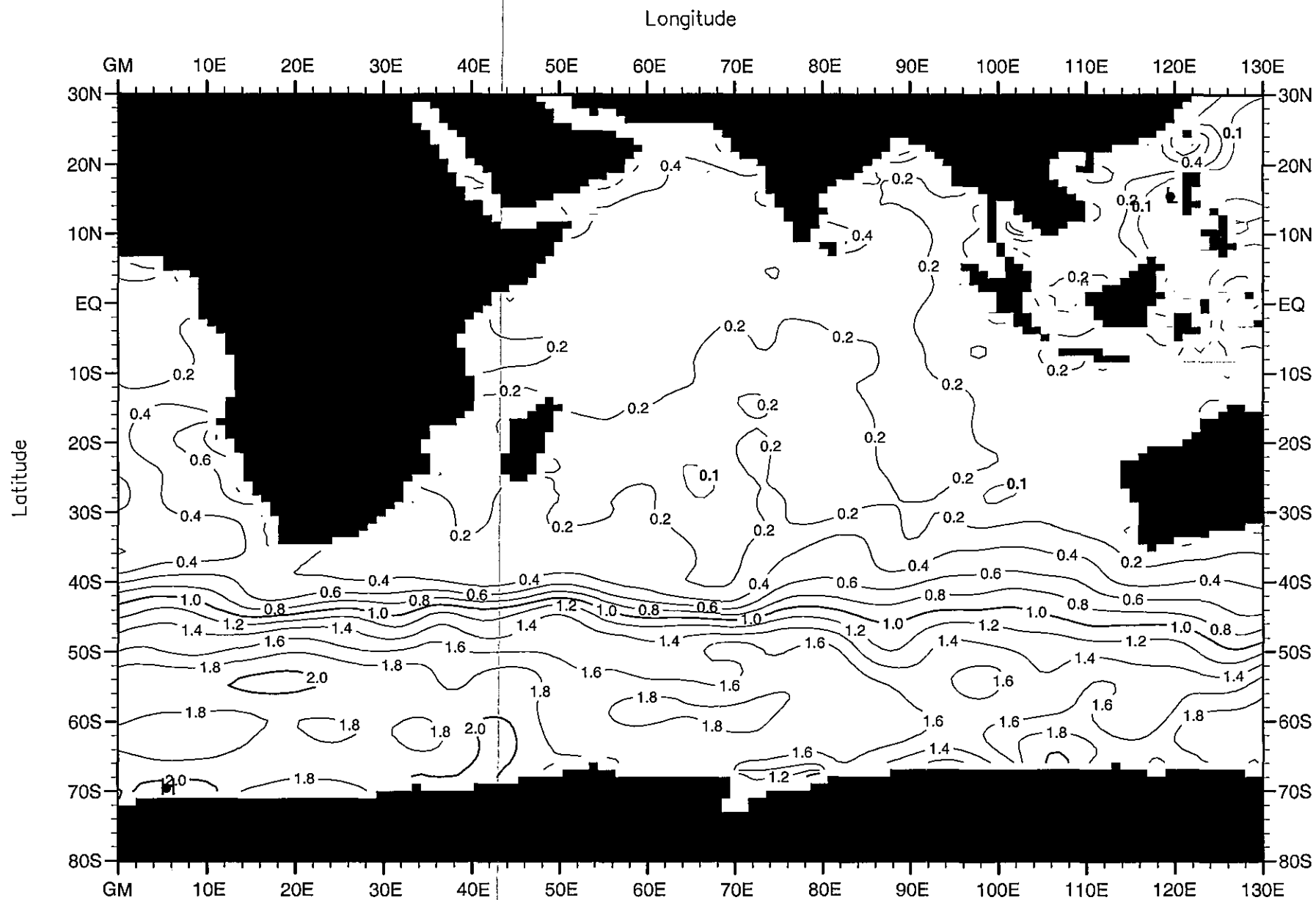
Fig. A17. Annual mean phosphate (μM) at the surface .

Minimum Value= 0.01   Maximum Value= 2.08   Contour Interval: 0.20
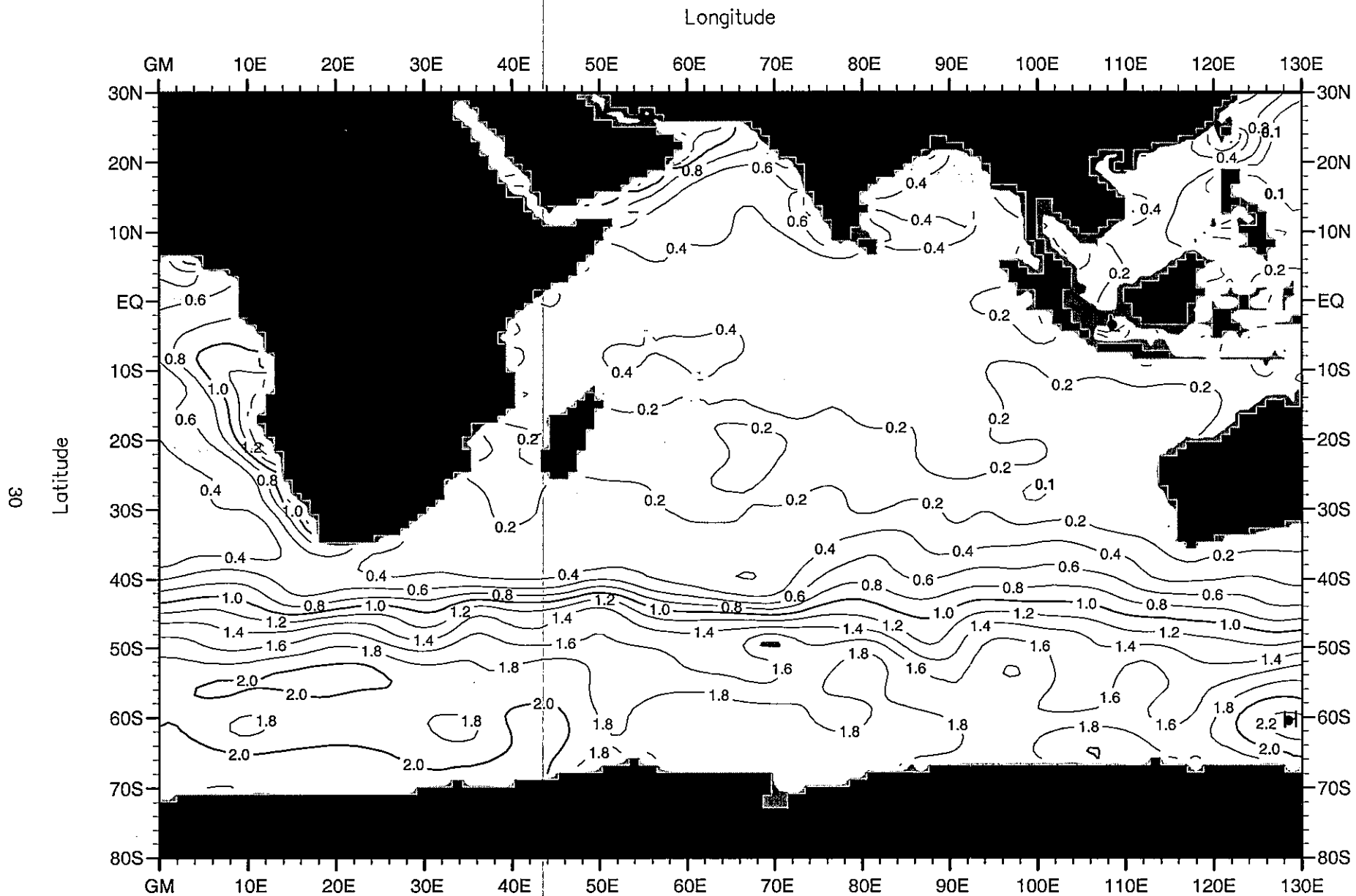
Fig. A18. Annual mean phosphate (μM) at 50 m. depth .

Minimum Value= 0.02   Maximum Value= 2.26   Contour Interval: 0.20
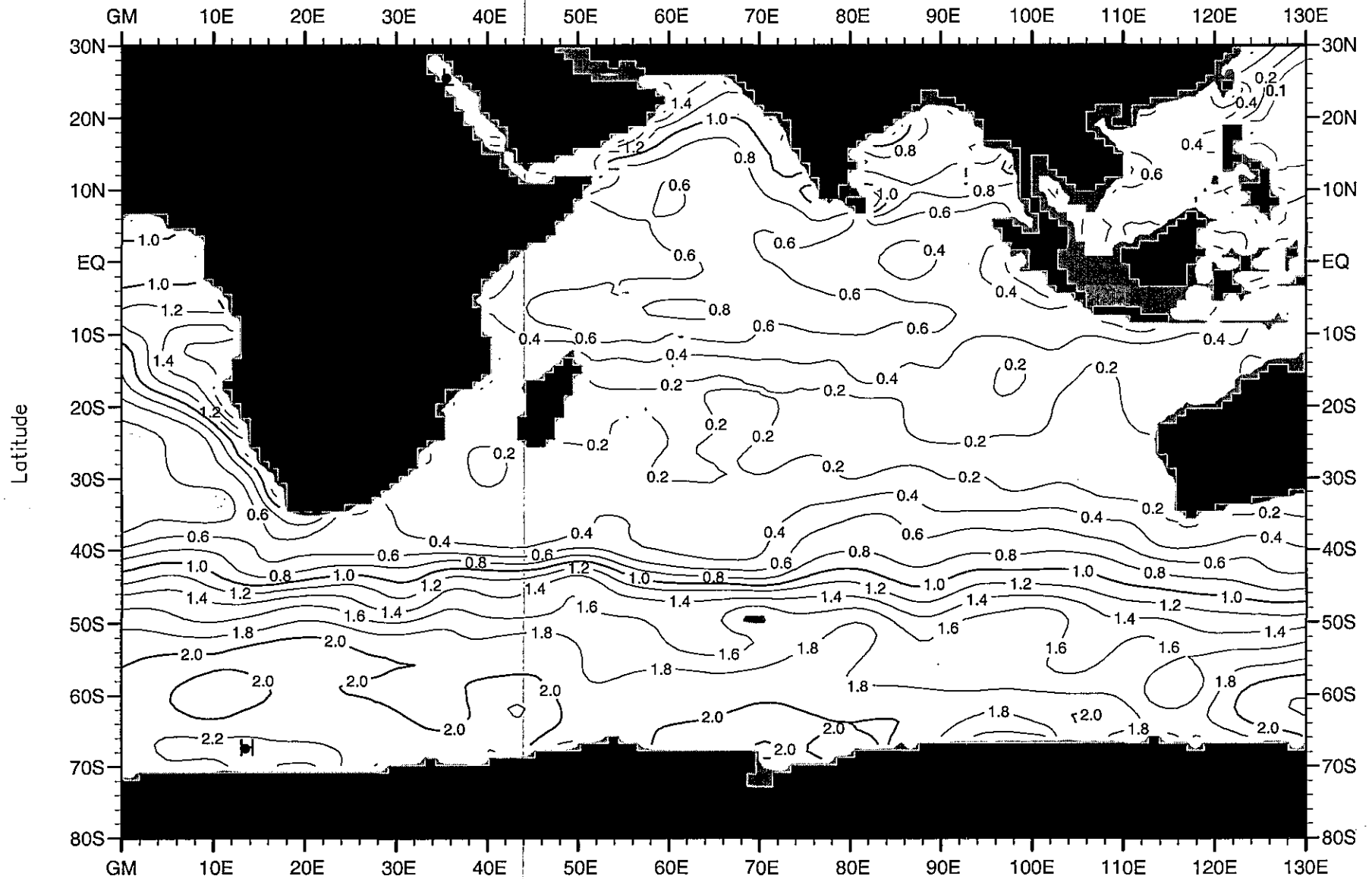
Fig. A19. Annual mean phosphate (μM) at 75 m. depth .

Minimum Value= 0.02   Maximum Value= 2.25   Contour Interval: 0.20
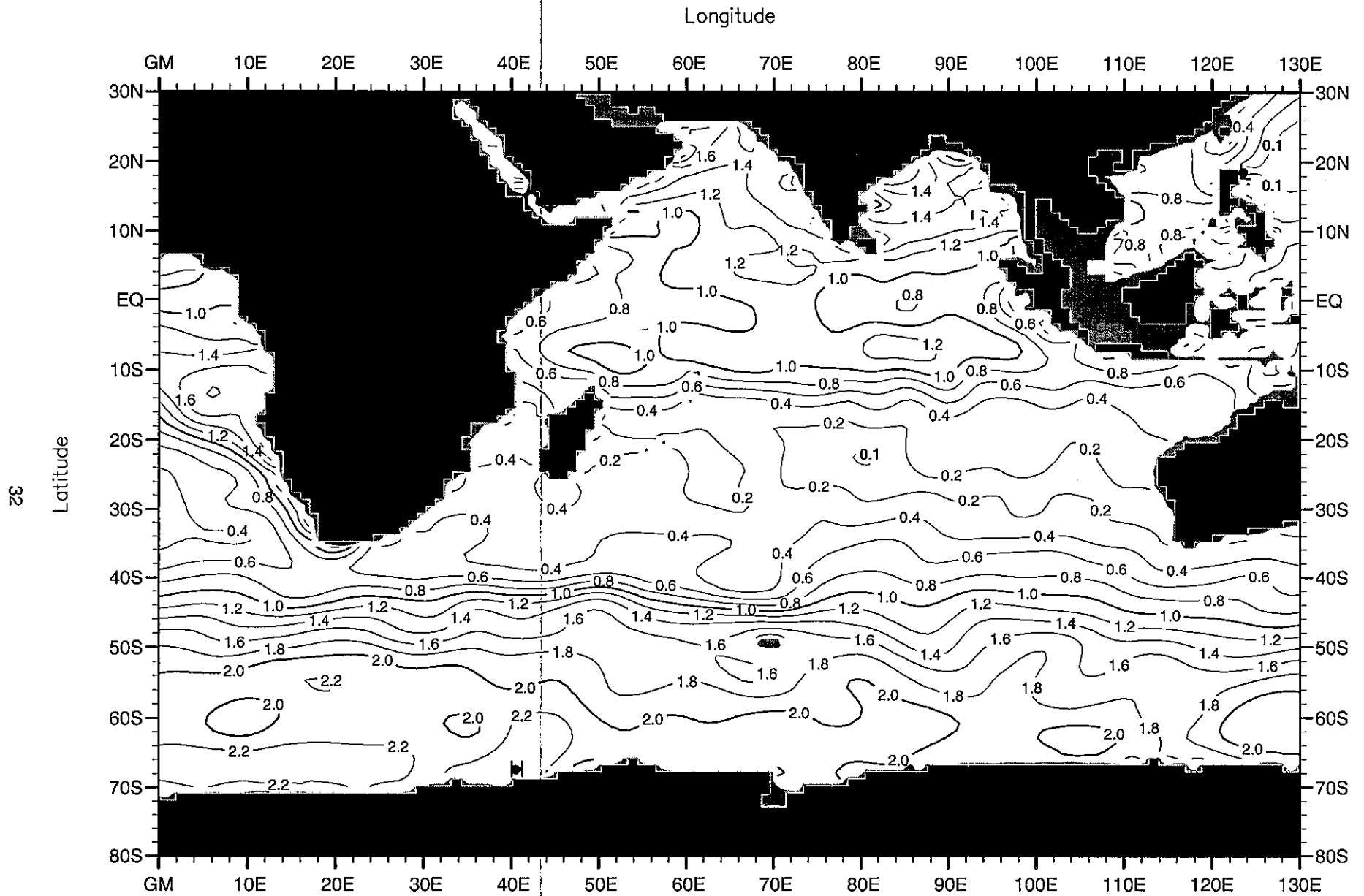
Fig. A20.   Annual mean phosphate (μM) at 100 m. depth .

Minimum Value= 0.04   Maximum Value= 2.43   Contour Interval: 0.20

32
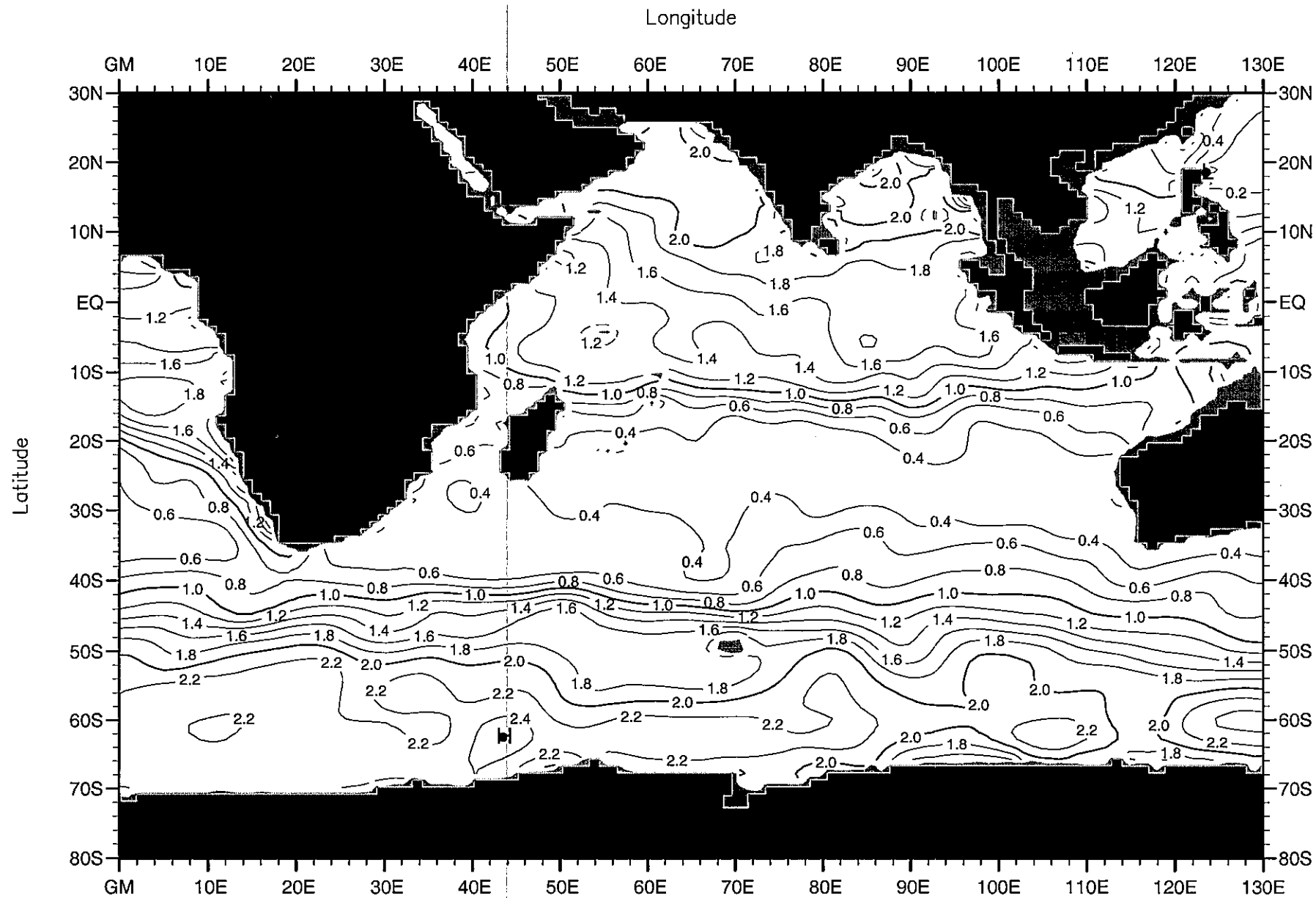
Fig. A21. Annual mean phosphate (μM) at 150 m. depth .

Minimum Value= 0.03   Maximum Value= 2.51   Contour Interval: 0.20
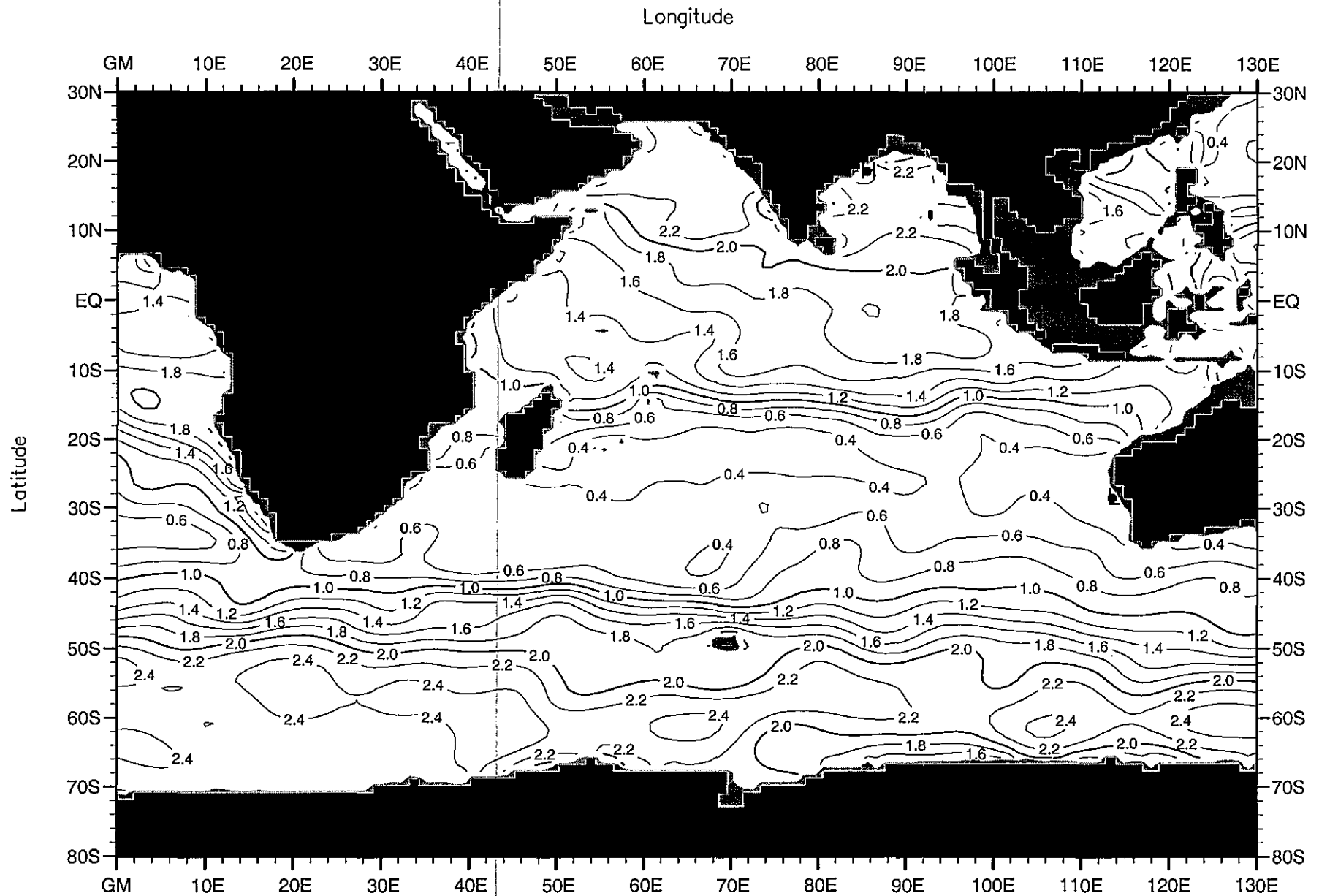
Fig. A22. Annual mean phosphate (μM) at 200 m. depth .

Minimum Value= 0.13   Maximum Value= 2.62   Contour Interval: 0.20
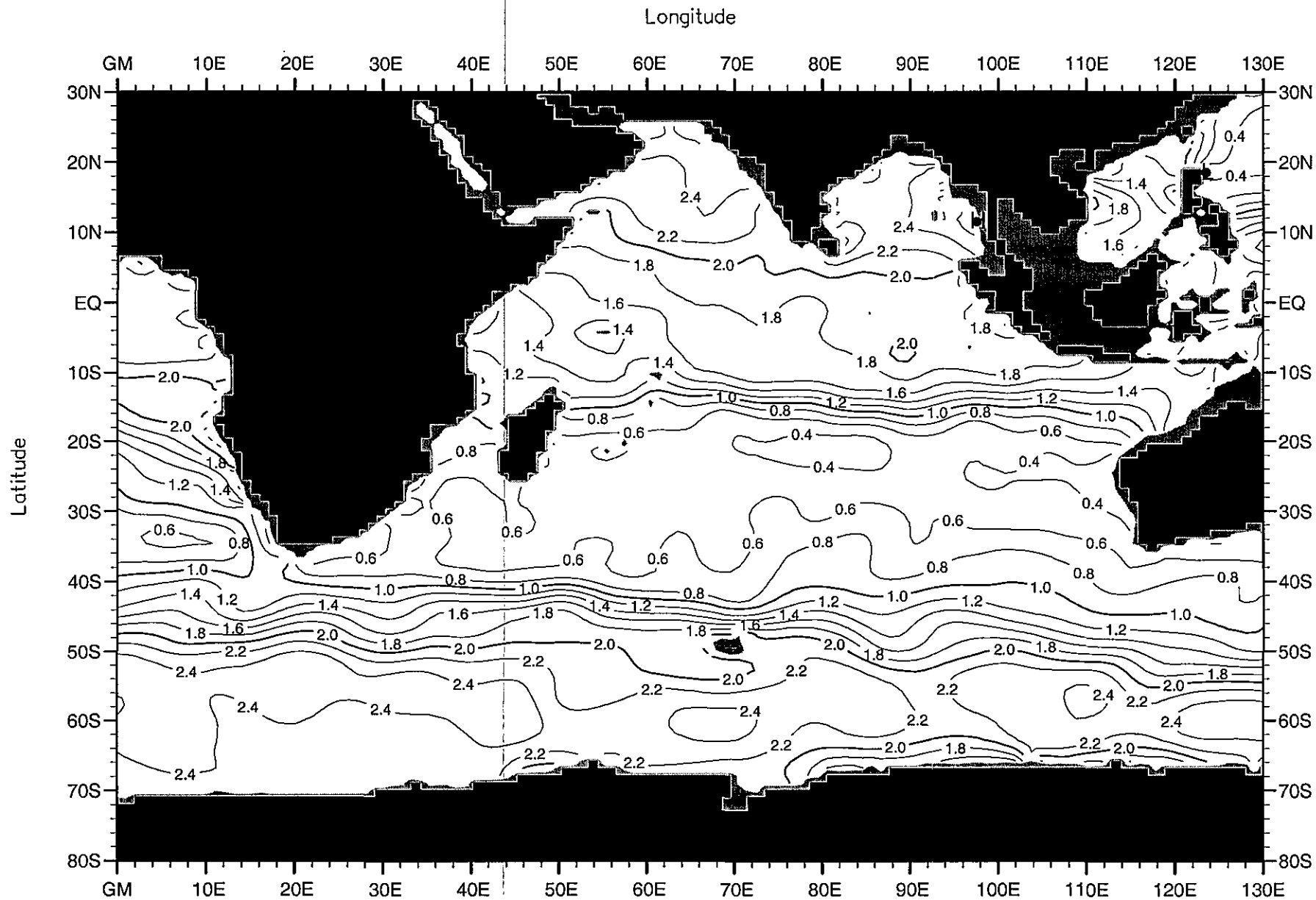
Fig. A23. Annual mean phosphate (μM) at 250 m. depth.

Minimum Value= 0.21   Maximum Value= 2.79   Contour Interval: 0.20
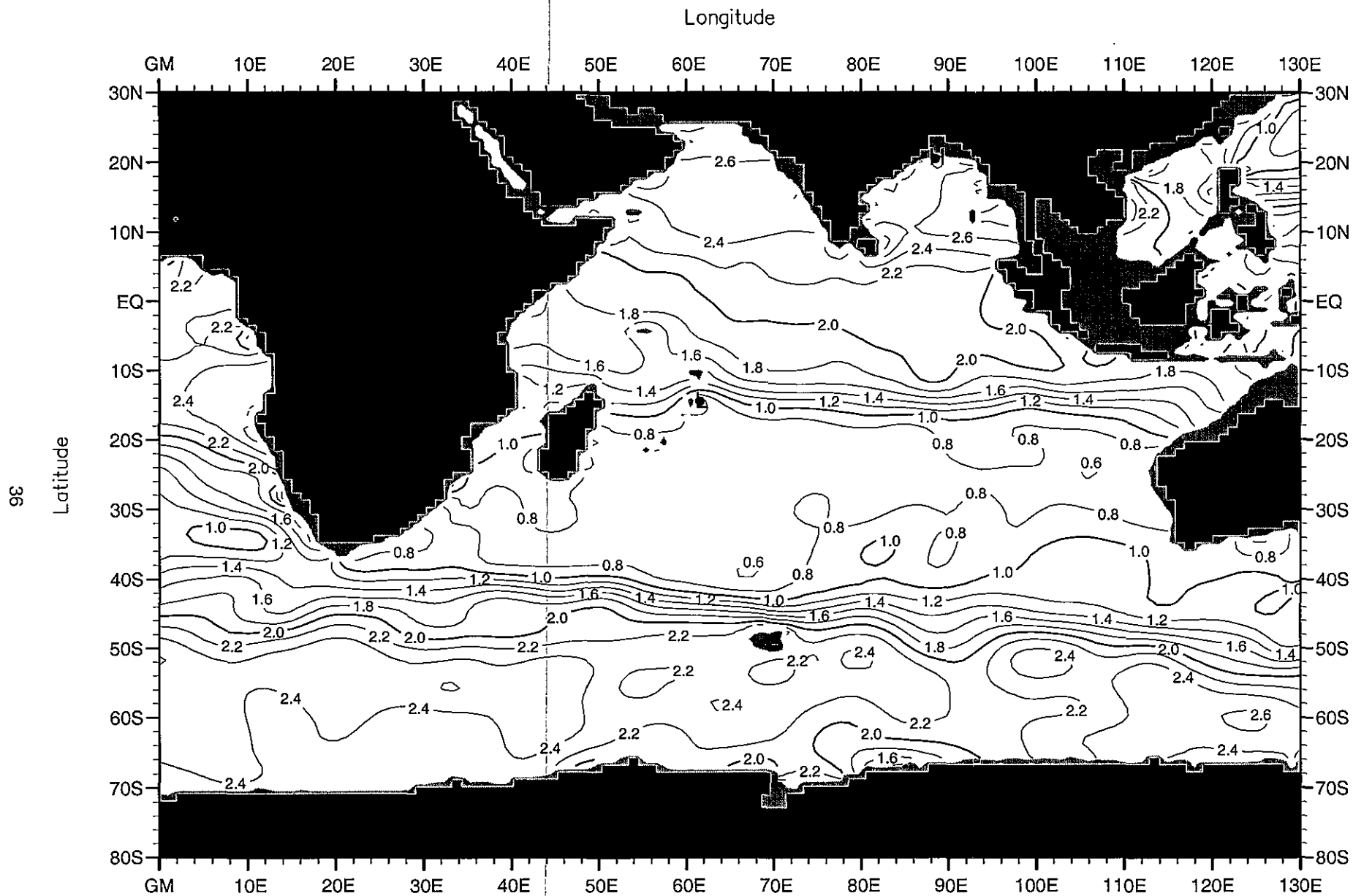
Fig. A24. Annual mean phosphate (μM) at 400 m. depth .

Minimum Value= 0.46   Maximum Value= 3.04   Contour Interval: 0.20
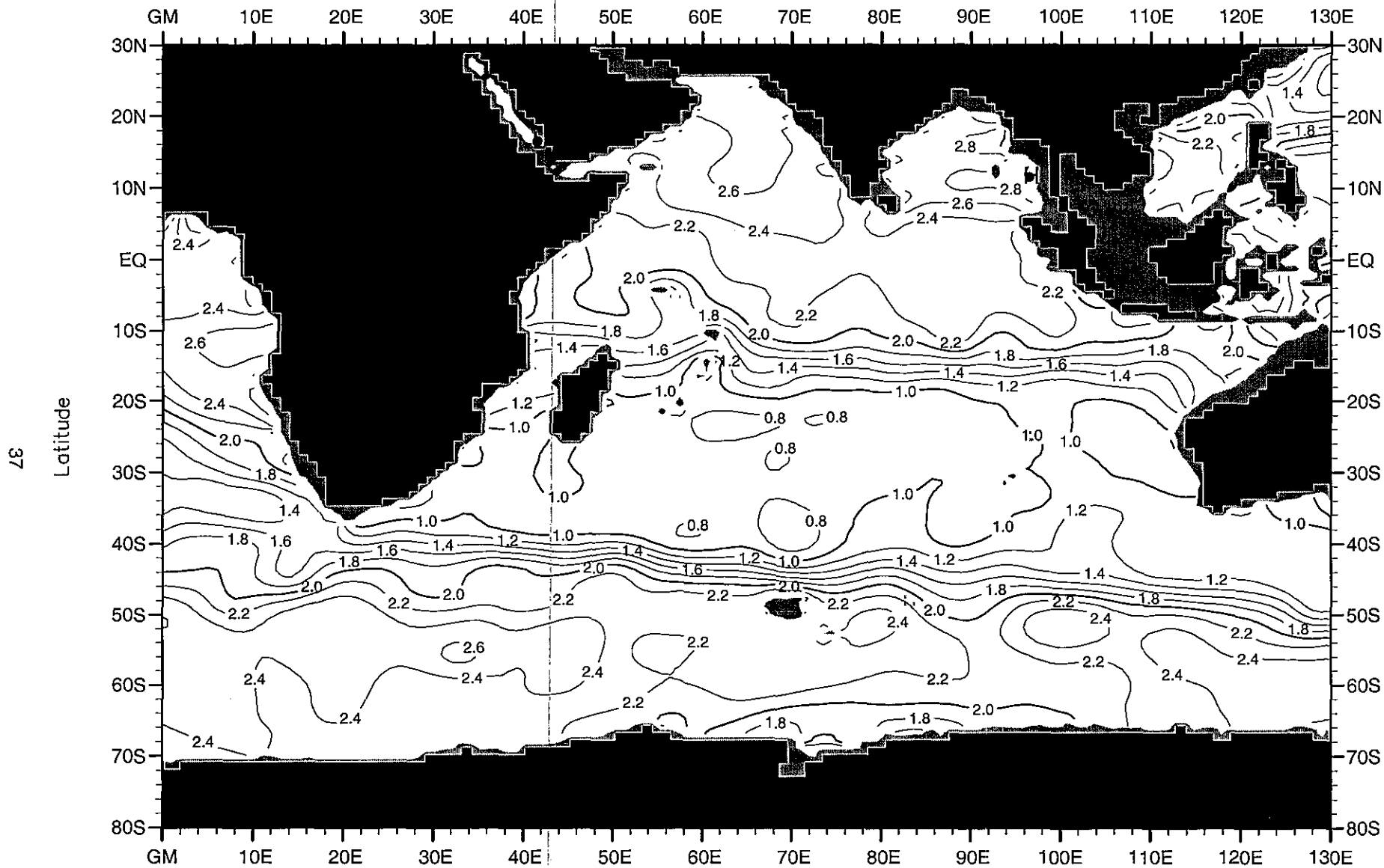
Fig. A25. Annual mean phosphate (μM) at 500 m. depth .

Minimum Value= 0.57   Maximum Value= 3.11   Contour Interval: 0.20
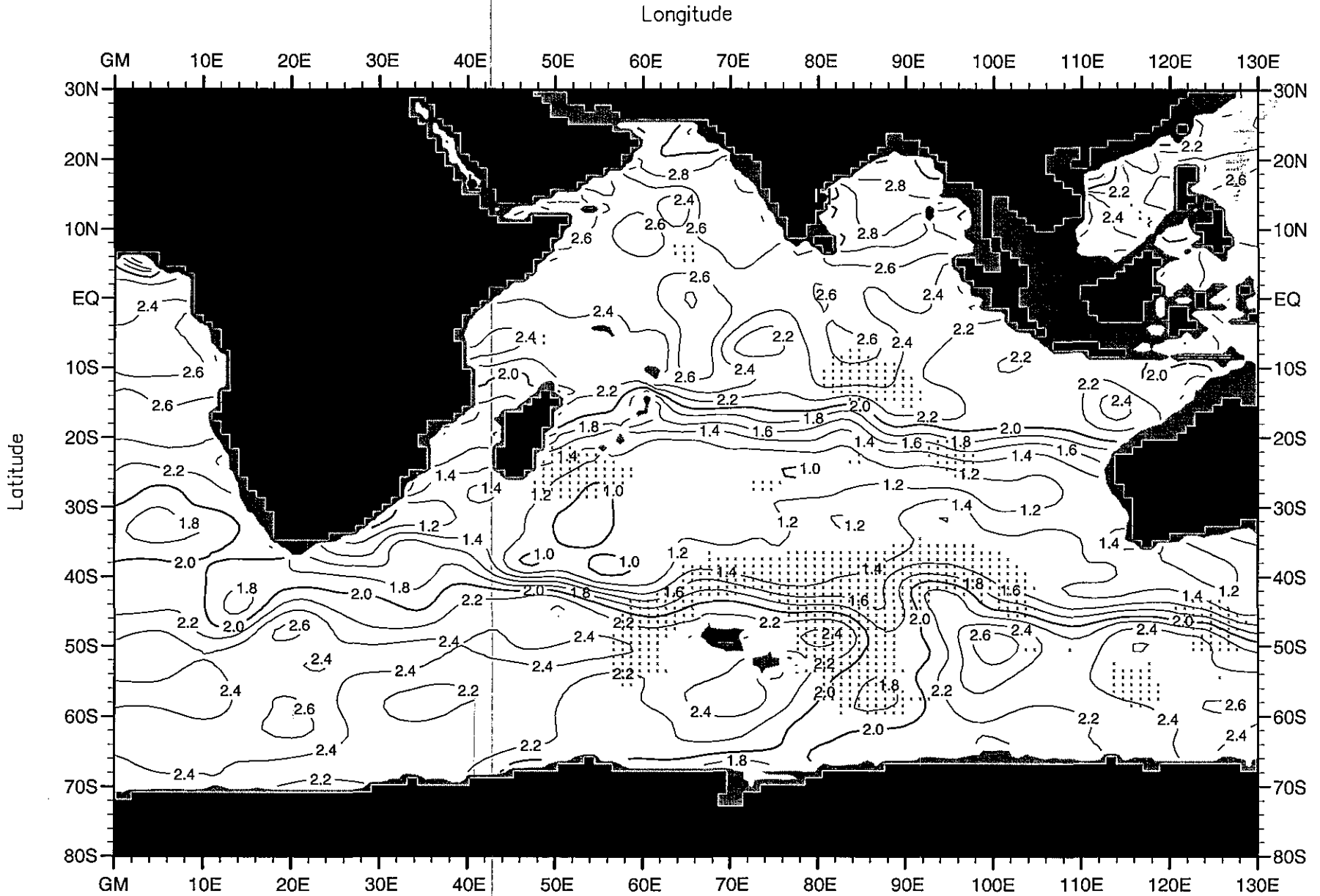
Fig. A26.   Annual mean phosphate (μM) at 700 m. depth .

Minimum Value=   0.32   Maximum Value=   3.56   Contour Interval: 0.20

38
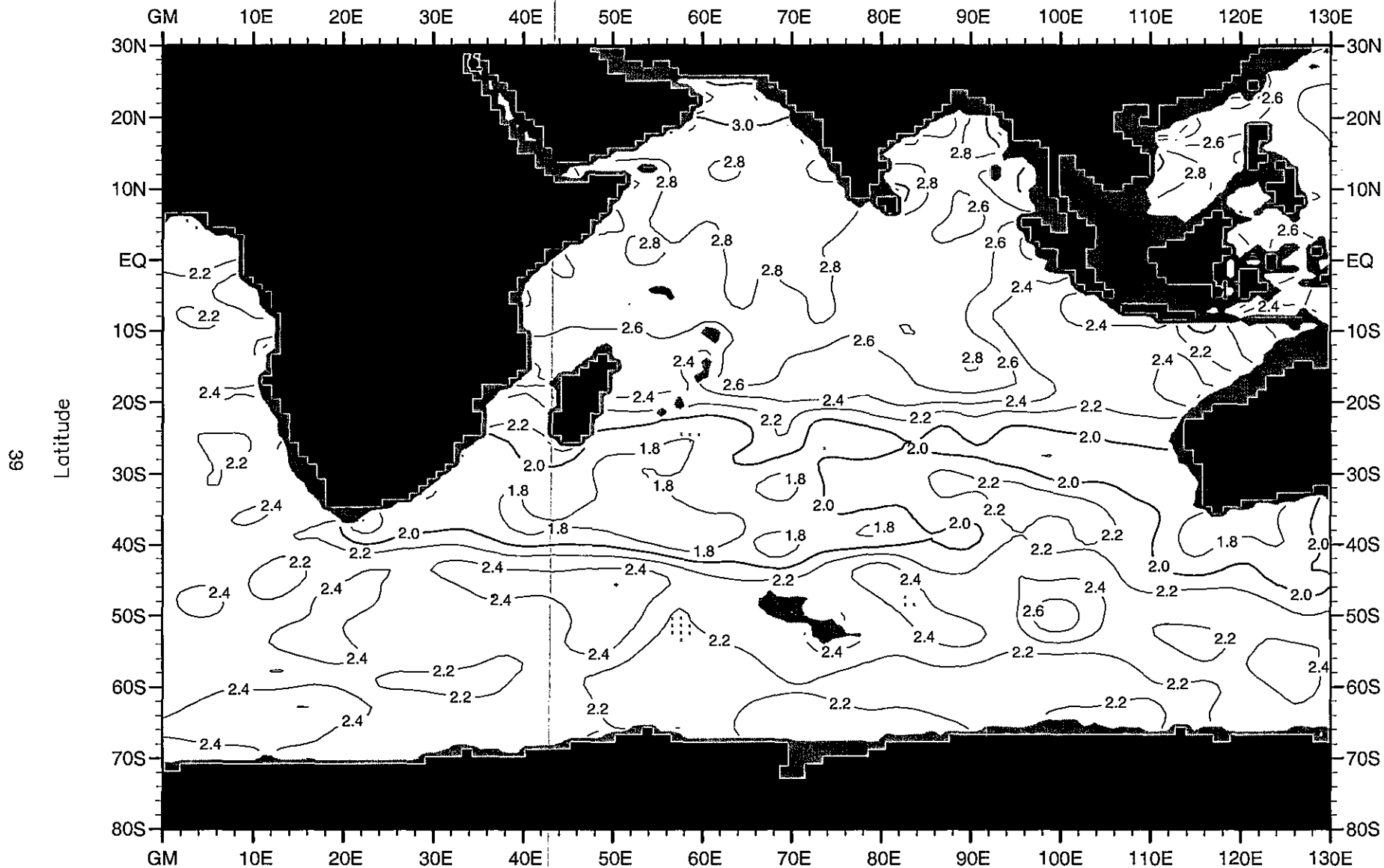
Fig. A27. Annual mean phosphate (μM) at 1000 m. depth.

Minimum Value= 0.57   Maximum Value= 3.59   Contour Interval: 0.20
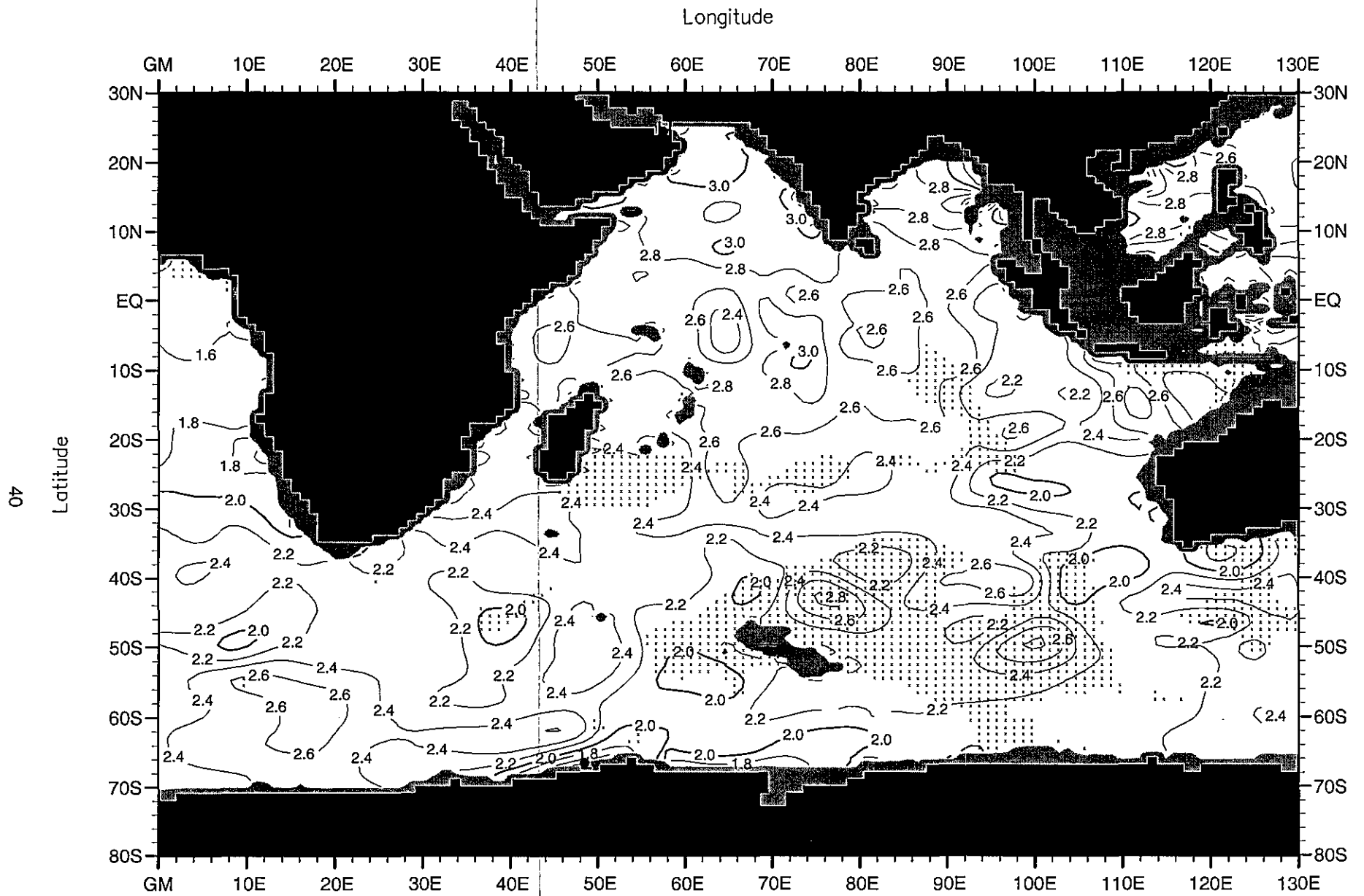
Fig. A28. Annual mean phosphate (μM) at 1500 m. depth .

Minimum Value= 1.30   Maximum Value= 3.93   Contour Interval: 0.20

40
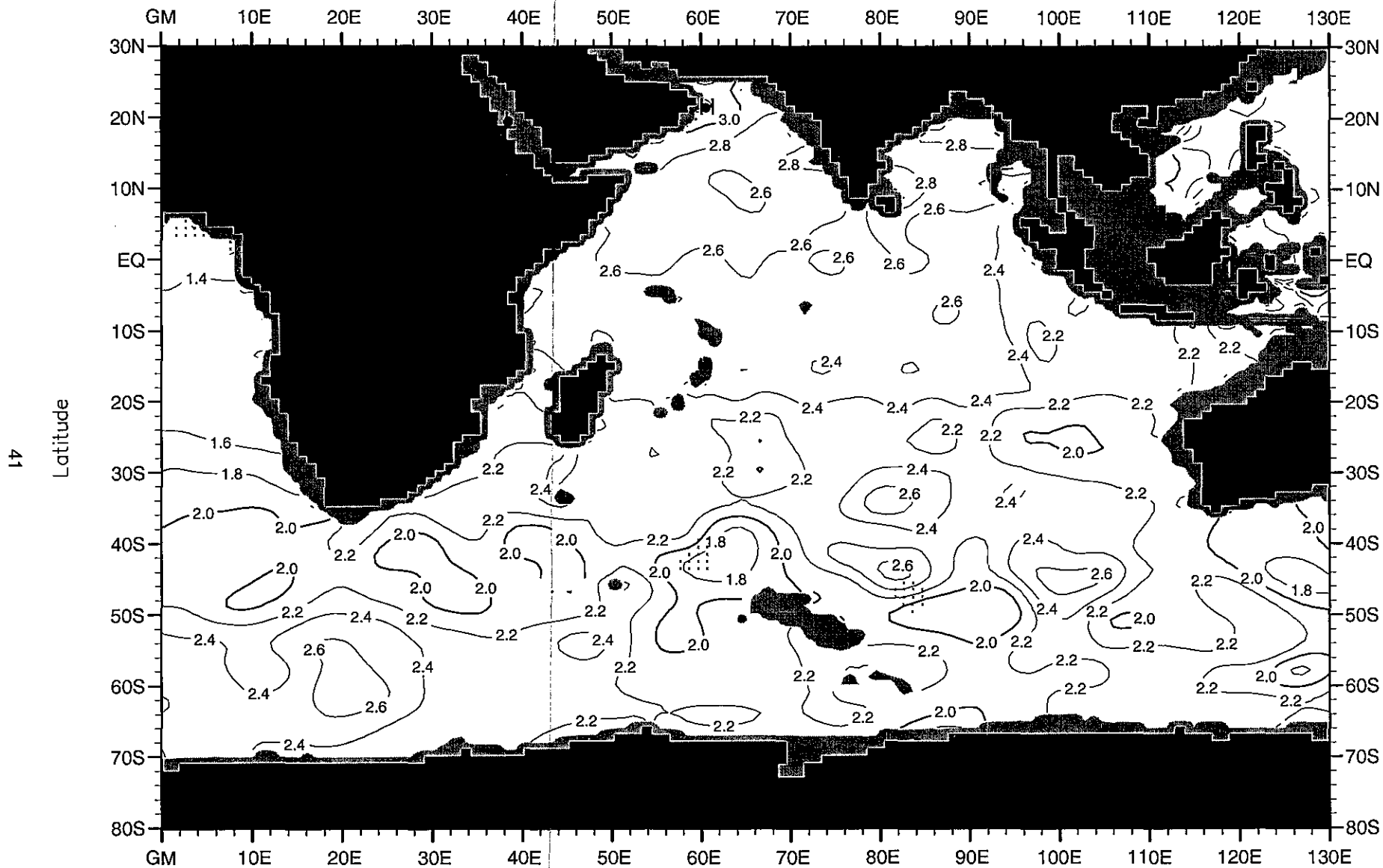
Fig. A29. Annual mean phosphate (μM) at 2000 m. depth .

Minimum Value= 0.67   Maximum Value= 3.27   Contour Interval: 0.20

41
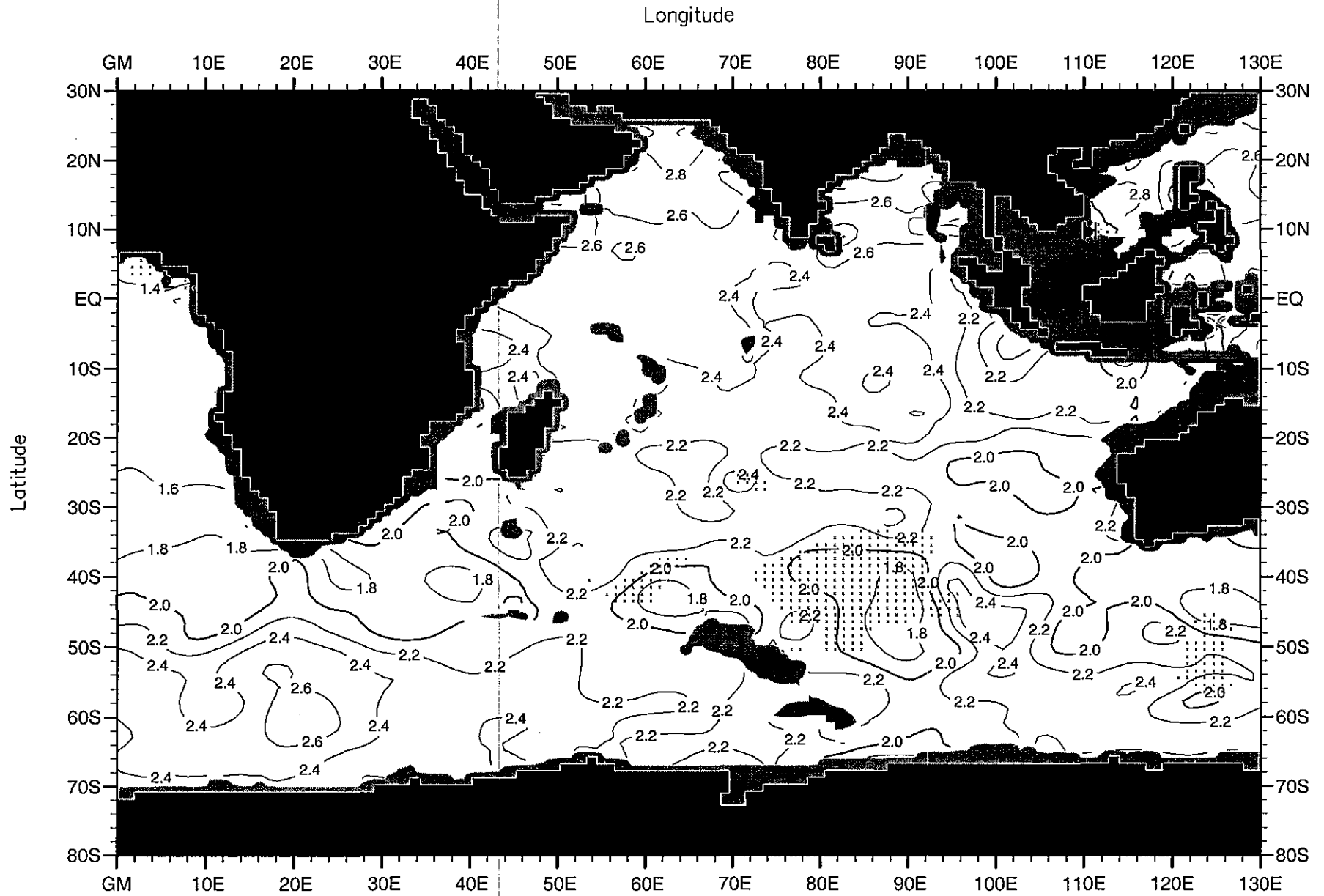
Fig. A30. Annual mean phosphate (μM) at 2500 m. depth .

Minimum Value= 1.31   Maximum Value= 3.27   Contour Interval: 0.20
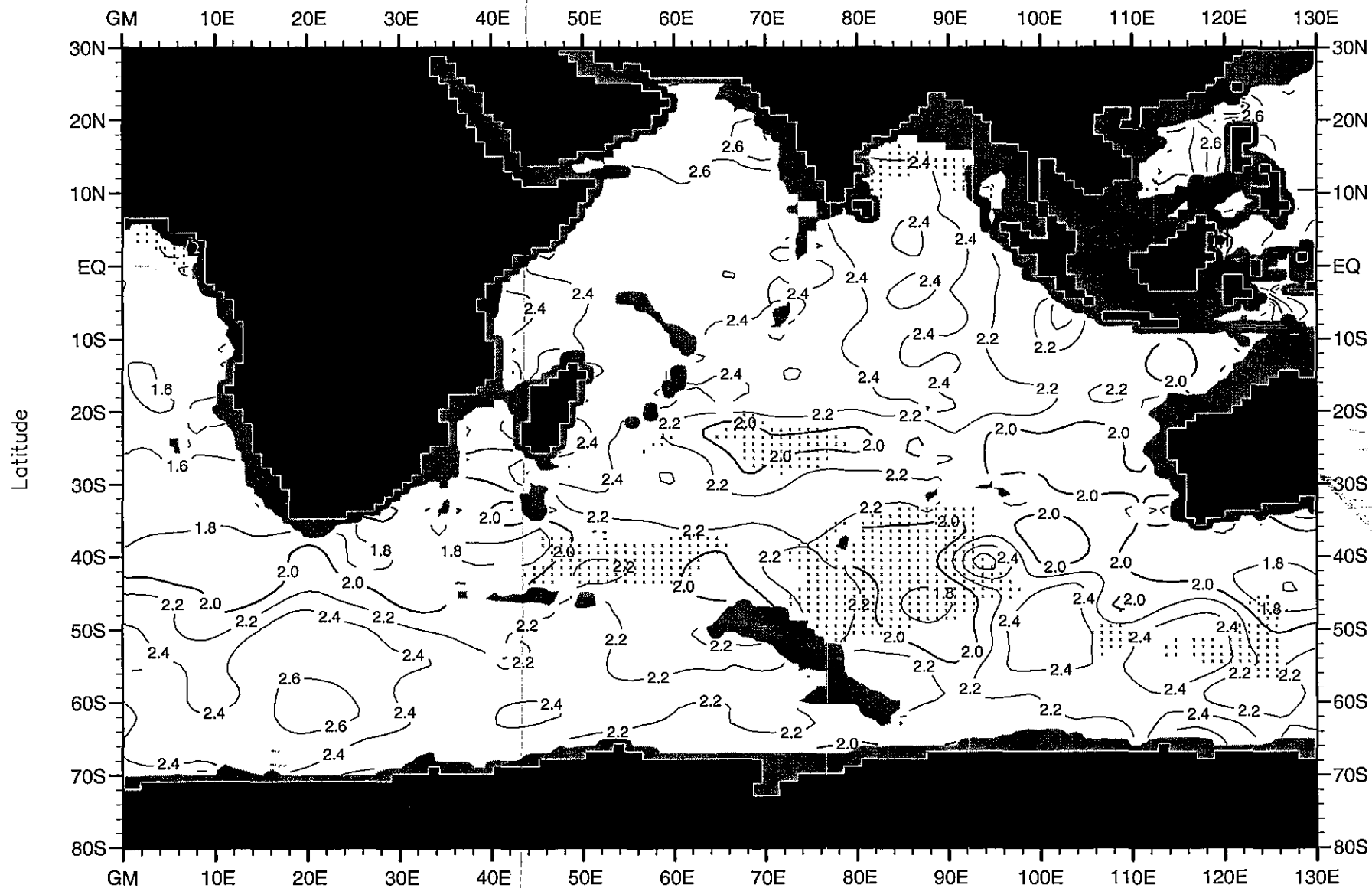
Fig. A31. Annual mean phosphate (μM) at 3000 m. depth .

Minimum Value= 1.32   Maximum Value= 3.23   Contour Interval: 0.20
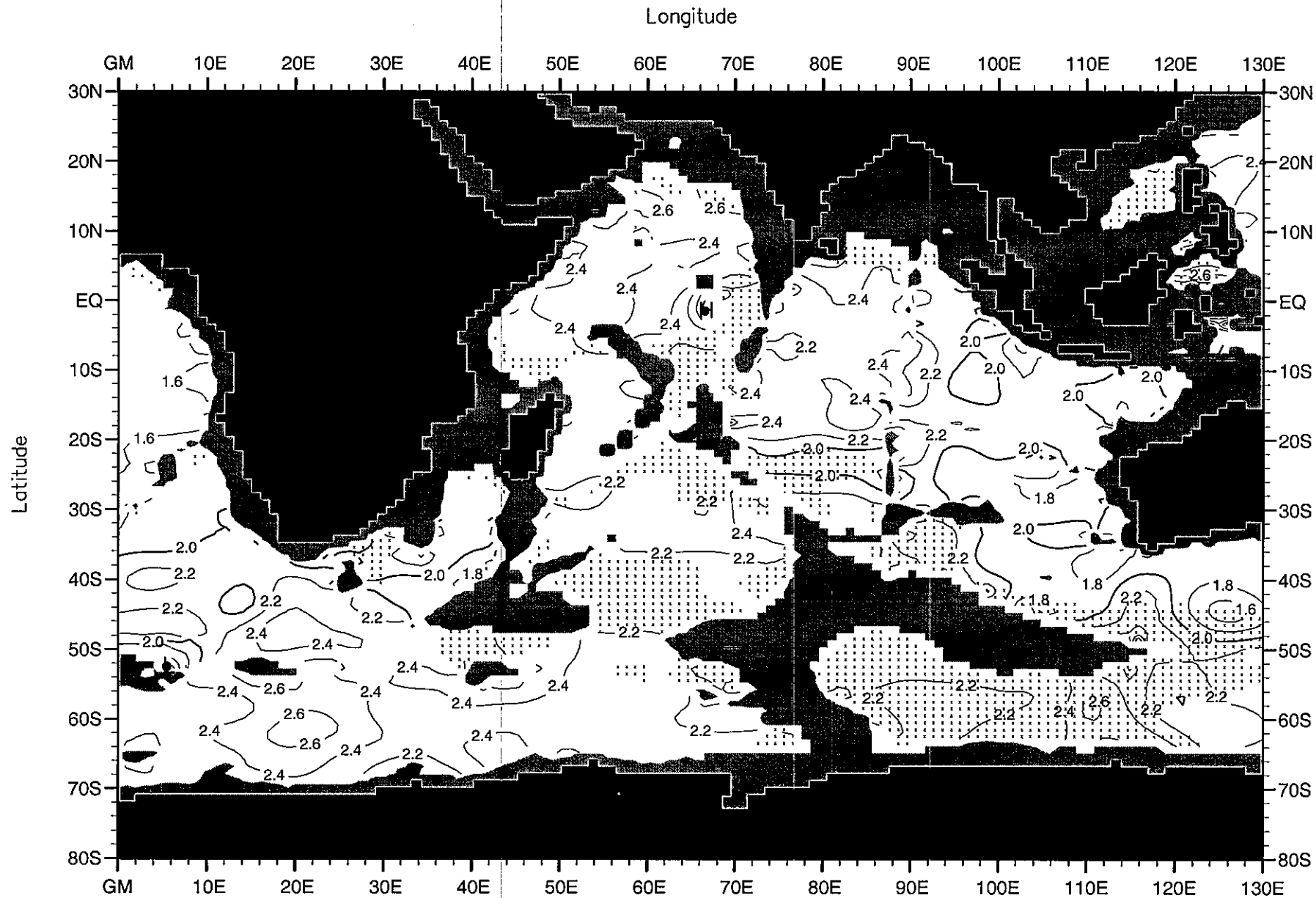
Fig. A32. Annual mean phosphate (μM) at 4000 m. depth .

Minimum Value= 1.29   Maximum Value= 3.11   Contour Interval: 0.20
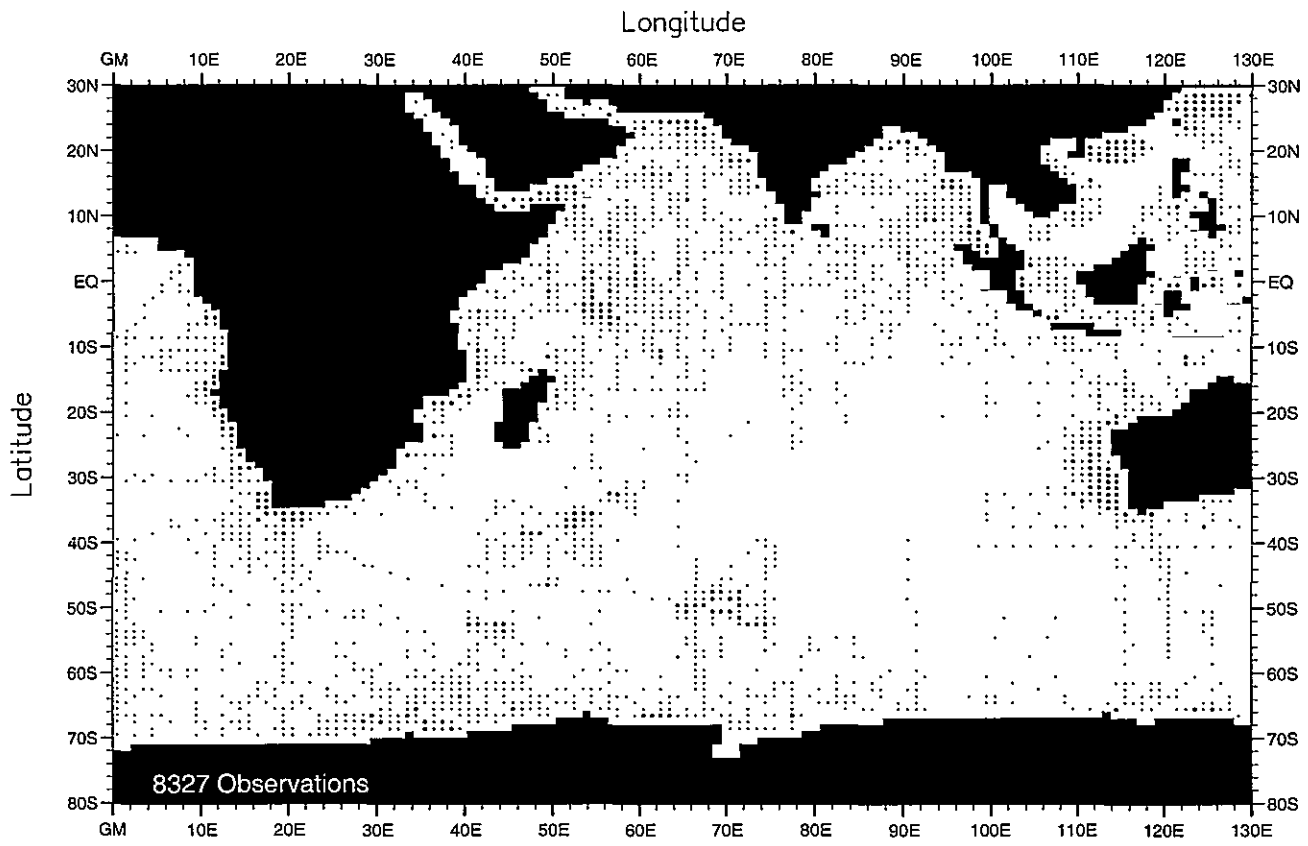
Fig. B1. Winter (Jan.-Mar.) phosphate observations at the surface .
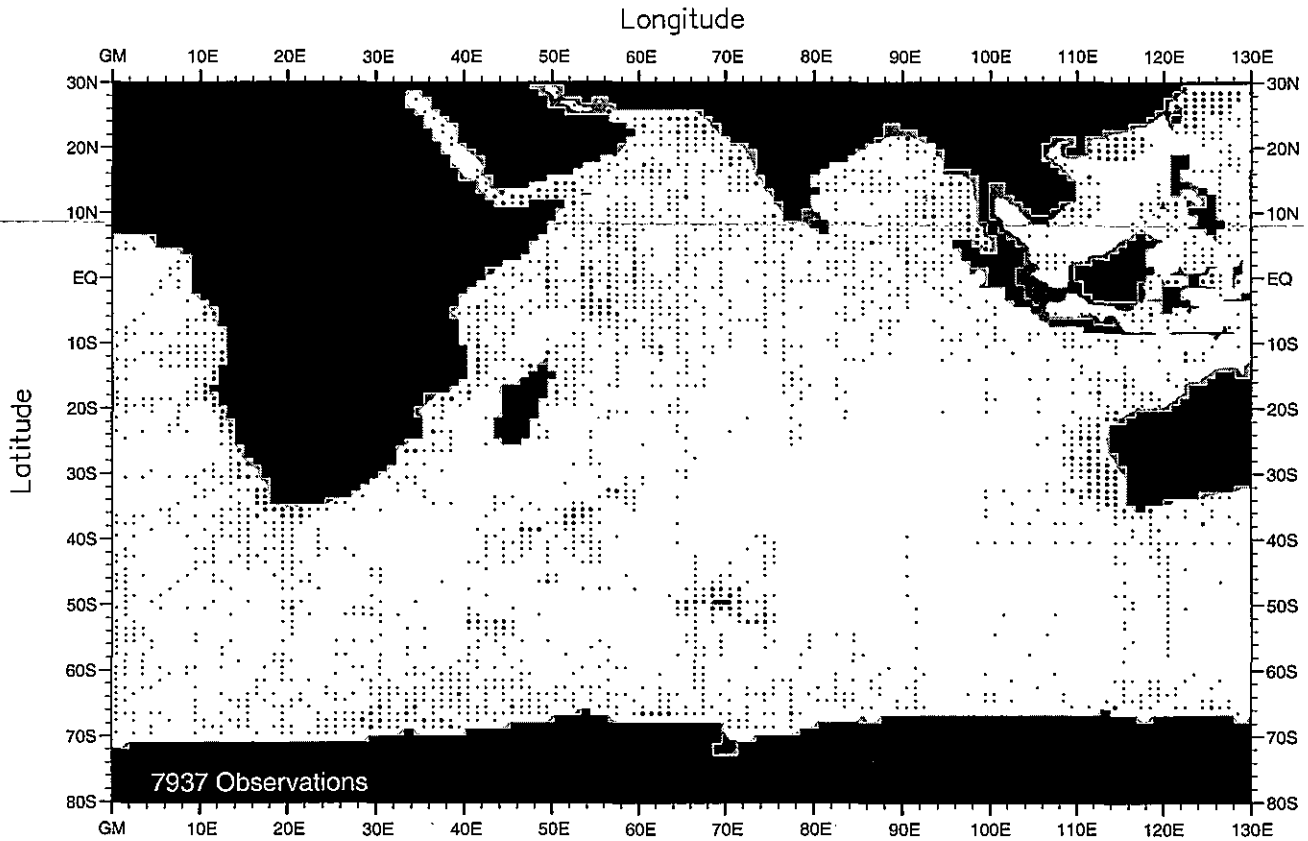
Fig. B2. Winter (Jan.-Mar.) phosphate observations at 50 m. depth .

45
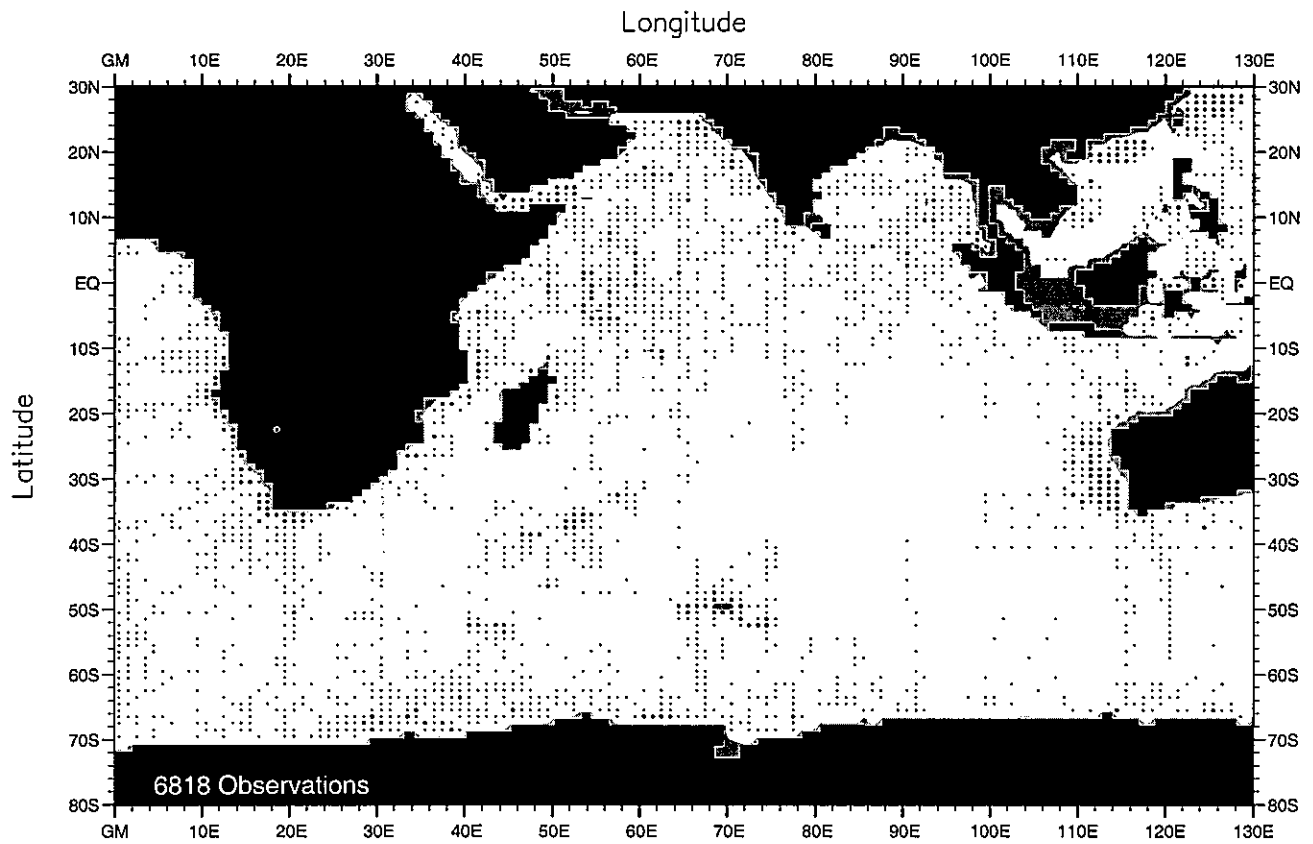
Fig. B3. Winter (Jan.-Mar.) phosphate observations at 75 m. depth .
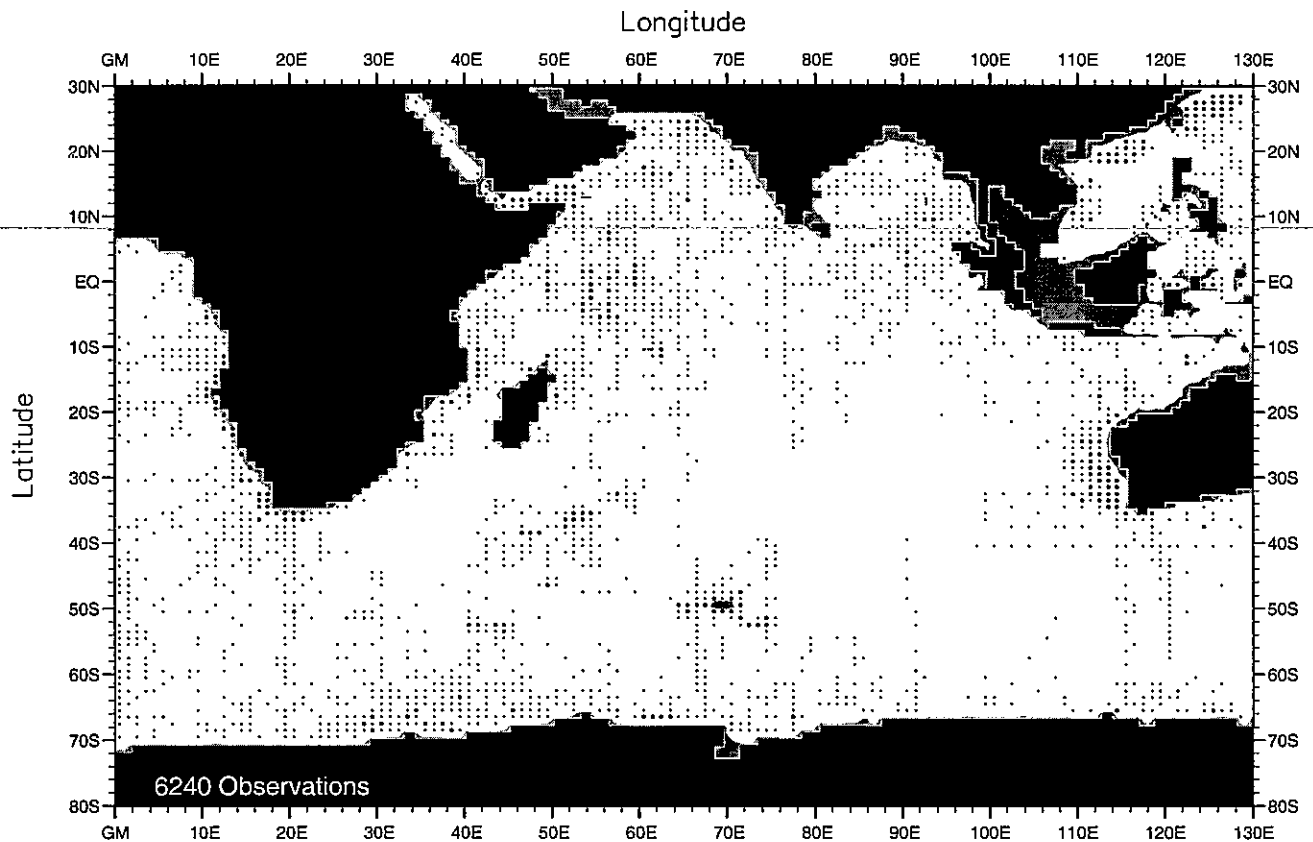
Fig. B4. Winter (Jan.-Mar.) phosphate observations at 100 m. depth .
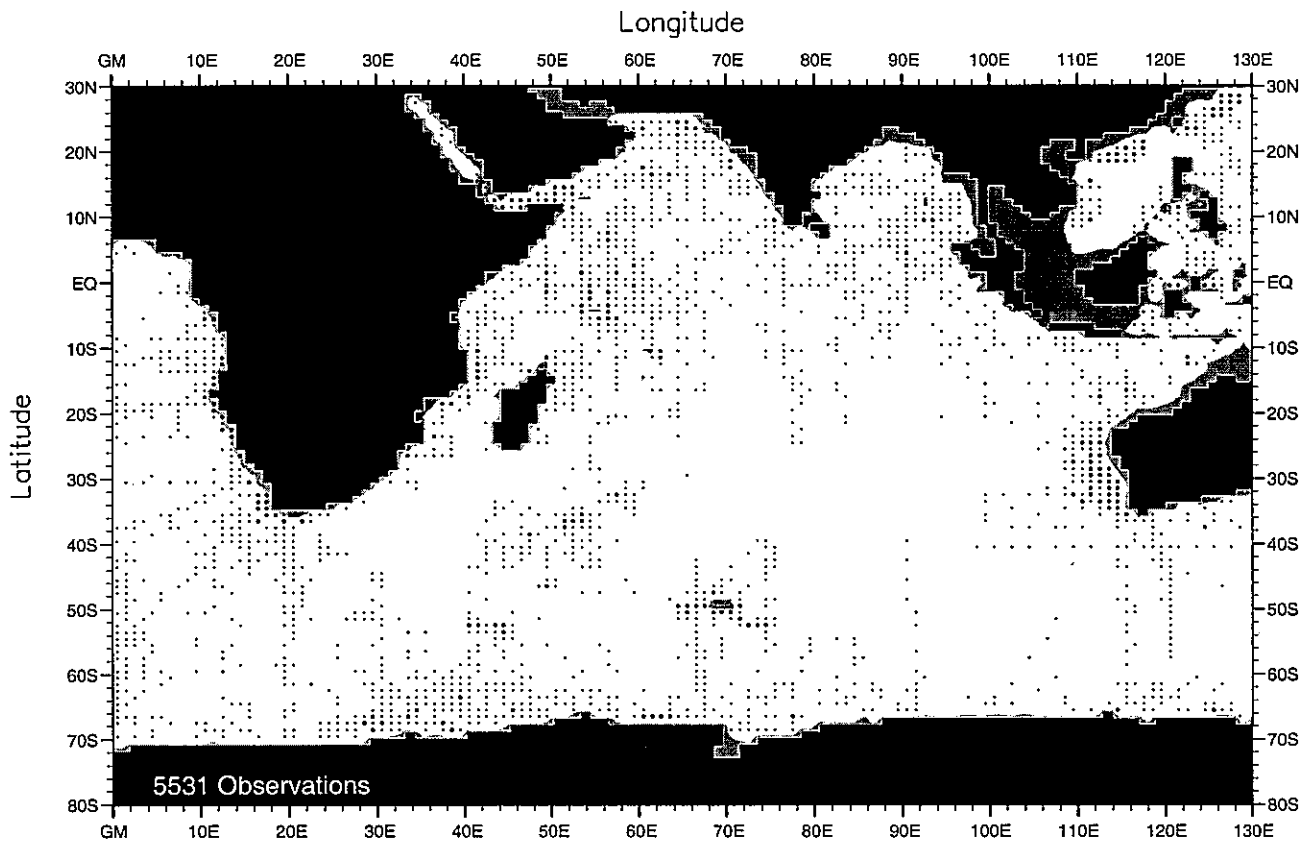
Fig. B5. Winter (Jan.-Mar.) phosphate observations at 150 m. depth .
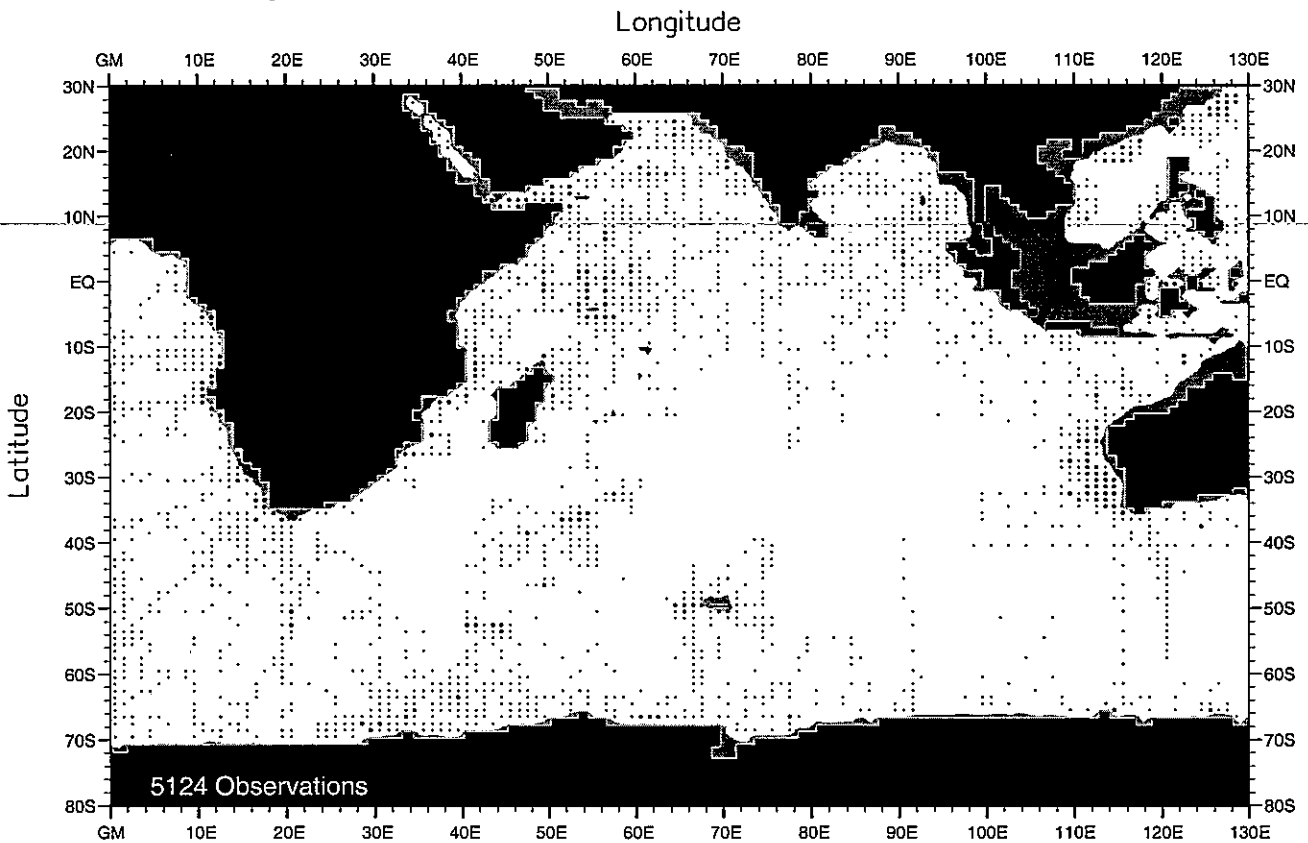
Fig. B6. Winter (Jan.-Mar.) phosphate observations at 250 m. depth .
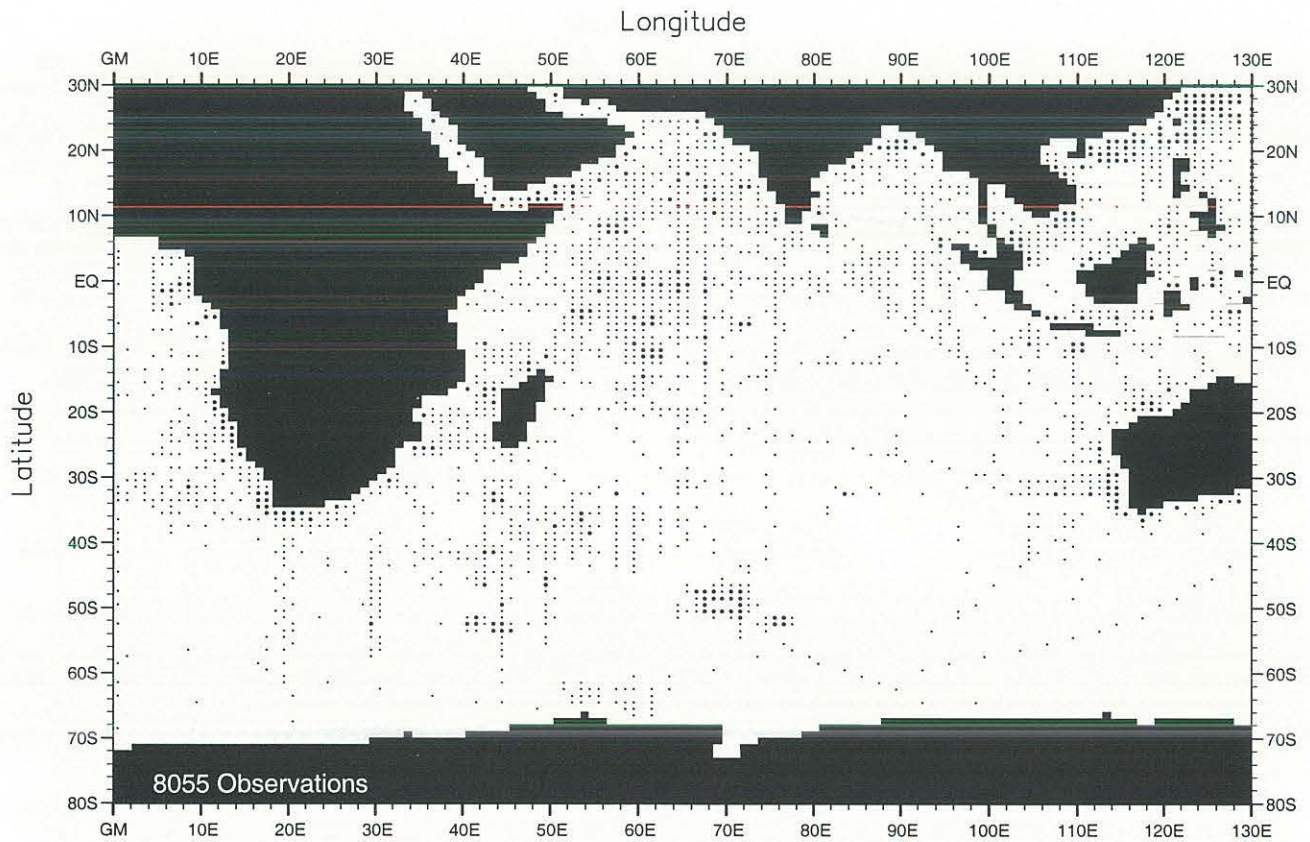
Fig. B7.   Spring (Apr.-Jun.) phosphate observations at the surface .
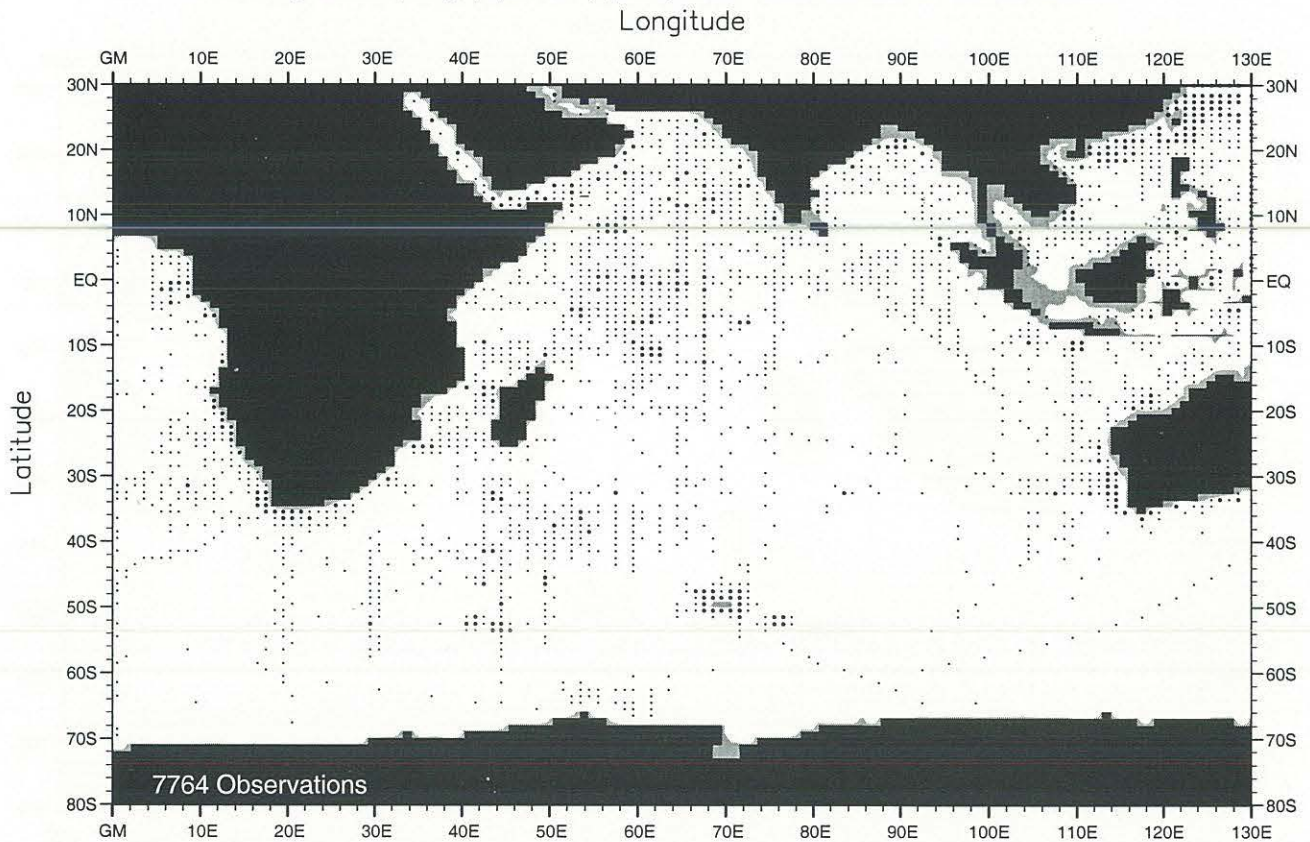
Fig. B8.   Spring (Apr.-Jun.) phosphate observations at   50 m. depth .
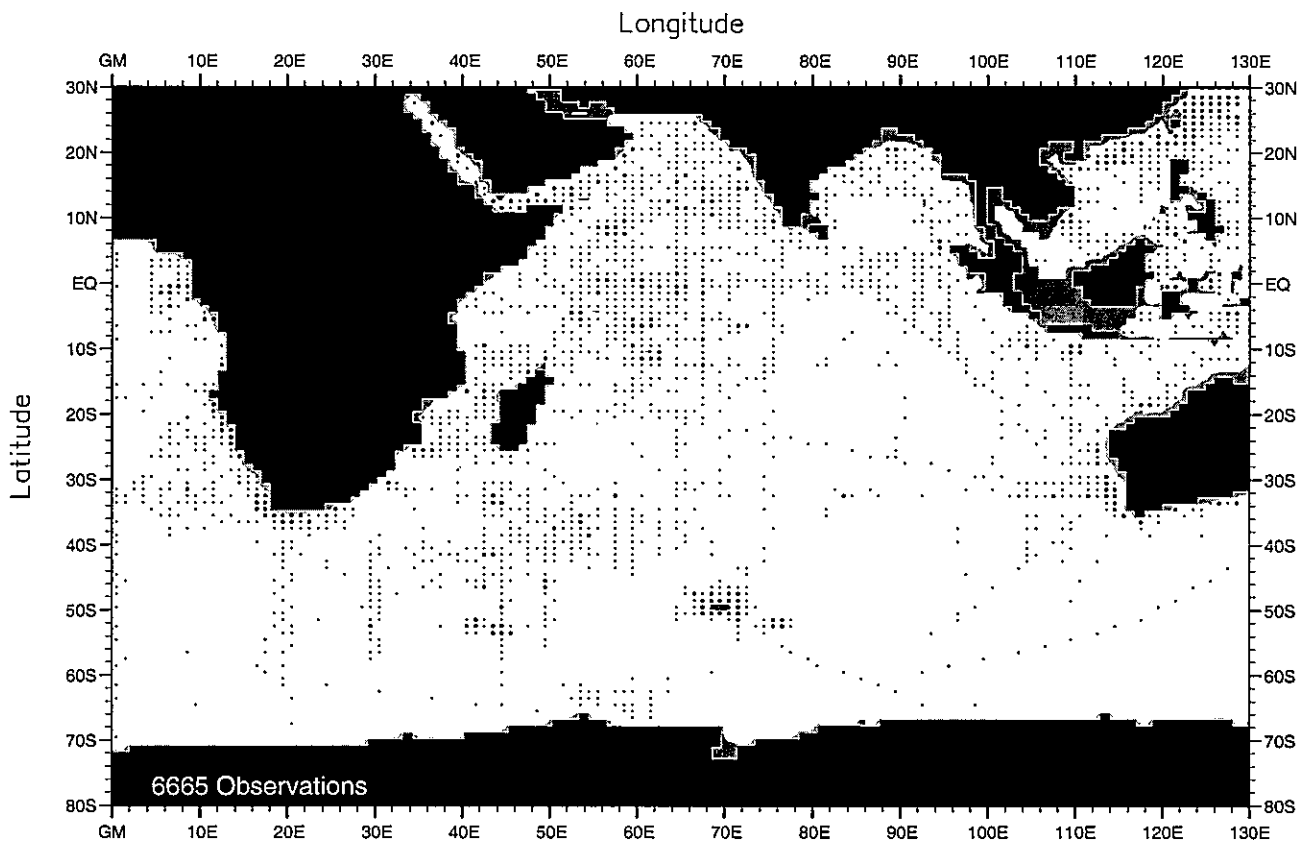
Fig. B9. Spring (Apr.-Jun.) phosphate observations at 75 m. depth .
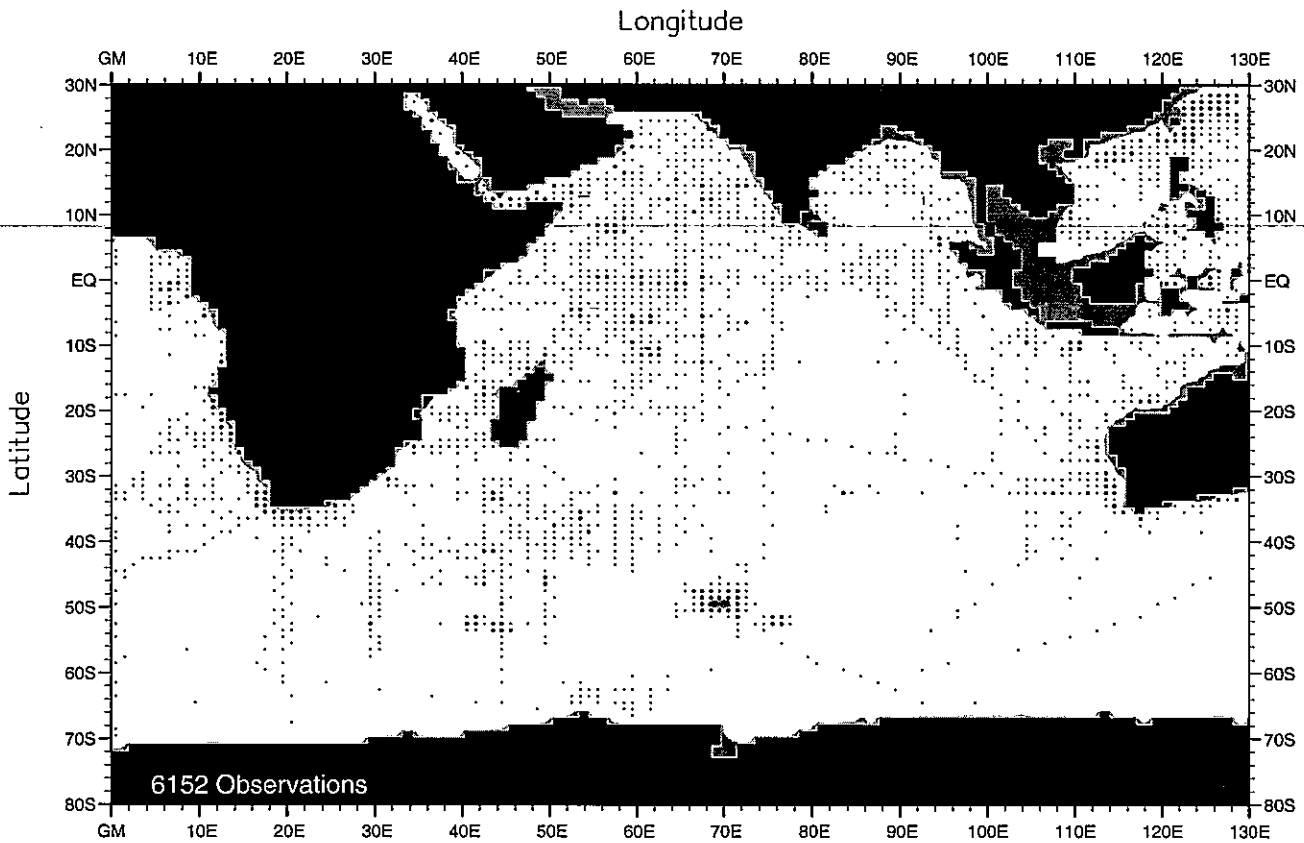
Fig. B10. Spring (Apr.-Jun.) phosphate observations at 100 m. depth .

Longitude
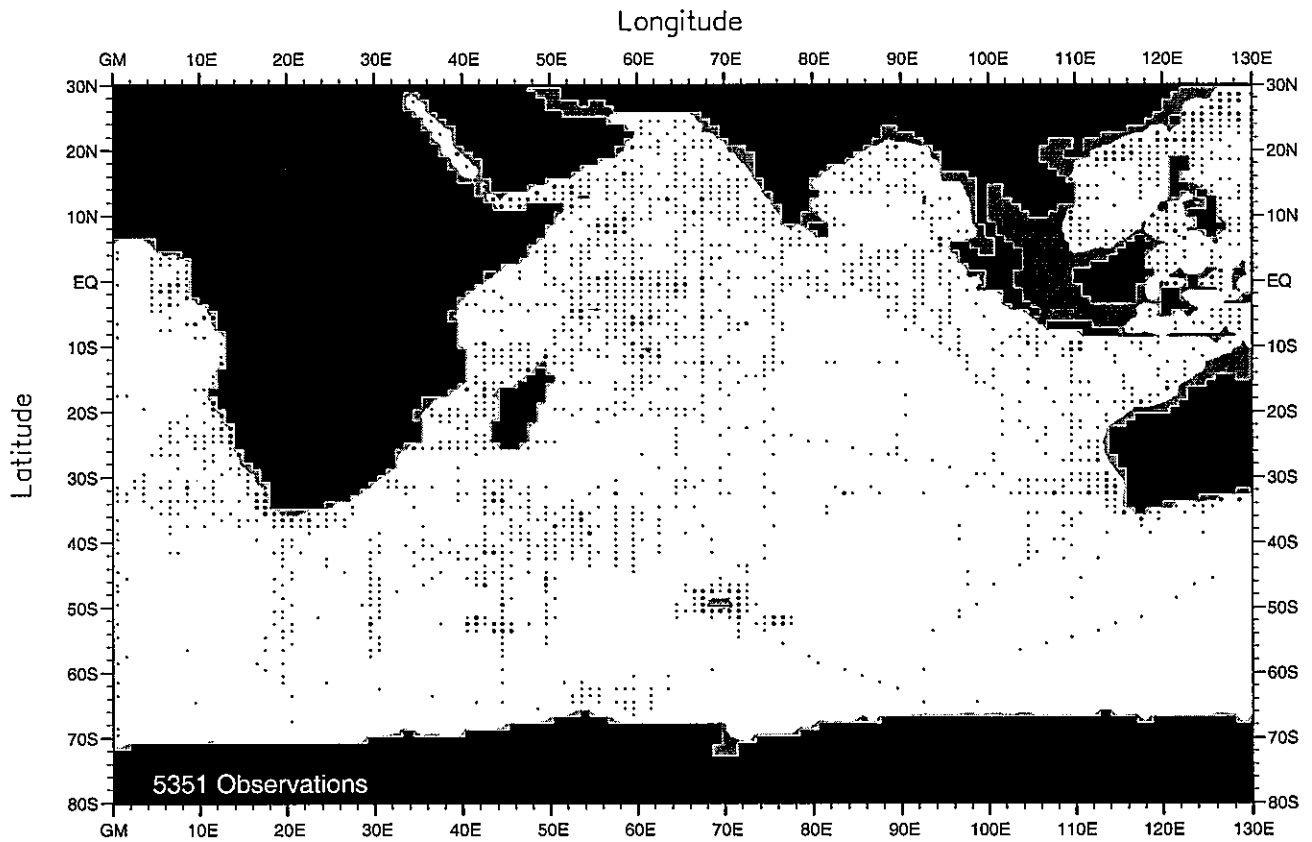
Fig. B11. Spring (Apr.-Jun.) phosphate observations at 150 m. depth .

Longitude
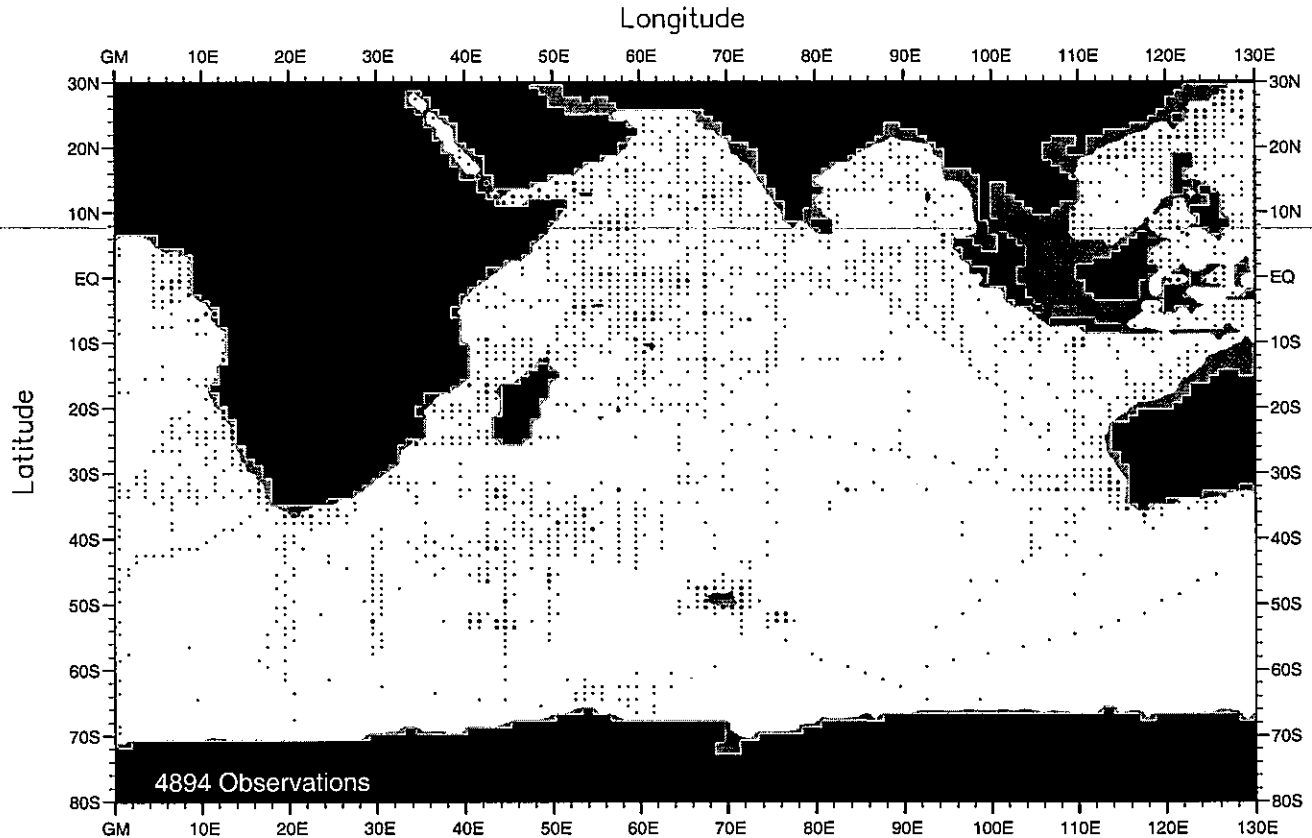
Fig. B12. Spring (Apr.-Jun.) phosphate observations at 250 m. depth .
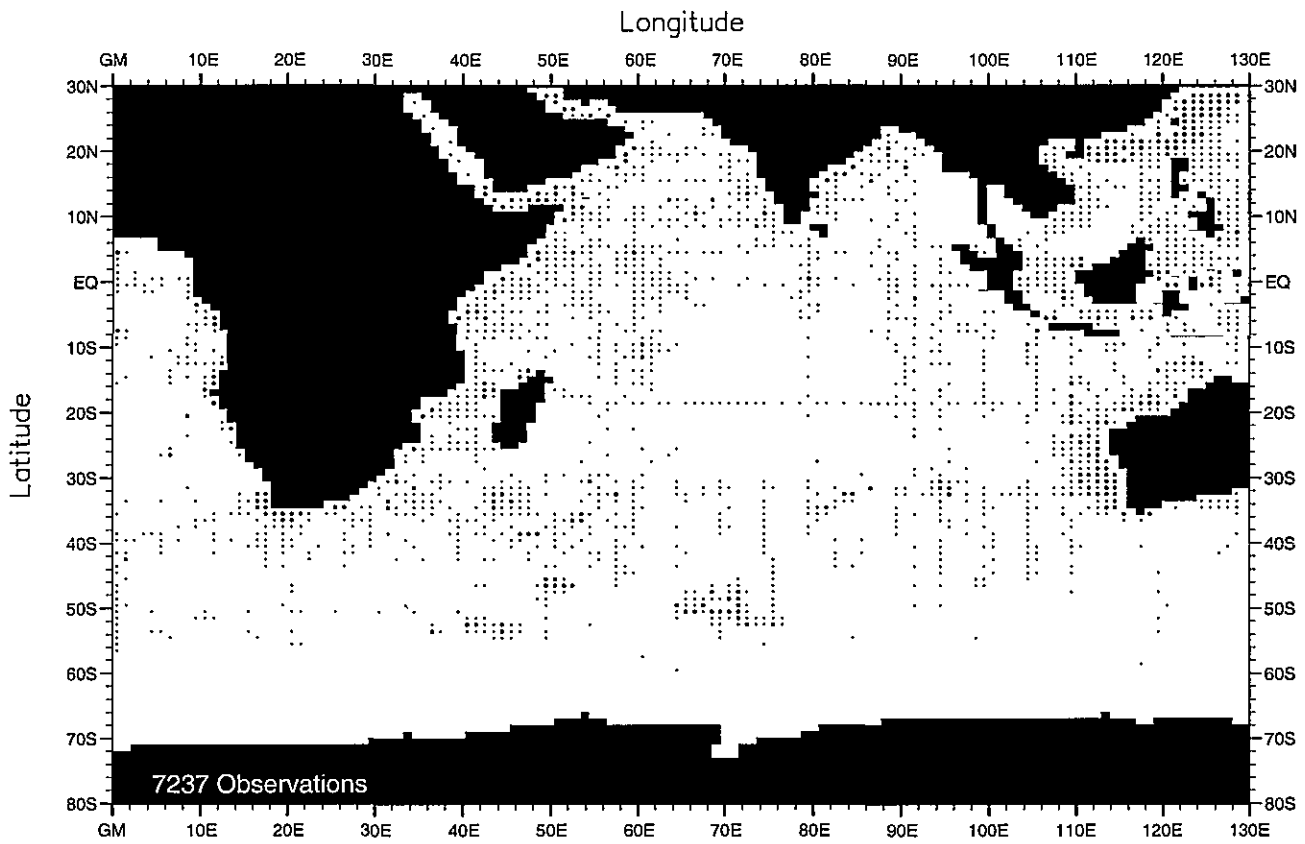
Fig. B13. Summer (Jul.-Sep.) phosphate observations at the surface .
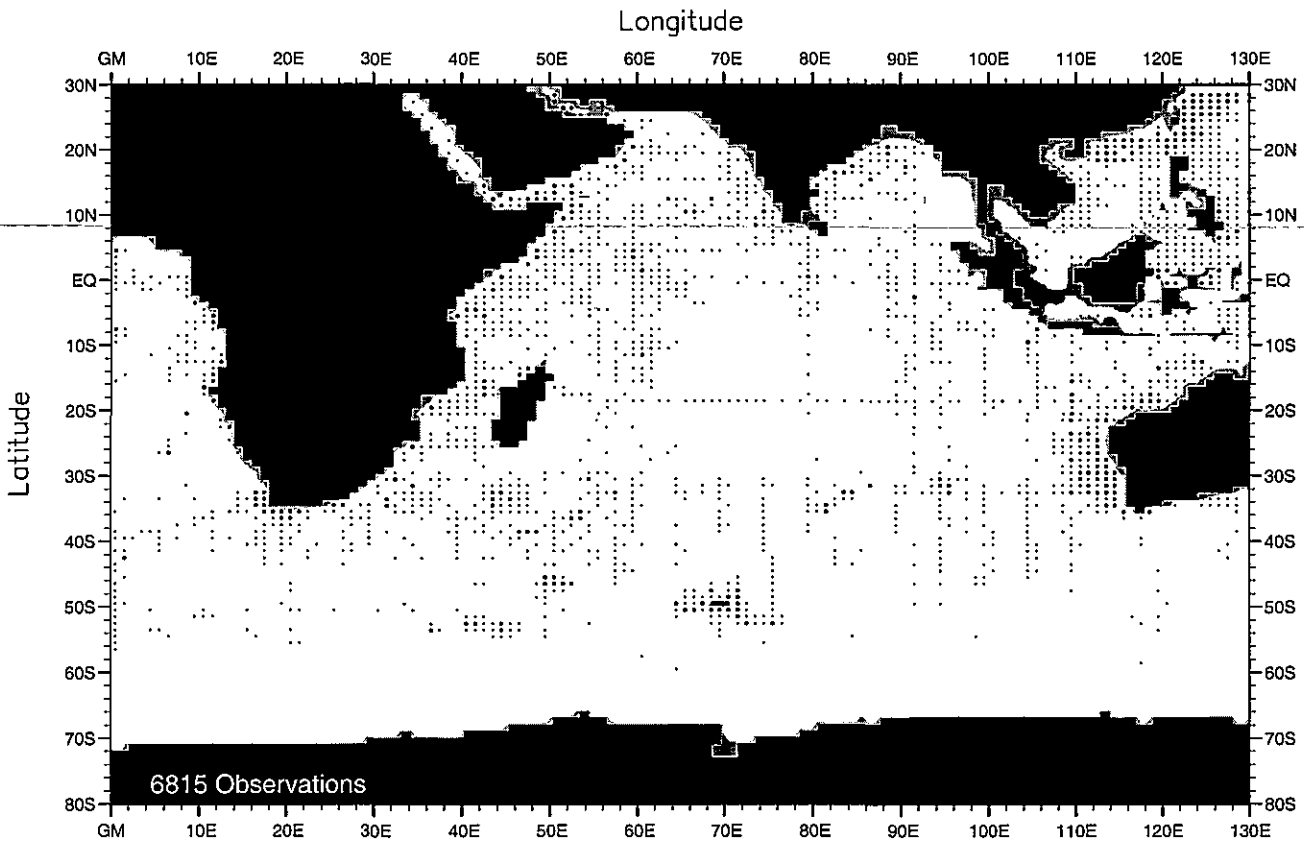
Fig. B14. Summer (Jul.-Sep.) phosphate observations at 50 m. depth .

51

Longitude
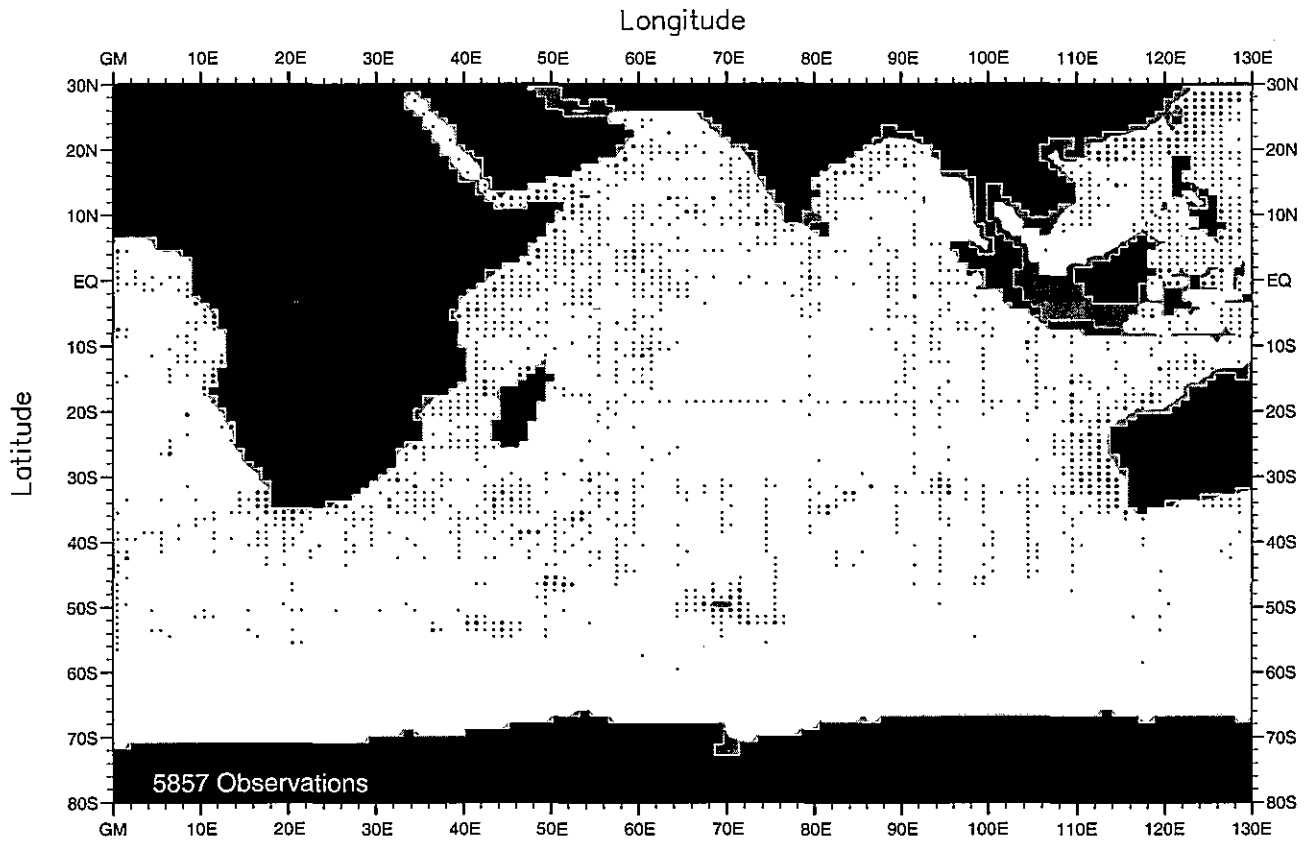
Fig. B15. Summer (Jul.-Sep.) phosphate observations at 75 m. depth .

Longitude
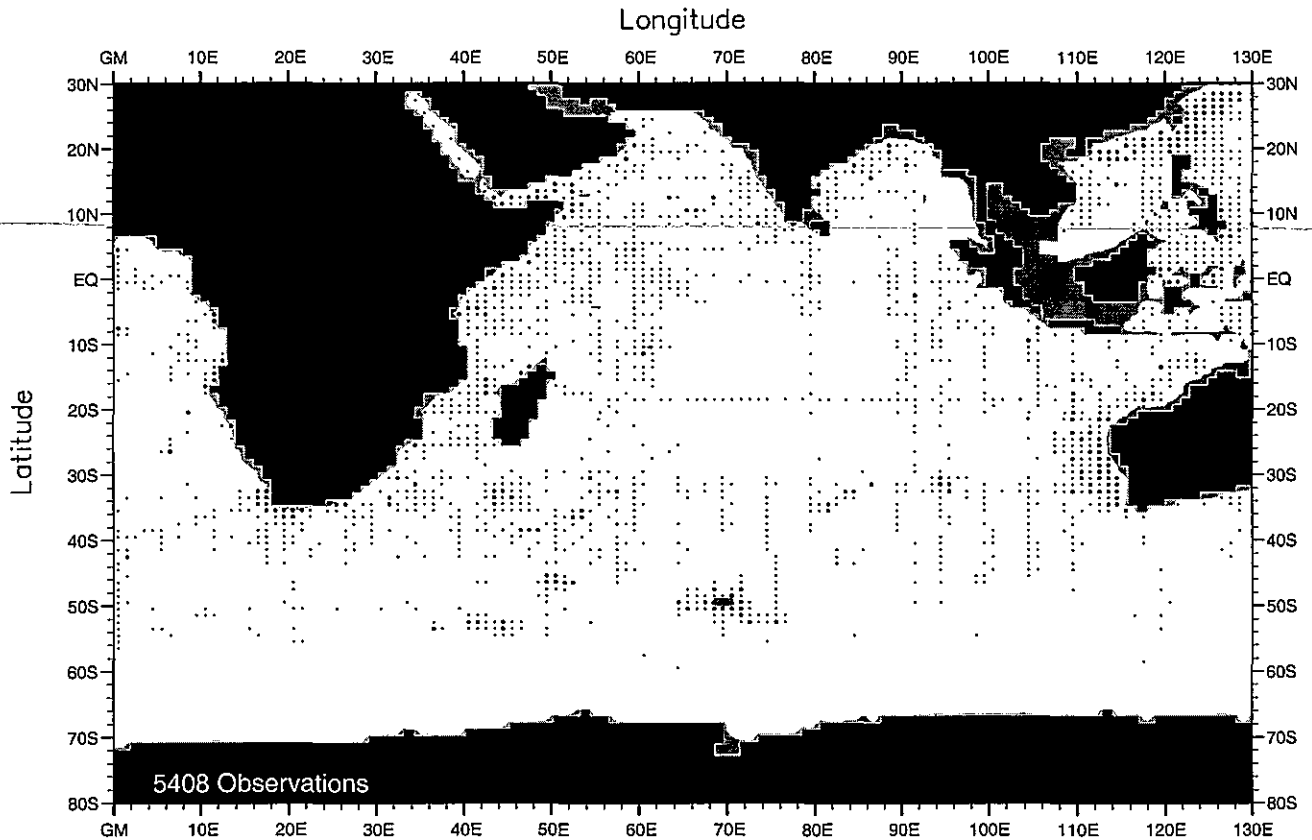
Fig. B16. Summer (Jul.-Sep.) phosphate observations at 100 m. depth .
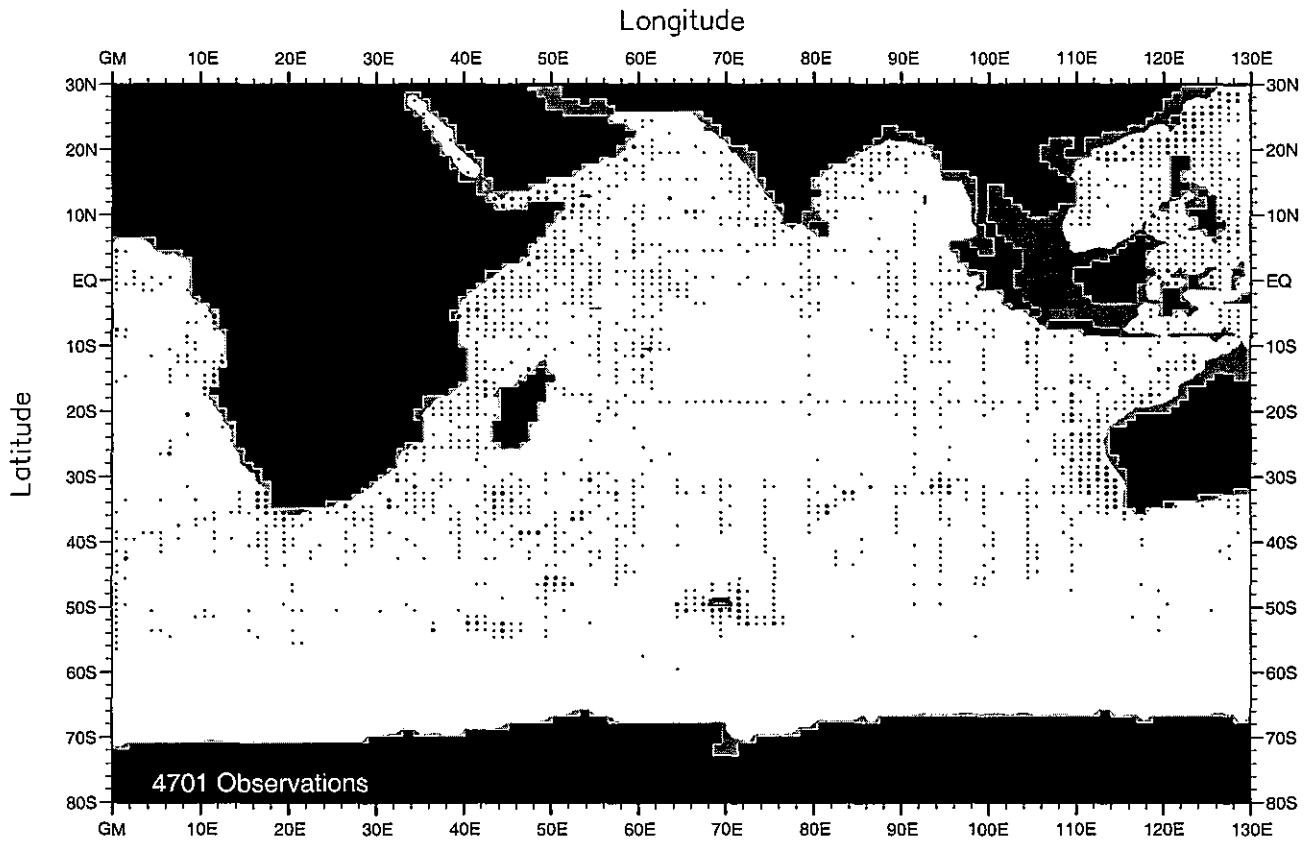
Fig. B17. Summer (Jul.-Sep.) phosphate observations at 150 m. depth .
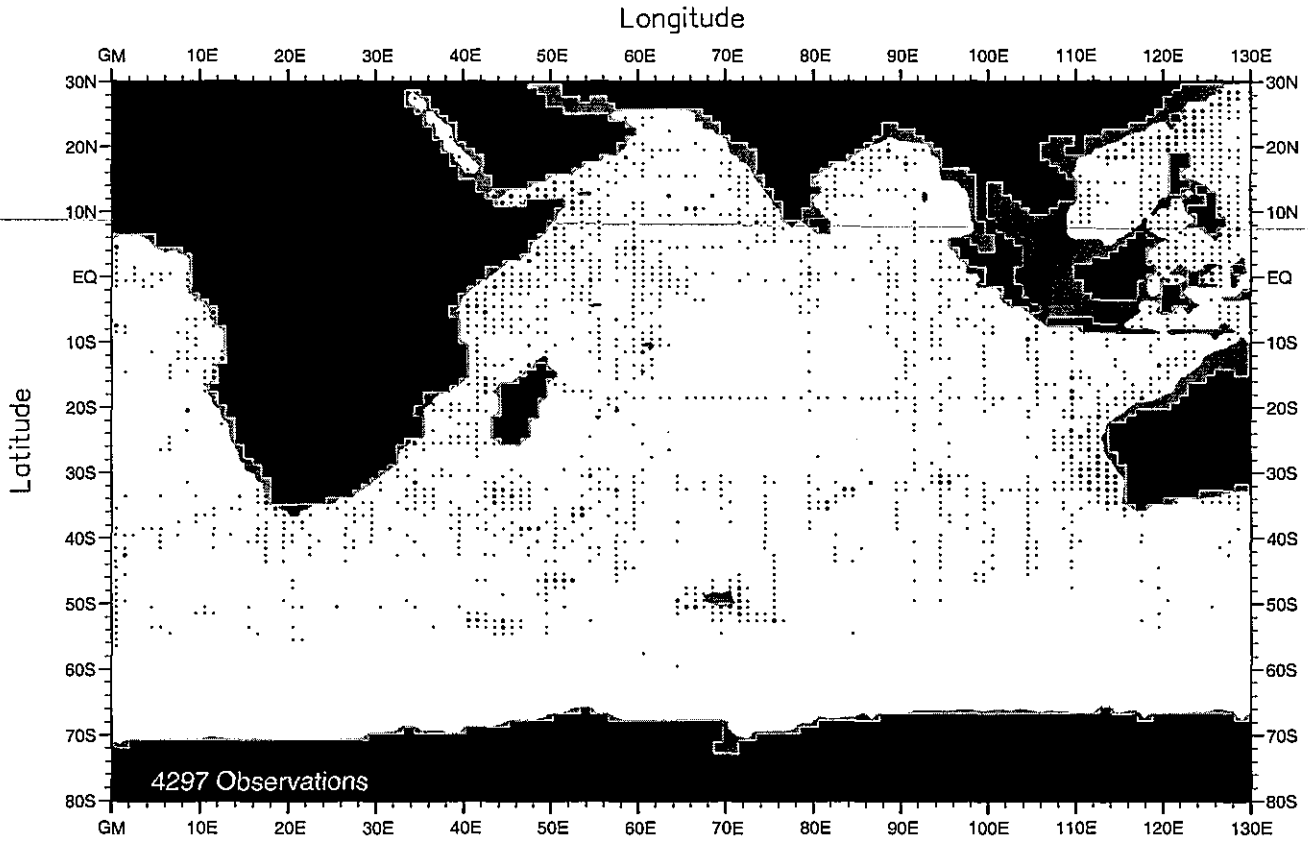
Fig. B18. Summer (Jul.-Sep.) phosphate observations at 250 m. depth .
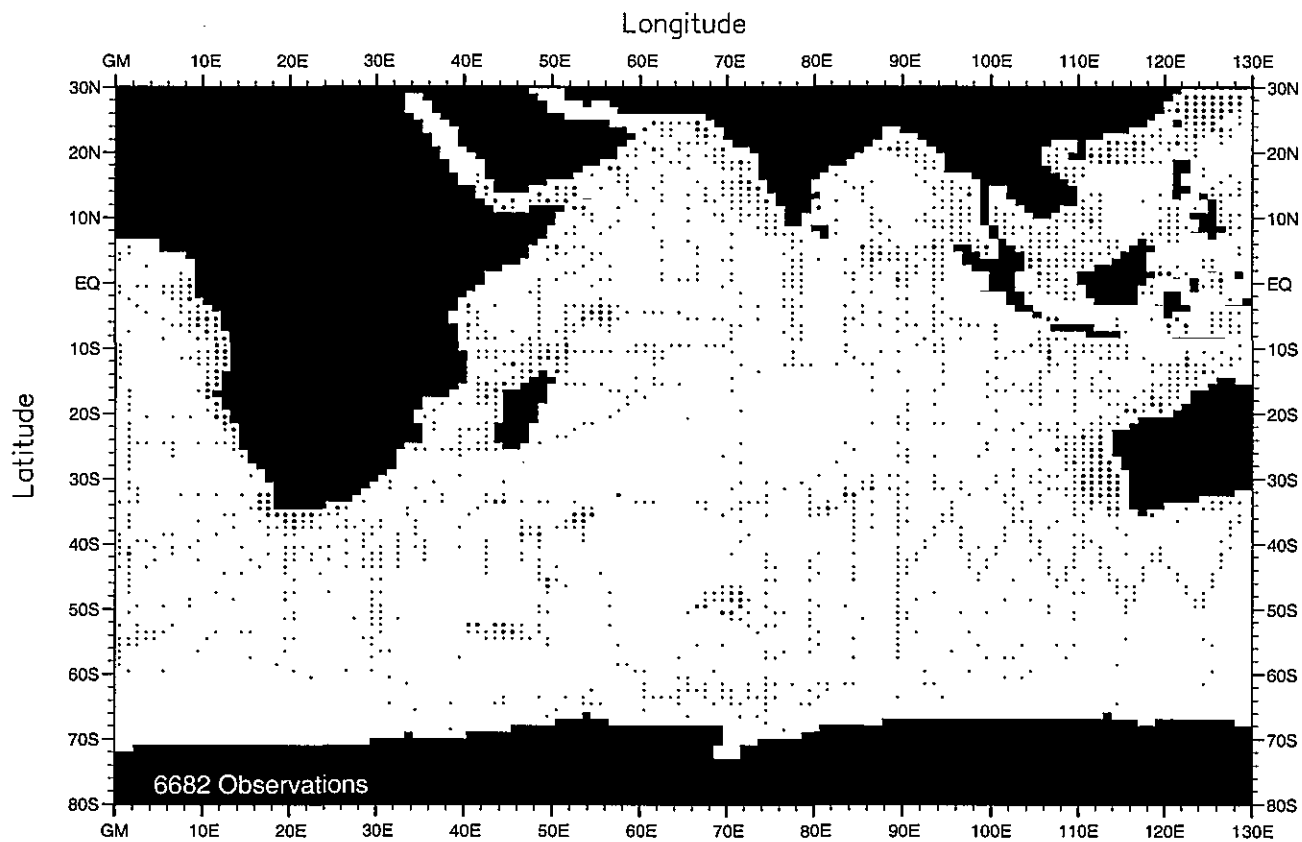
Fig. B19. Fall (Oct.-Dec.) phosphate observations at the surface .
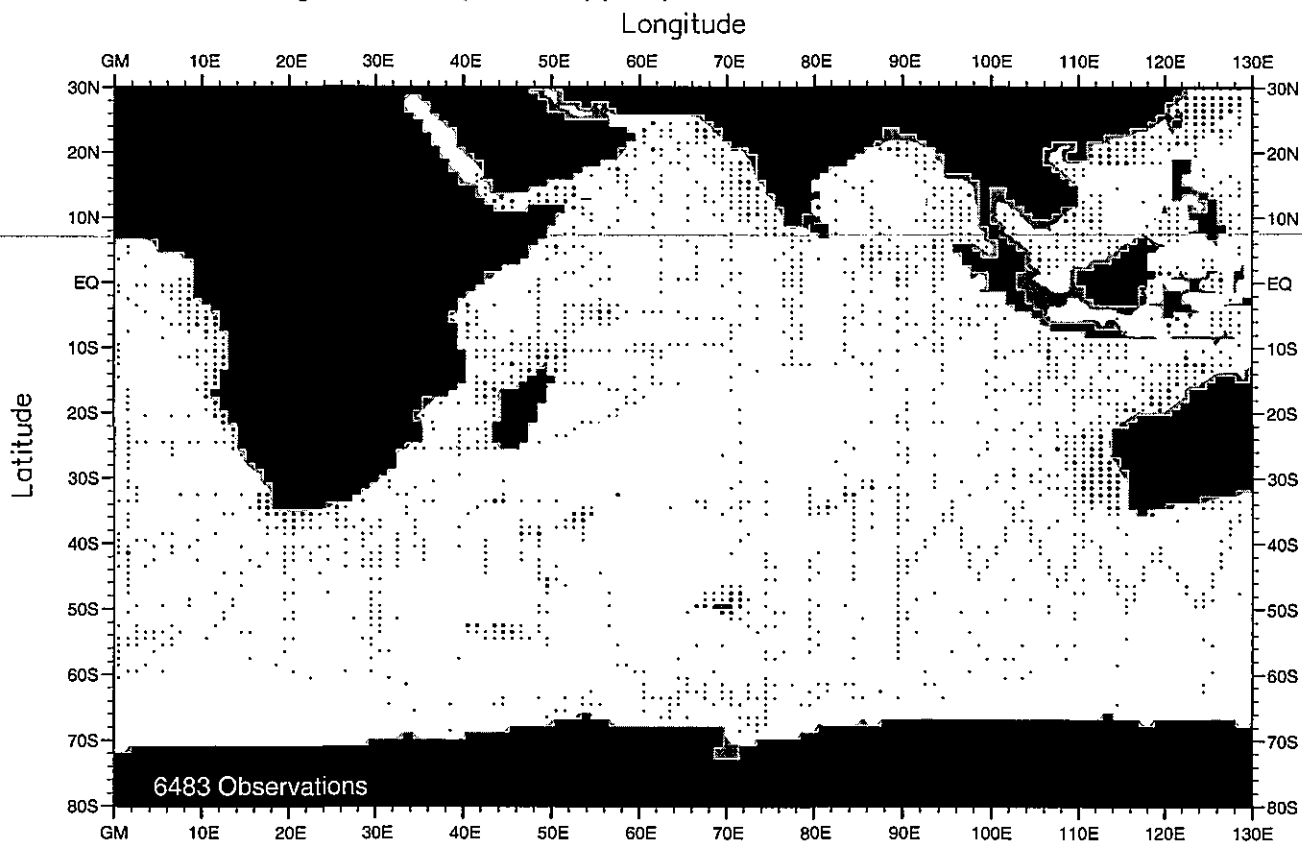
Fig. B20. Fall (Oct.-Dec.) phosphate observations at   50 m. depth .

54
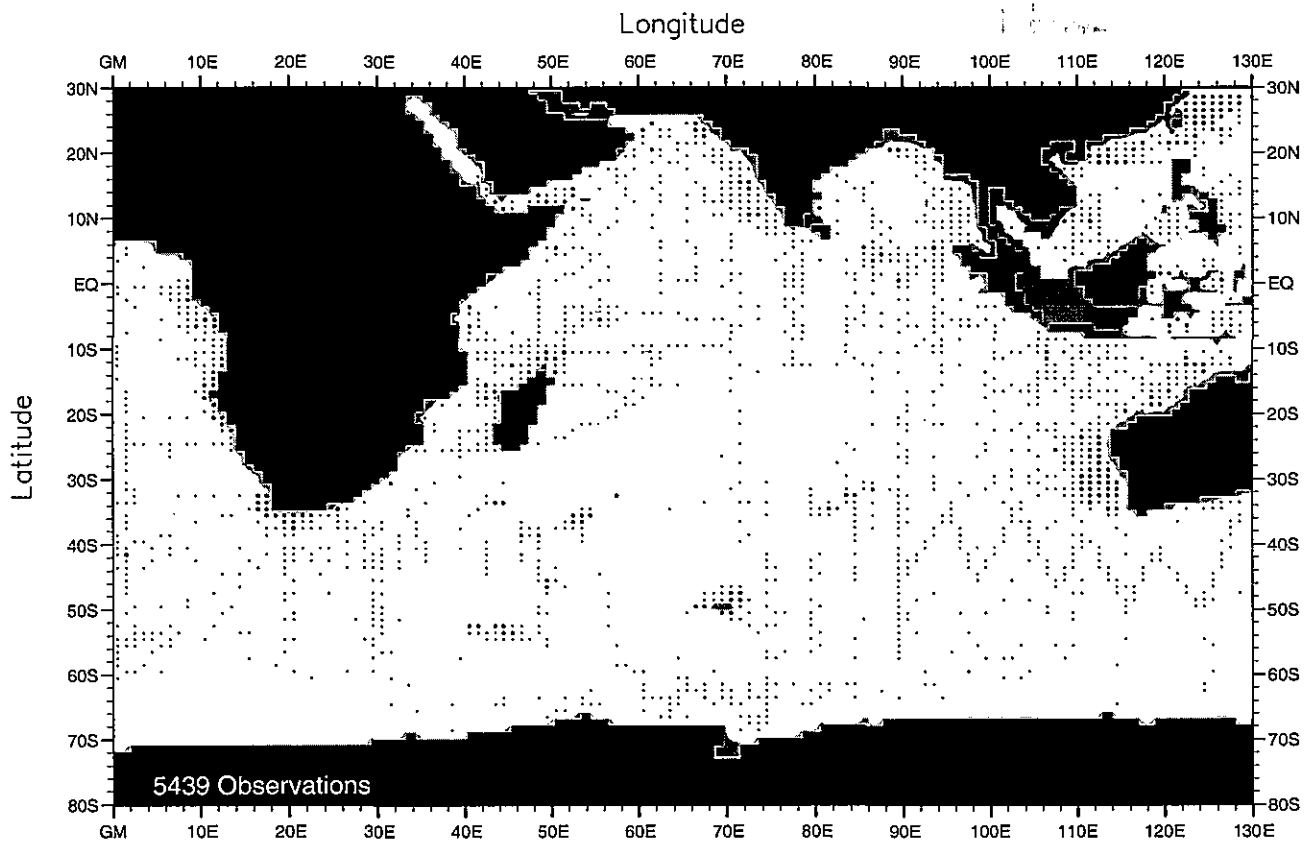
Fig. B21. Fall (Oct.-Dec.) phosphate observations at 75 m. depth .
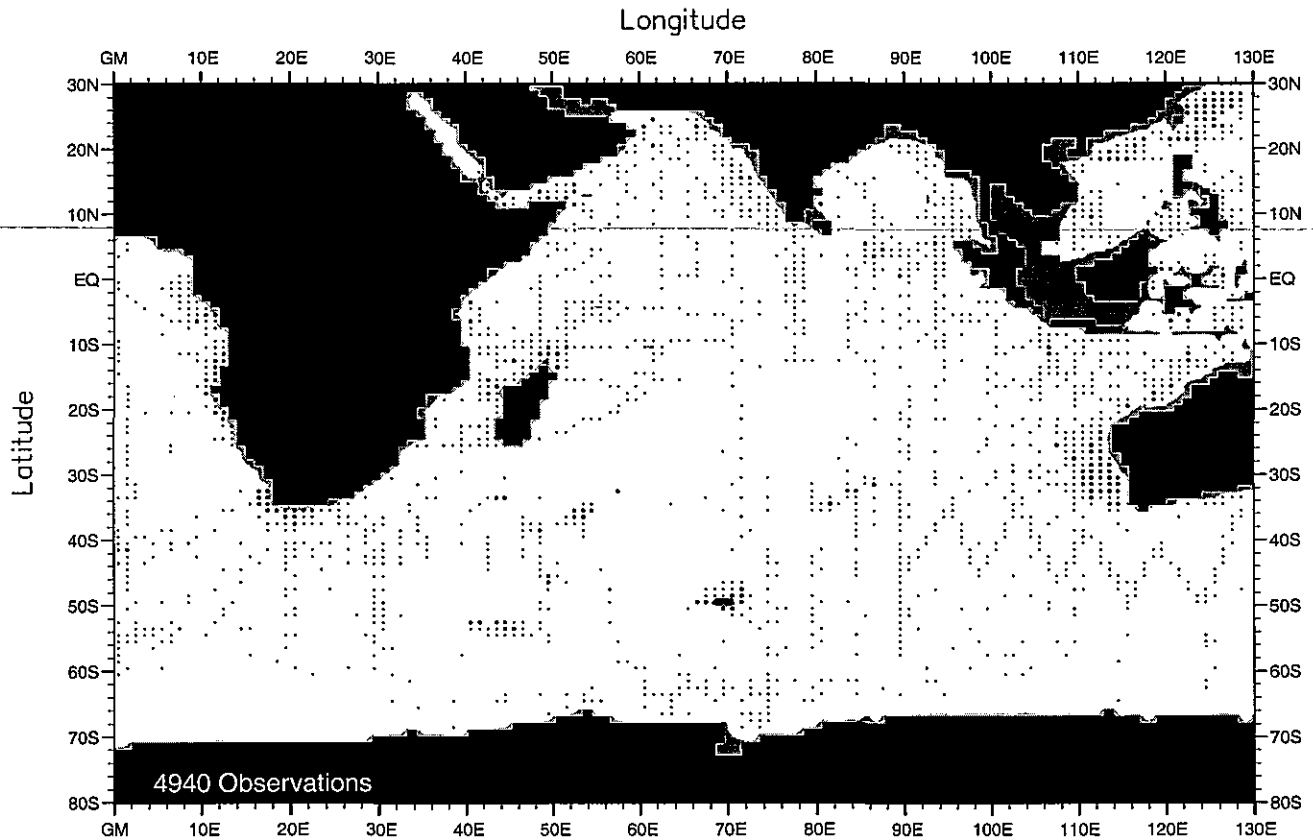
Fig. B22. Fall (Oct.-Dec.) phosphate observations at 100 m. depth .

55
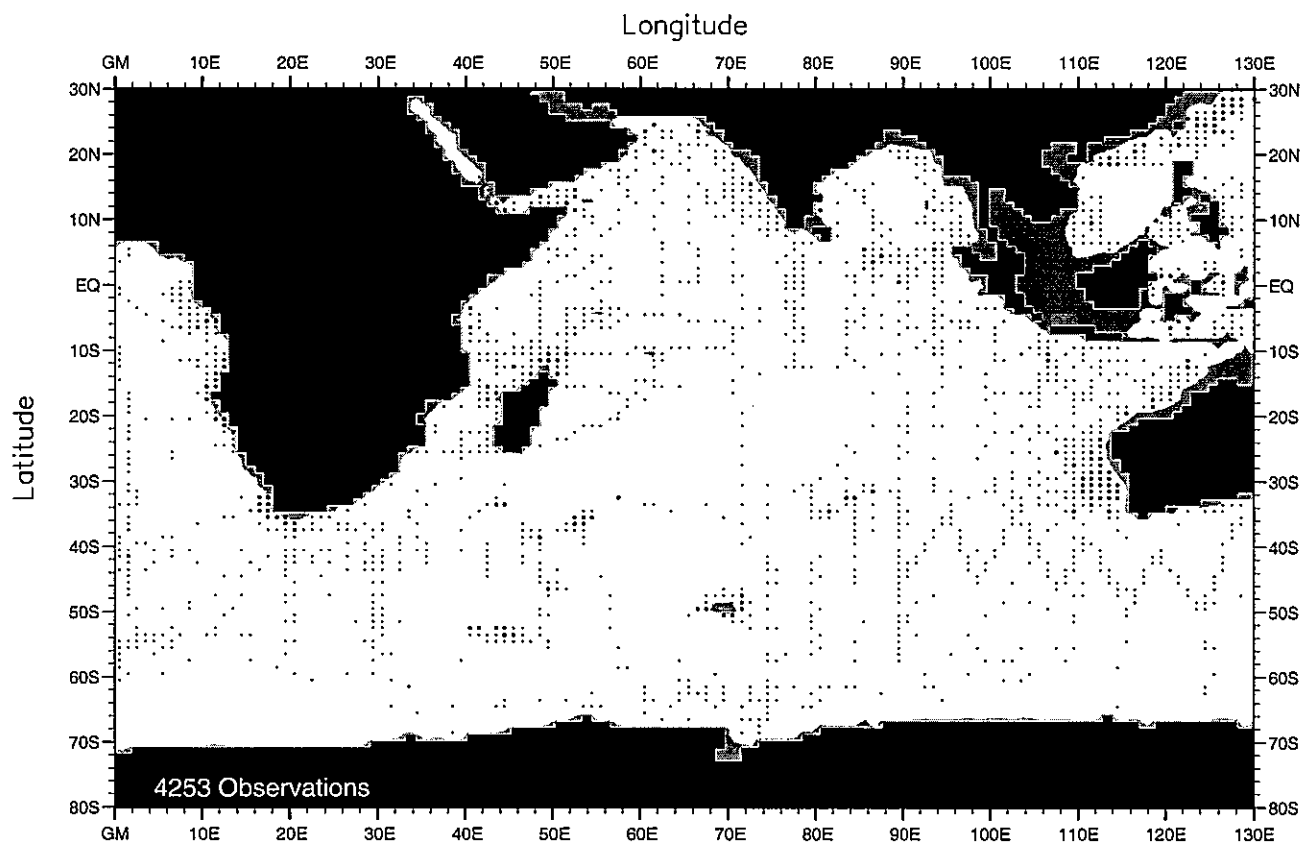
Fig. B23. Fall (Oct.-Dec.) phosphate observations at 150 m. depth.
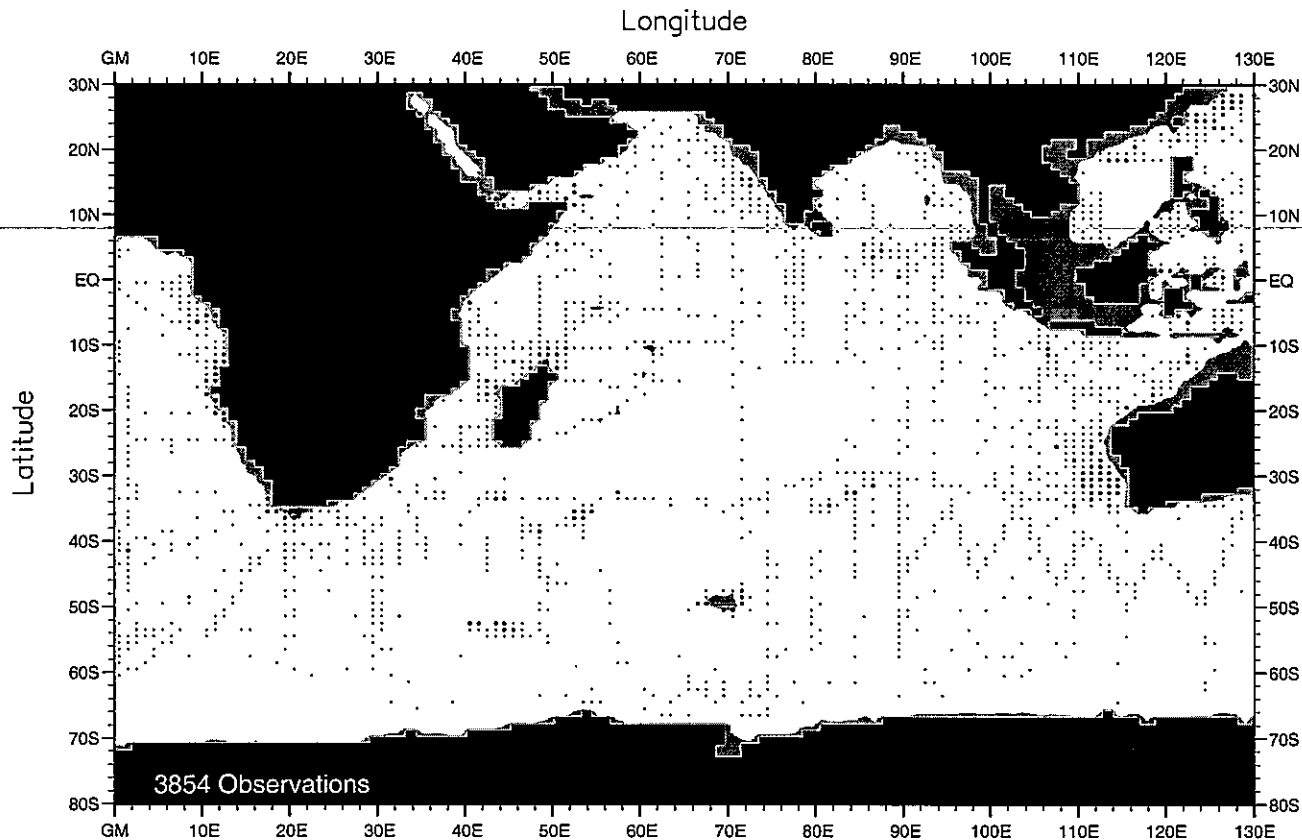
Fig. B24. Fall (Oct.-Dec.) phosphate observations at 250 m. depth.

56
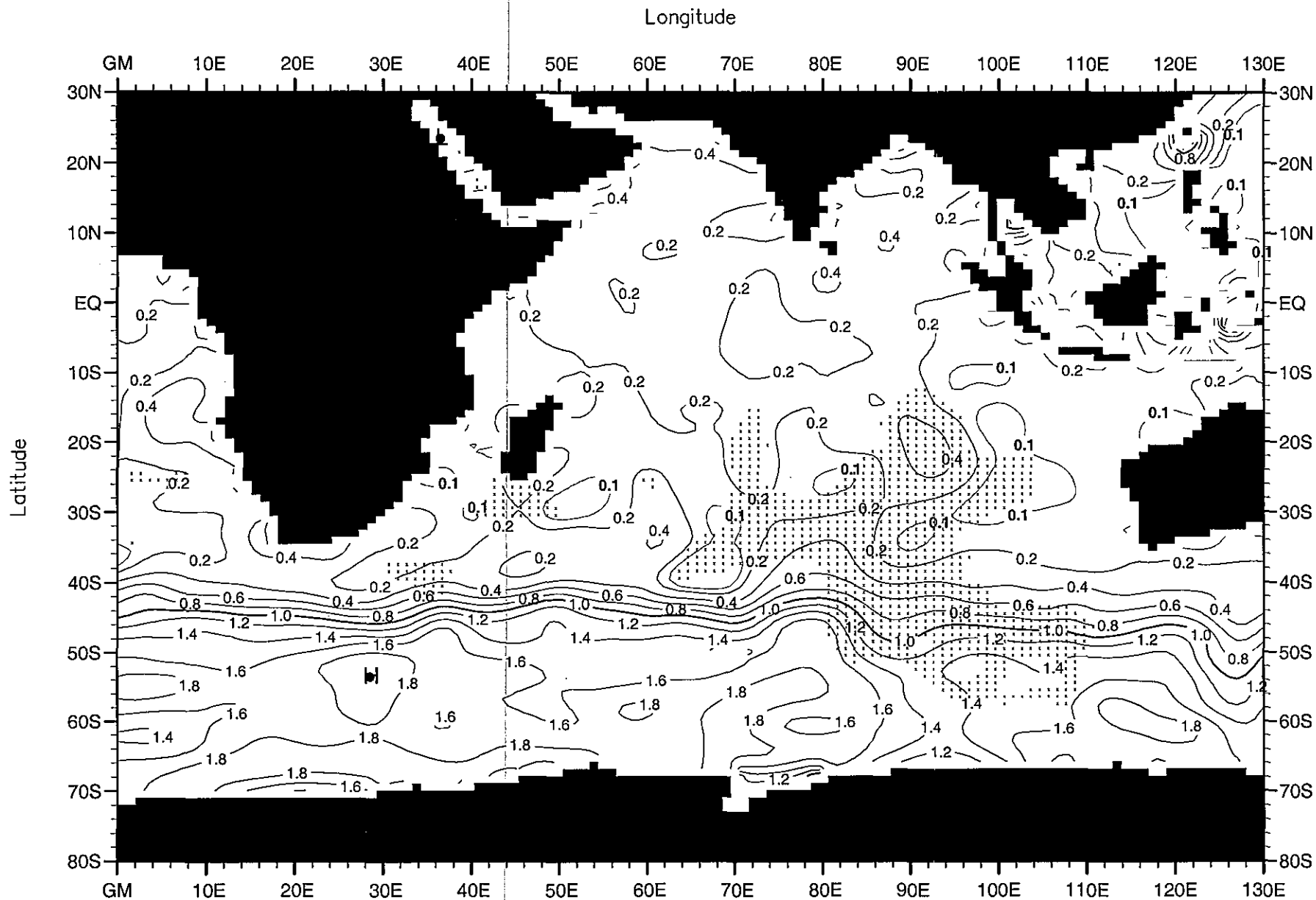
Fig. B25. Winter (Jan.-Mar.) mean phosphate (μM) at the surface .

Minimum Value= 0.00   Maximum Value= 2.00   Contour Interval: 0.20
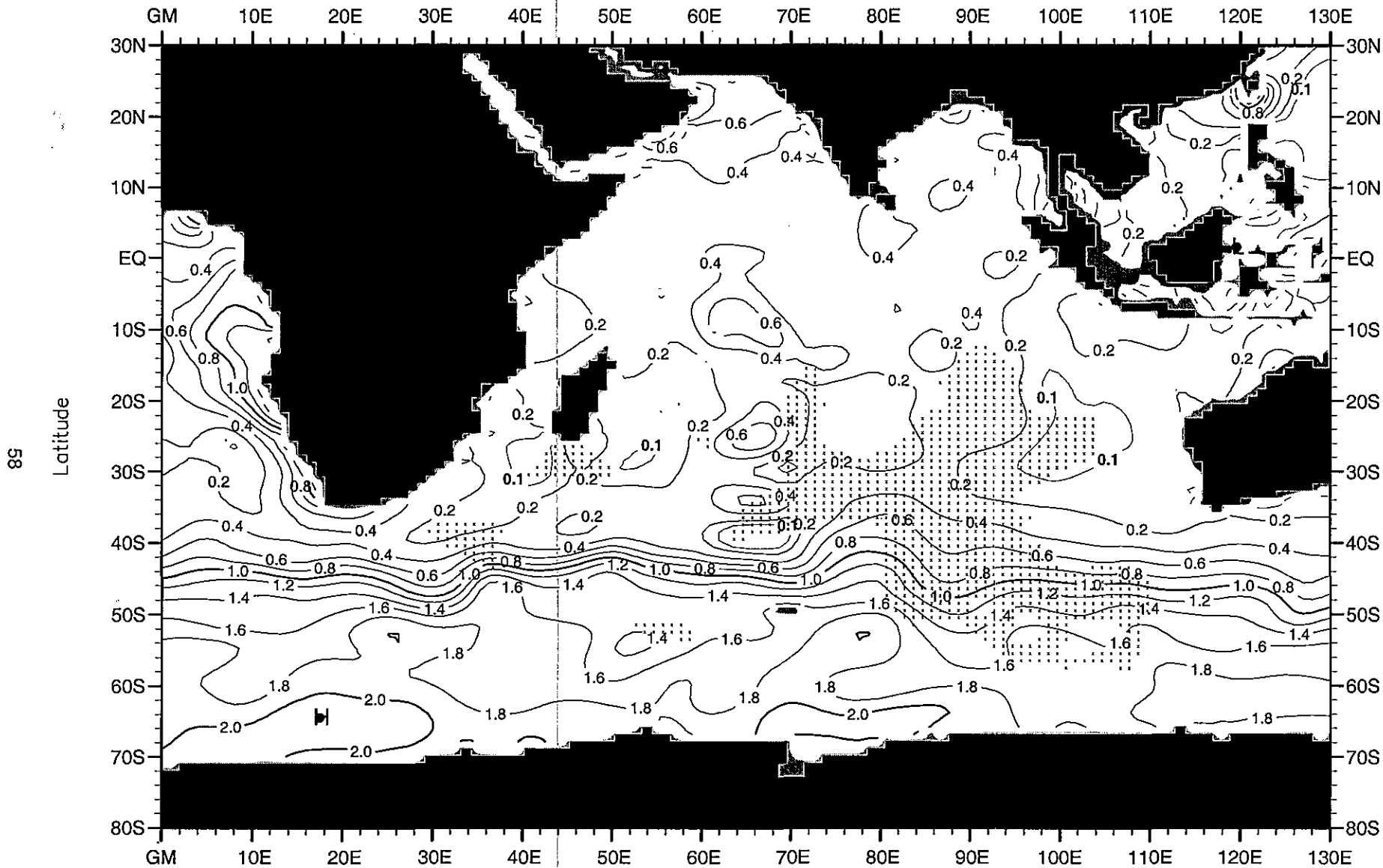
Fig. B26. Winter (Jan.-Mar.) mean phosphate (μM) at 50 m. depth.

Minimum Value= 0.00   Maximum Value= 2.18   Contour Interval: 0.20
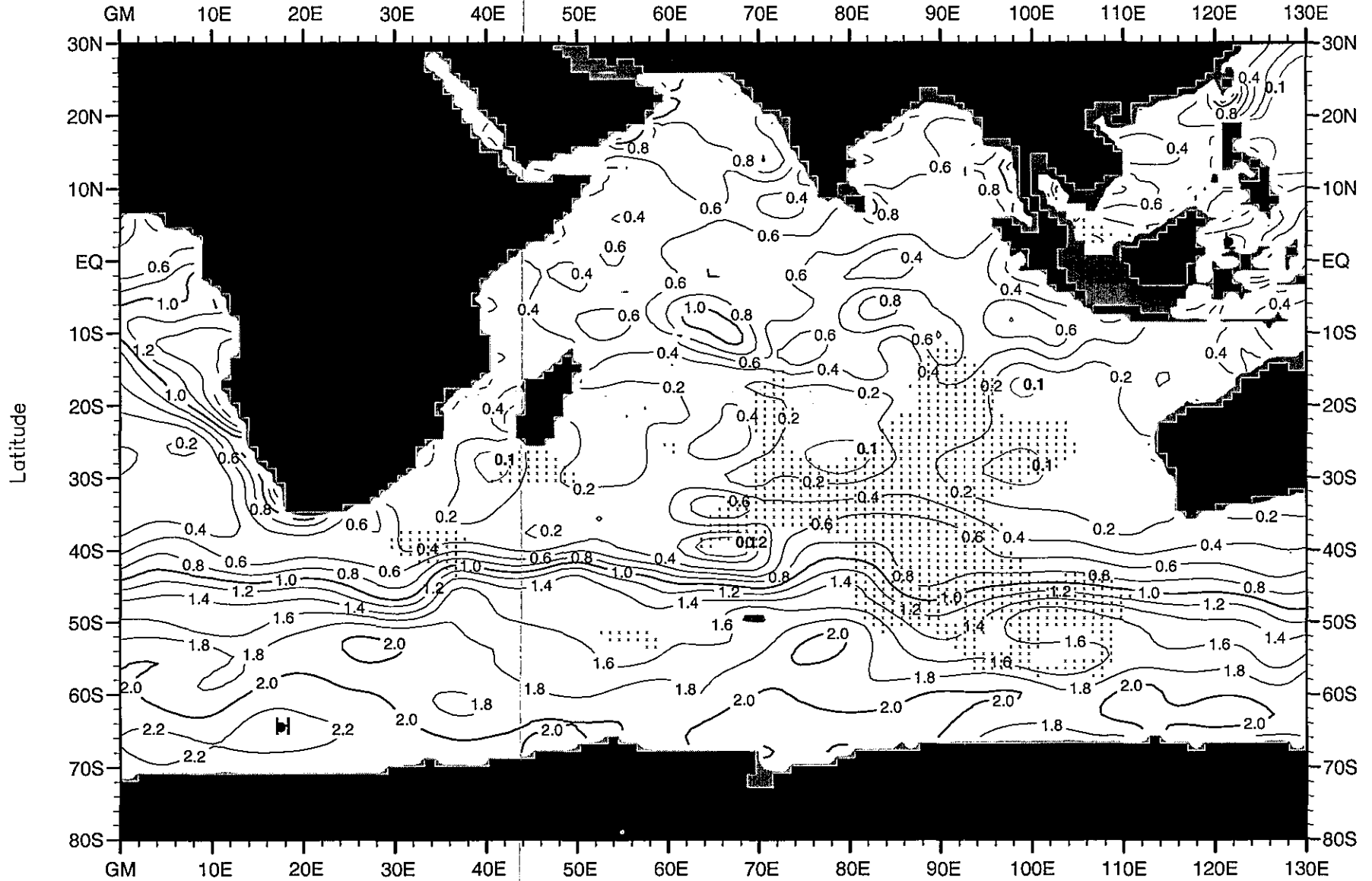
Fig. B27.   Winter (Jan.-Mar.) mean phosphate (μM) at   75 m. depth .

Minimum Value= 0.00   Maximum Value= 2.31   Contour Interval: 0.20
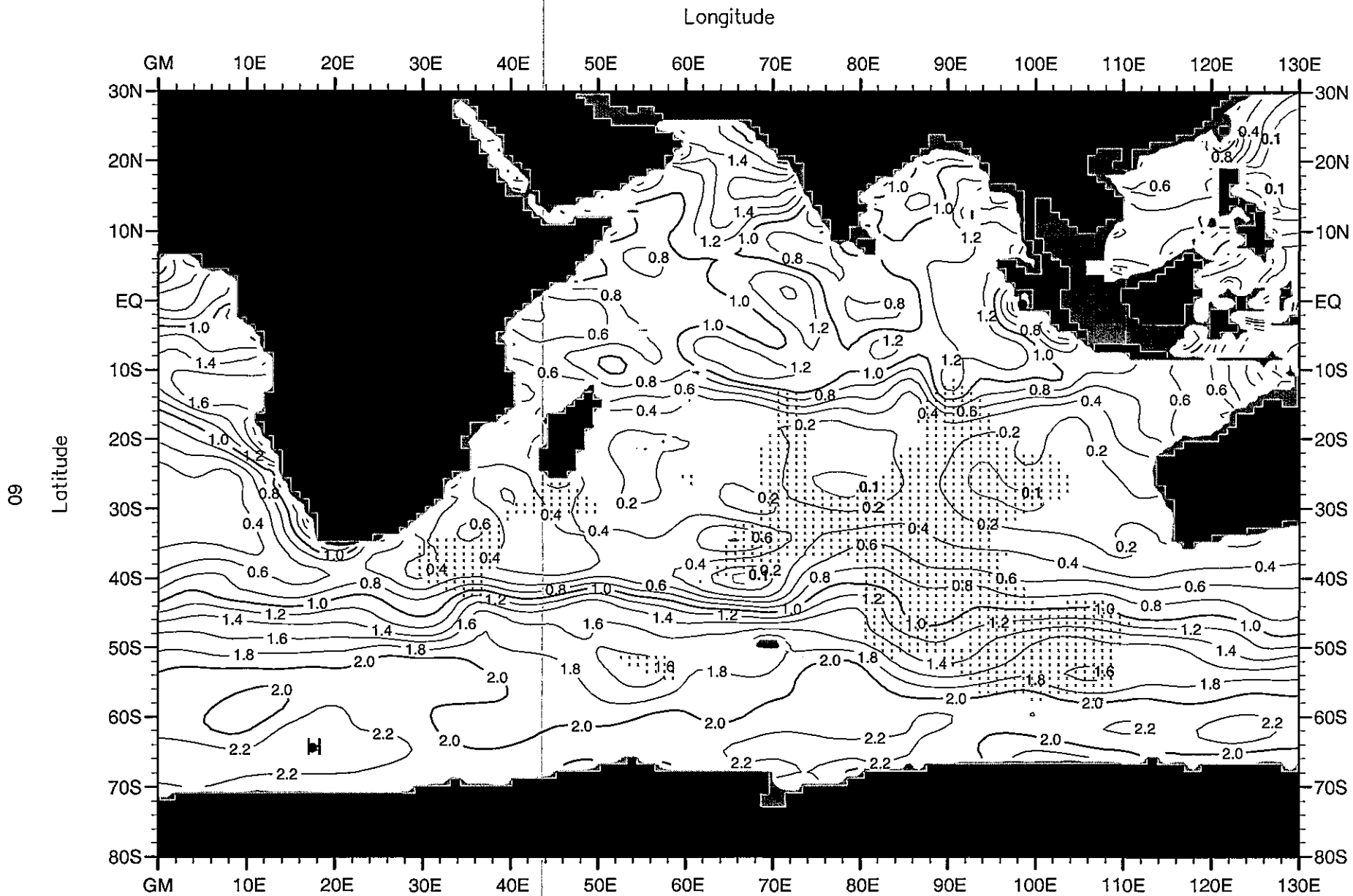
Fig. B28. Winter (Jan.-Mar.) mean phosphate (μM) at 100 m. depth .

Minimum Value= 0.01   Maximum Value= 2.40   Contour Interval: 0.20
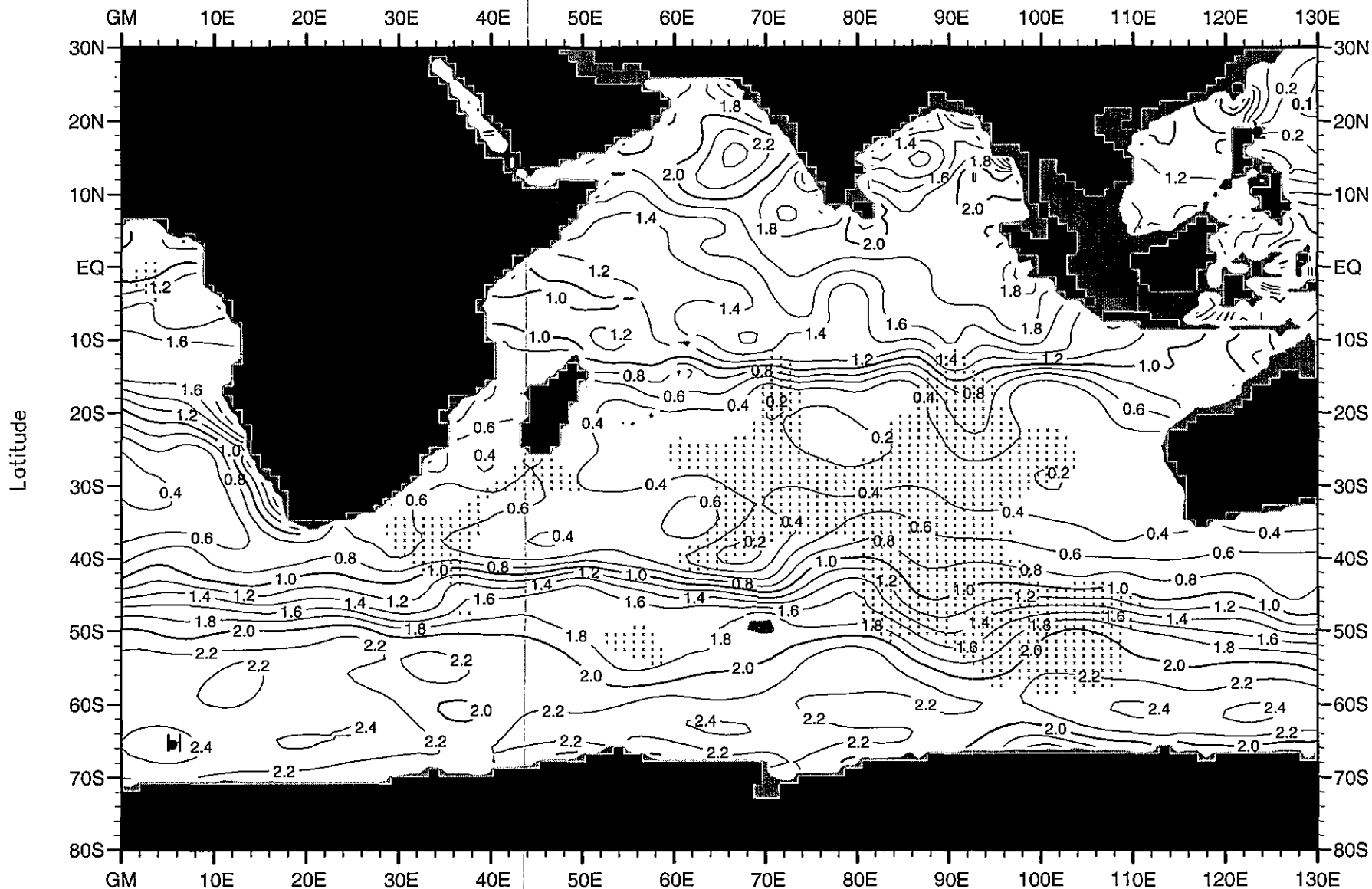
Fig. B29. Winter (Jan.-Mar.) mean phosphate (μM) at 150 m. depth.

Minimum Value= 0.06   Maximum Value= 2.48   Contour Interval: 0.20

61
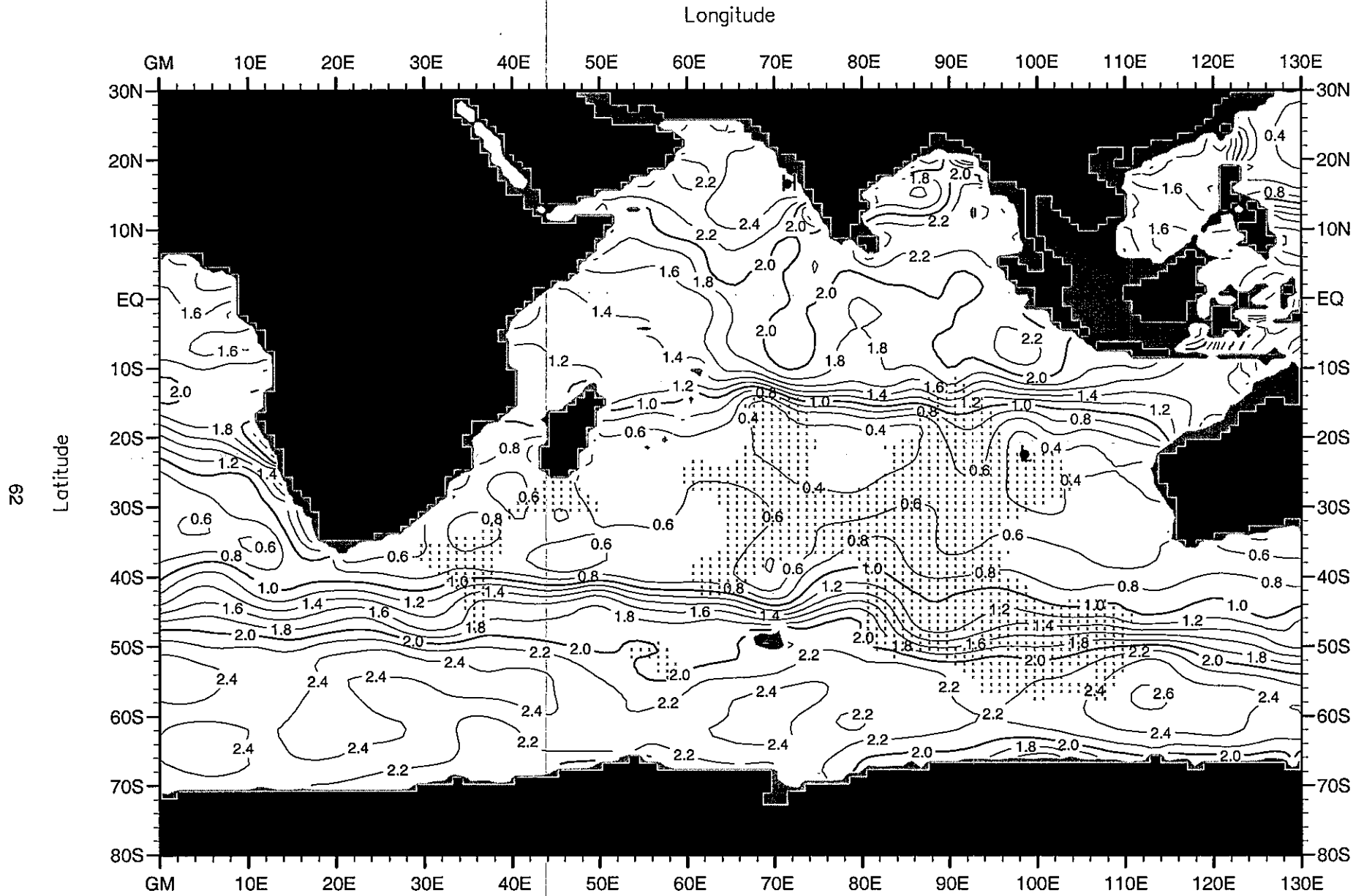
Fig. B30. Winter (Jan.-Mar.) mean phosphate (μM) at 250 m. depth .

Minimum Value= 0.23   Maximum Value= 2.67   Contour Interval: 0.20

62
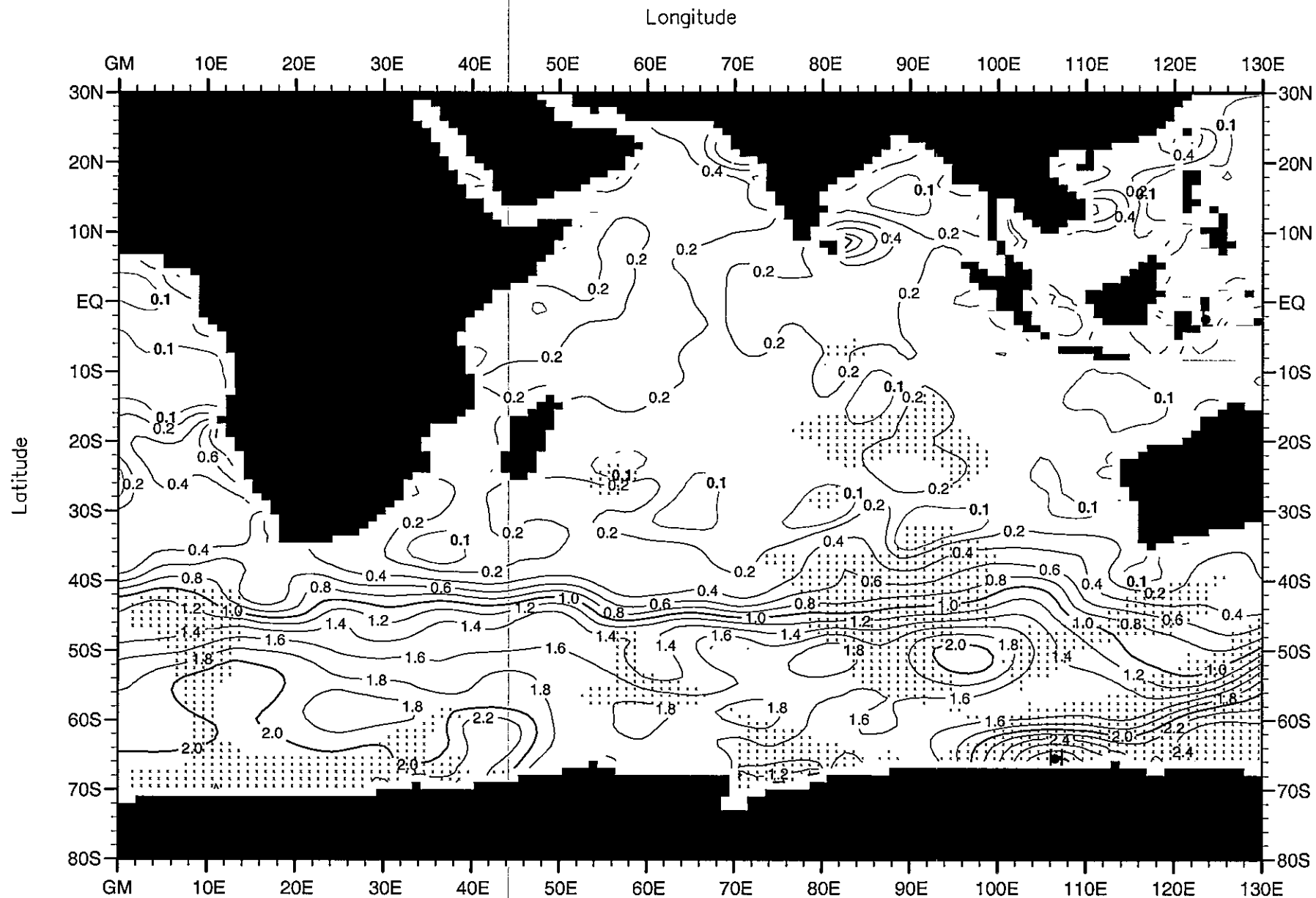
Fig. B31. Spring (Apr.-Jun.) mean phosphate (μM) at the surface.

Minimum Value= 0.00   Maximum Value= 3.05   Contour Interval: 0.20
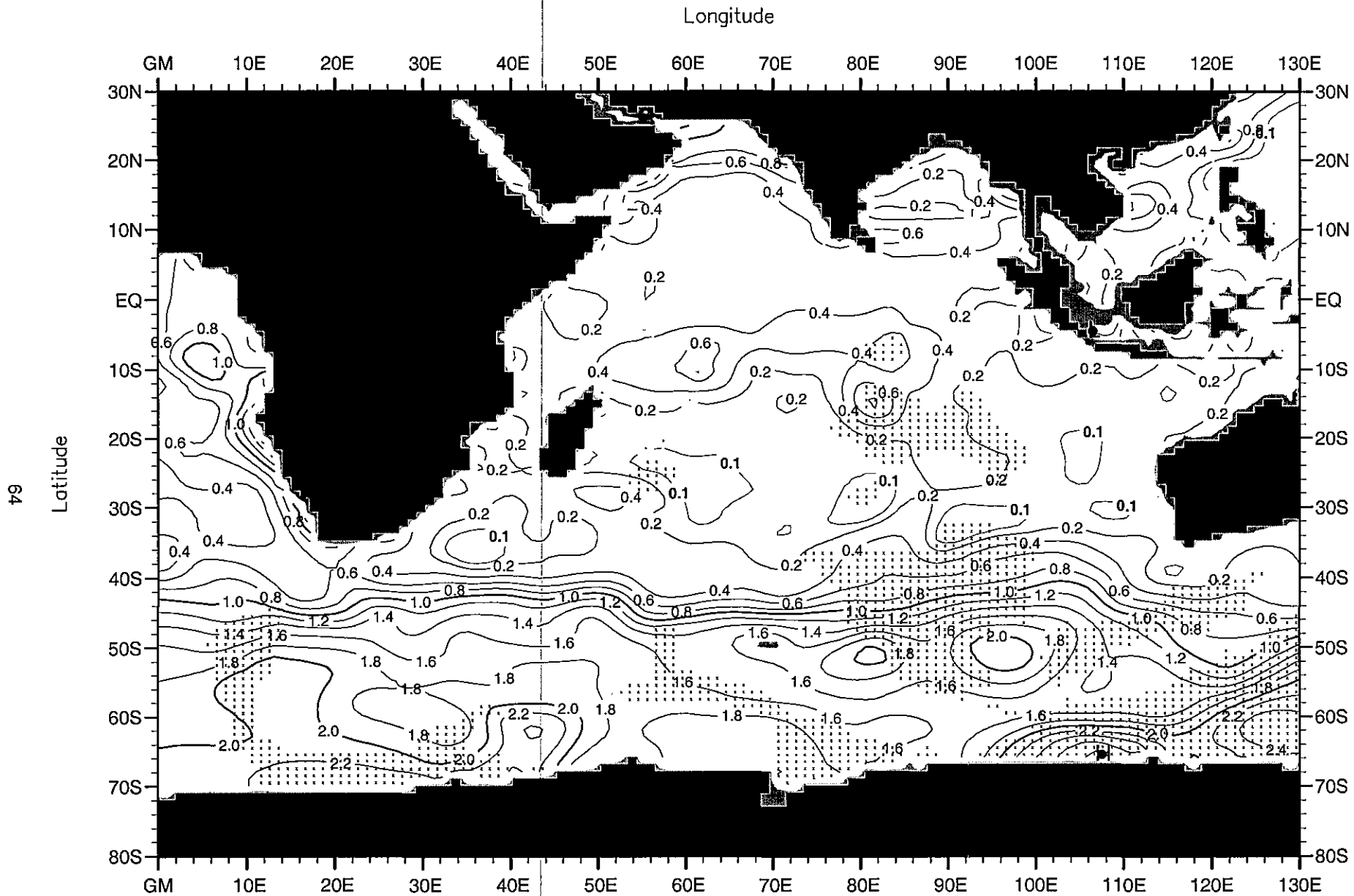
Fig. B32. Spring (Apr.-Jun.) mean phosphate (μM) at 50 m. depth .

Minimum Value= 0.00   Maximum Value= 2.90   Contour Interval: 0.20

64
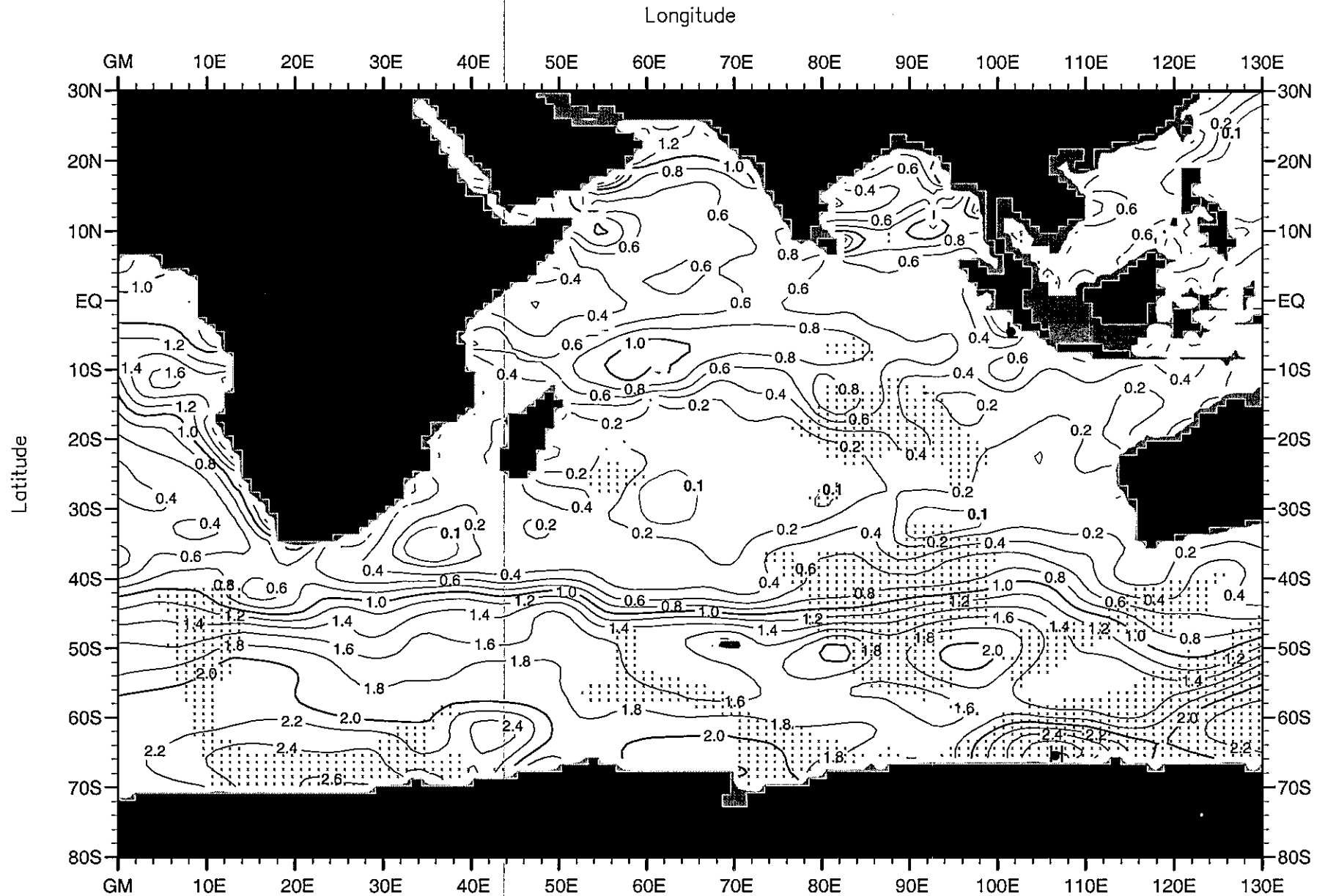
Fig. B33.   Spring (Apr.-Jun.) mean phosphate (μM) at 75 m. depth .

Minimum Value= 0.00   Maximum Value= 2.87   Contour Interval: 0.20
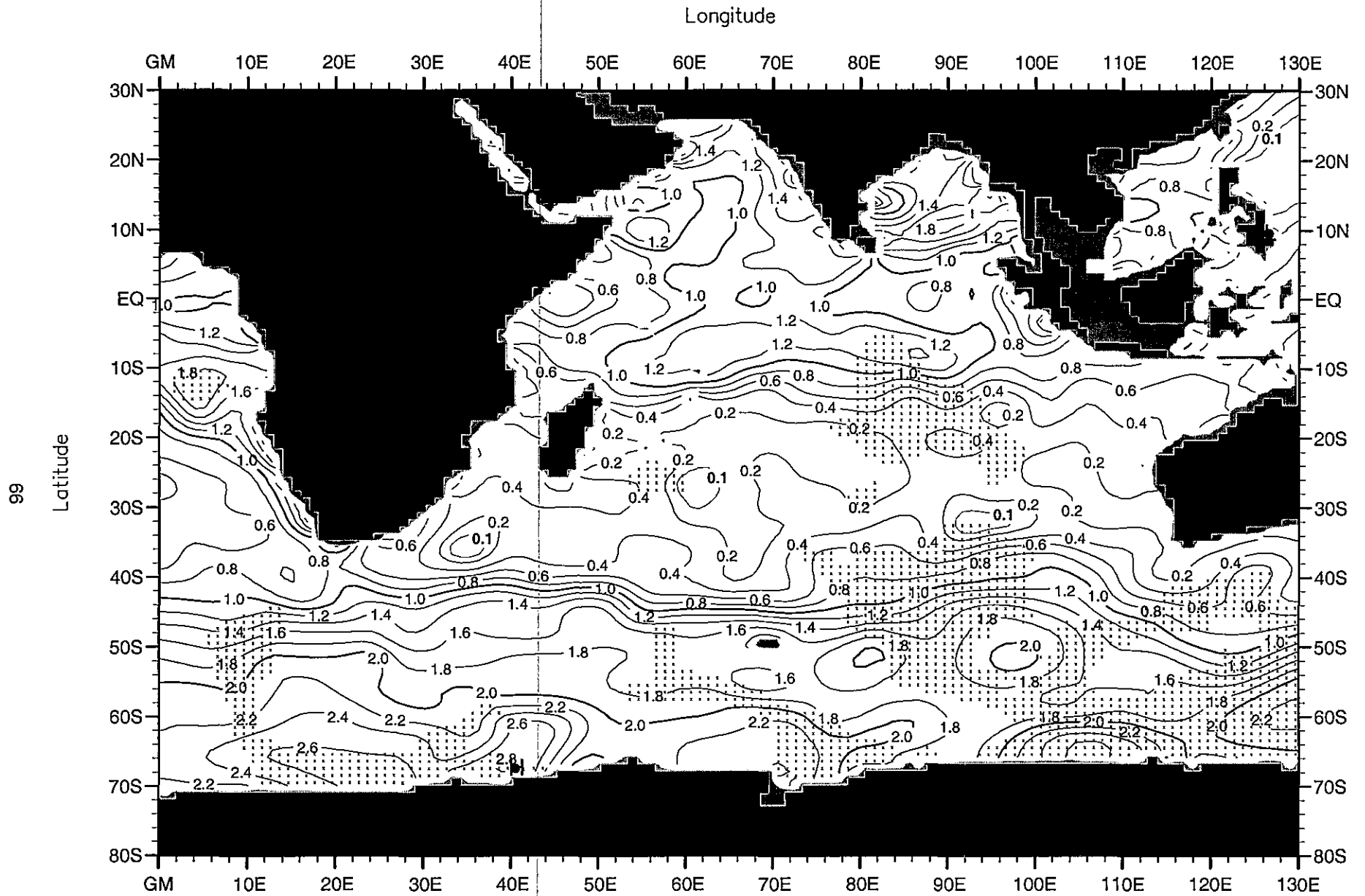
Fig. B34.   Spring (Apr.-Jun.) mean phosphate (μM) at 100 m. depth .

Minimum Value=   0.00   Maximum Value=   2.93   Contour Interval: 0.20
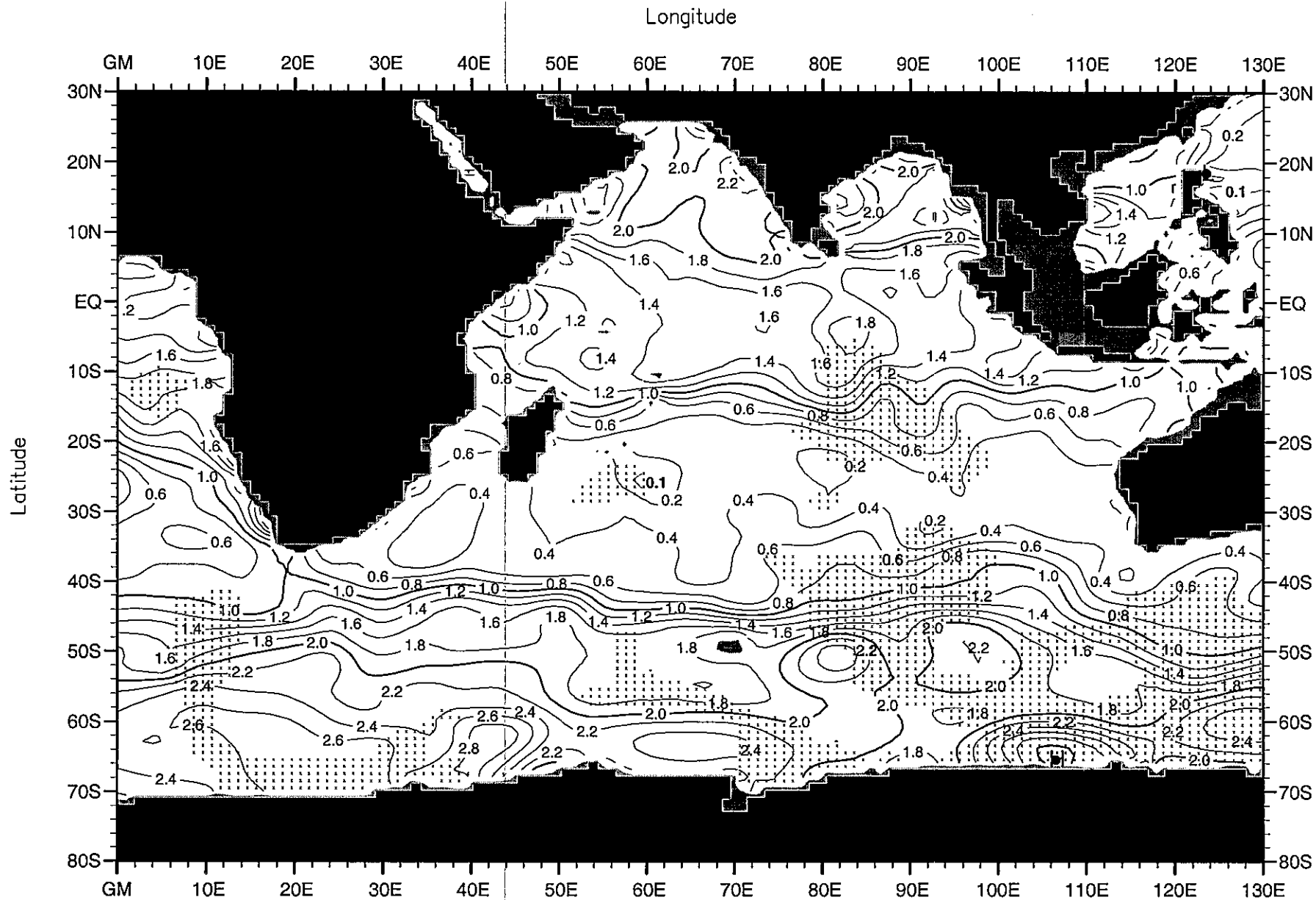
Fig. B35. Spring (Apr.-Jun.) mean phosphate (μM) at 150 m. depth.

Minimum Value= 0.00   Maximum Value= 3.12   Contour Interval: 0.20
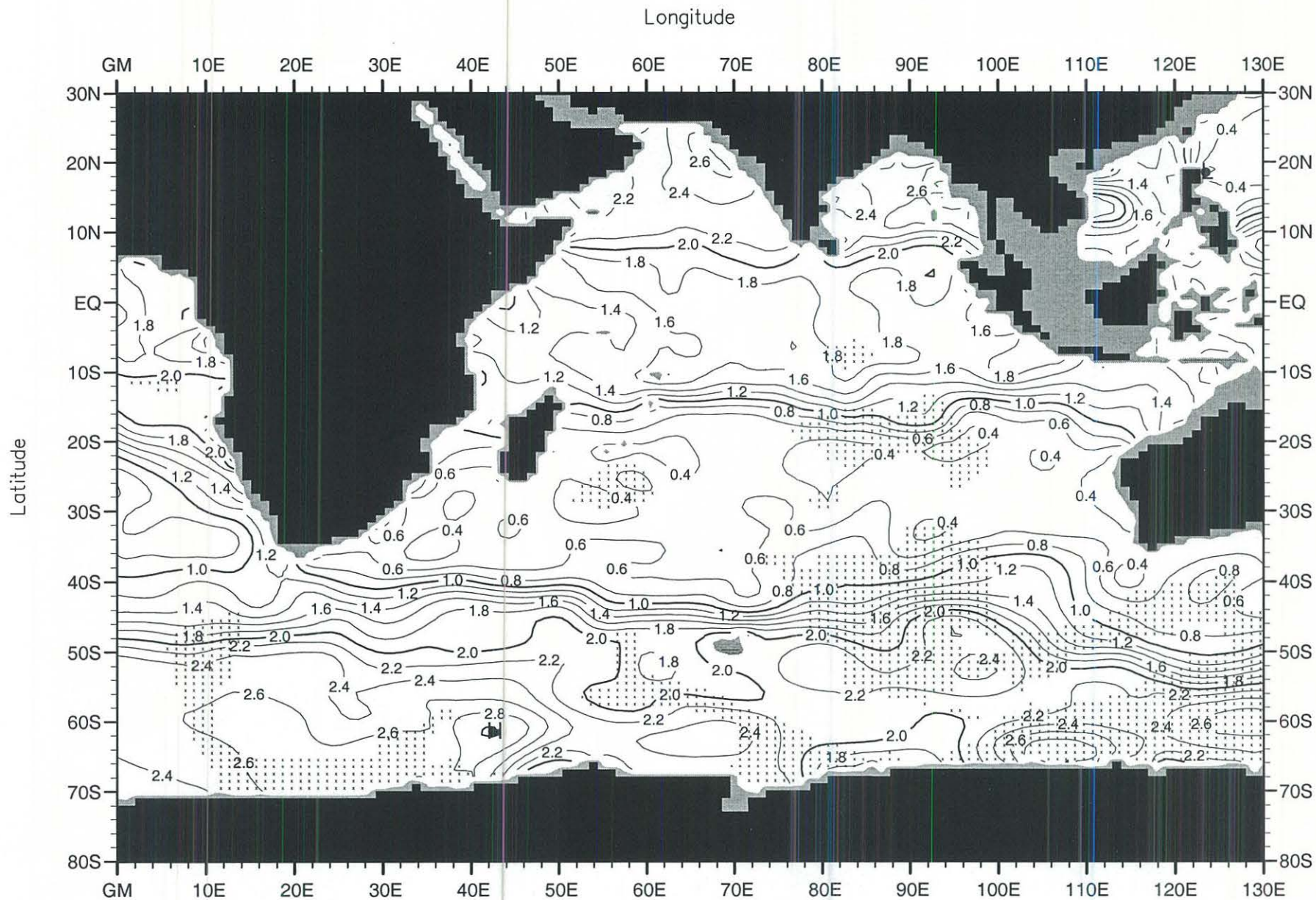
Fig. B36. Spring (Apr.-Jun.) mean phosphate (μM) at 250 m. depth .

Minimum Value= 0.11   Maximum Value= 3.02   Contour Interval: 0.20
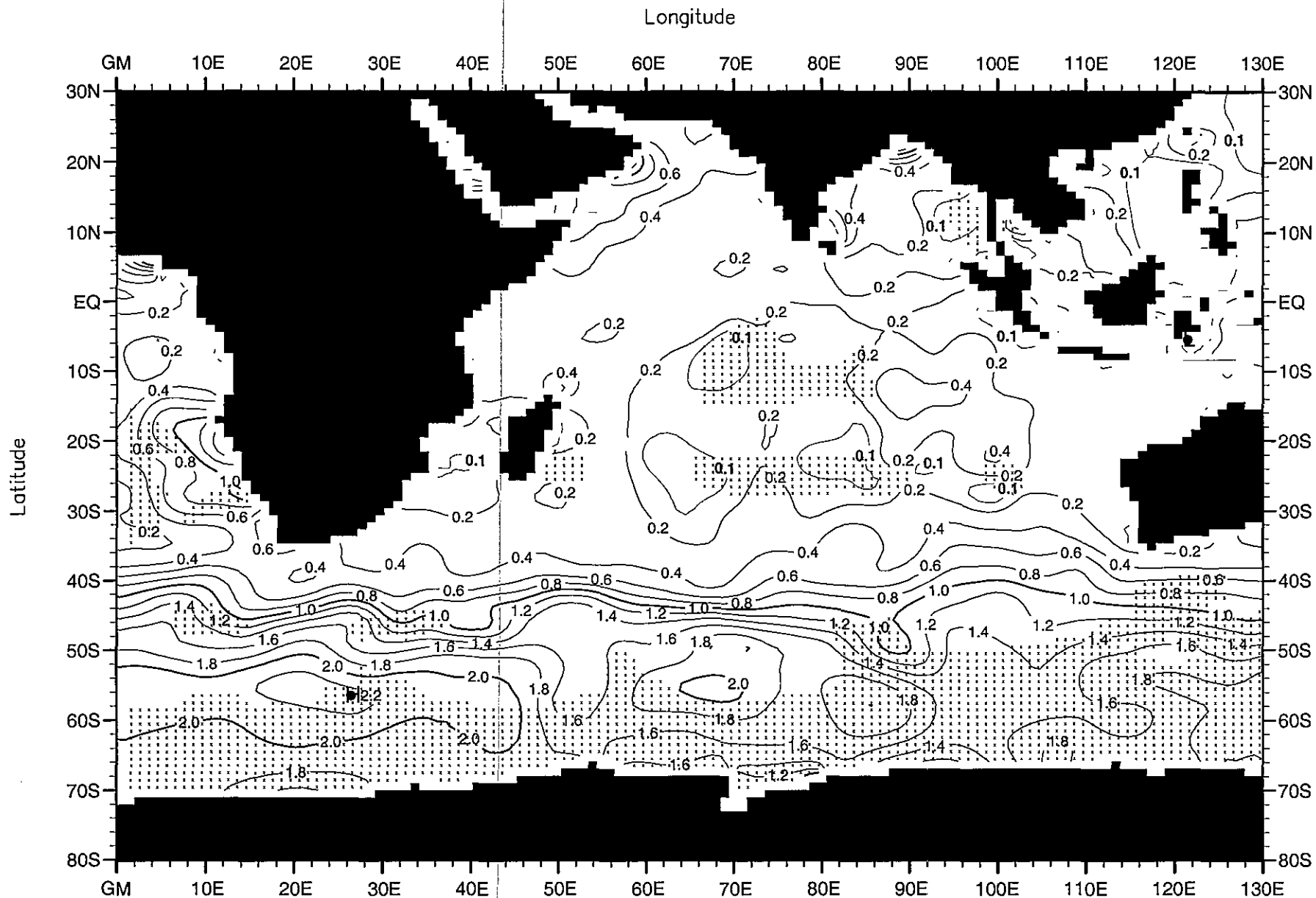
Fig. B37.   Summer (Jul.-Sep.) mean phosphate (μM) at the surface .

Minimum Value=   0.00   Maximum Value=   2.26   Contour Interval: 0.20
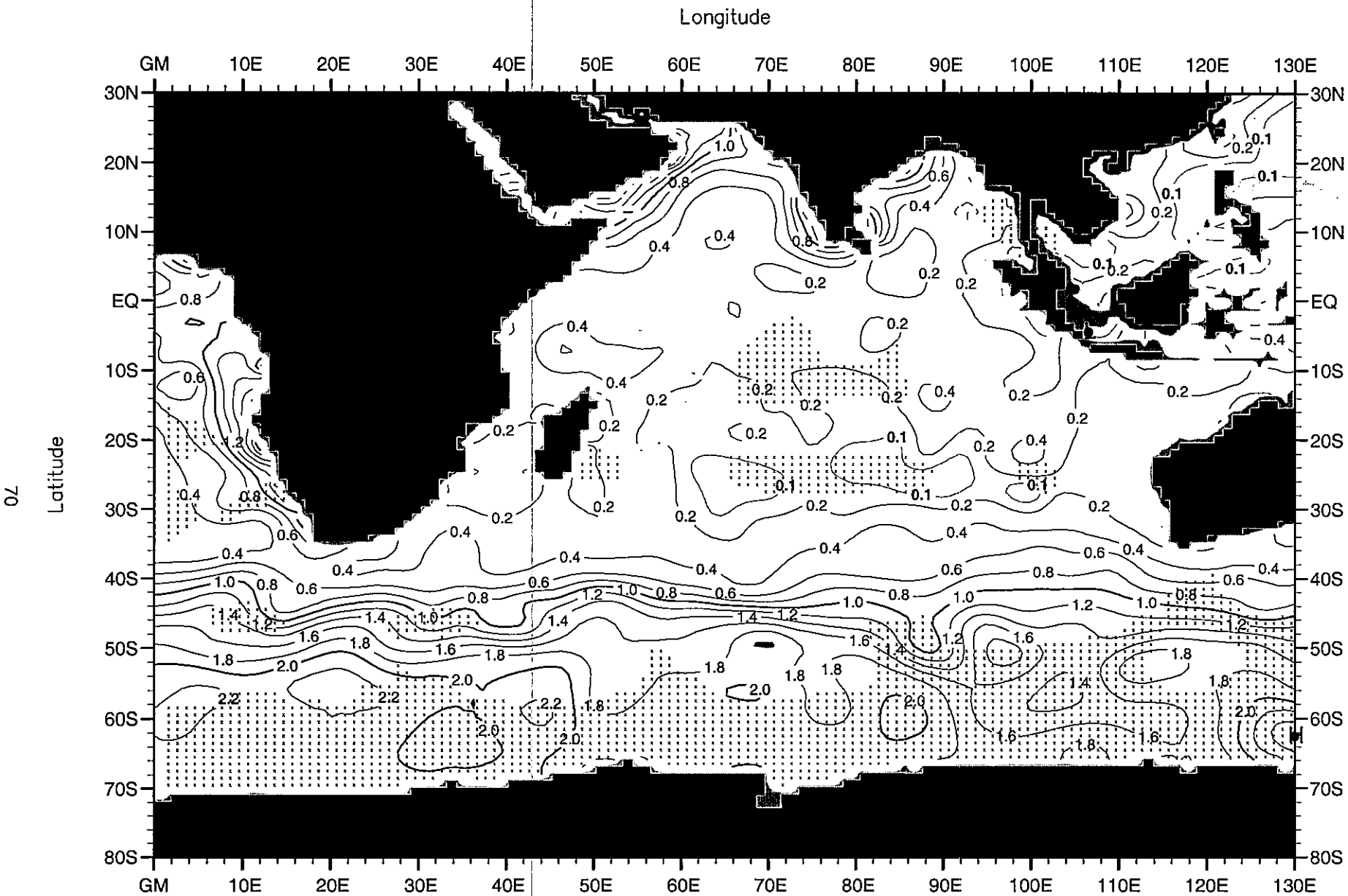
Fig. B38.   Summer (Jul.-Sep.) mean phosphate (μM) at 50 m. depth .

Minimum Value=   0.00   Maximum Value=   2.51   Contour Interval: 0.20
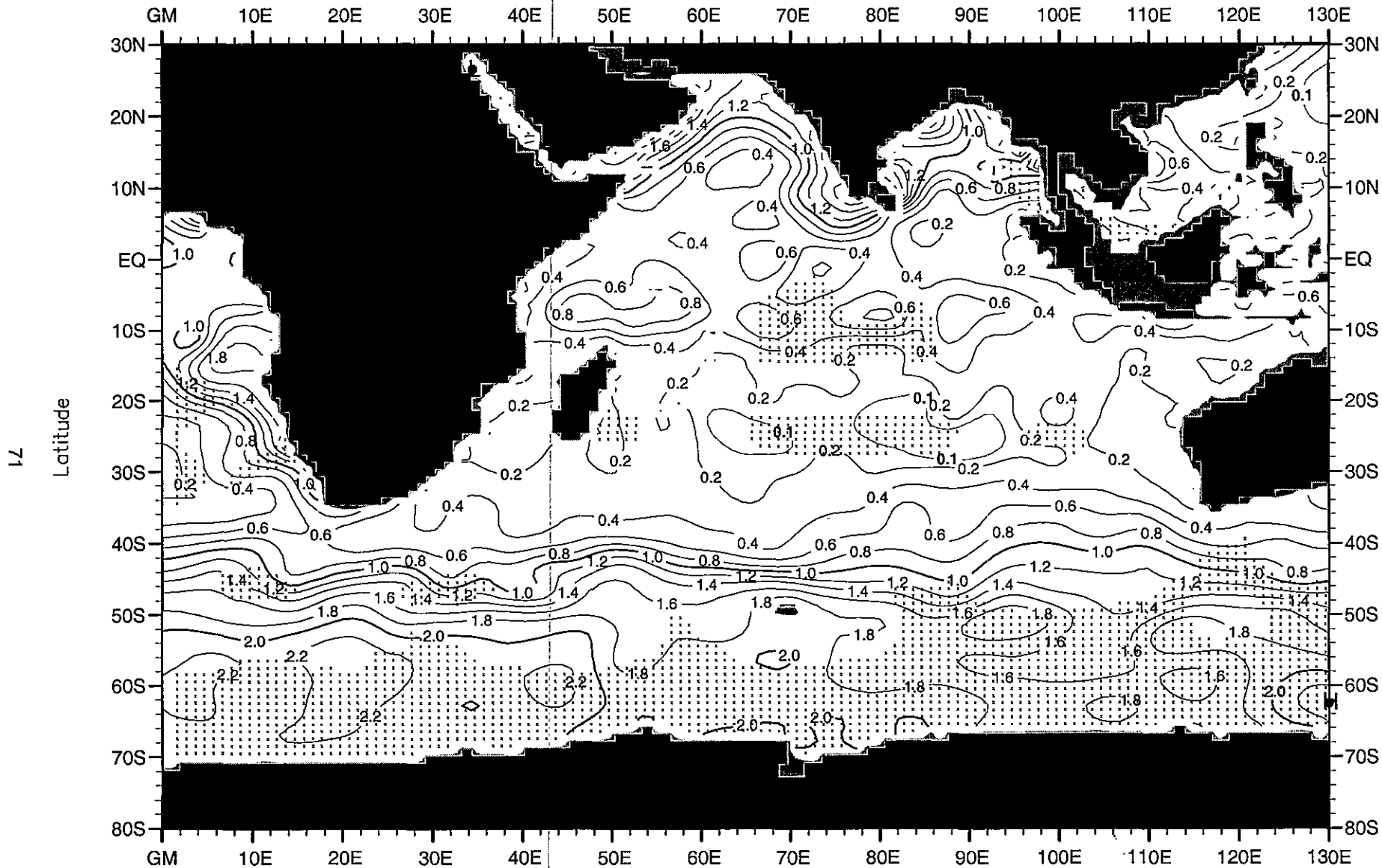
Fig. B39. Summer (Jul.-Sep.) mean phosphate (μM) at 75 m. depth .

Minimum Value= 0.00   Maximum Value= 2.32   Contour Interval: 0.20
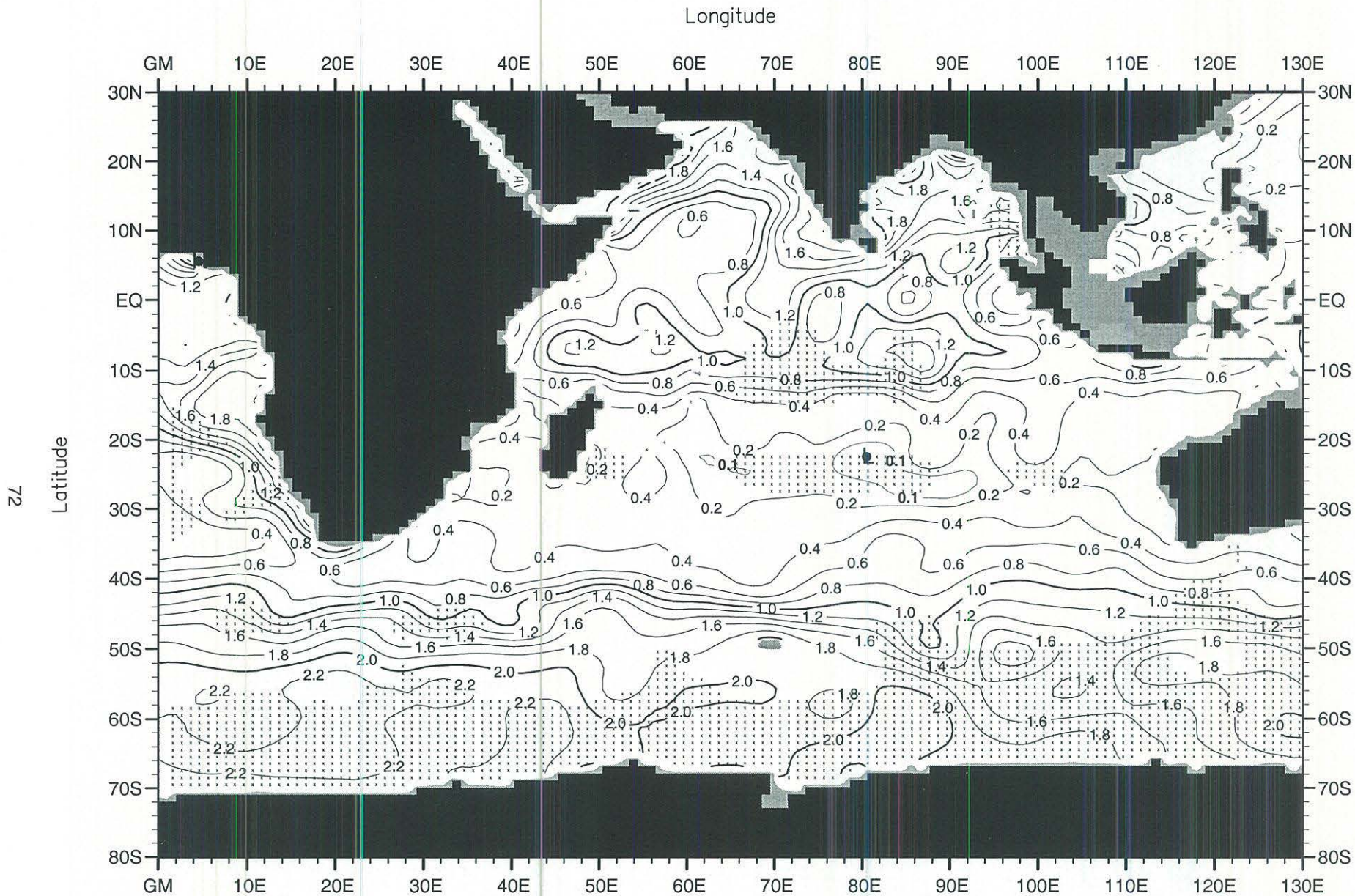
Fig. B40. Summer (Jul.-Sep.) mean phosphate (μM) at 100 m. depth .

Minimum Value= 0.01   Maximum Value= 2.44   Contour Interval: 0.20
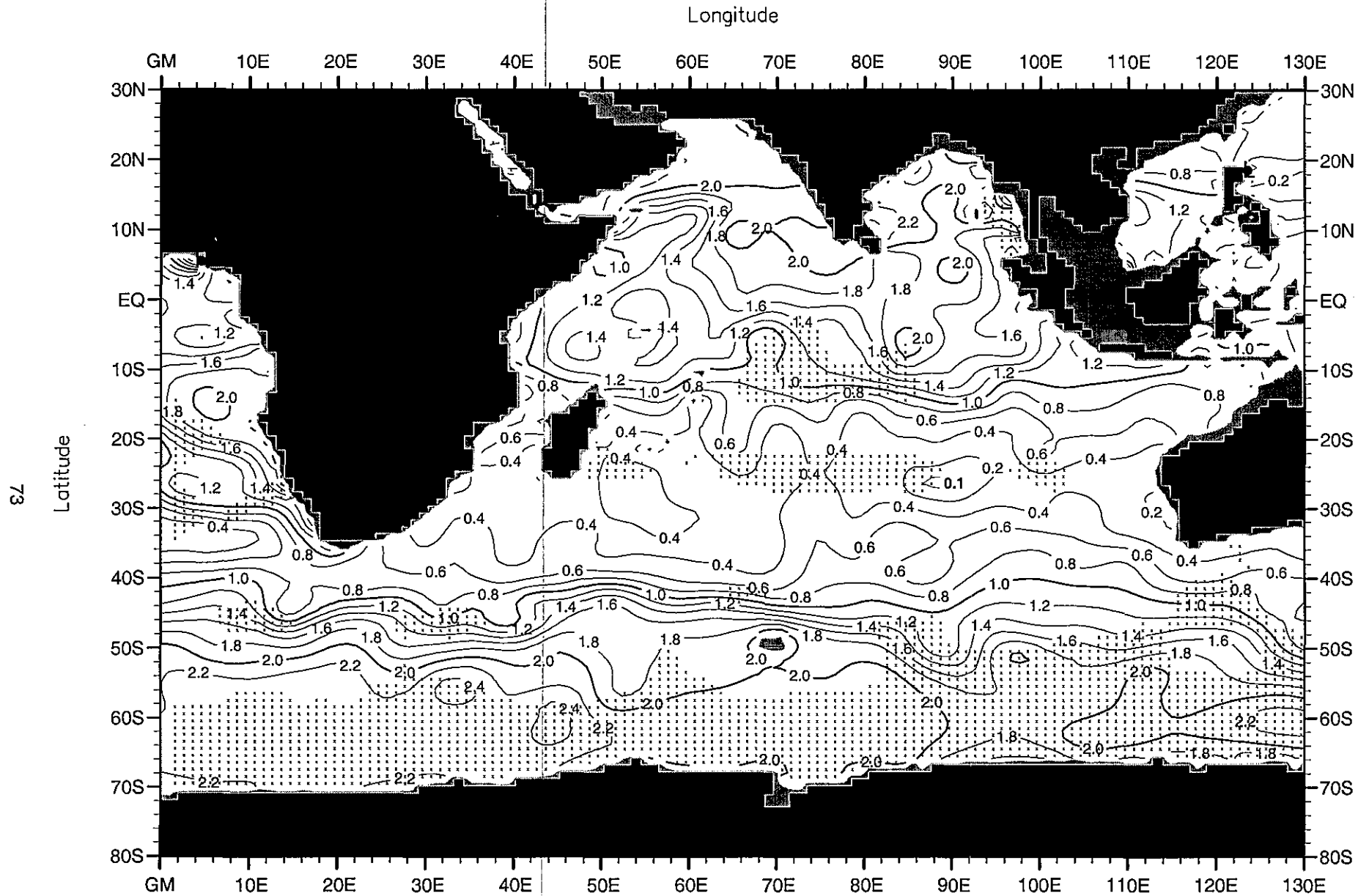
Fig. B41. Summer (Jul.-Sep.) mean phosphate (μM) at 150 m. depth .

Minimum Value= 0.05   Maximum Value= 2.98   Contour Interval: 0.20

Fig. B42. Summer (Jul.-Sep.) mean phosphate (μM) at 250 m. depth .

Minimum Value= 0.17   Maximum Value= 2.93   Contour Interval: 0.20
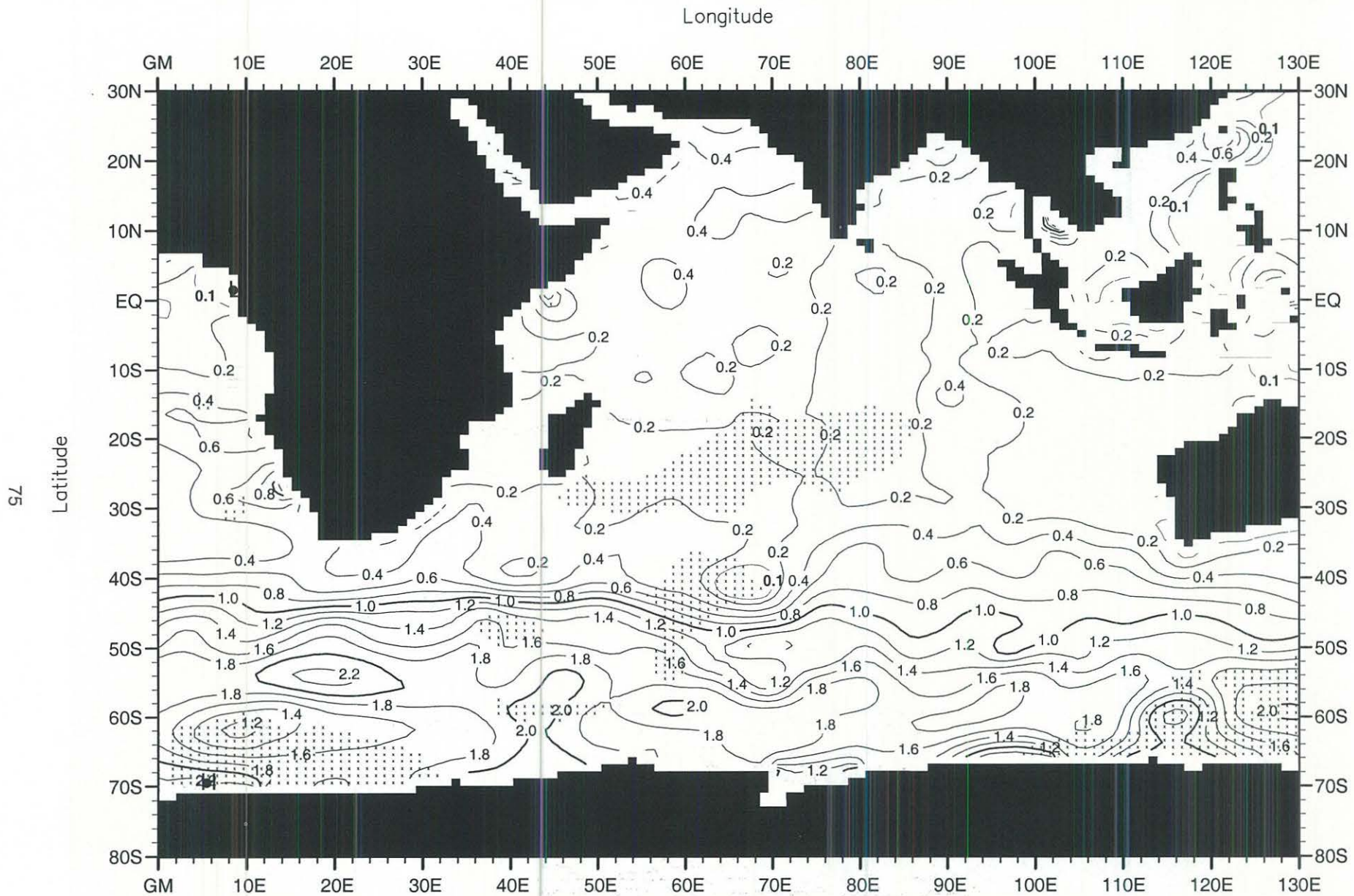
Fig. B43.   Fall (Oct.-Dec.) mean phosphate (μM) at the surface .

Minimum Value=   0.00   Maximum Value=   2.35   Contour Interval: 0.20
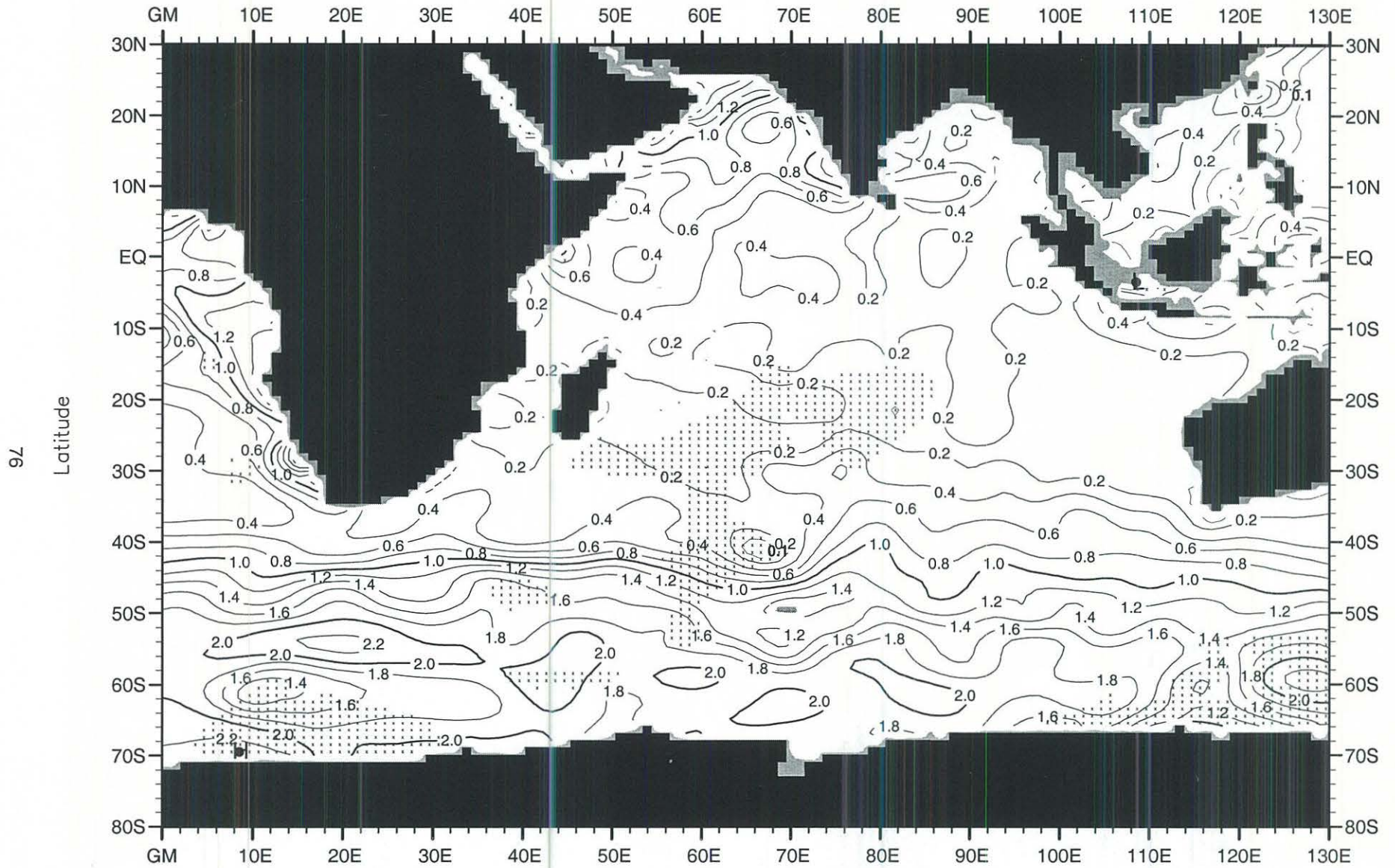
Fig. B44. Fall (Oct.-Dec.) mean phosphate (μM) at 50 m. depth .

Minimum Value= 0.00   Maximum Value= 2.32   Contour Interval: 0.20
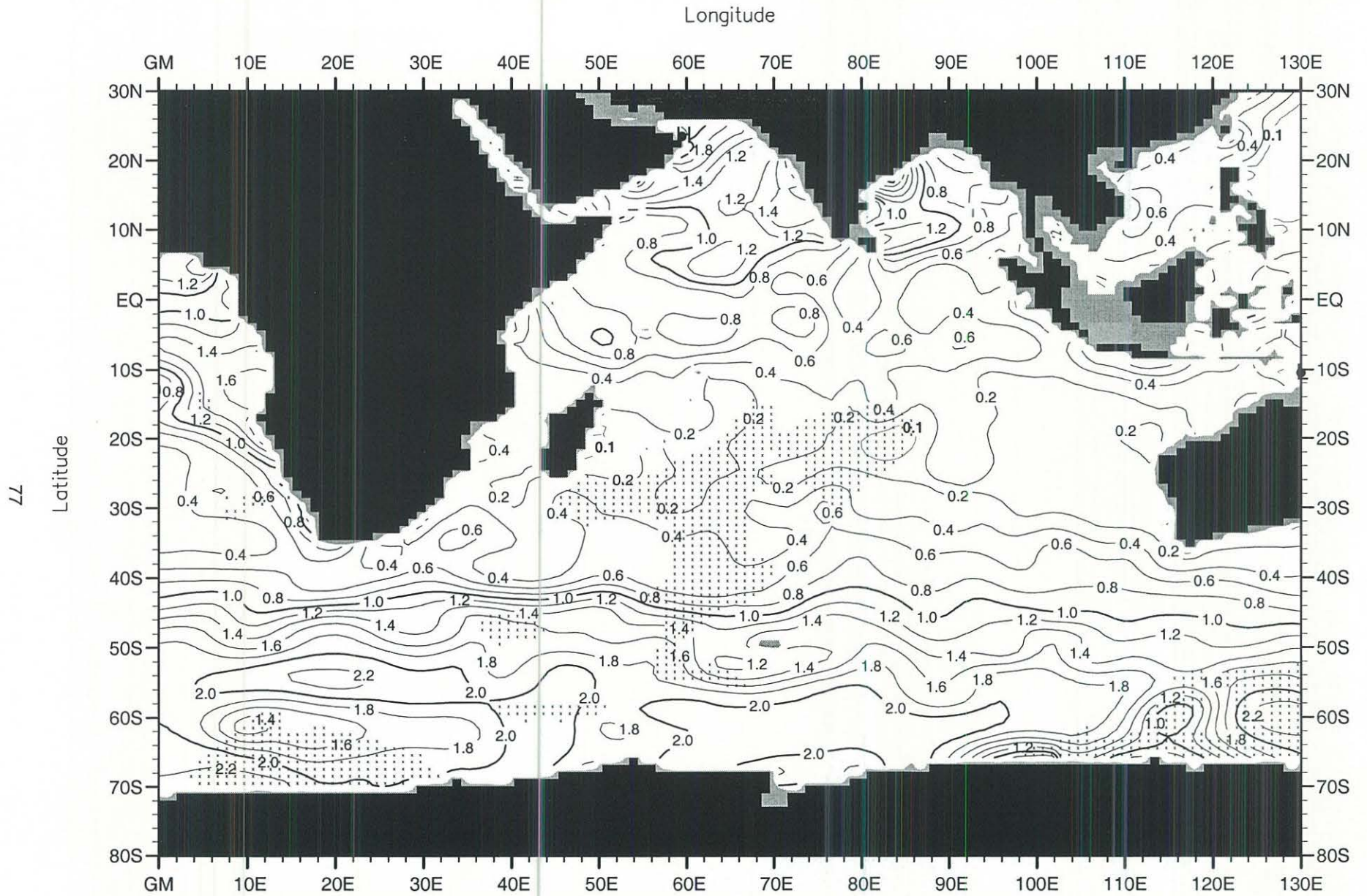
Fig. B45.   Fall (Oct.-Dec.) mean phosphate (μM) at 75 m. depth .

Minimum Value= 0.00   Maximum Value= 2.35   Contour Interval: 0.20
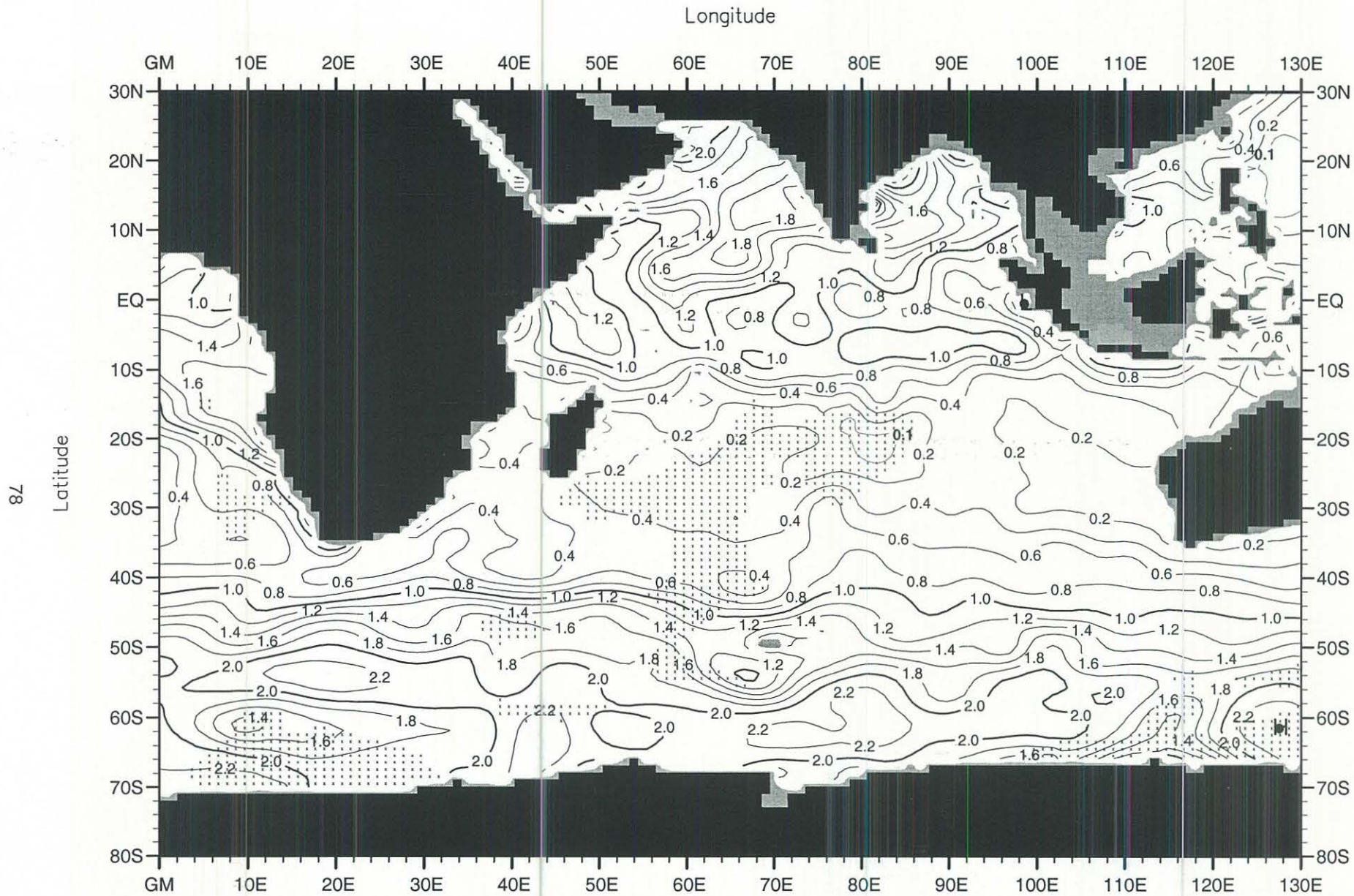
Fig. B46.   Fall (Oct.-Dec.) mean phosphate (μM) at 100 m. depth .

Minimum Value= 0.00   Maximum Value= 2.37   Contour Interval: 0.20
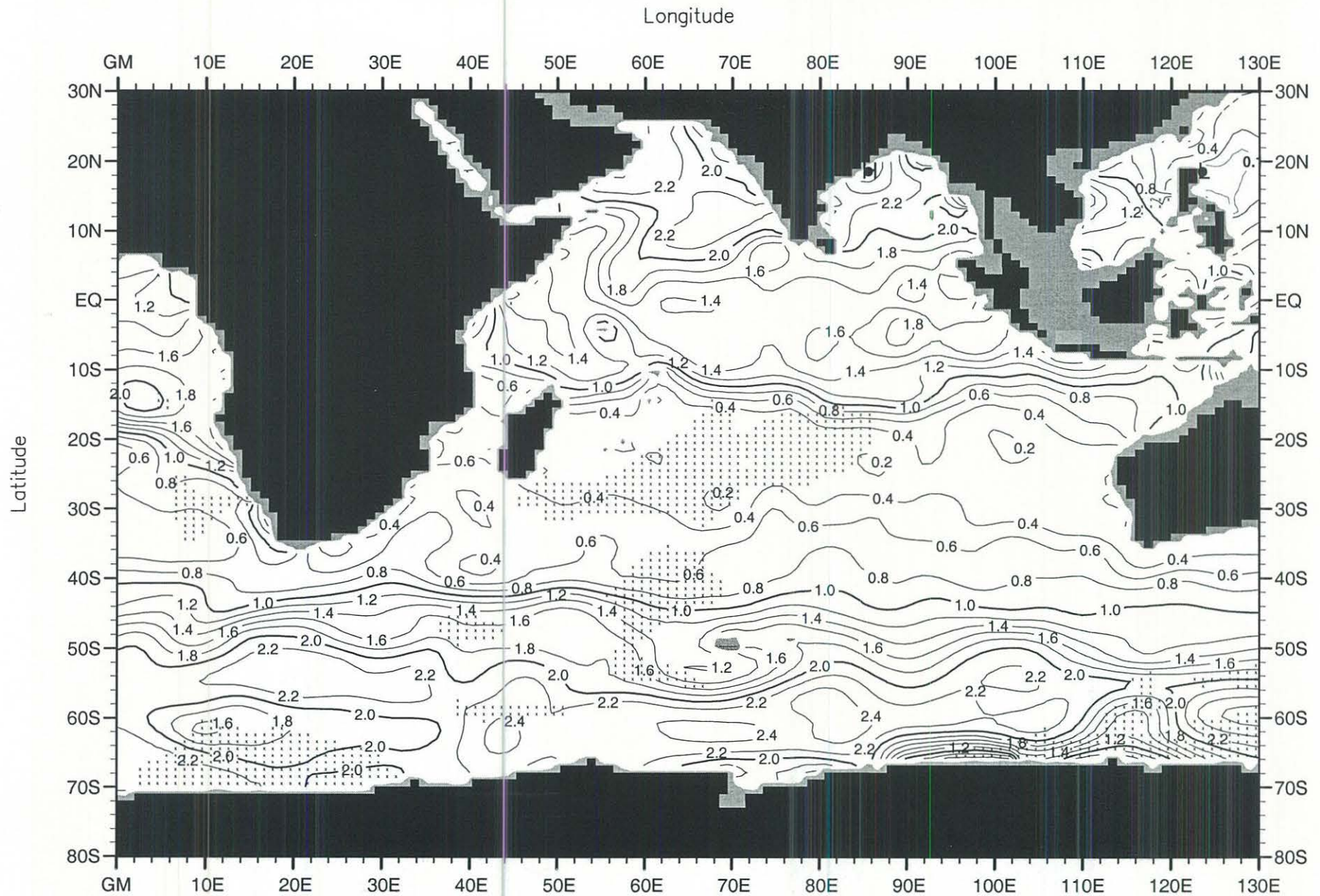
Fig. B47.   Fall (Oct.-Dec.) mean phosphate (μM) at 150 m. depth .

Minimum Value= 0.00   Maximum Value= 2.99   Contour Interval: 0.20
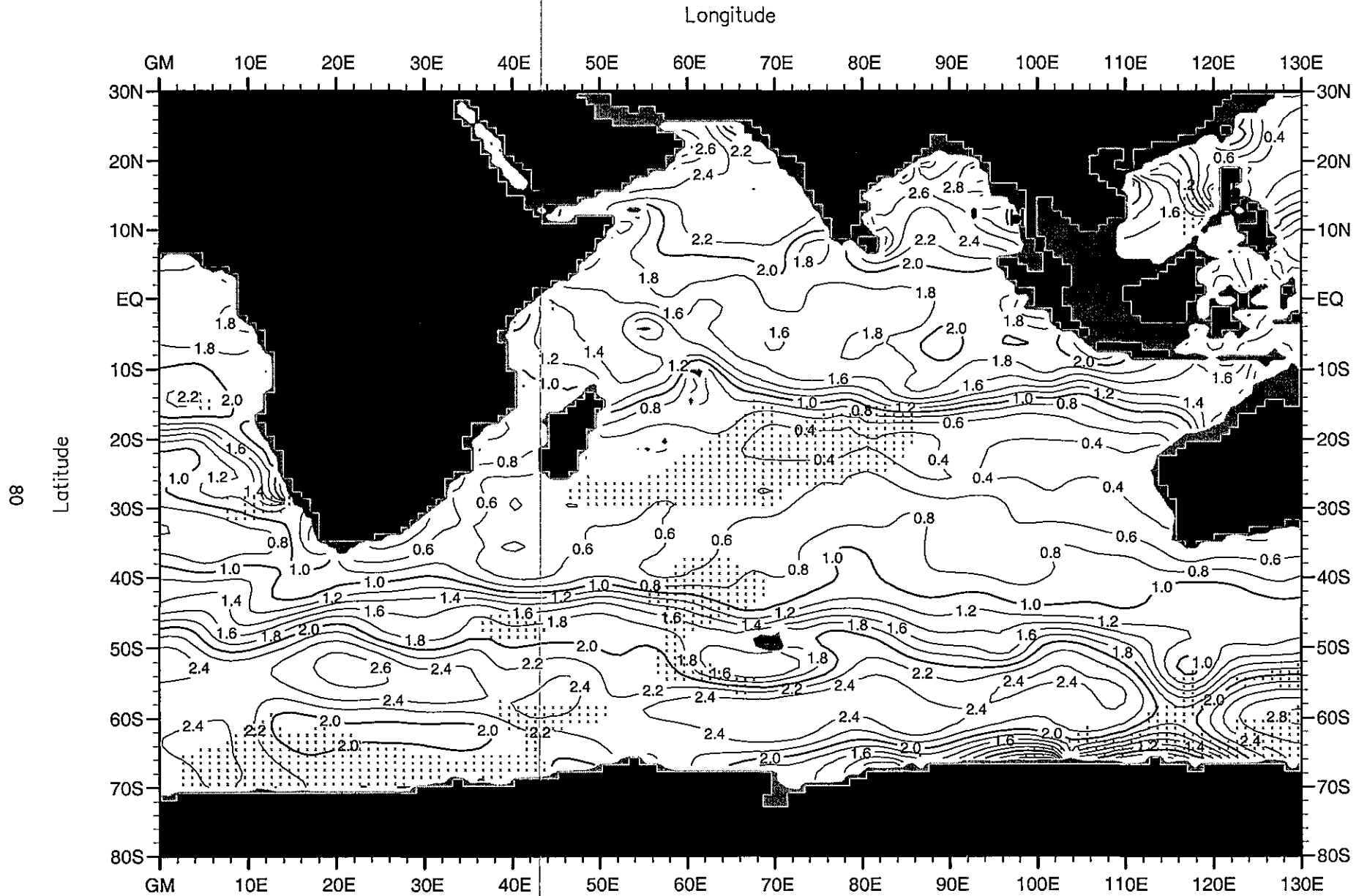
Fig. B48. Fall (Oct.-Dec.) mean phosphate (μM) at 250 m. depth.

Minimum Value= 0.03   Maximum Value= 3.15   Contour Interval: 0.20
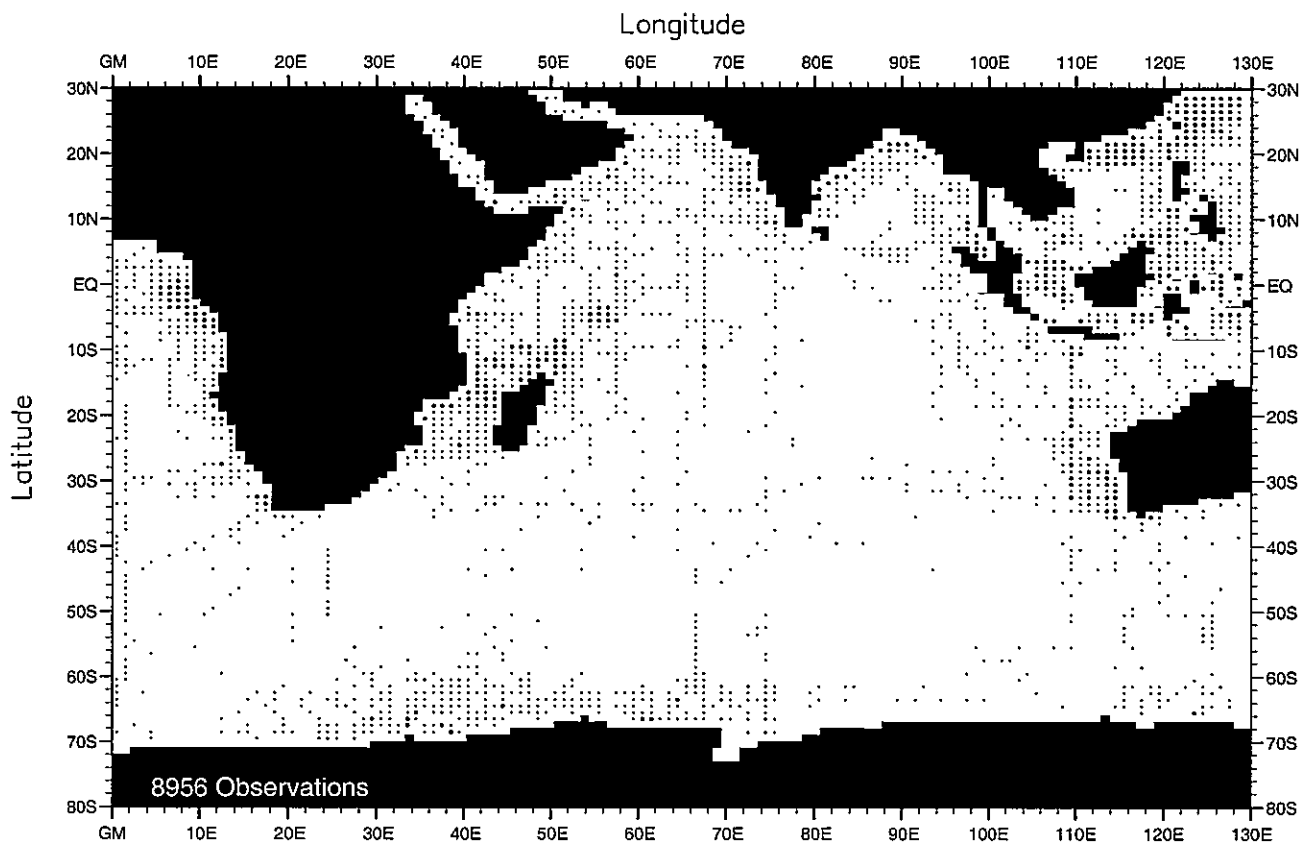
Fig. C1. Annual nitrate observations at the surface .
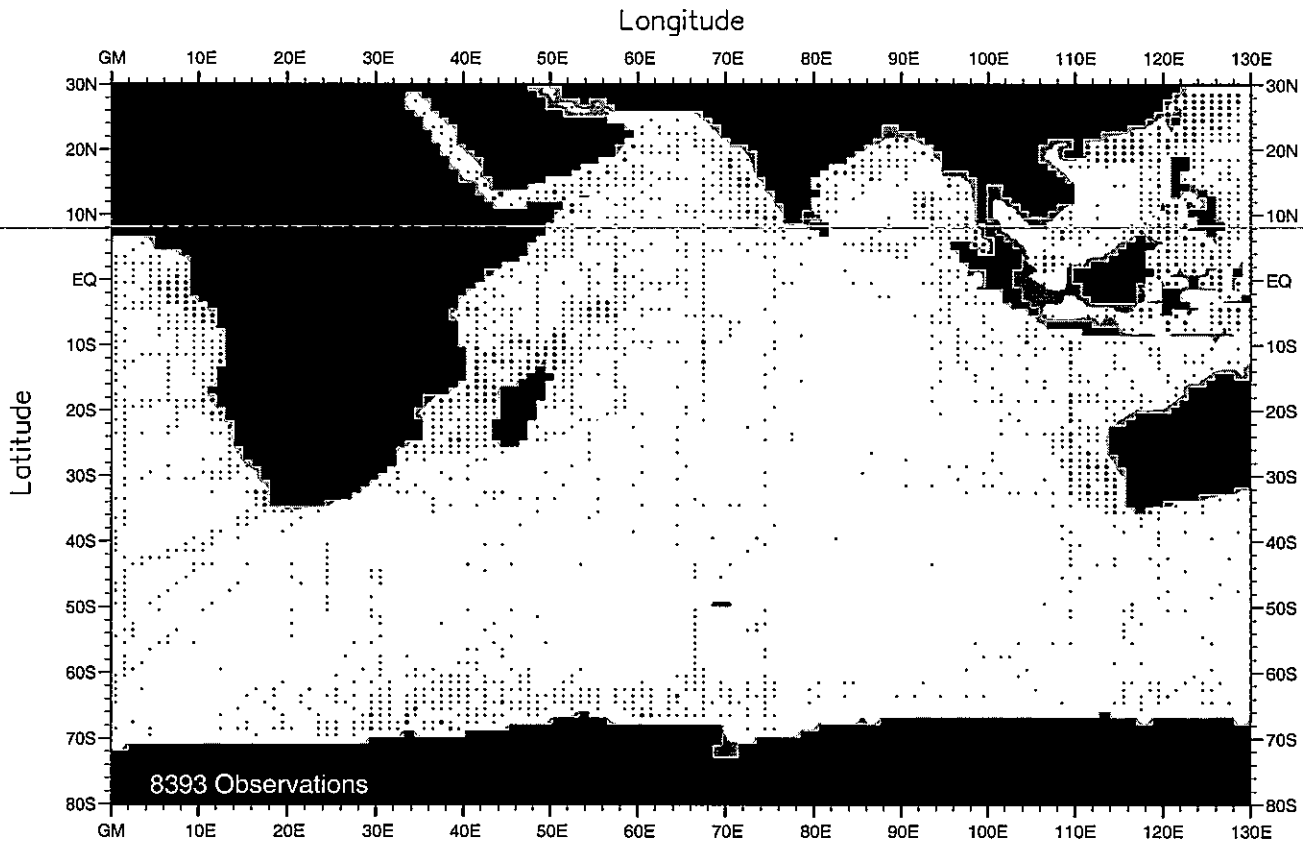
Fig. C2. Annual nitrate observations at 50 m. depth .
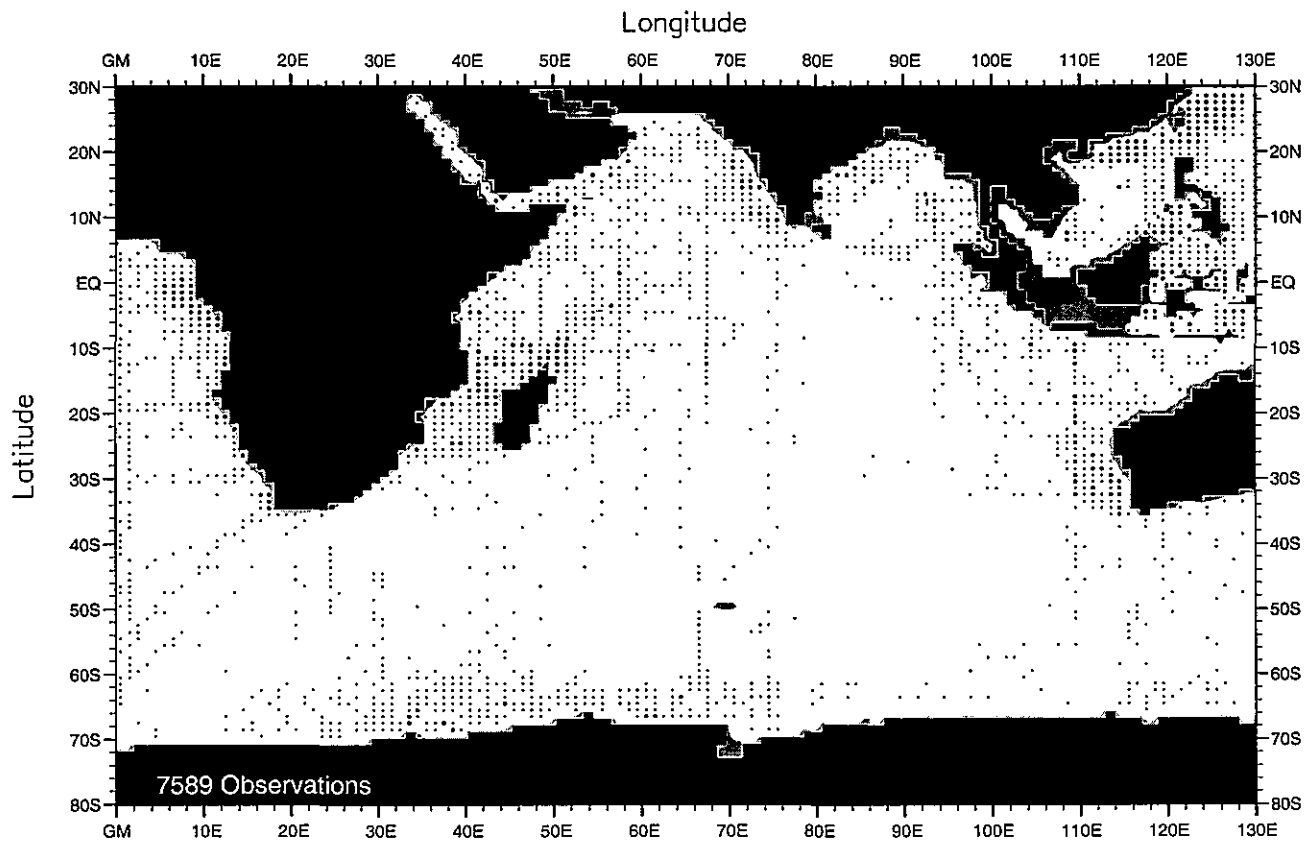
Fig. C3.   Annual nitrate observations at   75 m. depth .
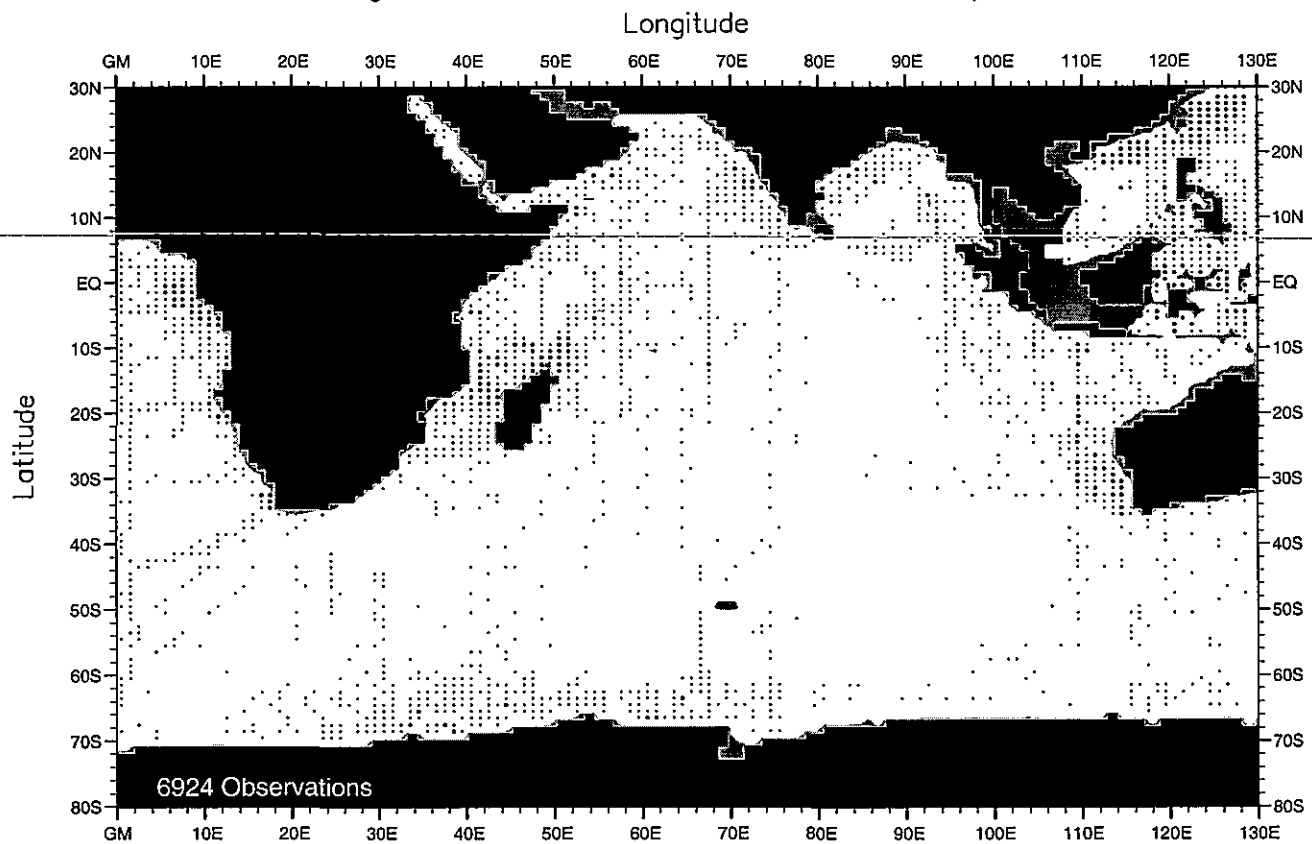
Fig. C4.   Annual nitrate observations at 100 m. depth .
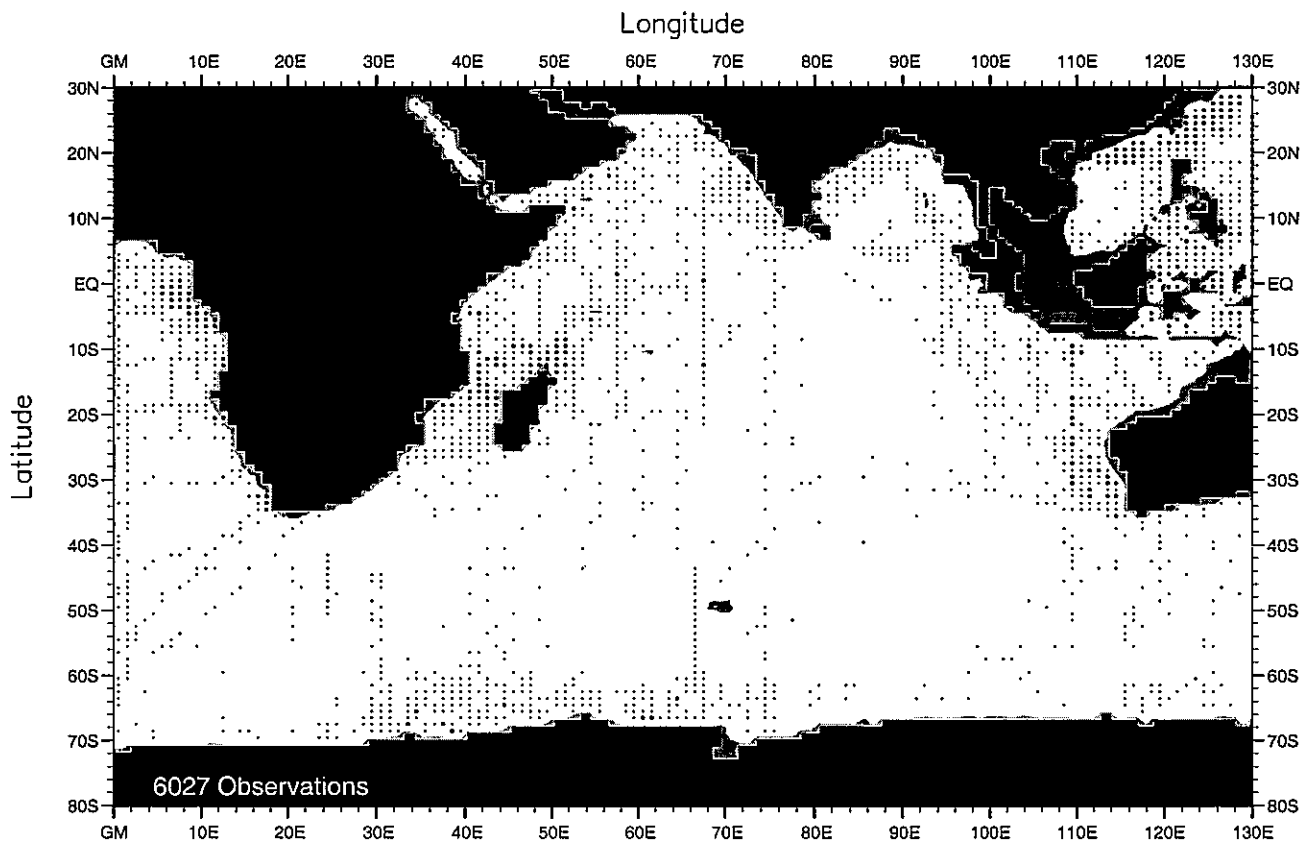
Fig. C5.   Annual nitrate observations at 150 m. depth .
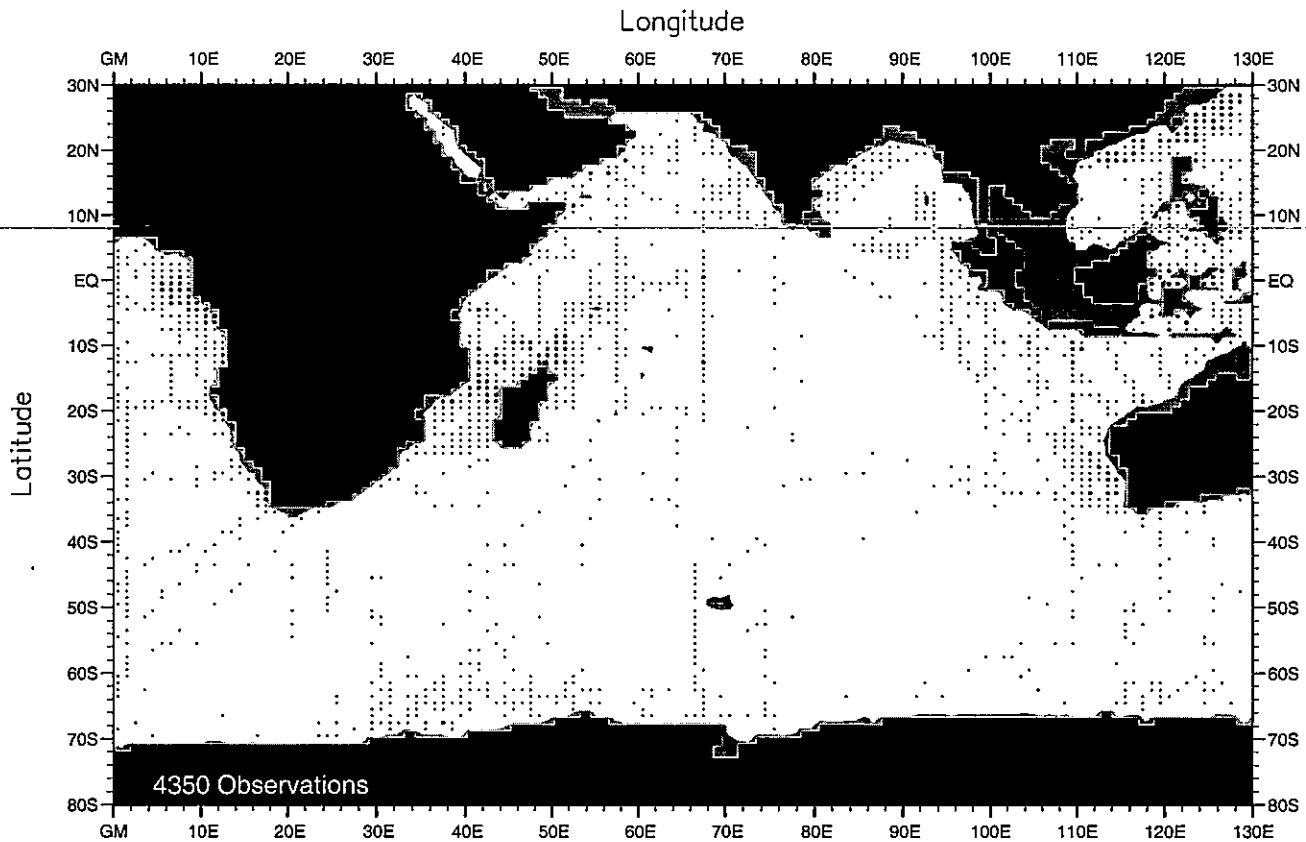
Fig. C6.   Annual nitrate observations at 200 m. depth .
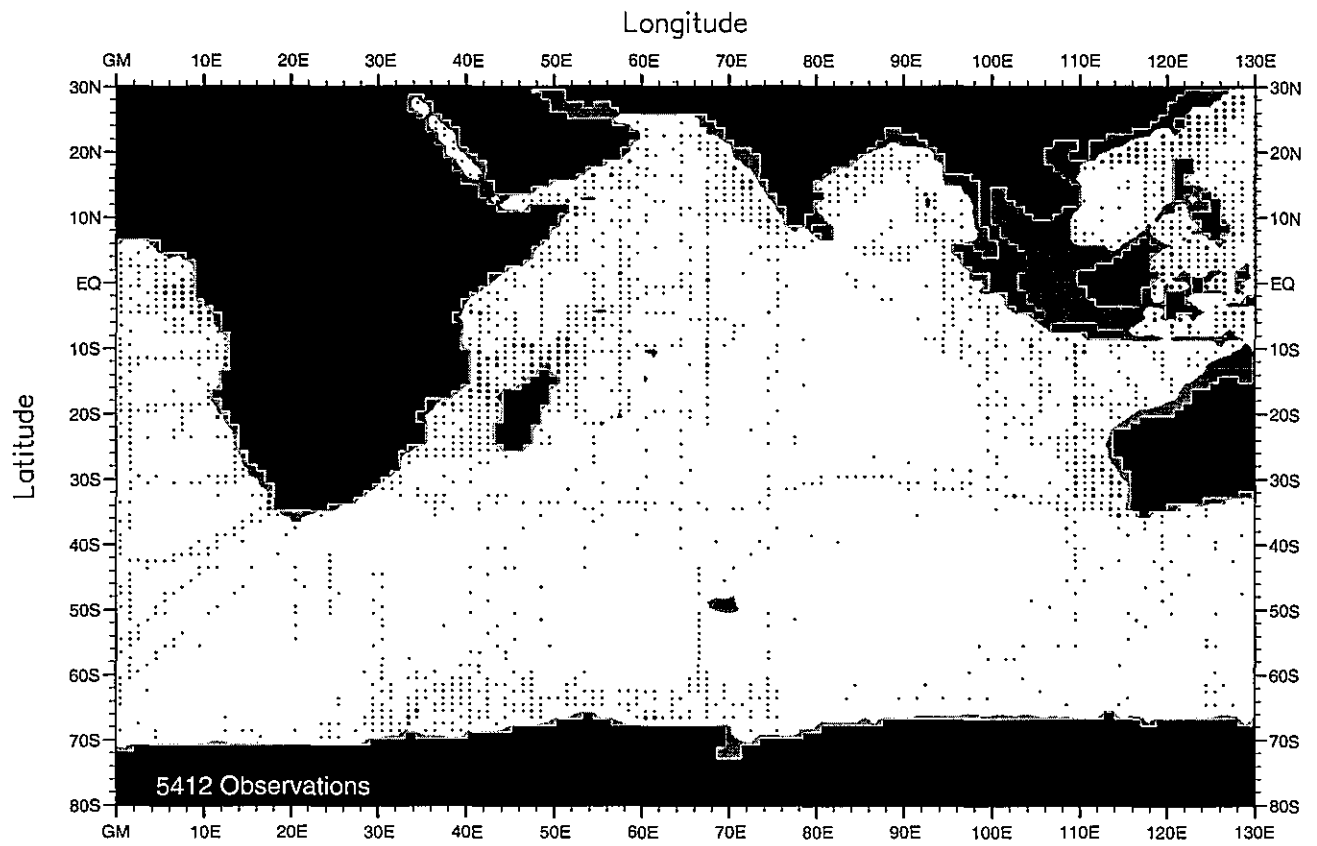
Fig. C7.   Annual nitrate observations at 250 m. depth .
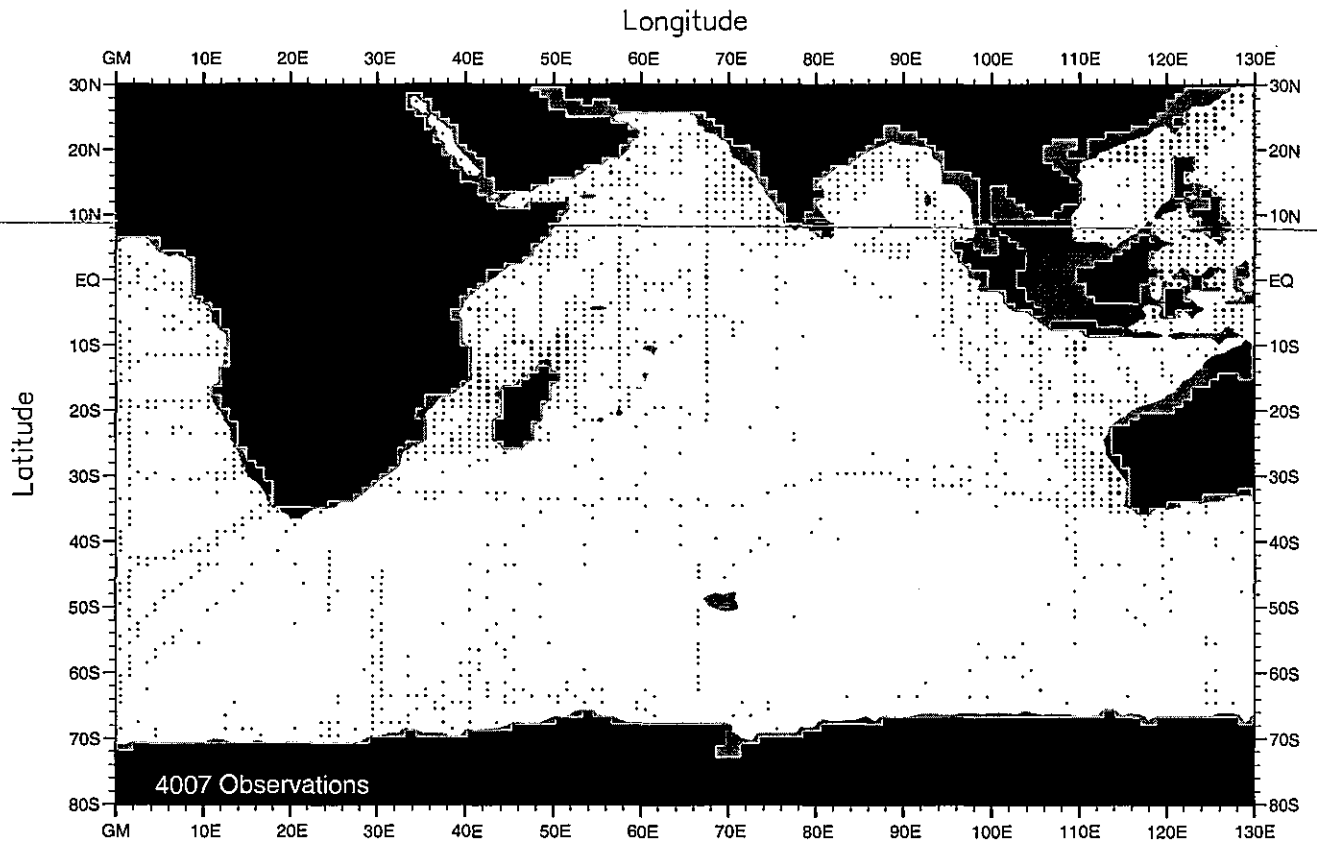
Fig. C8.   Annual nitrate observations at 400 m. depth .
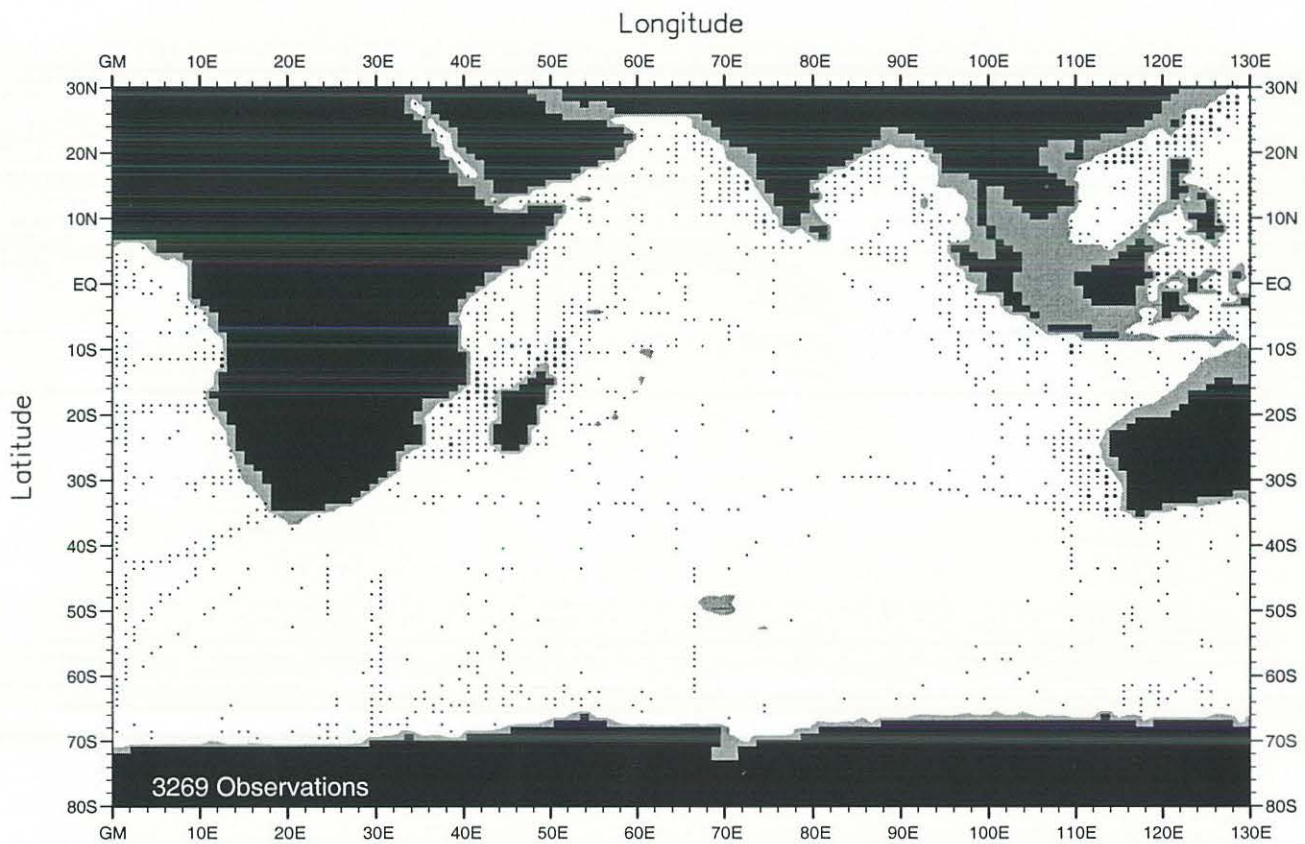
Fig. C9. Annual nitrate observations at 500 m. depth .
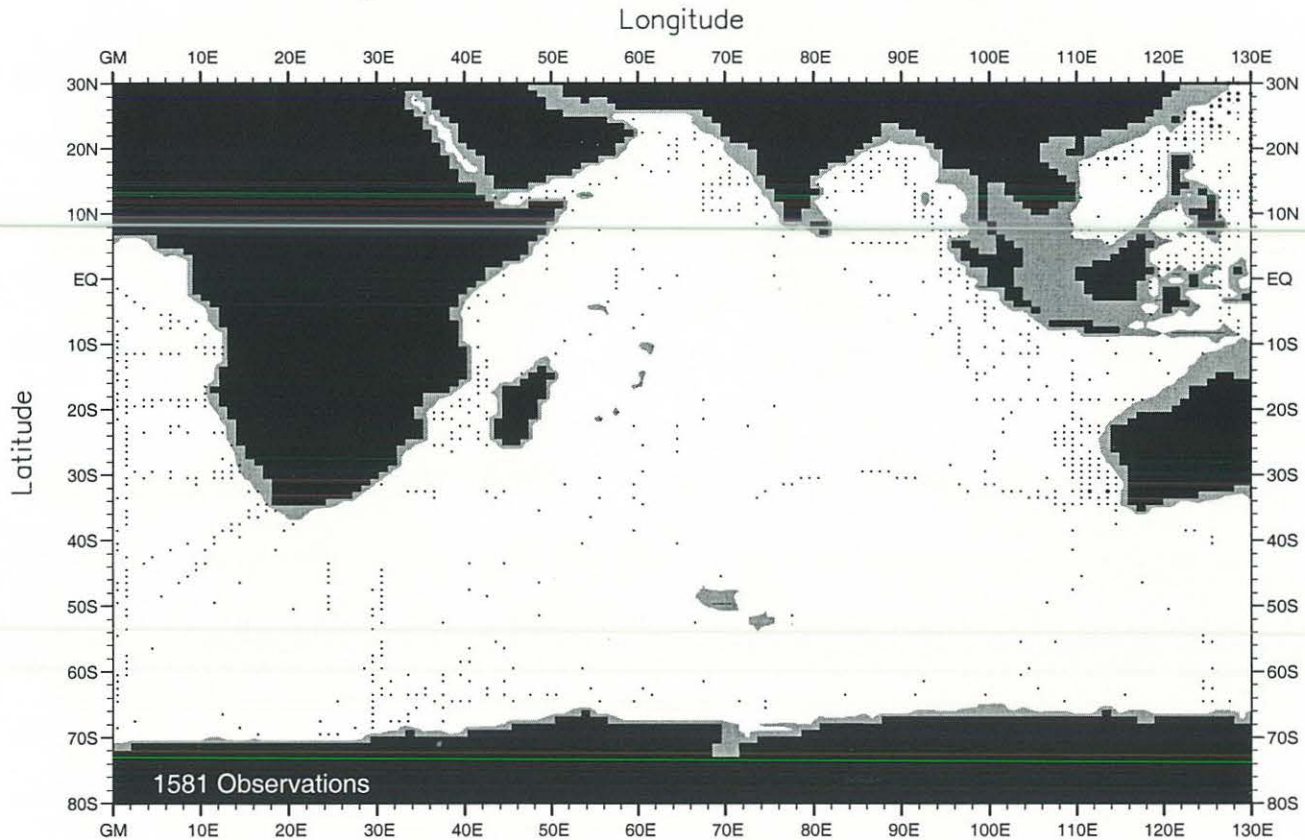
Fig. C10. Annual nitrate observations at 700 m. depth .
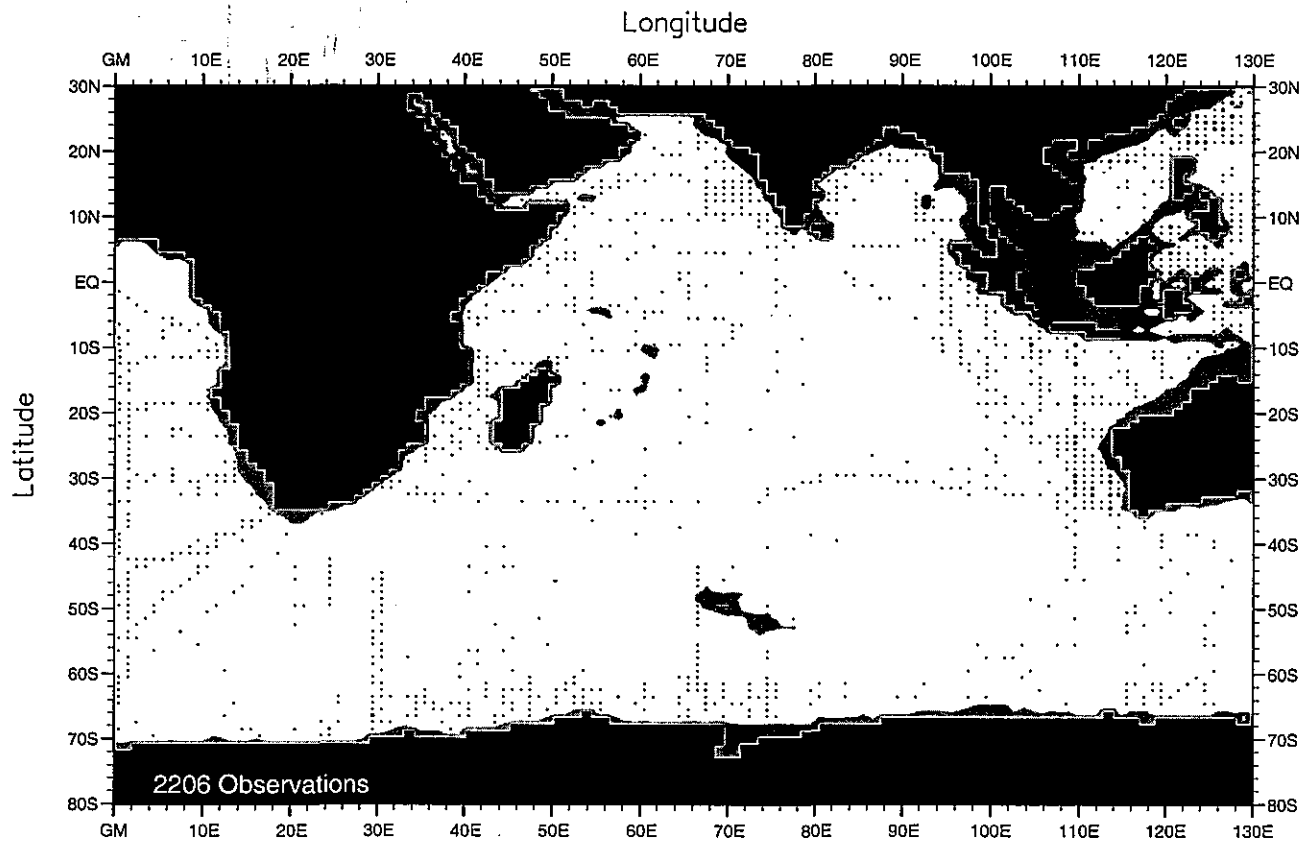
Fig. C11. Annual nitrate observations at 1000 m. depth .
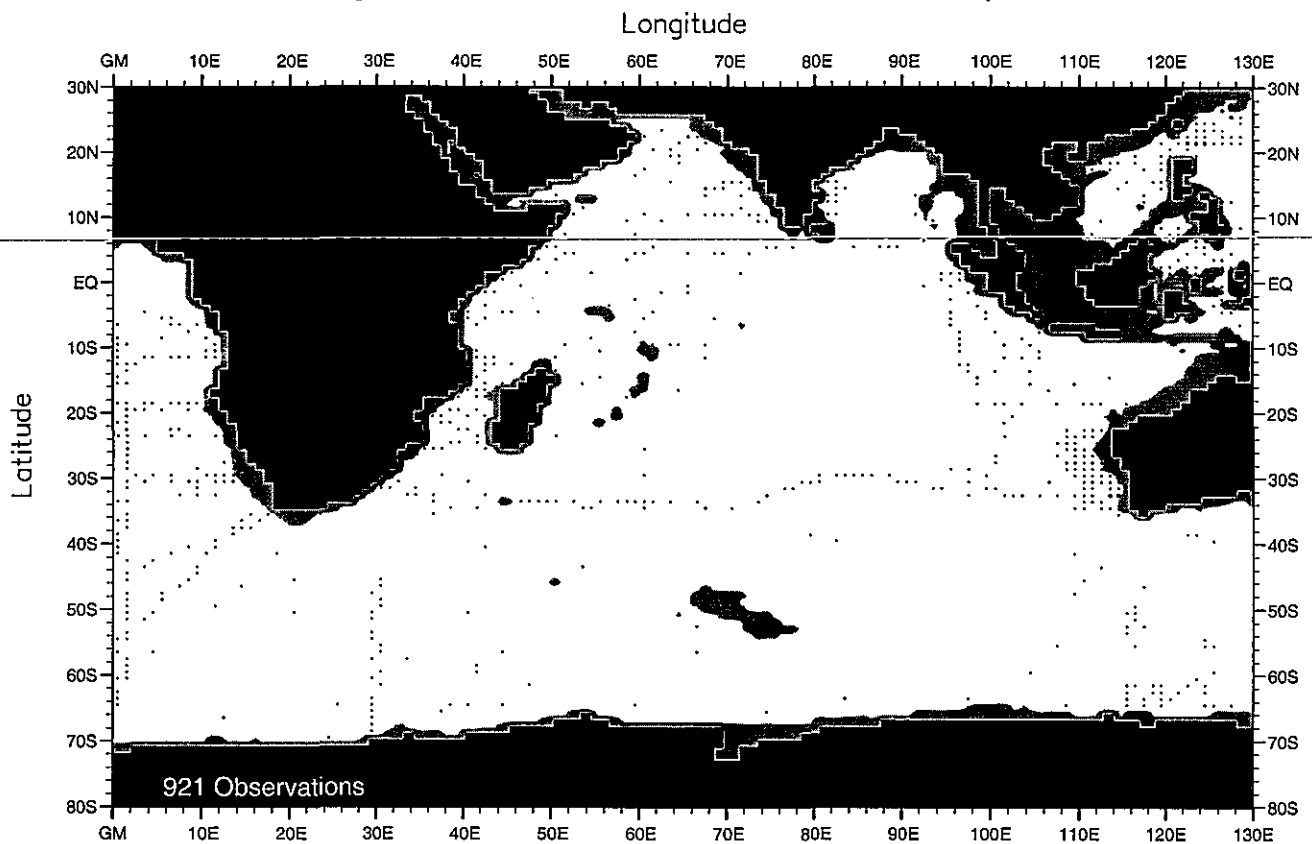
Fig. C12. Annual nitrate observations at 1500 m. depth .
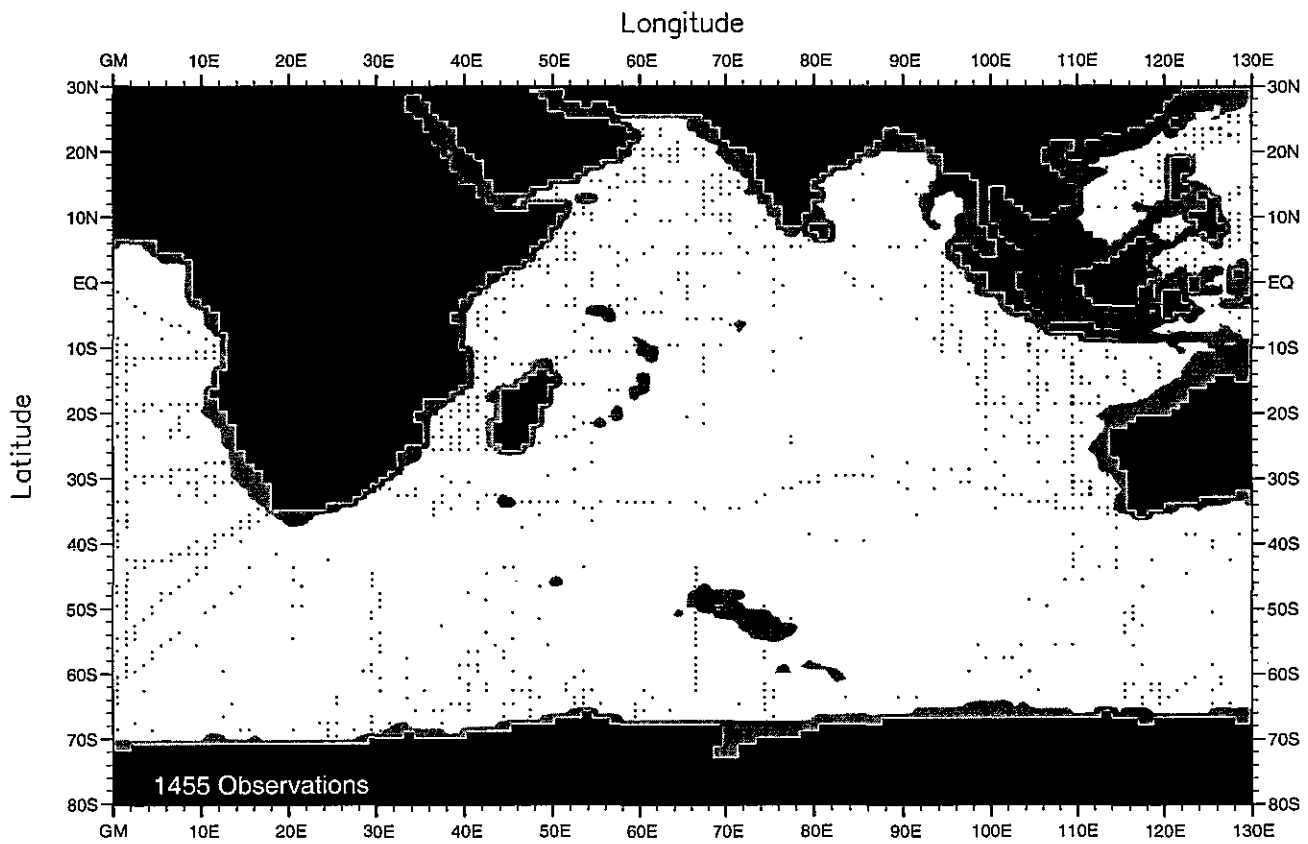
Fig. C13.   Annual nitrate observations at 2000 m. depth .
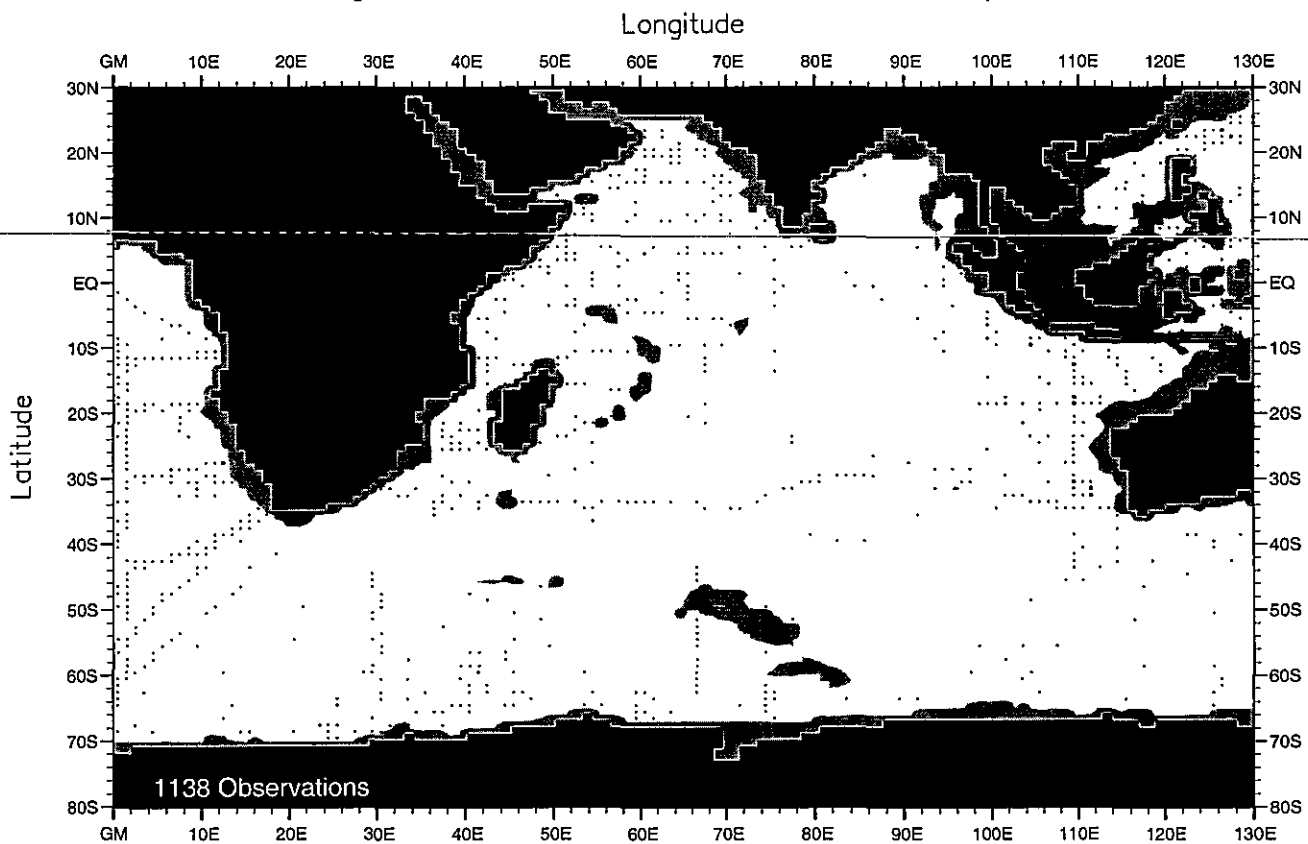
Fig. C14.   Annual nitrate observations at 2500 m. depth .
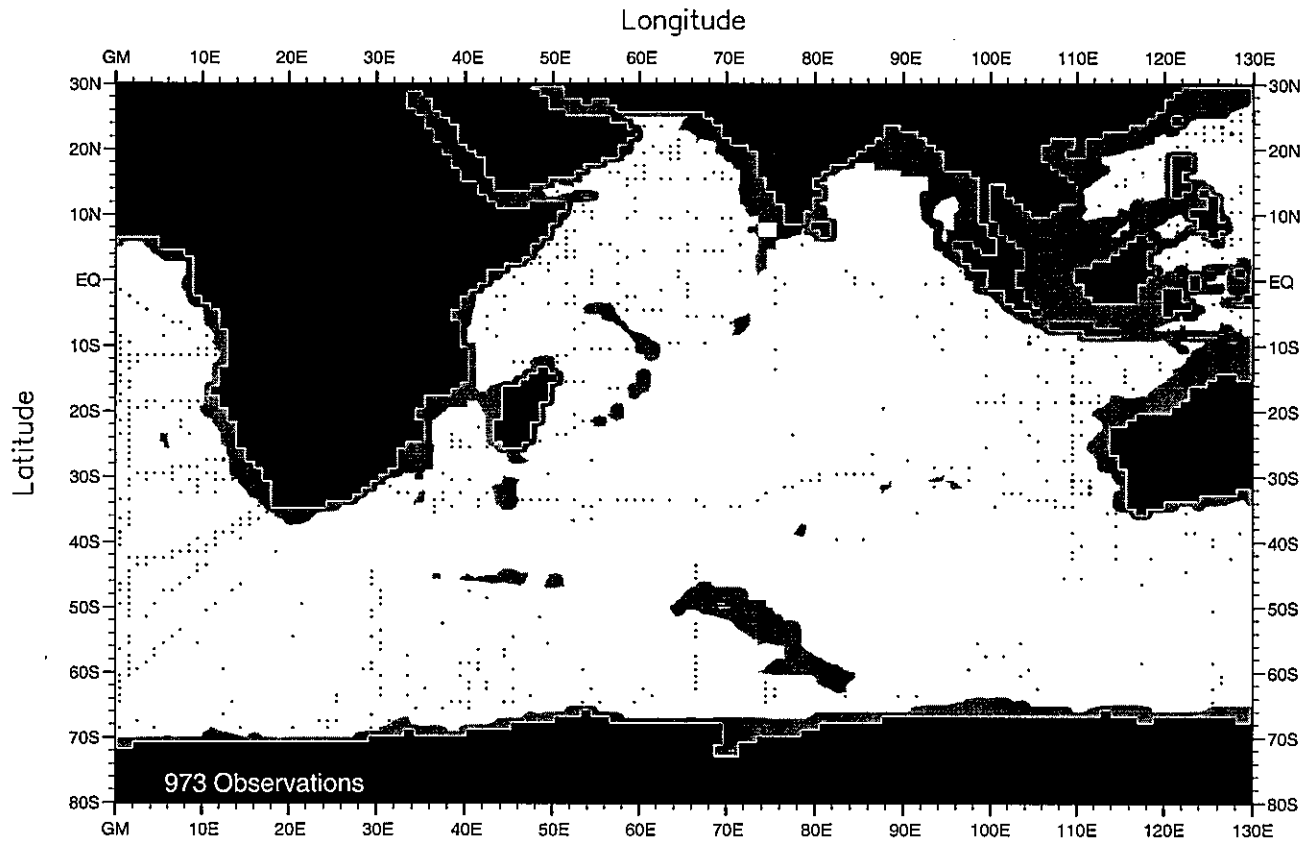
Fig. C15.   Annual nitrate observations at 3000 m. depth .
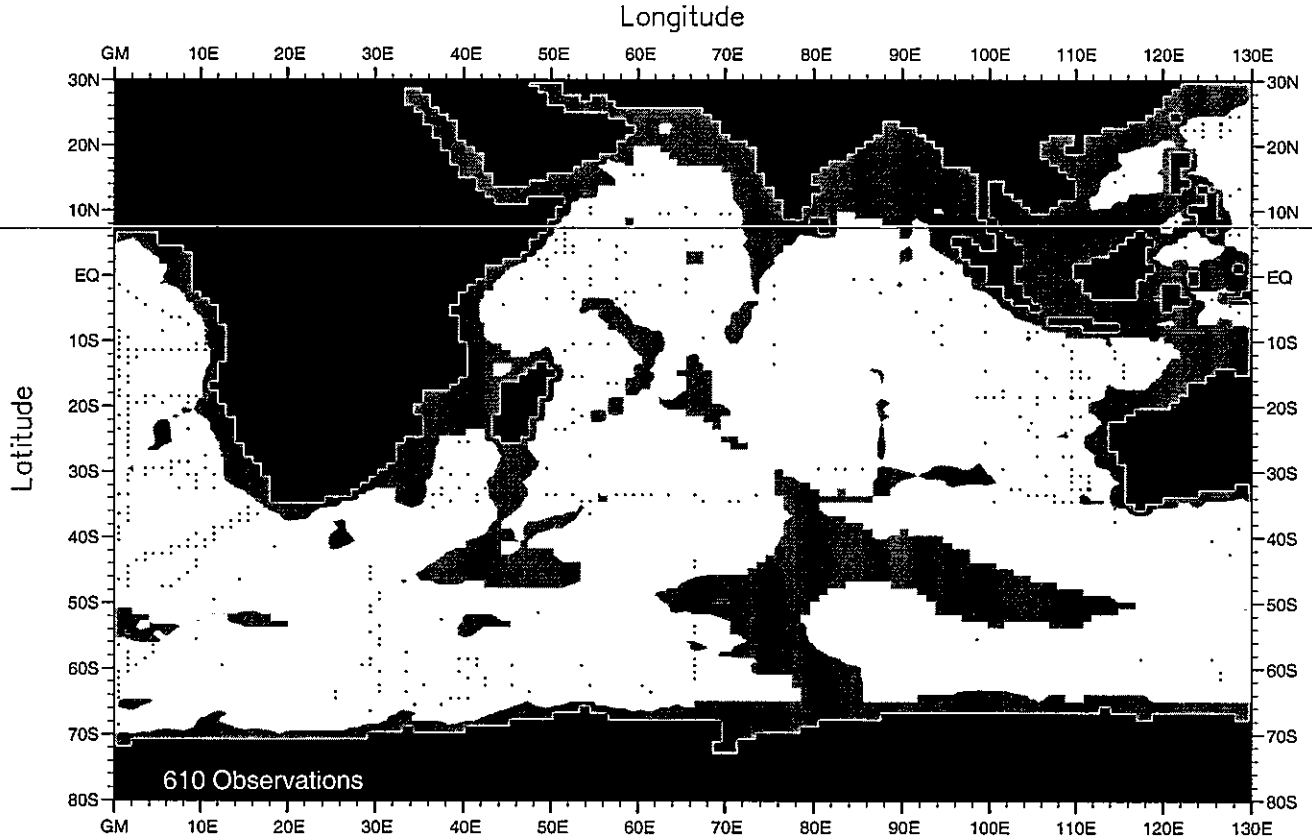
Fig. C16.   Annual nitrate observations at 4000 m. depth .
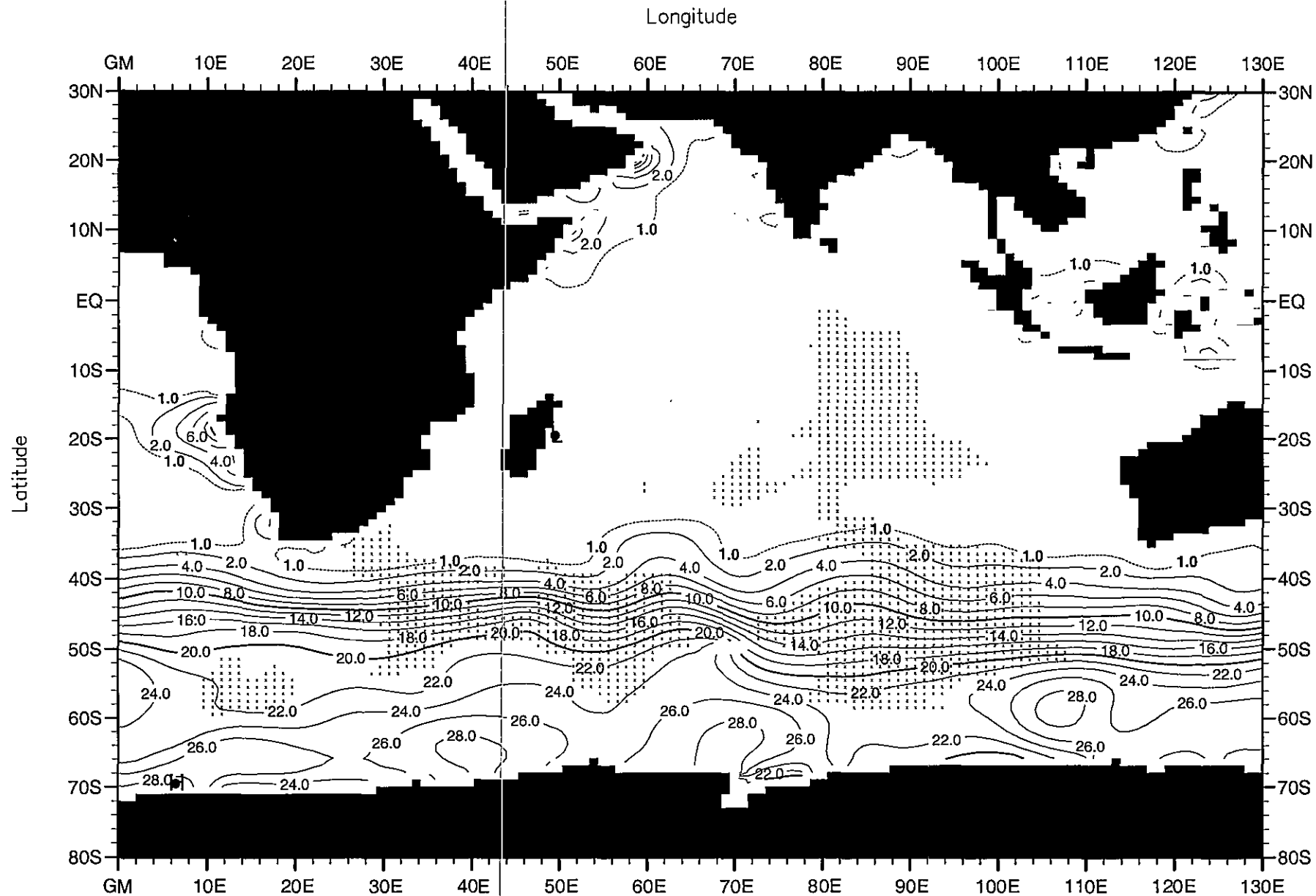
Fig. C17. Annual mean nitrate (μM) at the surface .

Minimum Value= 0.00   Maximum Value= 29.30   Contour Interval: 2.00
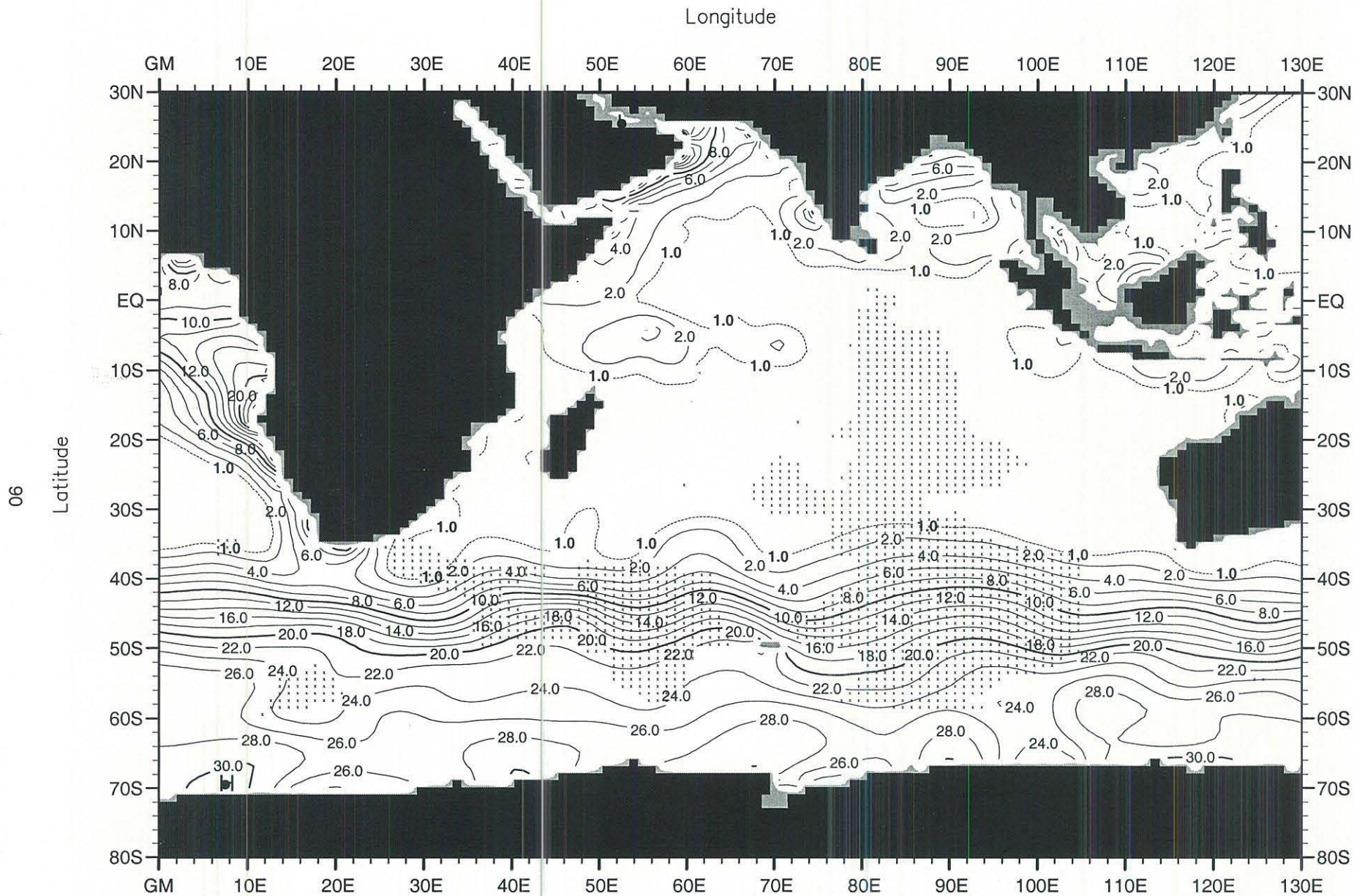
Fig. C18. Annual mean nitrate (μM) at 50 m. depth .

Minimum Value= 0.00   Maximum Value= 31.69   Contour Interval: 2.00
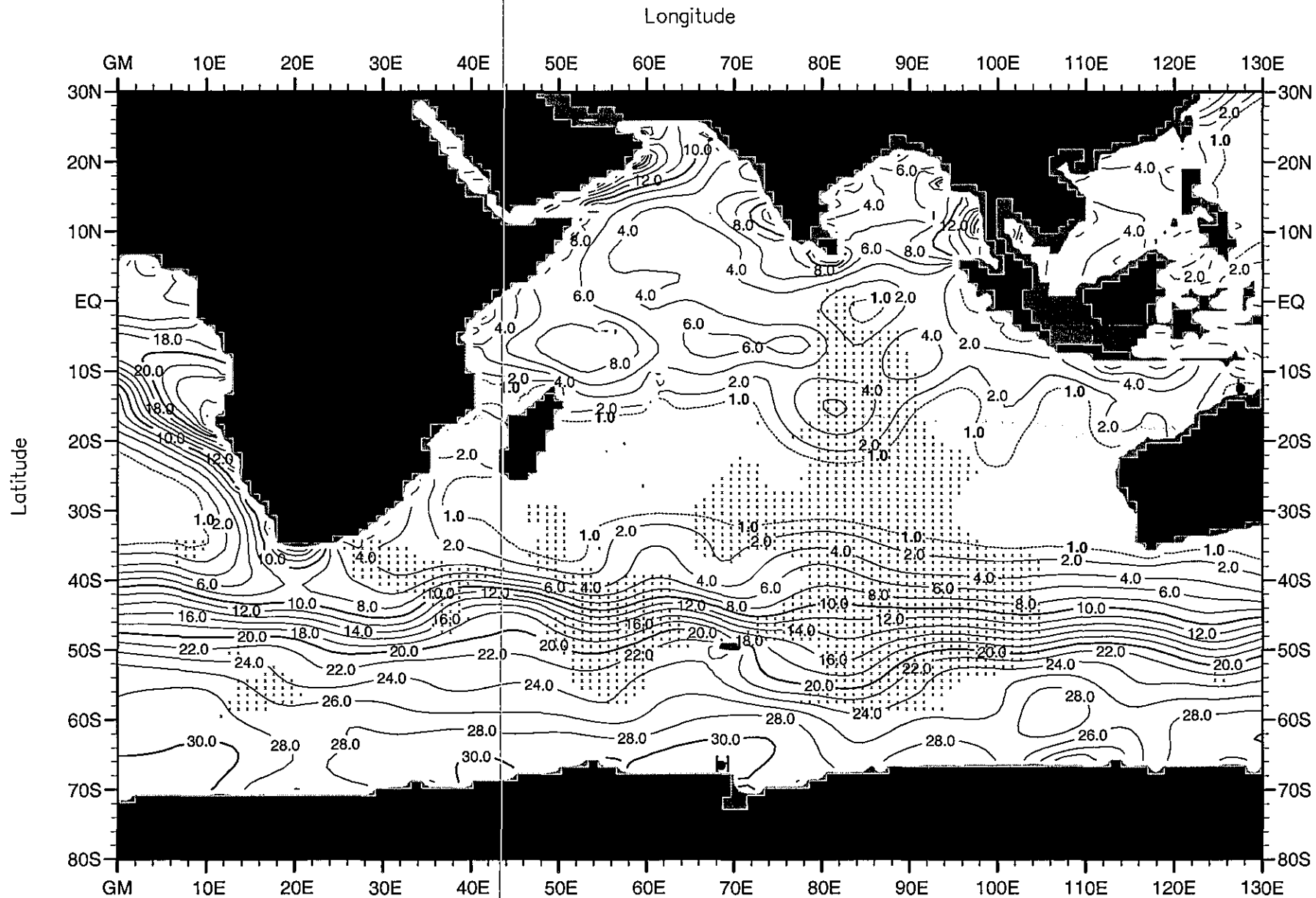
Fig. C19.   Annual mean nitrate (μM) at   75 m. depth .

Minimum Value=   0.06   Maximum Value=   31.80   Contour Interval: 2.00
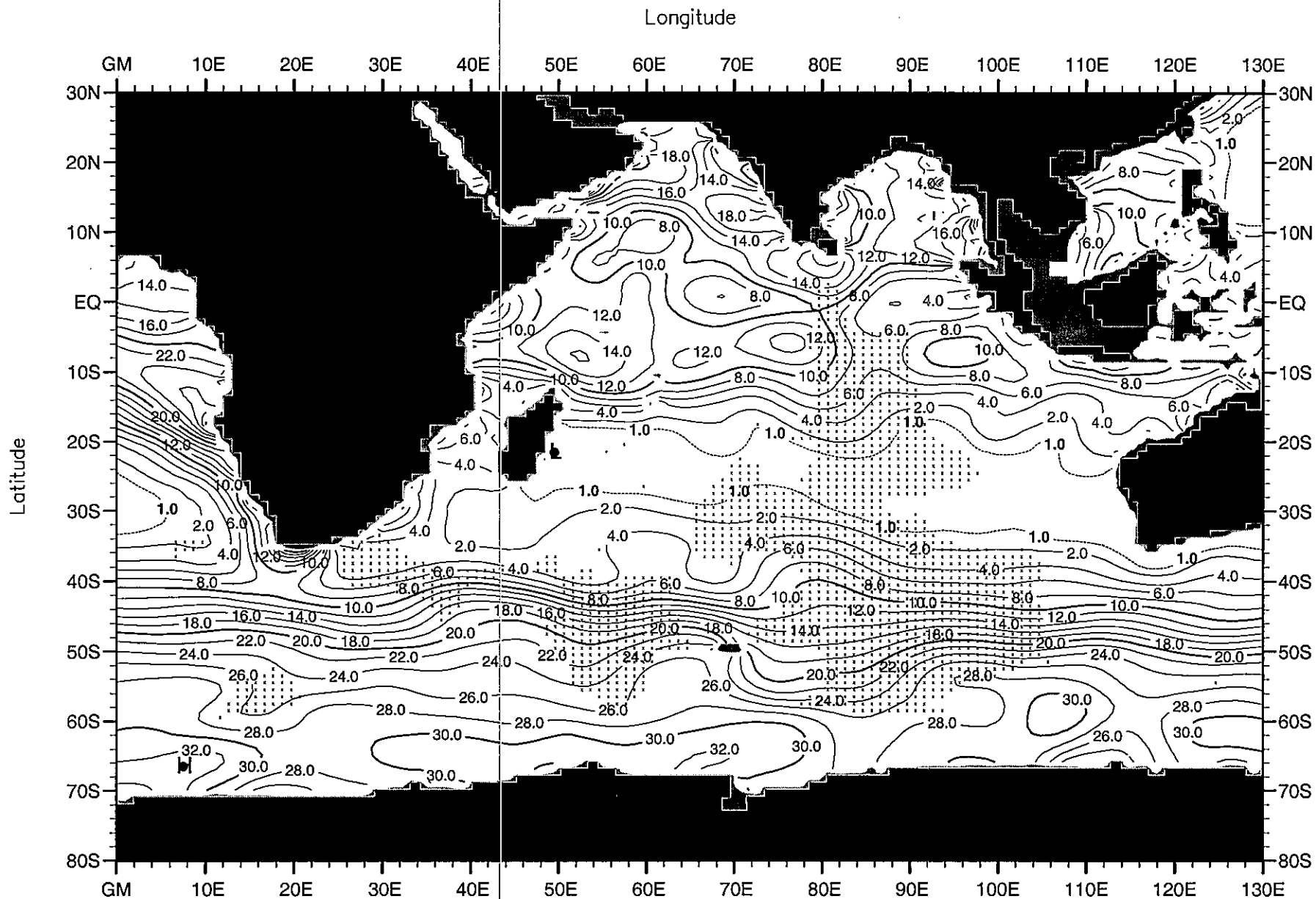
Fig. C20. Annual mean nitrate (μM) at 100 m. depth .

Minimum Value= 0.02   Maximum Value= 32.86   Contour Interval: 2.00
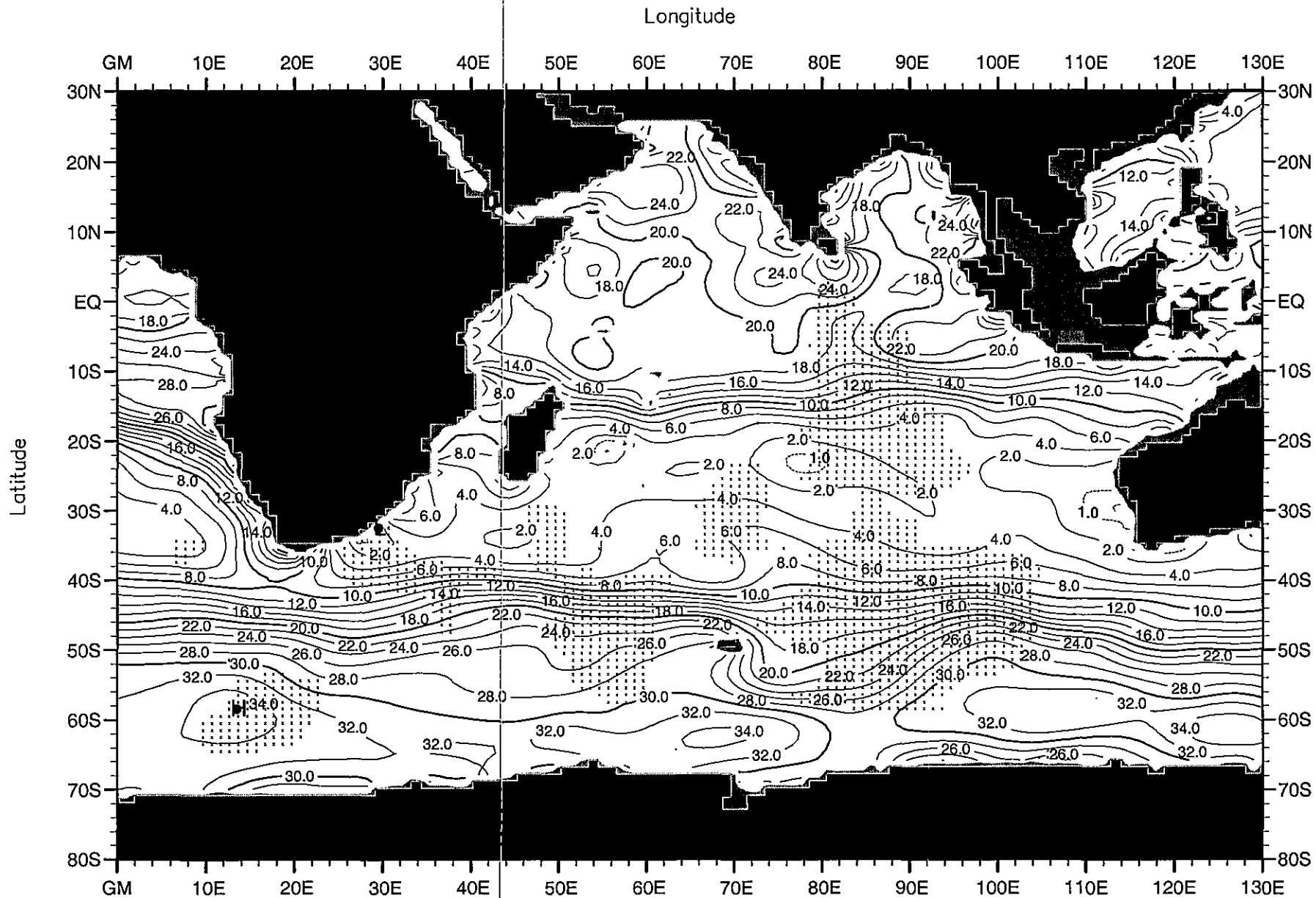
Fig. C21. Annual mean nitrate (μM) at 150 m. depth .

Minimum Value= 0.13   Maximum Value= 35.27   Contour Interval: 2.00
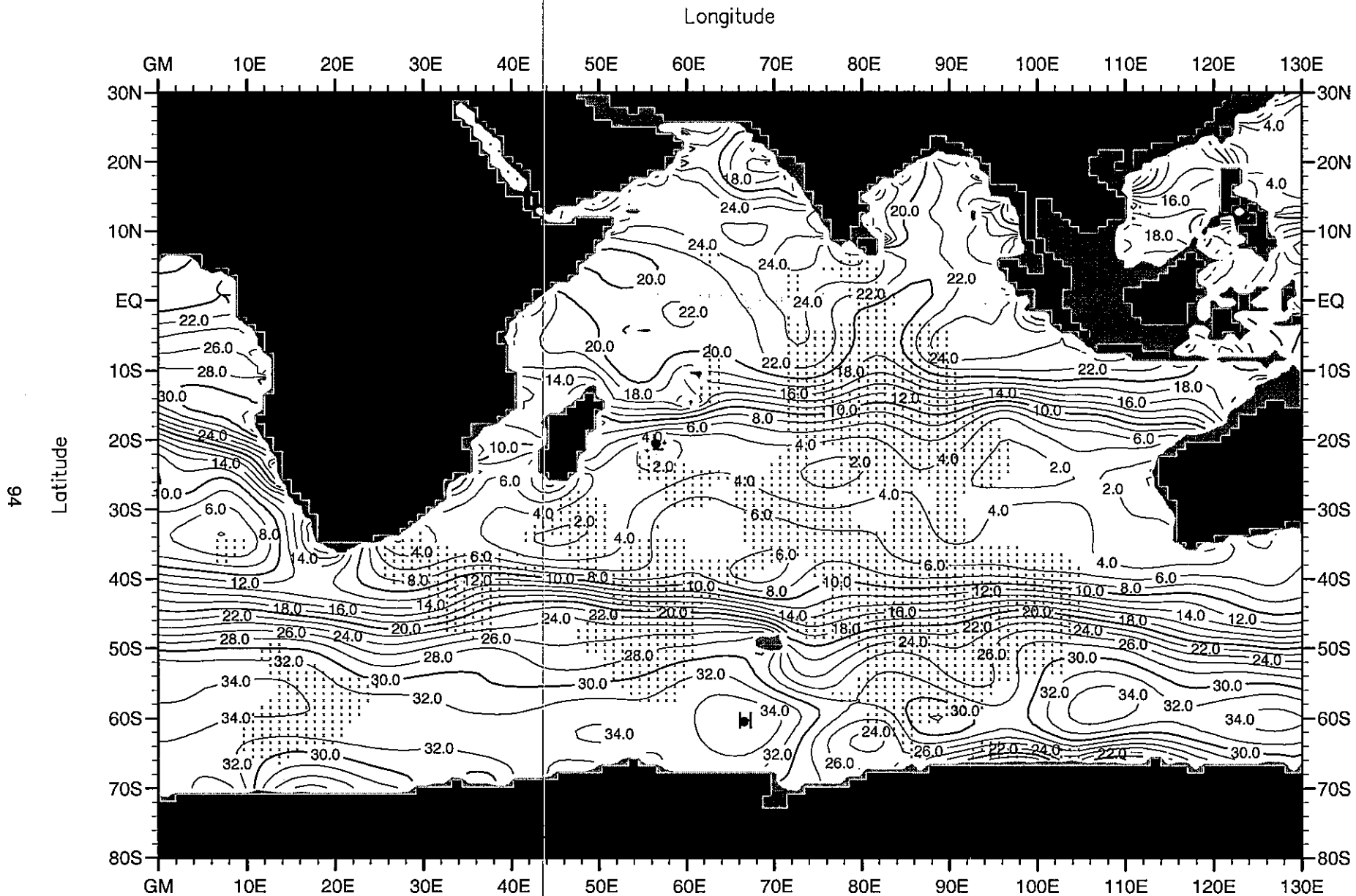
Fig. C22.   Annual mean nitrate (μM) at 200 m. depth .

Minimum Value=   0.67   Maximum Value=   35.89   Contour Interval: 2.00
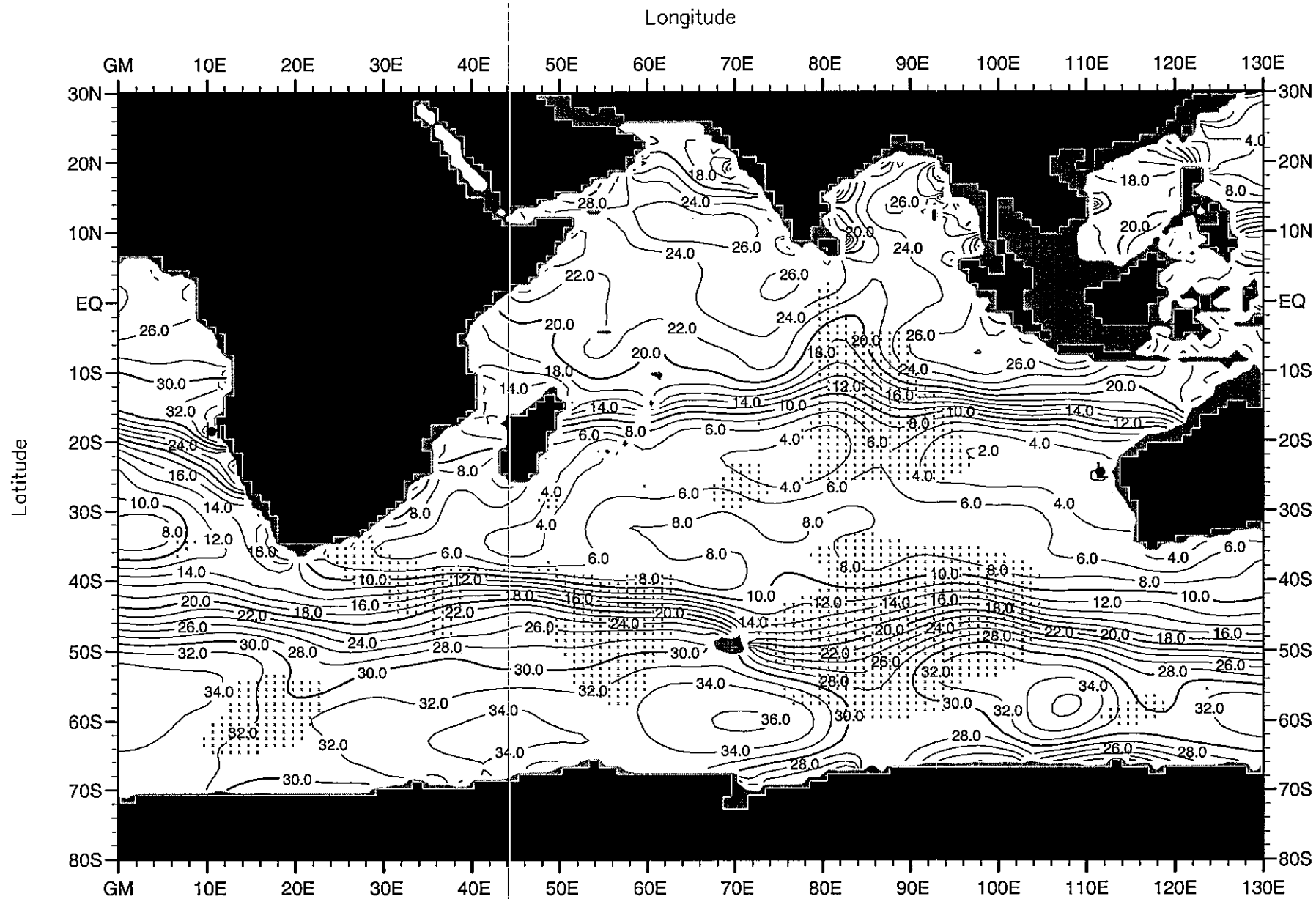
Fig. C23. Annual mean nitrate (μM) at 250 m. depth .

Minimum Value= 1.16   Maximum Value= 36.91   Contour Interval: 2.00
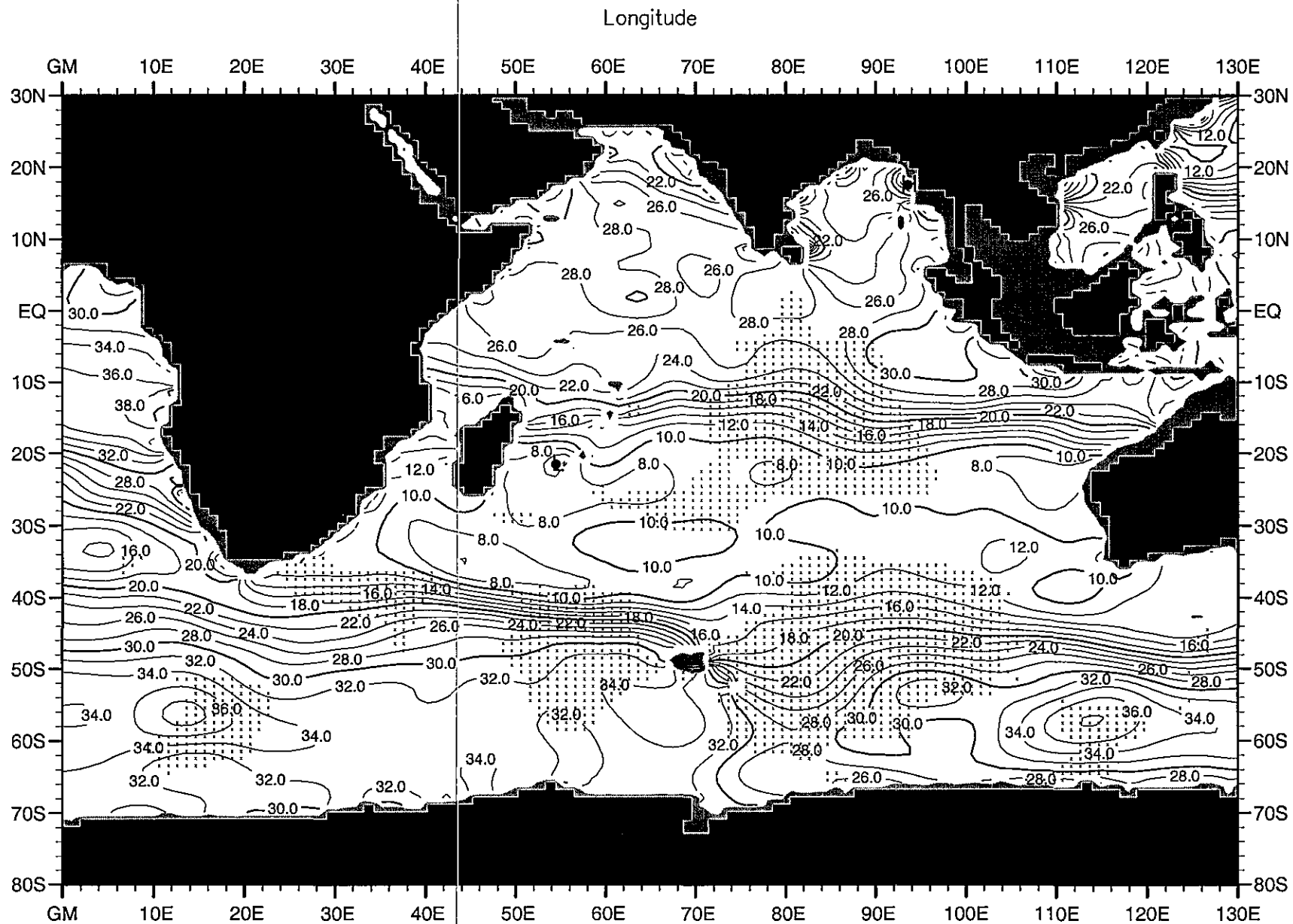
Fig. C24.   Annual mean nitrate (μM) at 400 m. depth .

Minimum Value=   3.84   Maximum Value=   42.49   Contour Interval: 2.00
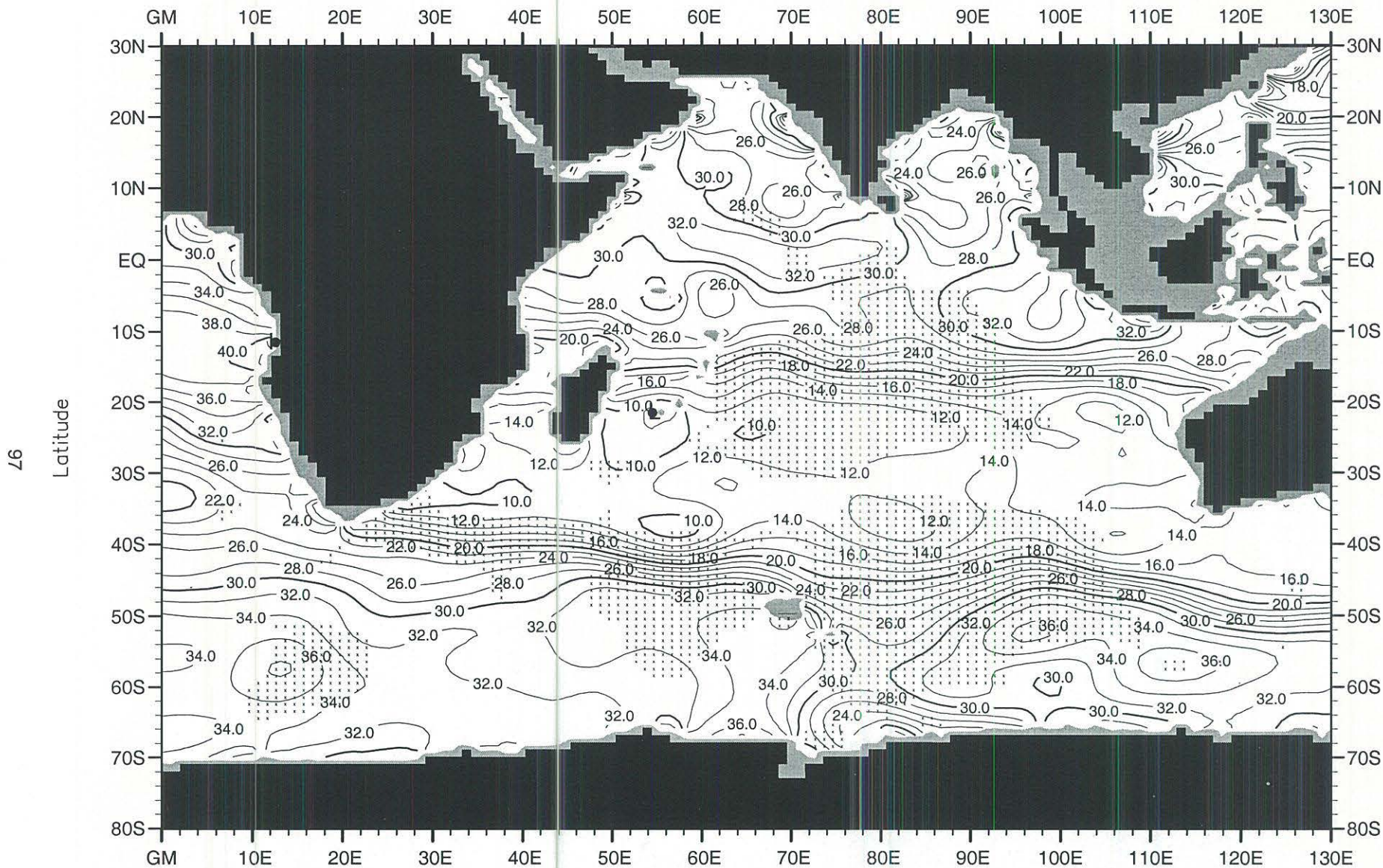
Fig. C25. Annual mean nitrate (μM) at 500 m. depth .

Minimum Value= 5.92   Maximum Value= 43.38   Contour Interval: 2.00
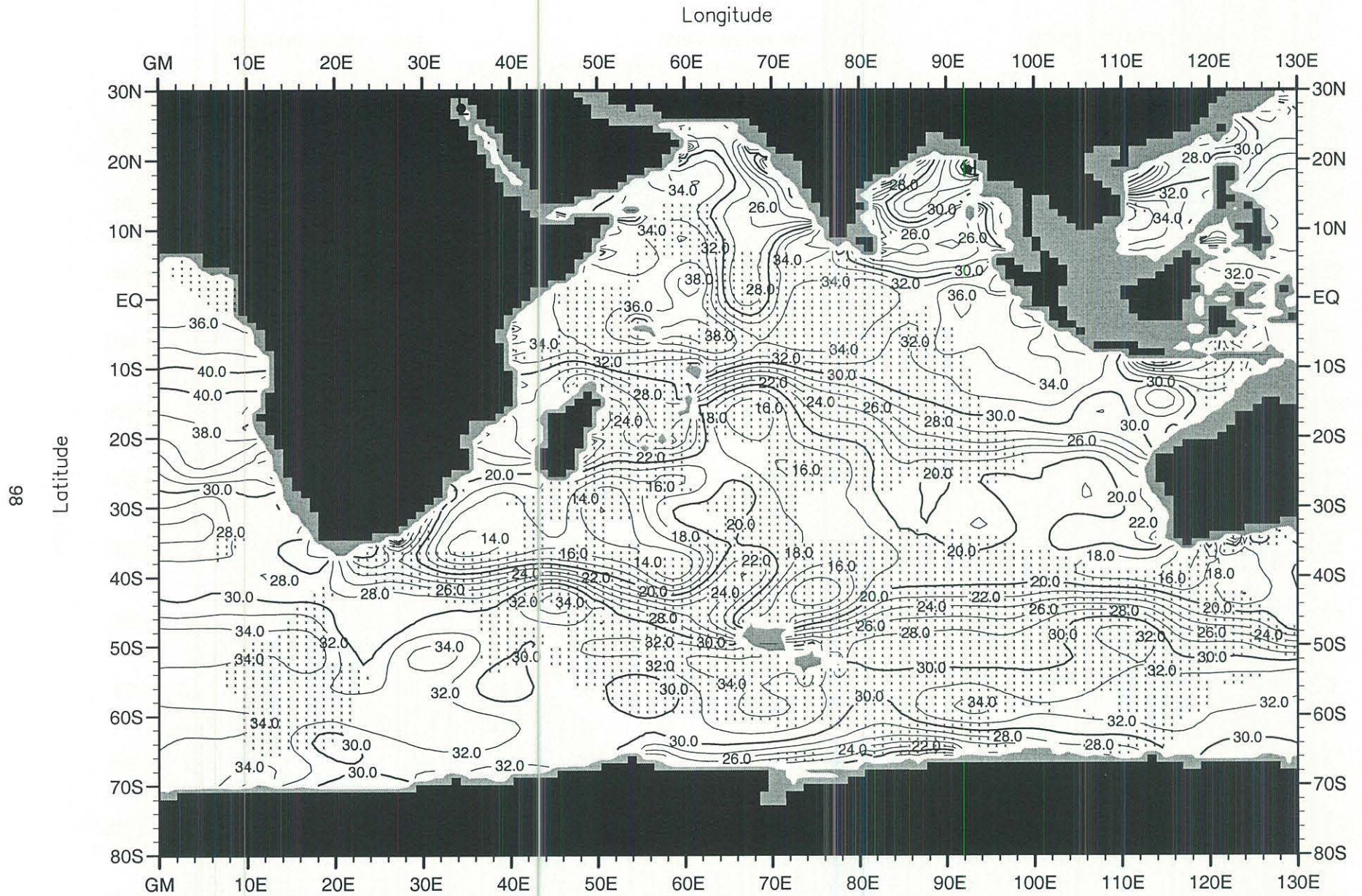
Fig. C26. Annual mean nitrate (μM) at 700 m. depth.

Minimum Value= 6.90   Maximum Value= 46.26   Contour Interval: 2.00
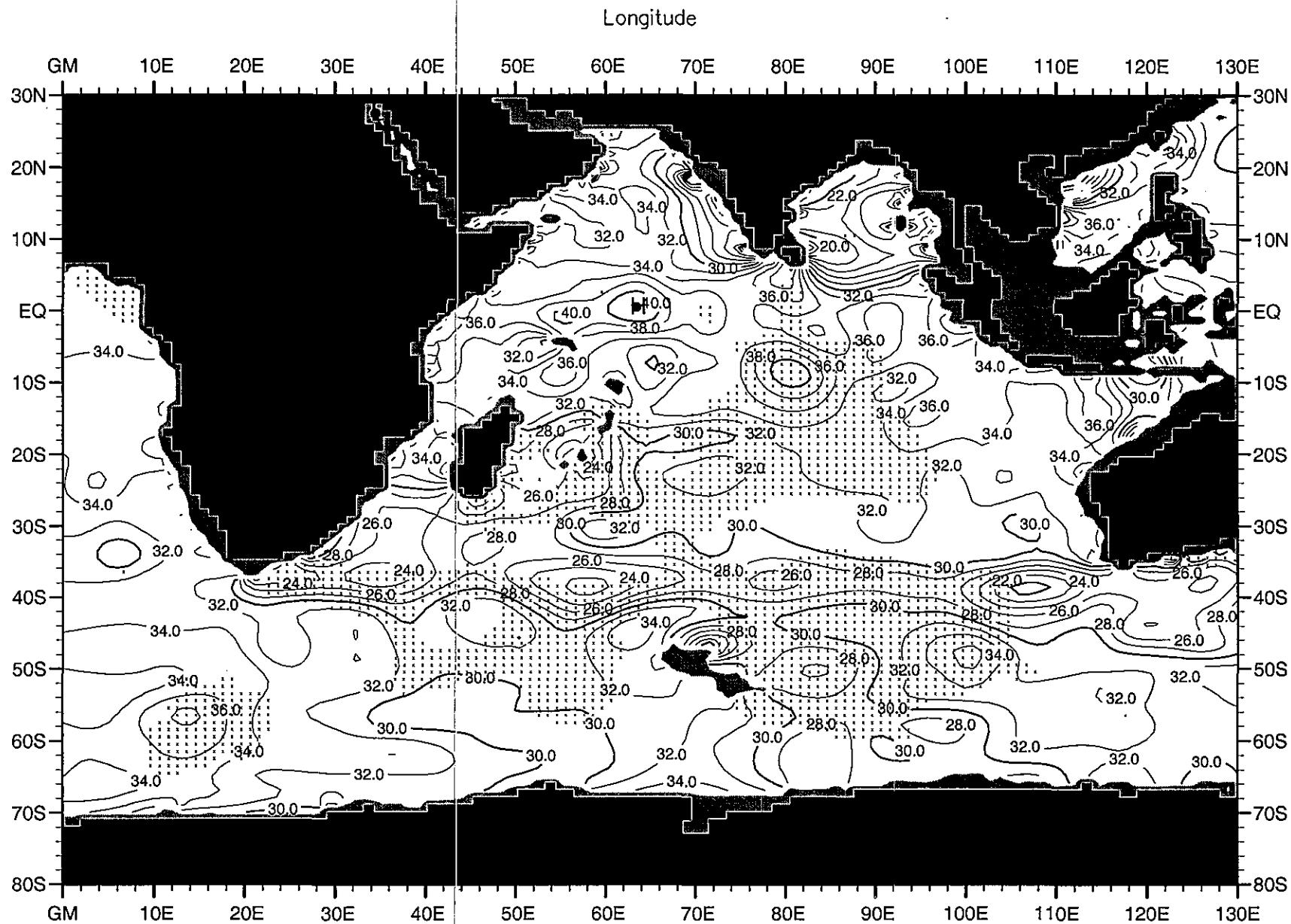
Fig. C27. Annual mean nitrate (μM) at 1000 m. depth .

Minimum Value= 6.60   Maximum Value= 42.05   Contour Interval: 2.00
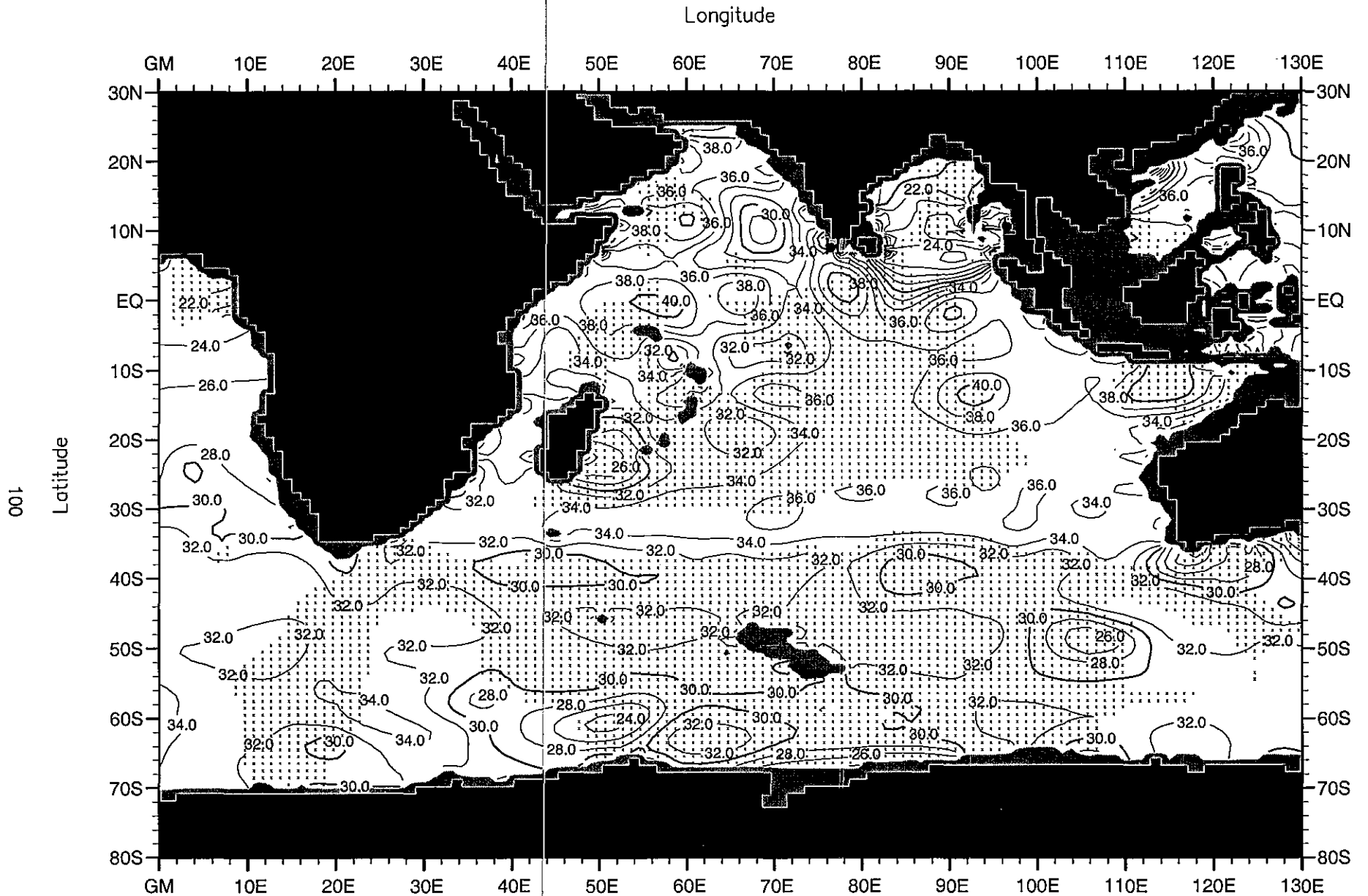
Fig. C28. Annual mean nitrate (μM) at 1500 m. depth .

Minimum Value= 7.89   Maximum Value= 45.62   Contour Interval: 2.00
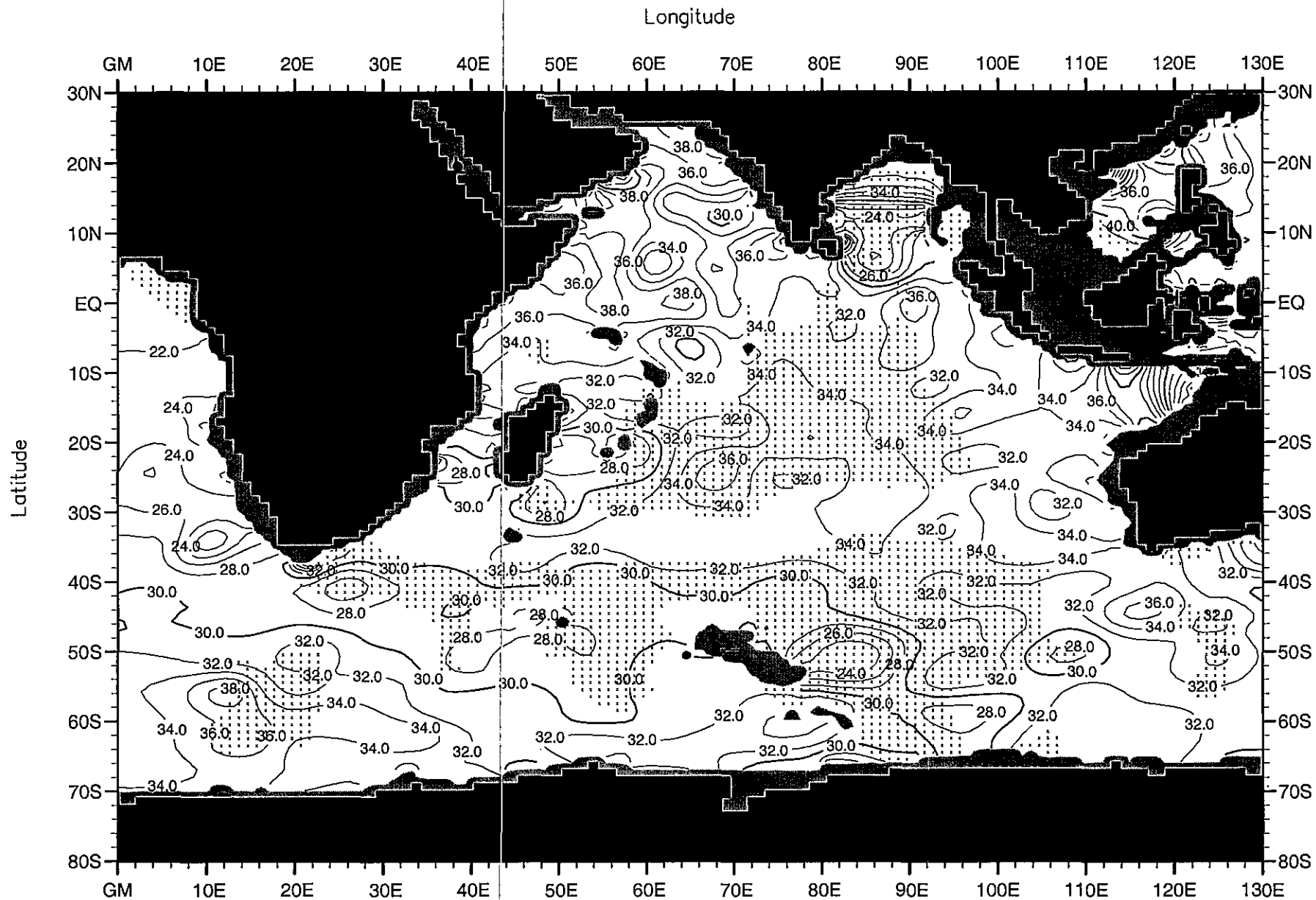
Fig. C29. Annual mean nitrate (μM) at 2000 m. depth .

Minimum Value= 12.31   Maximum Value= 46.73   Contour Interval: 2.00
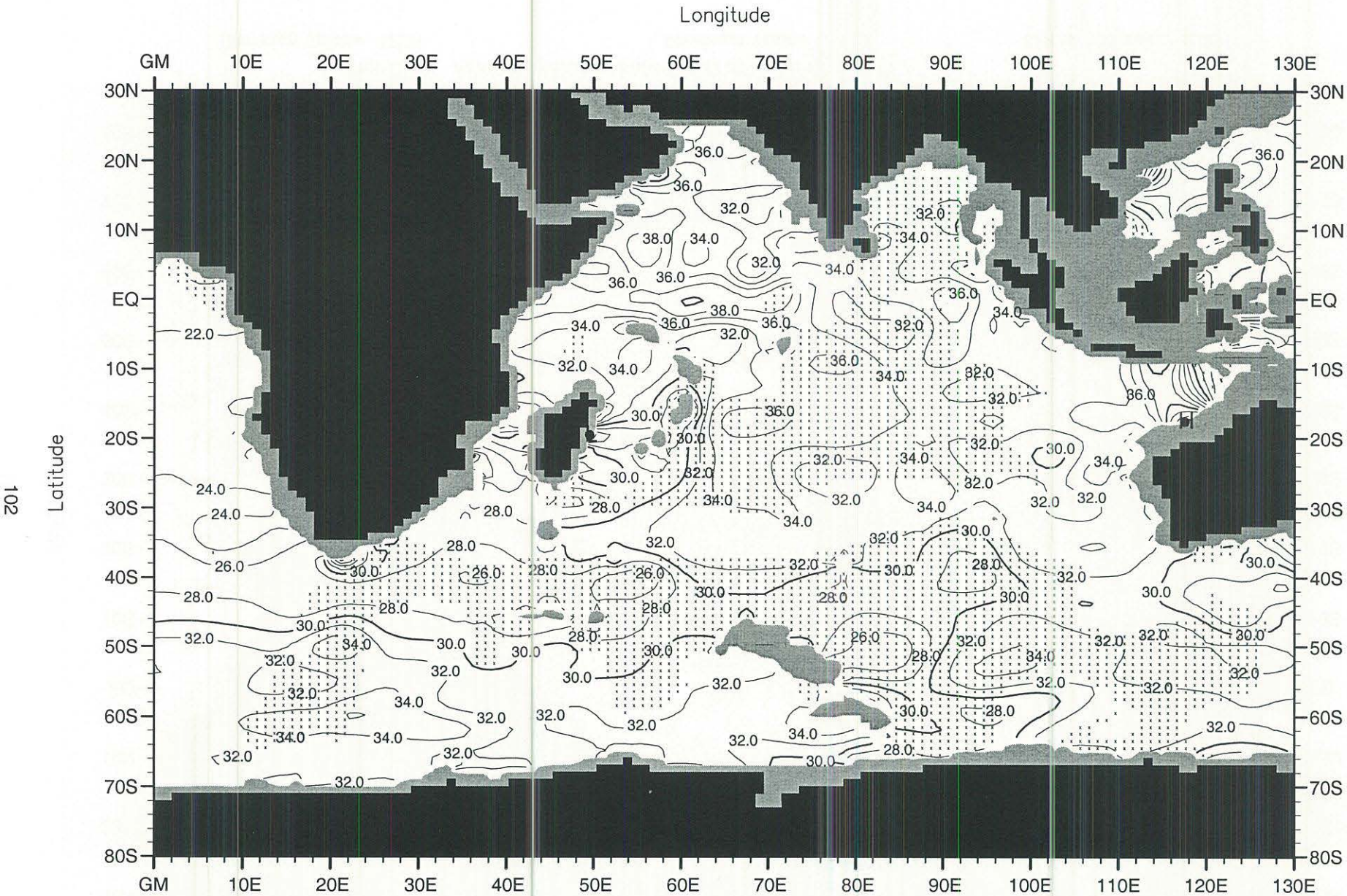
Fig. C30. Annual mean nitrate (μM) at 2500 m. depth .

Minimum Value= 19.00   Maximum Value= 46.09   Contour Interval: 2.00
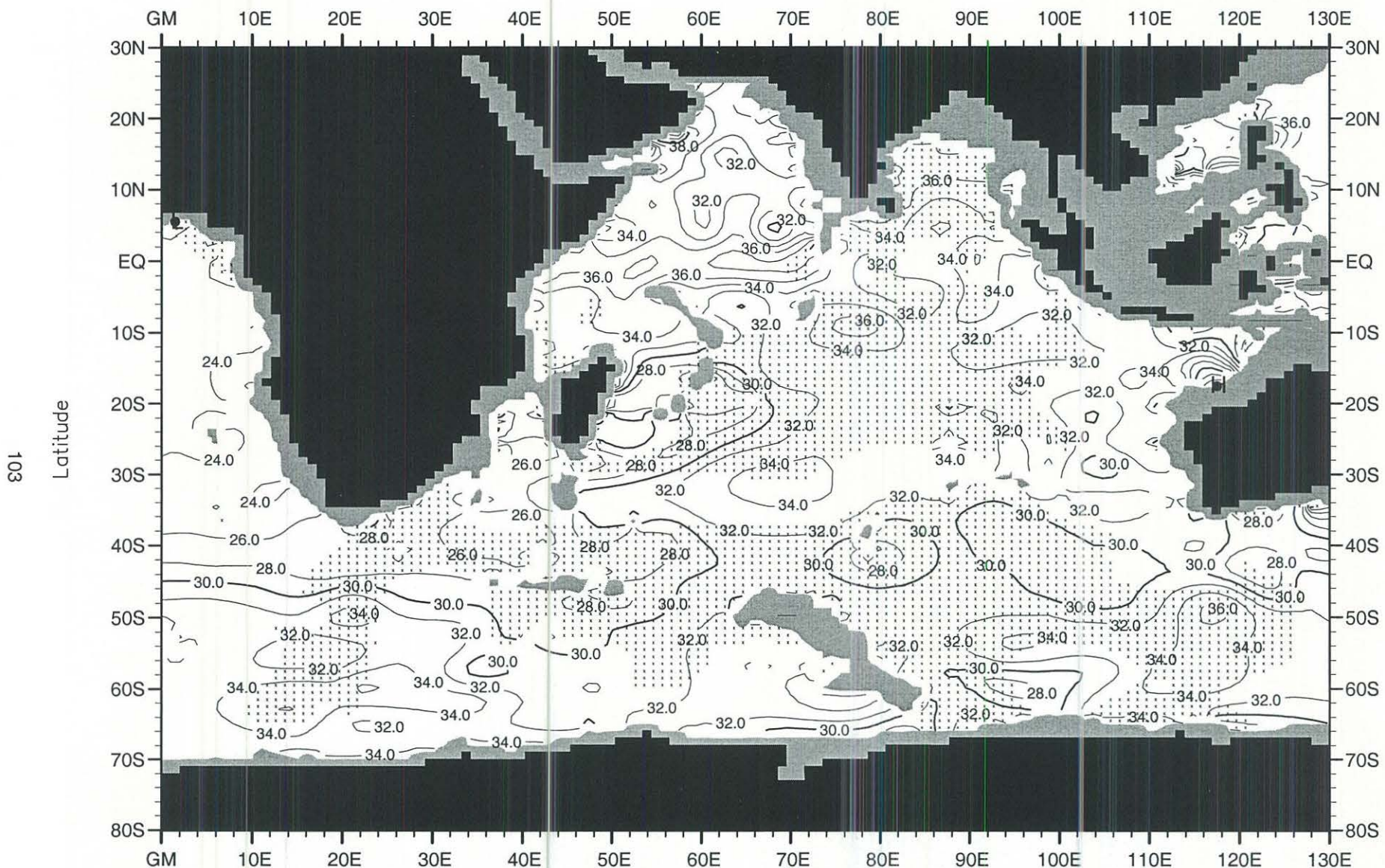
Fig. C31. Annual mean nitrate (μM) at 3000 m. depth .

Minimum Value= 20.84   Maximum Value= 46.79   Contour Interval: 2.00

Fig. C32.   Annual   mean nitrate (μM) at 4000 m. depth .

Minimum Value= 15.07   Maximum Value= 41.94   Contour Interval: 2.00
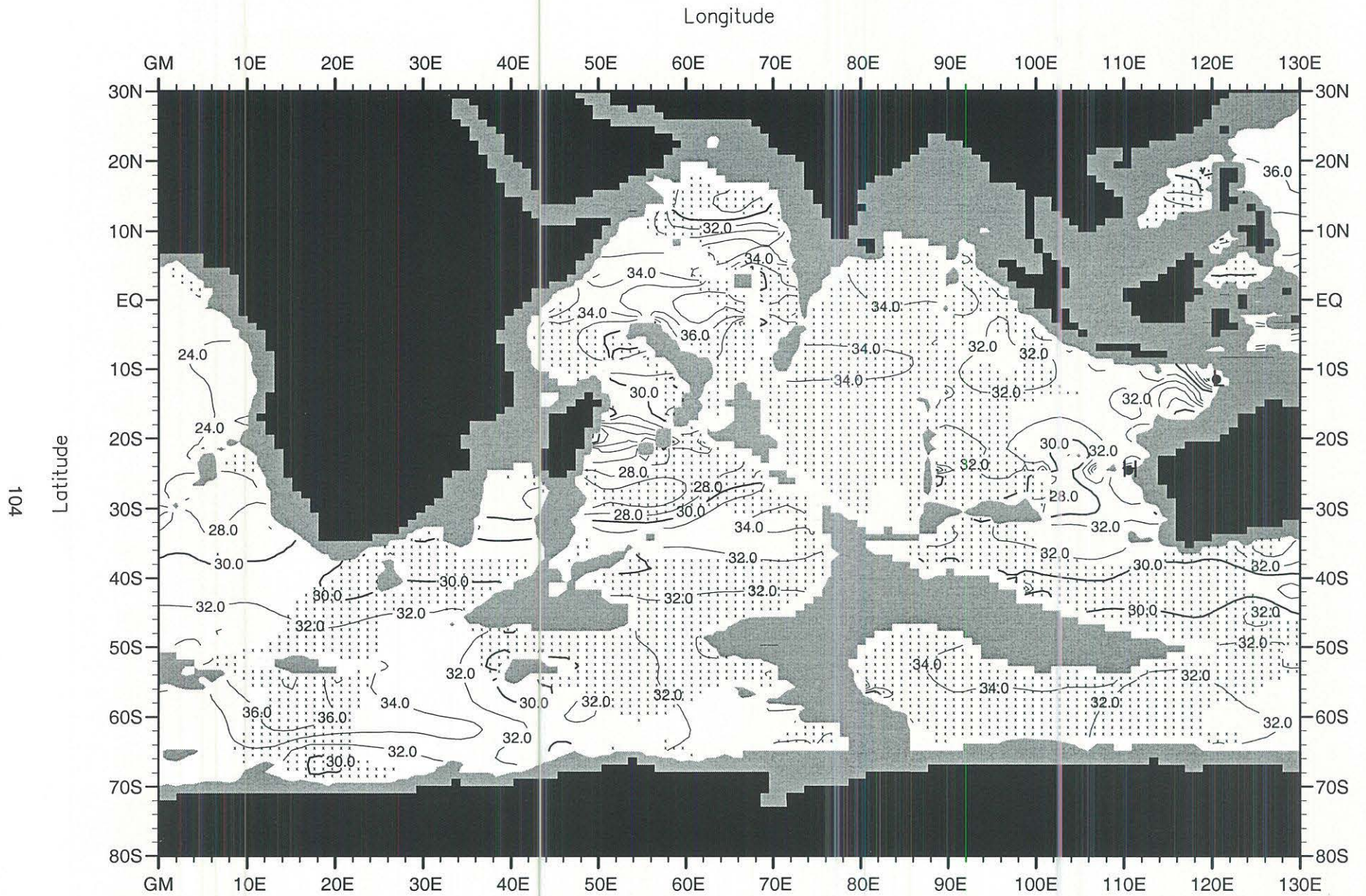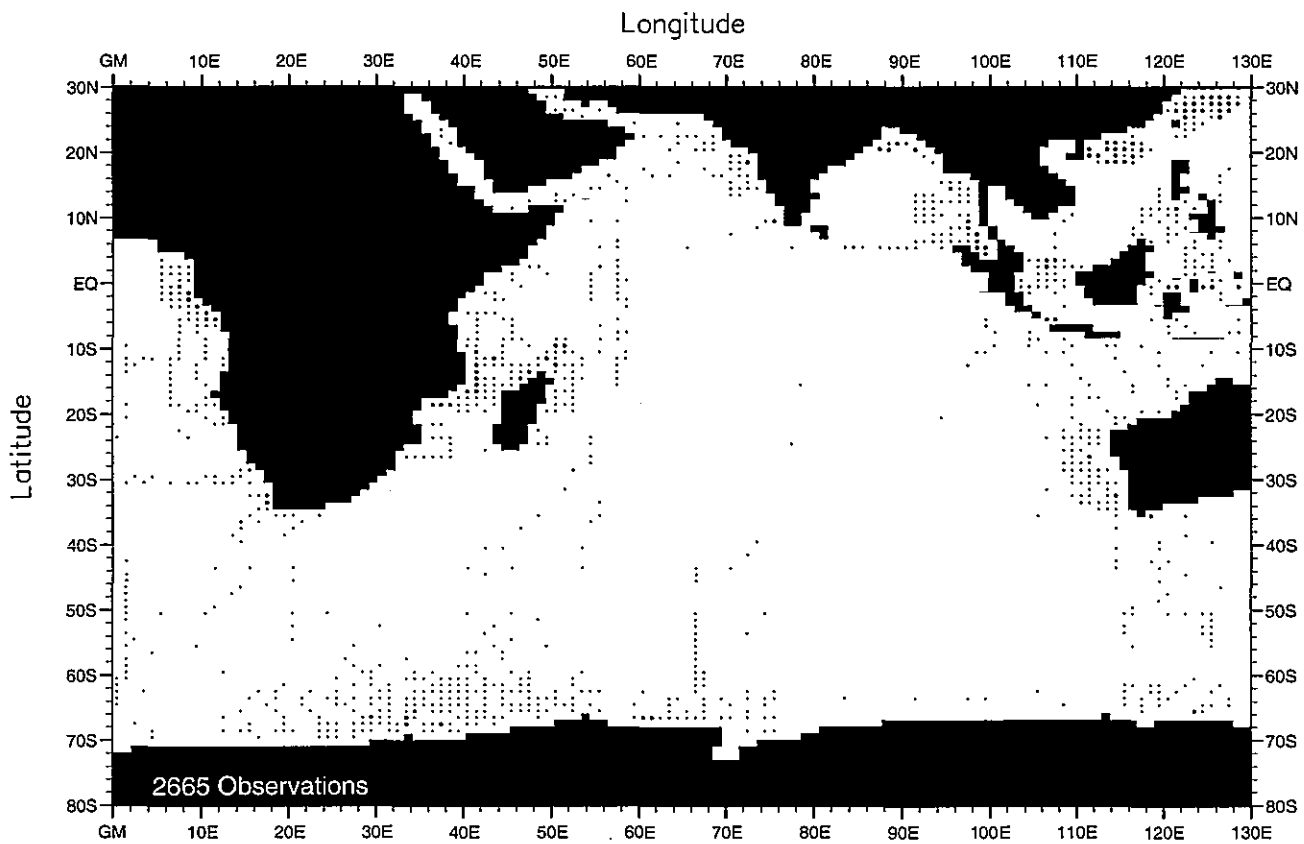
Fig. D1.   Winter (Jan.-Mar.) nitrate observations at the surface .
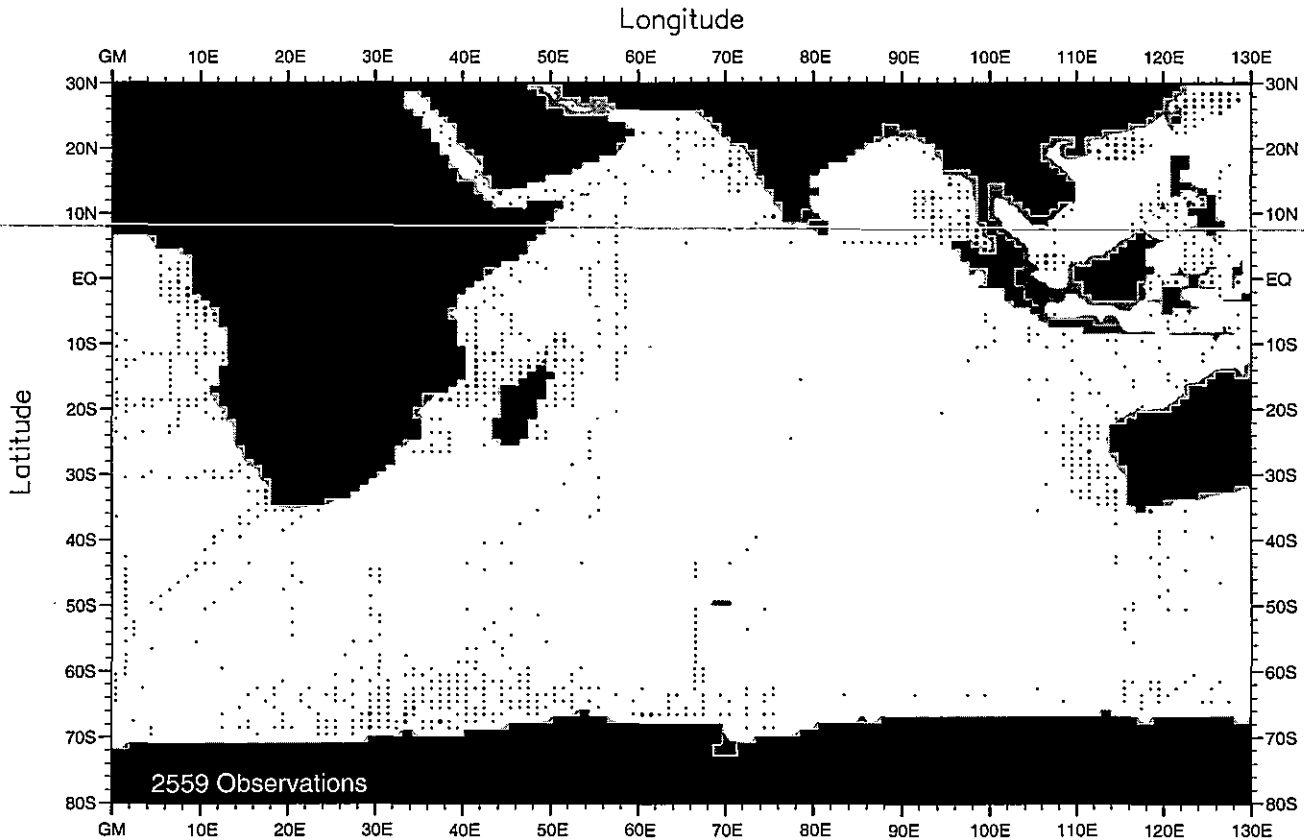
Fig. D2.   Winter (Jan.-Mar.) nitrate observations at   50 m. depth .

105
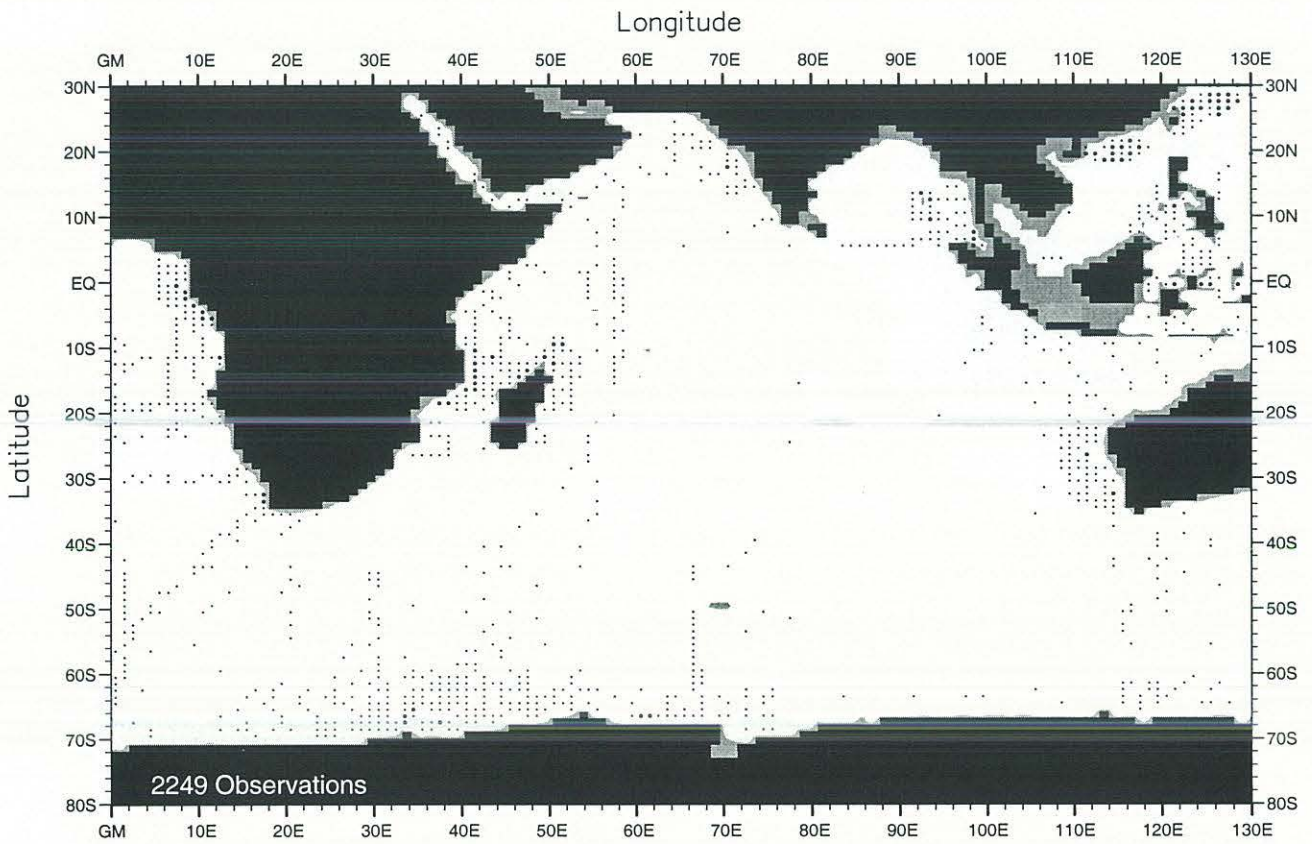
Fig. D3. Winter (Jan.-Mar.) nitrate observations at 75 m. depth .
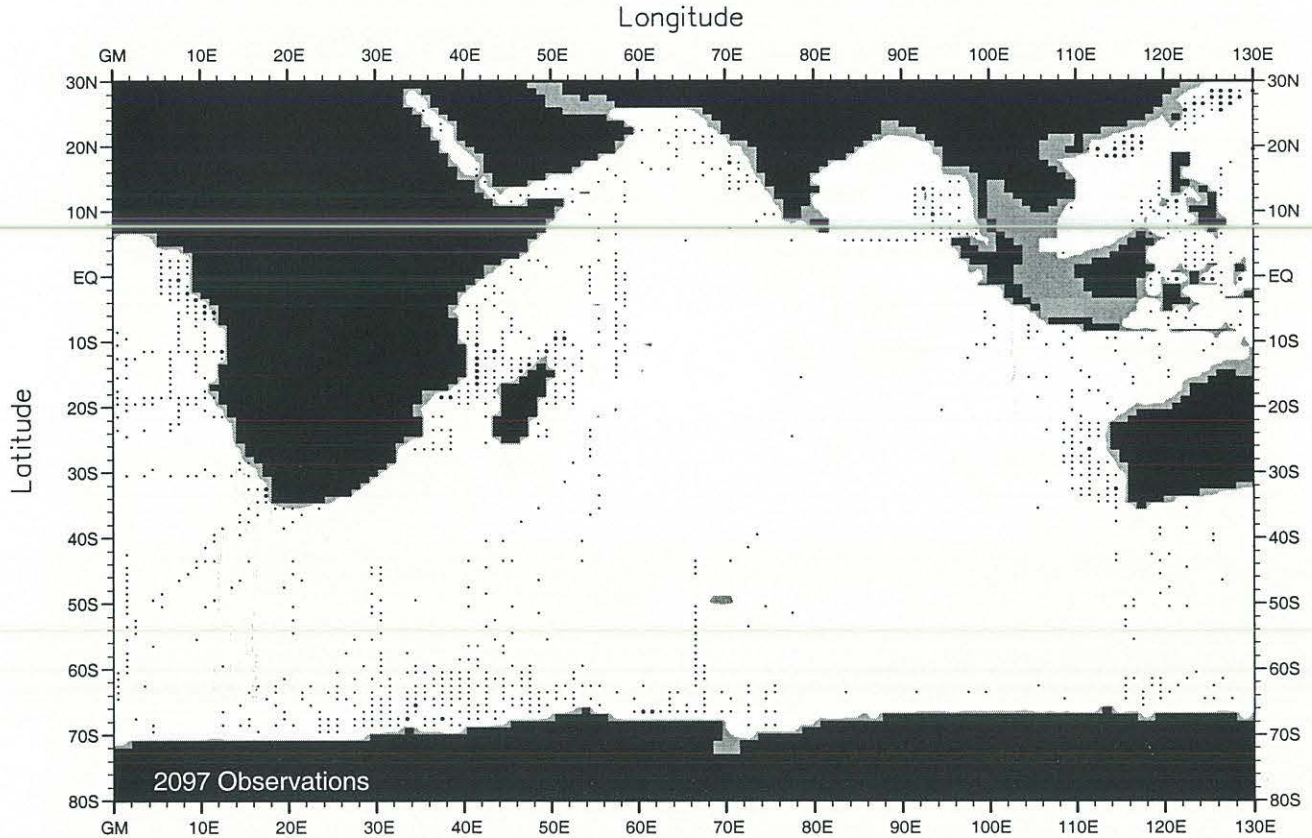
Fig. D4. Winter (Jan.-Mar.) nitrate observations at 100 m. depth .
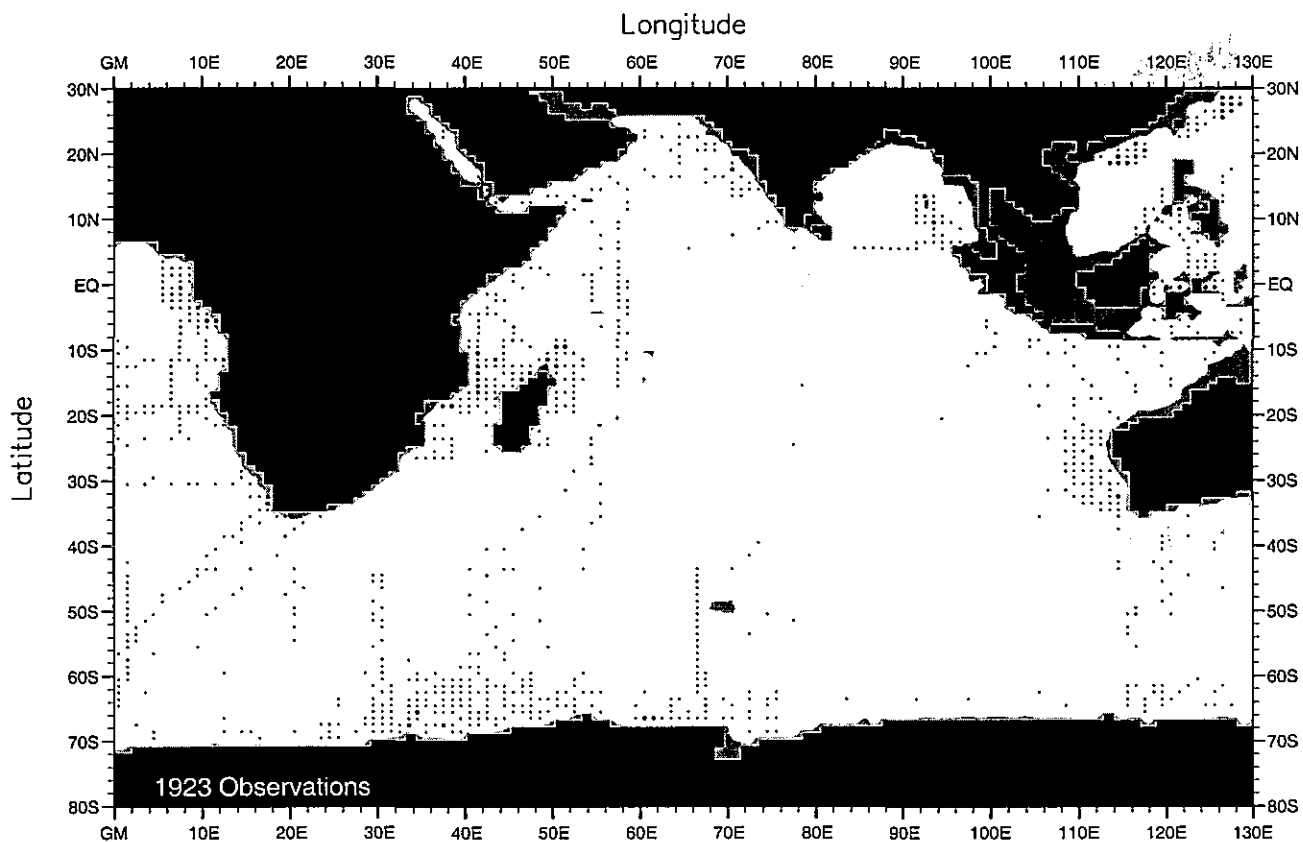
Fig. D5.   Winter (Jan.-Mar.) nitrate observations at 150 m. depth .
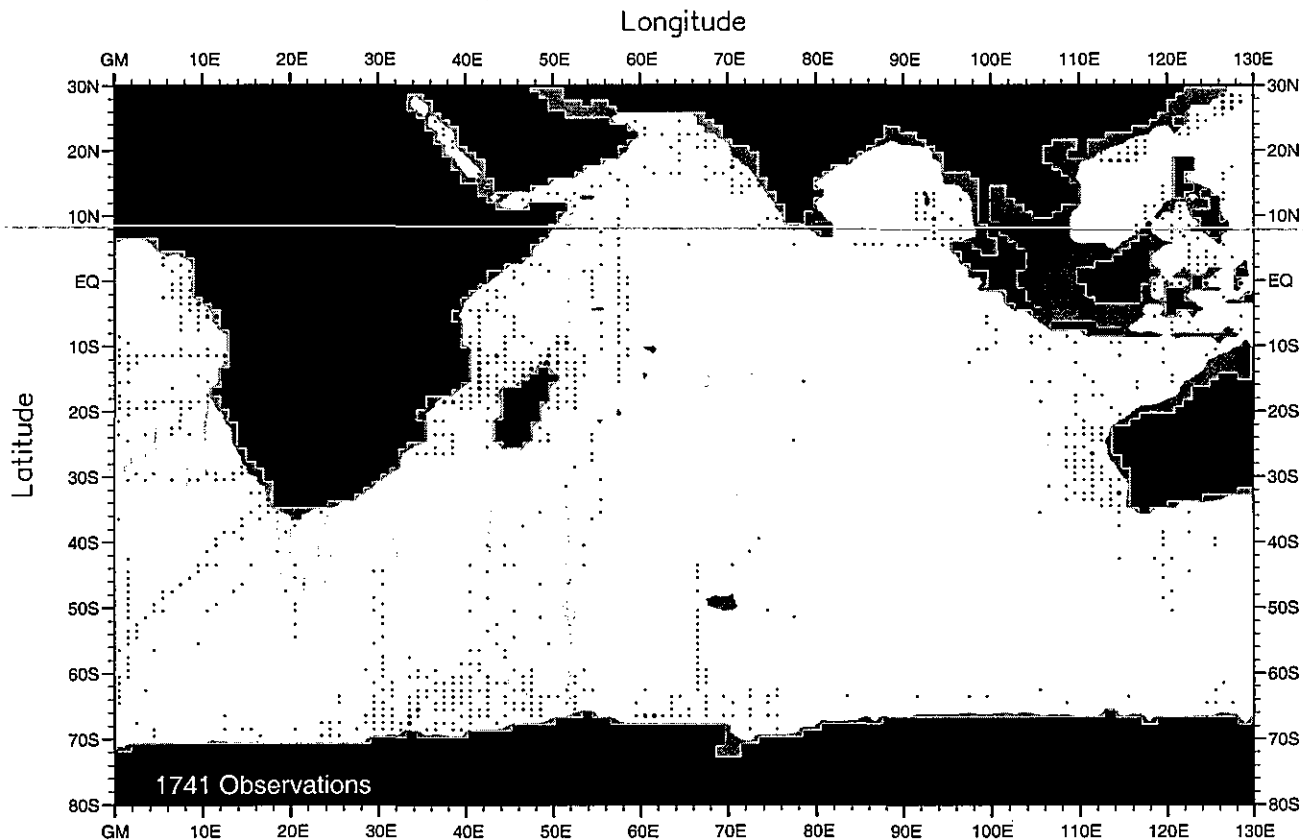
Fig. D6.   Winter (Jan.-Mar.) nitrate observations at 250 m. depth .
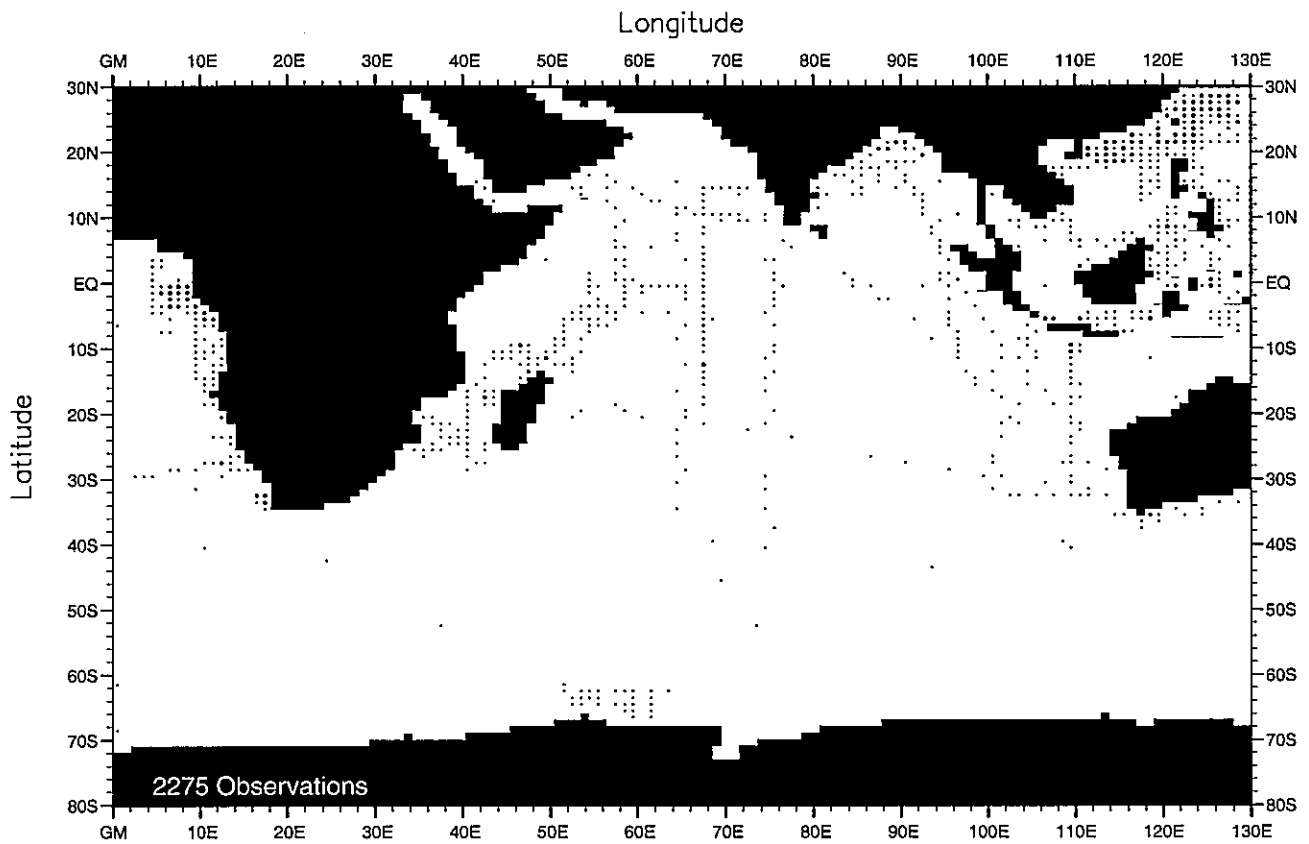
Fig. D7.   Spring (Apr.-Jun.) nitrate observations at the surface .
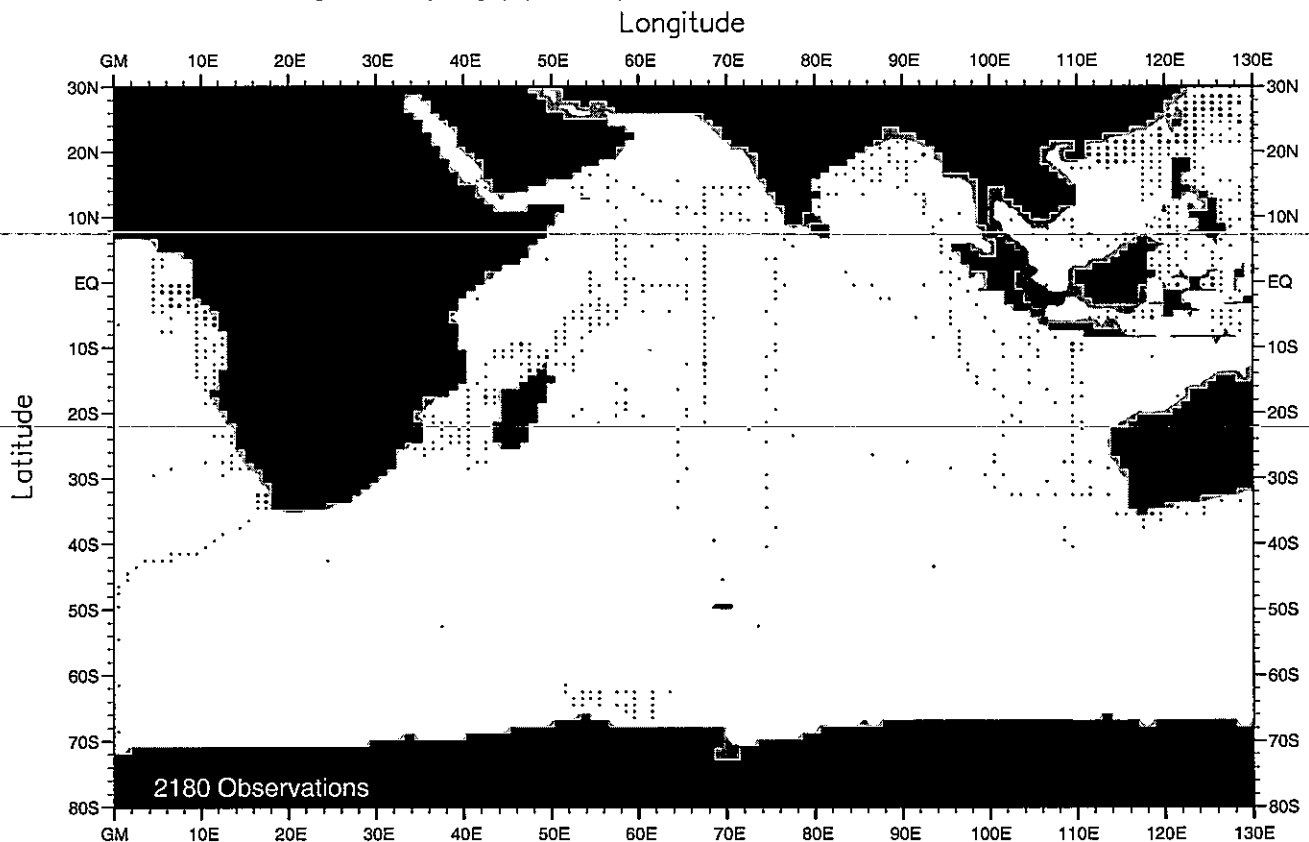
Fig. D8.   Spring (Apr.-Jun.) nitrate observations at   50 m. depth .

108

Longitude
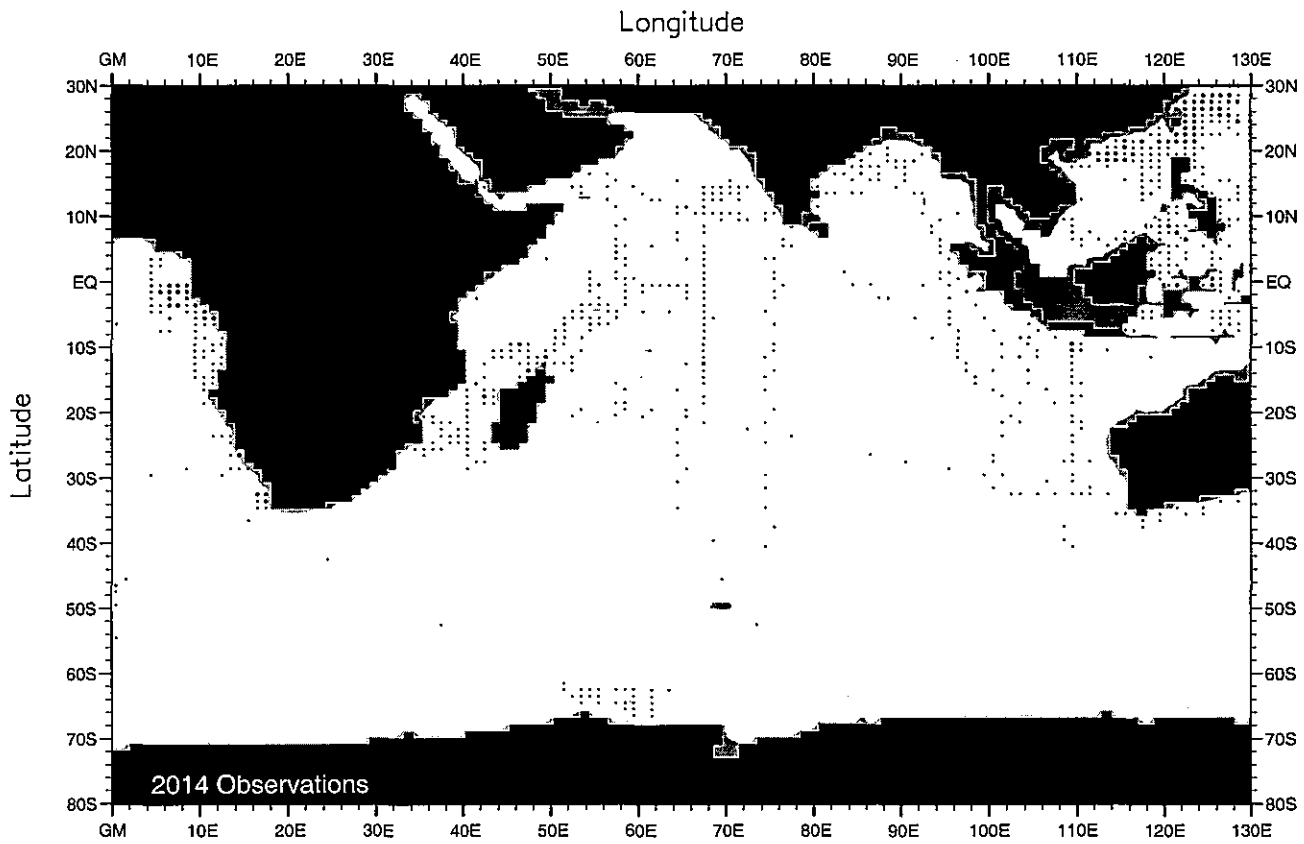
Fig. D9. Spring (Apr.-Jun.) nitrate observations at 75 m. depth .

Longitude
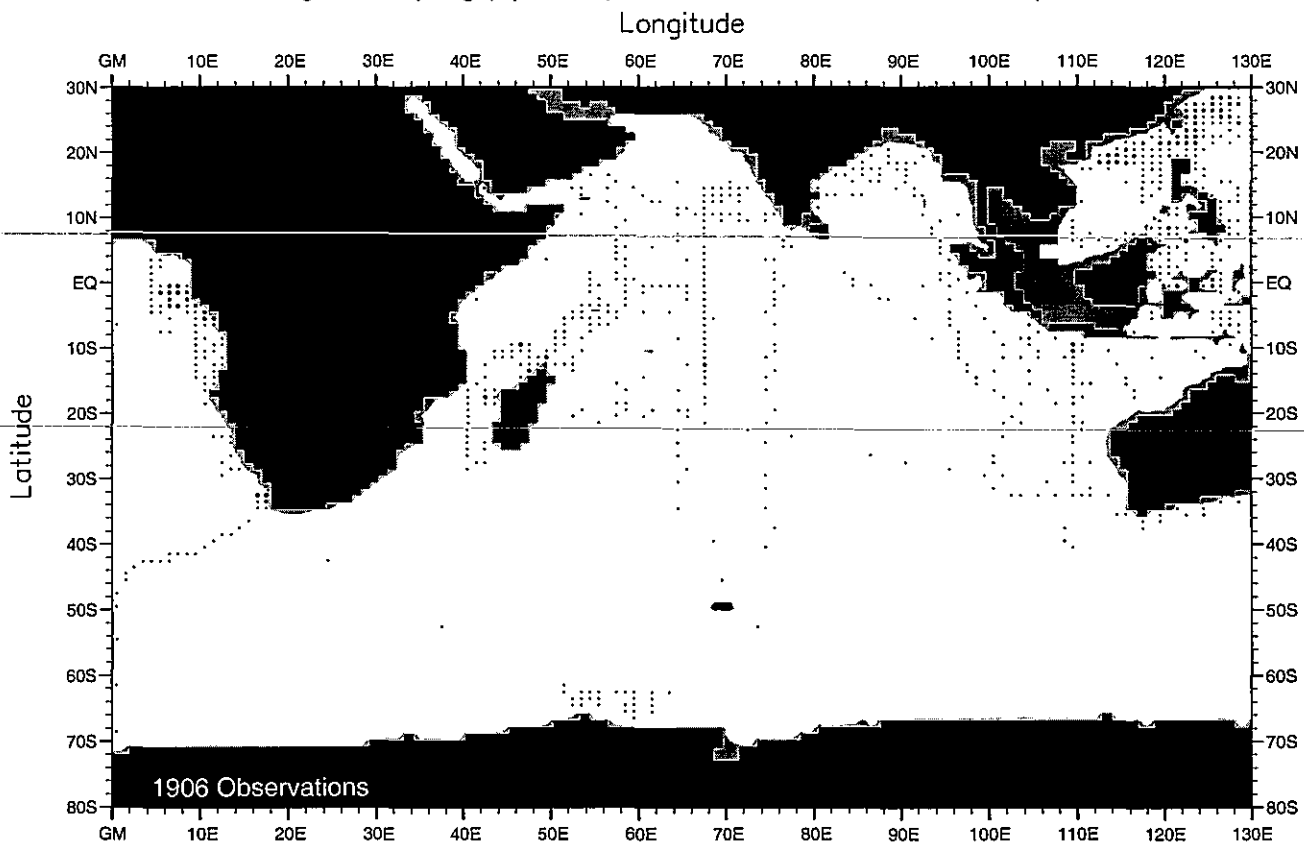
Fig. D10. Spring (Apr.-Jun.) nitrate observations at 100 m. depth .
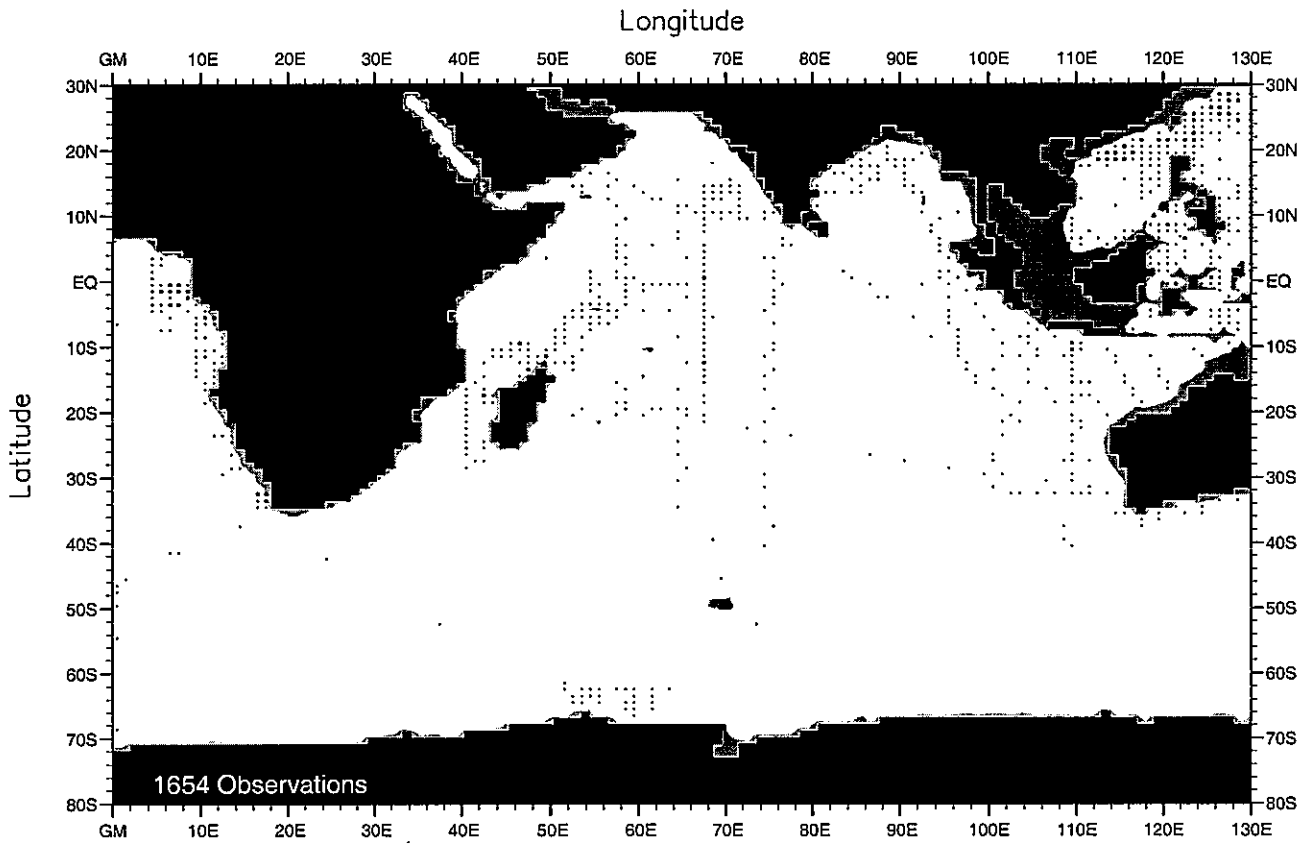
Fig. D11.   Spring (Apr.-Jun.) nitrate observations at 150 m. depth .
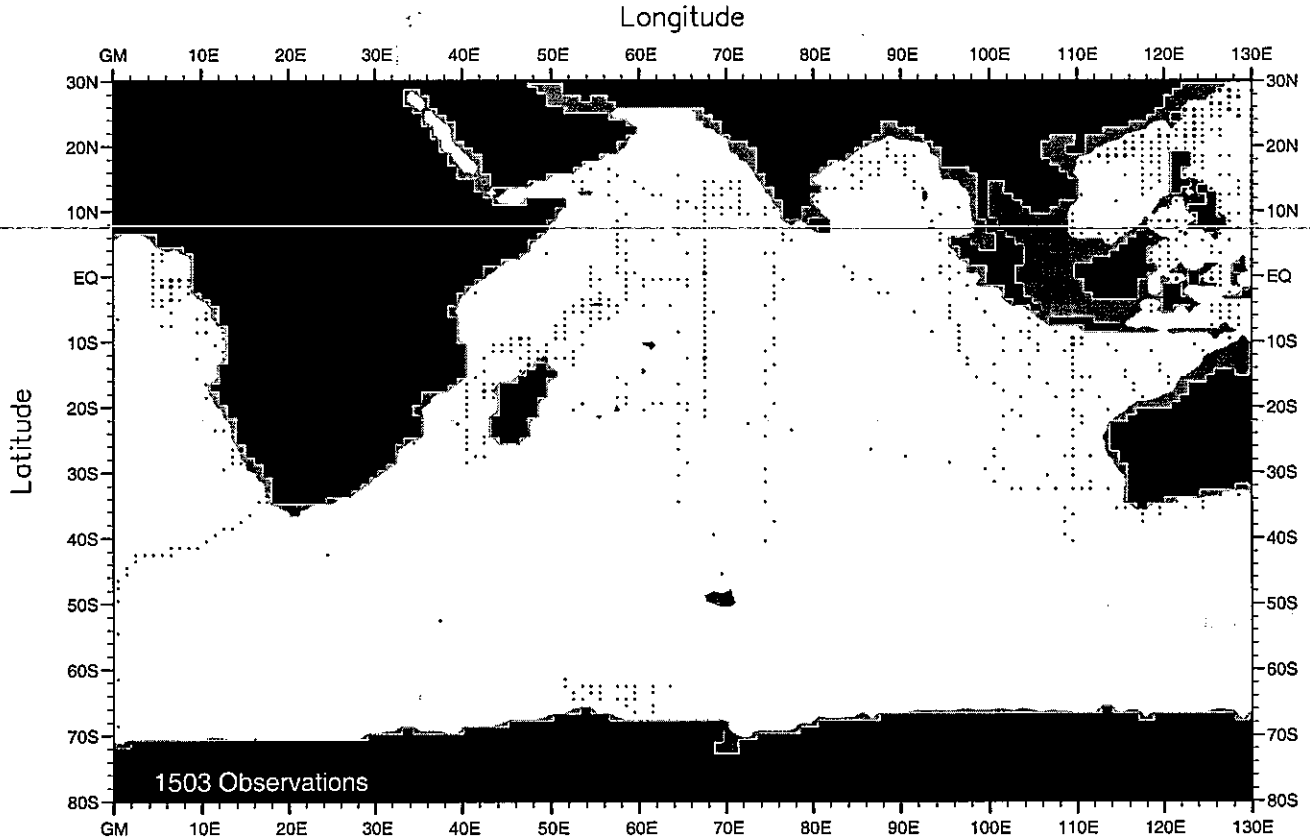
Fig. D12.   Spring (Apr.-Jun.) nitrate observations at 250 m. depth .

Longitude
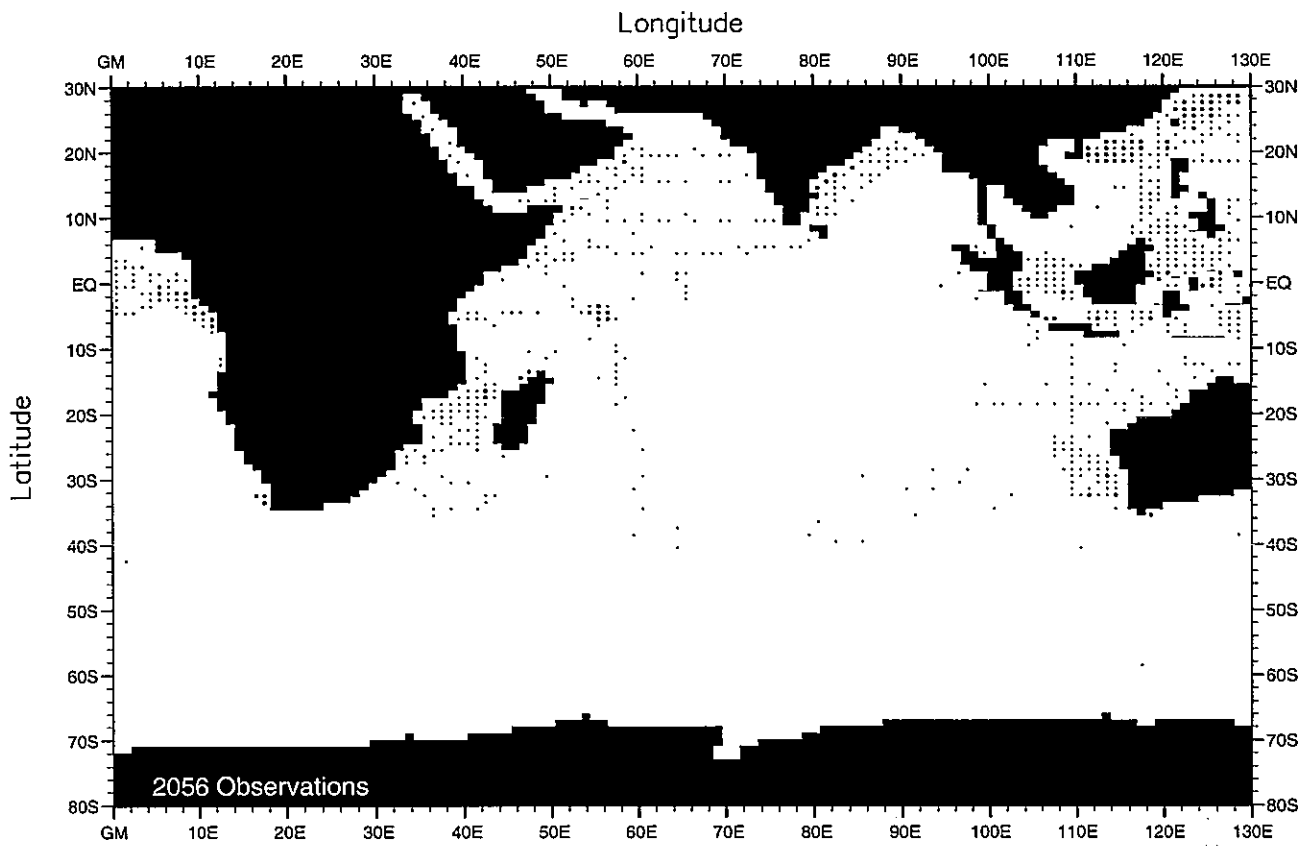
Fig. D13. Summer (Jul.-Sep.) nitrate observations at the surface .

Longitude
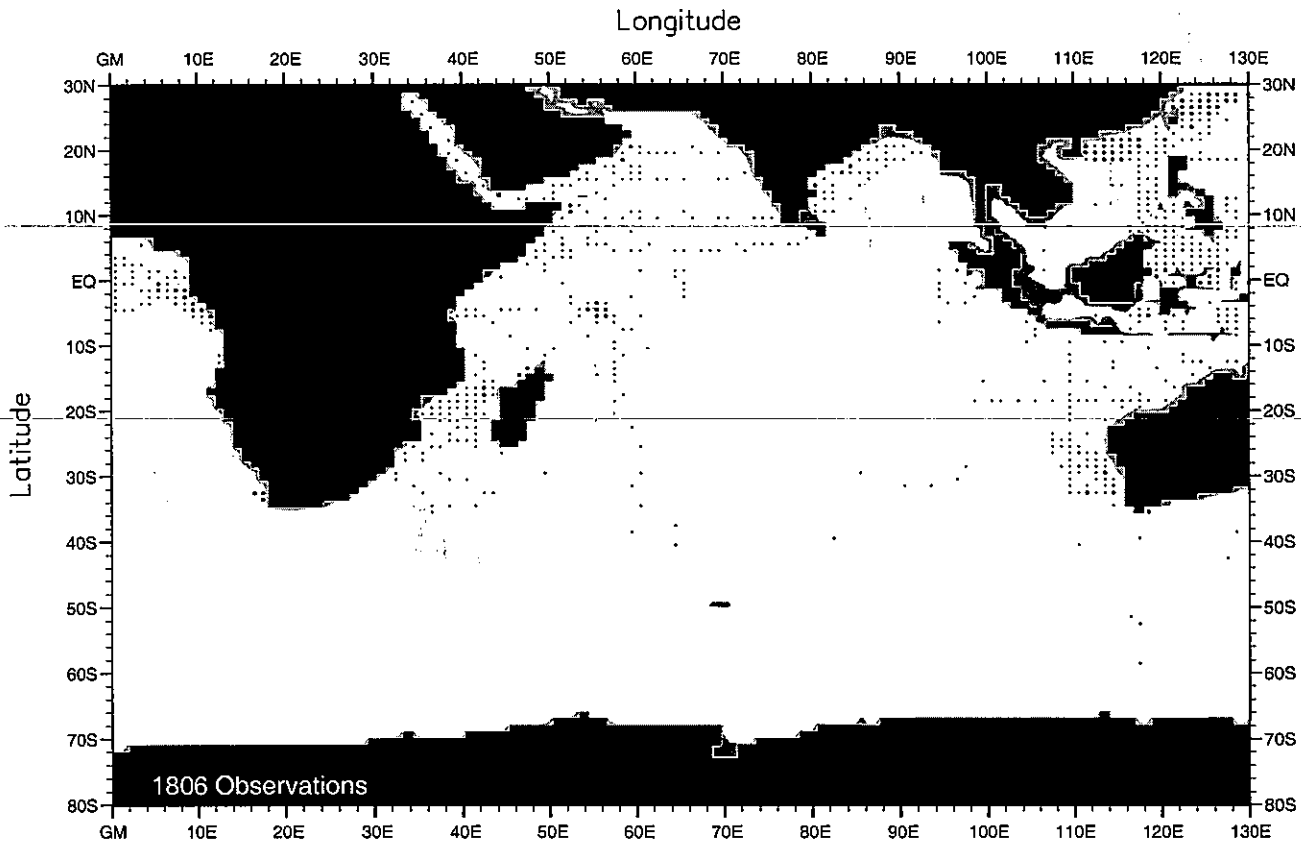
Fig. D14. Summer (Jul.-Sep.) nitrate observations at 50 m. depth .

111
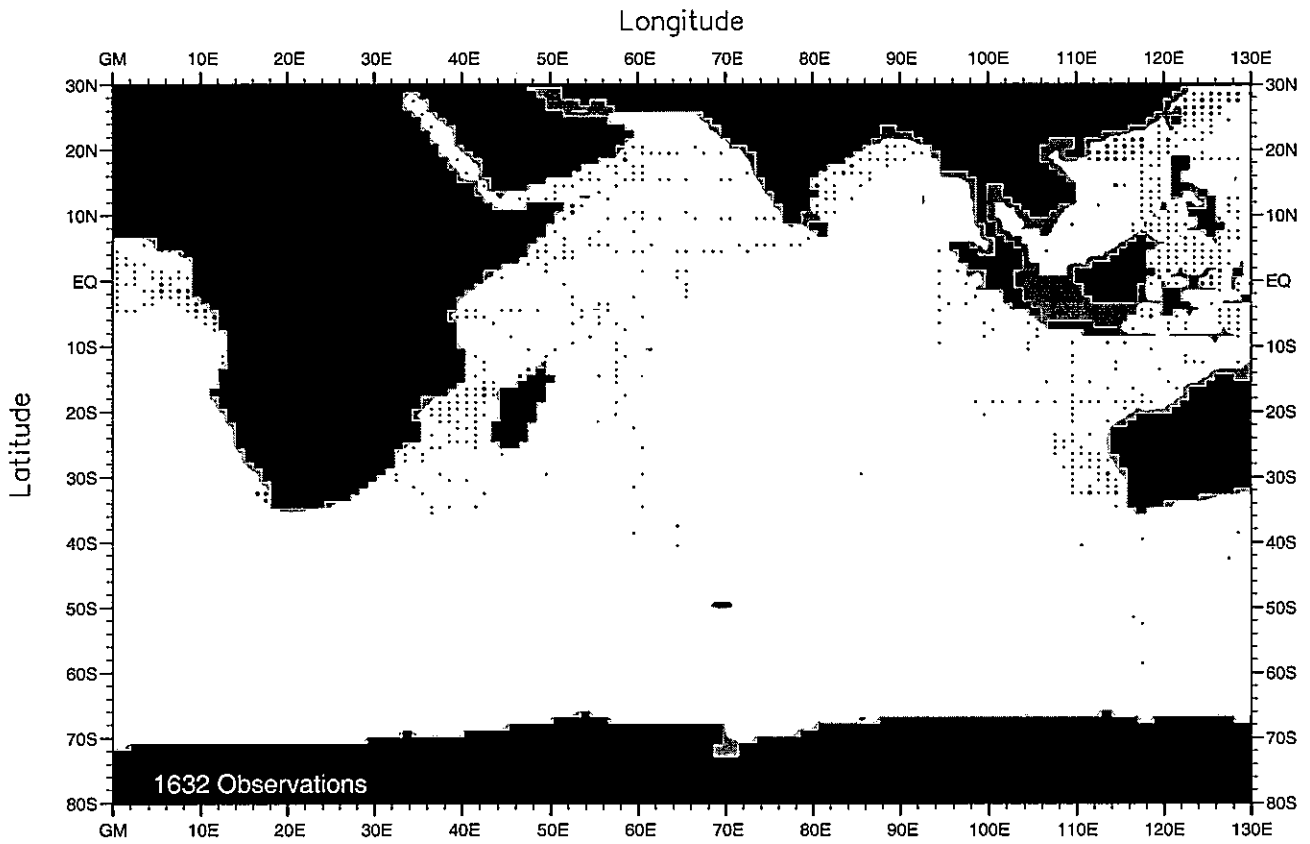
Fig. D15.   Summer (Jul.-Sep.) nitrate observations at   75 m. depth .
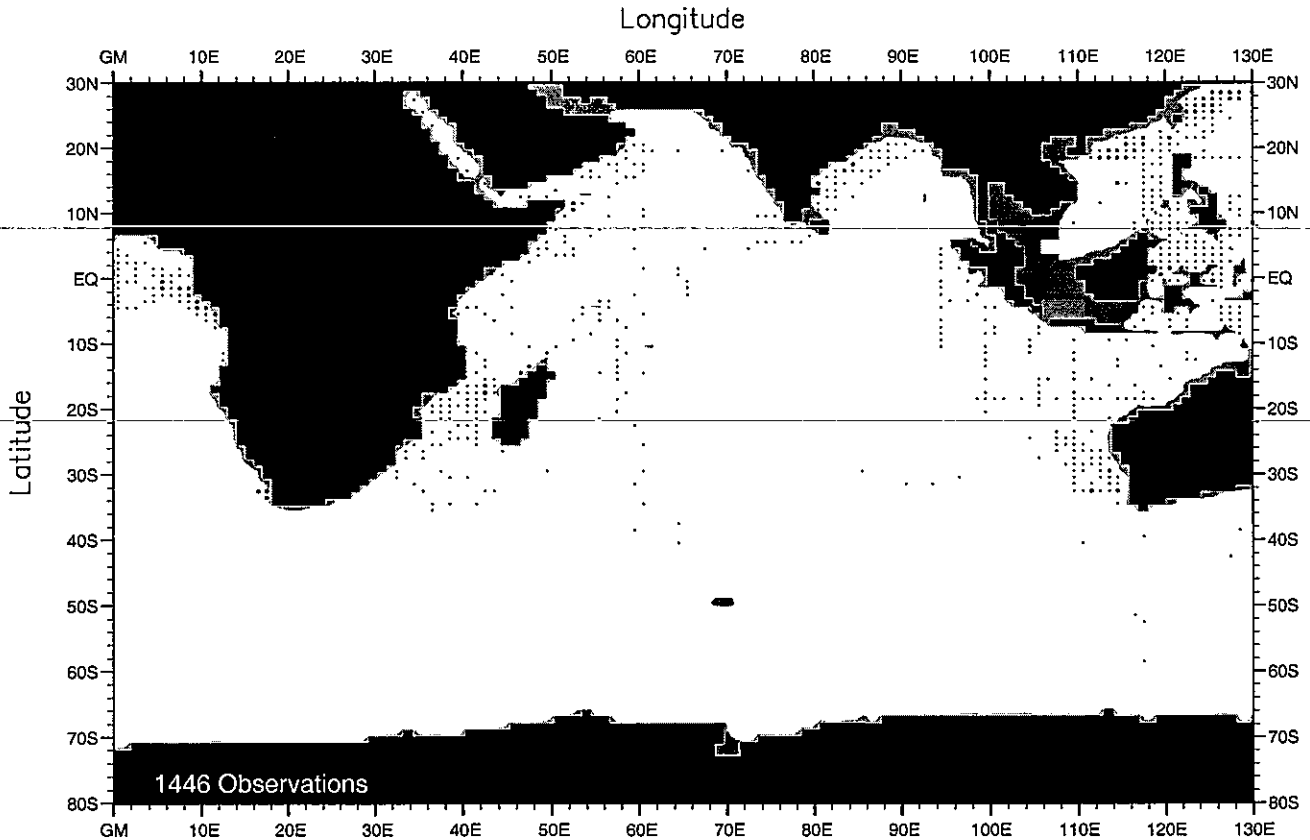
Fig. D16.   Summer (Jul.-Sep.) nitrate observations at 100 m. depth .
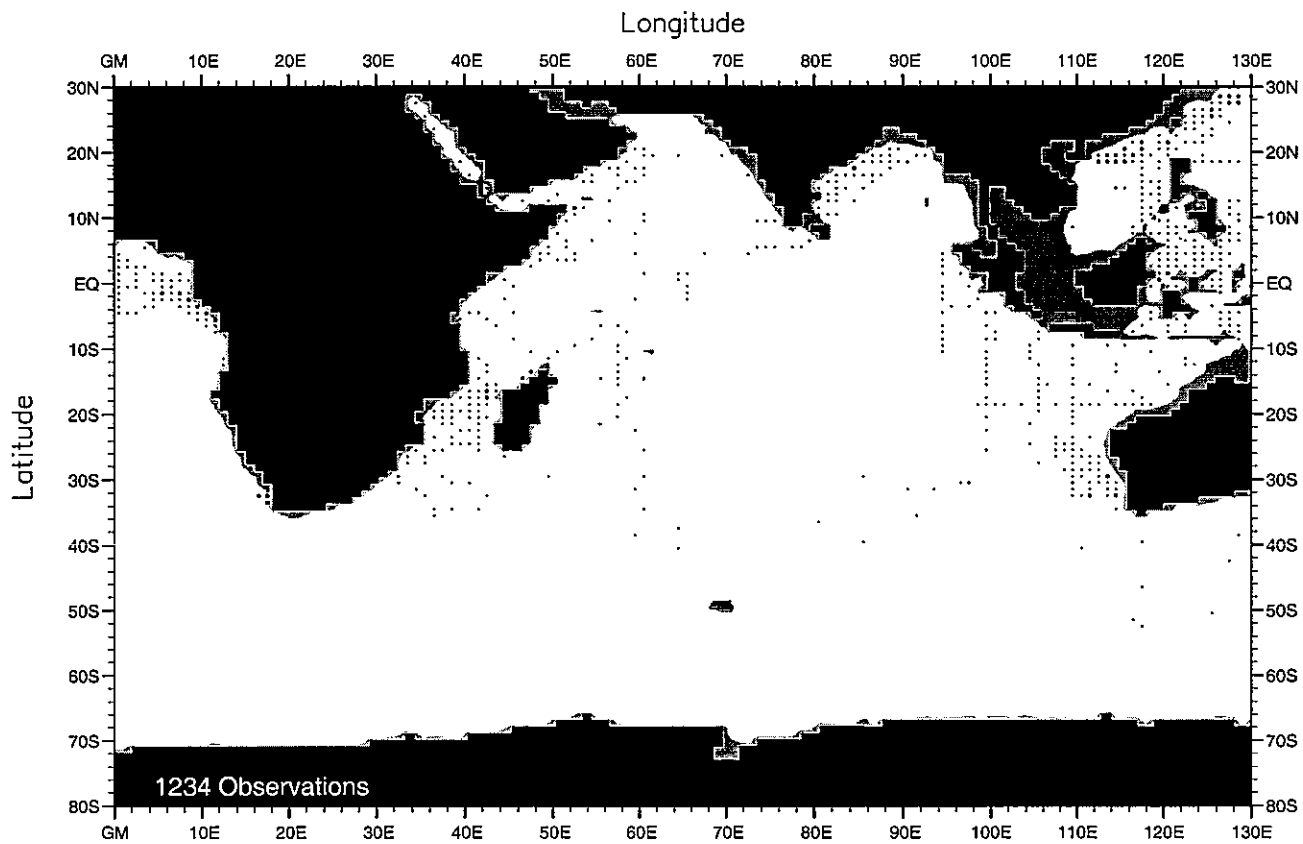
Fig. D17.   Summer (Jul.-Sep.) nitrate observations at 150 m. depth .
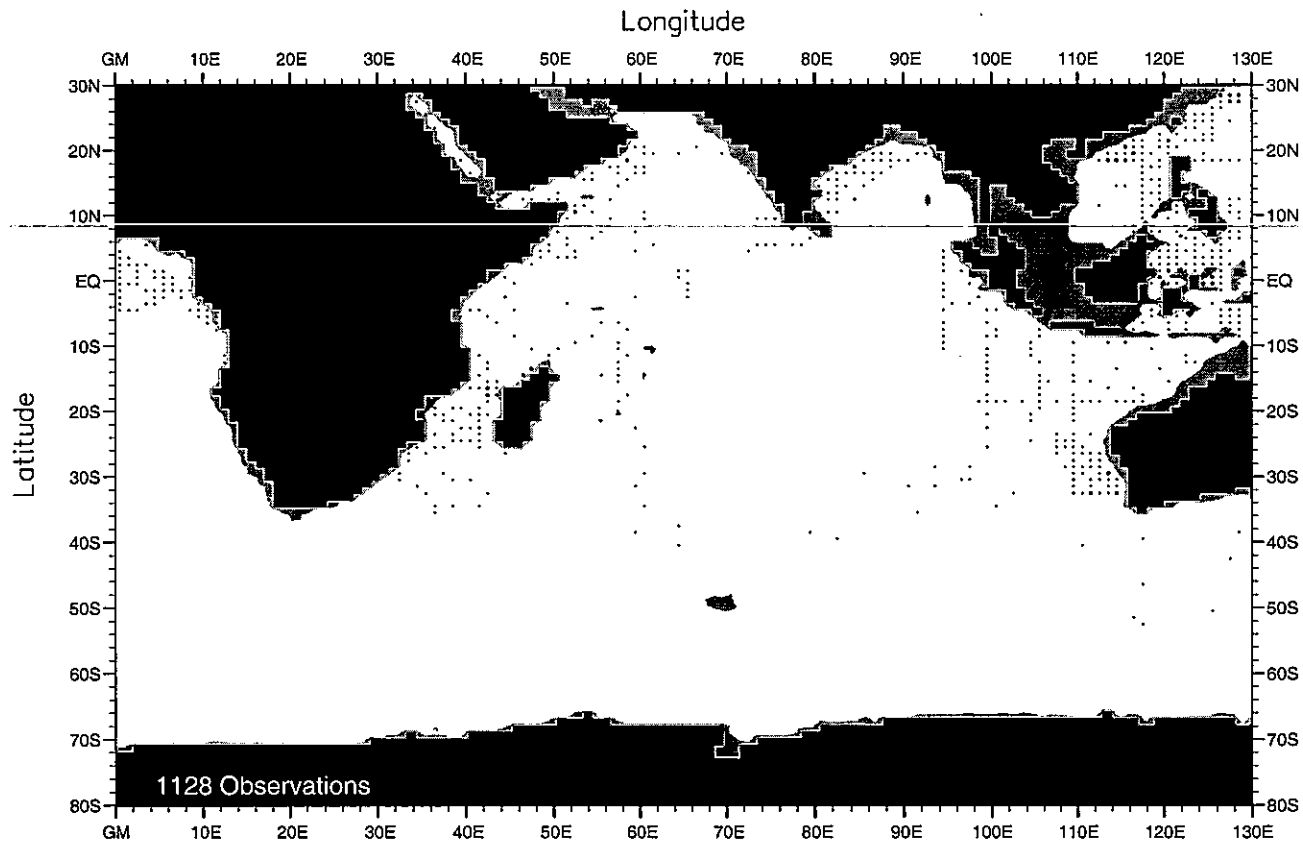
Fig. D18.   Summer (Jul.-Sep.) nitrate observations at 250 m. depth .
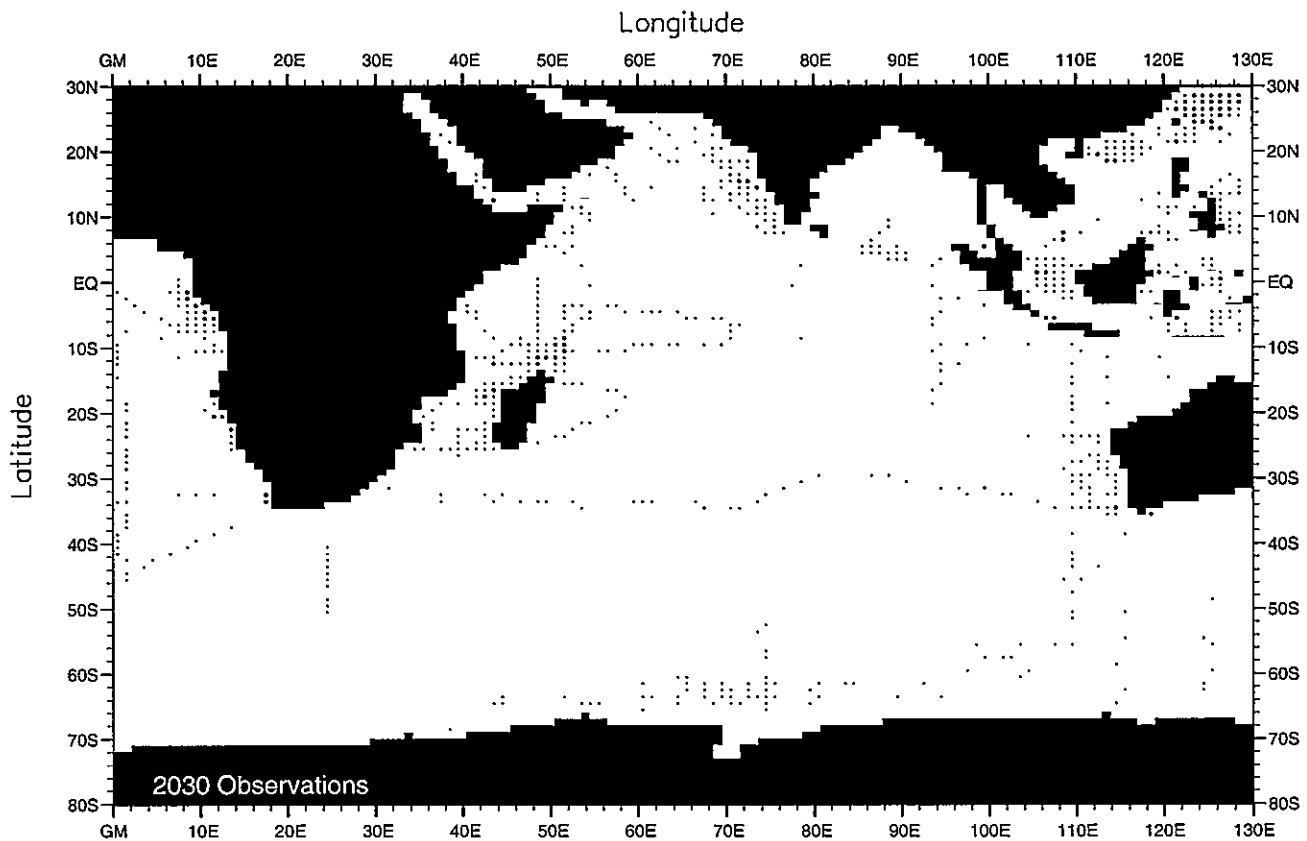
Fig. D19. Fall (Oct.-Dec.) nitrate observations at the surface .
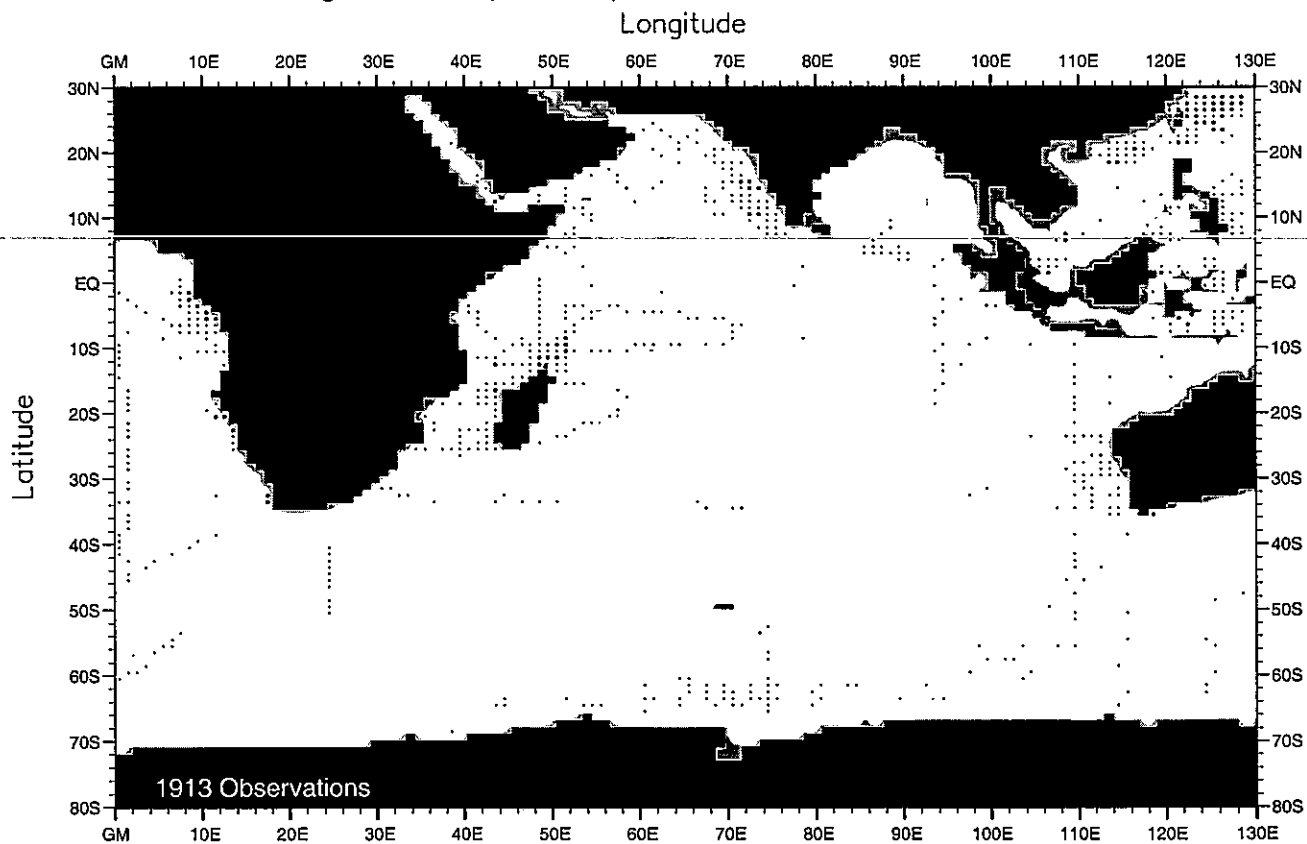
Fig. D20. Fall (Oct.-Dec.) nitrate observations at 50 m. depth .
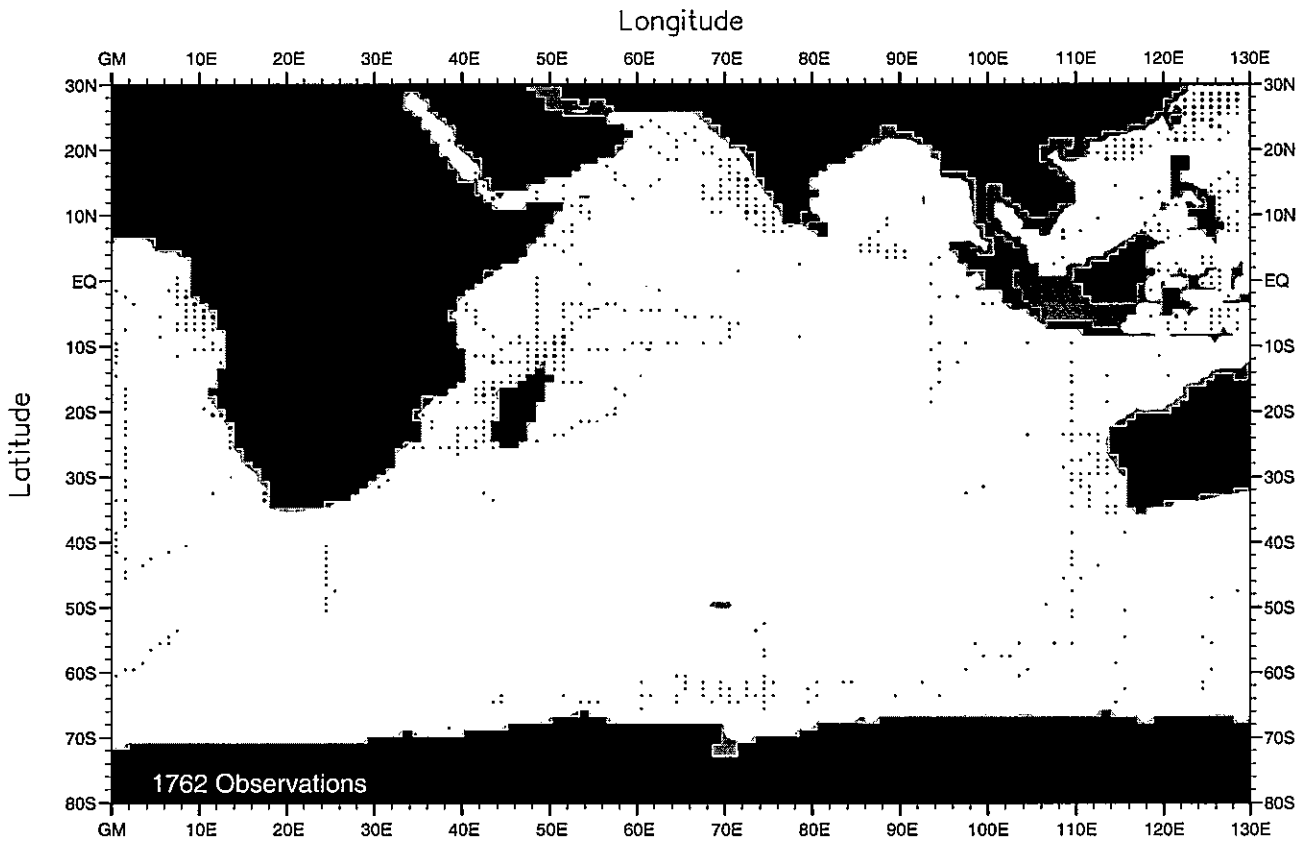
Fig. D21.   Fall (Oct.-Dec.) nitrate observations at 75 m. depth .
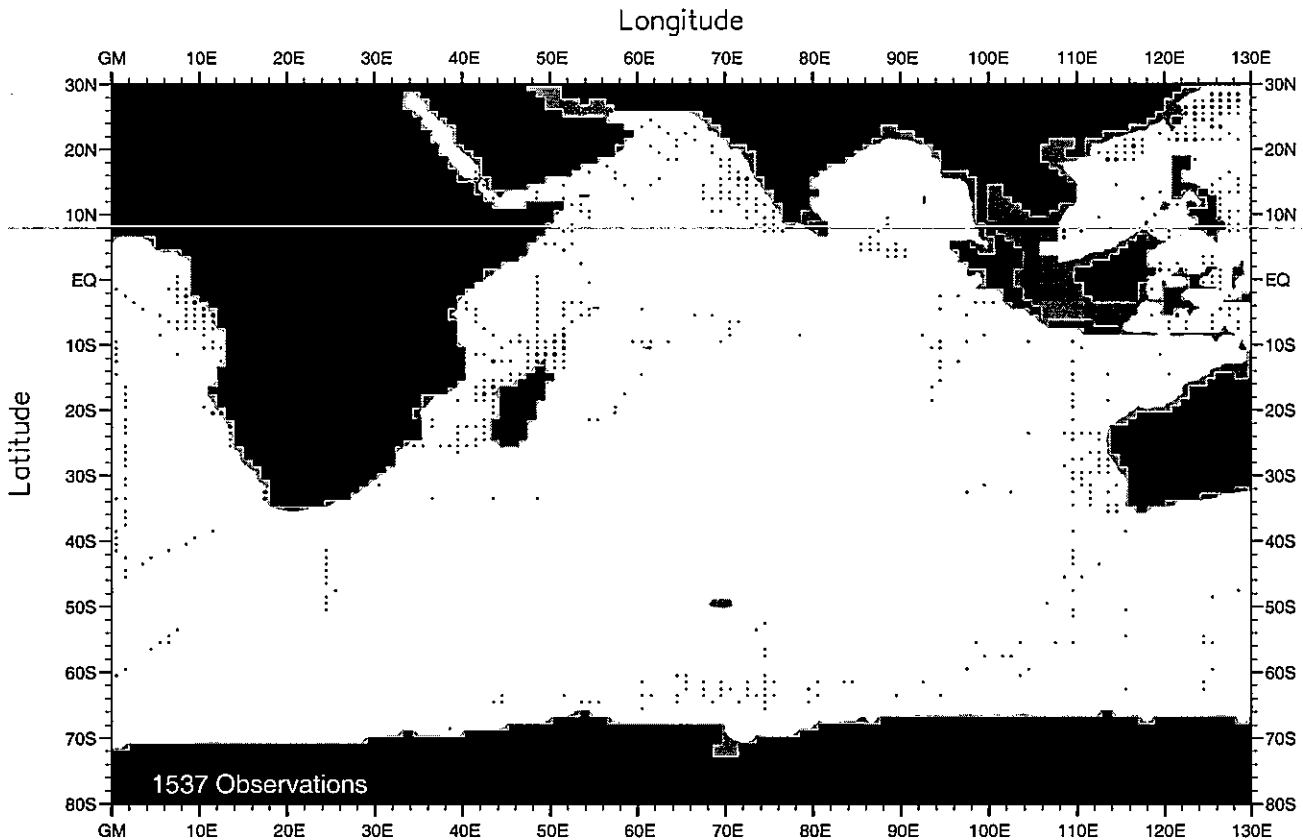
Fig. D22.   Fall (Oct.-Dec.) nitrate observations at 100 m. depth .
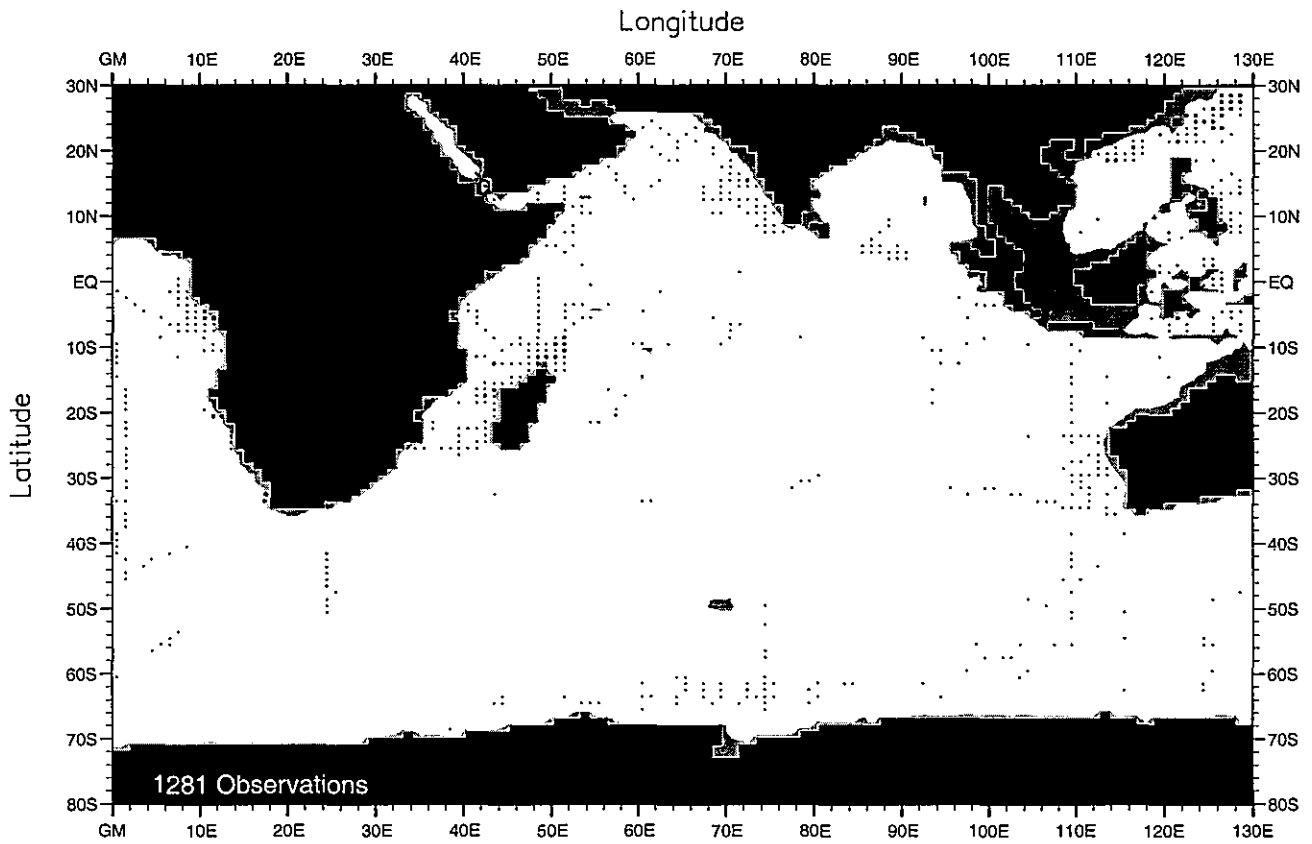
Fig. D23. Fall (Oct.-Dec.) nitrate observations at 150 m. depth .
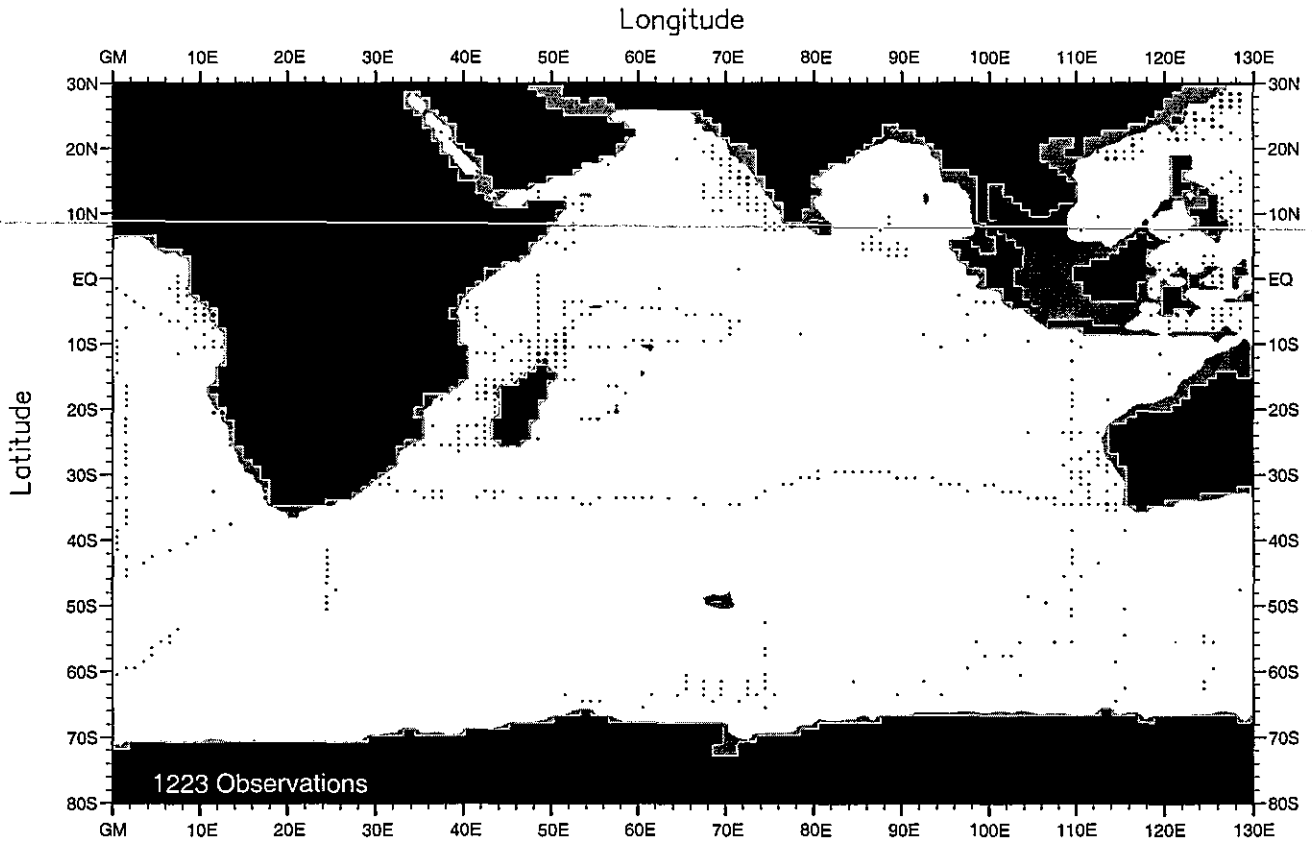
Fig. D24. Fall (Oct.-Dec.) nitrate observations at 250 m. depth .
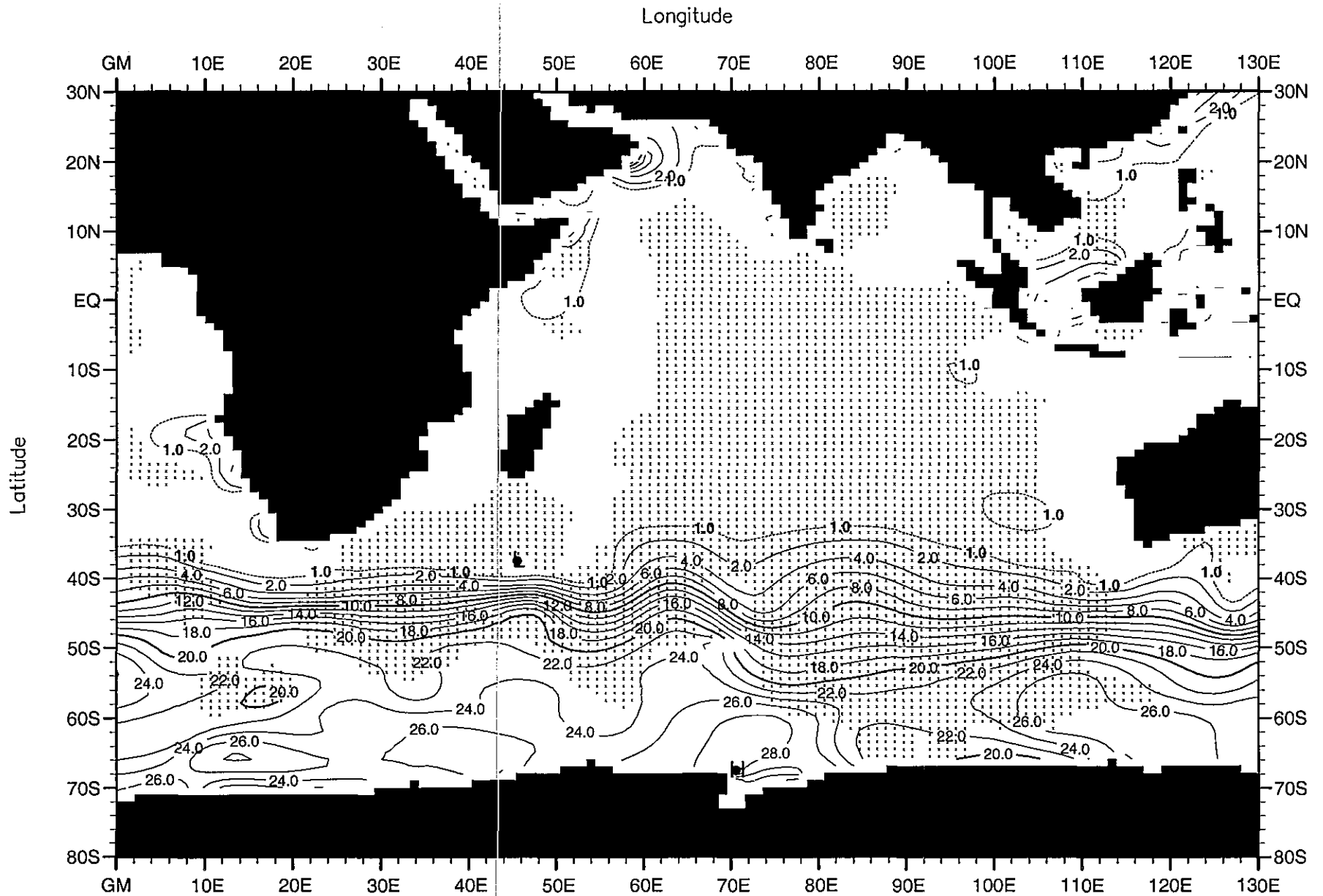
Fig. D25. Winter (Jan.-Mar.) mean nitrate (μM) at the surface.

Minimum Value= 0.00   Maximum Value= 29.89   Contour Interval: 2.00
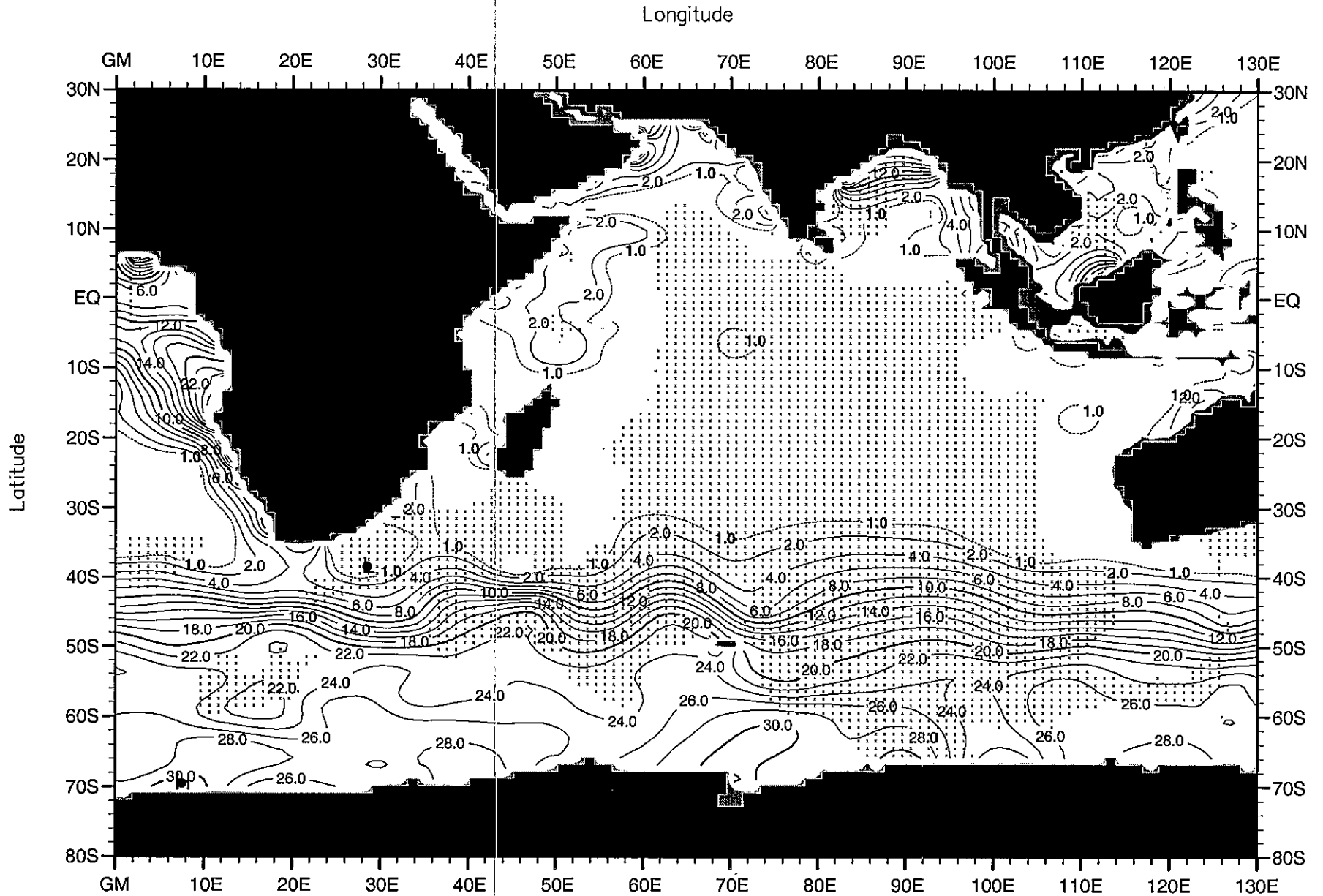
Fig. D26. Winter (Jan.-Mar.) mean nitrate (μM) at 50 m. depth .

Minimum Value= 0.00   Maximum Value= 31.78   Contour Interval: 2.00
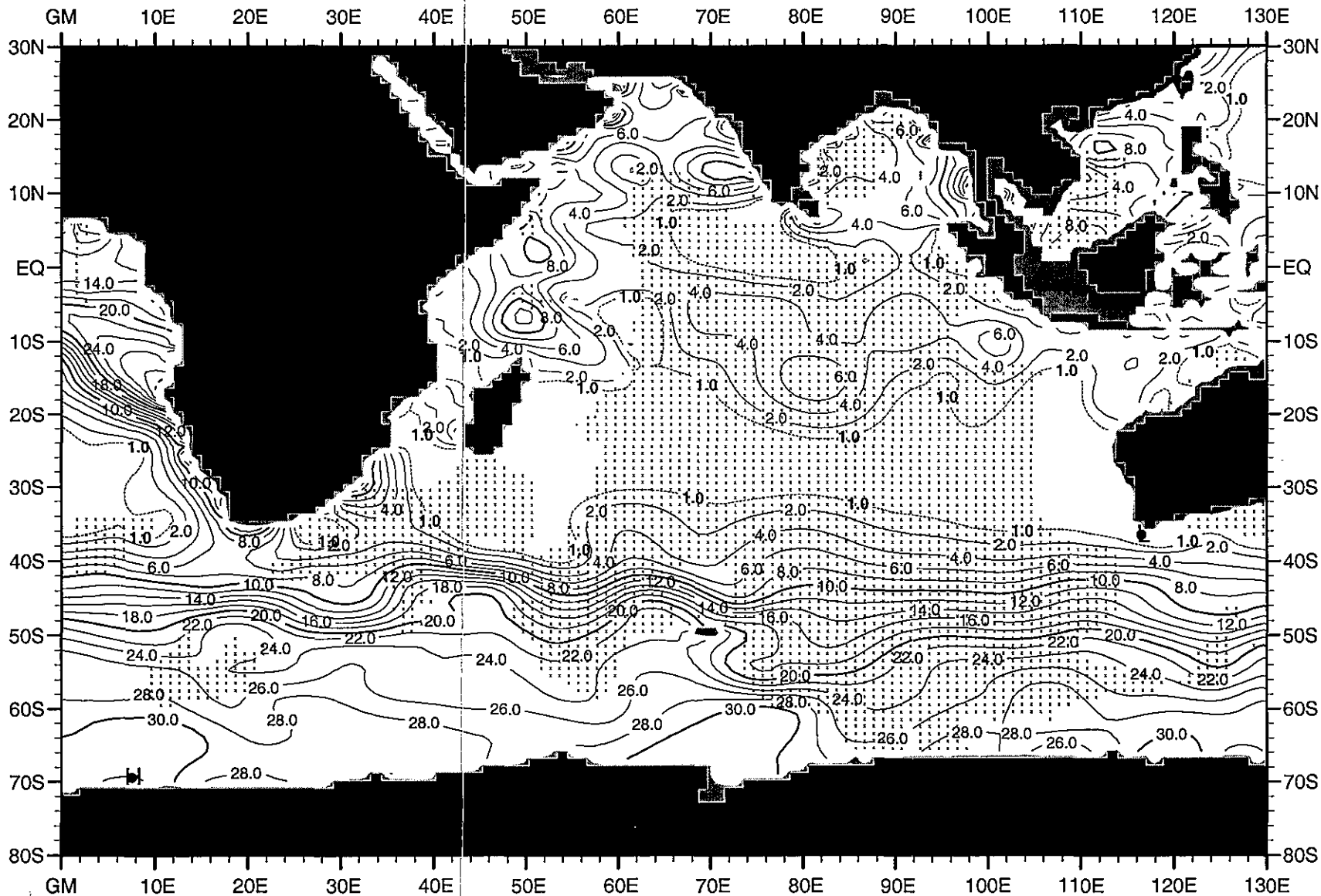
Fig. D27. Winter (Jan.-Mar.) mean nitrate (μM) at 75 m. depth .

Minimum Value= 0.00   Maximum Value= 32.64   Contour Interval: 2.00
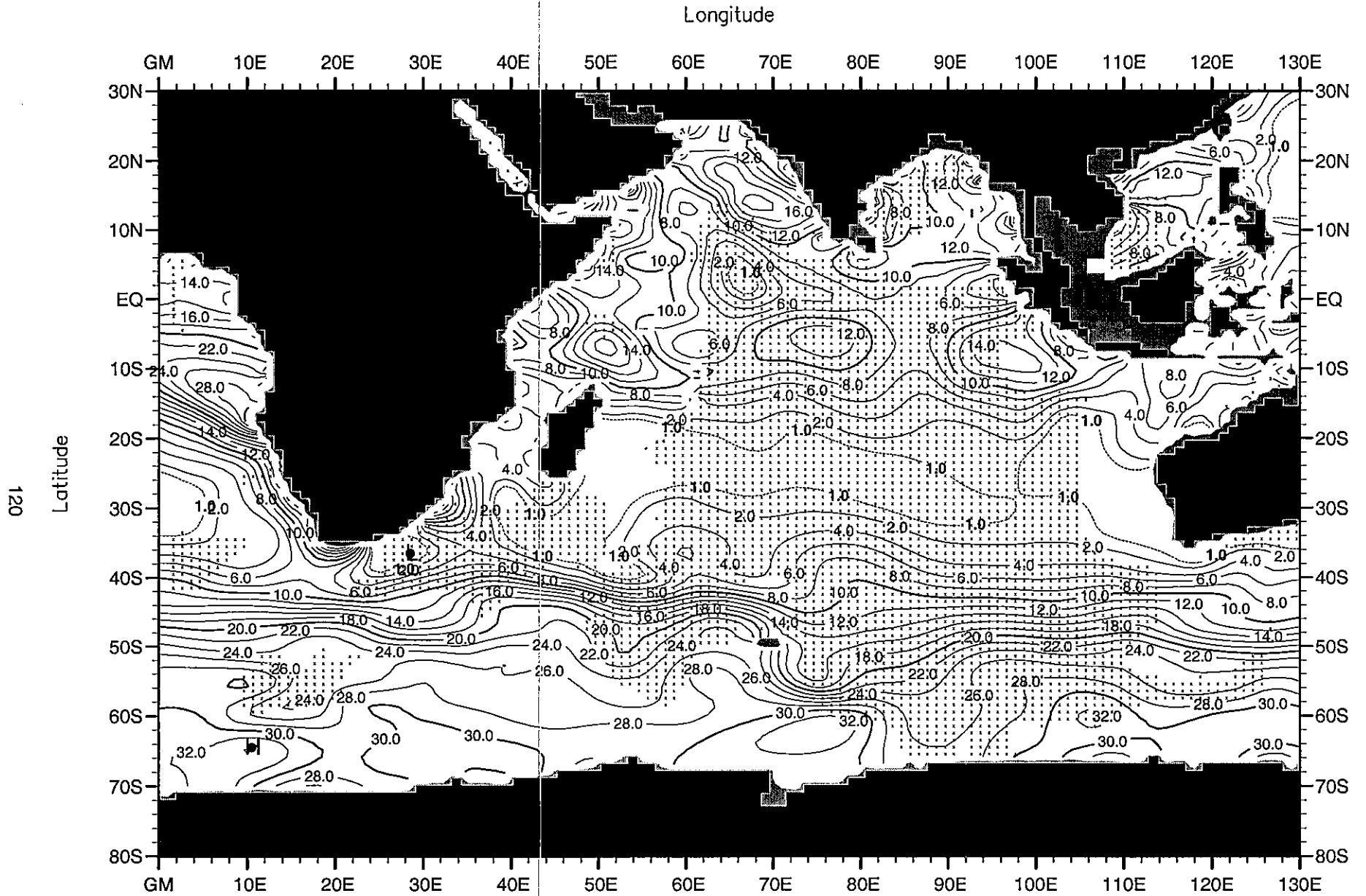
Fig. D28.   Winter (Jan.-Mar.) mean nitrate (μM) at 100 m. depth .

Minimum Value= 0.00   Maximum Value= 34.07   Contour Interval: 2.00
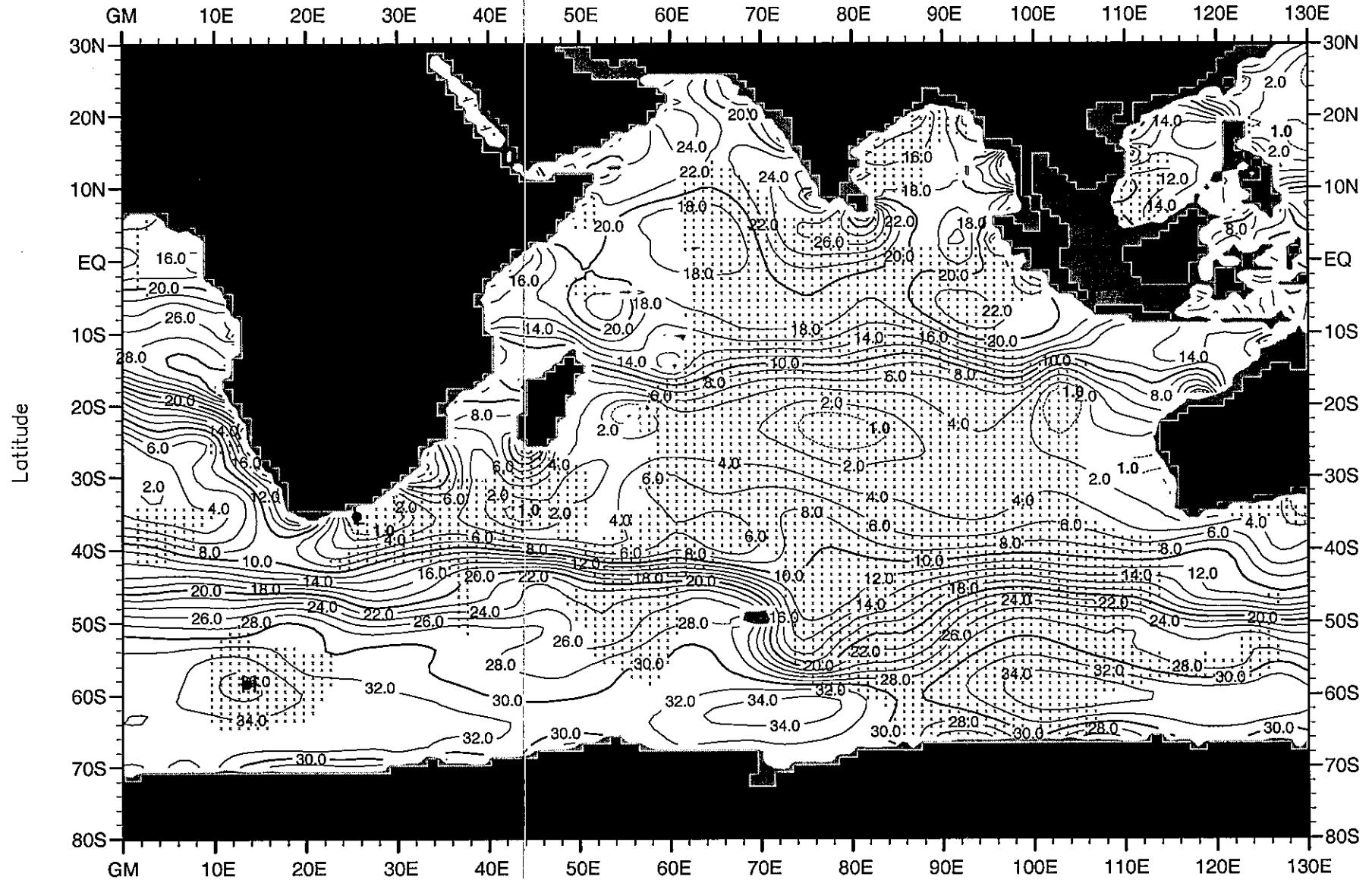
Fig. D29. Winter (Jan.-Mar.) mean nitrate (μM) at 150 m. depth .

Minimum Value= 0.00   Maximum Value= 36.46   Contour Interval: 2.00
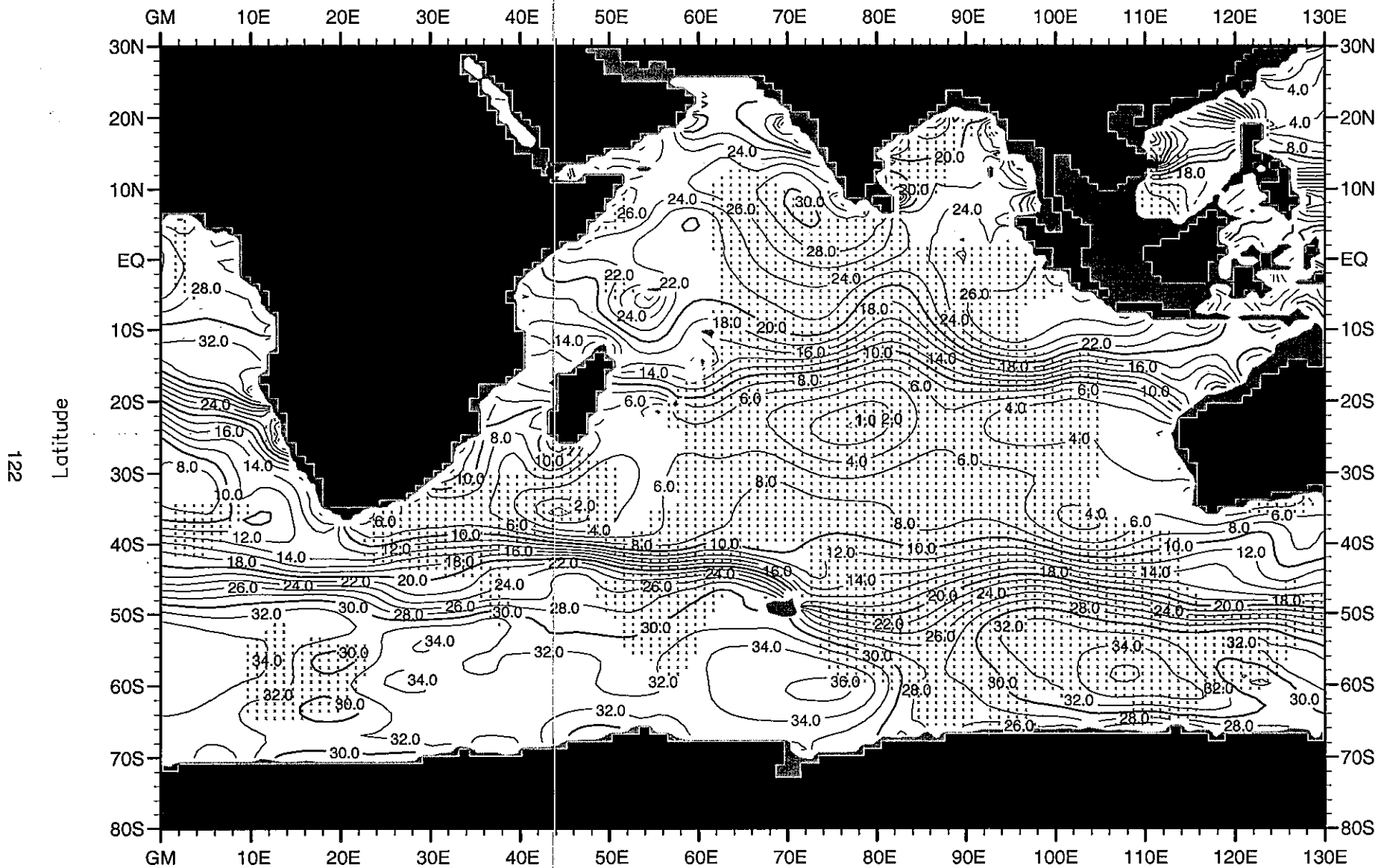
Fig. D30. Winter (Jan.-Mar.) mean nitrate (μM) at 250 m. depth .

Minimum Value= 0.20   Maximum Value= 38.76   Contour Interval: 2.00
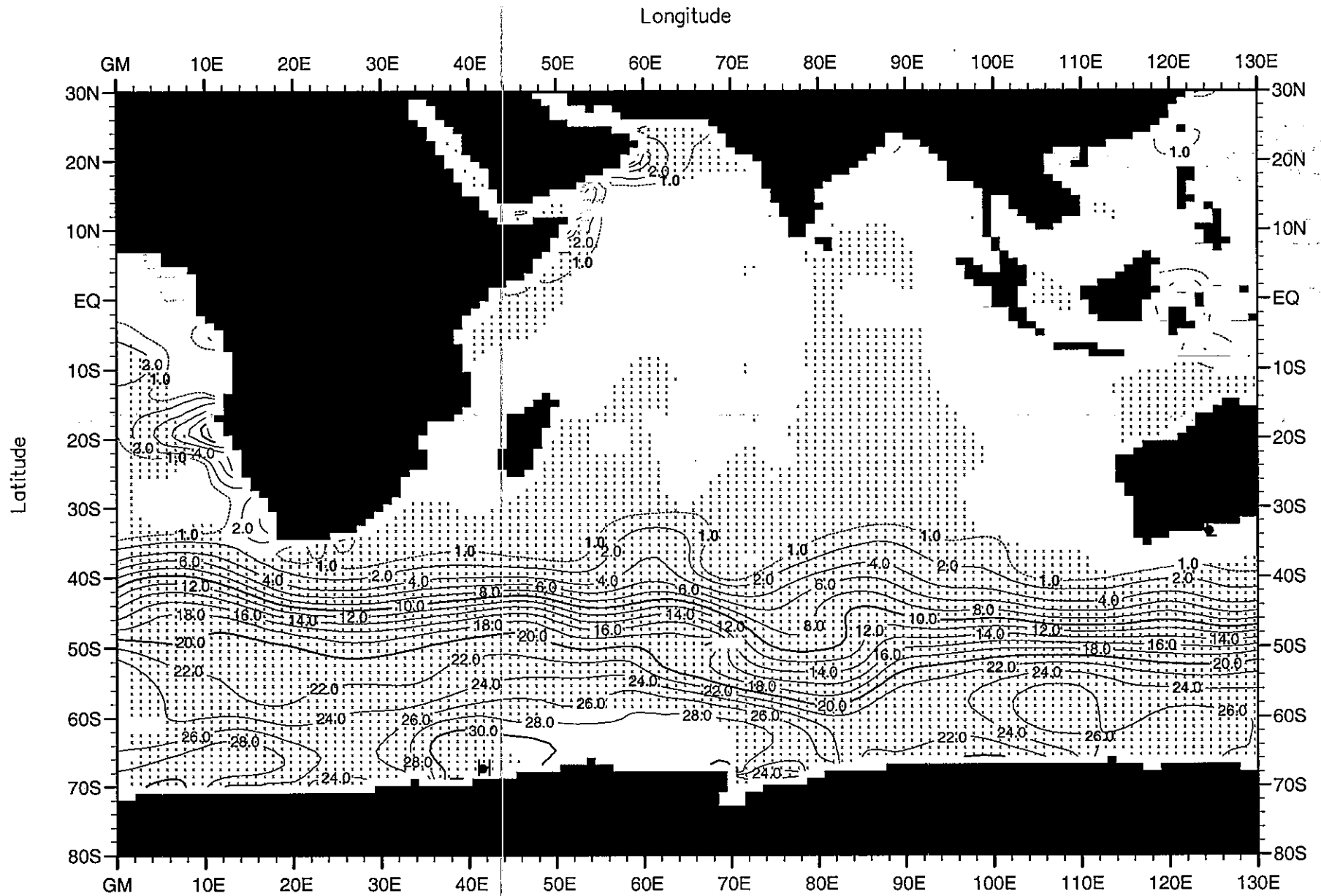
Fig. D31.   Spring (Apr.-Jun.) mean nitrate (μM) at the surface .

Minimum Value= 0.00   Maximum Value= 31.94   Contour Interval: 2.00

Fig. D32. Spring (Apr.-Jun.) mean nitrate (μM) at 50 m. depth.

Minimum Value= 0.00   Maximum Value= 34.34   Contour Interval: 2.00
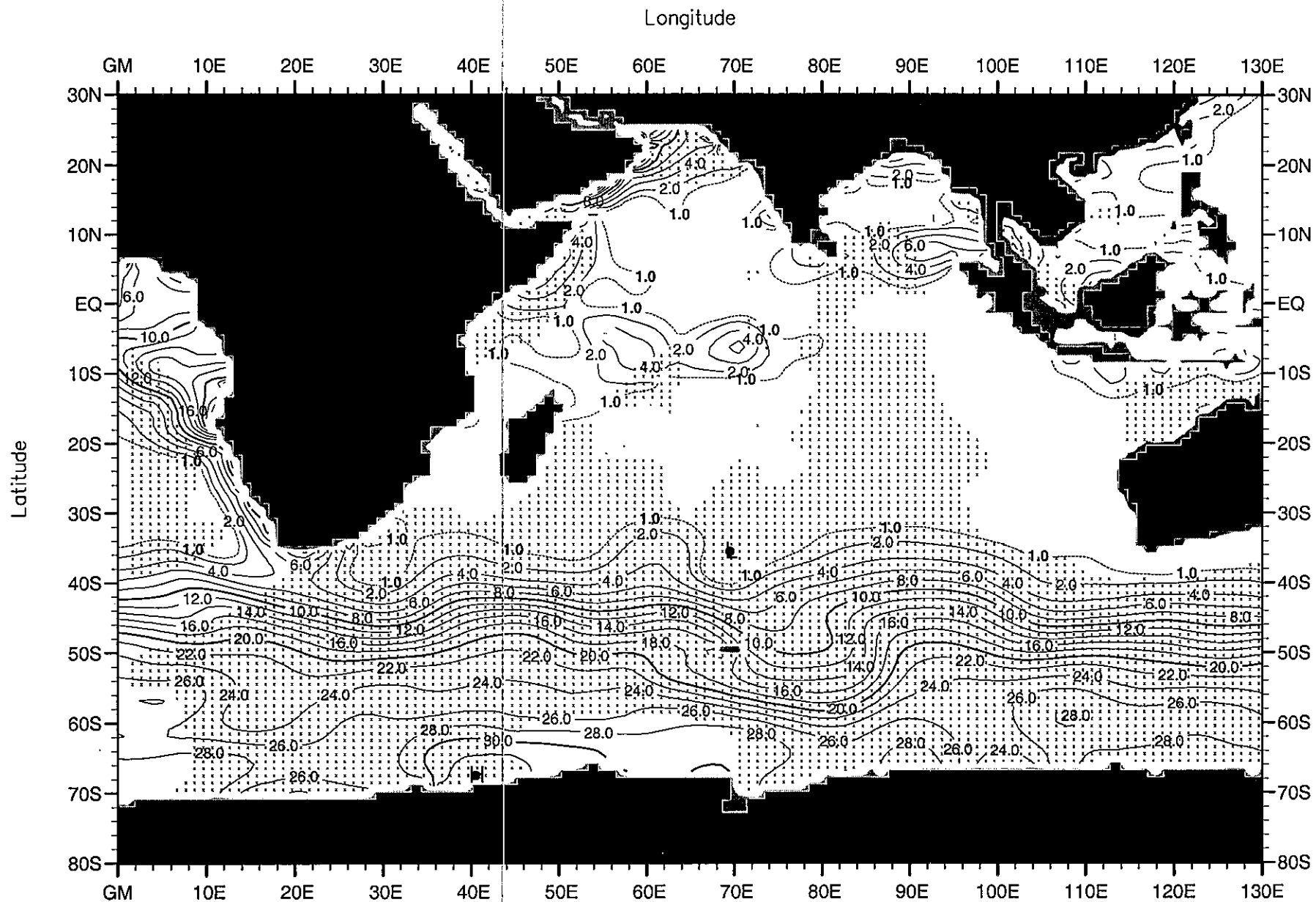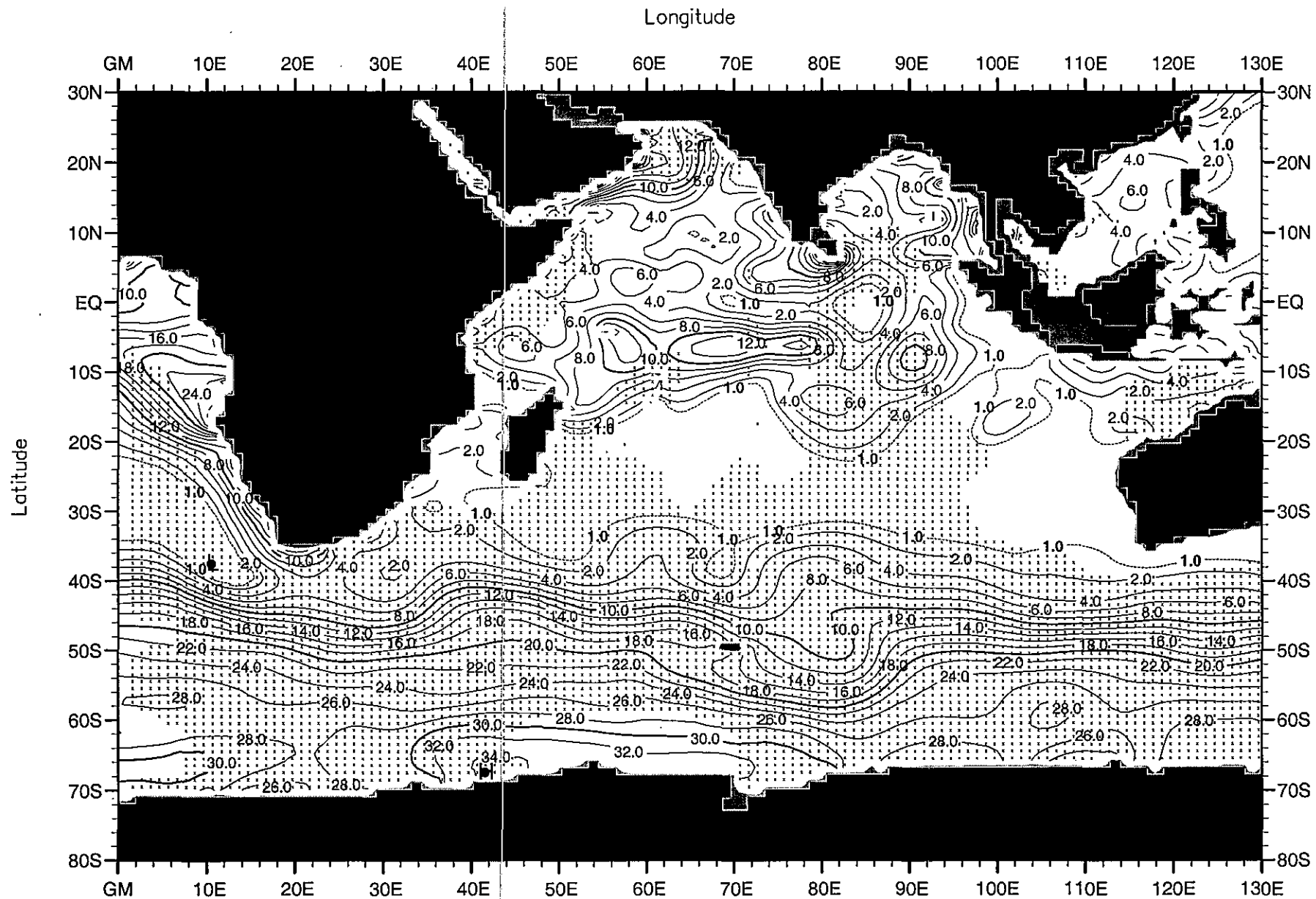
Fig. D33. Spring (Apr.-Jun.) mean nitrate (μM) at 75 m. depth .

Minimum Value= 0.00   Maximum Value= 35.54   Contour Interval: 2.00
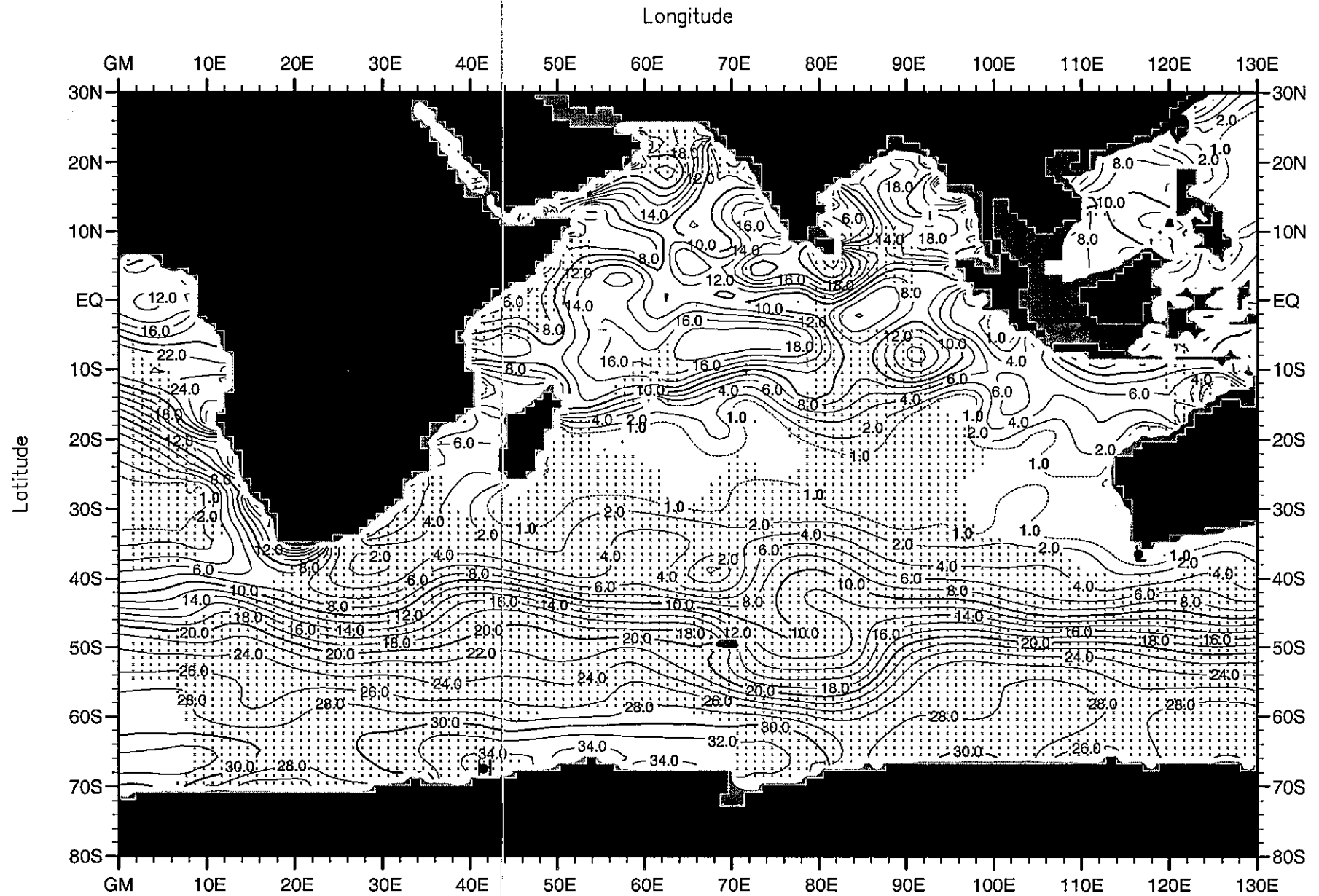
Fig. D34. Spring (Apr.-Jun.) mean nitrate (μM) at 100 m. depth .

Minimum Value= 0.00   Maximum Value= 35.75   Contour Interval: 2.00
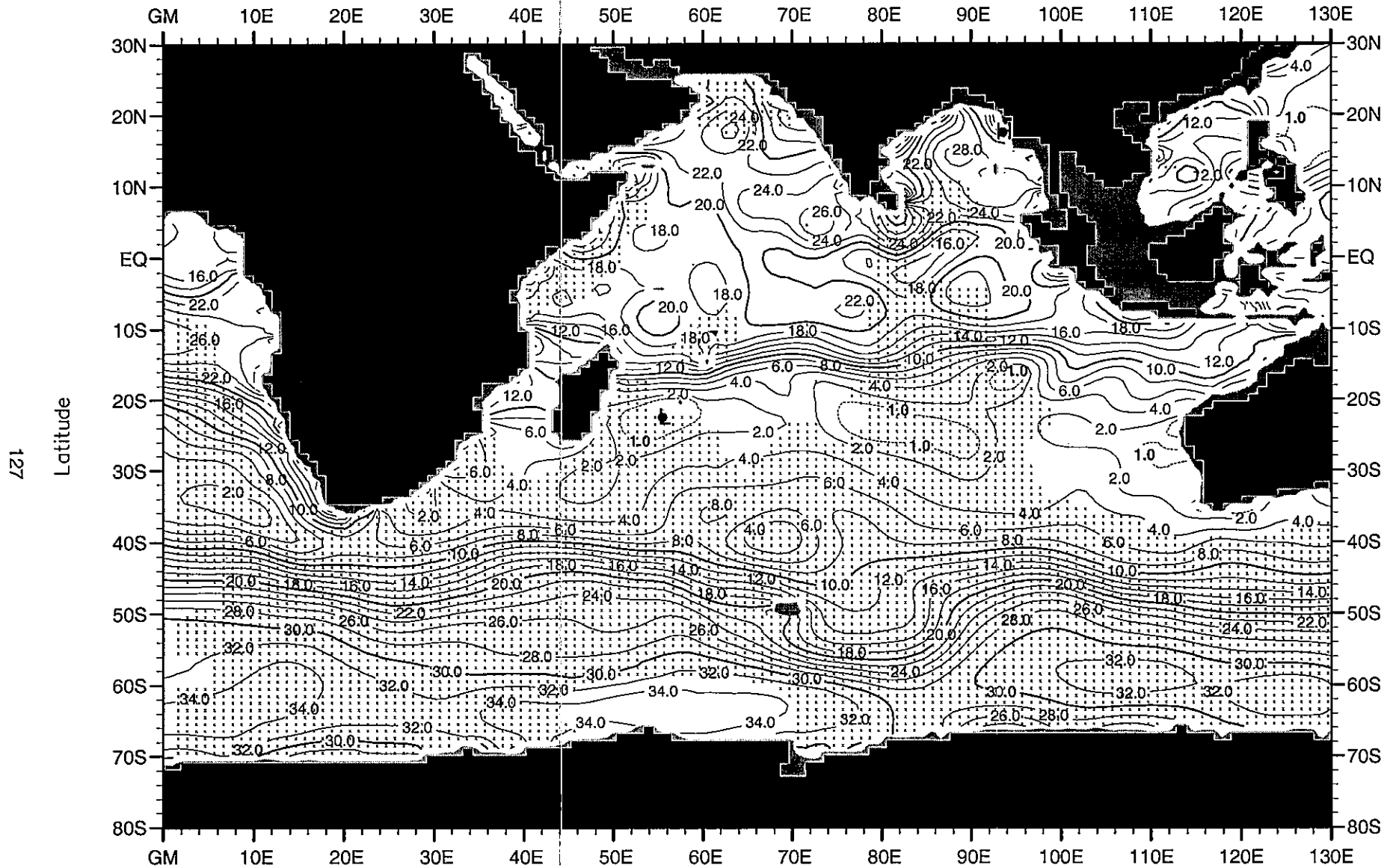
Fig. D35. Spring (Apr.-Jun.) mean nitrate (μM) at 150 m. depth .

Minimum Value= 0.00   Maximum Value= 37.93   Contour Interval: 2.00

127
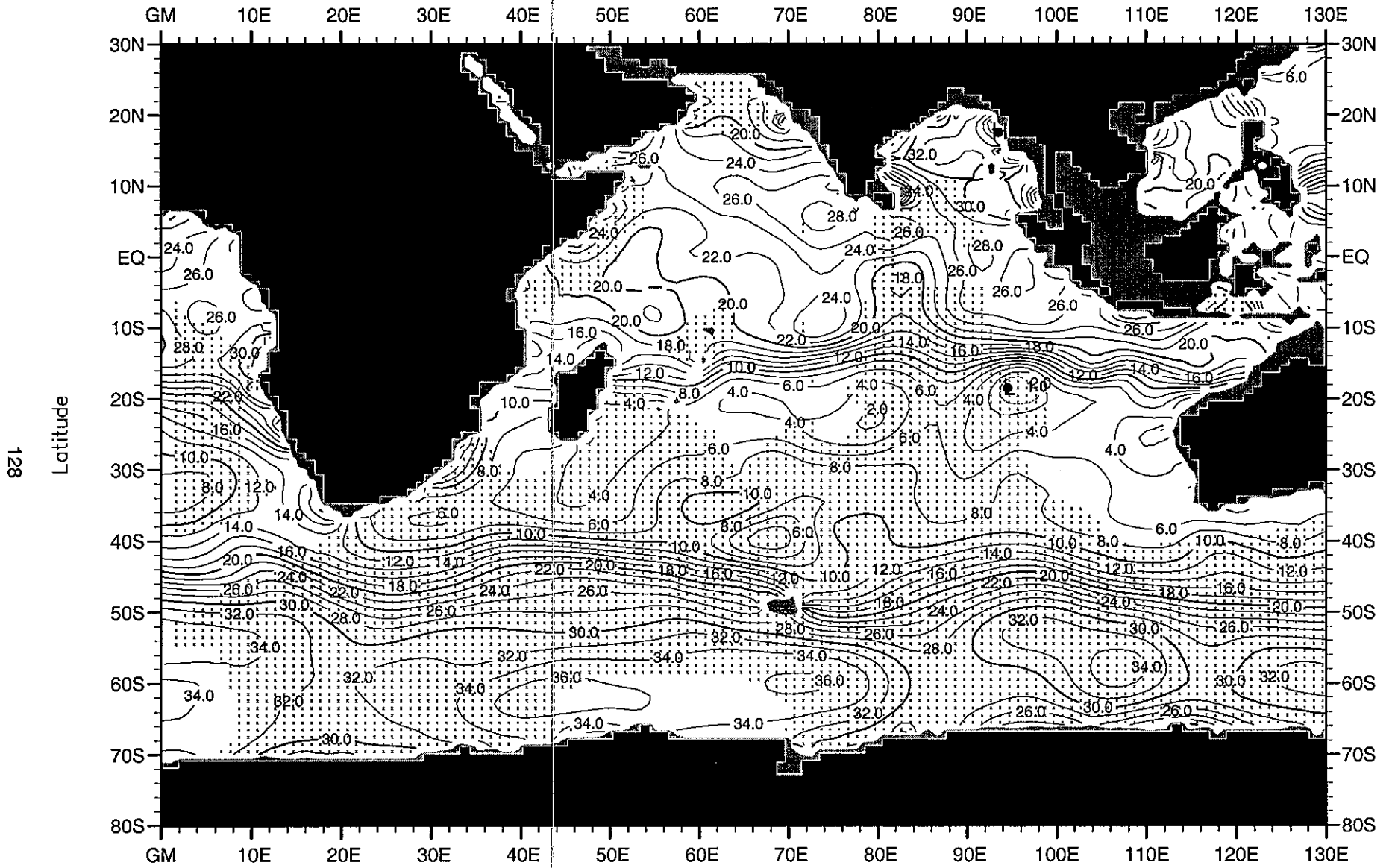
Fig. D36. Spring (Apr.-Jun.) mean nitrate (μM) at 250 m. depth .

Minimum Value= 0.00   Maximum Value= 44.74   Contour Interval: 2.00
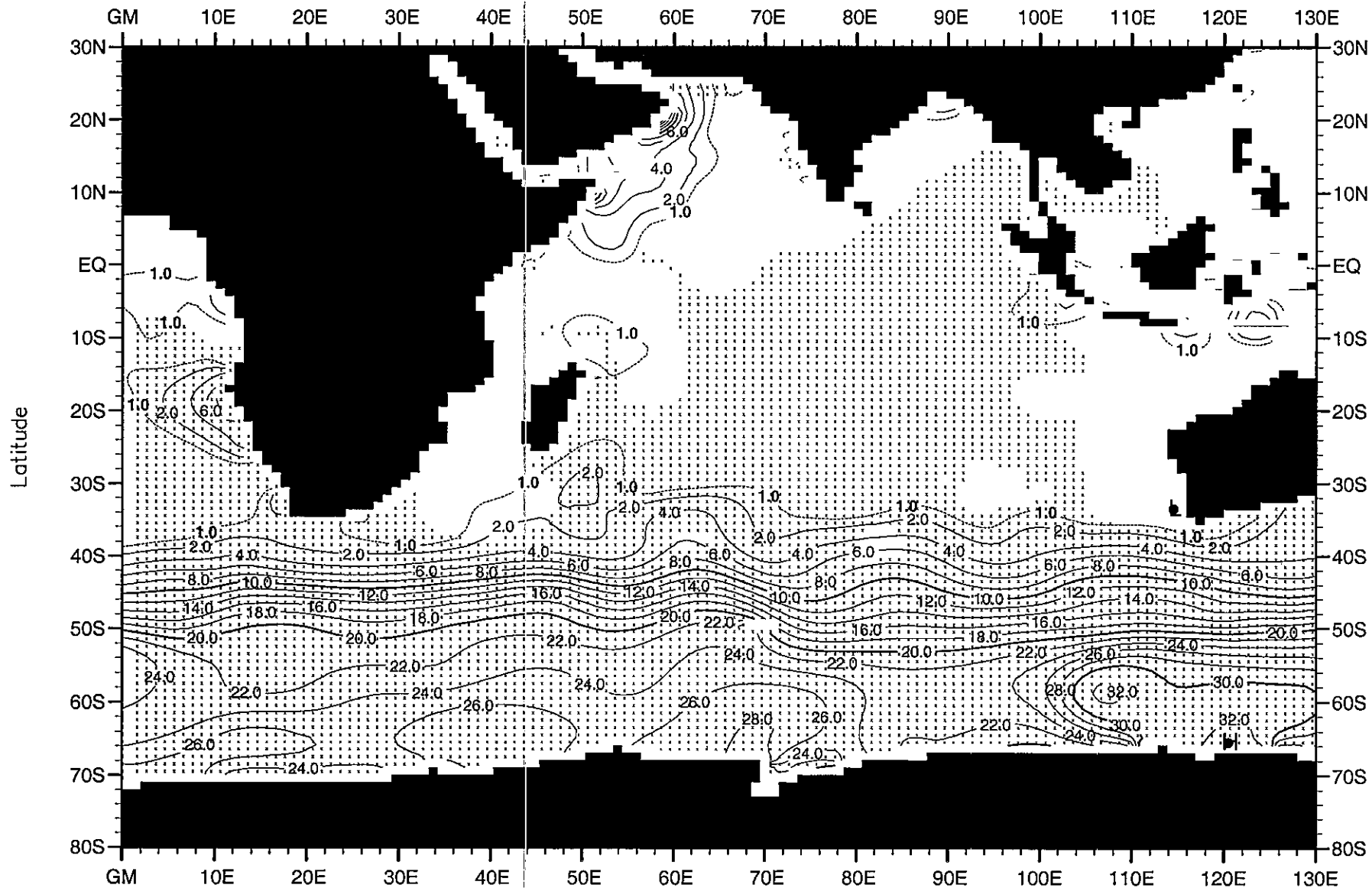
Fig. D37. Summer (Jul.-Sep.) mean nitrate (μM) at the surface .

Minimum Value= 0.00   Maximum Value= 32.50   Contour Interval: 2.00
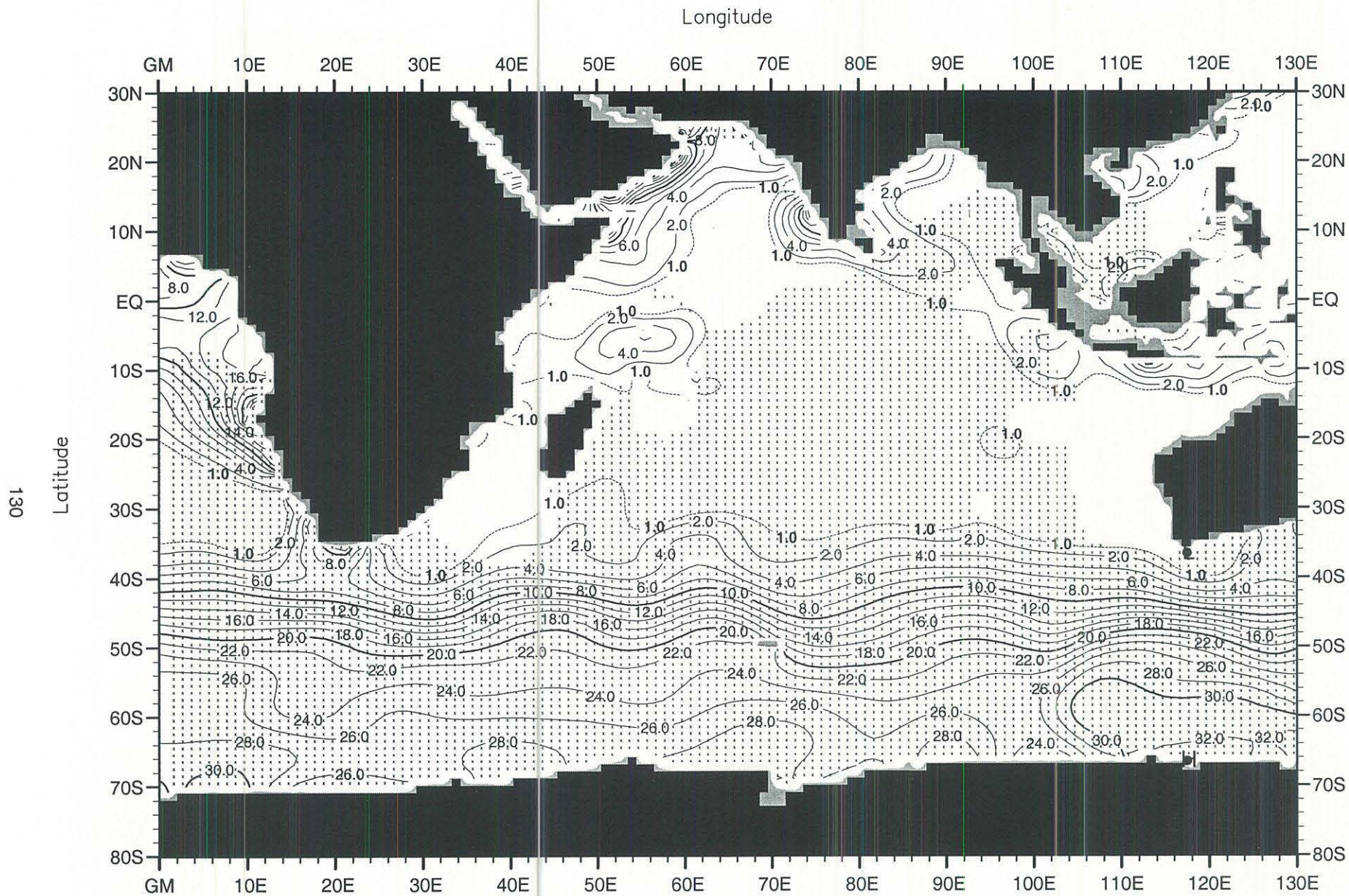
Fig. D38. Summer (Jul.-Sep.) mean nitrate (μM) at 50 m. depth.

Minimum Value= 0.00   Maximum Value= 33.58   Contour Interval: 2.00
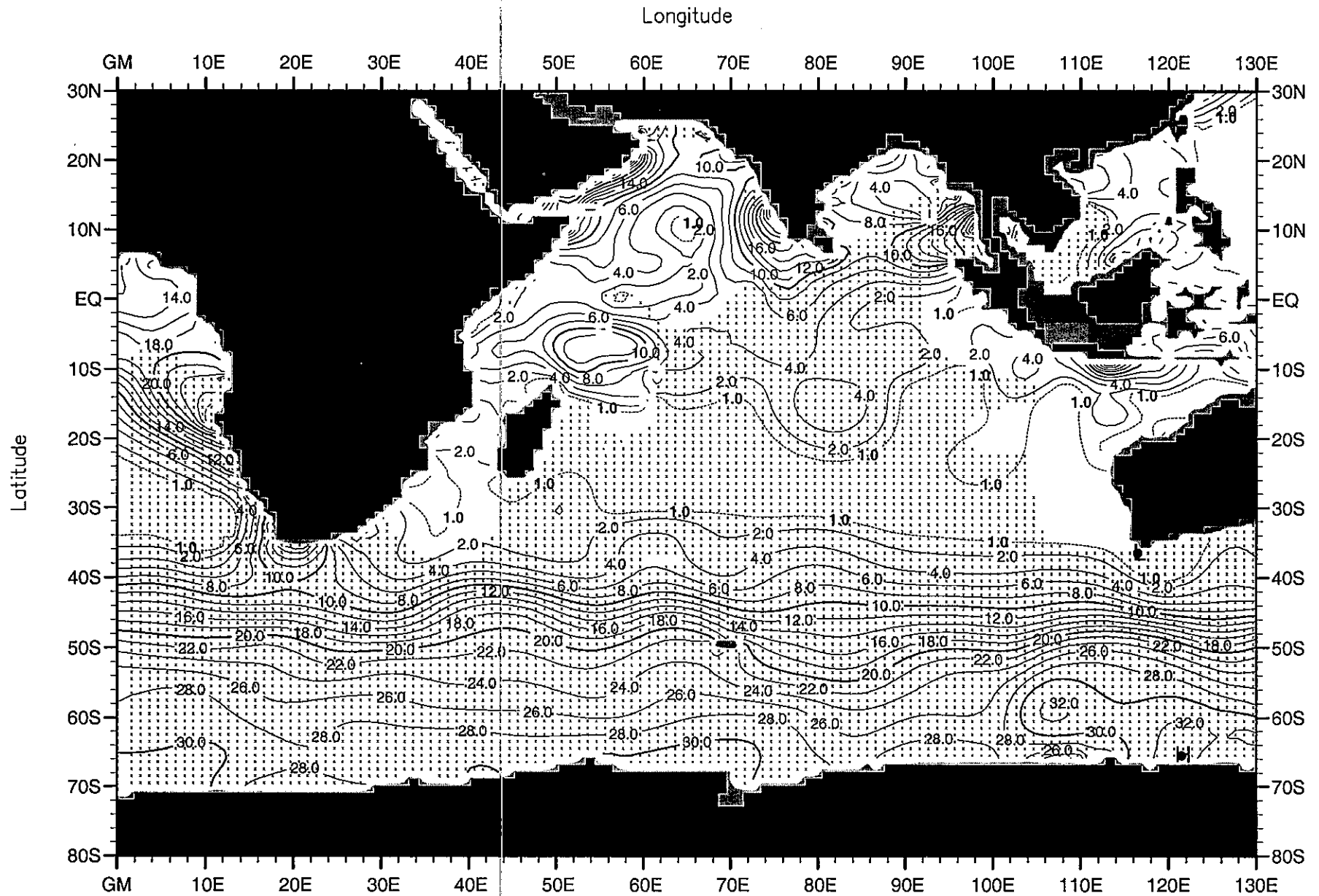
Fig. D39. Summer (Jul.-Sep.) mean nitrate (μM) at 75 m. depth .

Minimum Value= 0.00   Maximum Value= 33.33   Contour Interval: 2.00
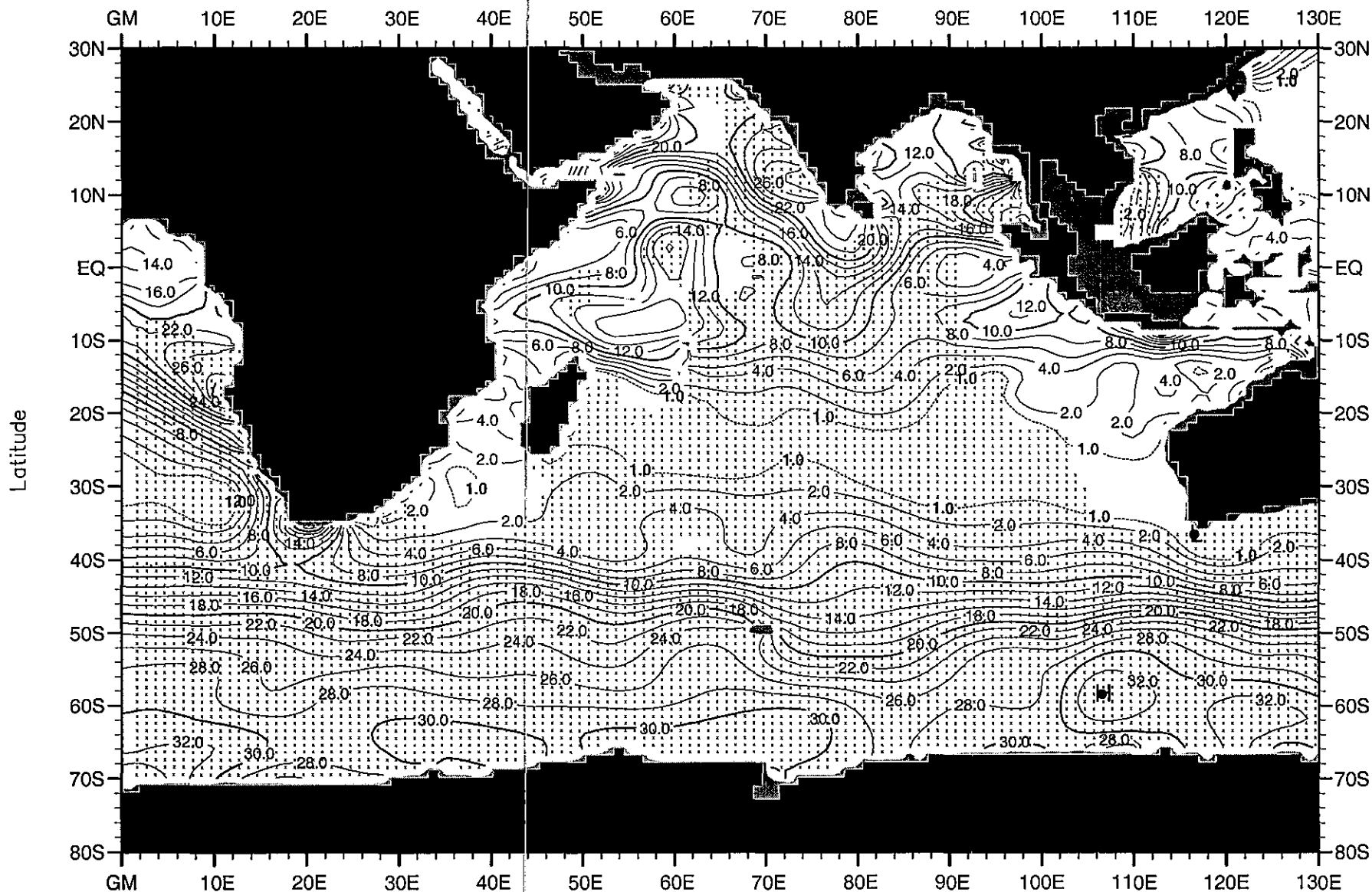
Fig. D40.   Summer (Jul.-Sep.) mean nitrate (μM) at 100 m. depth .

Minimum Value=   0.00   Maximum Value=   33.53   Contour Interval: 2.00
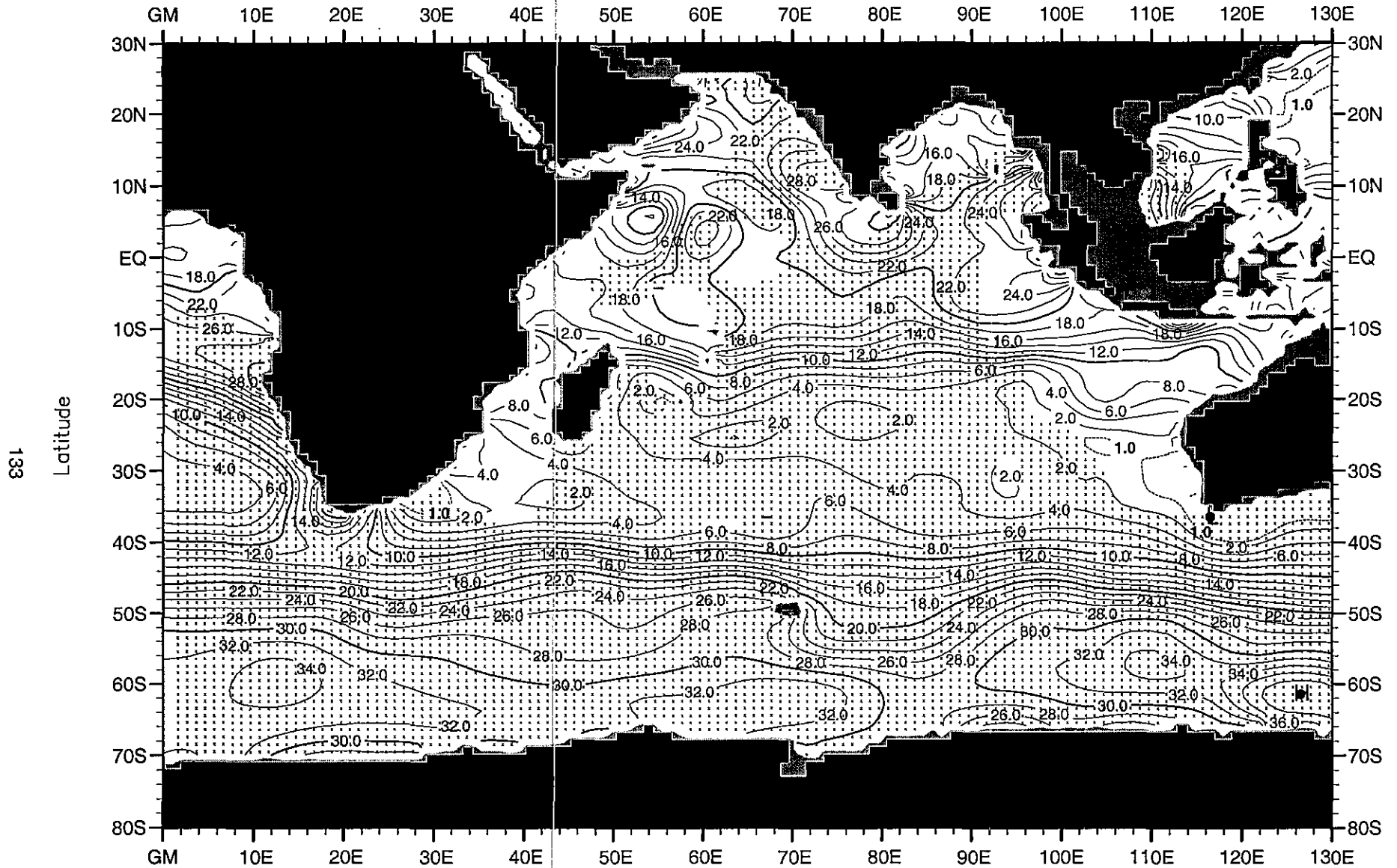
Fig. D41.   Summer (Jul.-Sep.) mean nitrate (μM) at 150 m. depth .

Minimum Value=   0.00   Maximum Value= 39.79   Contour Interval: 2.00

133
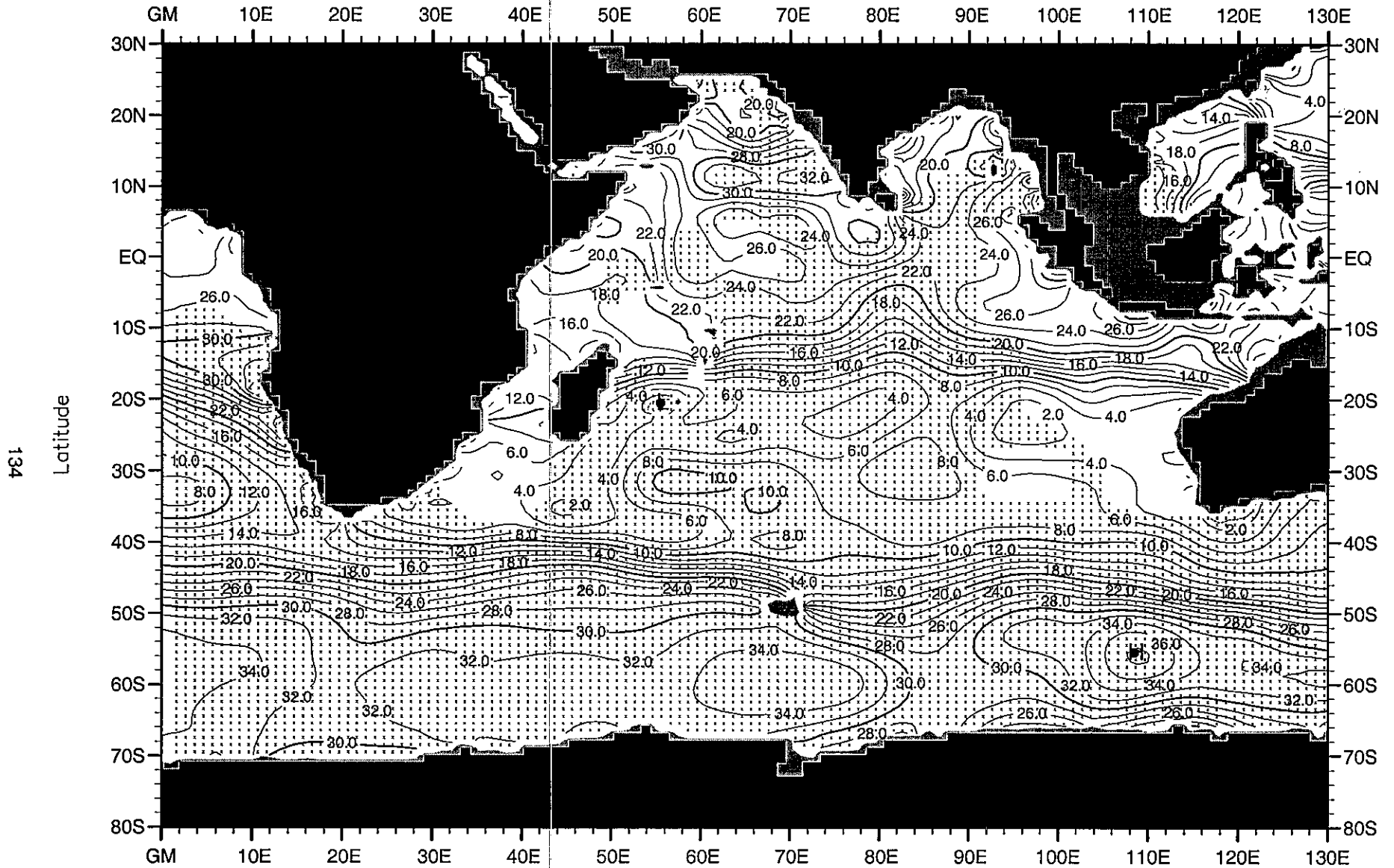
Fig. D42.   Summer (Jul.-Sep.) mean nitrate (μM) at 250 m. depth .

Minimum Value=   0.00   Maximum Value= 38.31   Contour Interval: 2.00

Fig. D43.   Fall (Oct.-Dec.) mean nitrate (μM) at the surface .

Minimum Value= 0.00   Maximum Value= 32.52   Contour Interval: 2.00
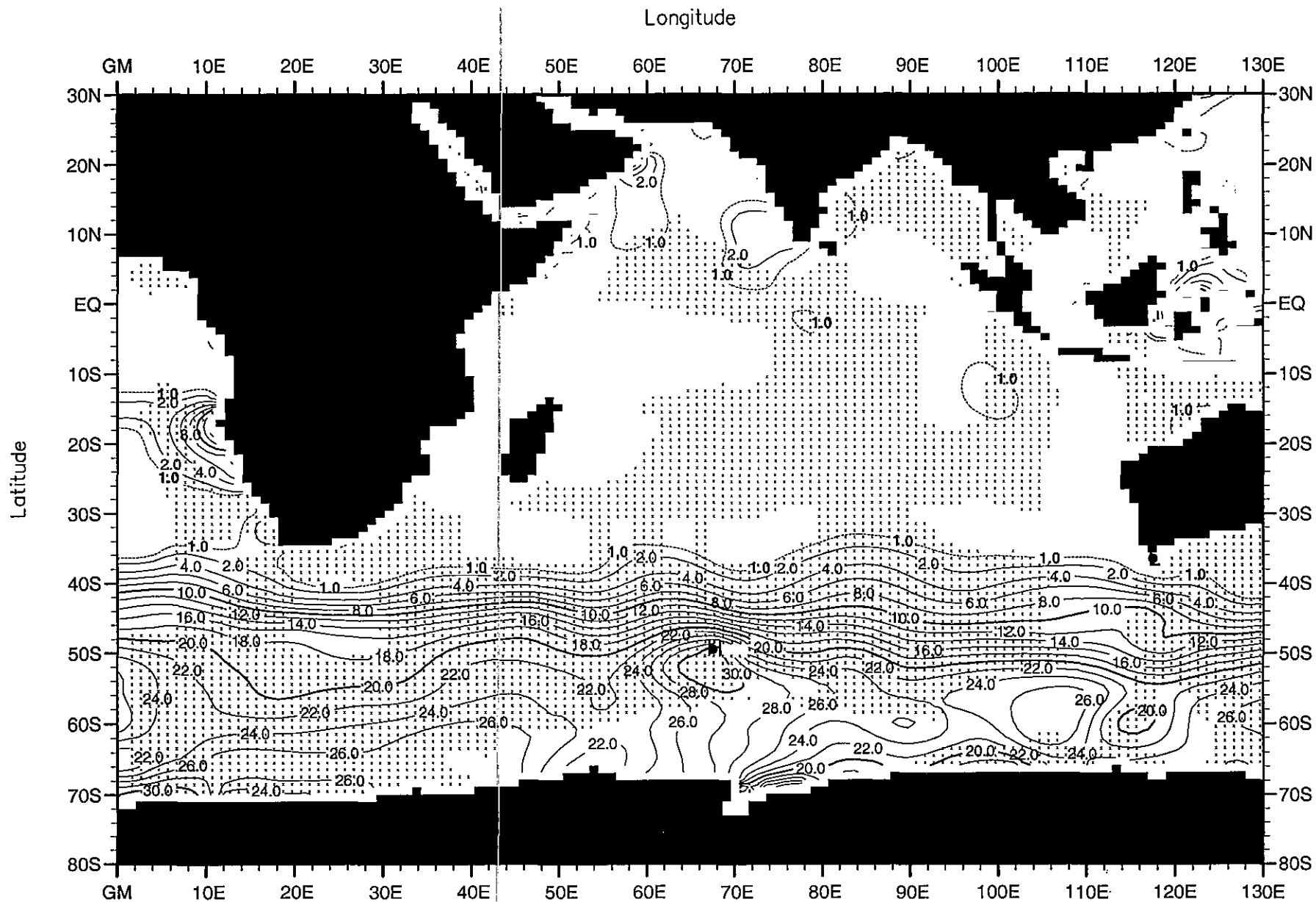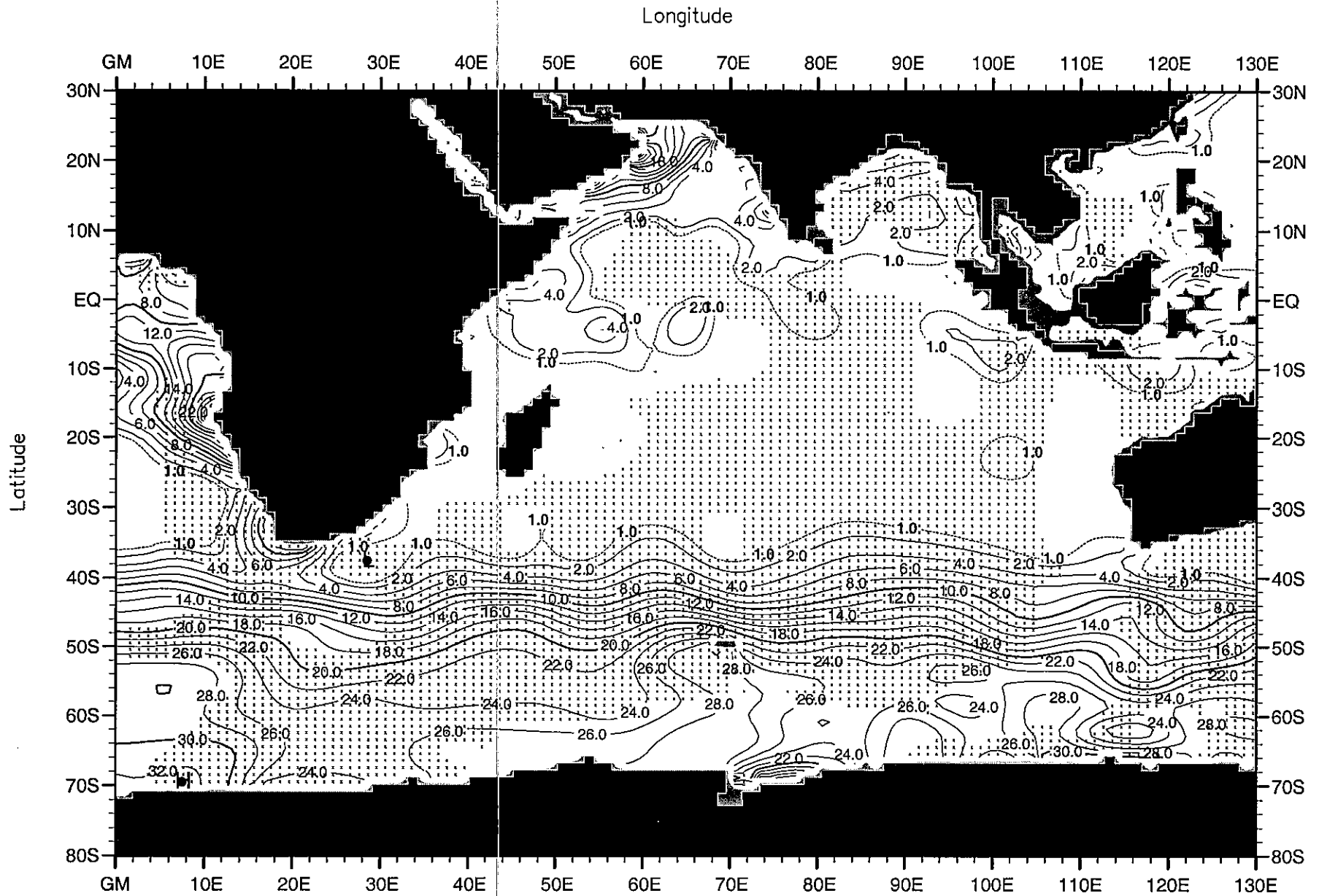
Fig. D44. Fall (Oct.-Dec.) mean nitrate (μM) at 50 m. depth .

Minimum Value= 0.00   Maximum Value= 33.67   Contour Interval: 2.00
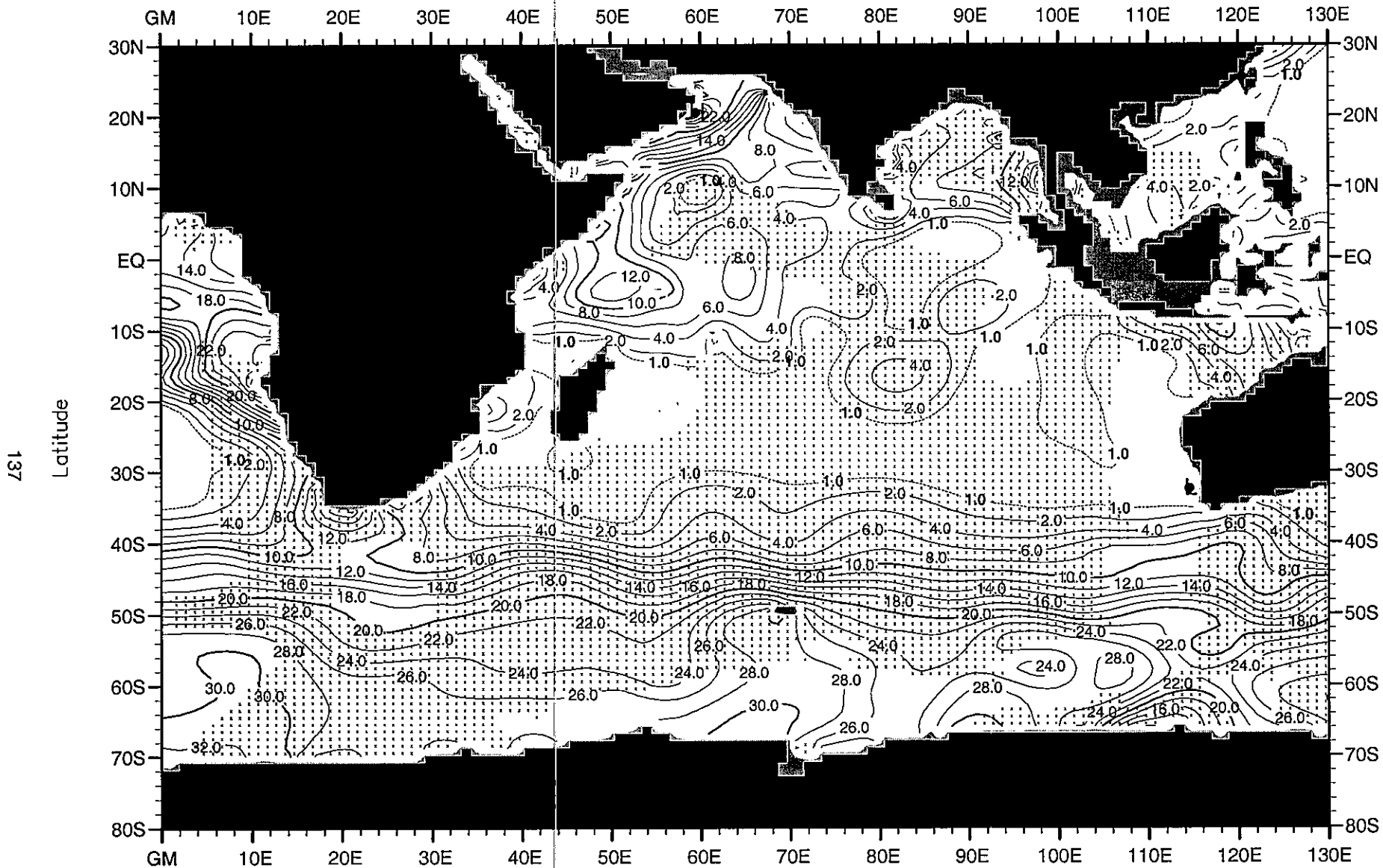
Fig. D45. Fall (Oct.-Dec.) mean nitrate (μM) at 75 m. depth .

Minimum Value= 0.00   Maximum Value= 34.15   Contour Interval: 2.00
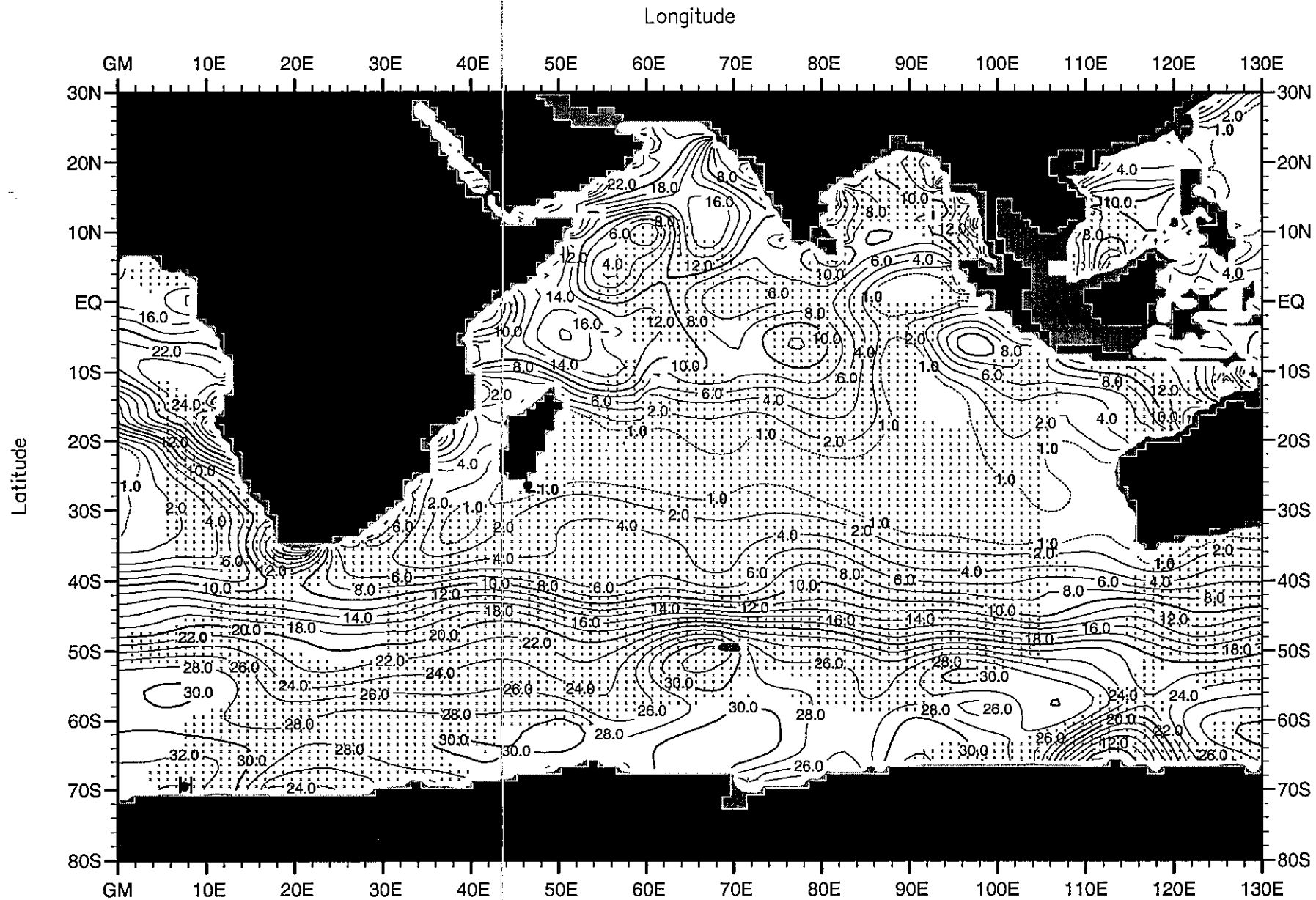
Fig. D46.   Fall (Oct.-Dec.) mean nitrate (μM) at 100 m. depth .

Minimum Value=   0.00   Maximum Value=   34.26   Contour Interval: 2.00
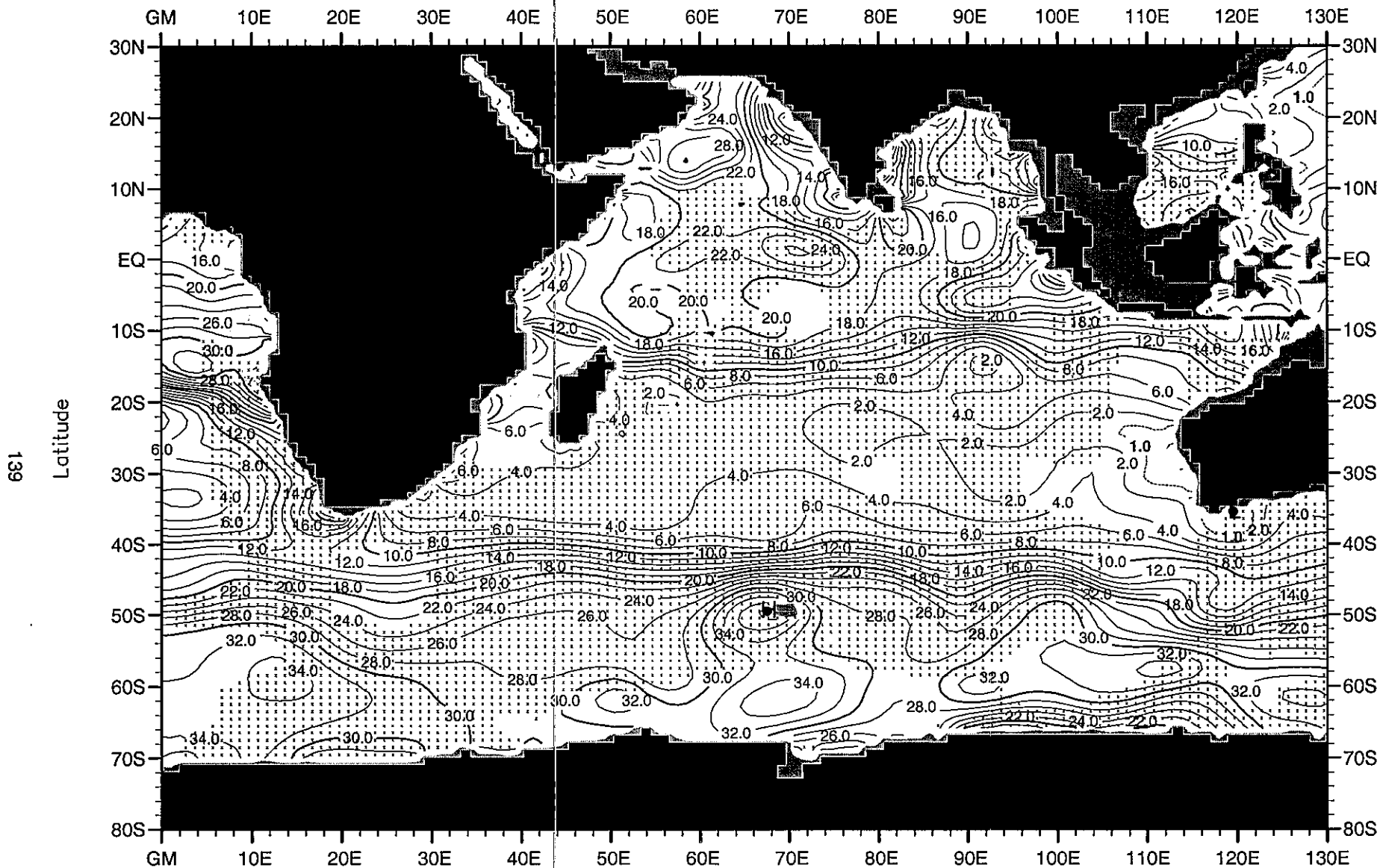
Fig. D47.   Fall (Oct.-Dec.) mean nitrate (μM) at 150 m. depth .

Minimum Value= 0.00   Maximum Value= 39.76   Contour Interval: 2.00

139
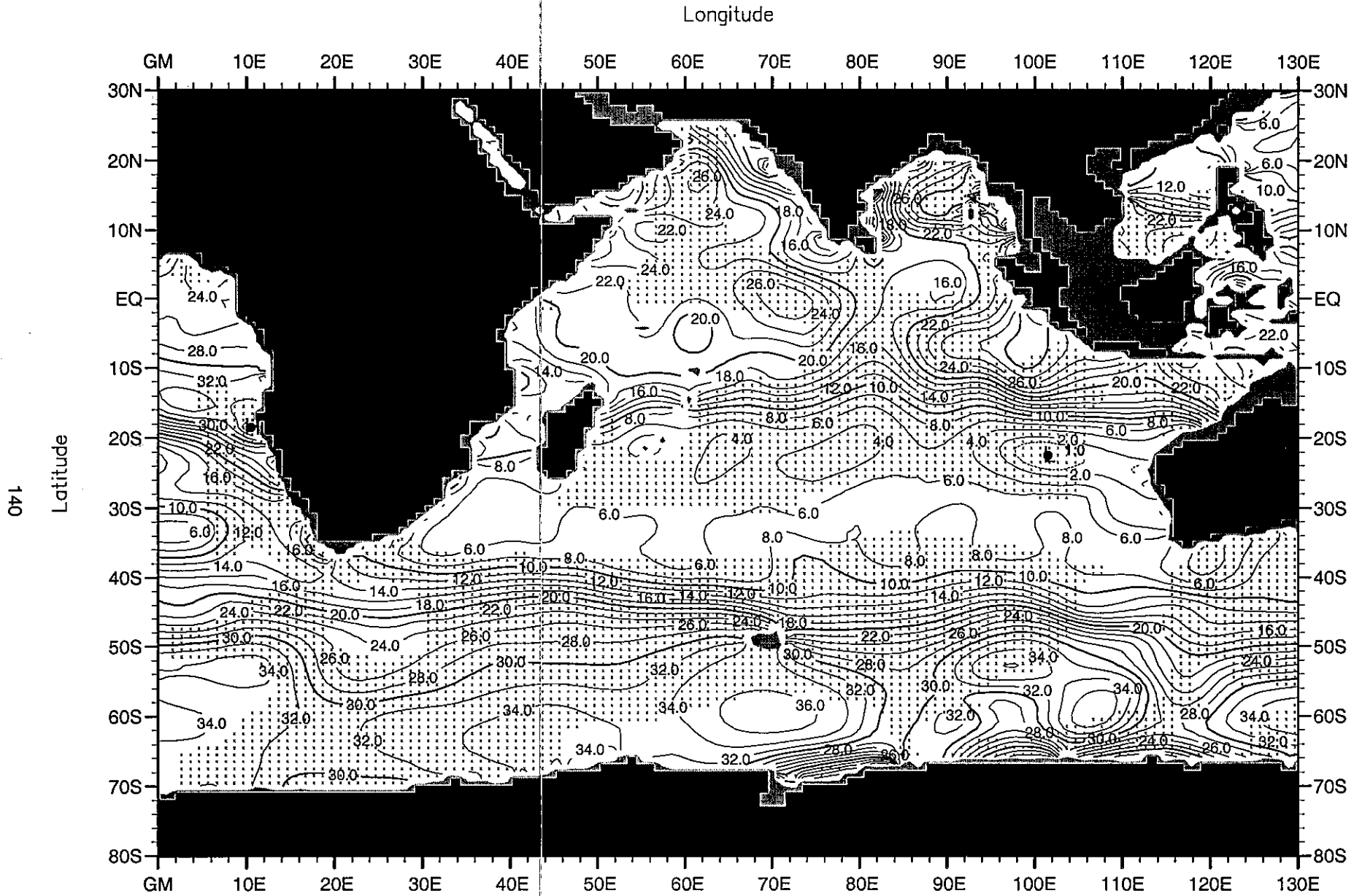
Fig. D48.   Fall (Oct.-Dec.) mean nitrate (μM) at 250 m. depth .

Minimum Value=   0.12   Maximum Value=   38.66   Contour Interval: 2.00
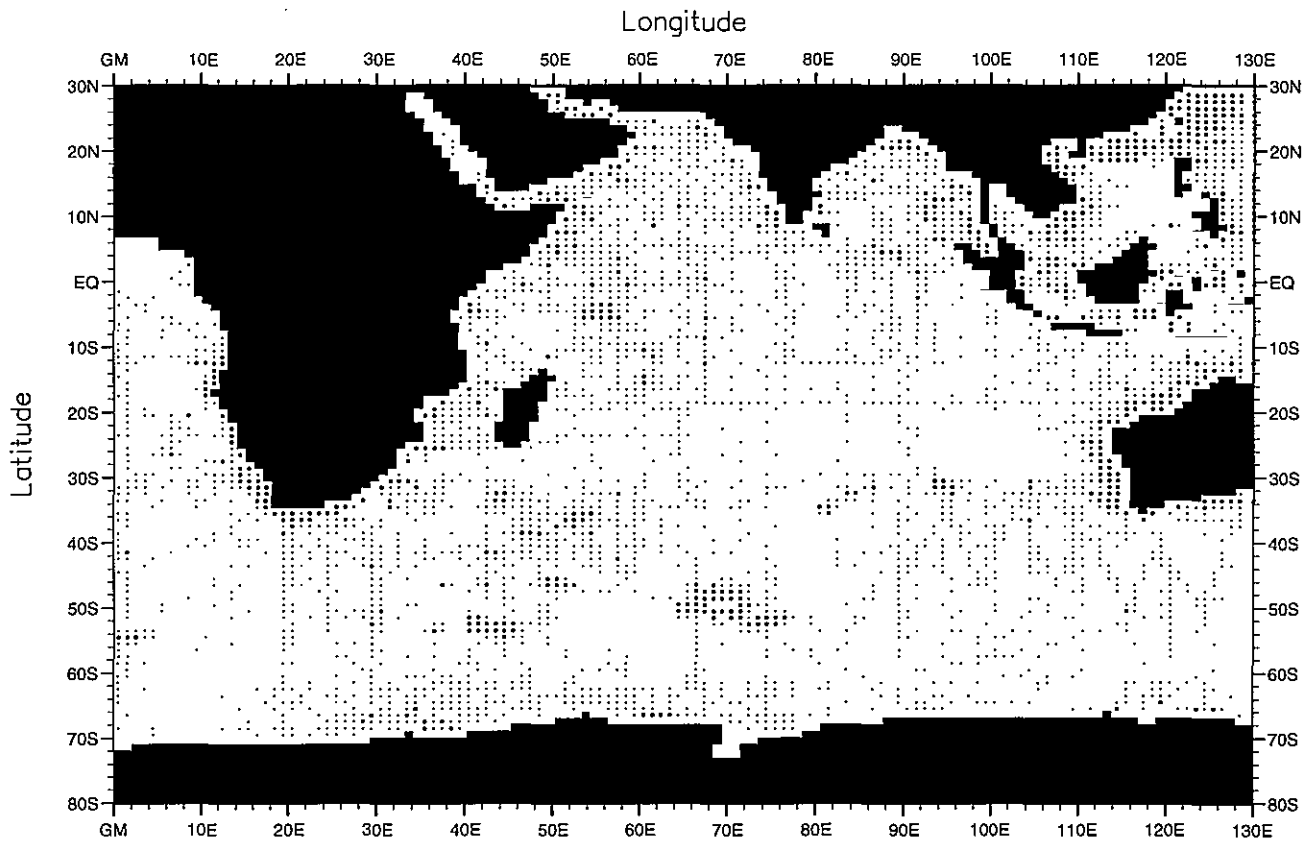
Fig. E1. Annual silicate observations at the surface .
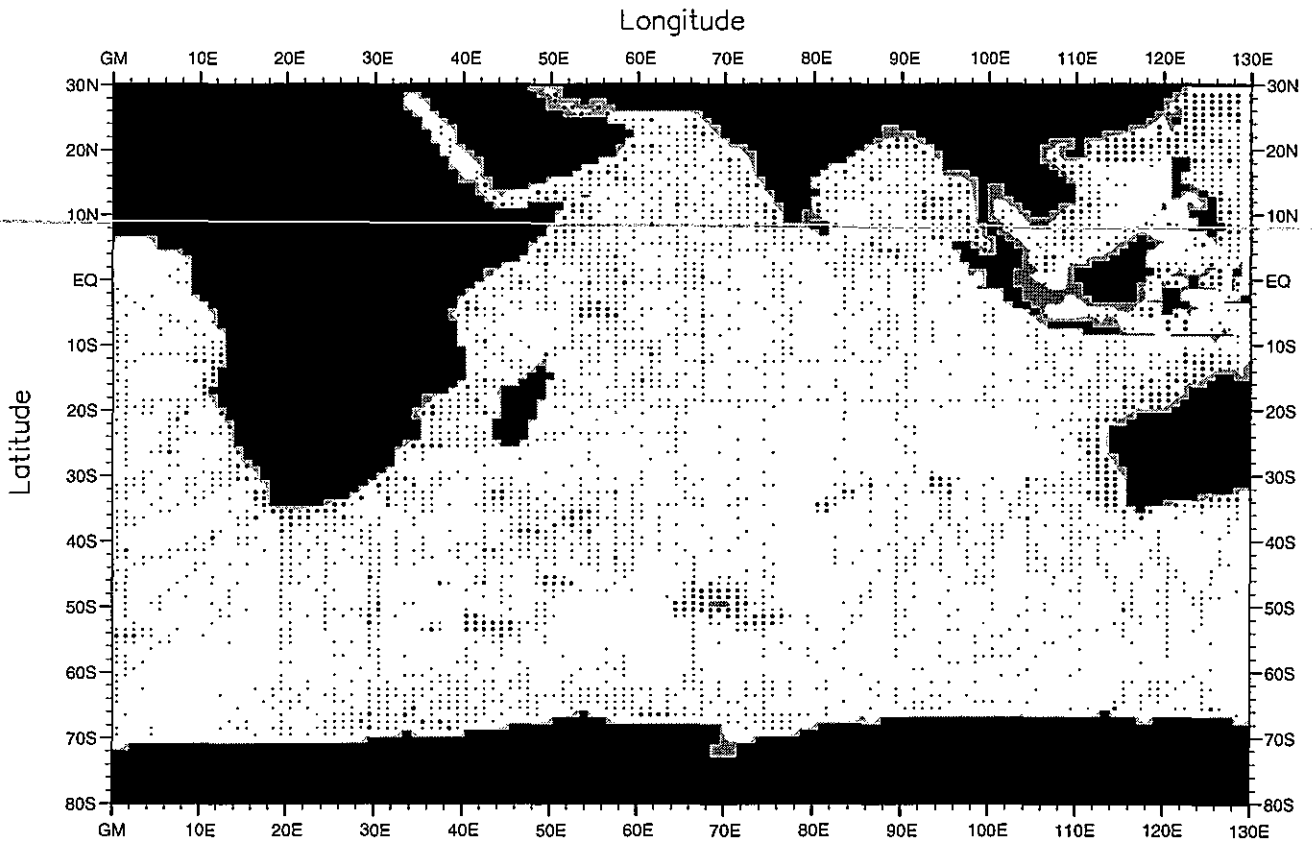
Fig. E2. Annual silicate observations at 50 m. depth .
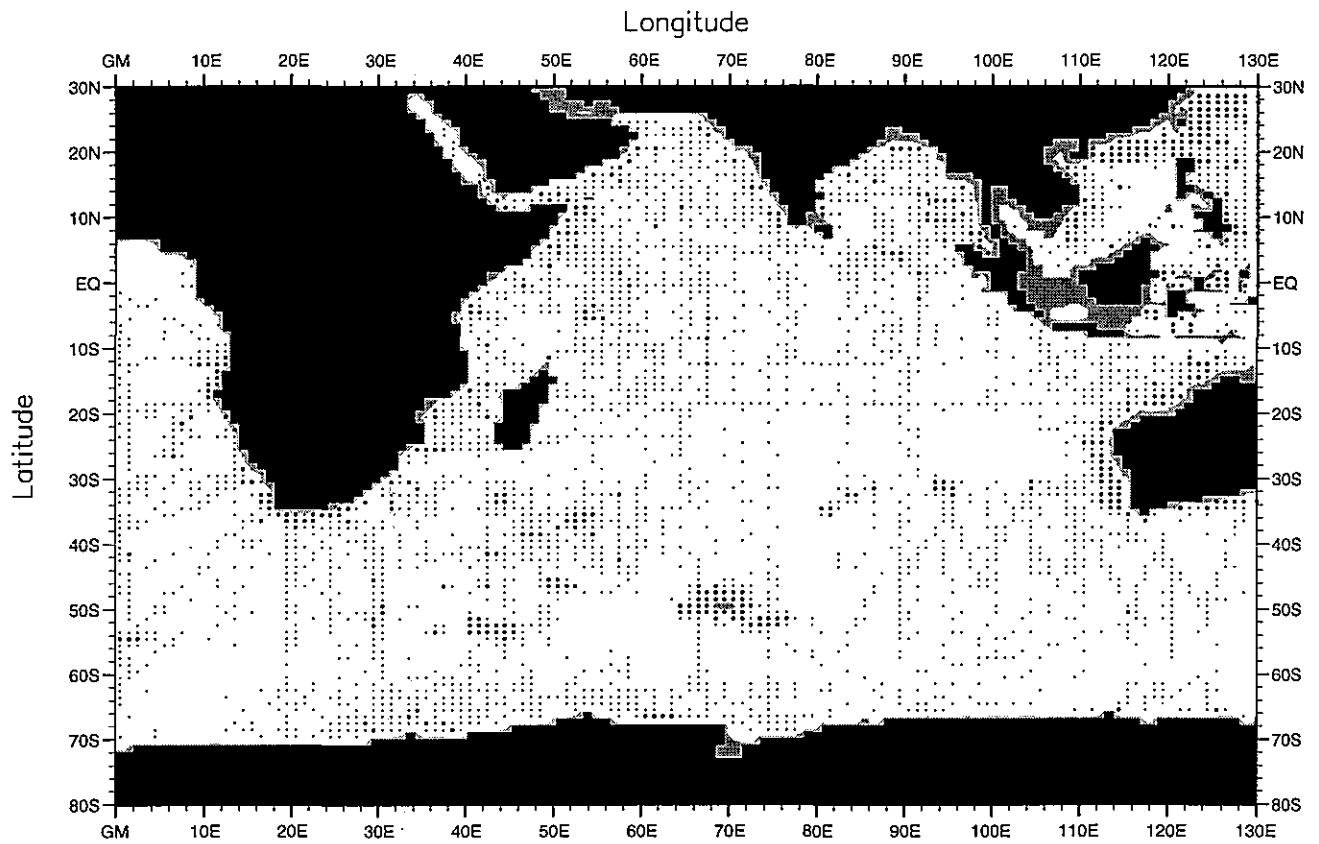
Fig. E3. Annual silicate observations at 75 m. depth .
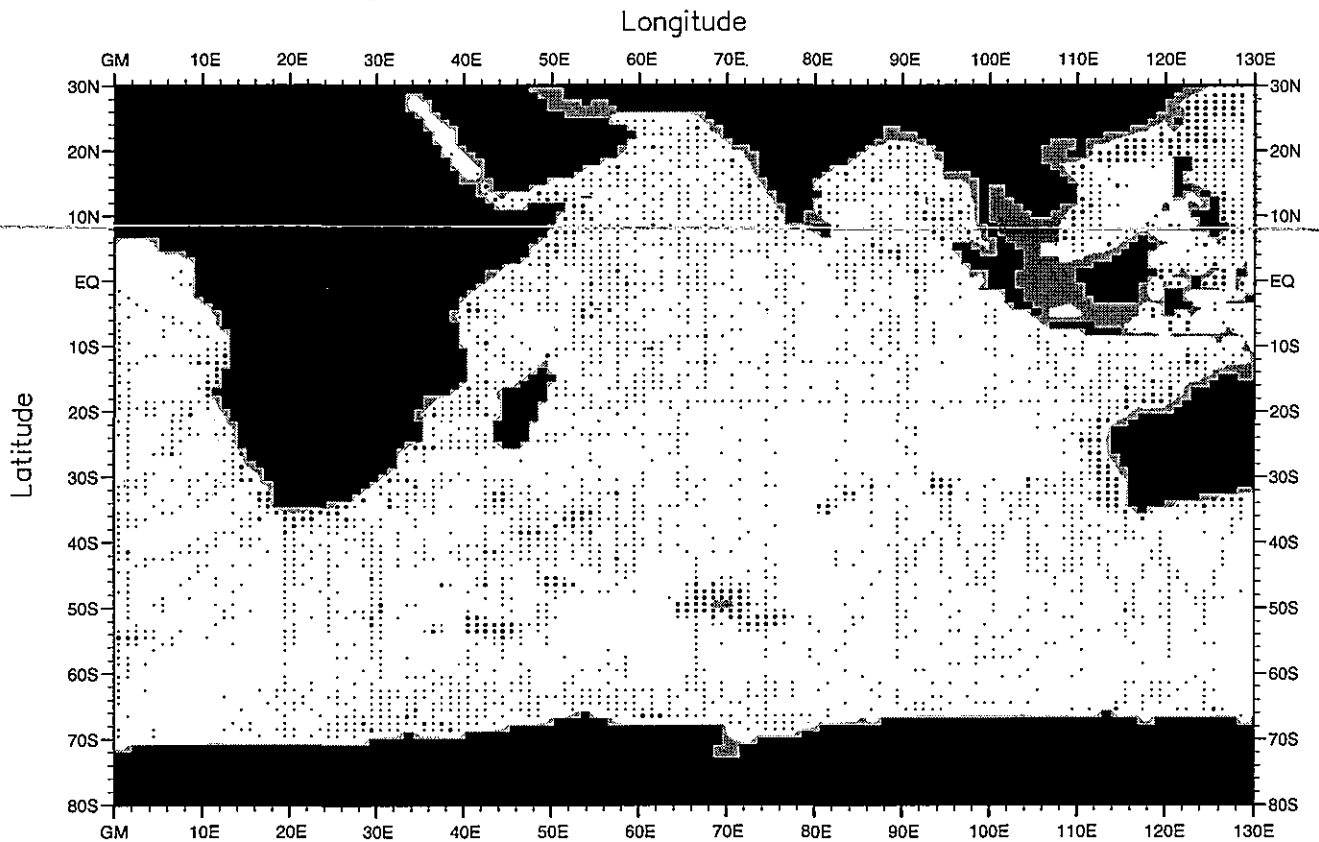
Fig. E4. Annual silicate observations at 100 m. depth .
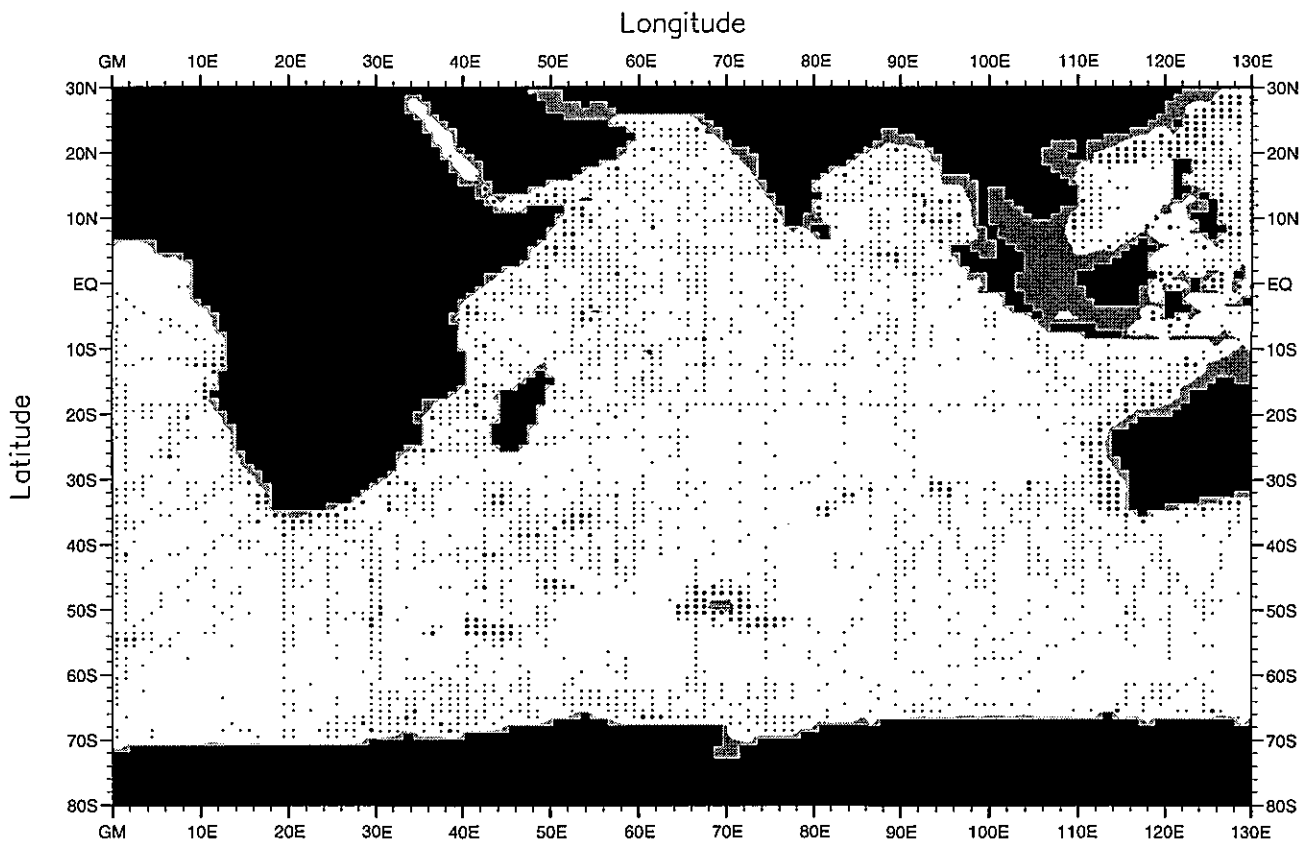
Fig. E5. Annual silicate observations at 150 m. depth .
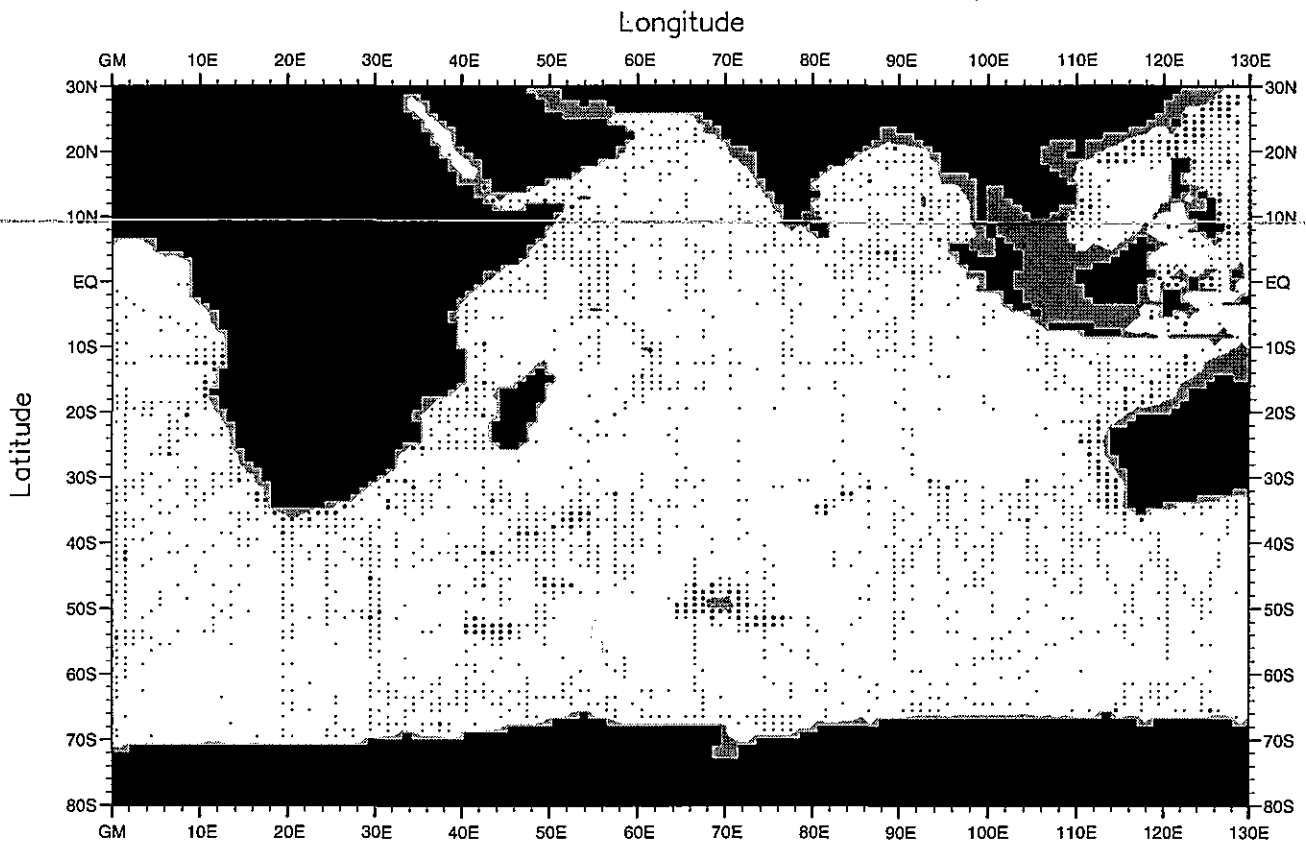
Fig. E6. Annual silicate observations at 200 m. depth .
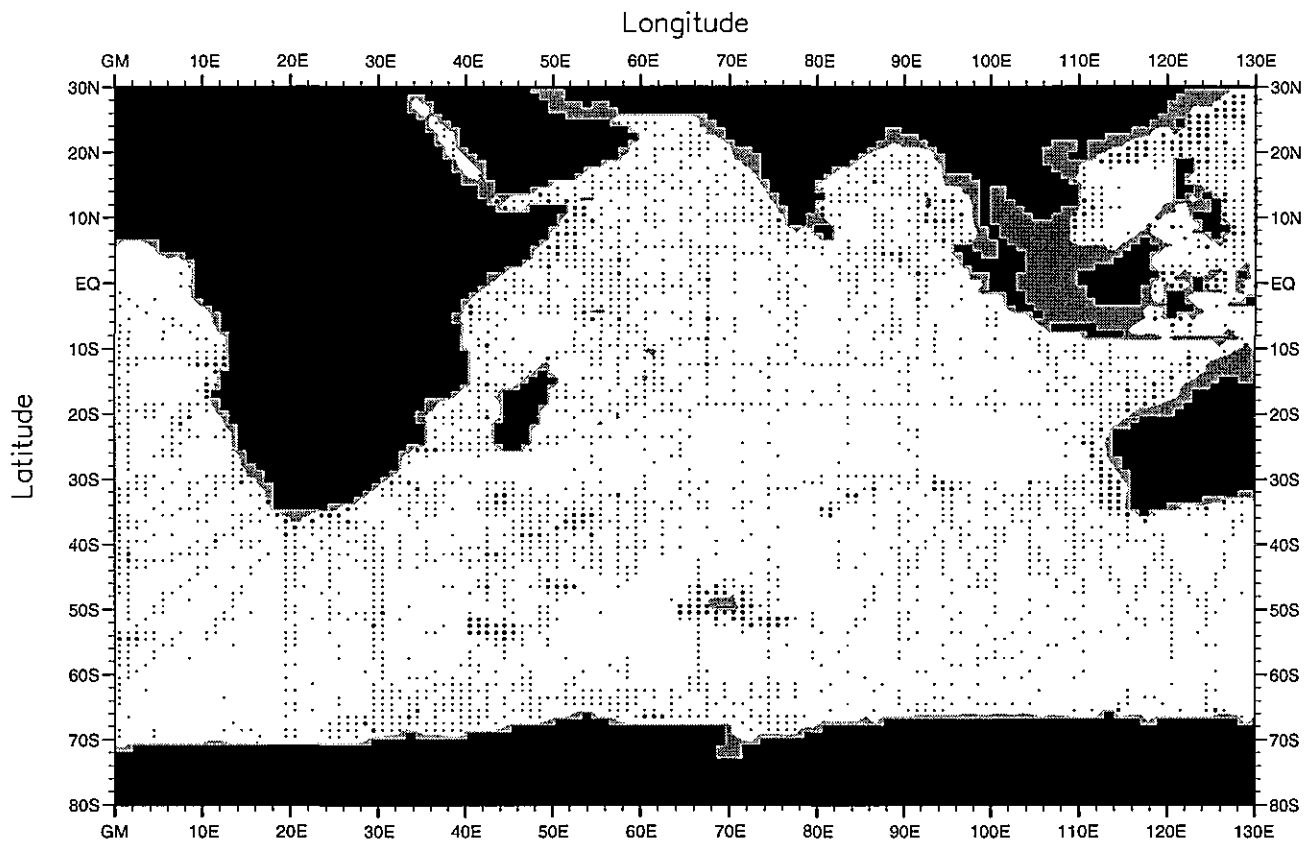
Fig. E7.   Annual silicate observations at 250 m. depth .
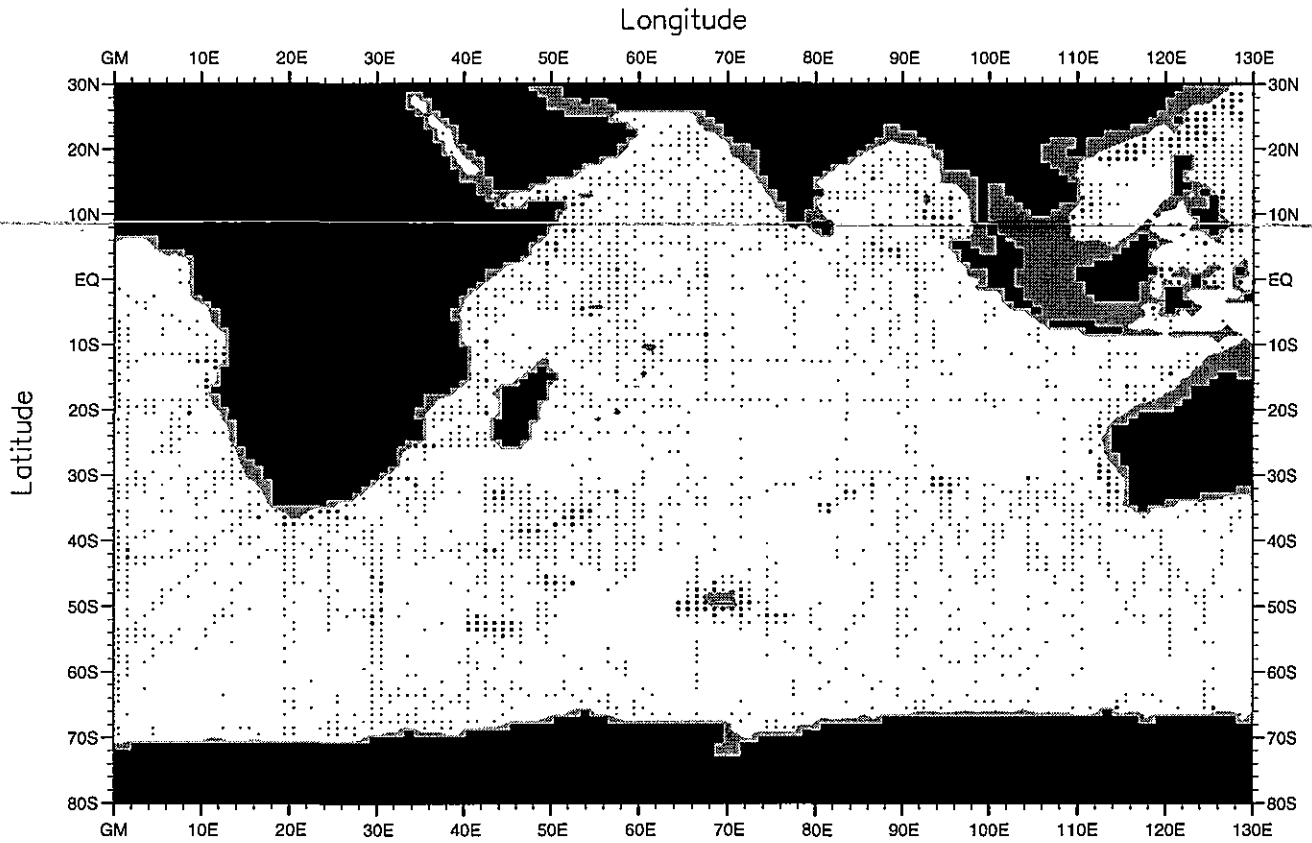
Fig. E8.   Annual silicate observations at 400 m. depth .

Longitude
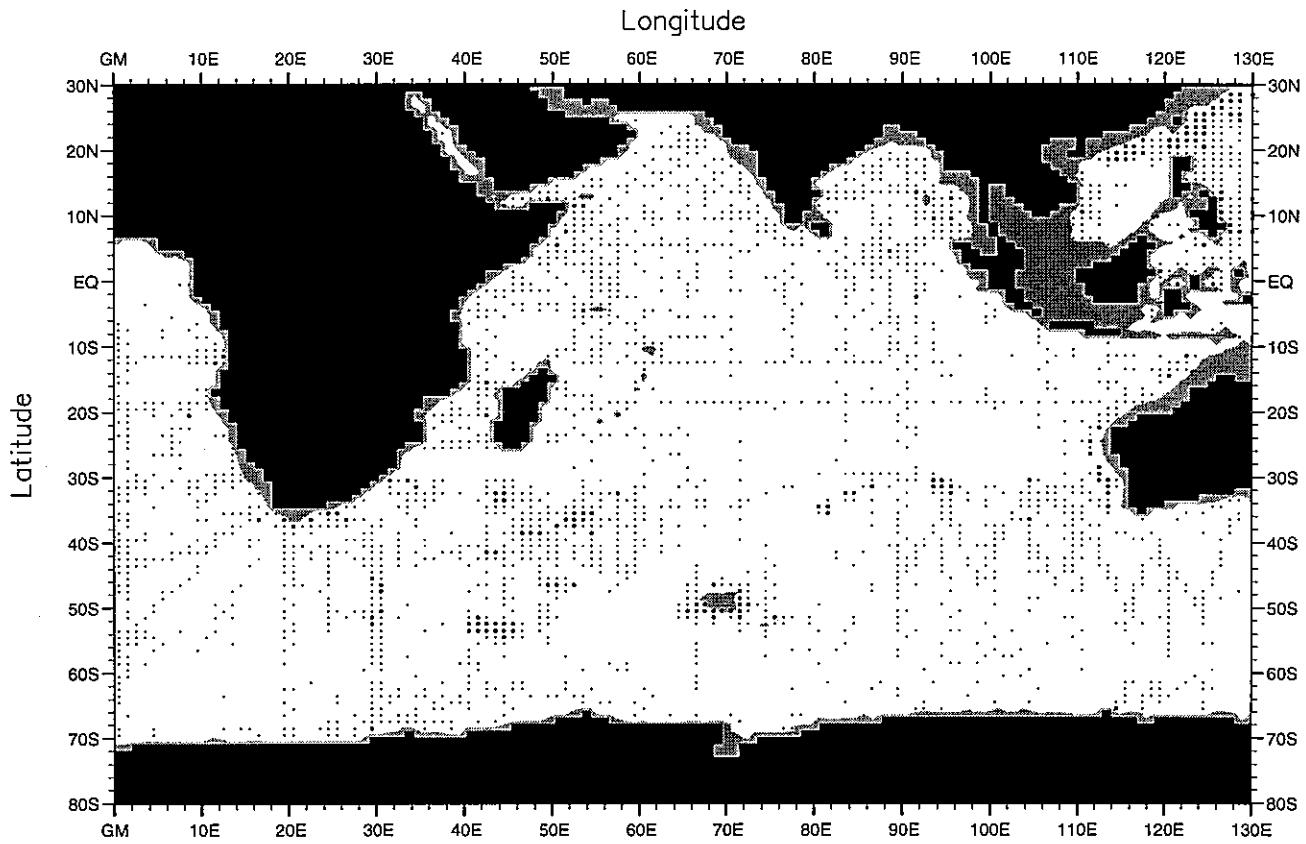
Fig. E9.   Annual silicate observations at 500 m. depth .

Longitude
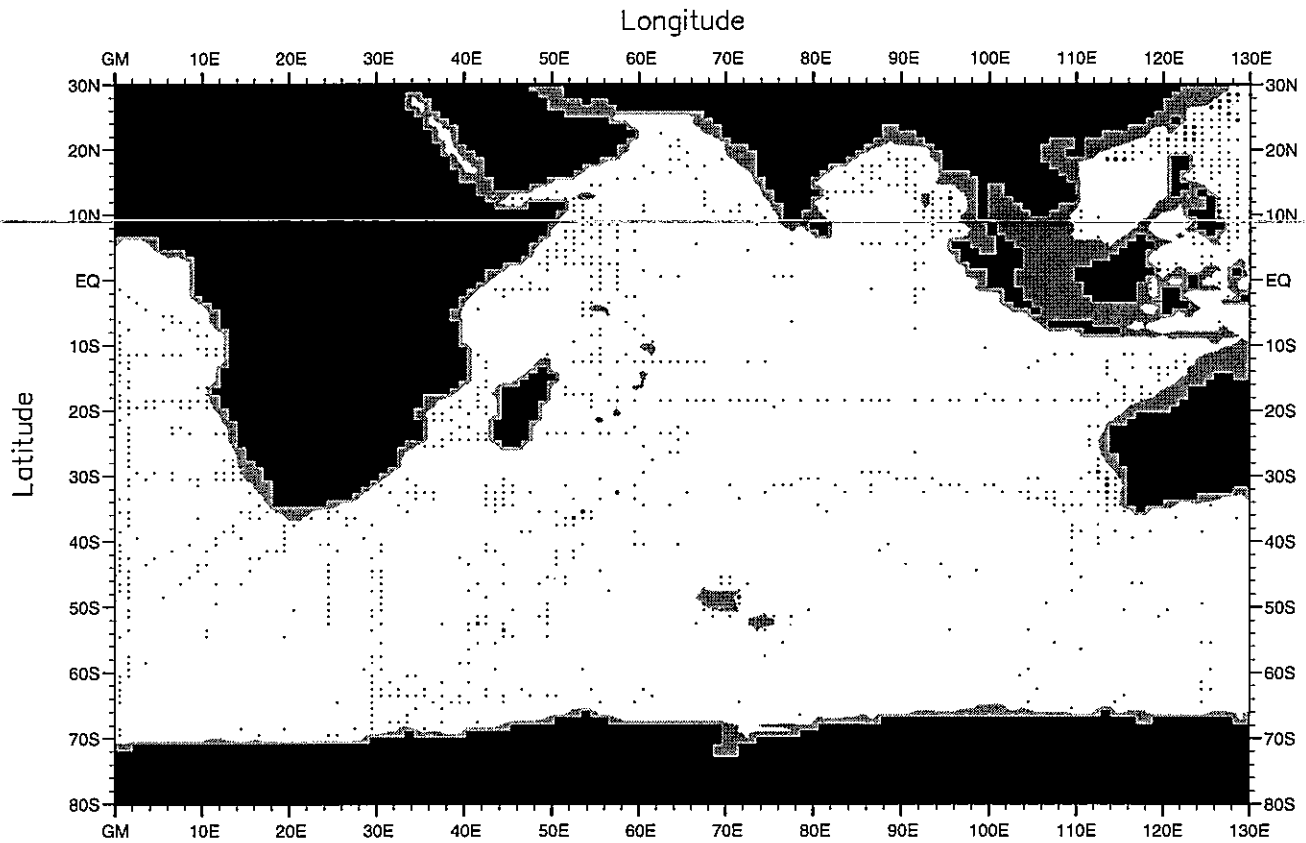
Fig. E10.   Annual silicate observations at 700 m. depth .

Longitude
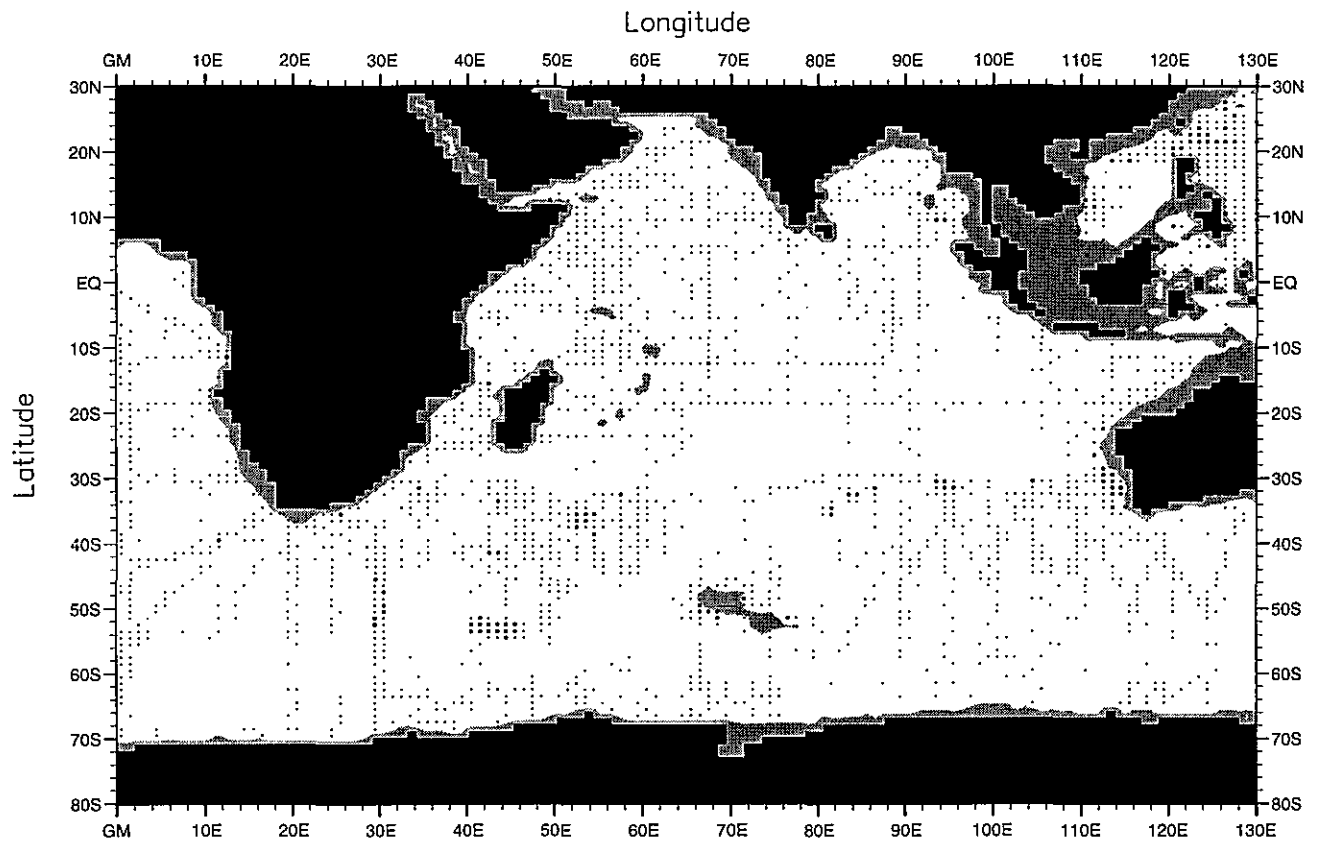
Fig. E11.   Annual silicate observations at 1000 m. depth .

Longitude
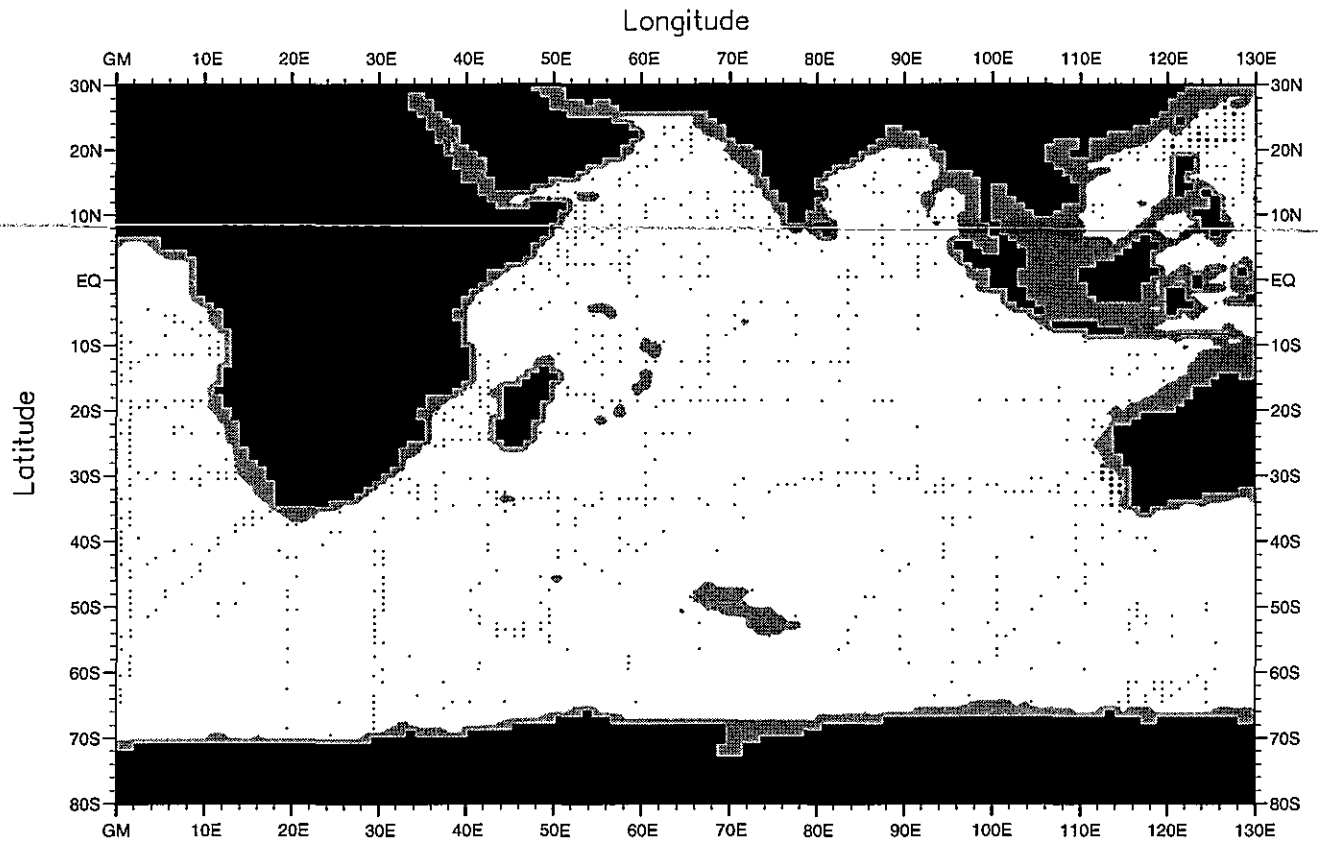
Fig. E12.   Annual silicate observations at 1500 m. depth .

146
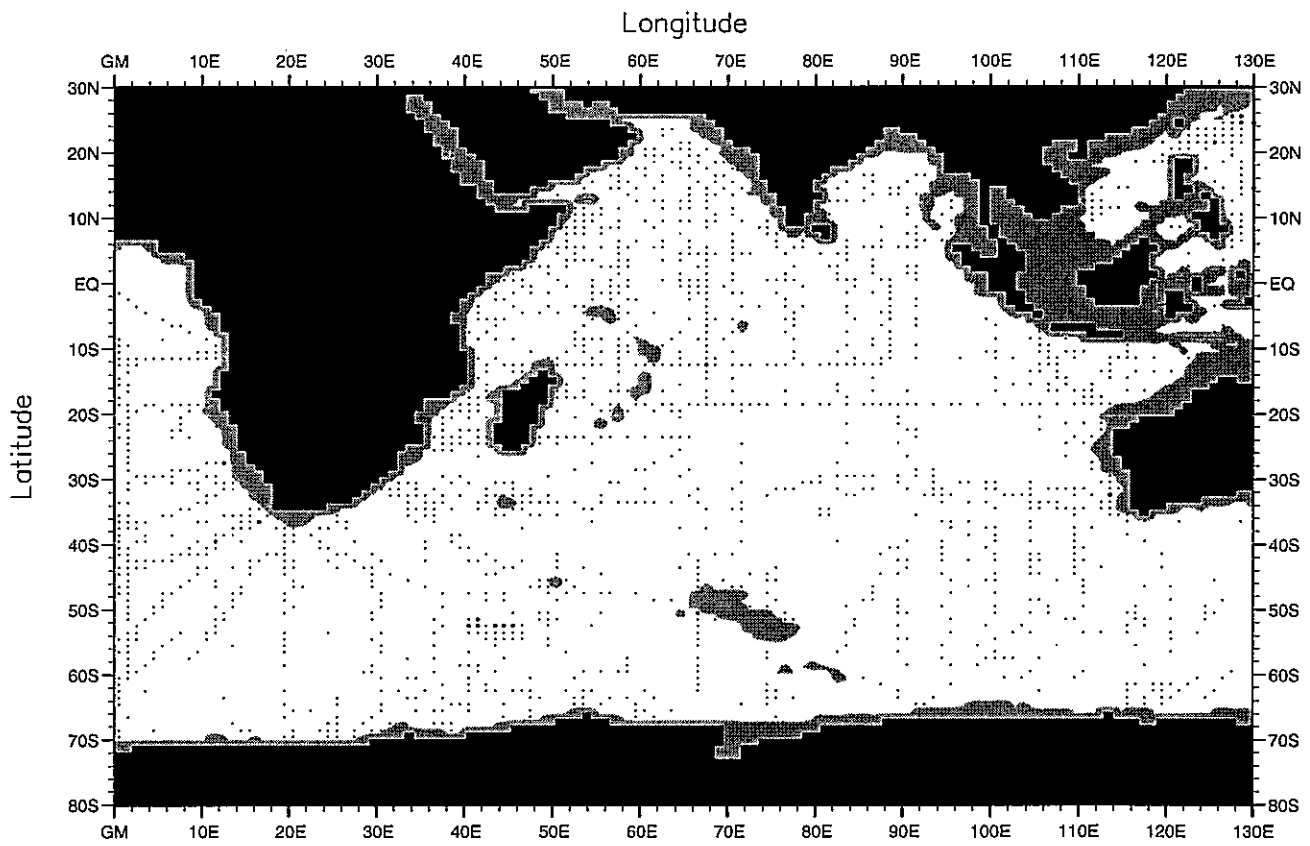
Fig. E13. Annual silicate observations at 2000 m. depth .
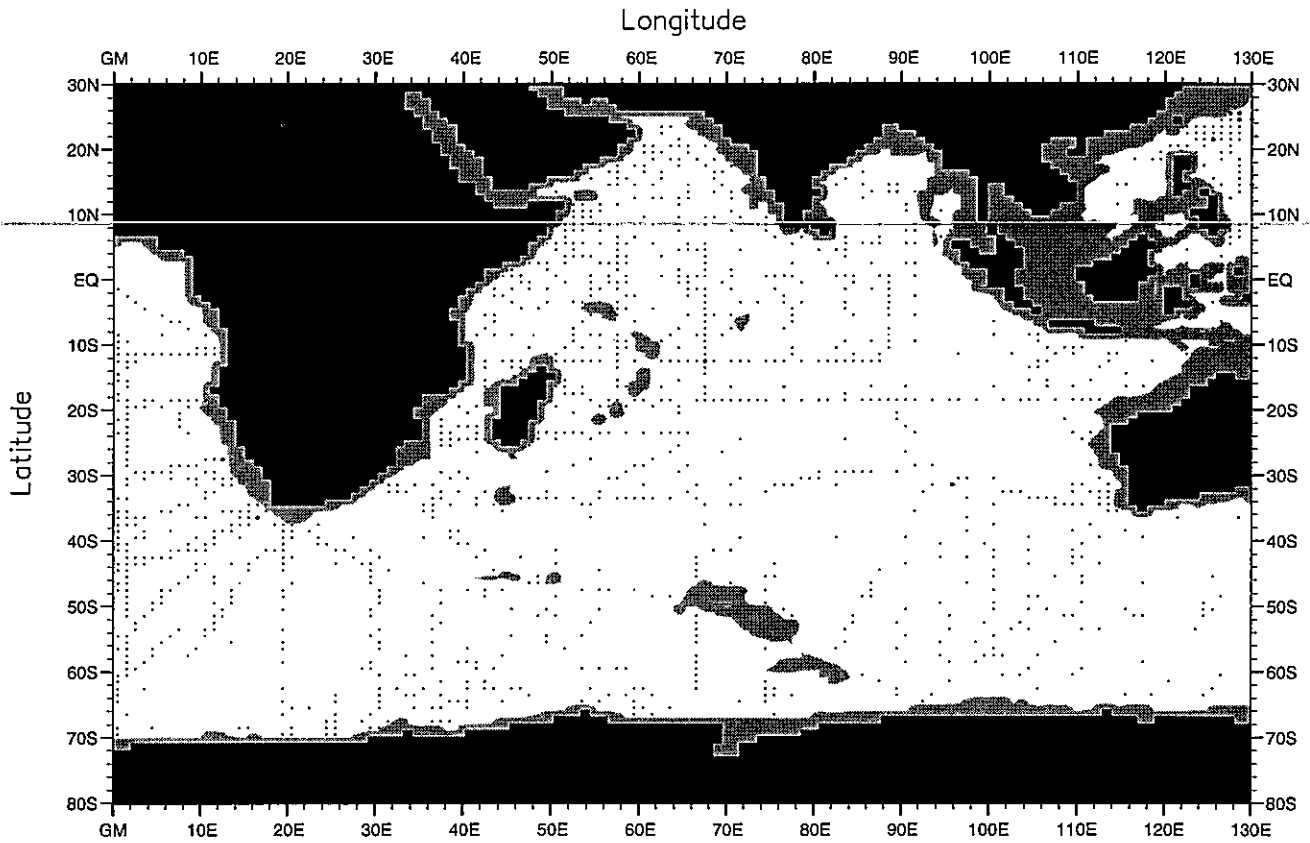
Fig. E14. Annual silicate observations at 2500 m. depth .
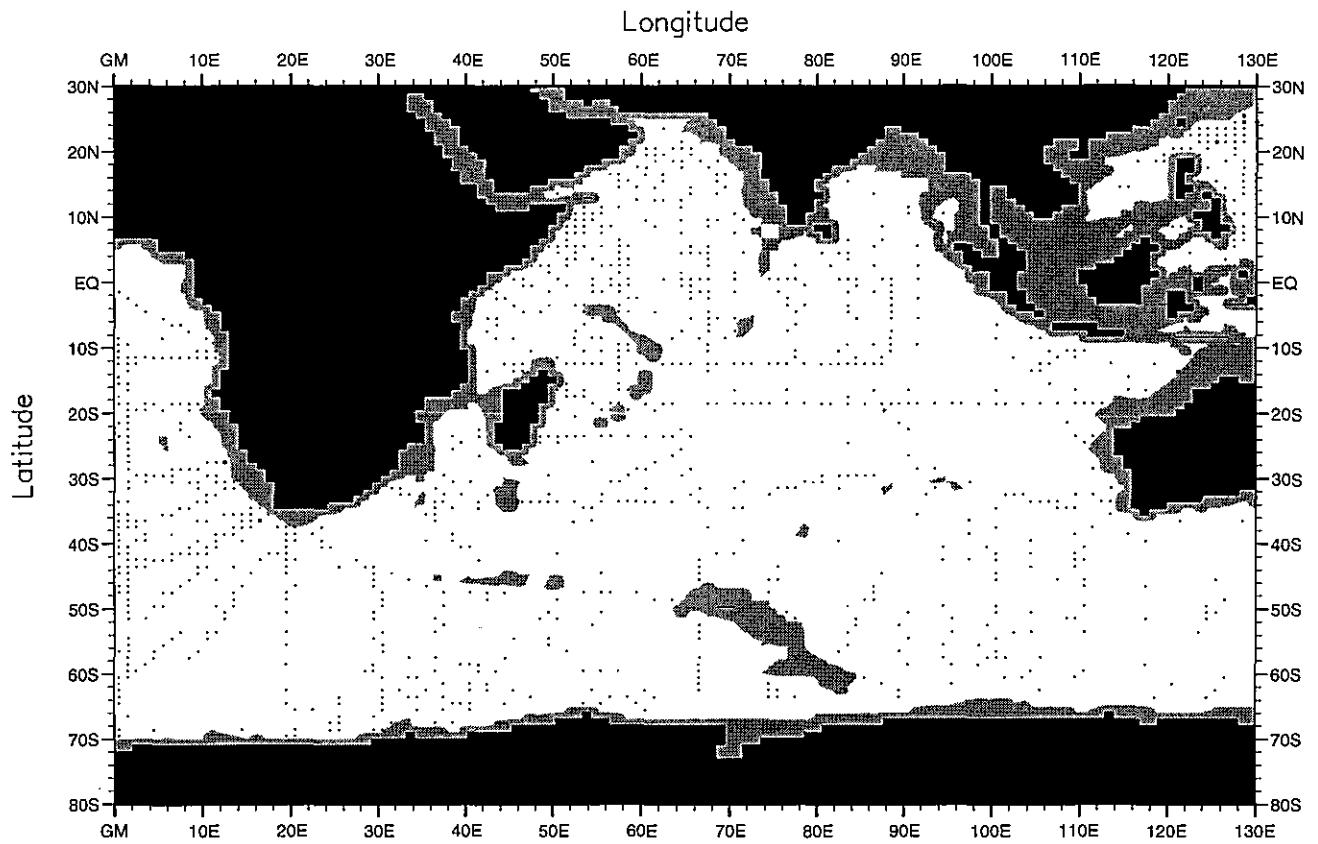
Fig. E15. Annual silicate observations at 3000 m. depth .
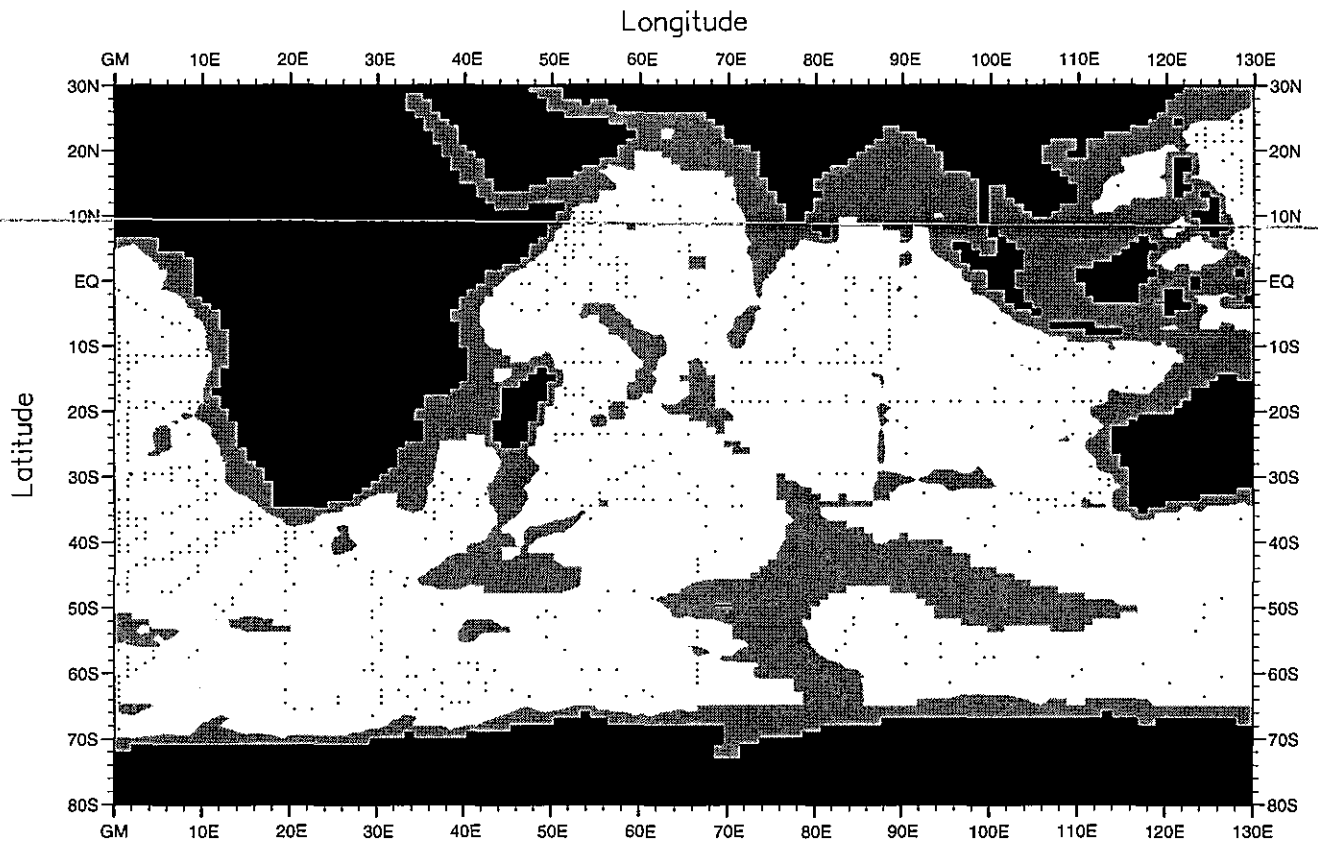
Fig. E16. Annual silicate observations at 4000 m. depth .
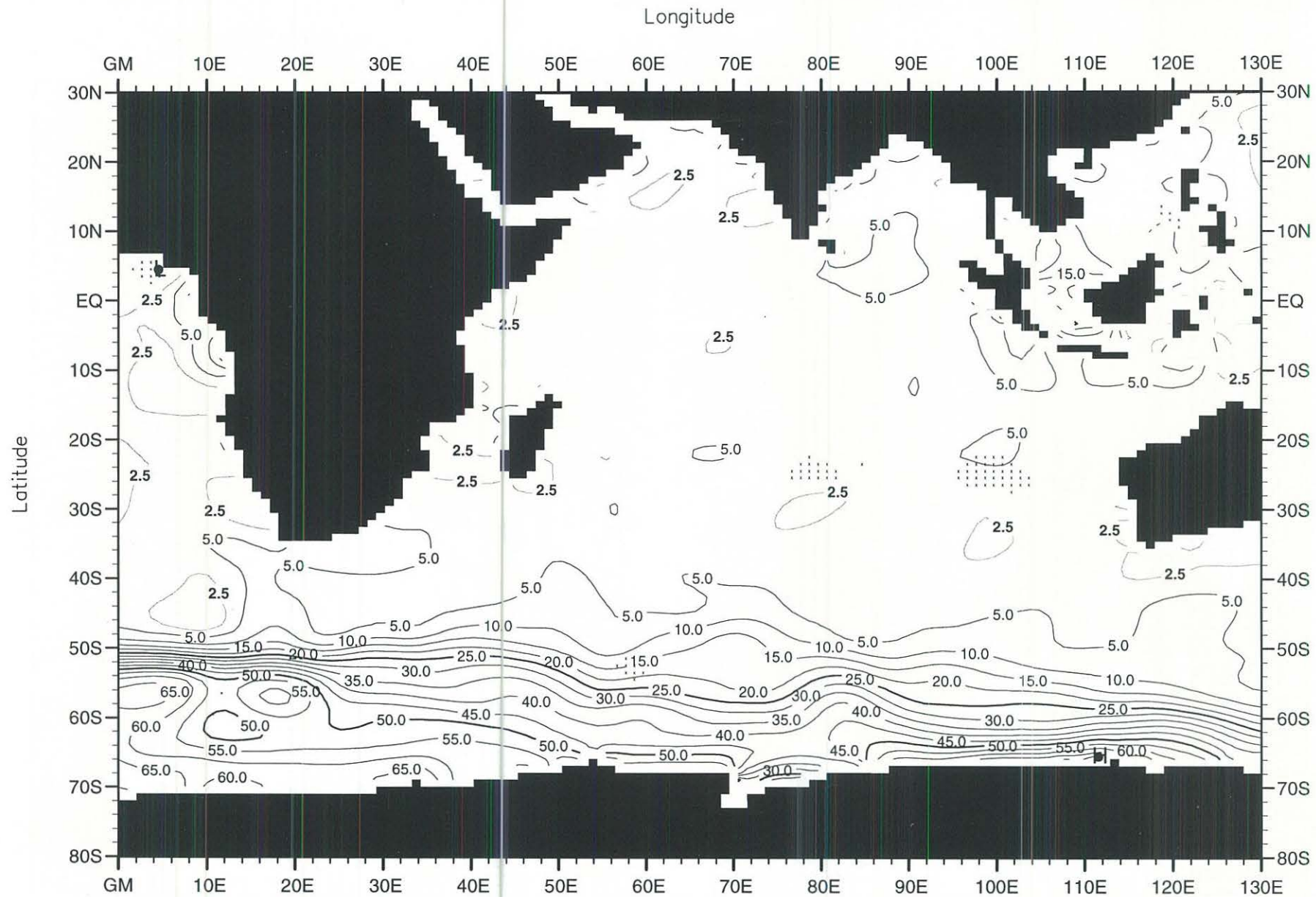
Fig. E17.   Annual mean silicate (μM) at the surface .

Minimum Value=   0.00   Maximum Value= 77.71   Contour Interval: 5.00
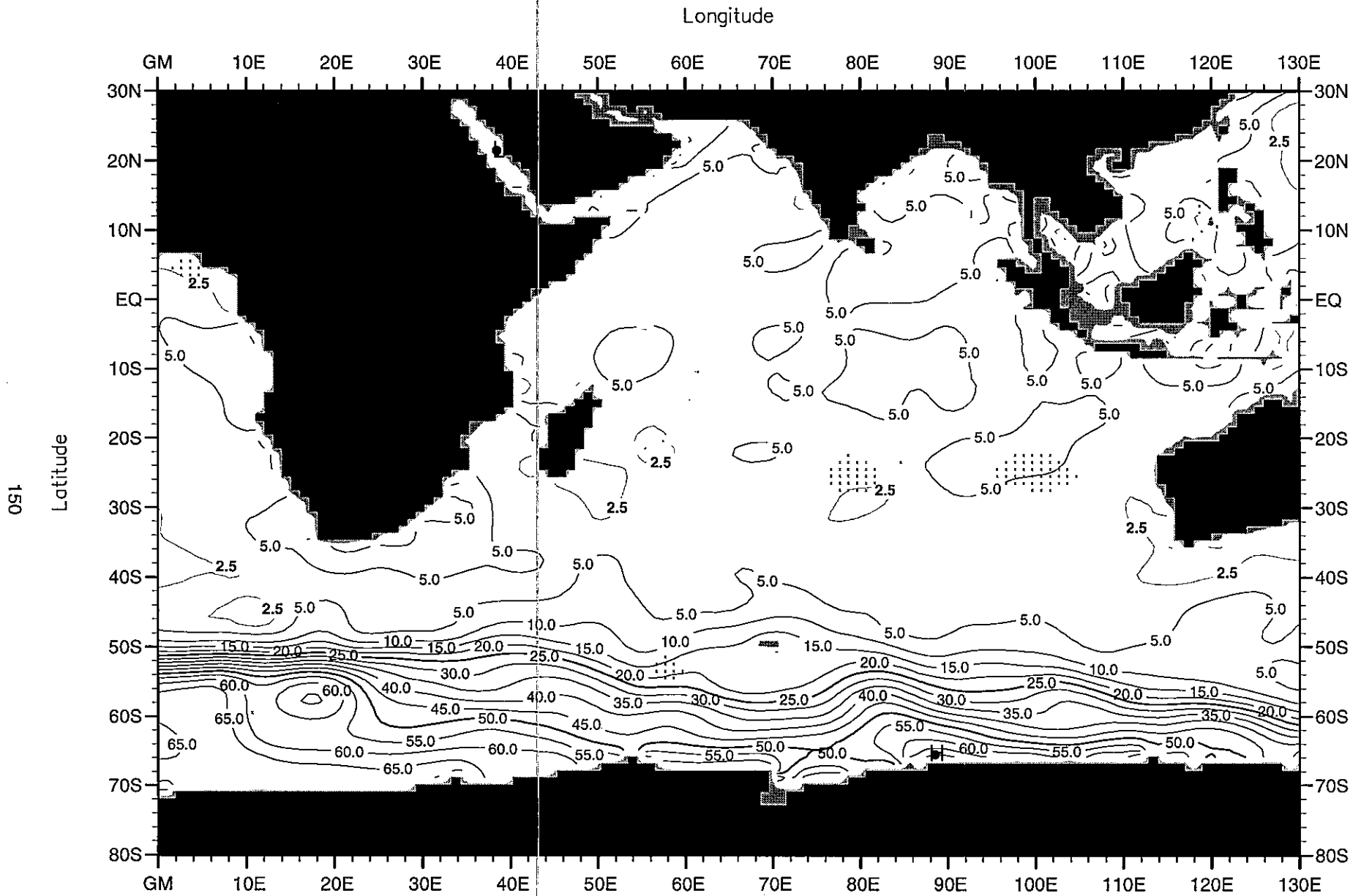
Fig. E18.   Annual mean silicate (μM) at   50 m. depth .

Minimum Value=   0.82   Maximum Value= 71.61   Contour Interval: 5.00
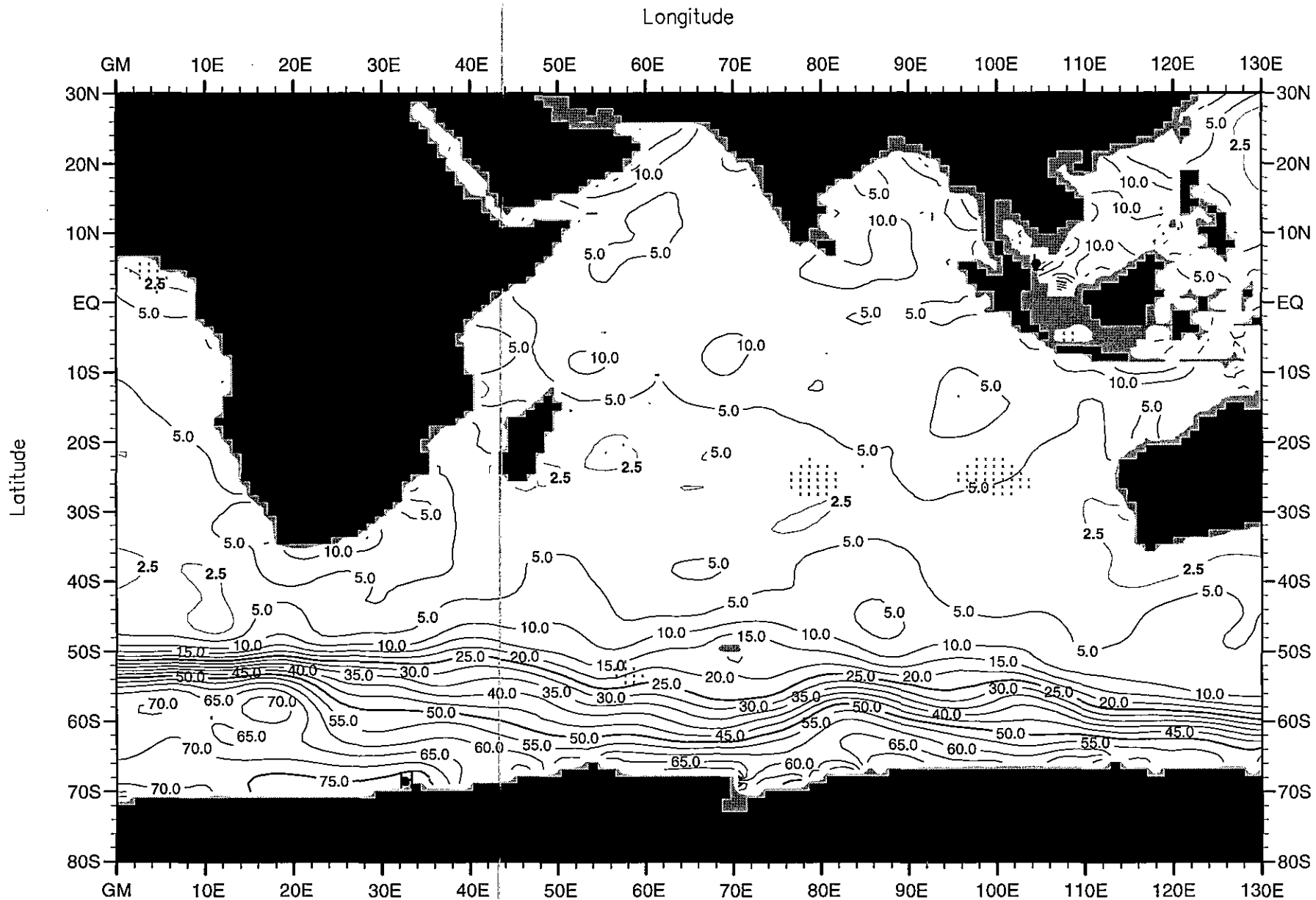
Fig. E19.   Annual mean silicate (μM) at   75 m. depth .

Minimum Value=   0.52   Maximum Value= 79.97   Contour Interval: 5.00

151
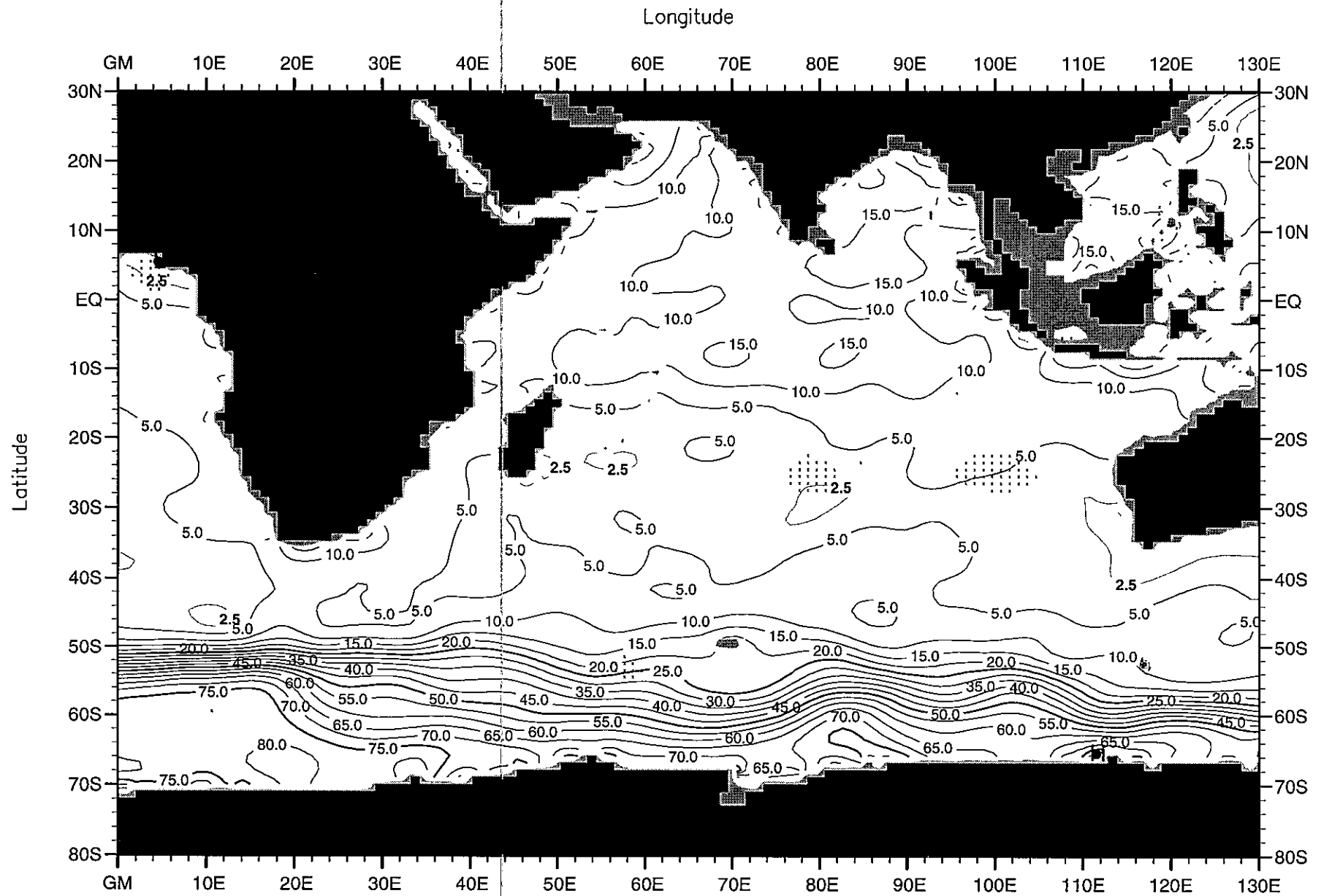
Fig. E20. Annual mean silicate (μM) at 100 m. depth .

Minimum Value= 0.22   Maximum Value= 87.64   Contour Interval: 5.00

152
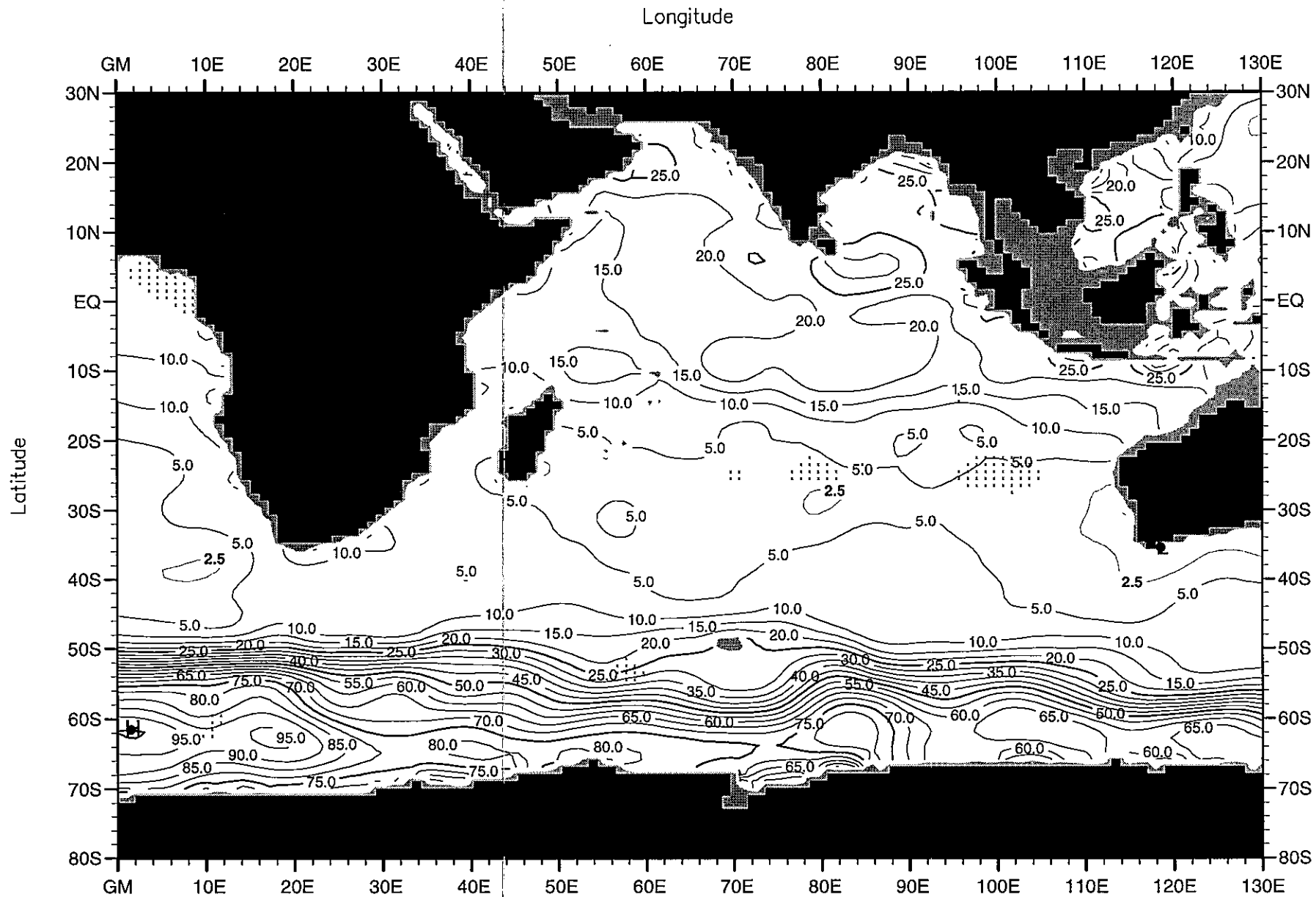
Fig. E21. Annual mean silicate (μM) at 150 m. depth .

Minimum Value= 1.08   Maximum Value= 100.36   Contour Interval: 5.00
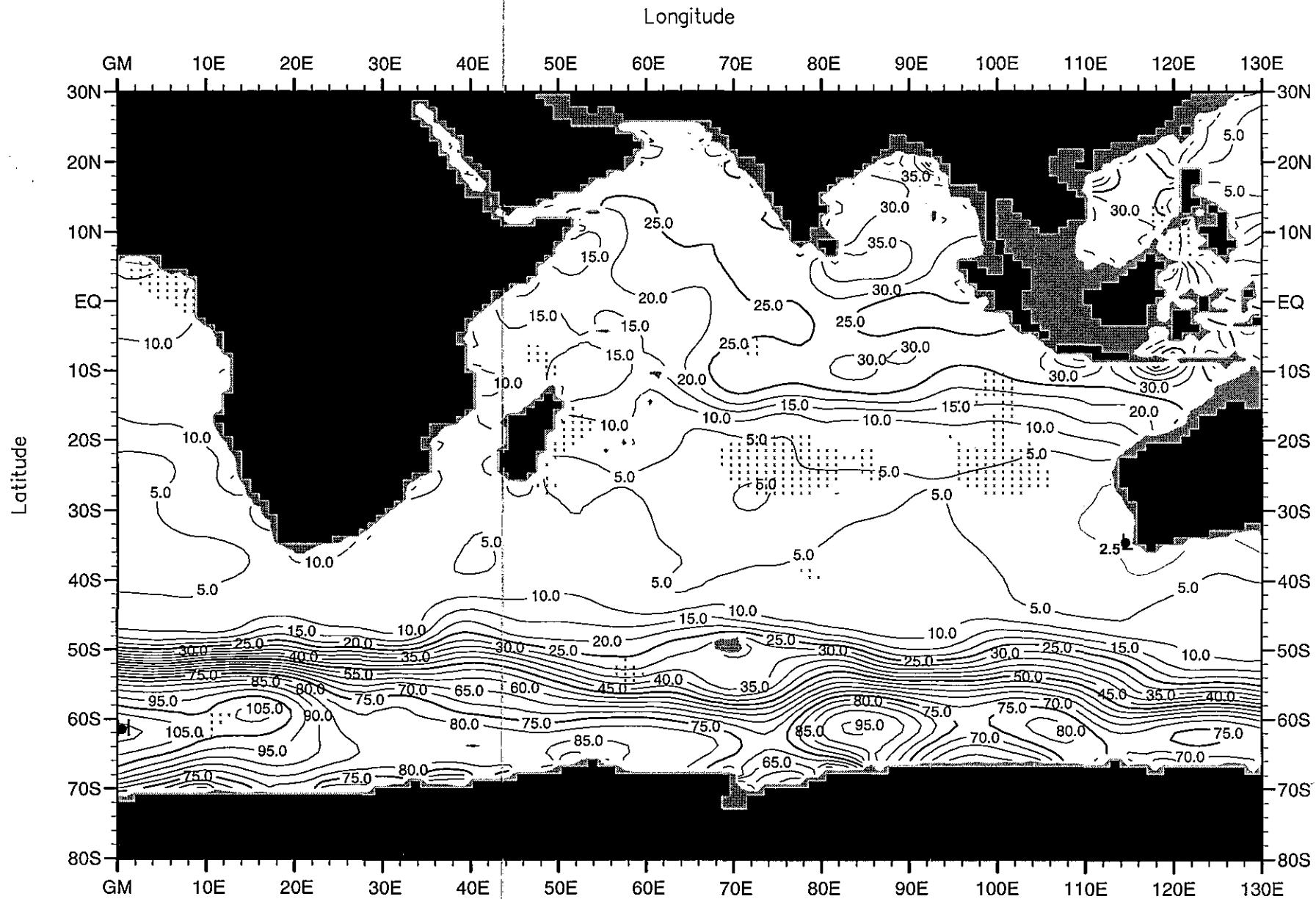
Fig. E22. Annual mean silicate (μM) at 200 m. depth .

Minimum Value= 1.25   Maximum Value= 111.94   Contour Interval: 5.00
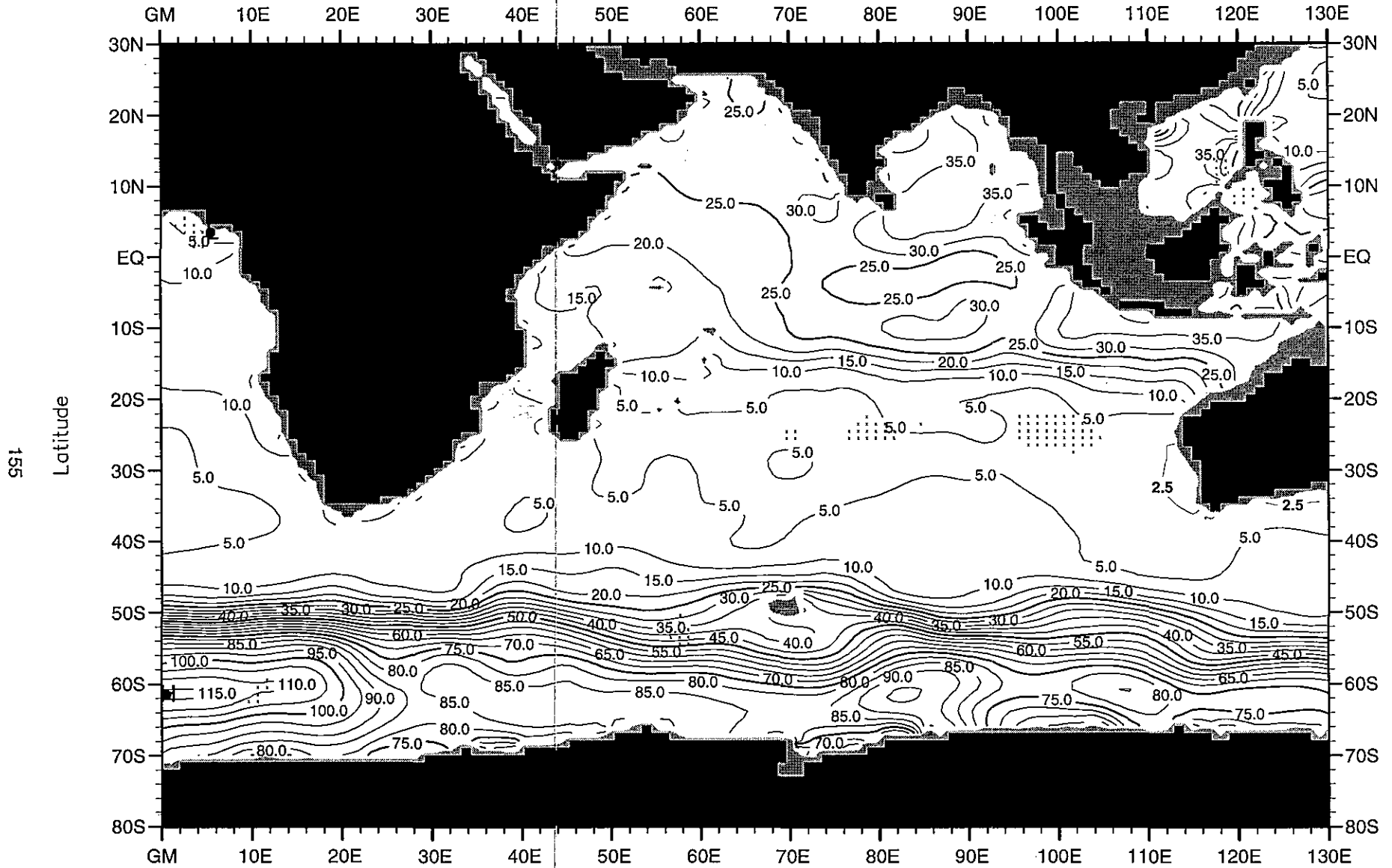
Fig. E23. Annual mean silicate (μM) at 250 m. depth .

Minimum Value= 1.26   Maximum Value= 115.67   Contour Interval: 5.00
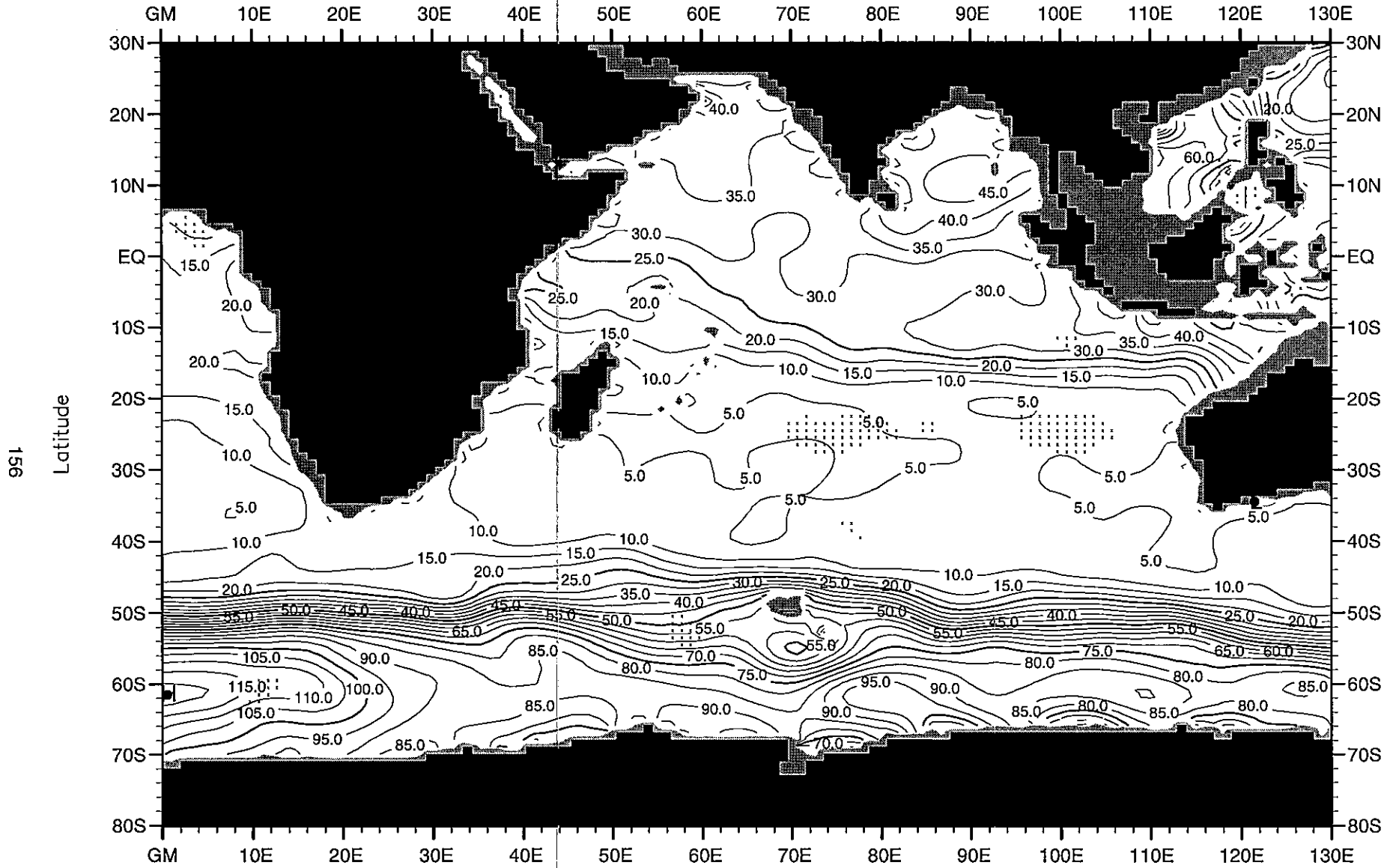
Fig. E24. Annual mean silicate (μM) at 400 m. depth .

Minimum Value= 1.37   Maximum Value= 122.17   Contour Interval: 5.00
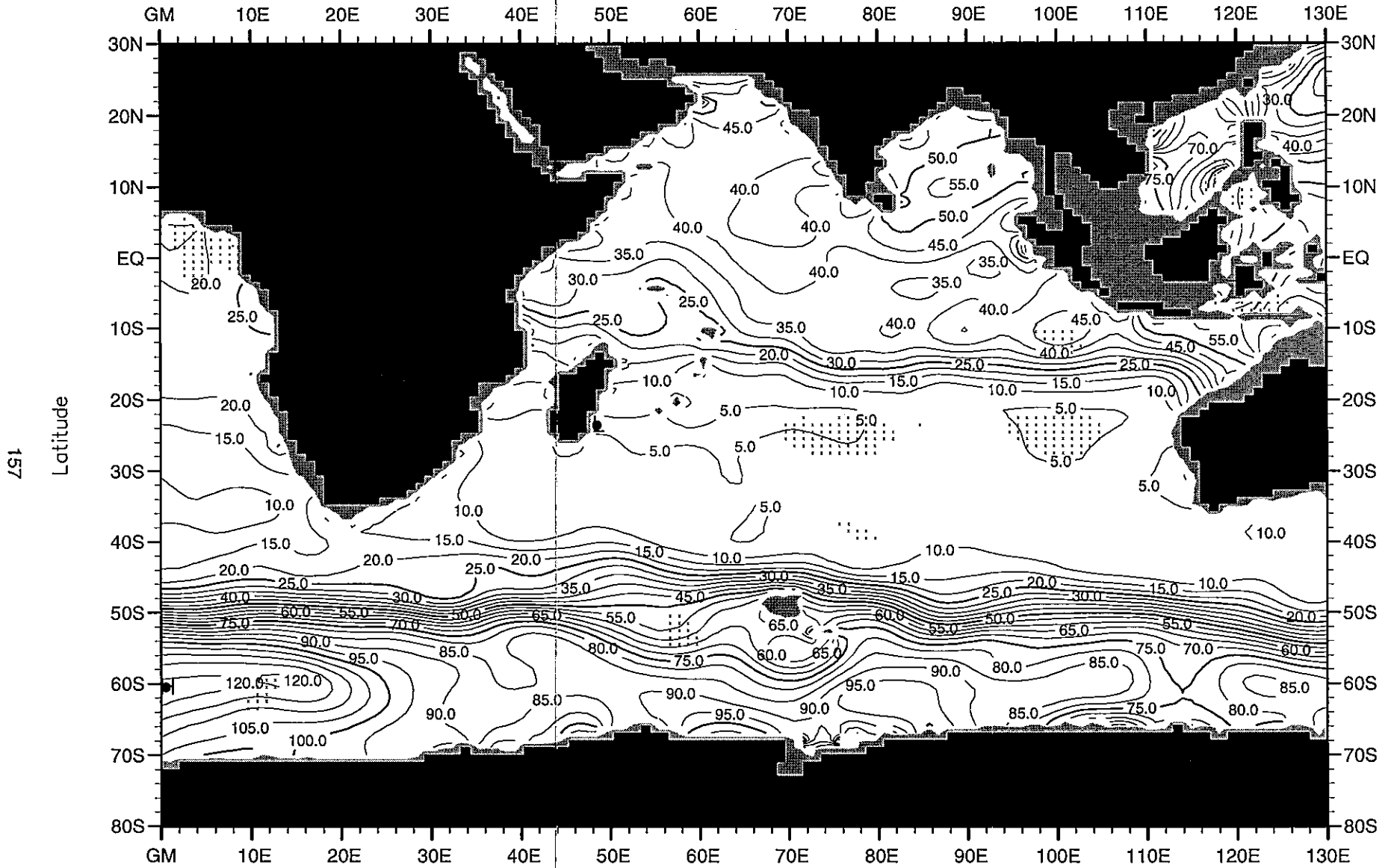
Fig. E25. Annual mean silicate (μM) at 500 m. depth.

Minimum Value= 2.68   Maximum Value= 121.88   Contour Interval: 5.00

157
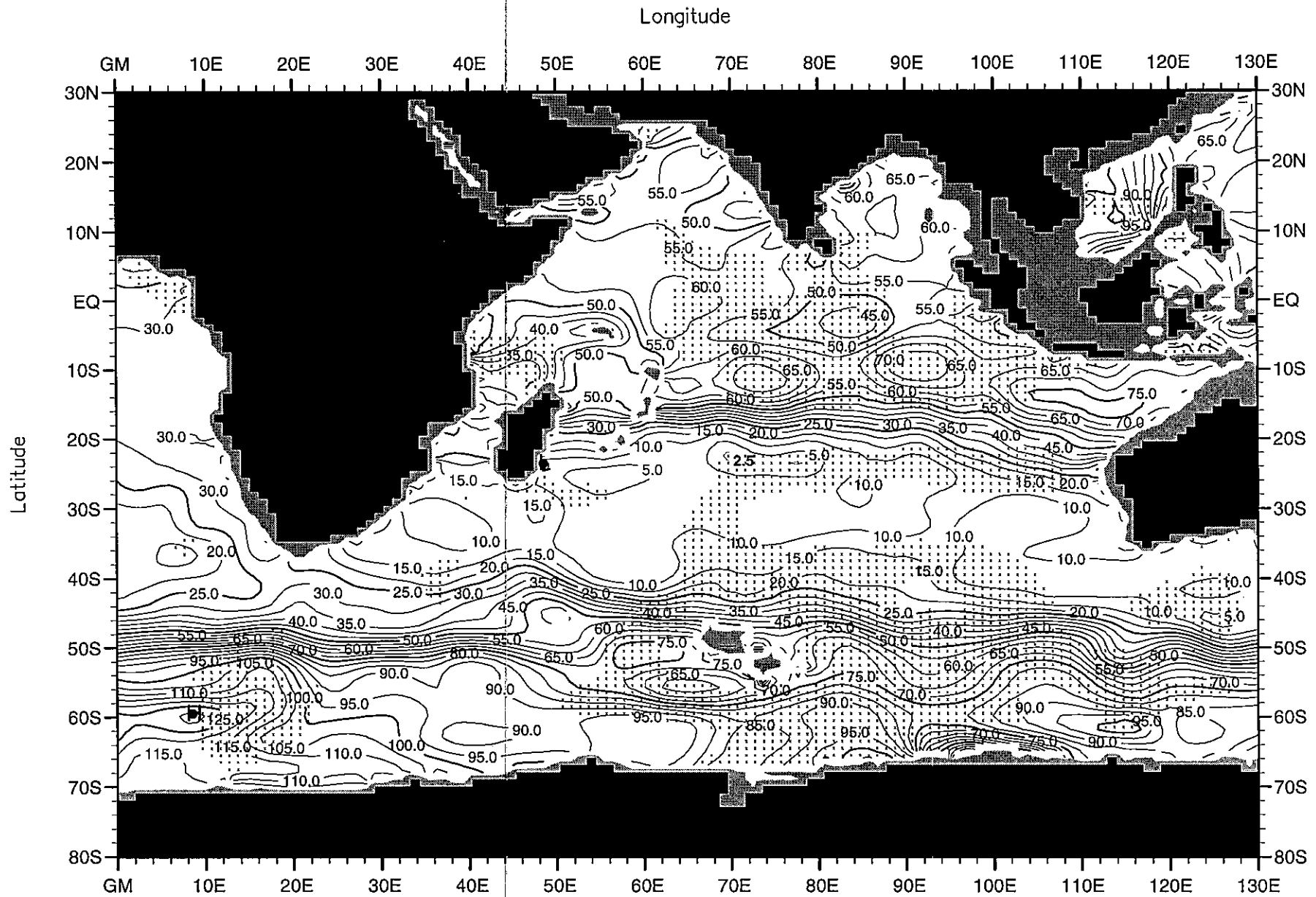
Fig. E26. Annual mean silicate (μM) at 700 m. depth .

Minimum Value= 0.93   Maximum Value= 131.57   Contour Interval: 5.00
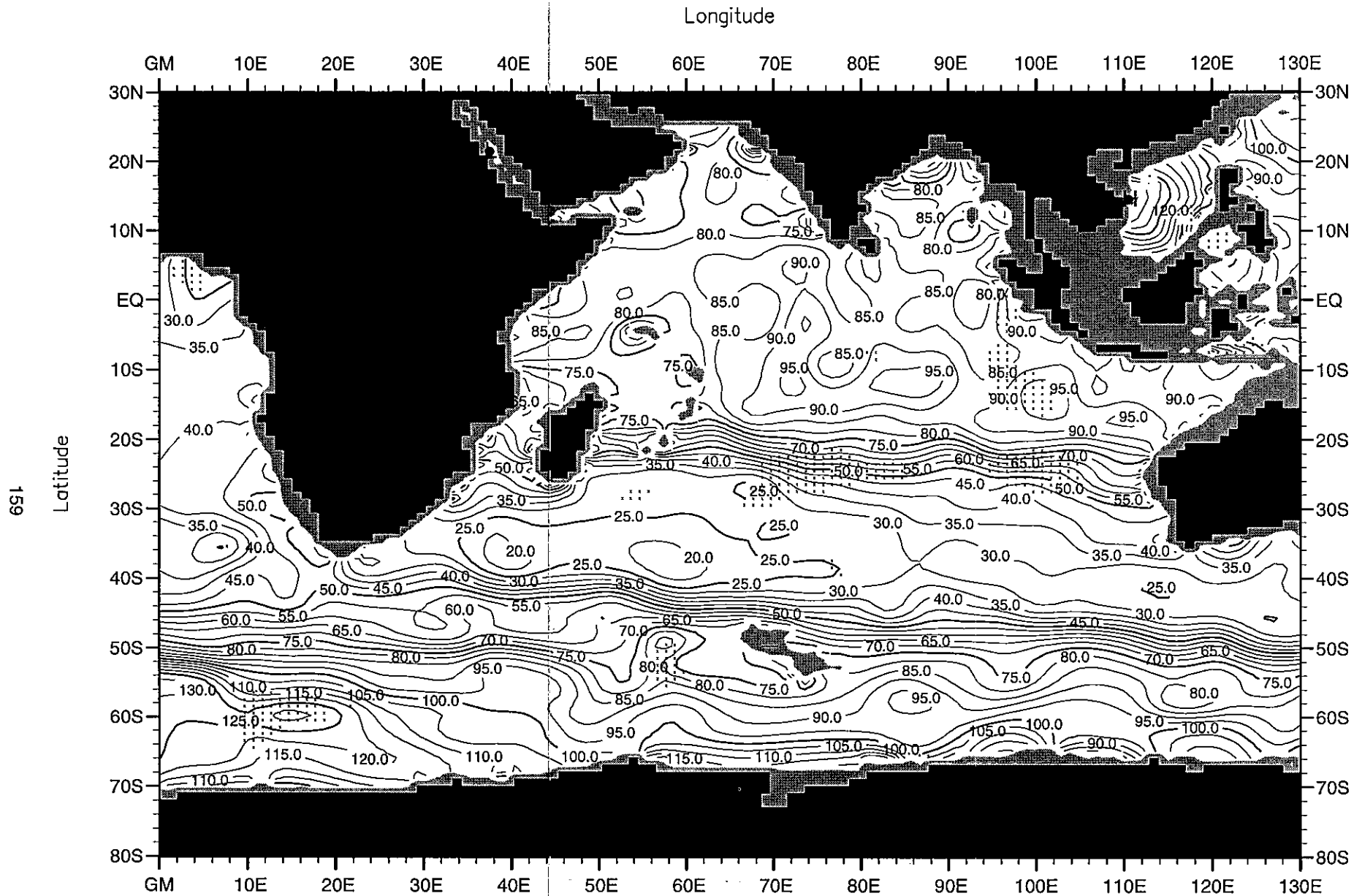
Fig. E27. Annual mean silicate (μM) at 1000 m. depth .

Minimum Value= 11.00   Maximum Value= 144.23   Contour Interval: 5.00
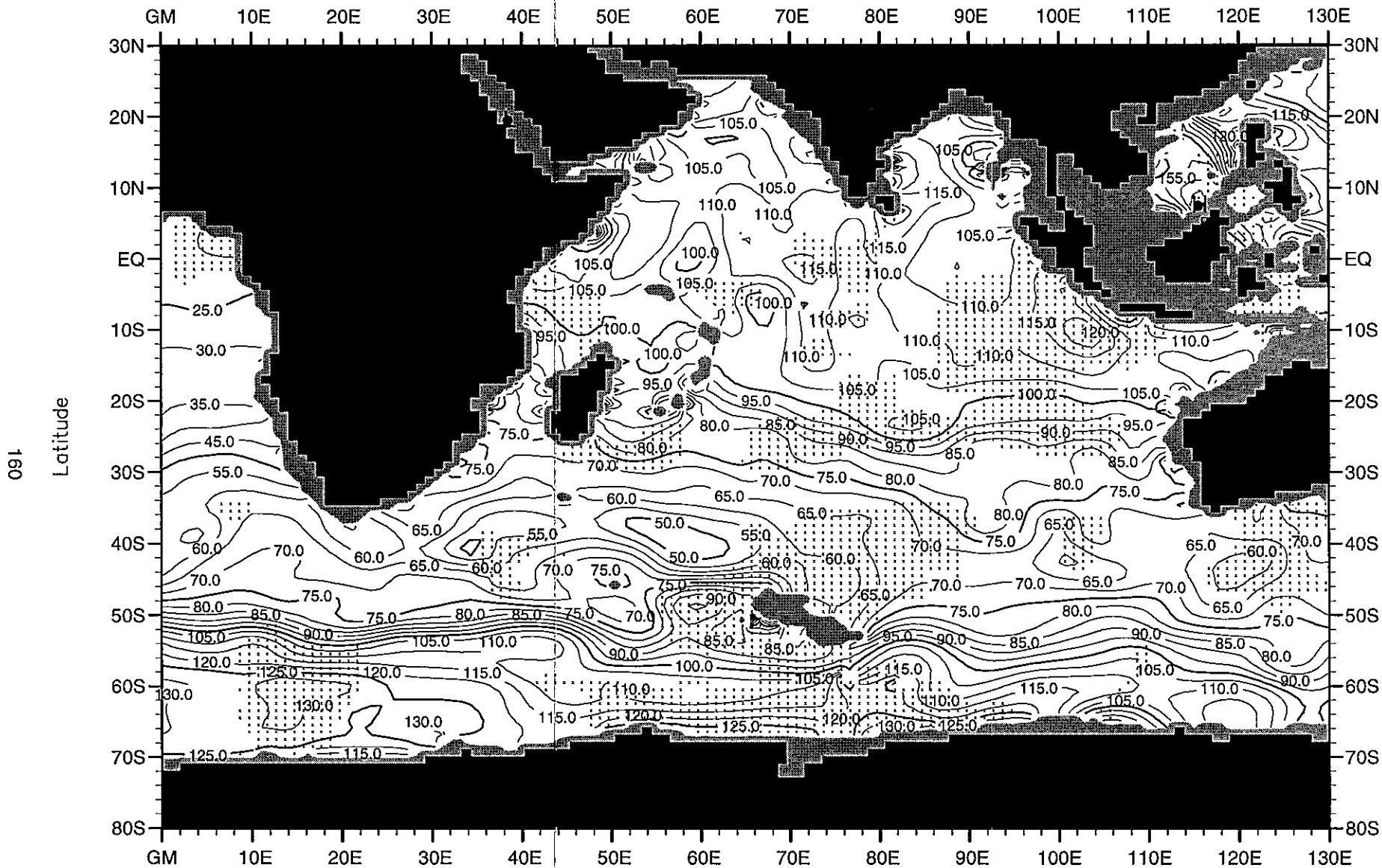
Fig. E28. Annual mean silicate (μM) at 1500 m. depth .

Minimum Value= 13.66   Maximum Value= 175.99   Contour Interval: 5.00

160
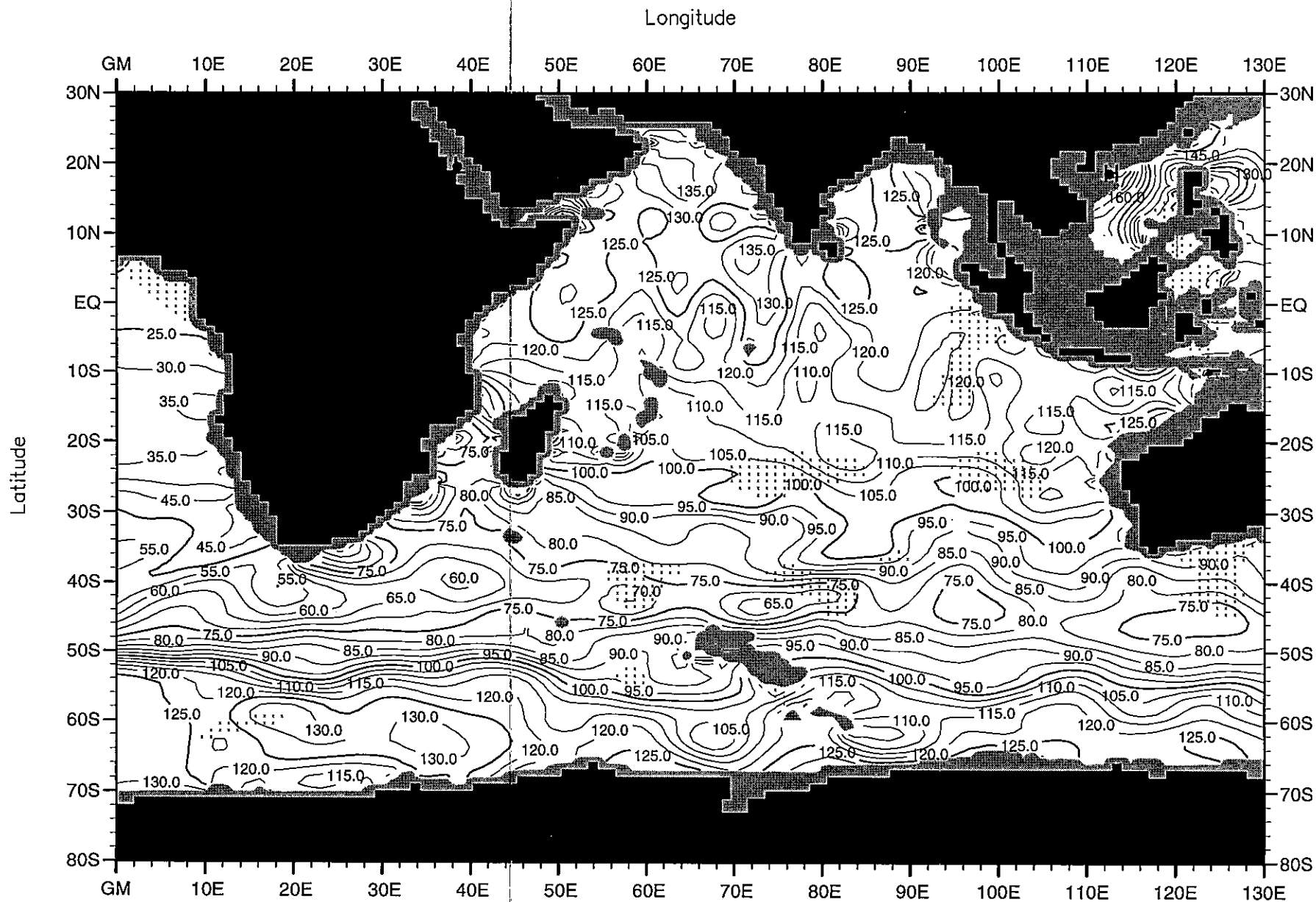
Fig. E29.   Annual mean silicate (μM) at 2000 m. depth .

Minimum Value= 14.00   Maximum Value= 185.46   Contour Interval: 5.00

161
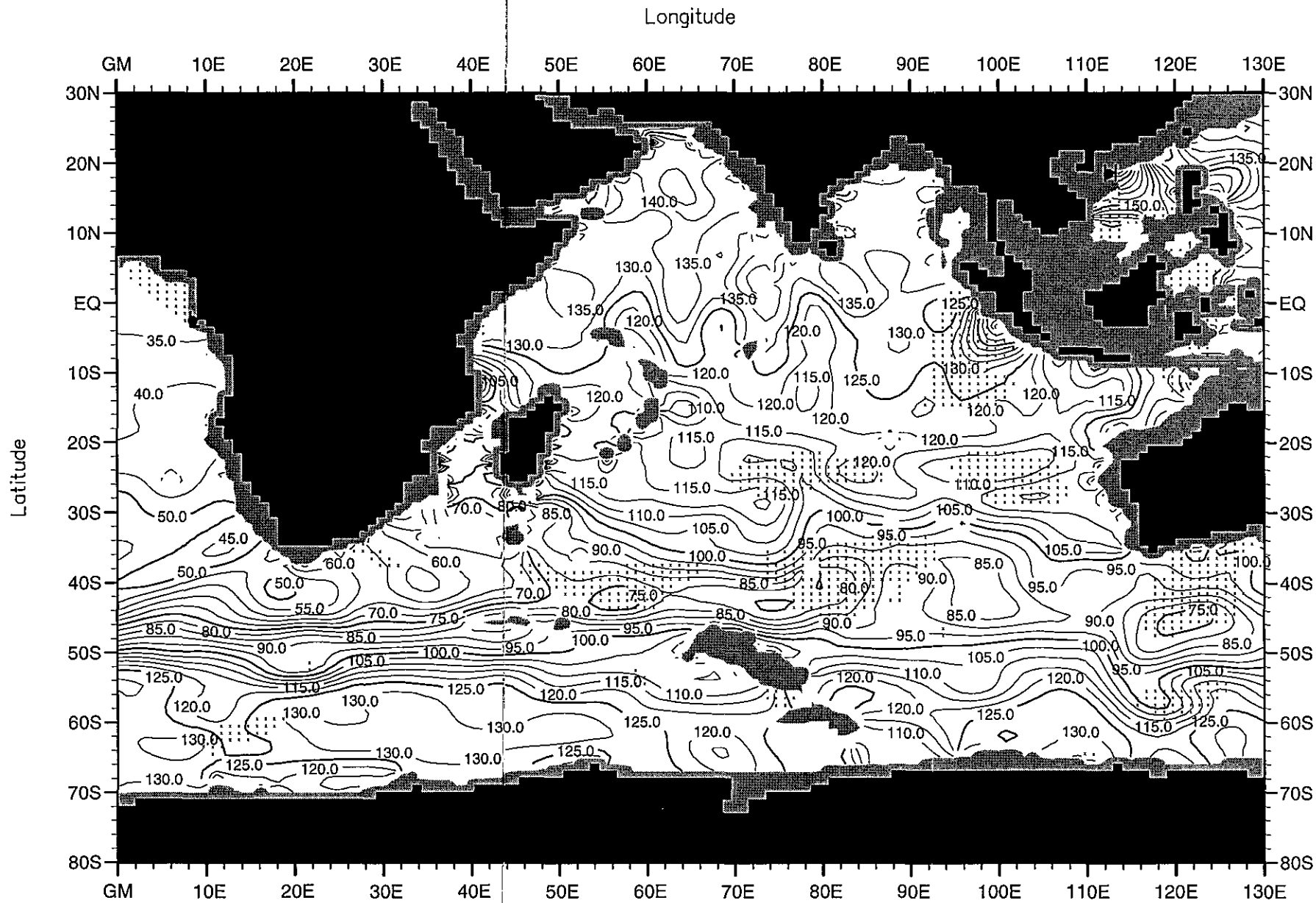
Fig. E30.   Annual mean silicate (μM) at 2500 m. depth .

Minimum Value= 29.80   Maximum Value= 190.47   Contour Interval: 5.00

162
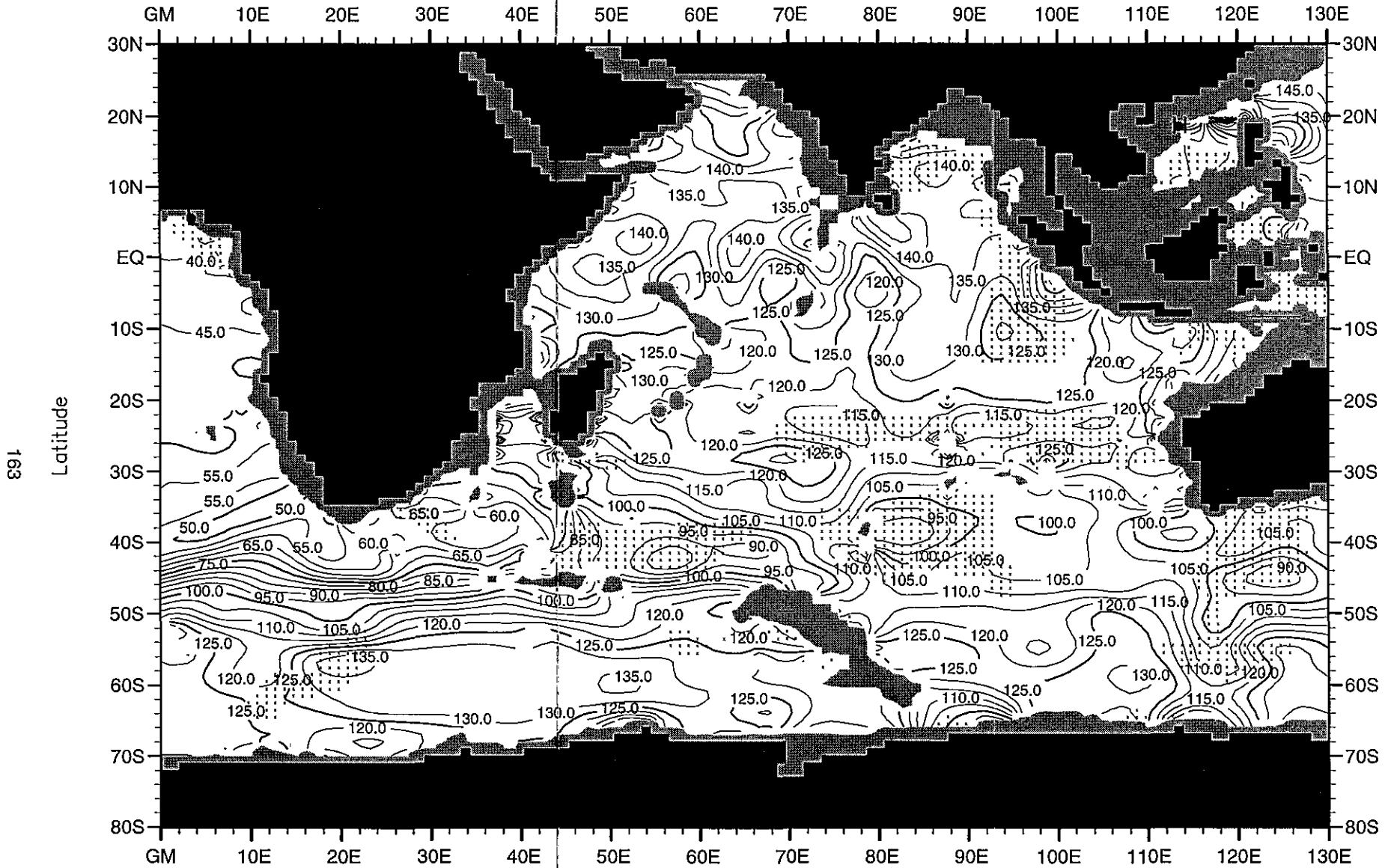
Fig. E31. Annual mean silicate (μM) at 3000 m. depth .

Minimum Value= 37.52   Maximum Value= 191.02   Contour Interval: 5.00
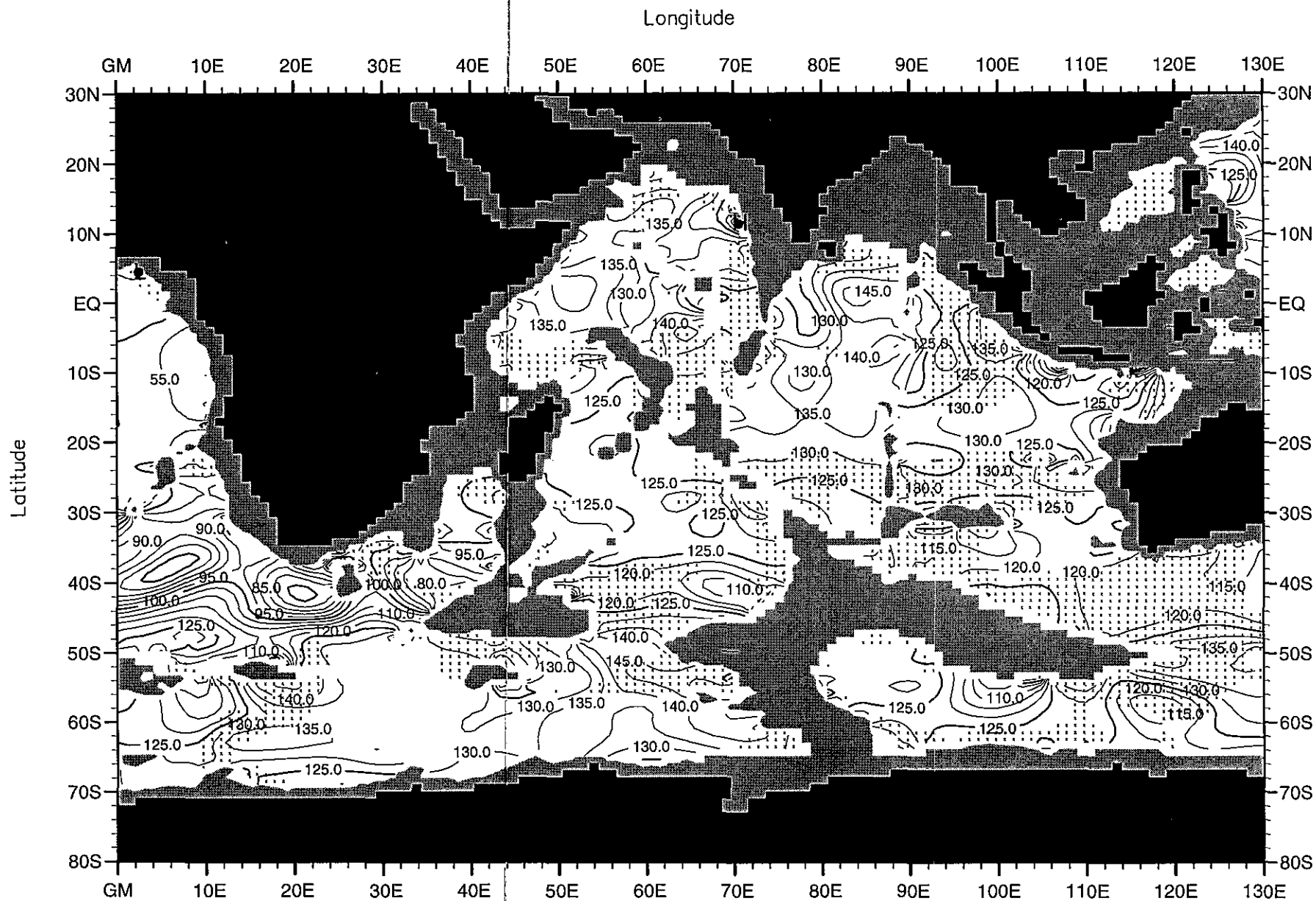
Fig. E32. Annual mean silicate (μM) at 4000 m. depth .

Minimum Value= 42.20   Maximum Value= 174.91   Contour Interval: 5.00
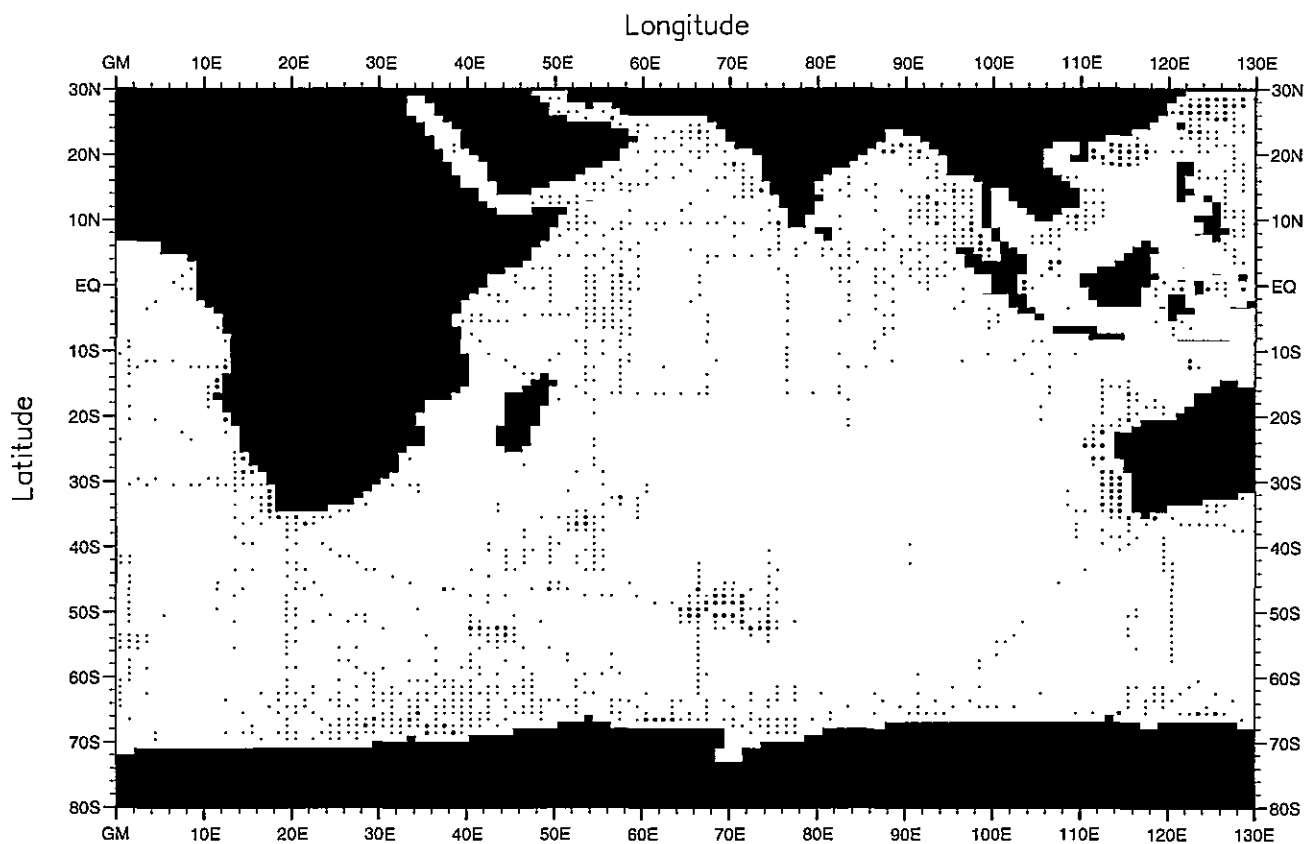
Fig. F1.   Winter (Jan.-Mar.) silicate observations at the surface .
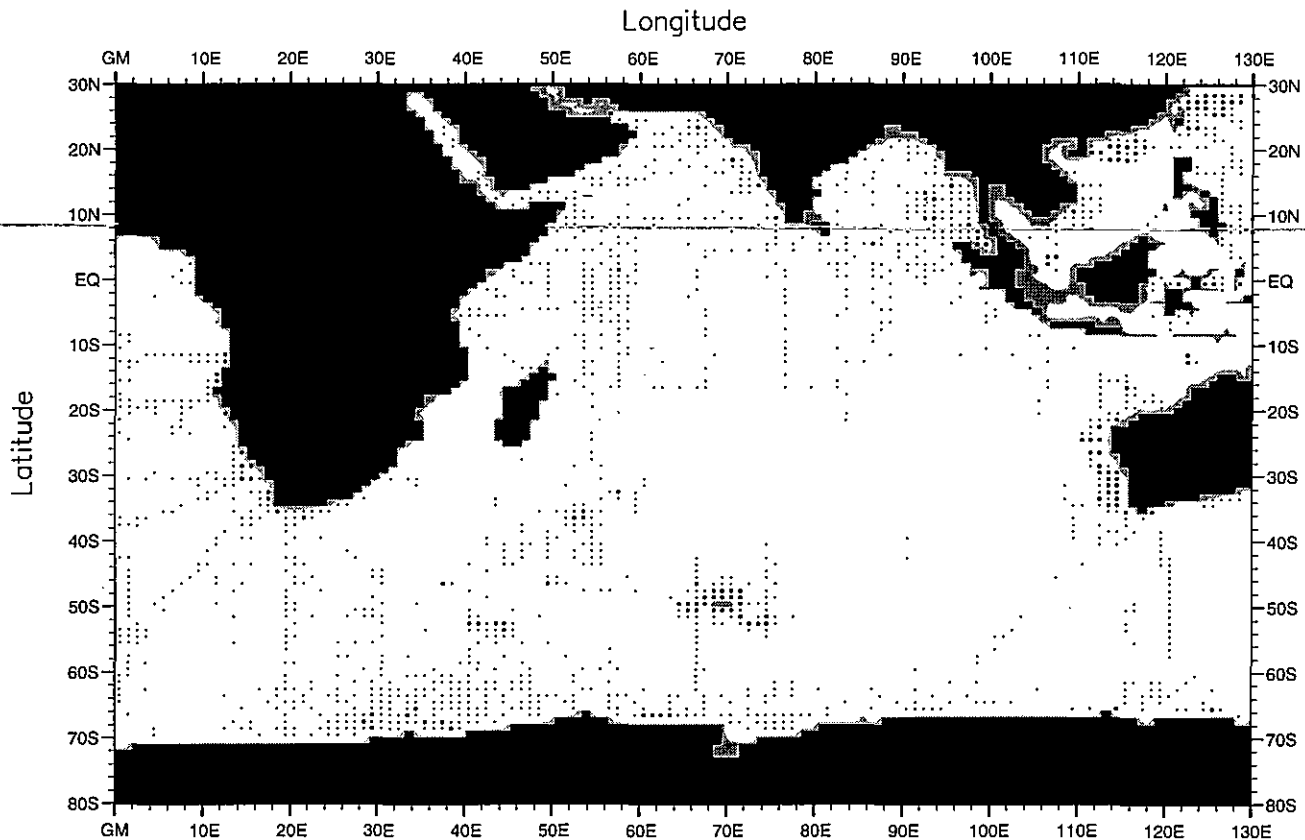
Fig. F2.   Winter (Jan.-Mar.) silicate observations at   50 m. depth .
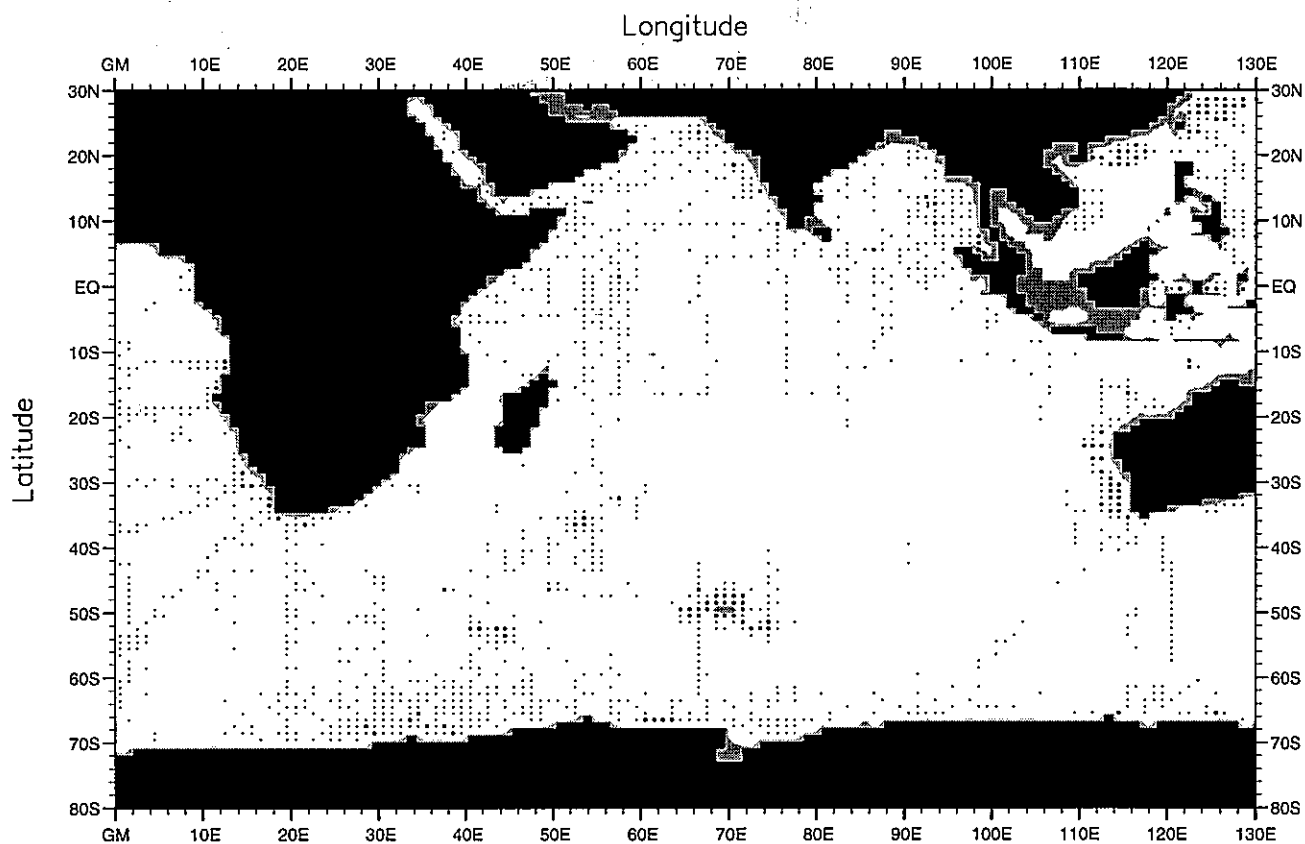
Fig. F3. Winter (Jan.-Mar.) silicate observations at 75 m. depth .
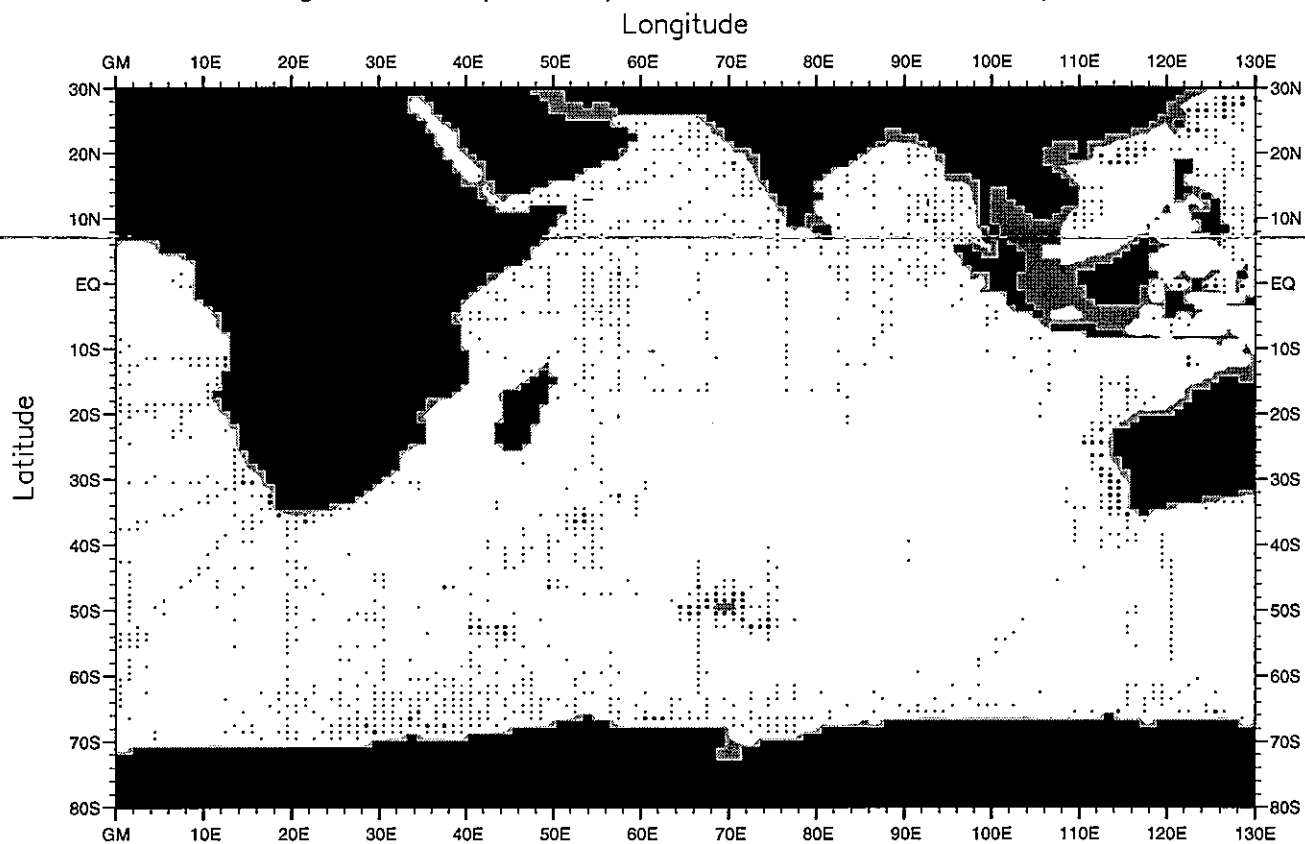
Fig. F4. Winter (Jan.-Mar.) silicate observations at 100 m. depth .
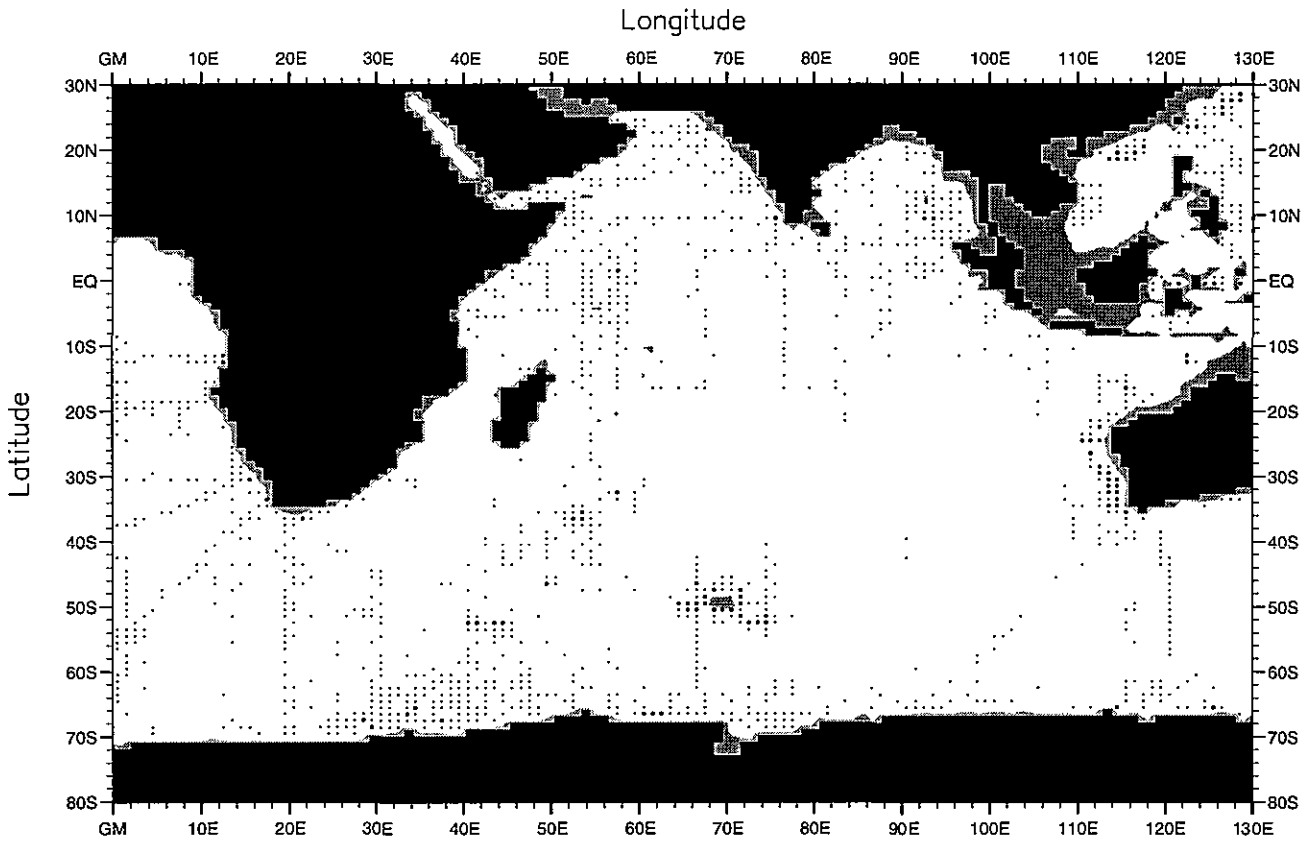
Fig. F5. Winter (Jan.-Mar.) silicate observations at 150 m. depth .
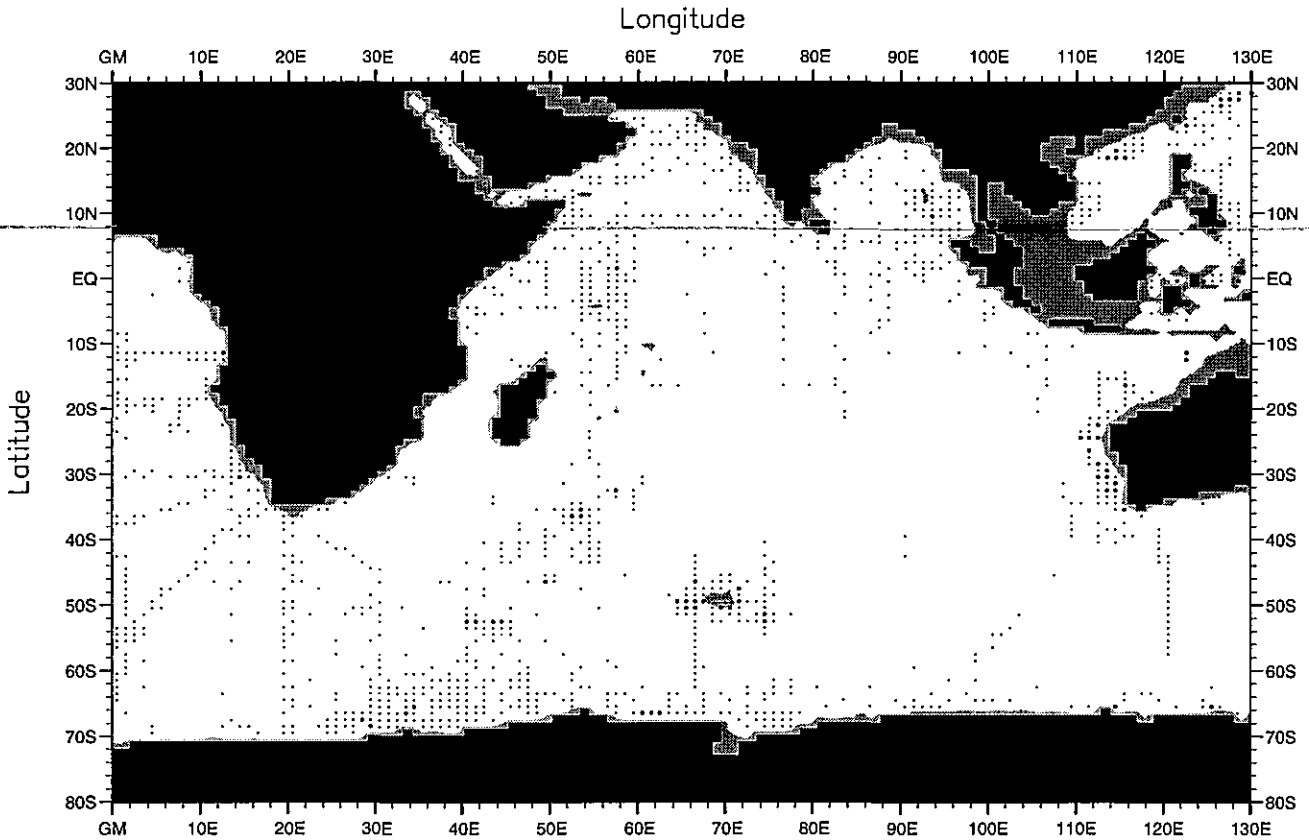
Fig. F6. Winter (Jan.-Mar.) silicate observations at 250 m. depth .
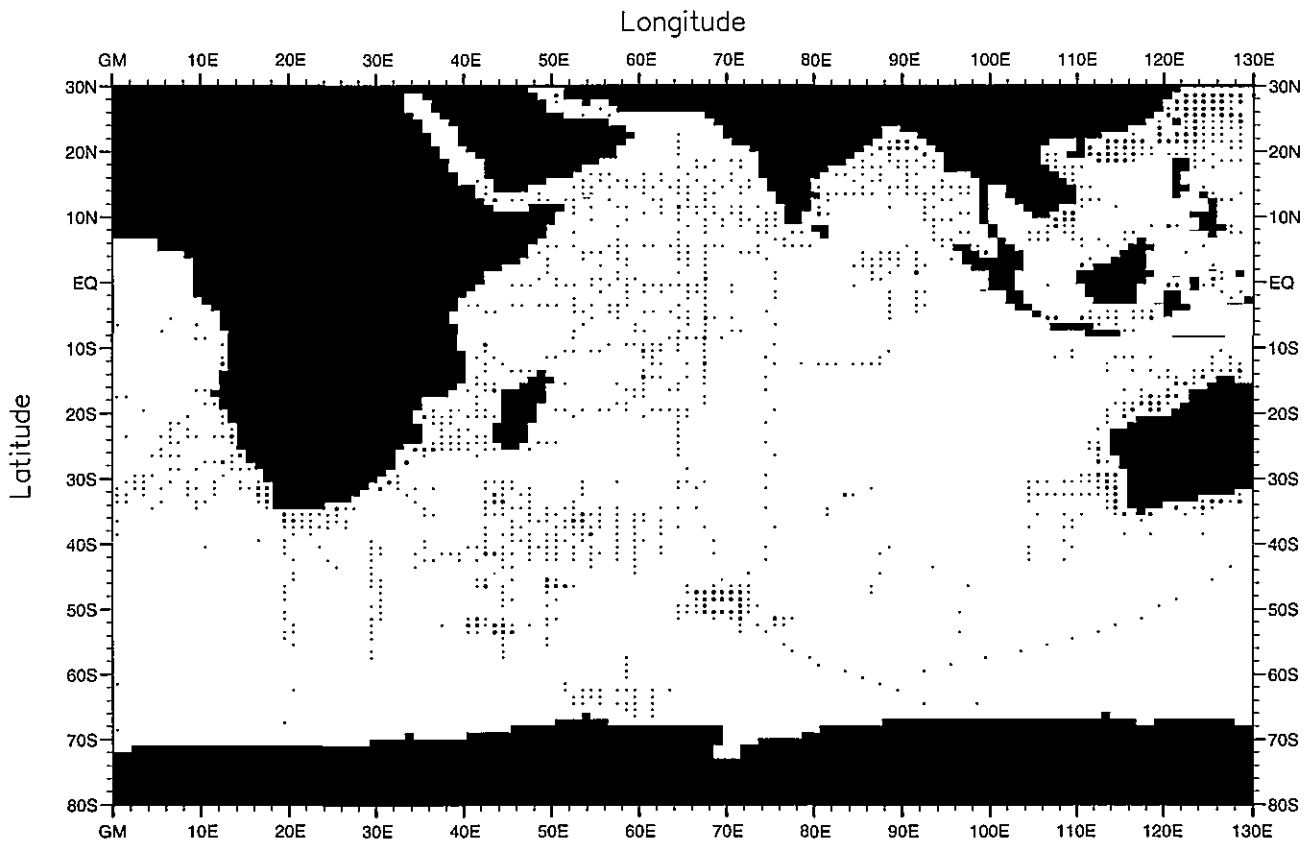
Fig. F7.   Spring (Apr.-Jun.) silicate observations at the surface .
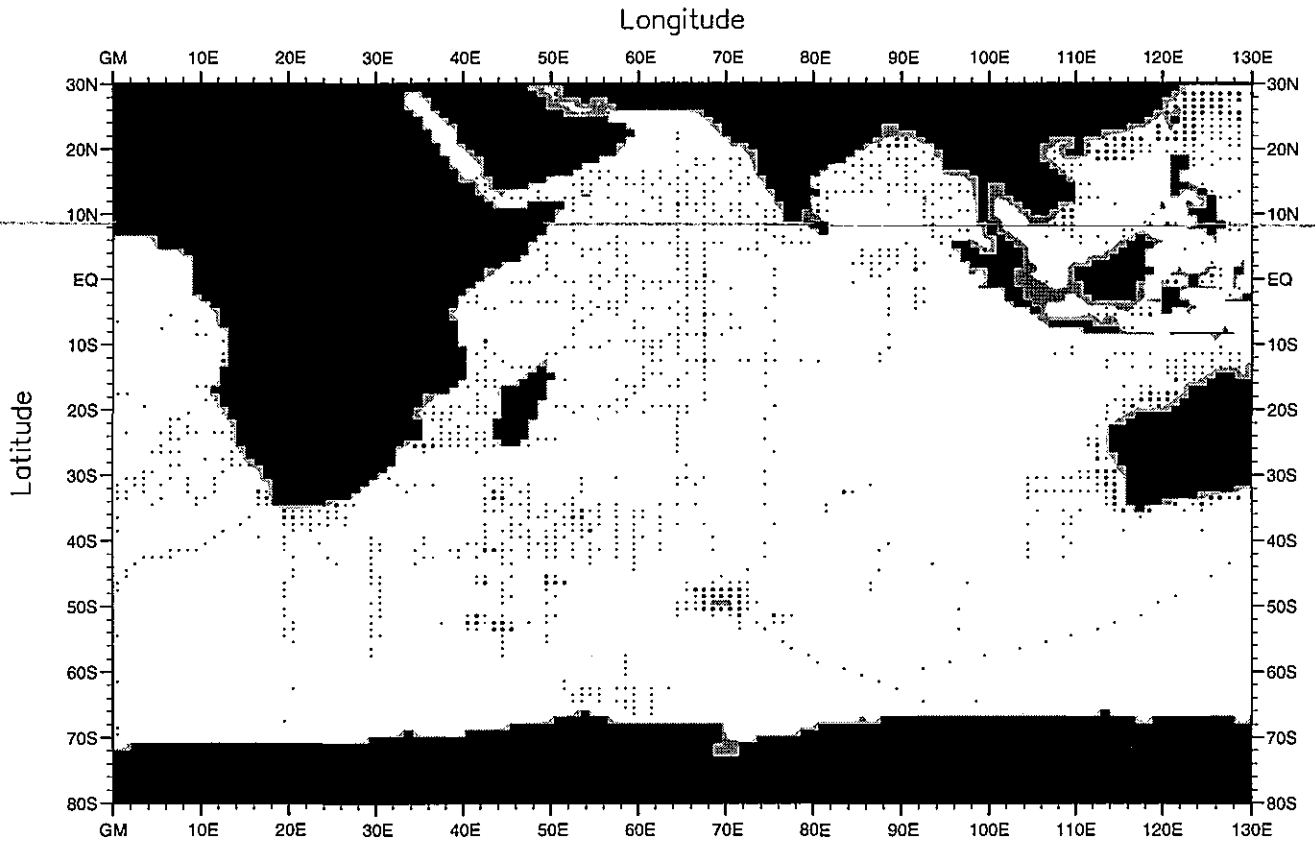
Fig. F8.   Spring (Apr.-Jun.) silicate observations at   50 m. depth .
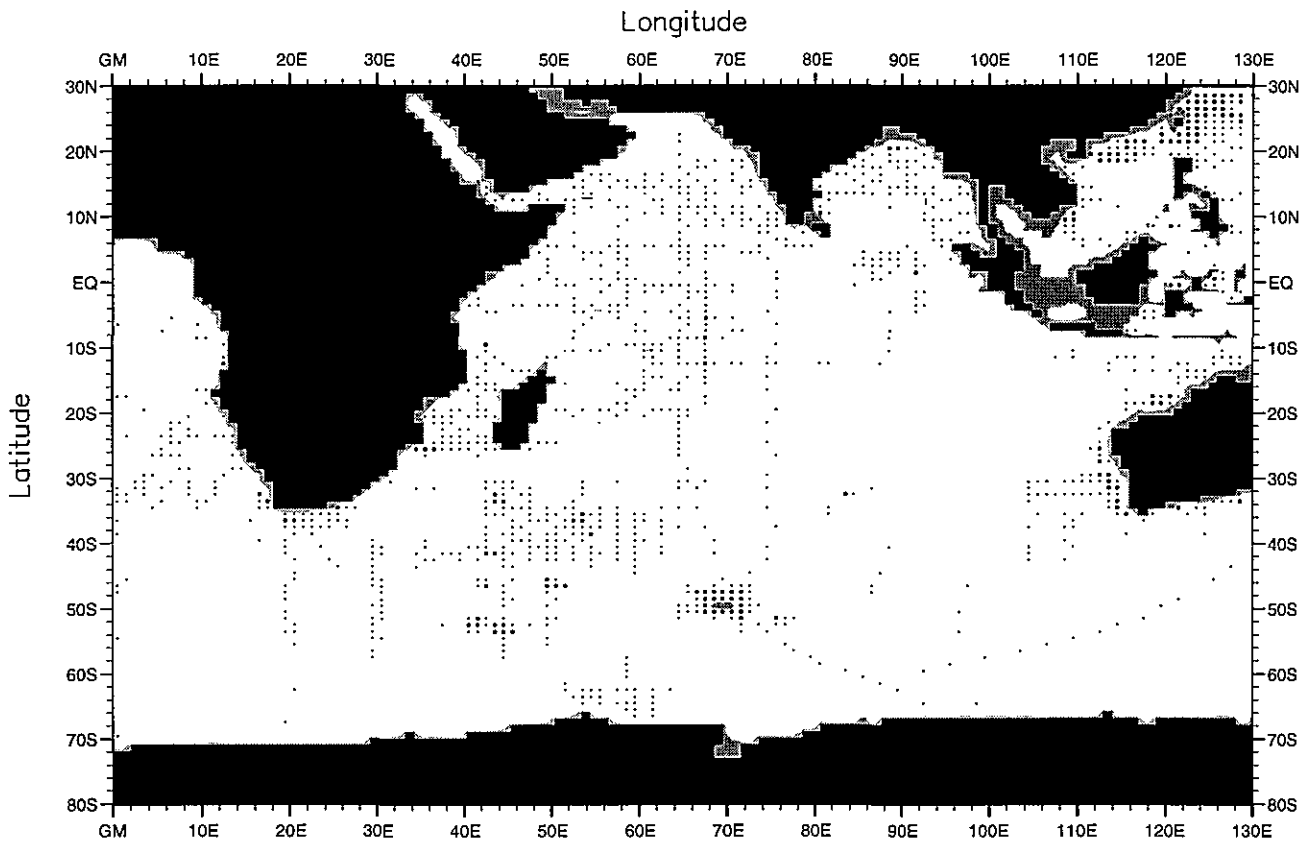
Fig. F9. Spring (Apr.-Jun.) silicate observations at 75 m. depth .
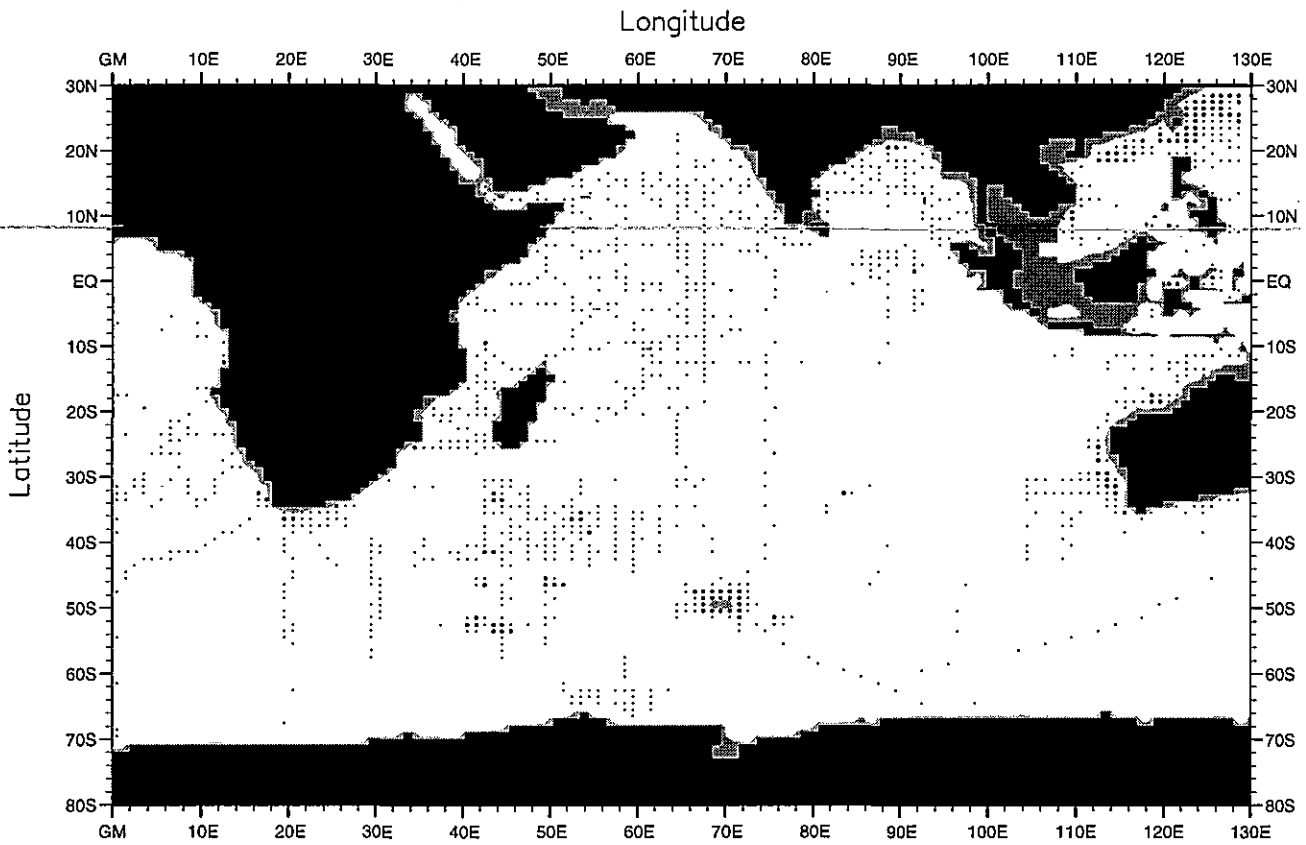
Fig. F10. Spring (Apr.-Jun.) silicate observations at 100 m. depth .
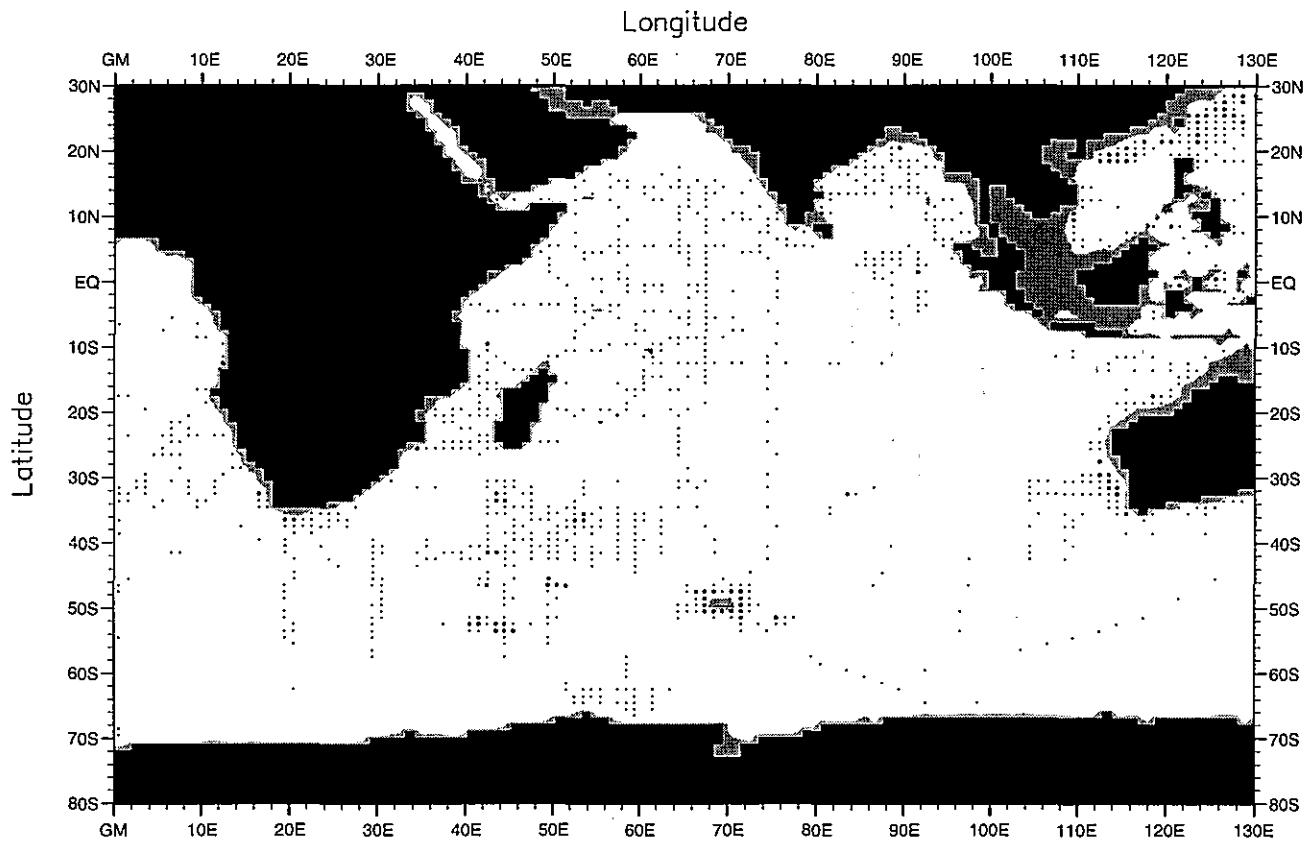
Fig. F11. Spring (Apr.-Jun.) silicate observations at 150 m. depth.
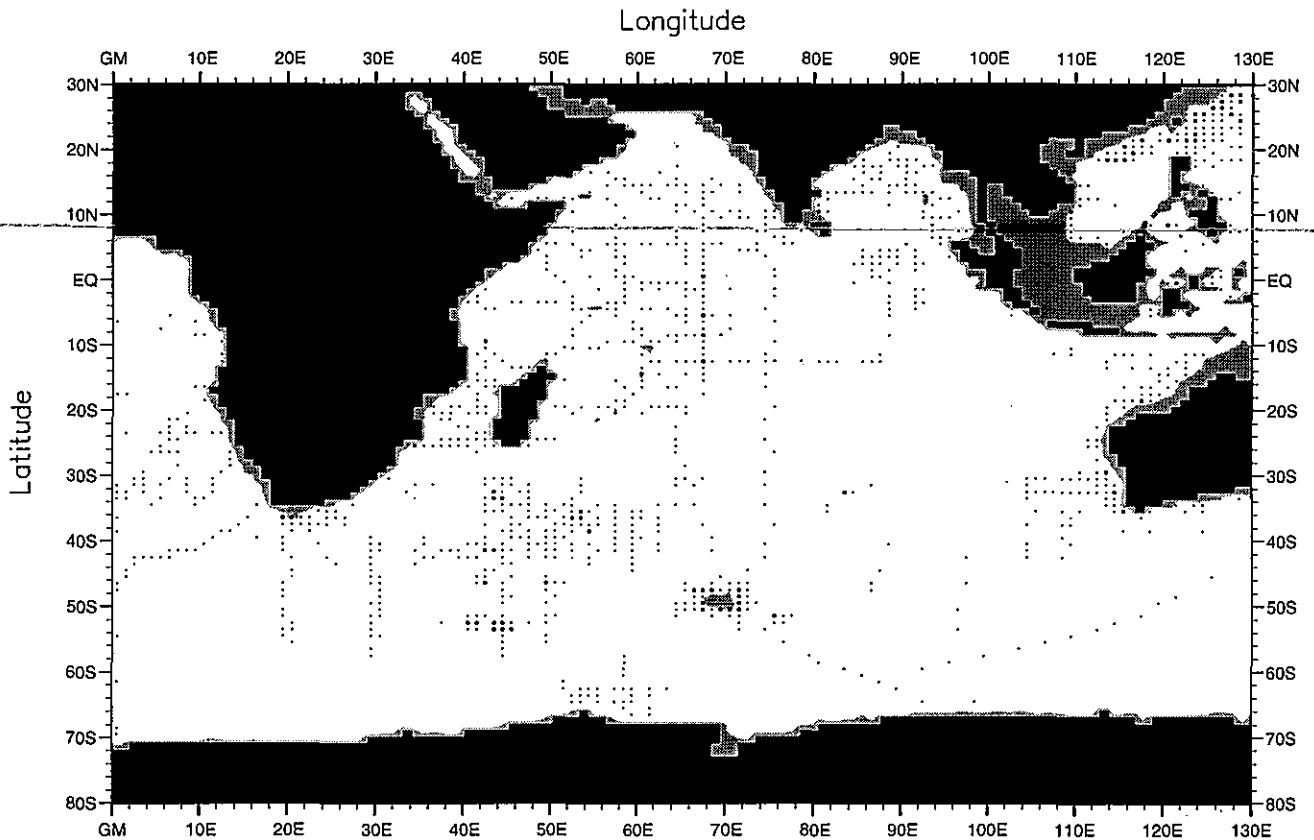
Fig. F12. Spring (Apr.-Jun.) silicate observations at 250 m. depth.

Longitude
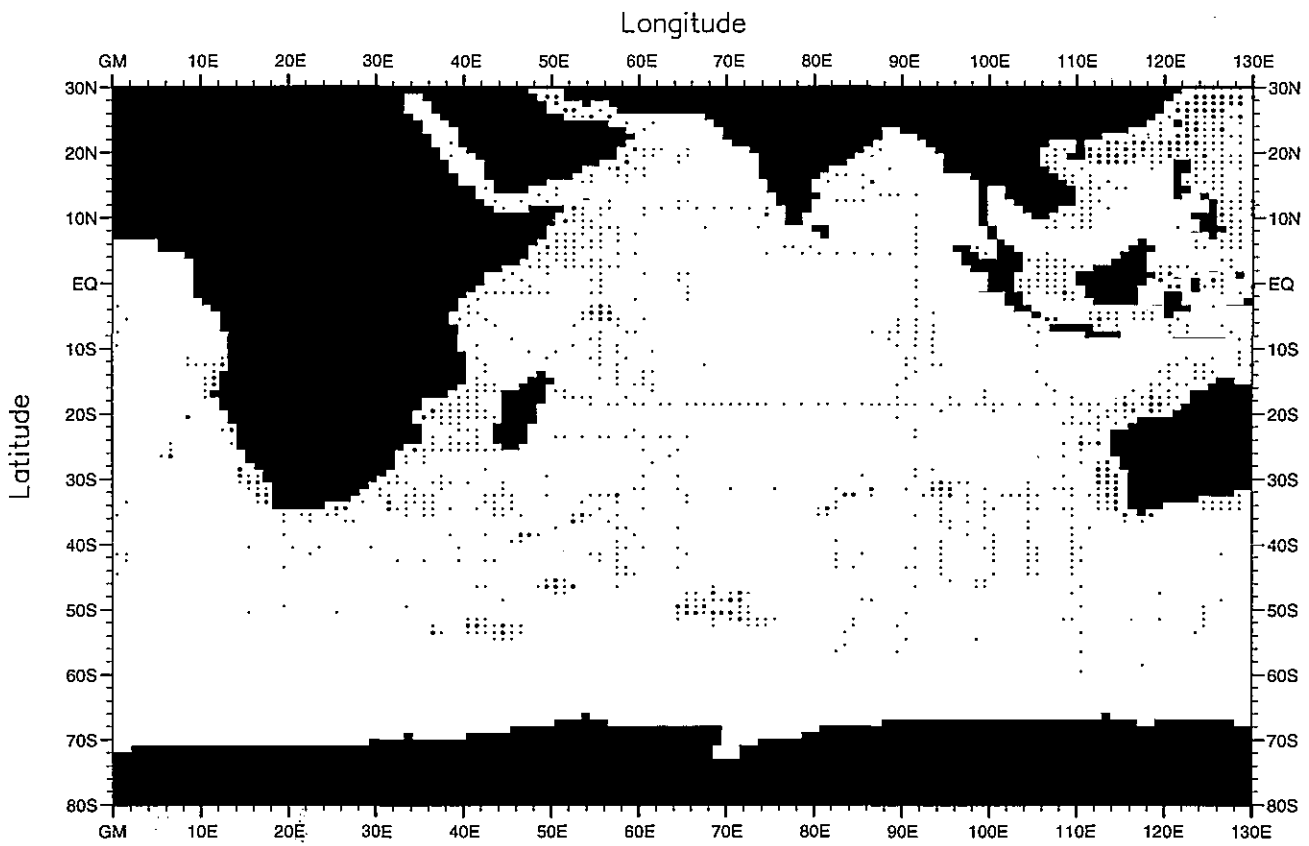
Fig. F13. Summer (Jul.-Sep.) silicate observations at the surface .

Longitude
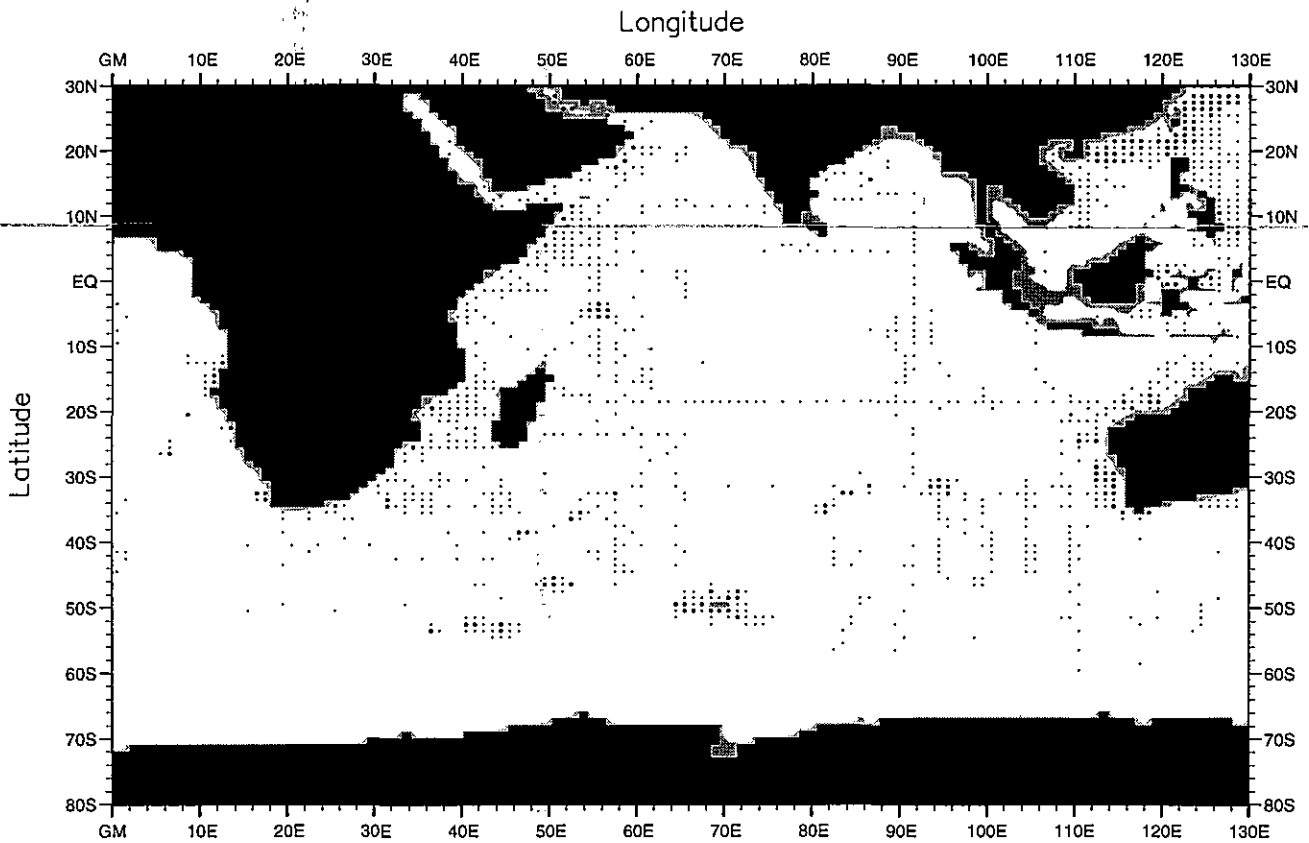
Fig. F14. Summer (Jul.-Sep.) silicate observations at 50 m. depth .

171
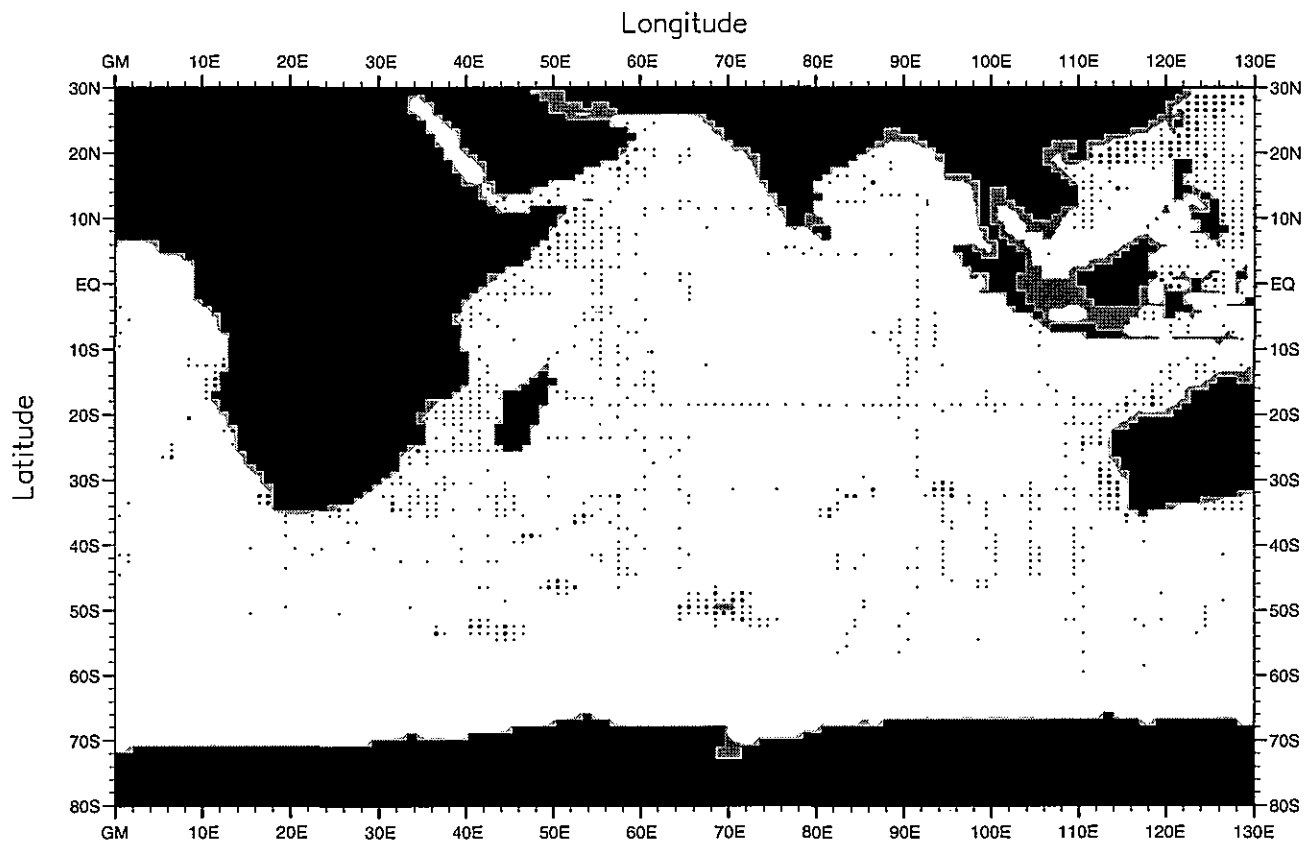
Fig. F15. Summer (Jul.-Sep.) silicate observations at 75 m. depth .
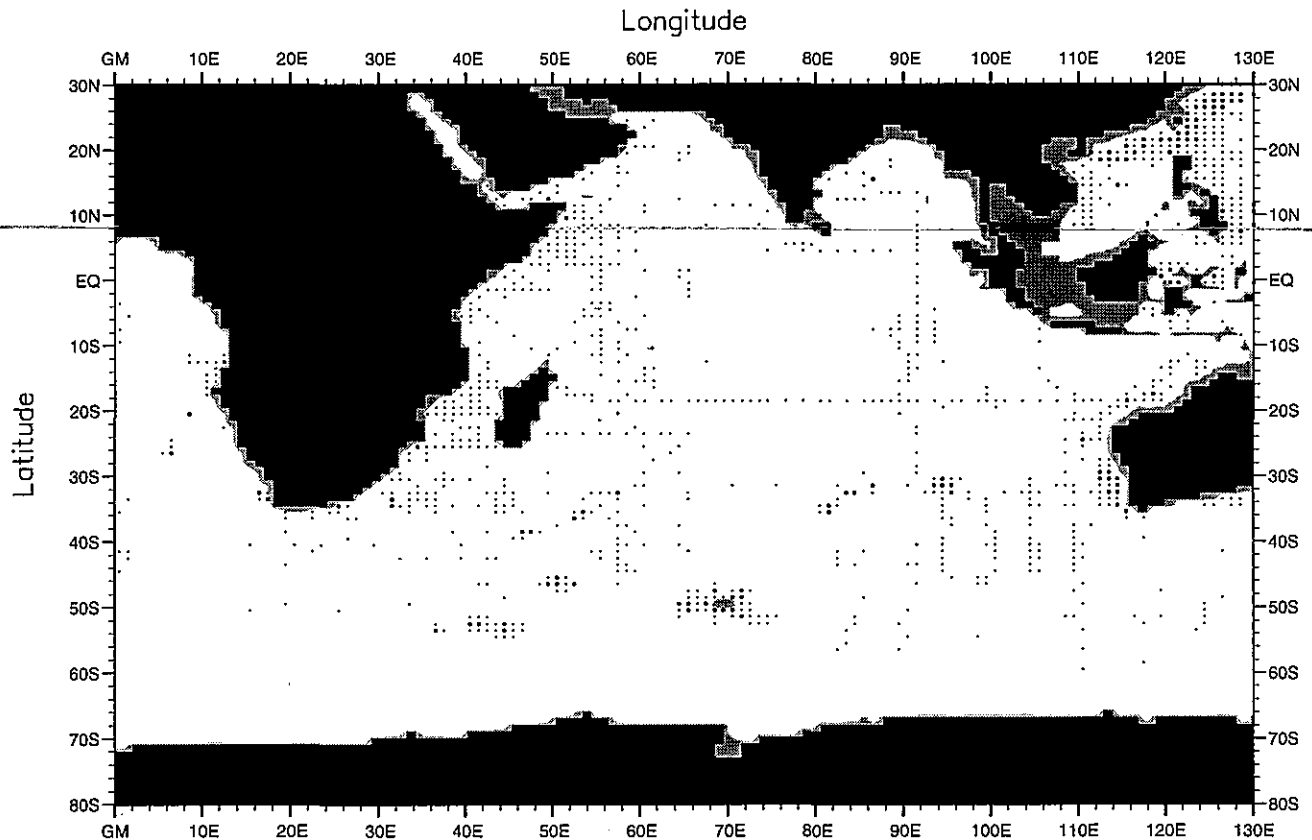
Fig. F16. Summer (Jul.-Sep.) silicate observations at 100 m. depth .
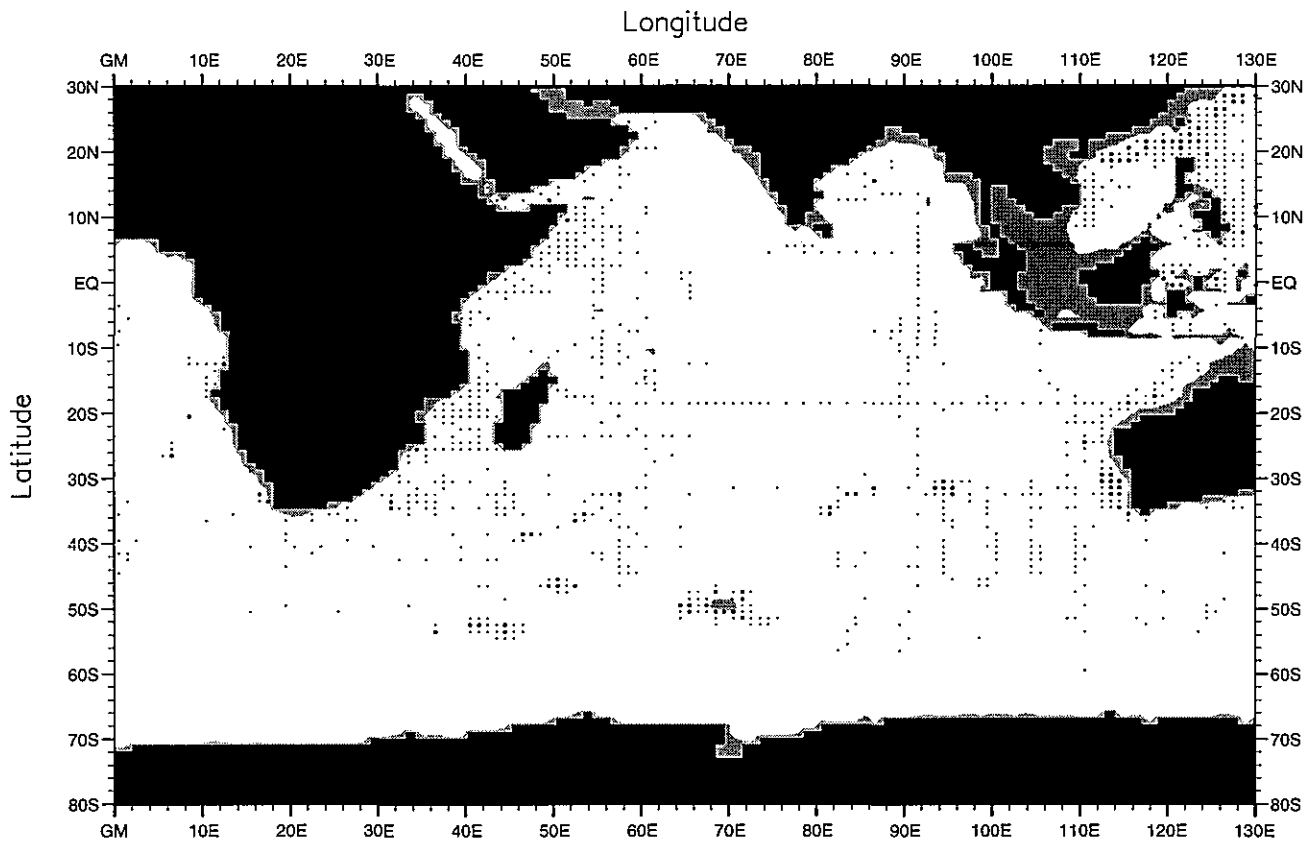
Fig. F17. Summer (Jul.-Sep.) silicate observations at 150 m. depth .
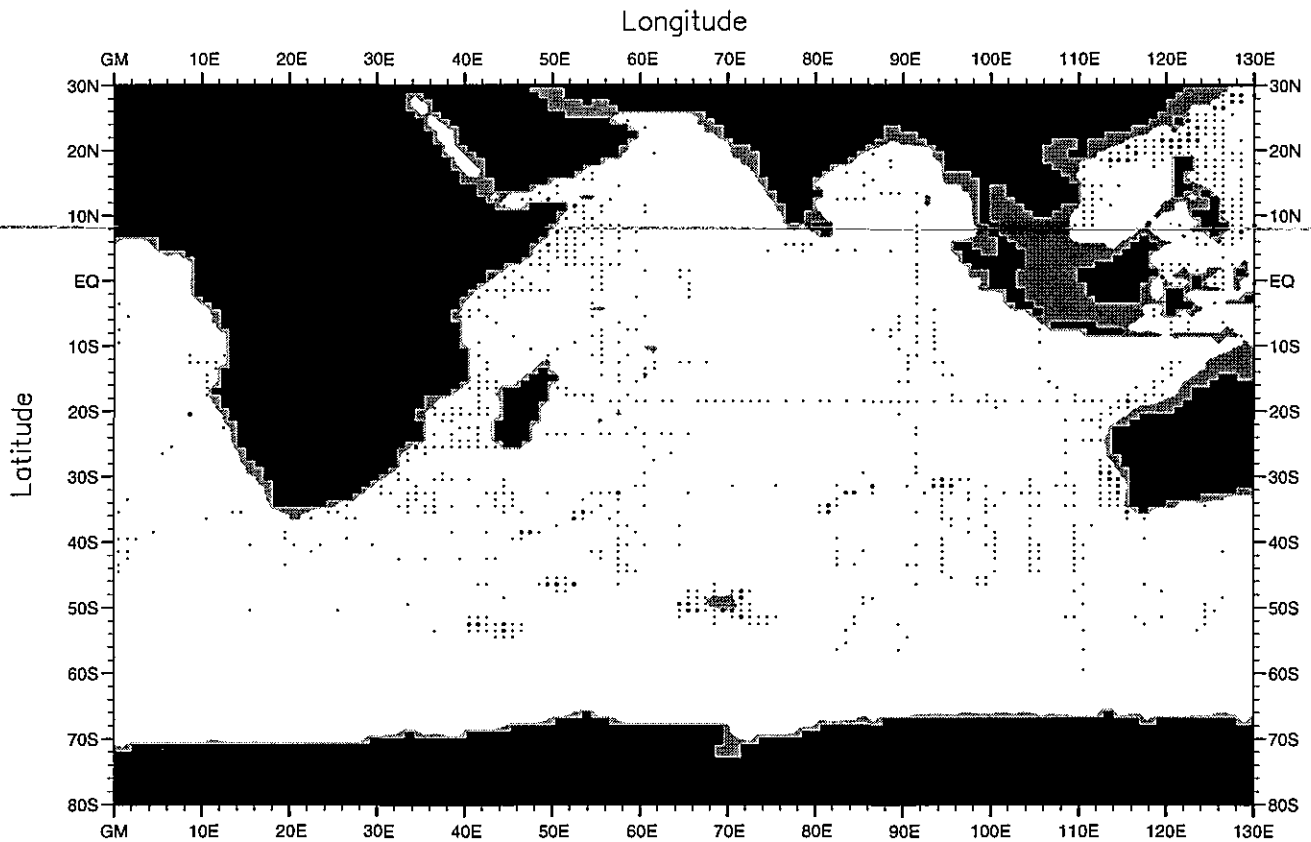
Fig. F18. Summer (Jul.-Sep.) silicate observations at 250 m. depth .
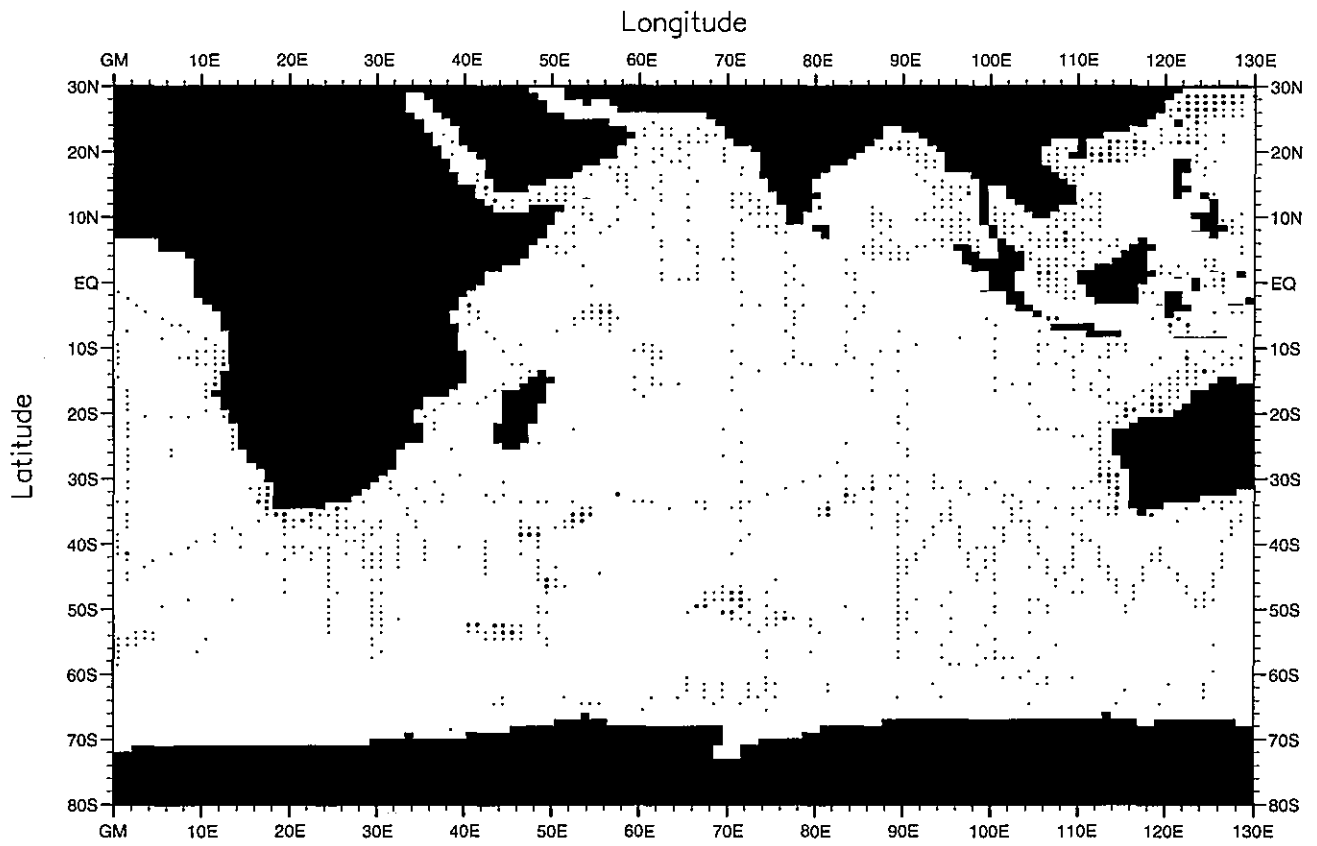
Fig. F19. Fall (Oct.-Dec.) silicate observations at the surface .
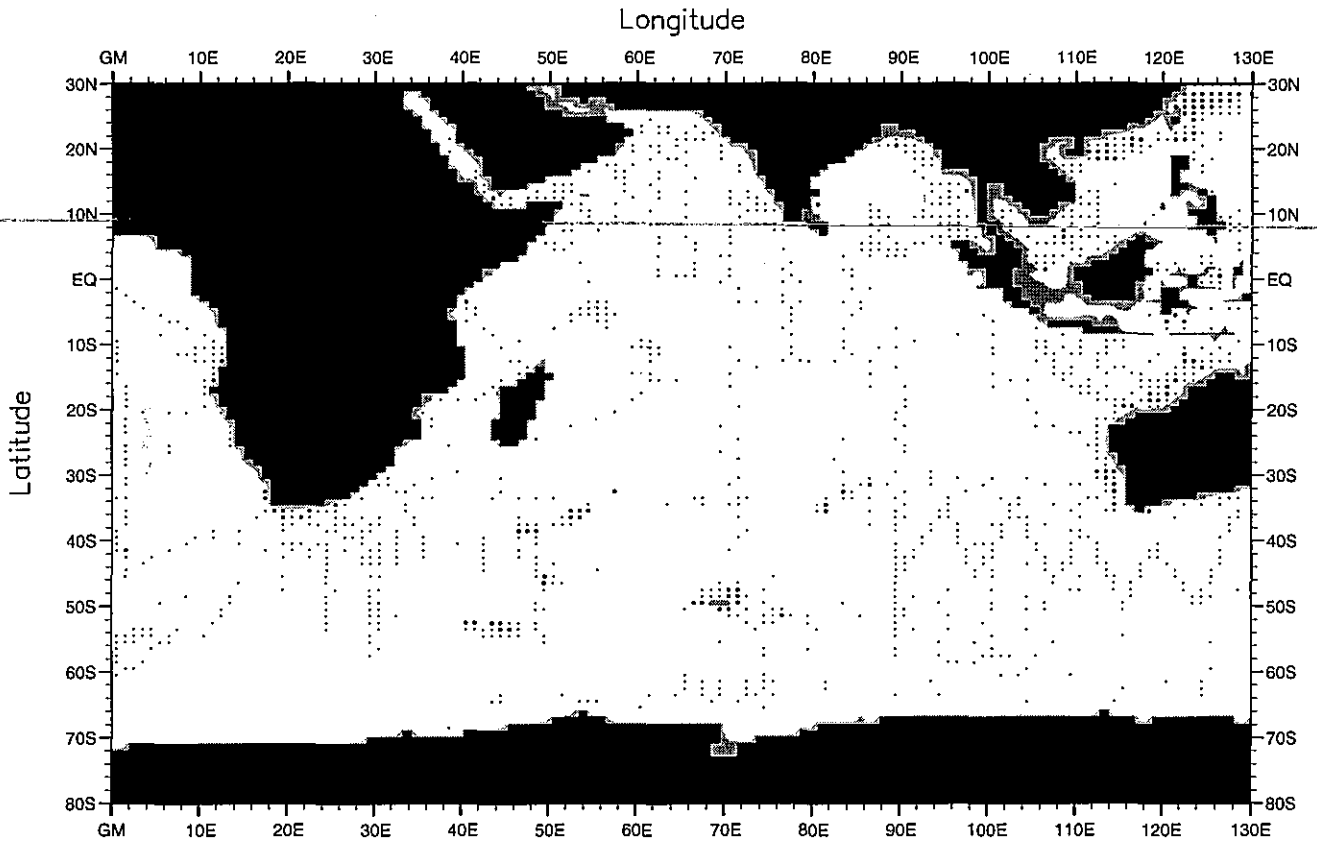
Fig. F20.   Fall (Oct.-Dec.) silicate observations at   50 m. depth .
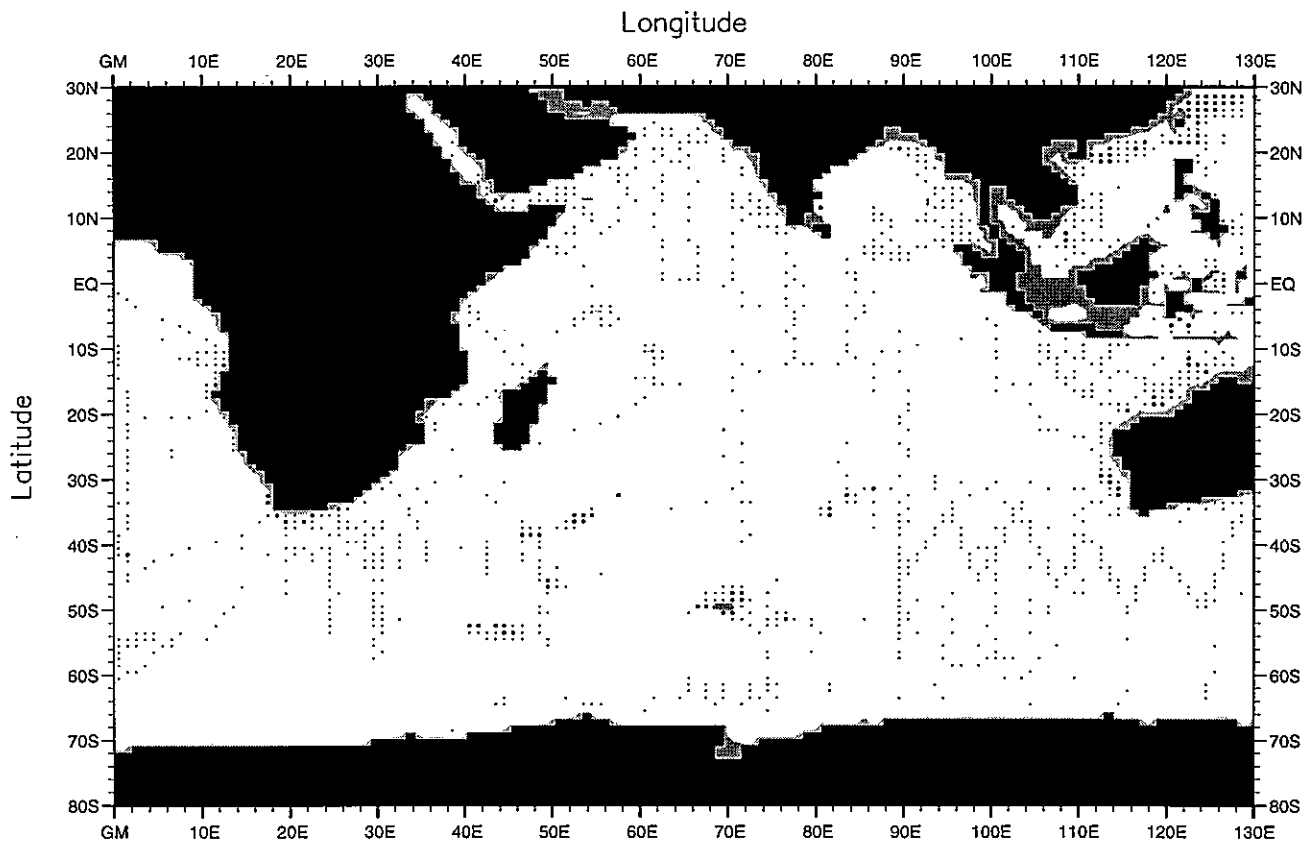
Fig. F21.   Fall (Oct.-Dec.) silicate observations at   75 m. depth .
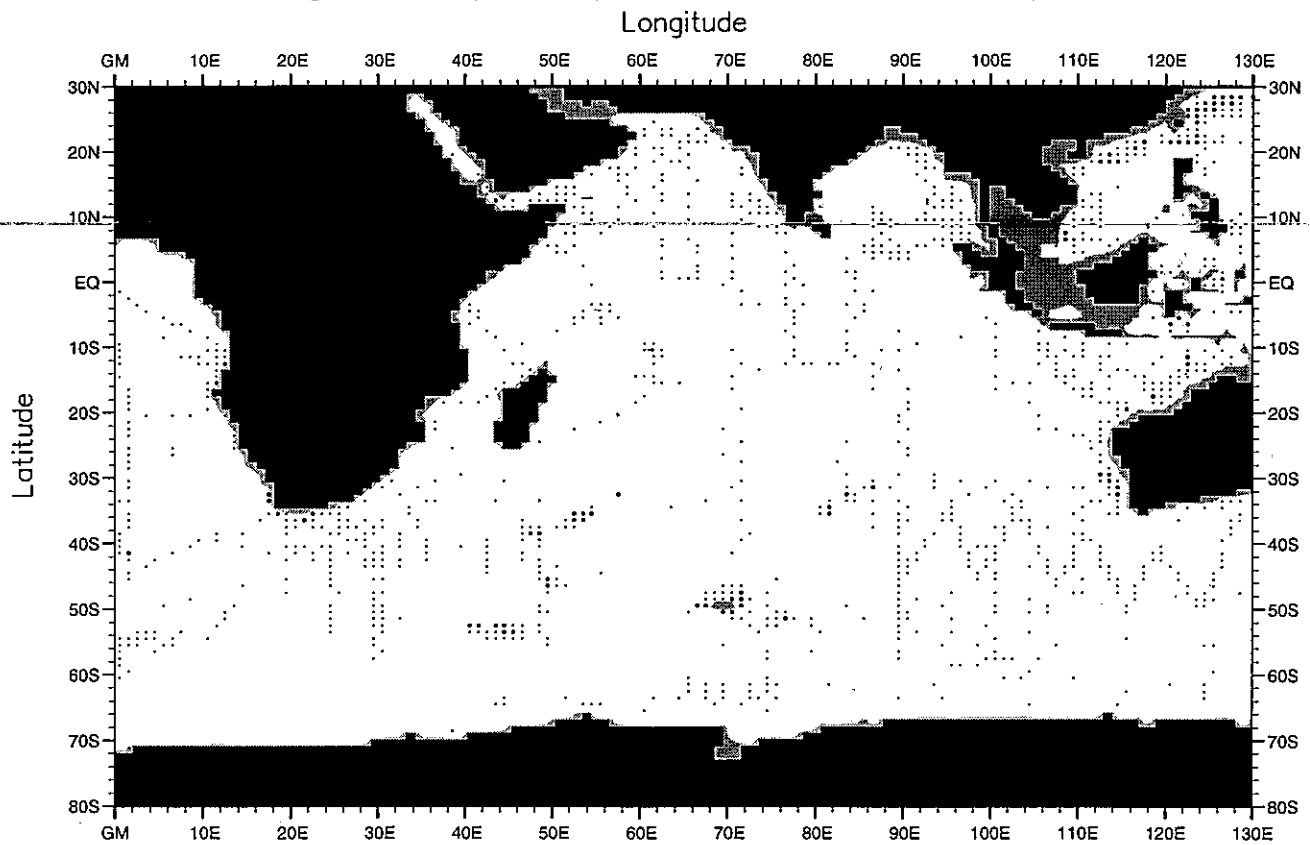
Fig. F22.   Fall (Oct.-Dec.) silicate observations at 100 m. depth .
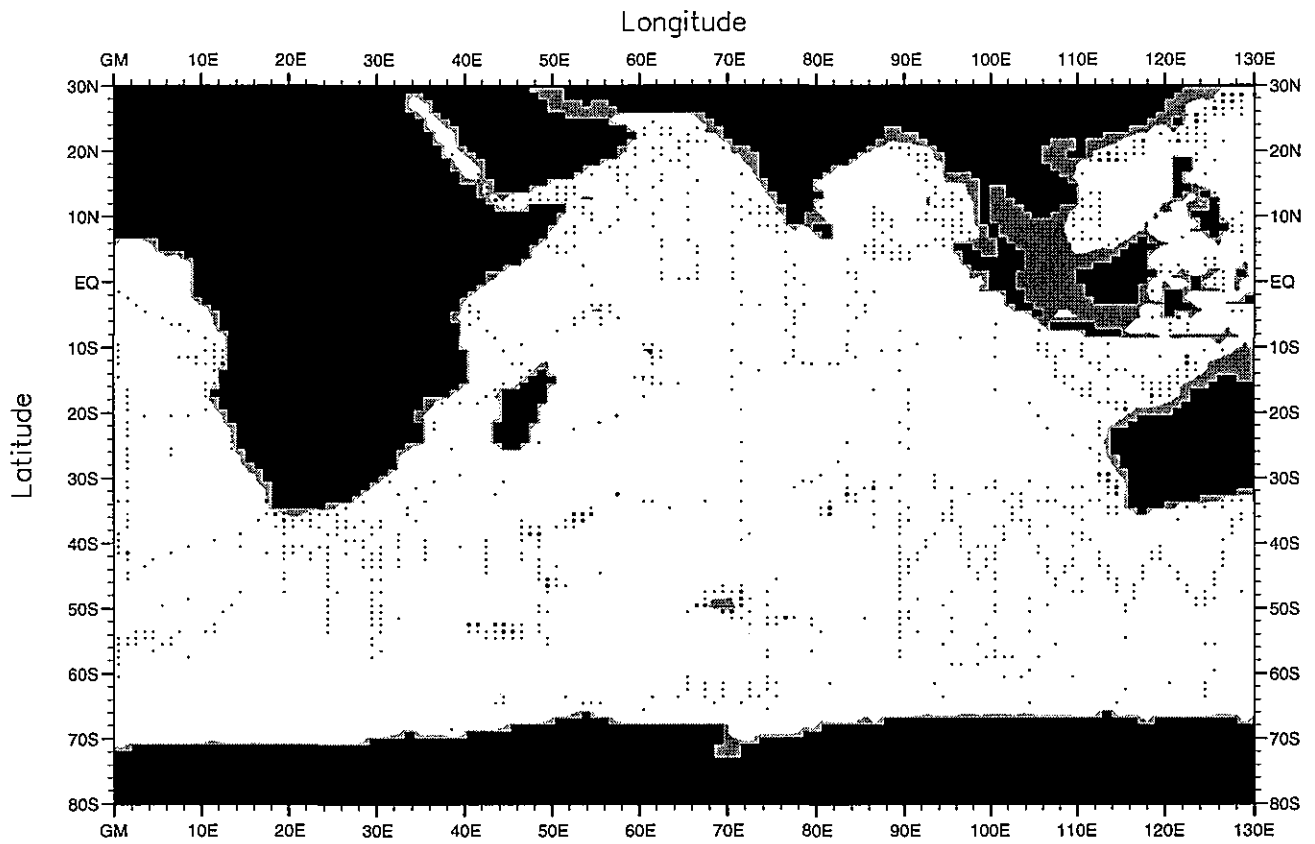
Fig. F23.   Fall (Oct.-Dec.) silicate observations at 150 m. depth .
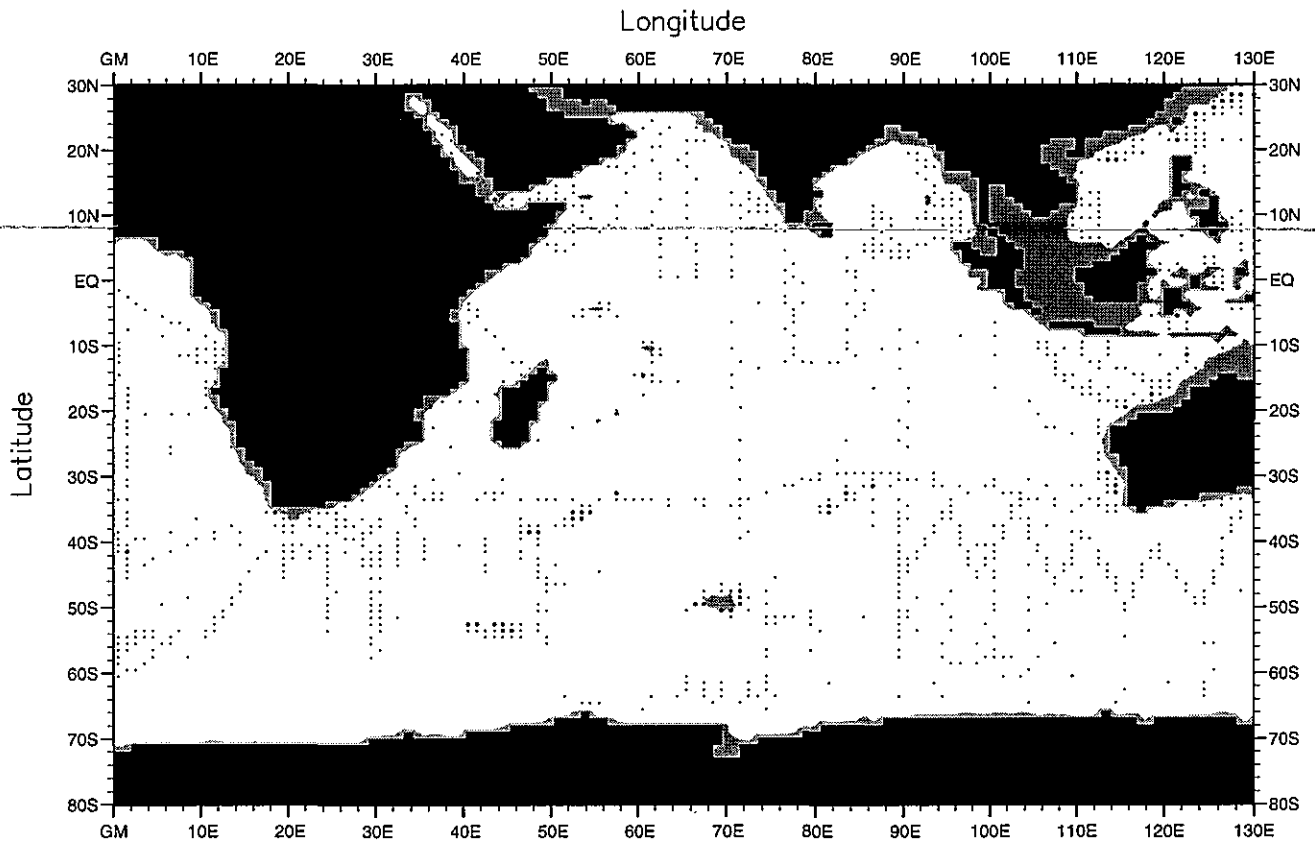
Fig. F24.   Fall (Oct.-Dec.) silicate observations at 250 m. depth .
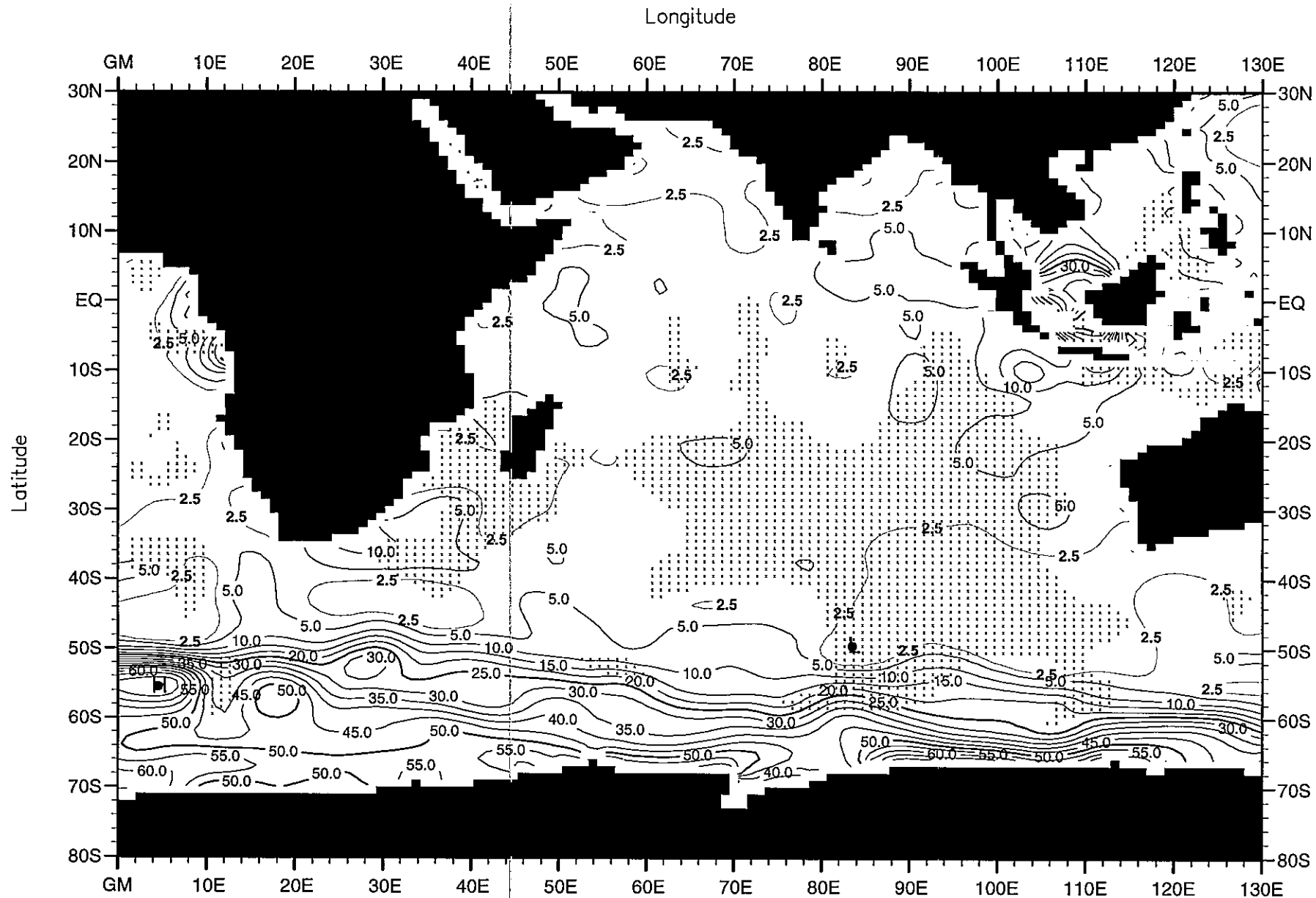
Fig. F25.   Winter (Jan.-Mar.) mean silicate (μM) at the surface .

Minimum Value=   0.00   Maximum Value= 74.76   Contour Interval: 5.00
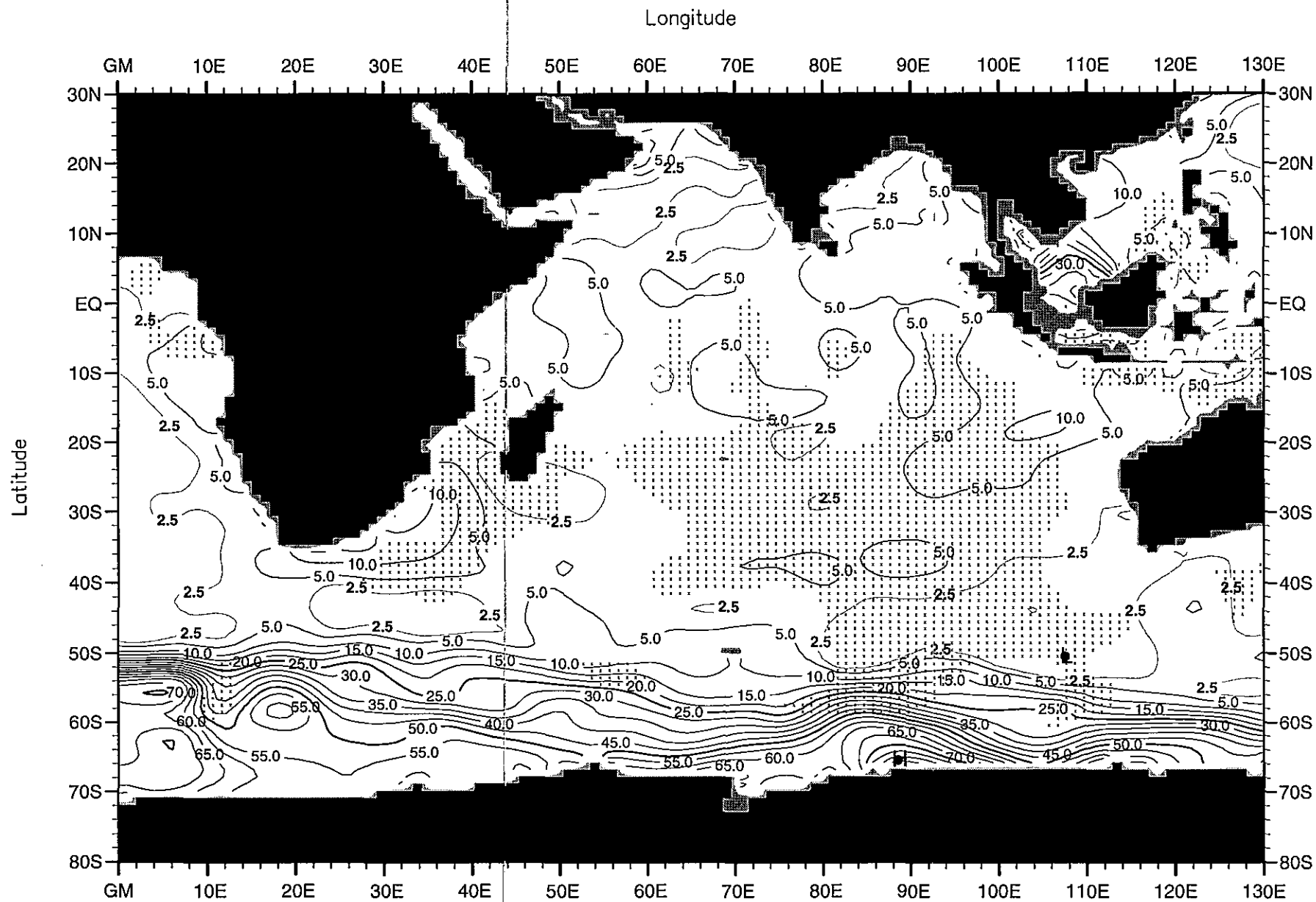
Fig. F26.   Winter (Jan.-Mar.) mean silicate (μM) at 50 m. depth .

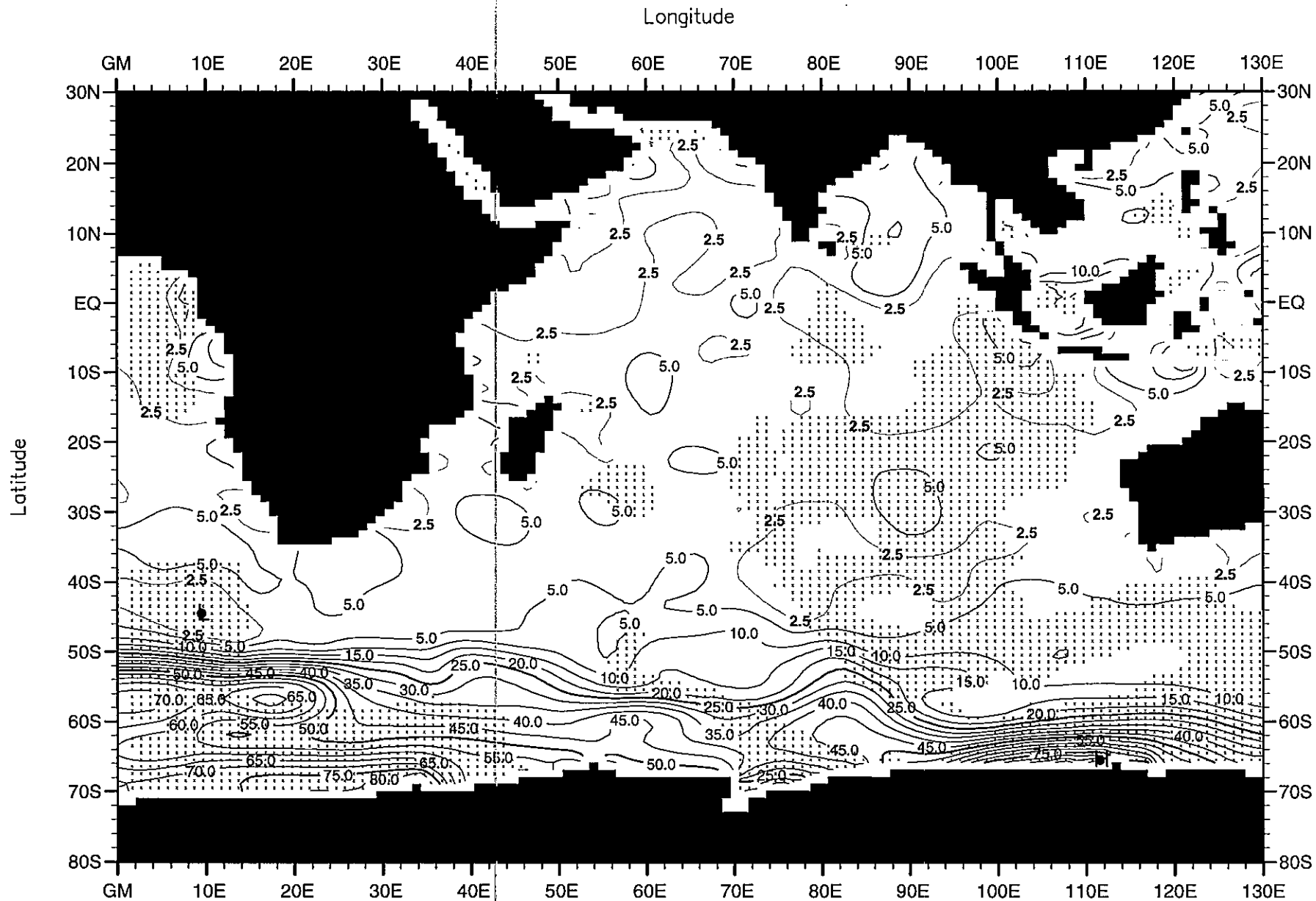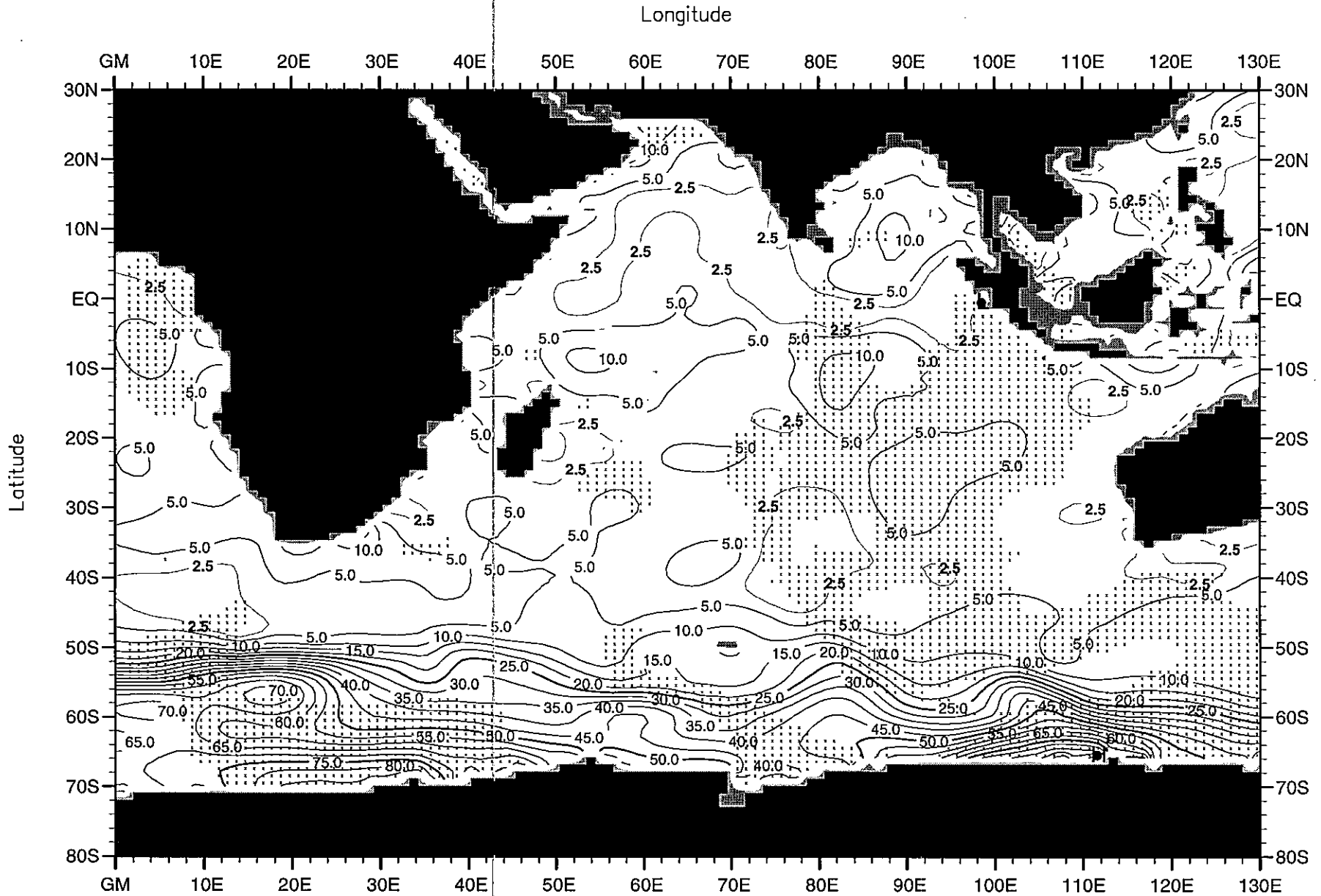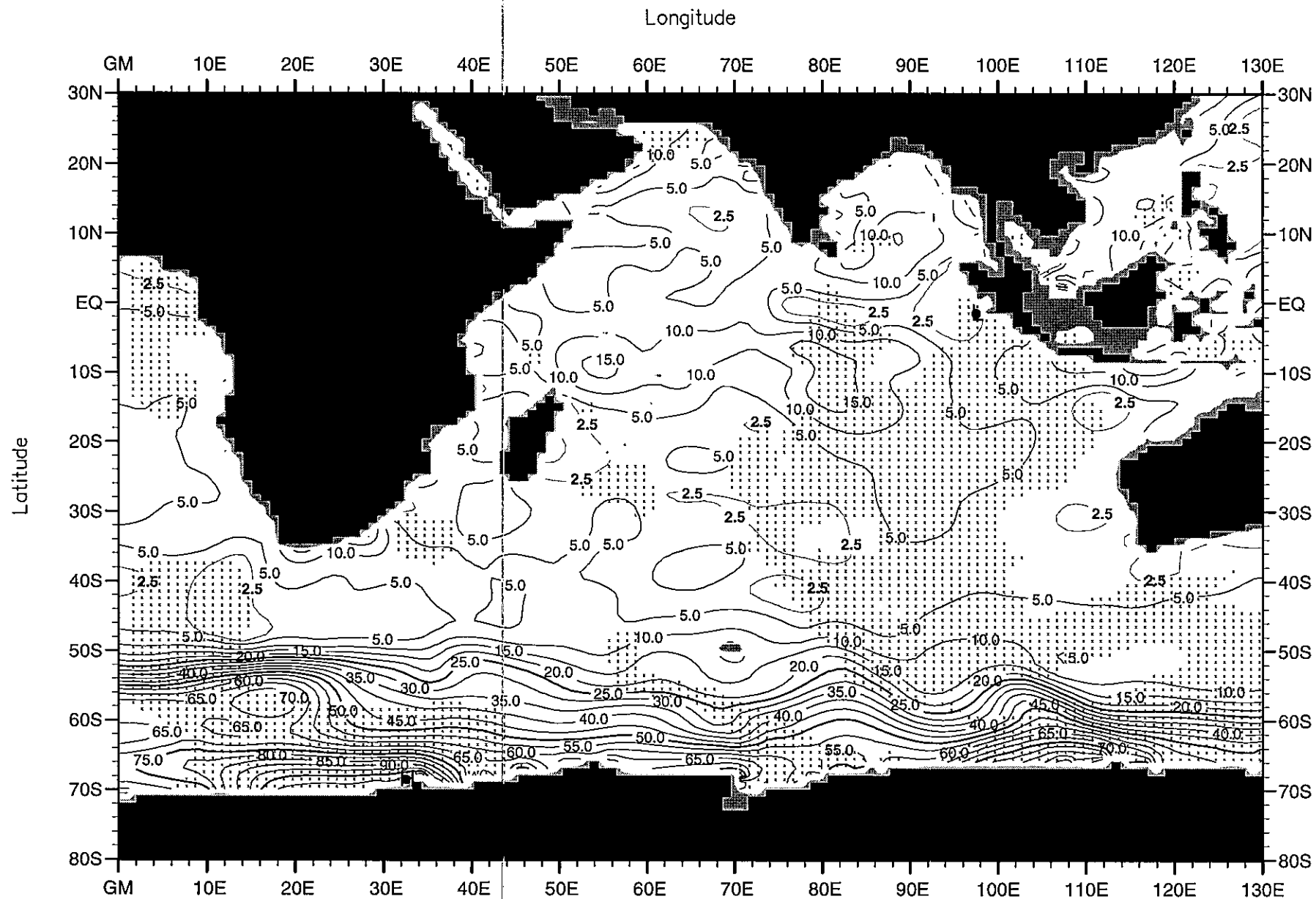Minimum Value= 0.00   Maximum Value= 91.96   Contour Interval: 5.00
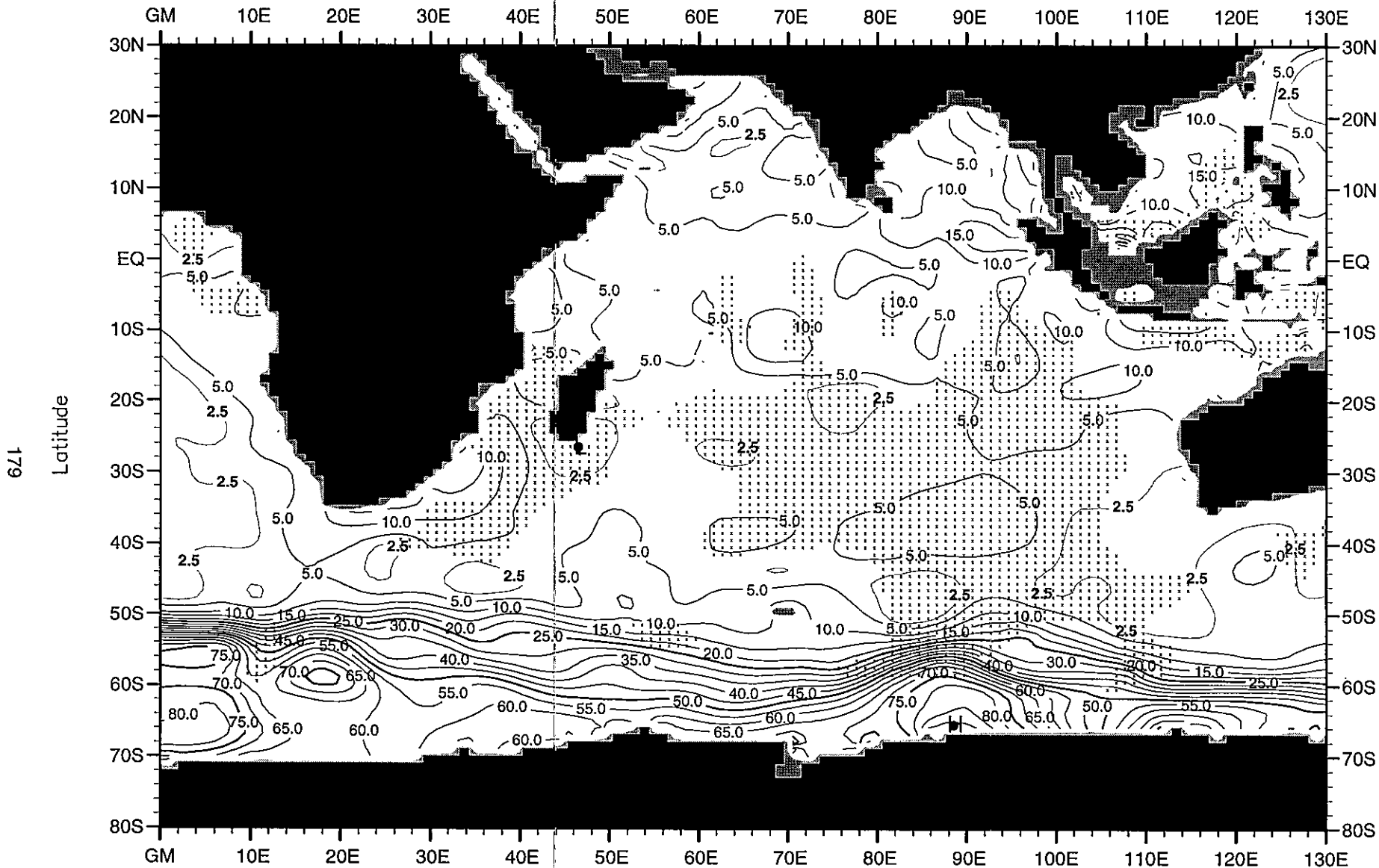
Fig. F27. Winter (Jan.-Mar.) mean silicate (μM) at 75 m. depth .

Minimum Value= 0.00   Maximum Value= 94.62   Contour Interval: 5.00
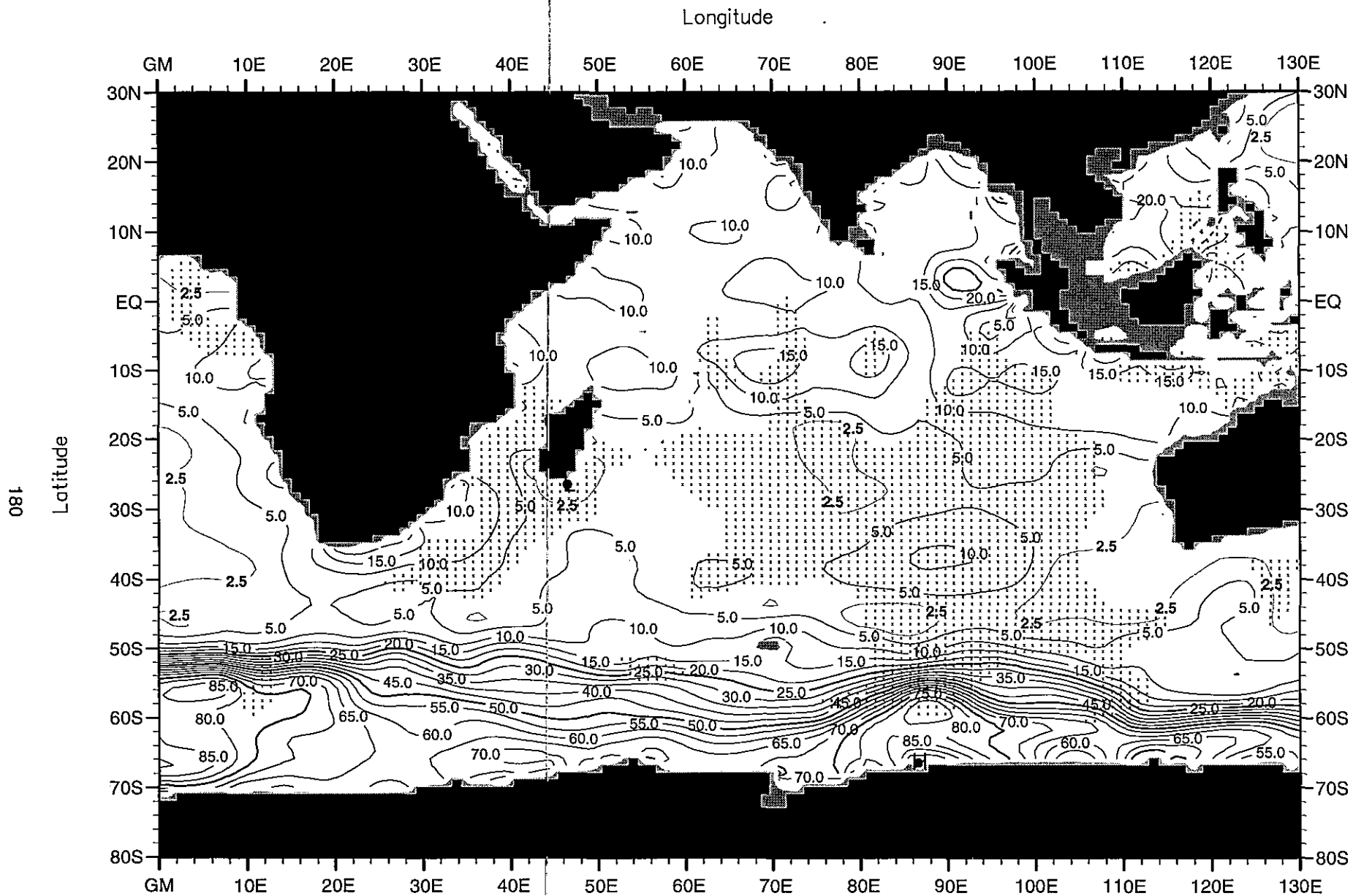
Fig. F28.   Winter (Jan.-Mar.) mean silicate (μM) at 100 m. depth .

Minimum Value= 0.00   Maximum Value= 101.34   Contour Interval: 5.00
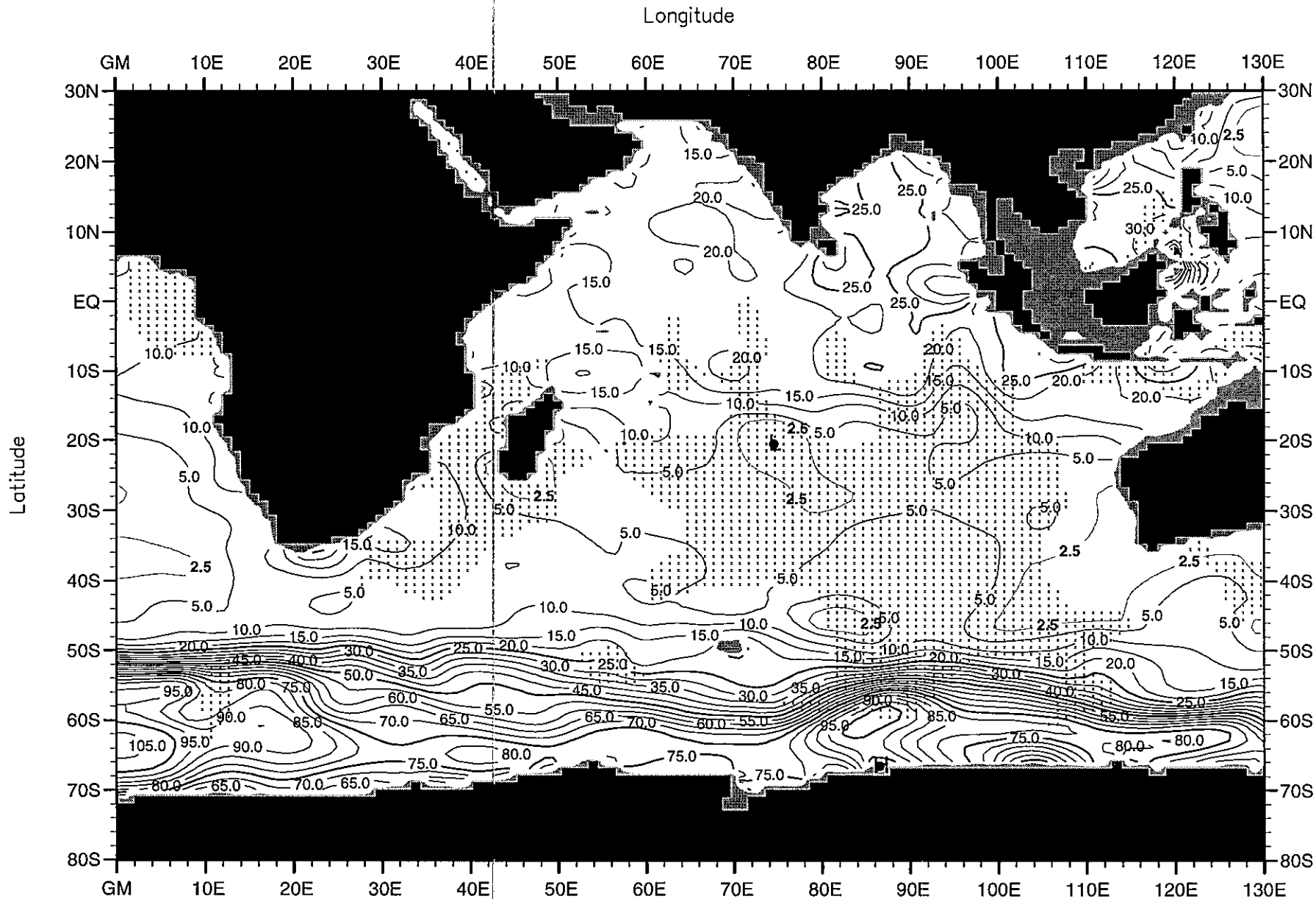
Fig. F29.   Winter (Jan.-Mar.) mean silicate (μM) at 150 m. depth .

Minimum Value= 0.00   Maximum Value= 107.10   Contour Interval: 5.00
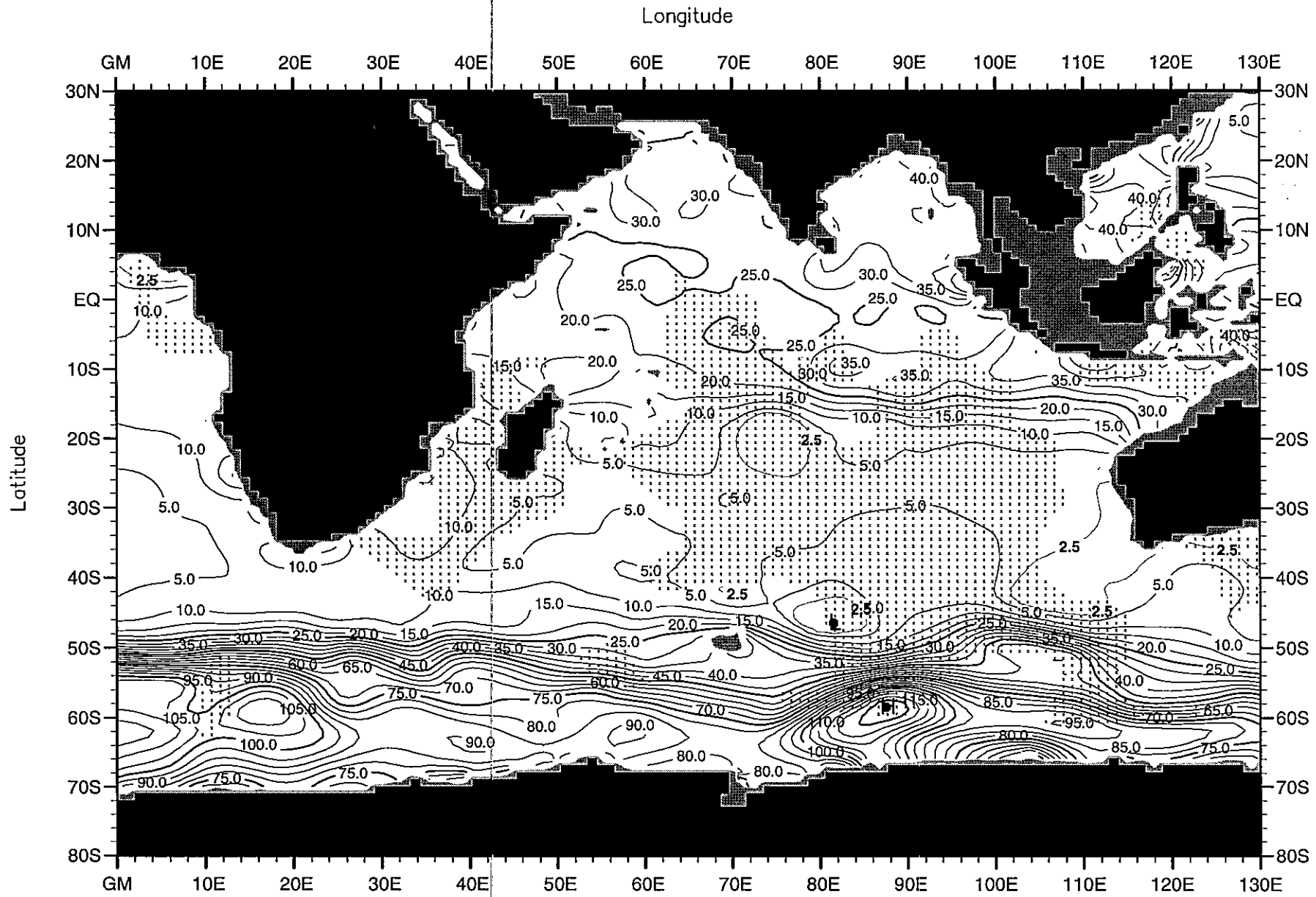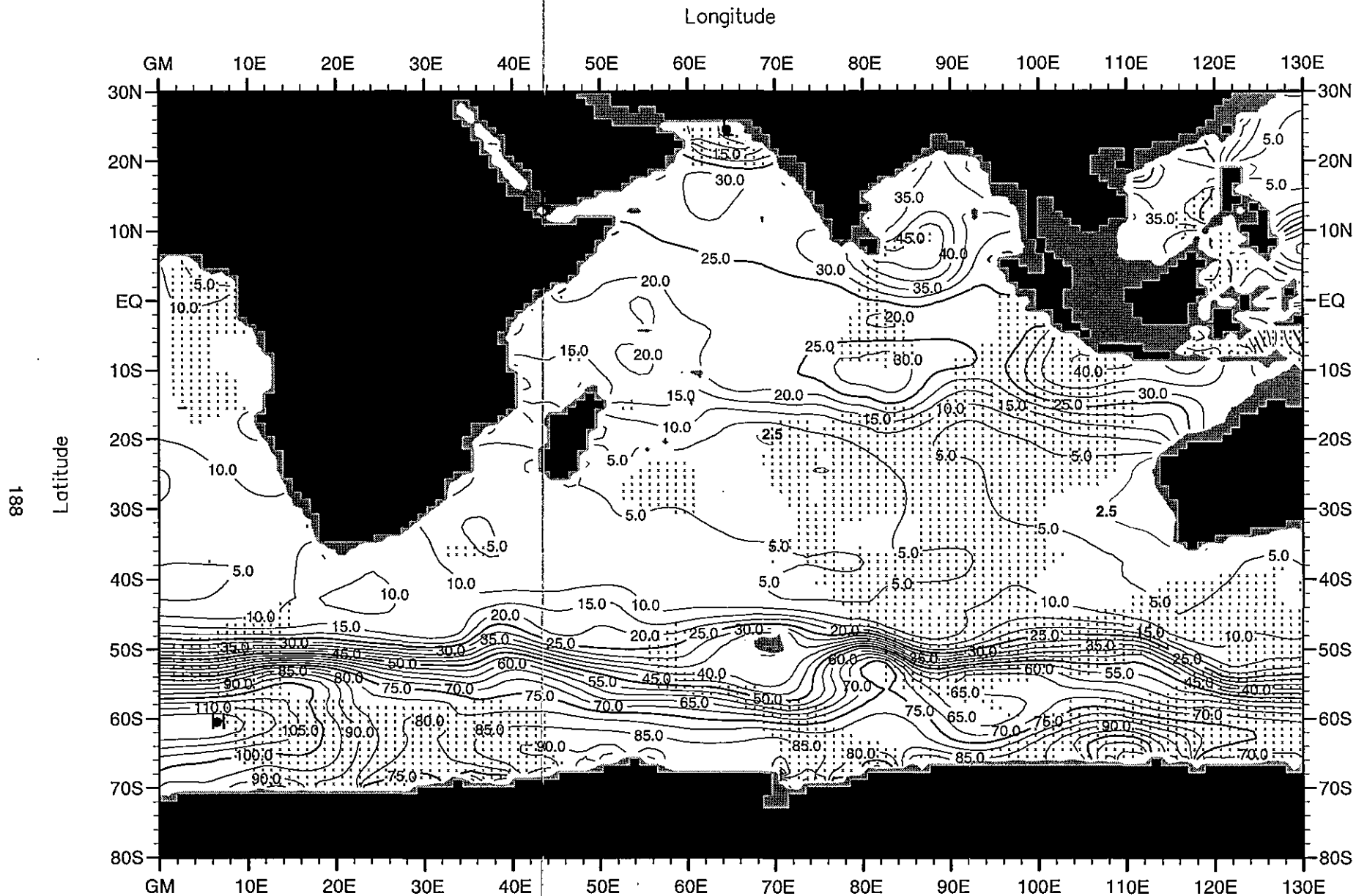
Fig. F30.   Winter (Jan.-Mar.) mean silicate (μM) at 250 m. depth .

Minimum Value=   0.00   Maximum Value= 130.20   Contour Interval: 5.00

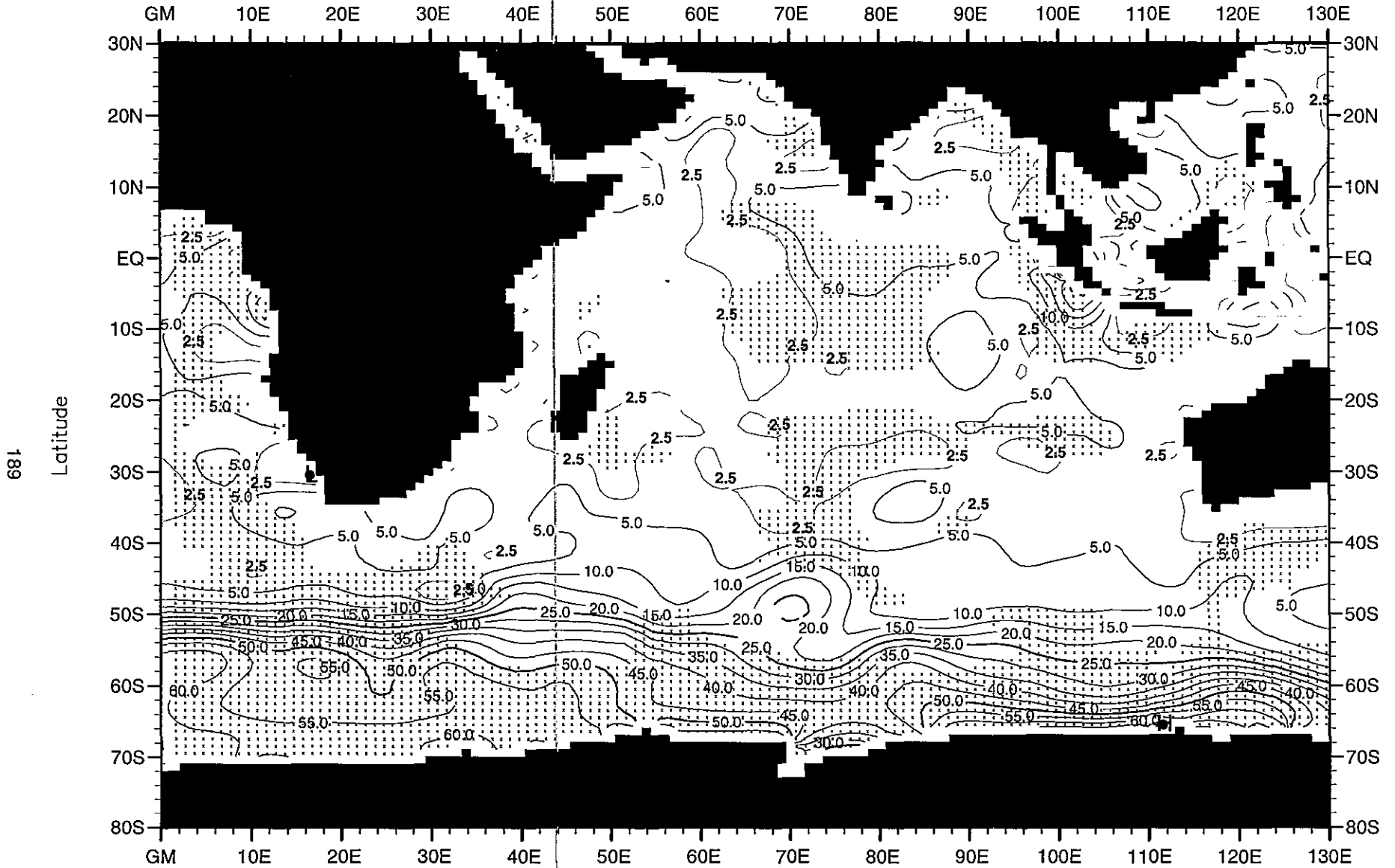Fig. F31.   Spring (Apr.-Jun.) mean silicate (μM) at the surface .

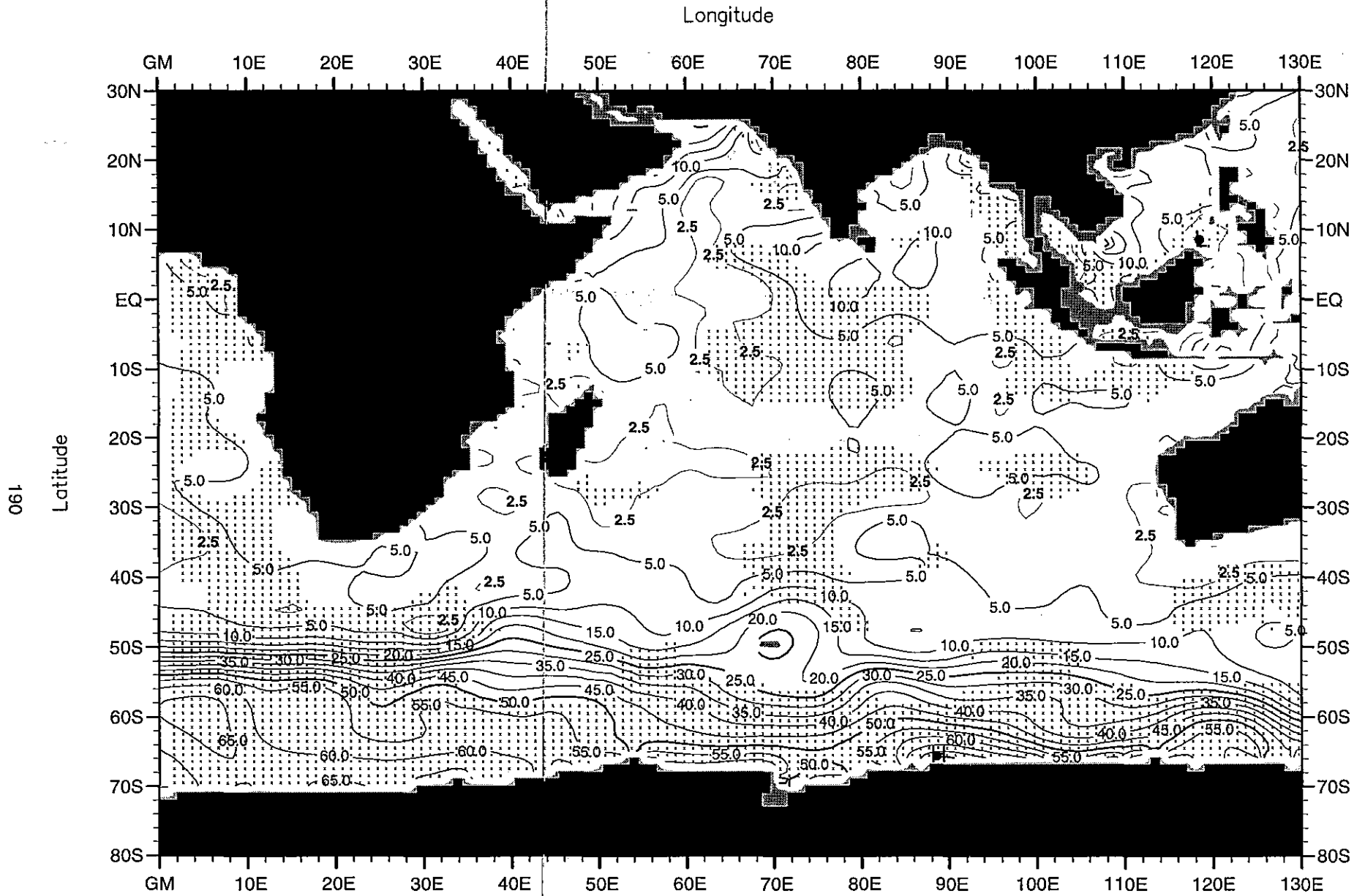Minimum Value= 0.00   Maximum Value= 97.46   Contour Interval: 5.00

Fig. F32. Spring (Apr.-Jun.) mean silicate (μM) at 50 m. depth .

Minimum Value= 0.00   Maximum Value= 101.89   Contour Interval: 5.00

Fig. F33. Spring (Apr.-Jun.) mean silicate (μM) at 75 m. depth .

Minimum Value= 0.00   Maximum Value= 109.53   Contour Interval: 5.00
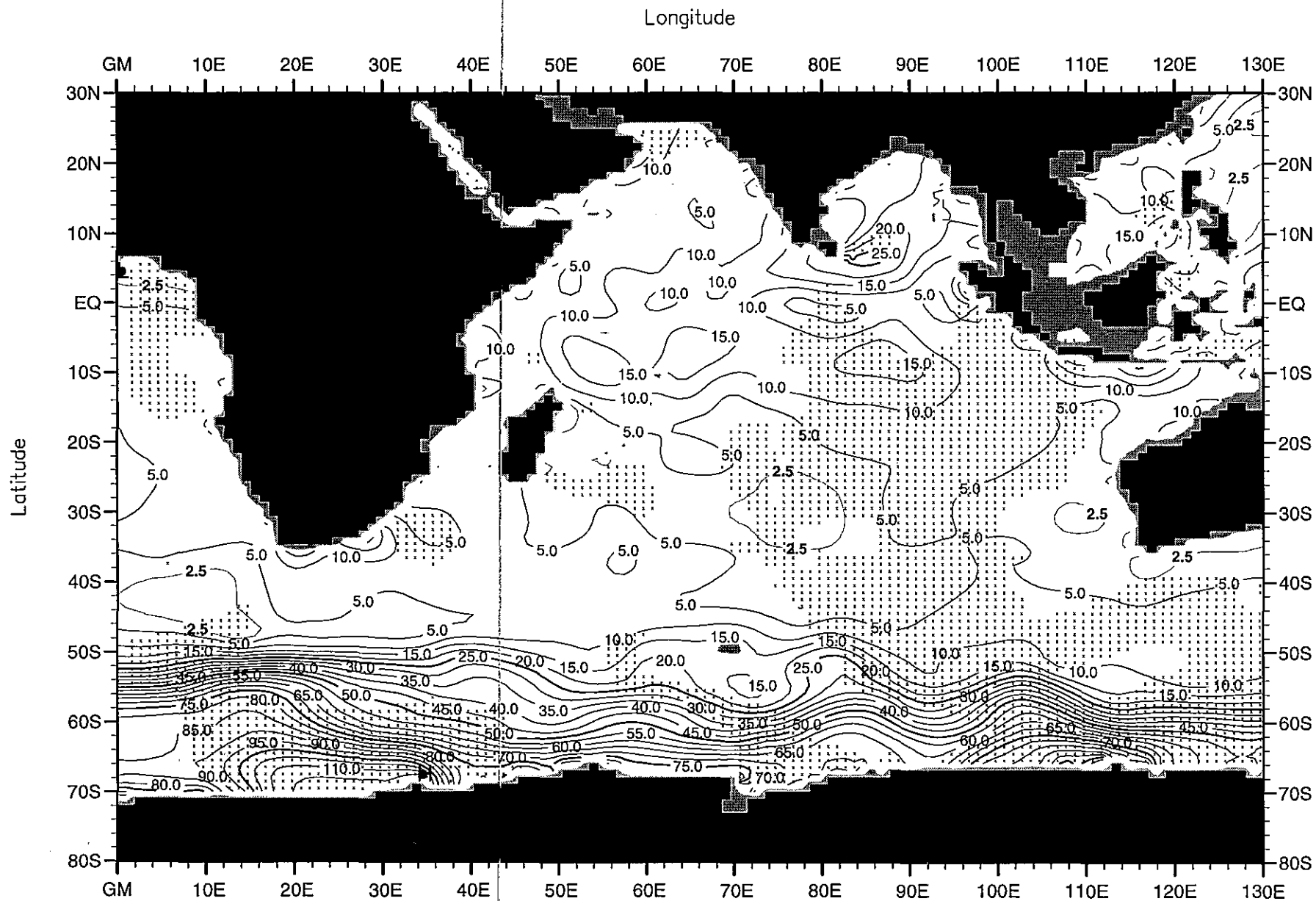
Fig. F34. Spring (Apr.-Jun.) mean silicate (μM) at 100 m. depth.

Minimum Value= 0.00   Maximum Value= 120.75   Contour Interval: 5.00
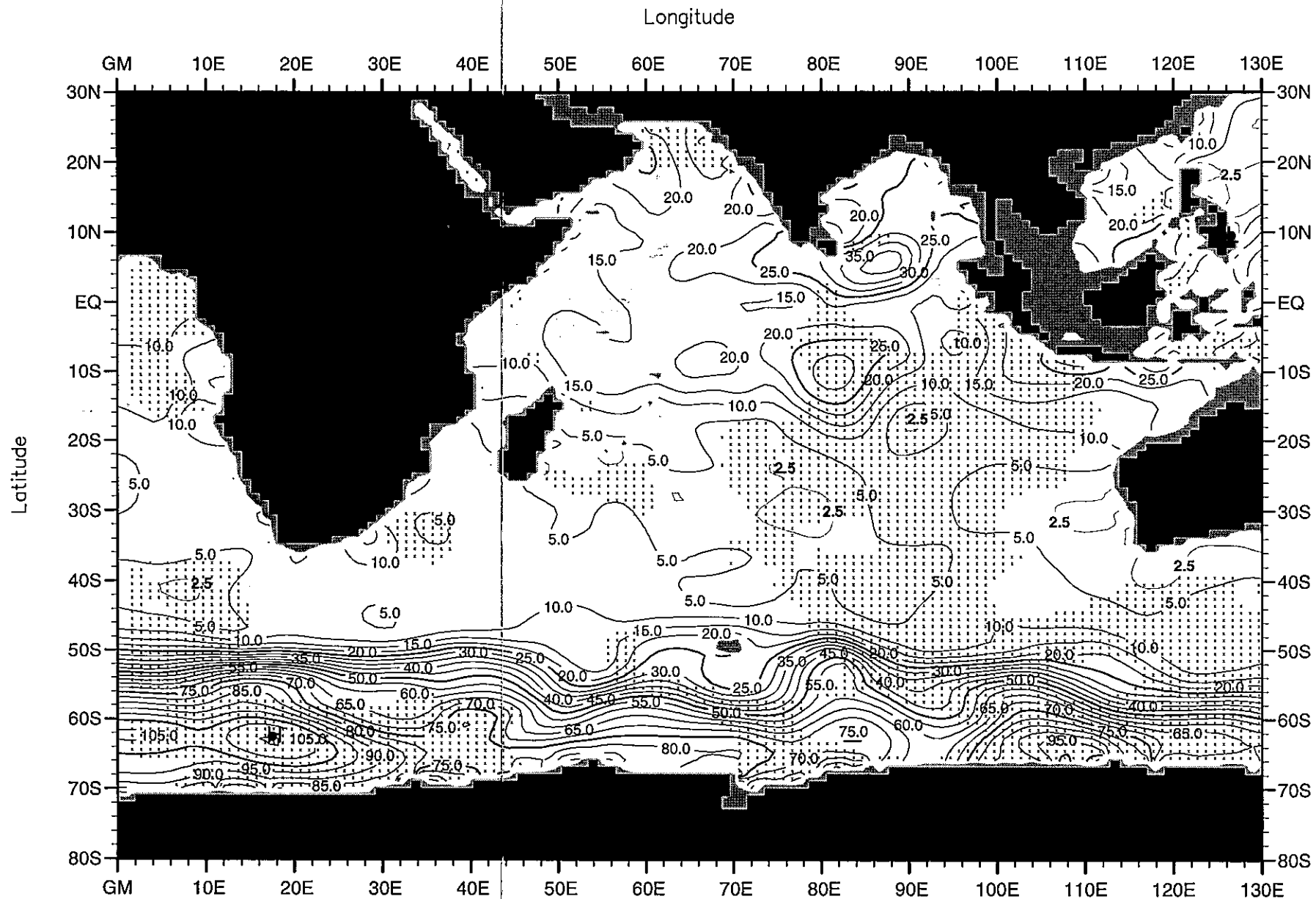
Fig. F35. Spring (Apr.-Jun.) mean silicate (μM) at 150 m. depth .

Minimum Value= 0.60   Maximum Value= 110.31   Contour Interval: 5.00
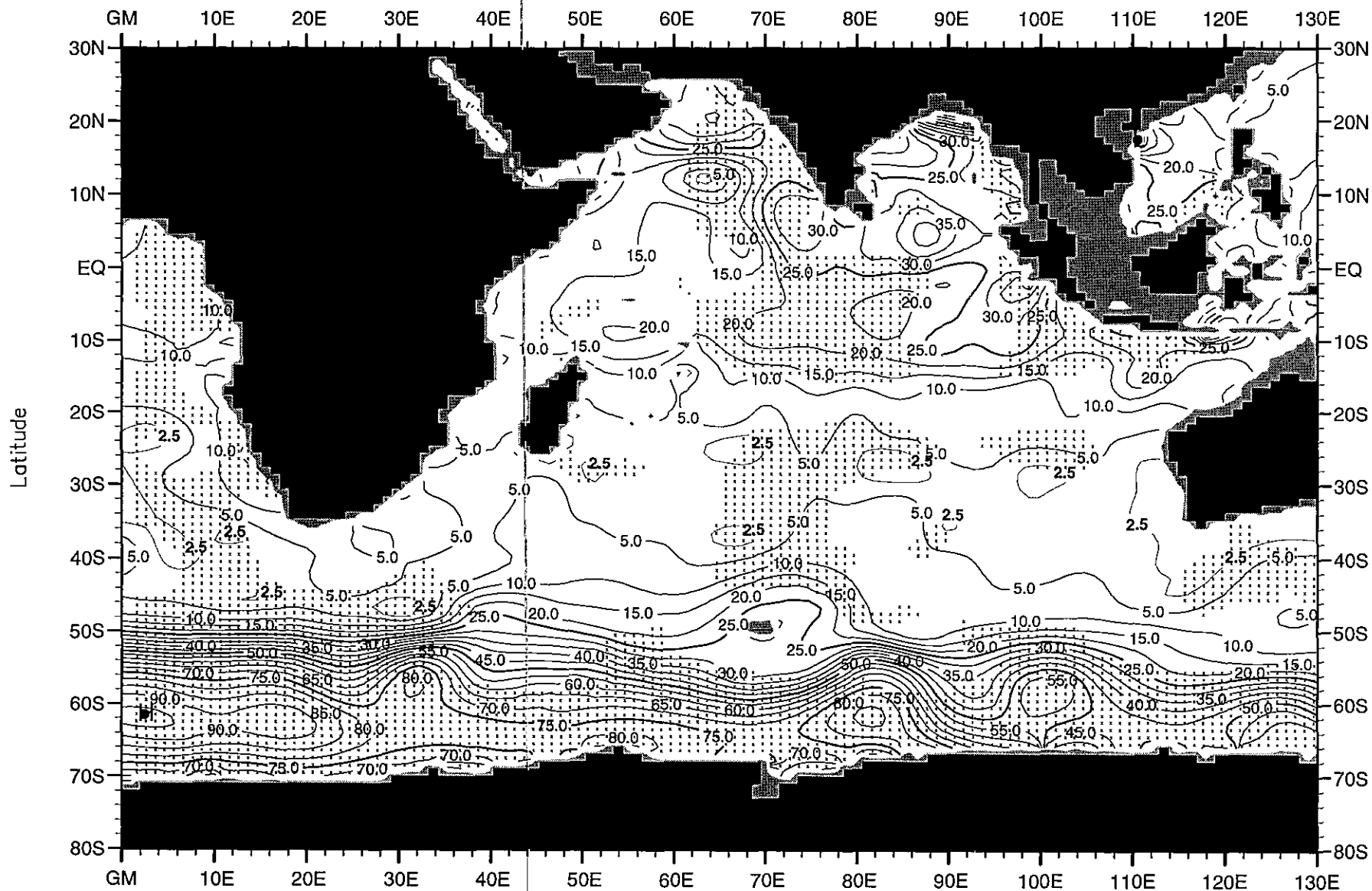
Fig. F36.   Spring (Apr.-Jun.) mean silicate (μM) at 250 m. depth .

Minimum Value=   0.00   Maximum Value= 119.35   Contour Interval: 5.00

Fig. F37. Summer (Jul.-Sep.) mean silicate (μM) at the surface .

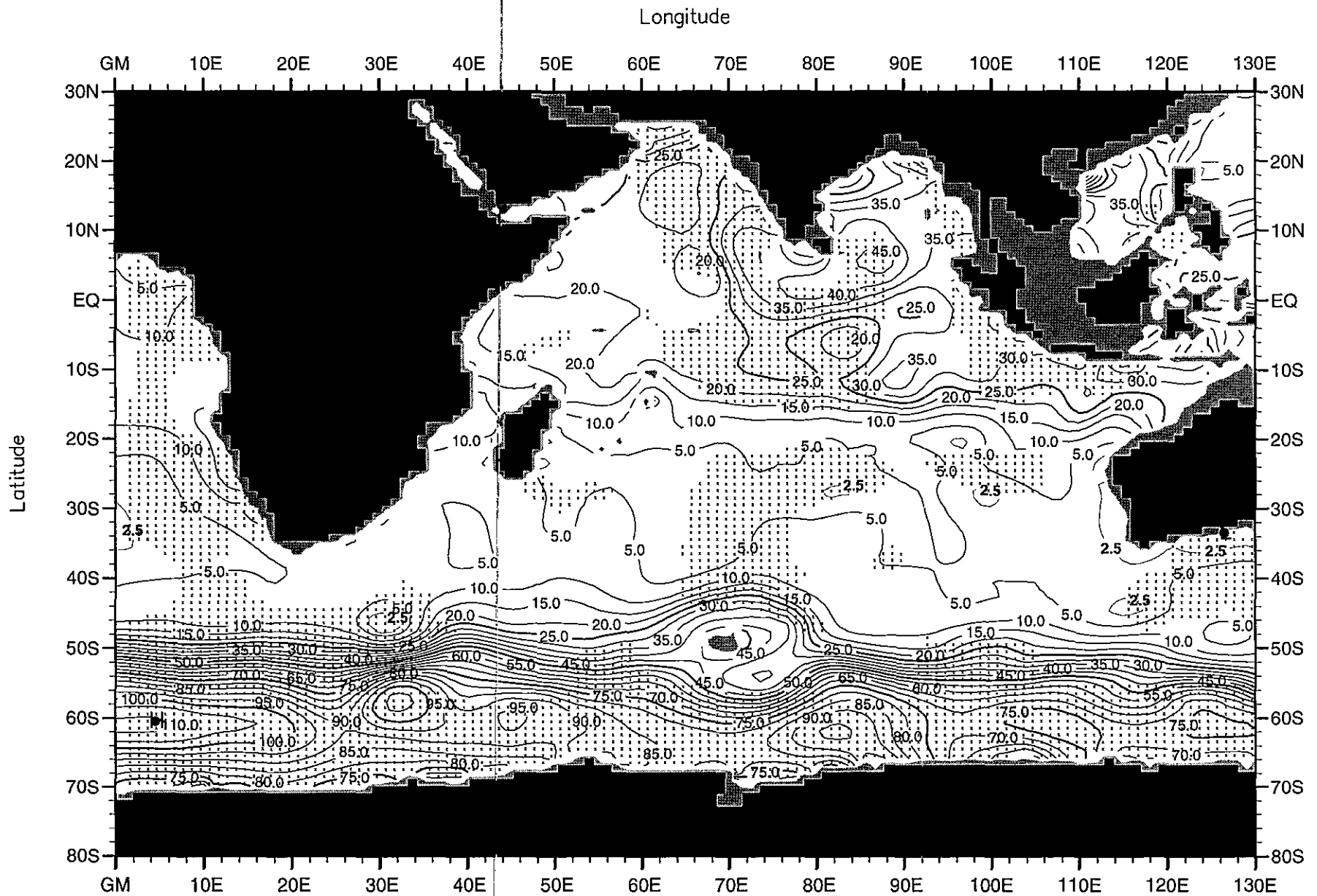Minimum Value= 0.00   Maximum Value= 74.09   Contour Interval: 5.00

189

Fig. F38. Summer (Jul.-Sep.) mean silicate (μM) at 50 m. depth .

Minimum Value= 0.00   Maximum Value= 75.86   Contour Interval: 5.00
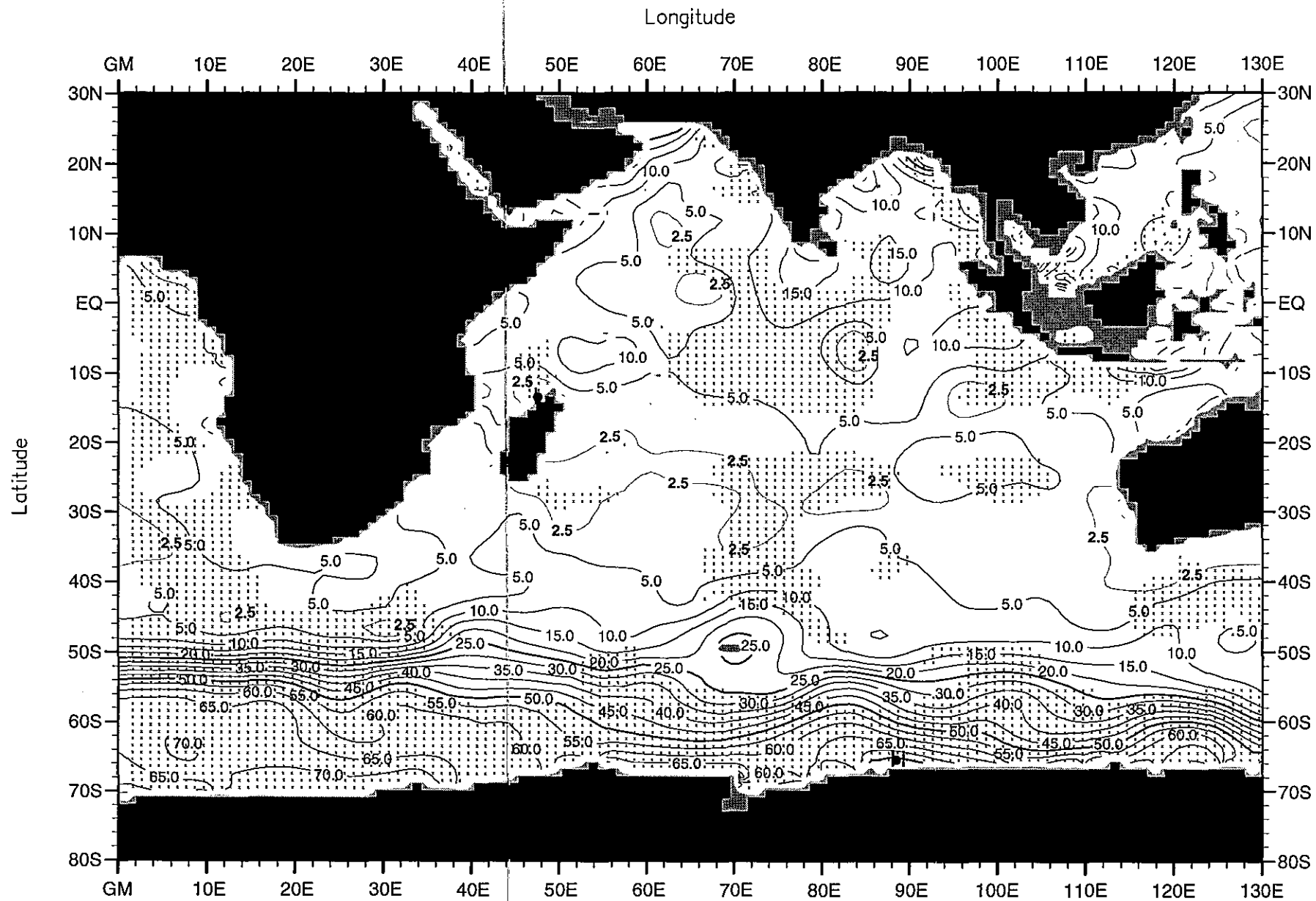
Fig. F39.   Summer (Jul.-Sep.) mean silicate (μM) at 75 m. depth .

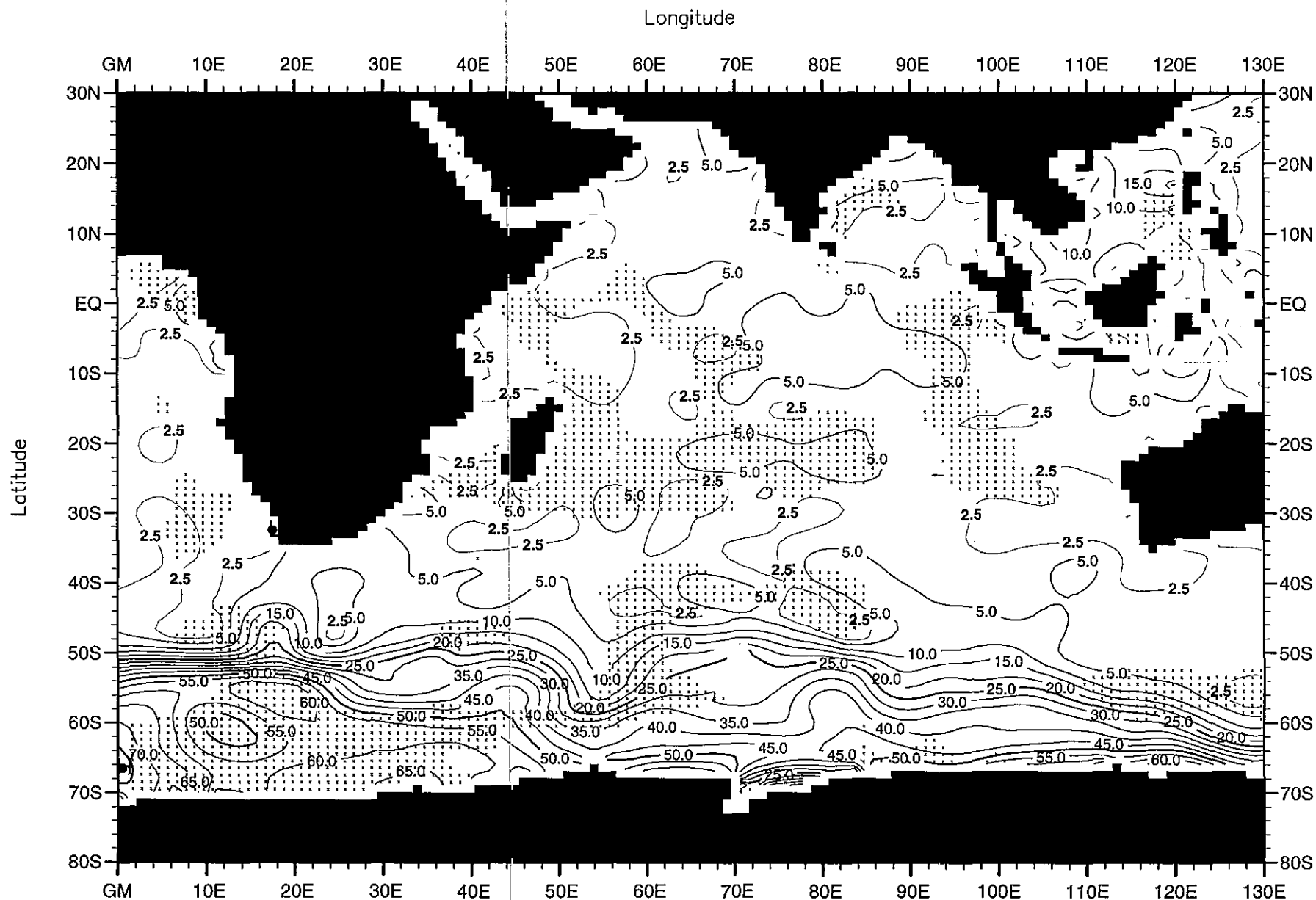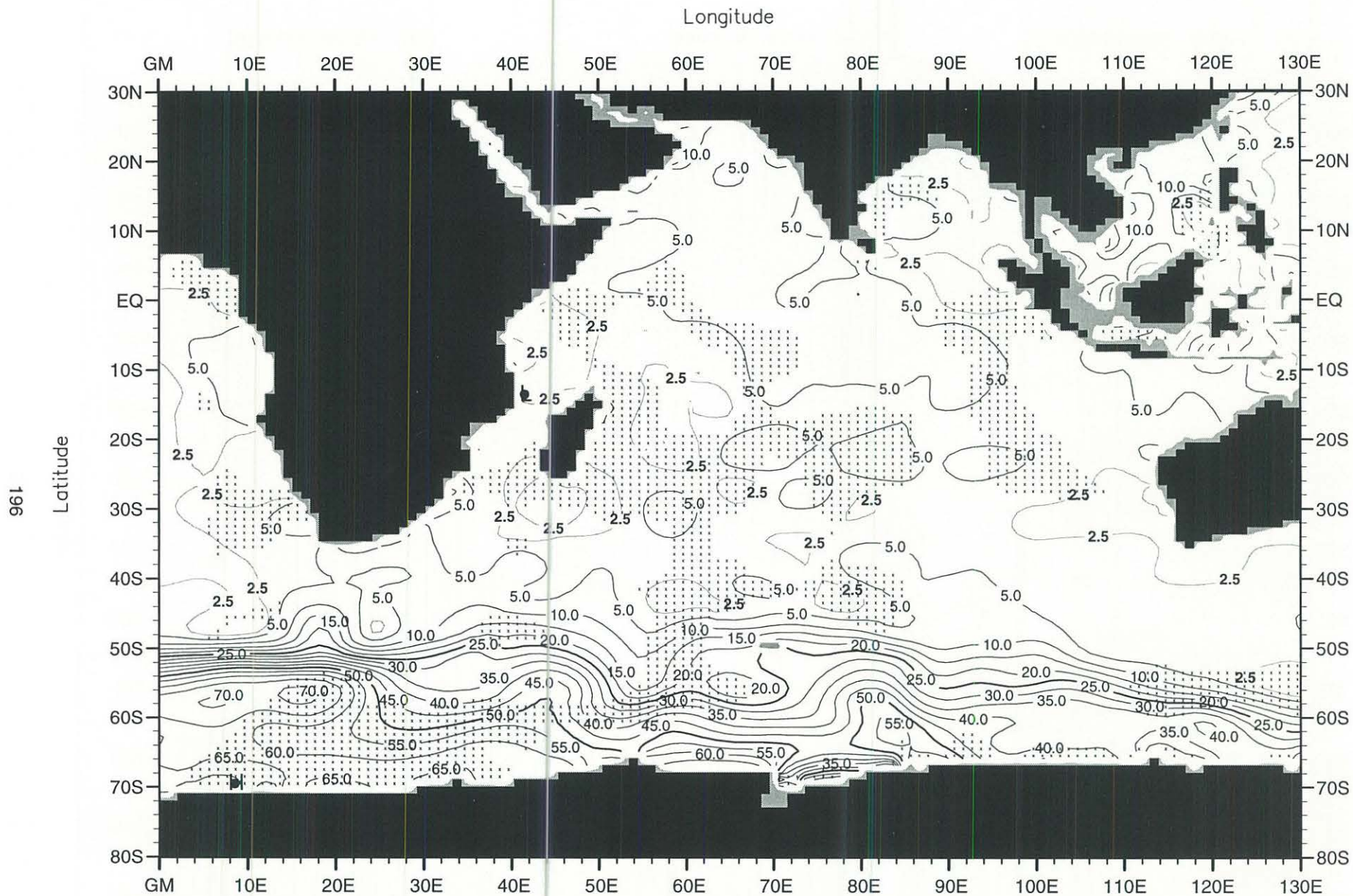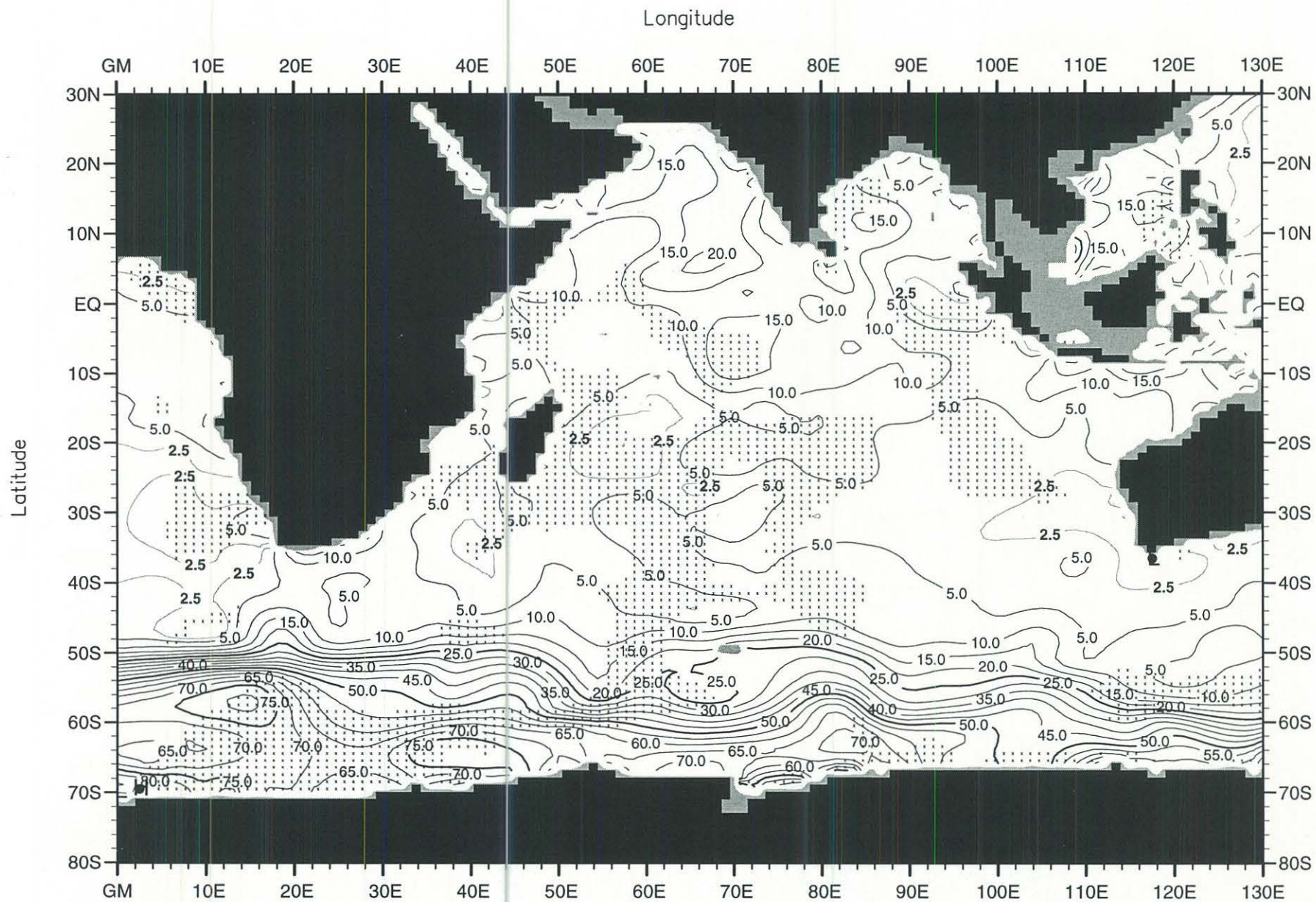Minimum Value=   0.00   Maximum Value= 79.06   Contour Interval: 5.00

Fig. F40. Summer (Jul.-Sep.) mean silicate (μM) at 100 m. depth .

Minimum Value= 0.04   Maximum Value= 85.58   Contour Interval: 5.00
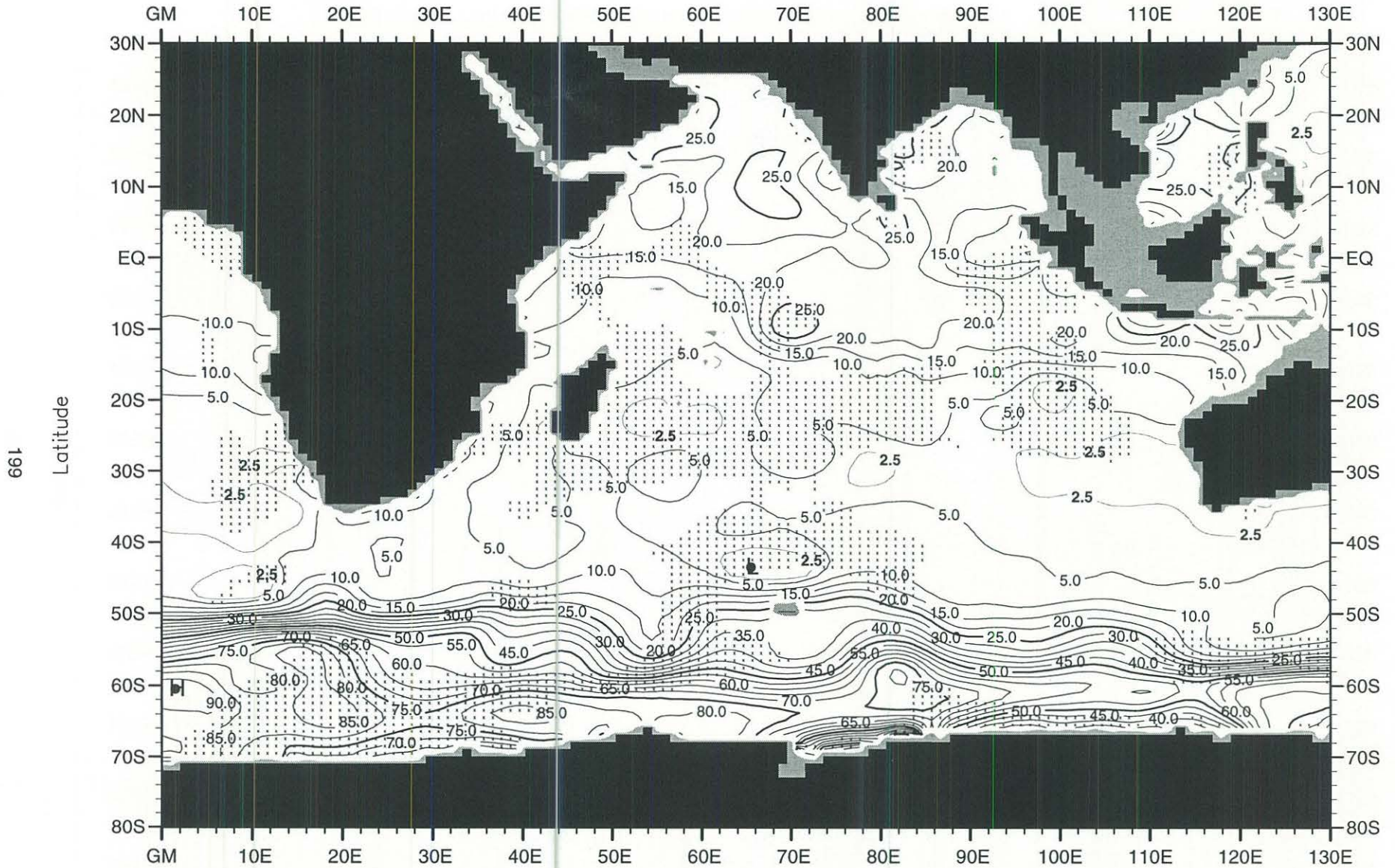
Fig. F41. Summer (Jul.-Sep.) mean silicate (μM) at 150 m. depth .

Minimum Value= 0.00   Maximum Value= 96.55   Contour Interval: 5.00

Fig. F42.   Summer (Jul.-Sep.) mean silicate (μM) at 250 m. depth .

Minimum Value=   0.76   Maximum Value= 111.26   Contour Interval: 5.00

Fig. F43. Fall (Oct.-Dec.) mean silicate (μM) at the surface .

Minimum Value= 0.00   Maximum Value= 78.80   Contour Interval: 5.00

Fig. F44. Fall (Oct.-Dec.) mean silicate (μM) at 50 m. depth.

Minimum Value= 0.00   Maximum Value= 74.13   Contour Interval: 5.00

Fig. F45. Fall (Oct.-Dec.) mean silicate (μM) at 75 m. depth .

Minimum Value= 0.00   Maximum Value= 77.53   Contour Interval: 5.00

Fig. F46.   Fall (Oct.-Dec.) mean silicate (μM) at 100 m. depth .

Minimum Value=   0.00   Maximum Value=   86.08   Contour Interval: 5.00

Fig. F47.   Fall (Oct.-Dec.) mean silicate (μM) at 150 m. depth .

Minimum Value= 0.00   Maximum Value= 94.57   Contour Interval: 5.00
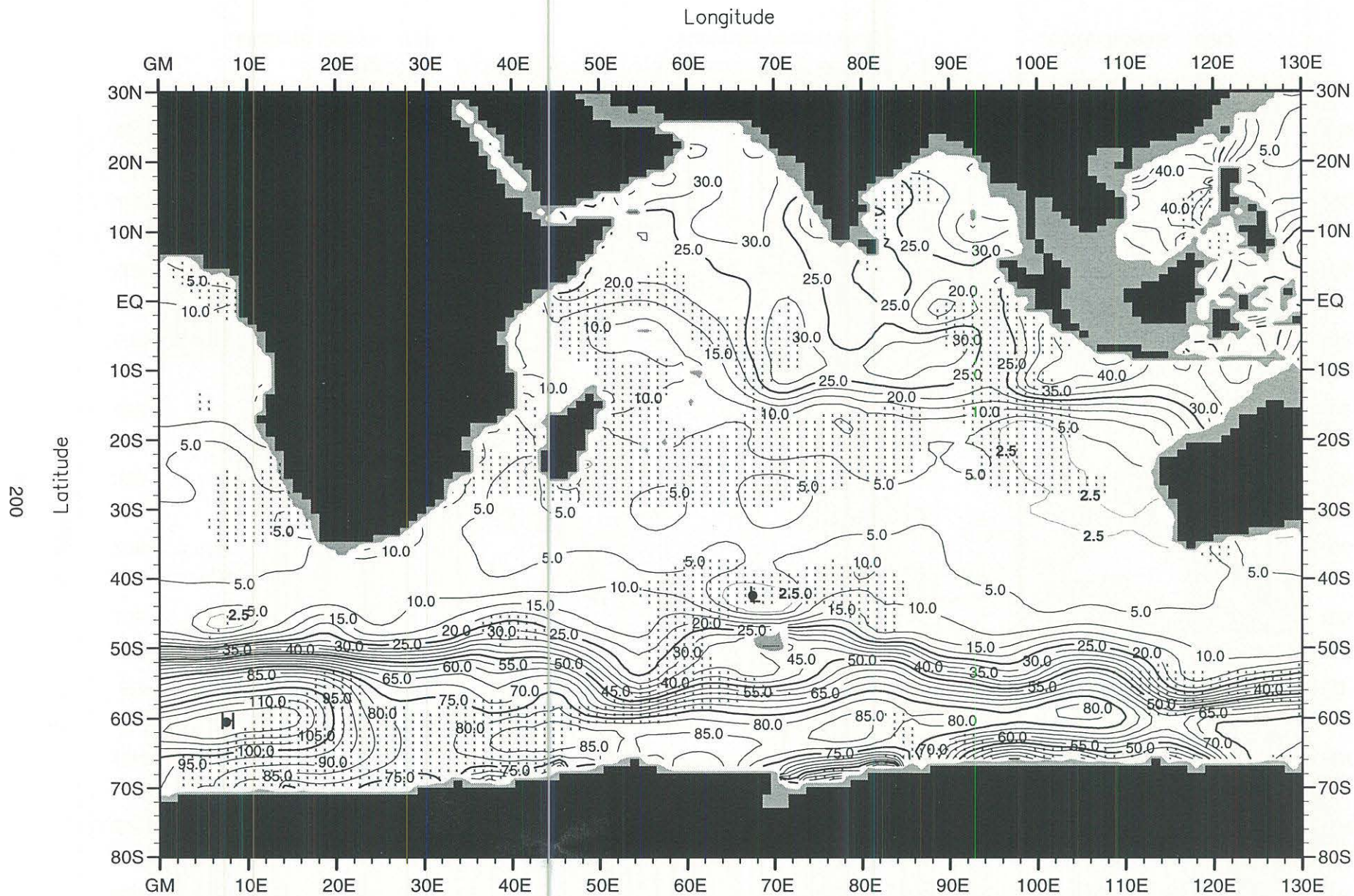
Fig. F48. Fall (Oct.-Dec.) mean silicate (μM) at 250 m. depth .

Minimum Value= 0.00   Maximum Value= 119.88   Contour Interval: 5.00

Longitude
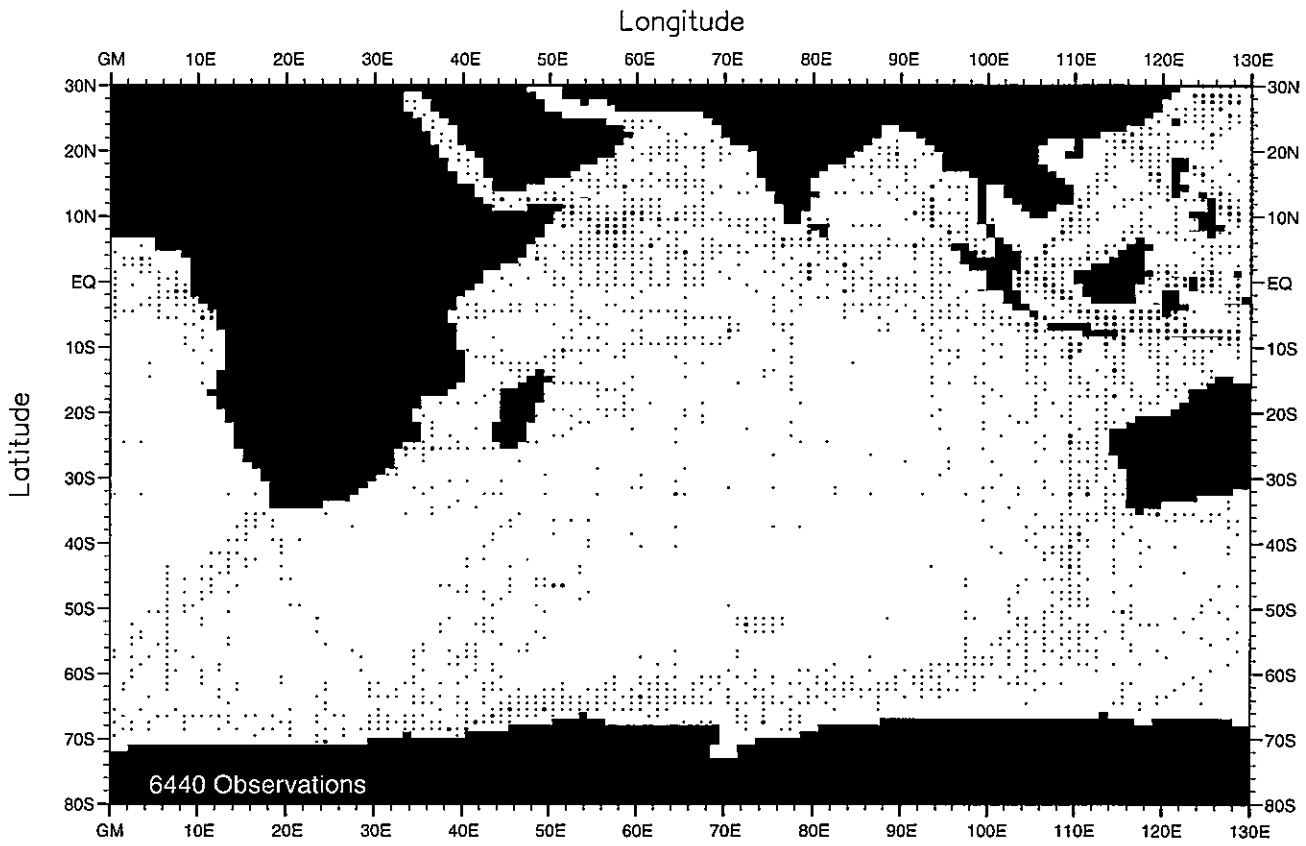
Fig. G1. Annual chlorophyll observations at the surface .

Longitude
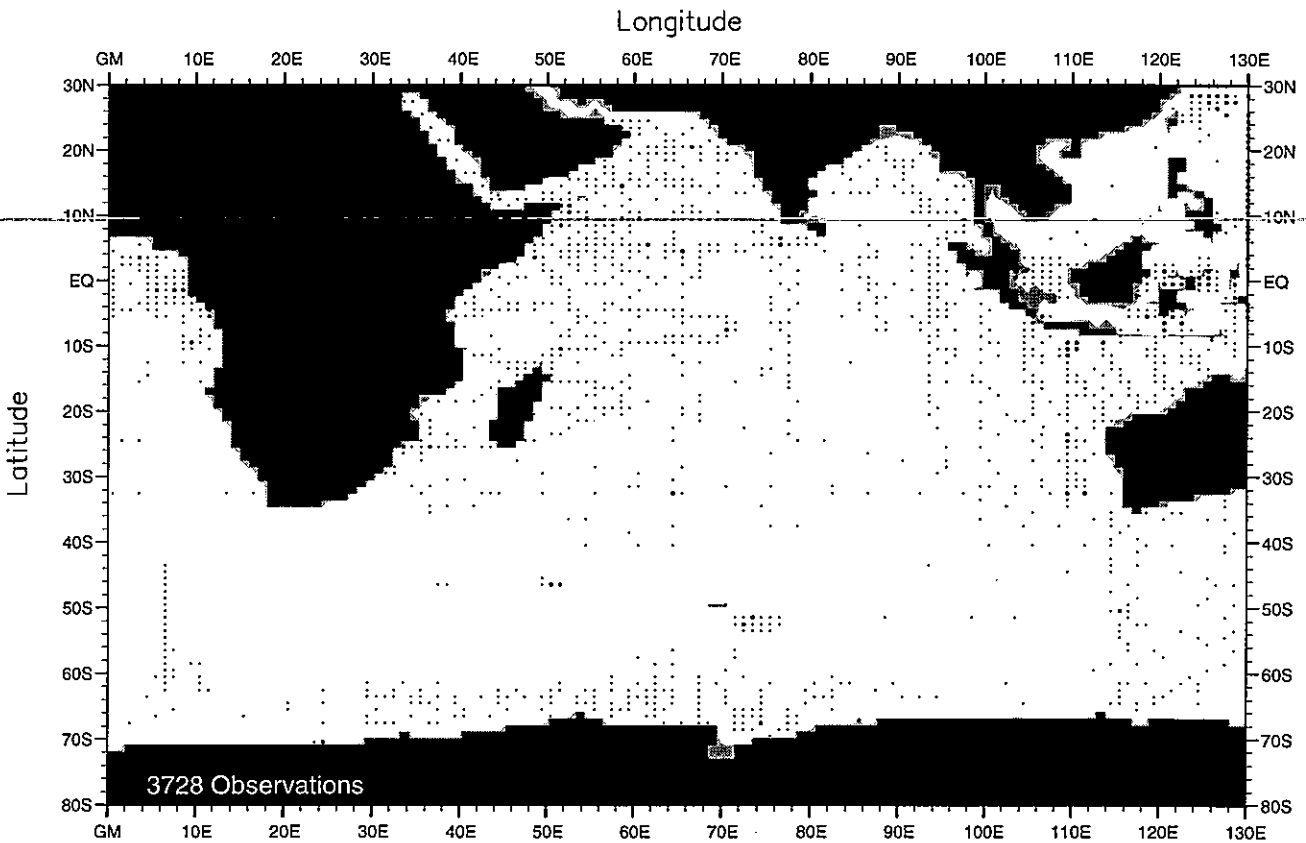
Fig. G2. Annual chlorophyll observations at   20 m. depth .
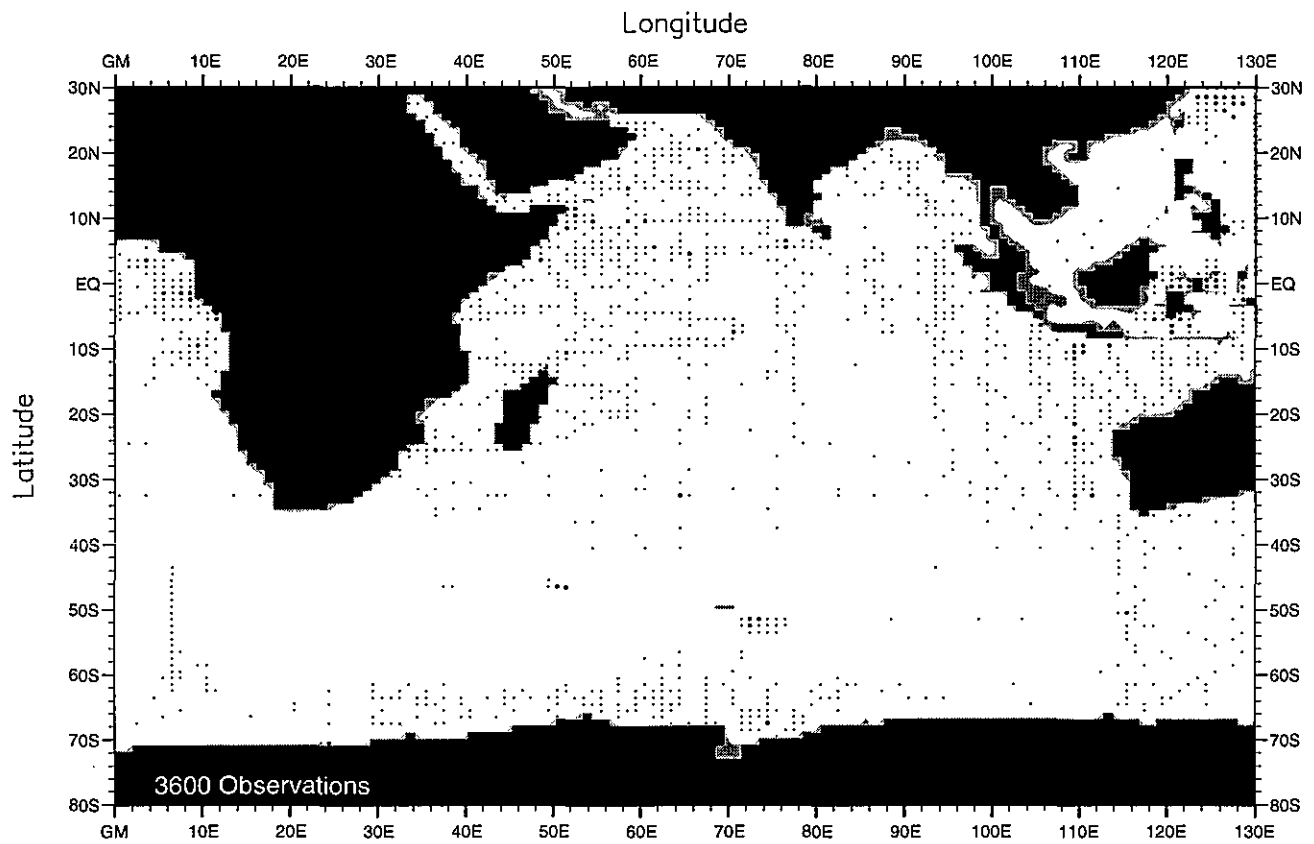
Fig. G3. Annual chlorophyll observations at   30 m. depth .
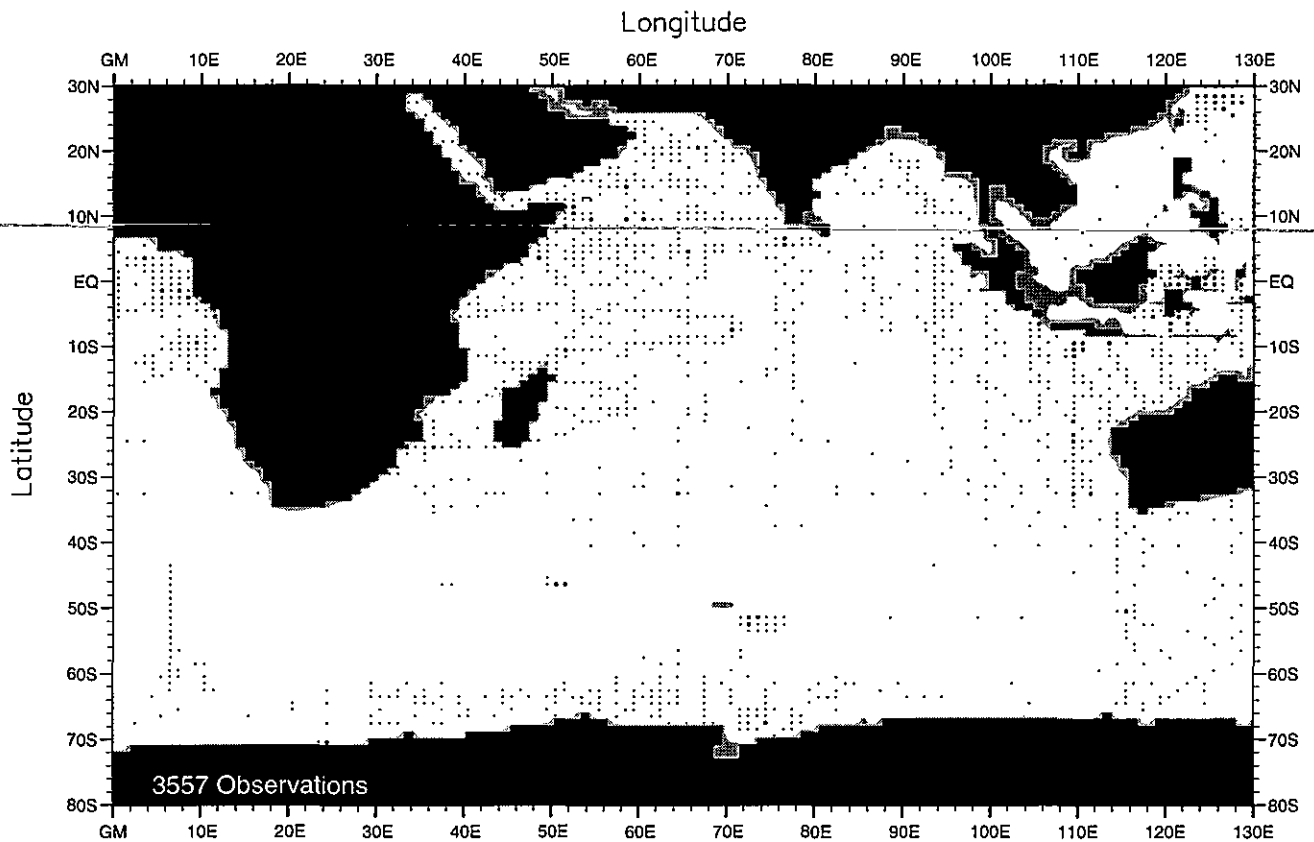
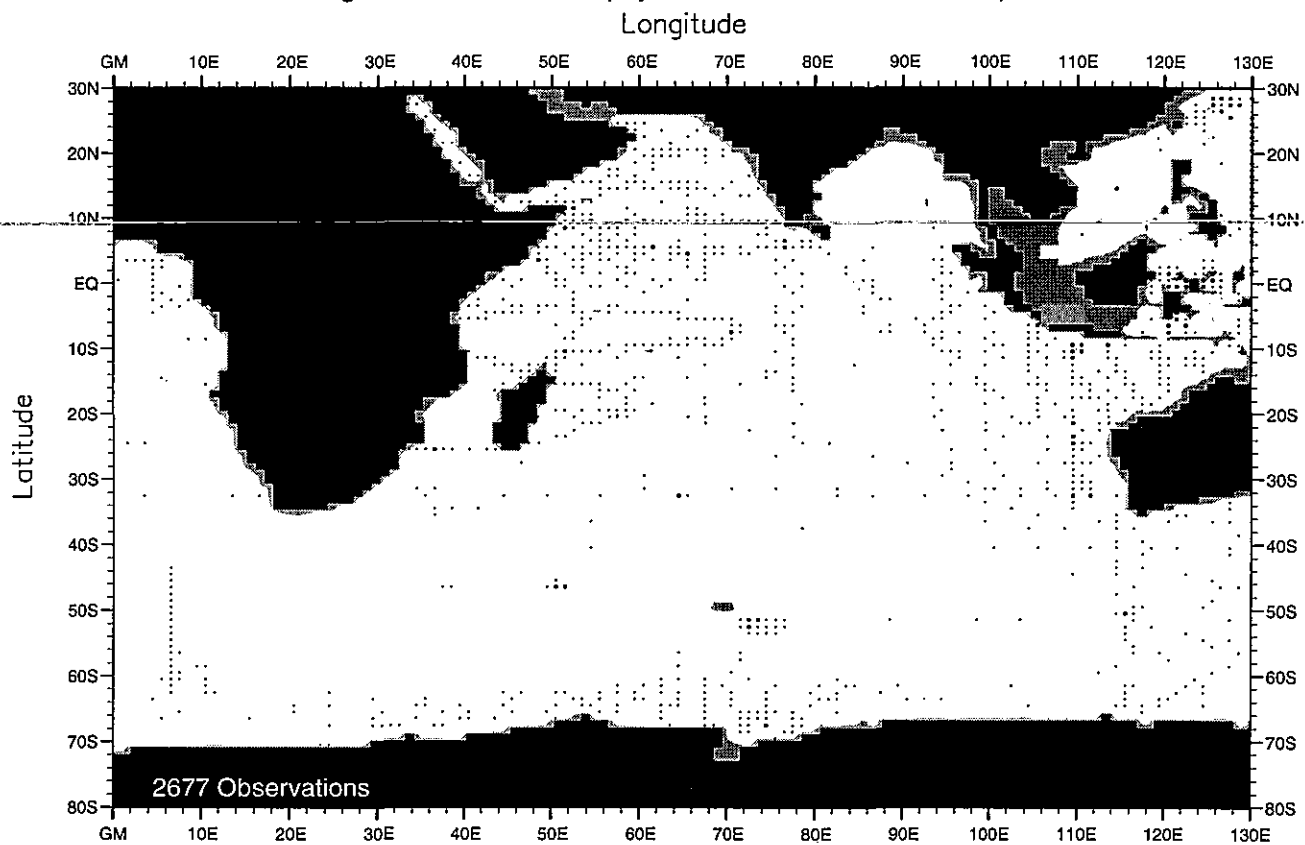Fig. G4. Annual chlorophyll observations at   50 m. depth .
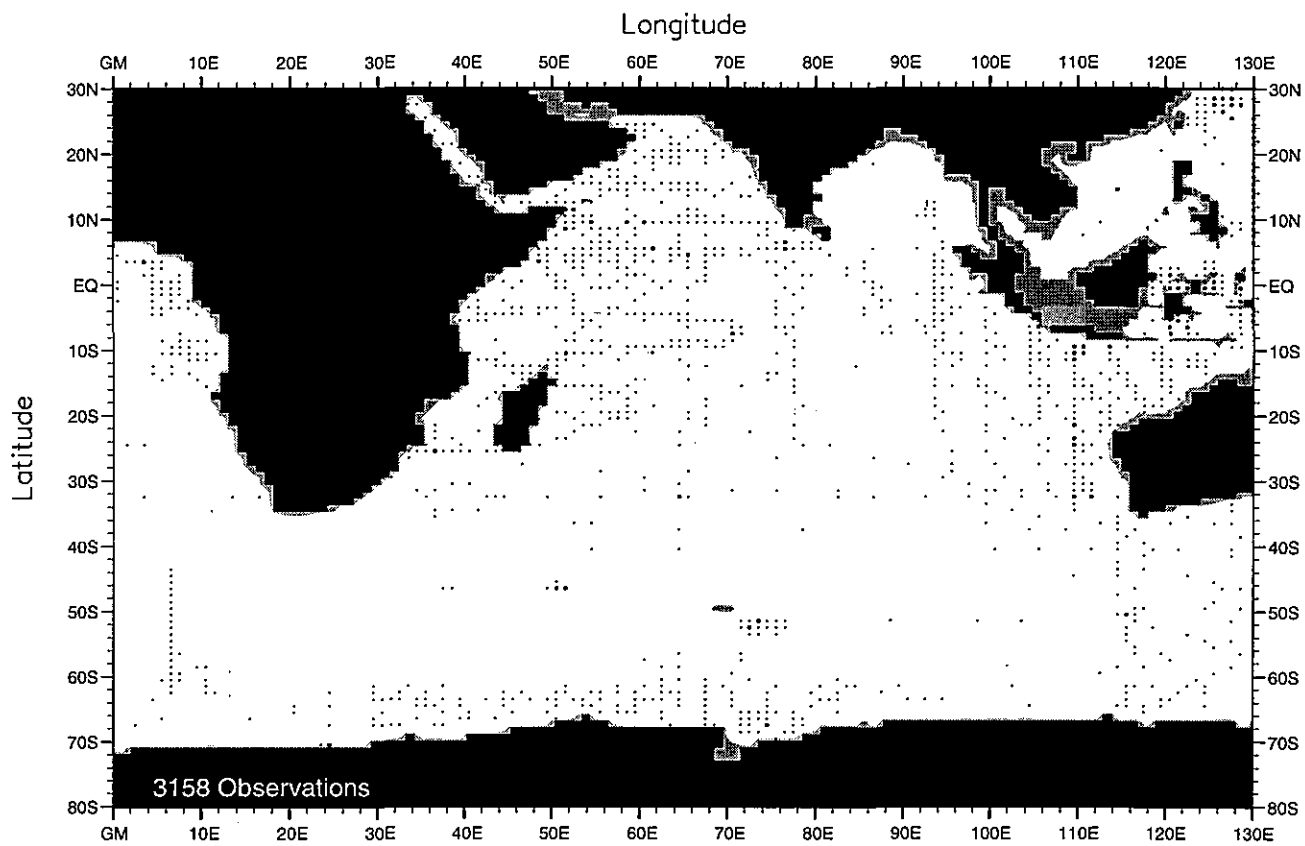
Fig. G5. Annual chlorophyll observations at 75 m. depth .

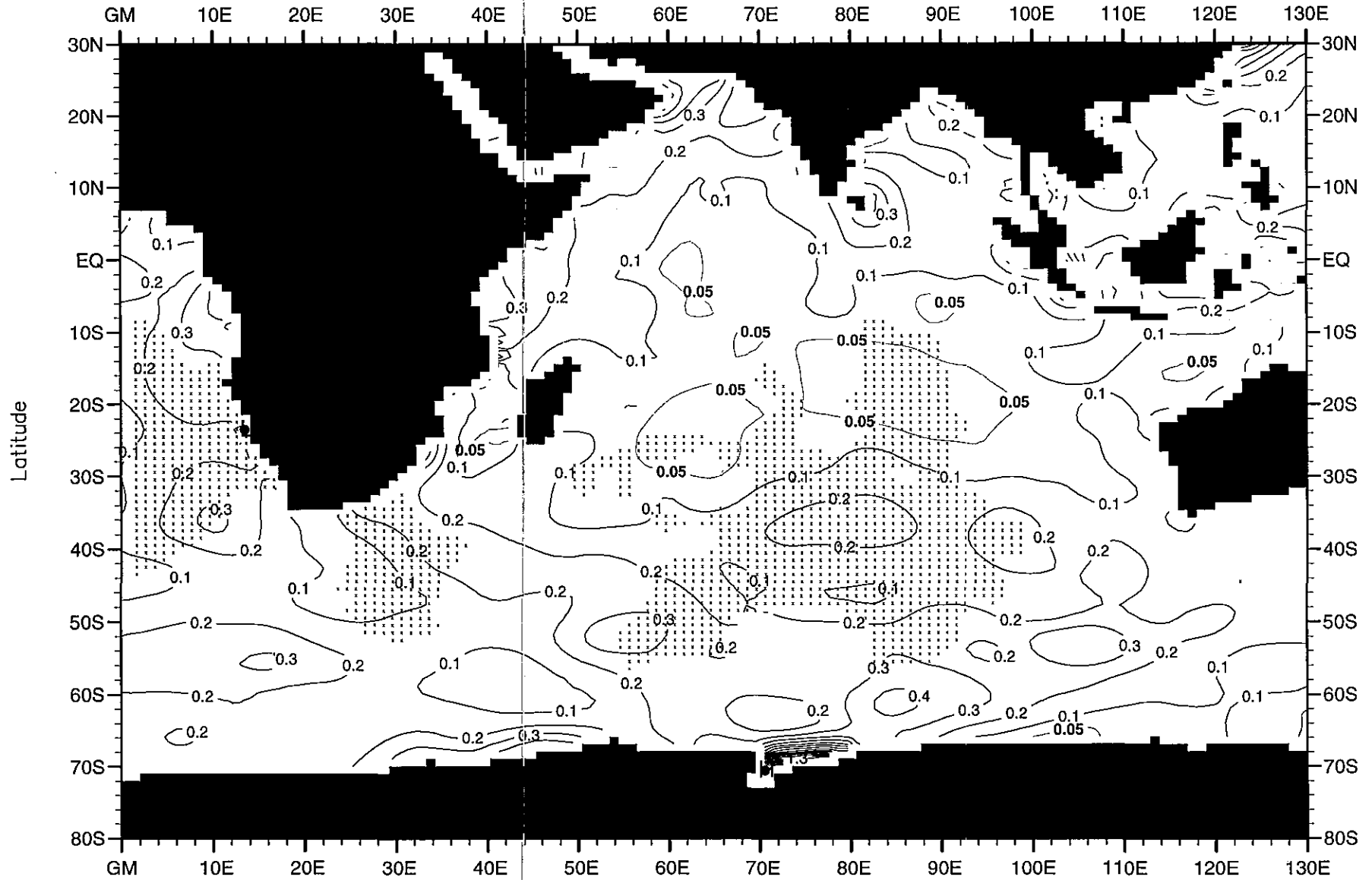Fig. G6. Annual chlorophyll observations at 100 m. depth .

Fig. G7. Annual mean chlorophyll (μg/l) at the surface .

Minimum Value= 0.00   Maximum Value= 2.45   Contour Interval: 0.10

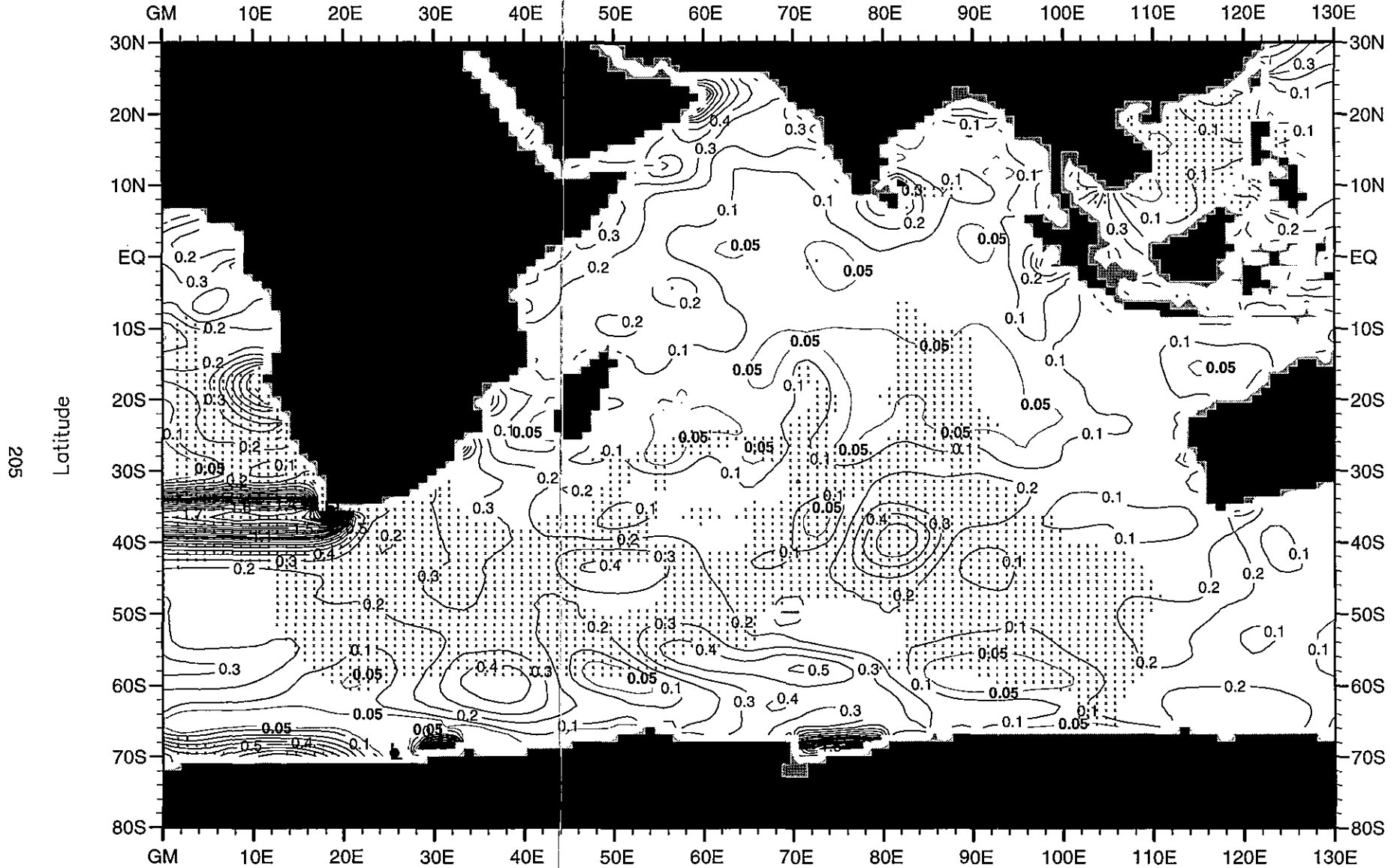Fig. G8. Annual mean chlorophyll (μg/l) at 20 m. depth .

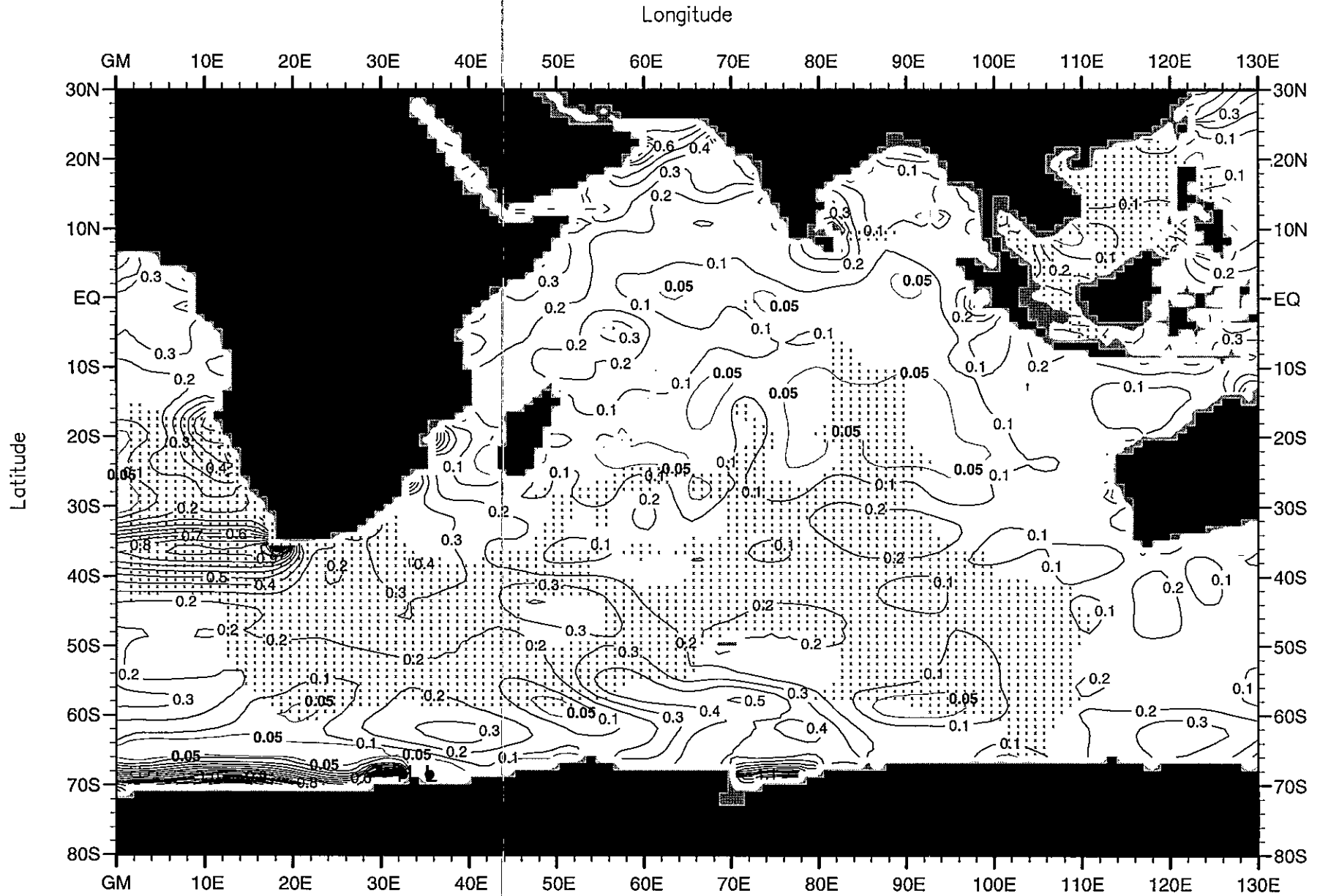Minimum Value= 0.00   Maximum Value=   4.17   Contour Interval: 0.10

Fig. G9. Annual mean chlorophyll (μg/l) at 30 m. depth .

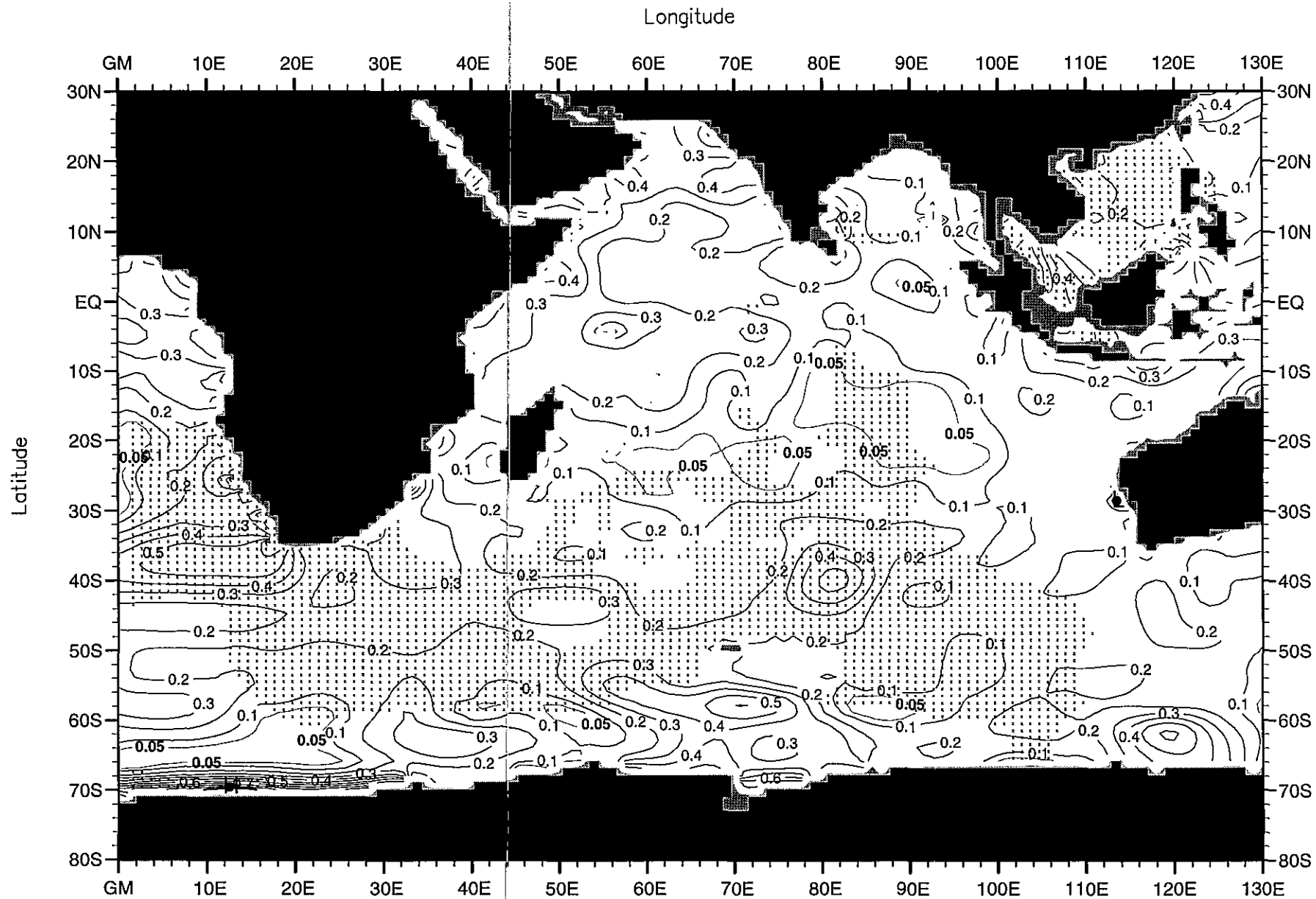Minimum Value= 0.00   Maximum Value= 1.92   Contour Interval: 0.10

Fig. G10.   Annual mean chlorophyll (μg/l) at   50 m. depth .

Minimum Value=   0.00   Maximum Value=   1.07   Contour Interval: 0.10
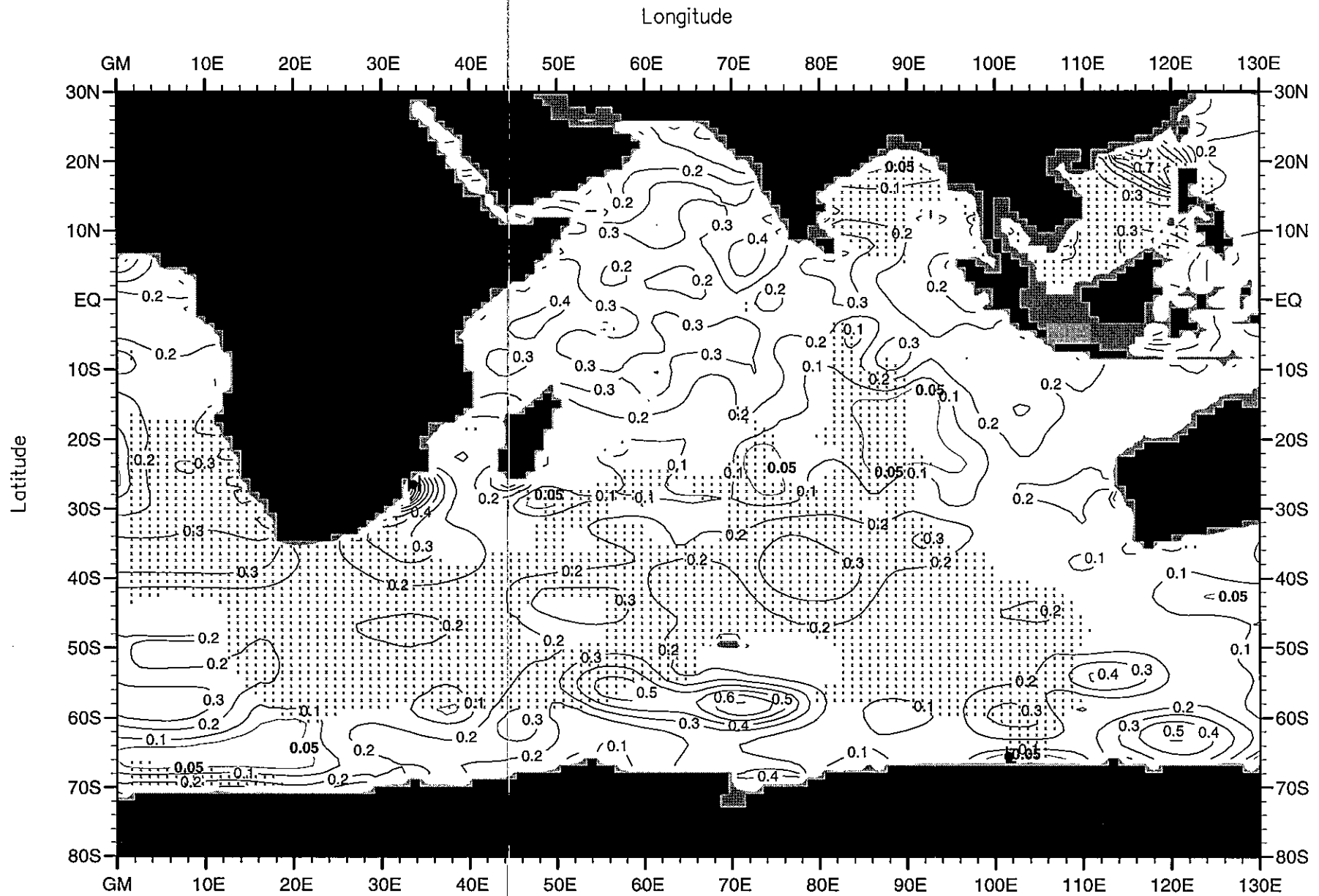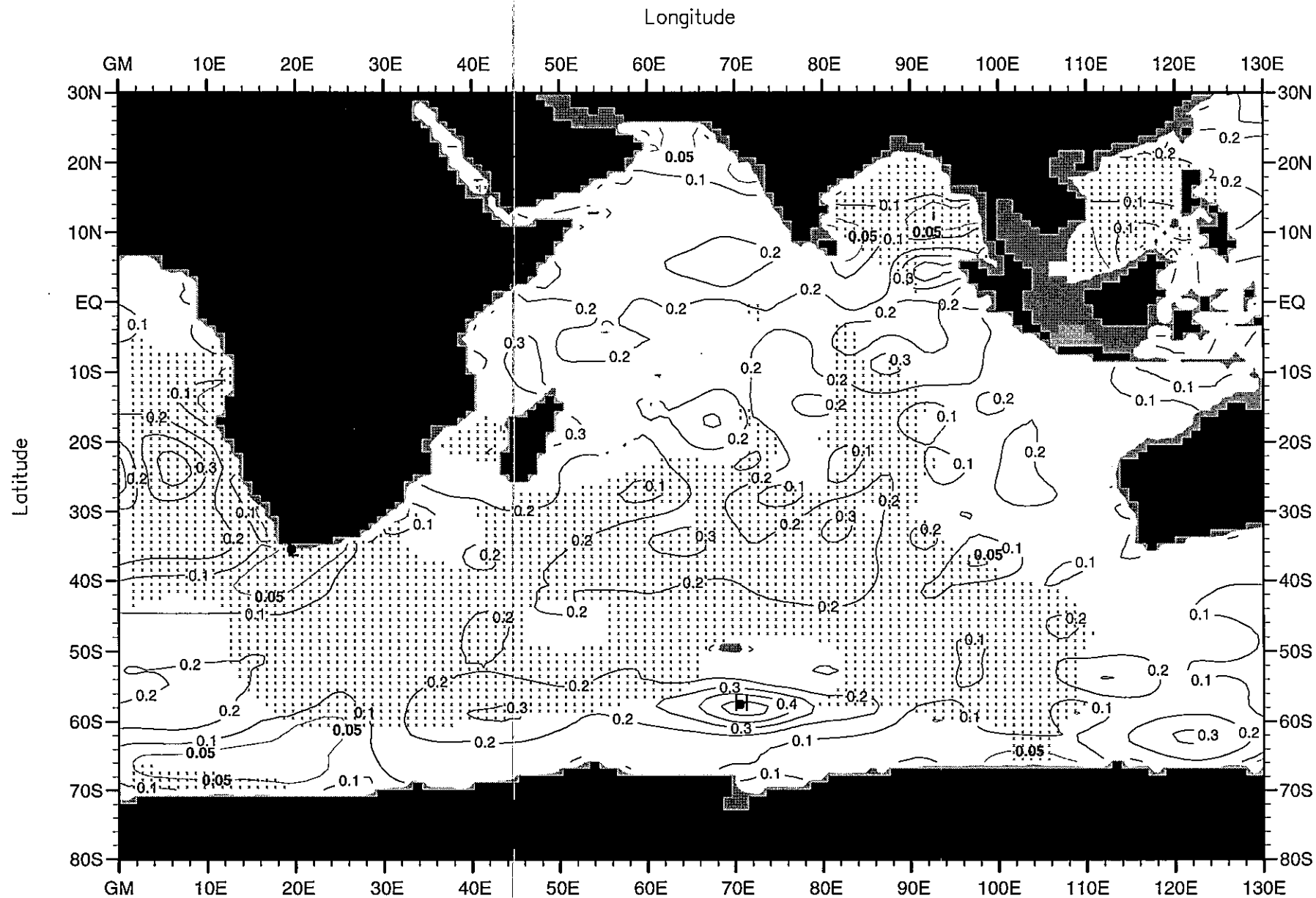
Fig. G11. Annual mean chlorophyll (μg/l) at 75 m. depth .

Minimum Value= 0.00   Maximum Value= 1.25   Contour Interval: 0.10

Fig. G12.   Annual mean chlorophyll (μg/l) at 100 m. depth .

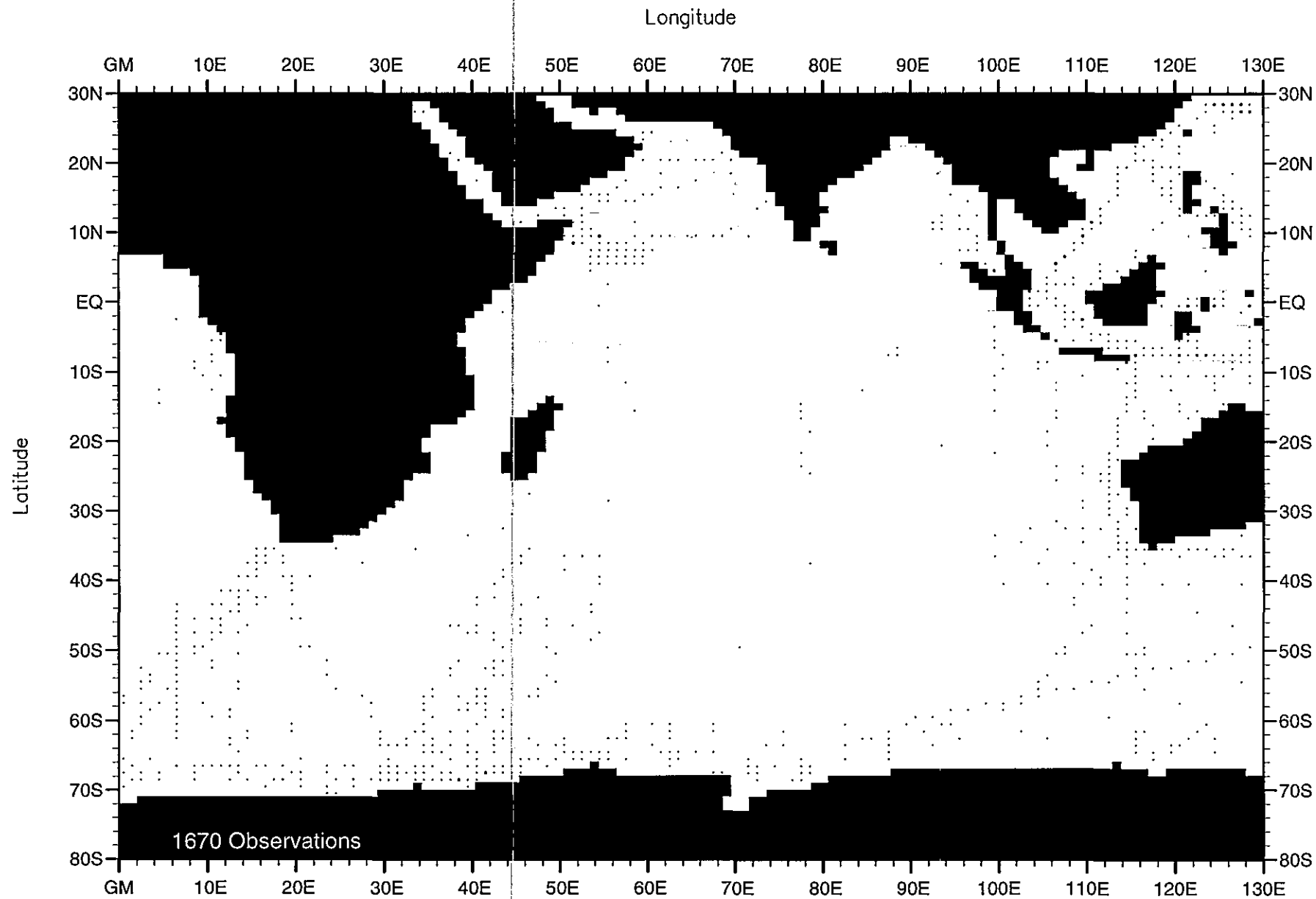Minimum Value=   0.00   Maximum Value=   0.55   Contour Interval: 0.10

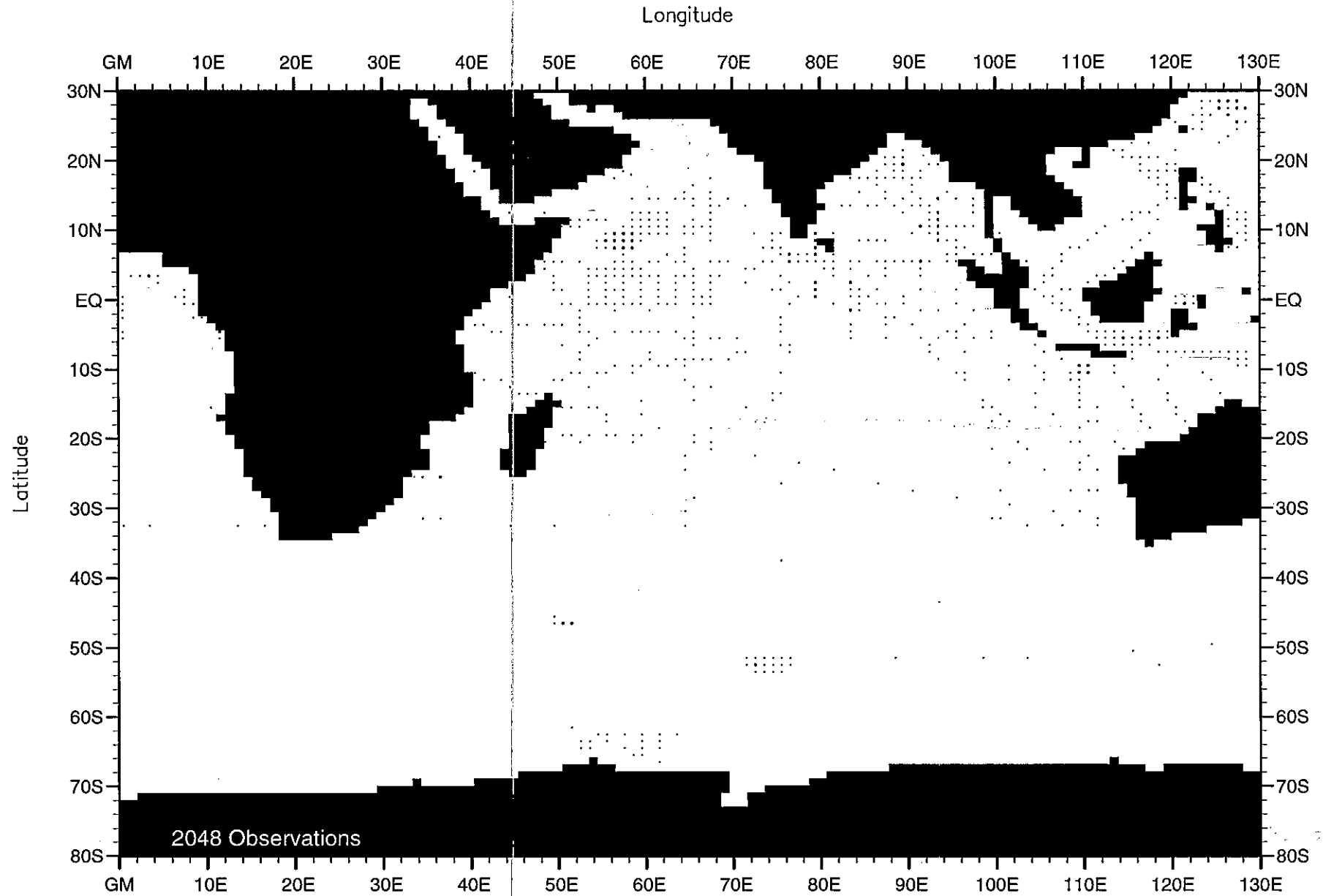Fig. H1. Winter (Jan.-Mar.) chlorophyll observations at the surface .

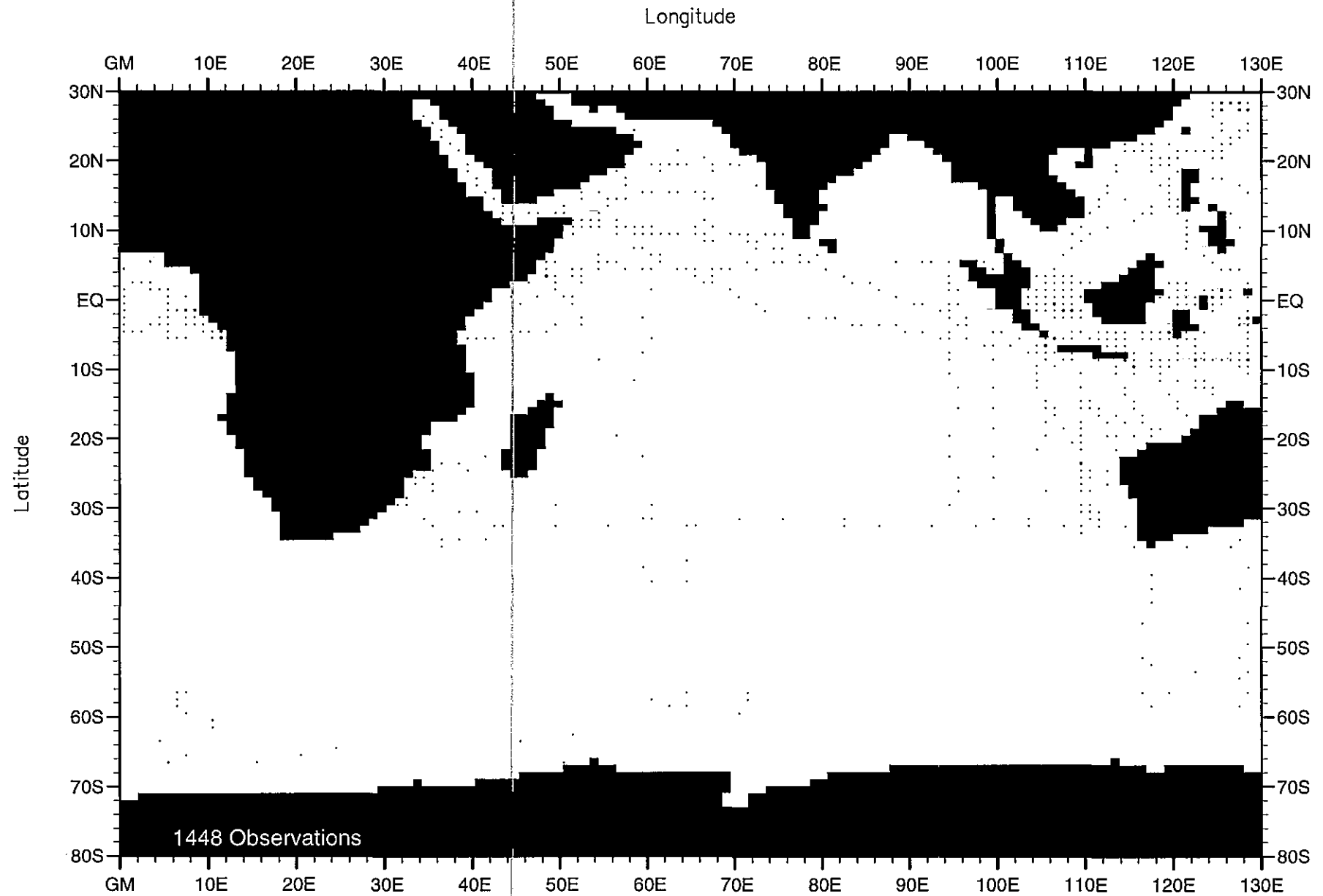Fig. H2.   Spring (Apr.-Jun.) chlorophyll observations at the surface .

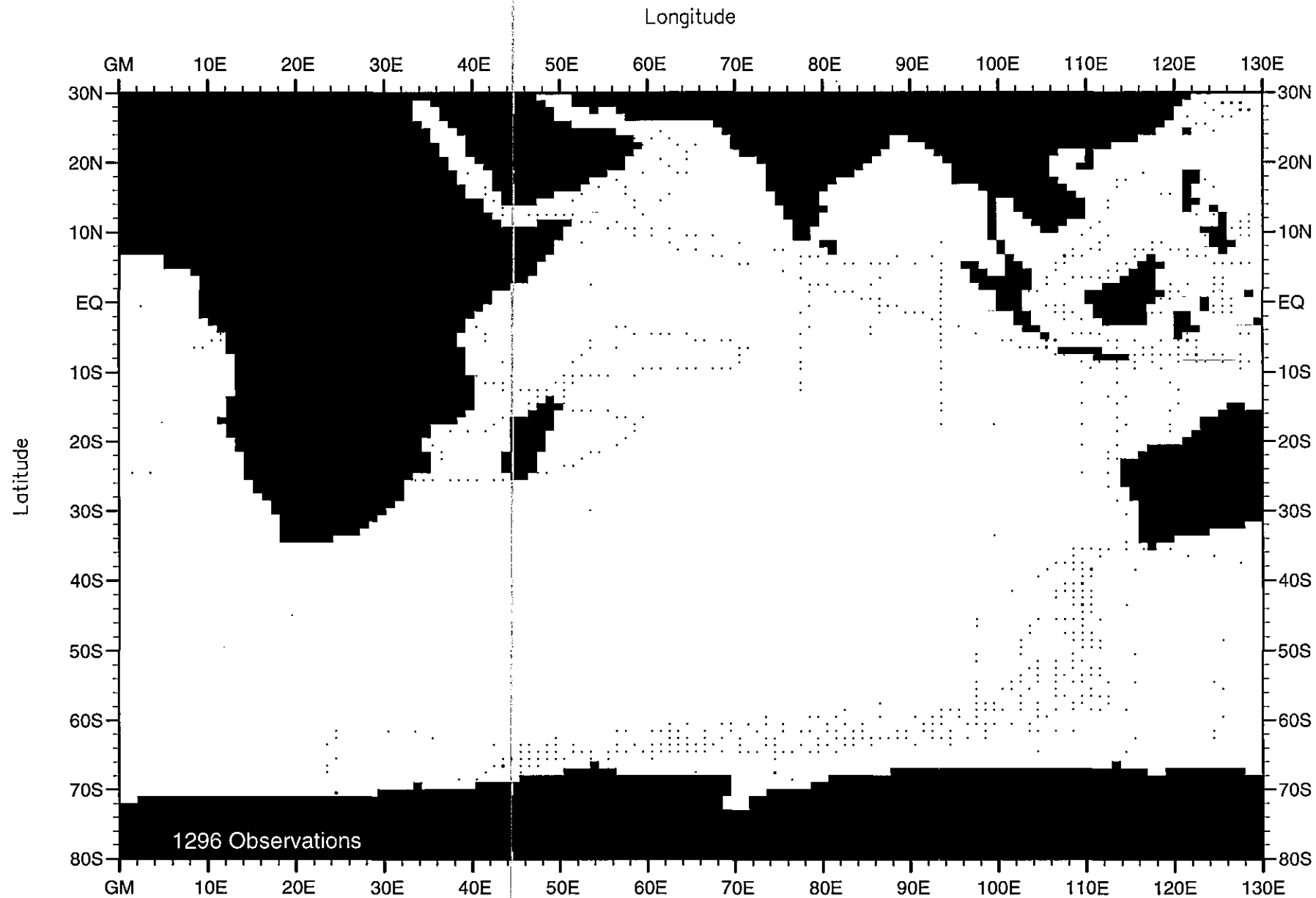Fig. H3. Summer (Jul.-Sep.) chlorophyll observations at the surface .

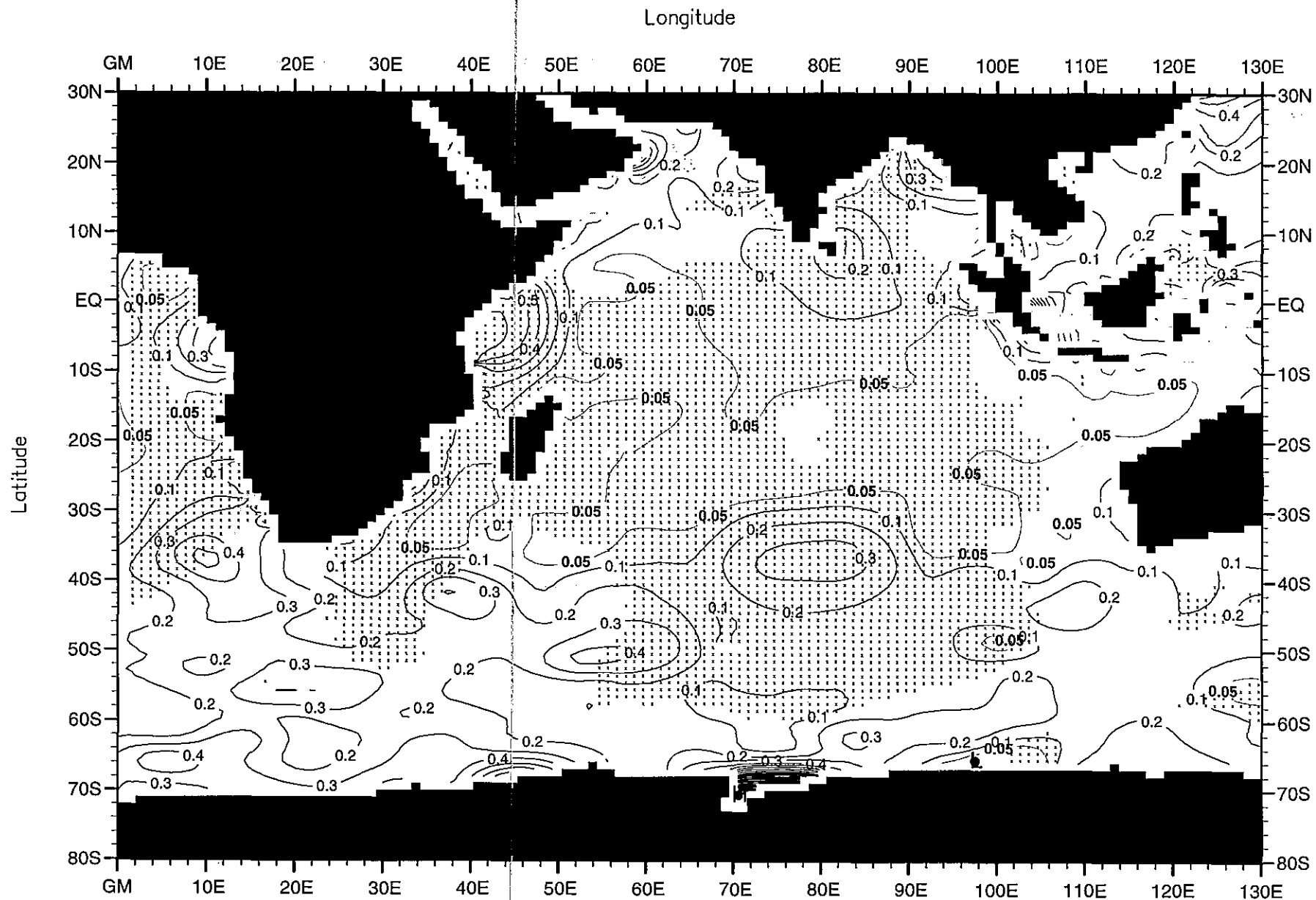Fig. H4. Fall (Oct.-Dec.) chlorophyll observations at the surface .

1296 Observations

213

Fig. H5. Winter (Jan.-Mar.) mean chlorophyll (μg/l) at the surface .

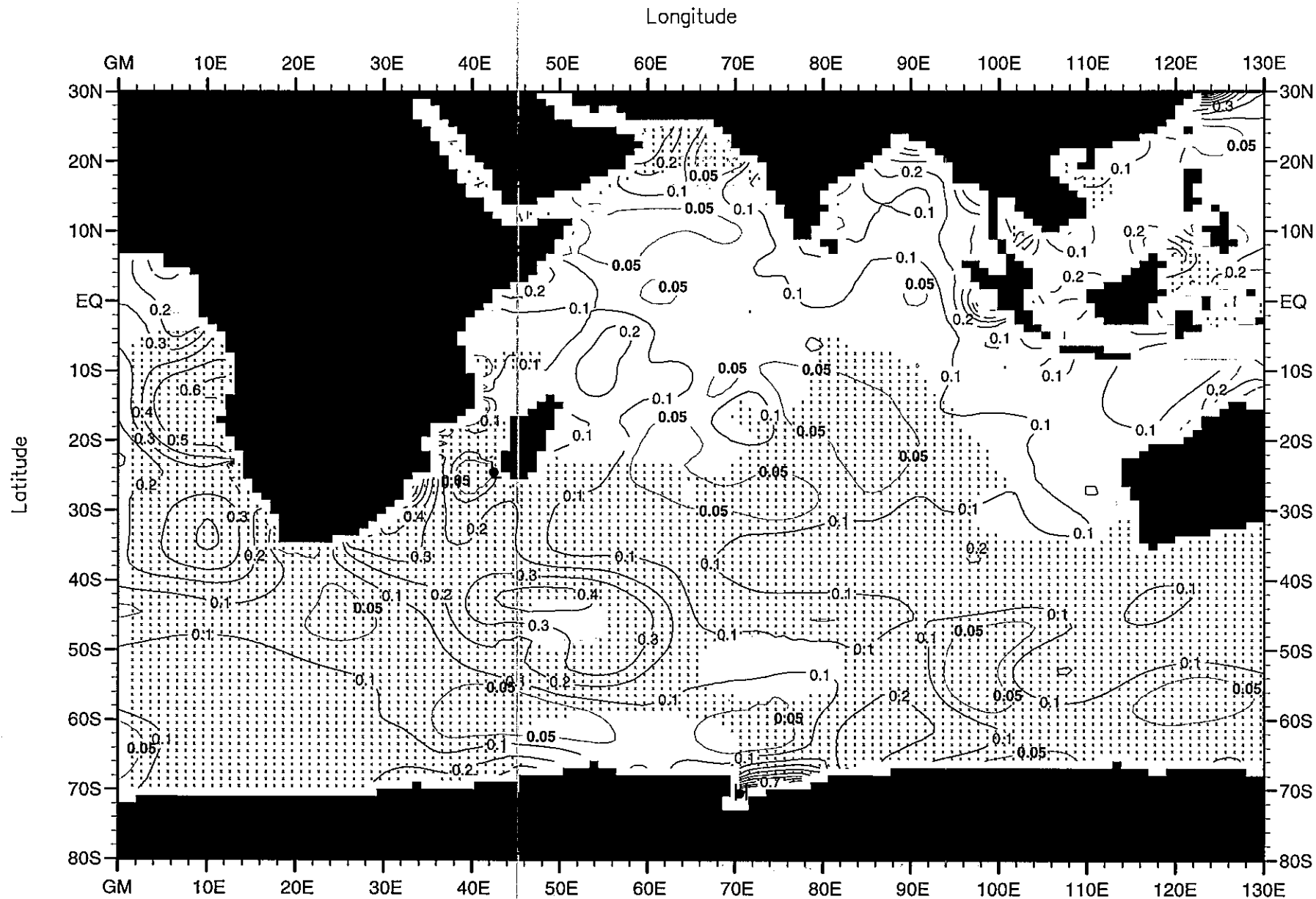Minimum Value= 0.00   Maximum Value= 3.12   Contour Interval: 0.10

Fig. H6. Spring (Apr.-Jun.) mean chlorophyll (μg/l) at the surface .

Minimum Value= 0.00   Maximum Value= 1.34   Contour Interval: 0.10
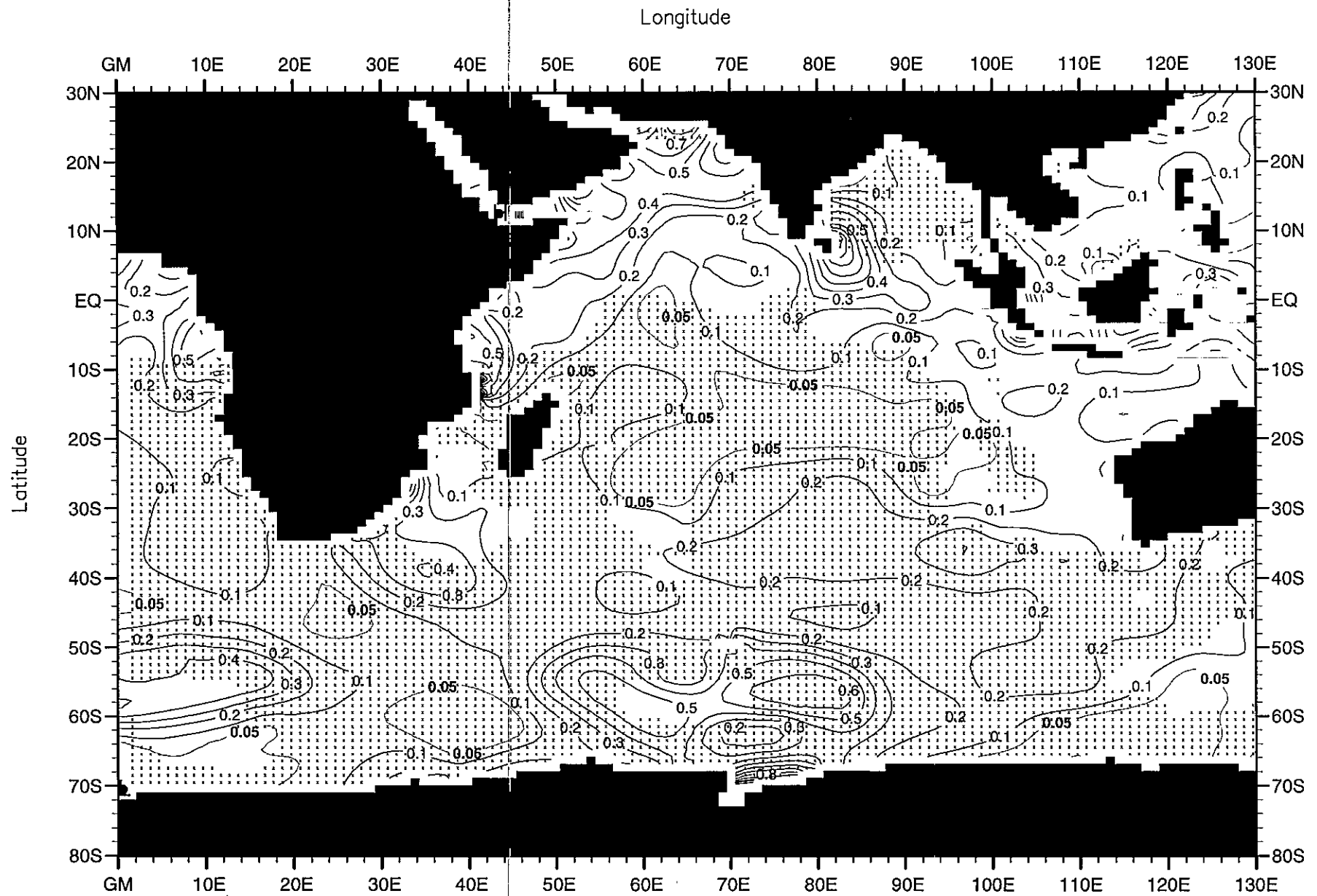
Fig. H7.   Summer (Jul. Sep.) mean chlorophyll (μg/l) at the surface .

Minimum Value=   0.00   Maximum Value=   2.44   Contour Interval: 0.10
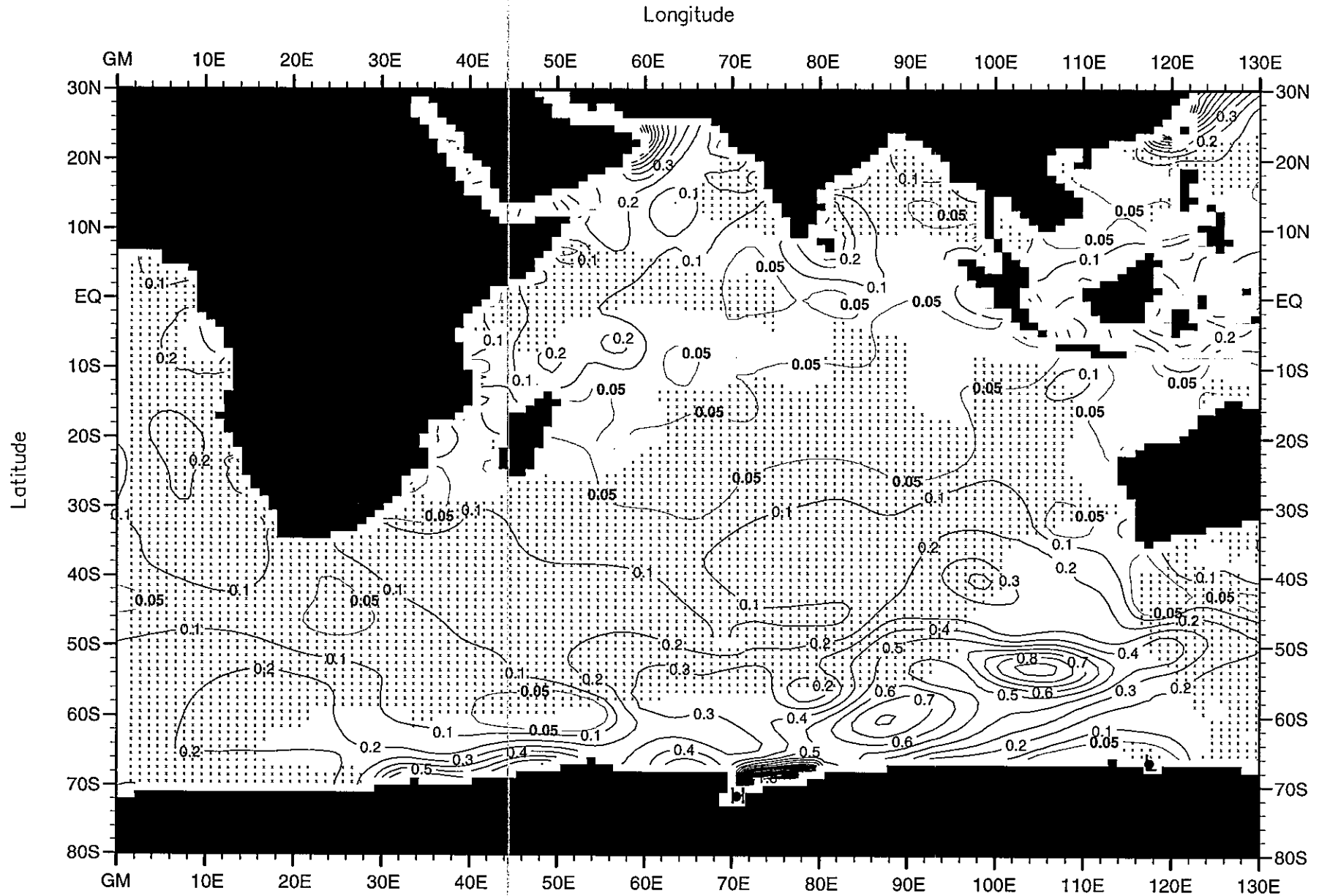
Fig. H8. Fall (Oct.-Dec.) mean chlorophyll (μg/l) at the surface .

Minimum Value= 0.00   Maximum Value= 5.91   Contour Interval: 0.10